
SECOND EDITION
OFFSHORE STRUCTURES
DESIGN, CONSTRUCTION AND MAINTENANCE
MOHAMED ABDALLAH EL-REEDY
G P
P

Offshore Structures

Offshore Structures

Design, Construction and Maintenance

Second Edition

Mohamed Abdallah El-Reedy, Ph.D.
Consultant Engineer and International Instructor

ELSEVIER

Gulf Professional Publishing
An imprint of Elsevier

Gulf Professional Publishing is an imprint of Elsevier
50 Hampshire Street, 5th Floor, Cambridge, MA 02139, United States
The Boulevard, Langford Lane, Kidlington, Oxford, OX5 1GB, United Kingdom

Notices
Knowledge and best practice in this field are constantly changing. As new research and experience broaden our understanding, changes in research methods, professional practices, or medical treatment may become necessary.

Practitioners and researchers must always rely on their own experience and knowledge in evaluating and using any information, methods, compounds, or experiments described herein. In using such information or methods they should be mindful of their own safety and the safety of others, including parties for whom they have a professional responsibility.

To the fullest extent of the law, neither the Publisher nor the authors, contributors, or editors, assume any liability for any injury and/or damage to persons or property as a matter of products liability, negligence or otherwise, or from any use or operation of any methods, products, instructions, or ideas contained in the material herein.

British Library Cataloguing-in-Publication Data
A catalogue record for this book is available from the British Library

Library of Congress Cataloging-in-Publication Data
A catalog record for this book is available from the Library of Congress

ISBN: 978-0-12-816191-3

Publisher: Matthew Deans
Acquisition Editor: Matthew Deans
Editorial Project Manager: Peter Llewellyn
Production Project Manager: Sruthi Satheesh
Cover Designer: Greg Harris

Typeset by MPS Limited, Chennai, India

Dedication

This book is dedicated to the spirits of my mother and my father.
To my wife and my children, Maey, Hisham, and Mayar.
And to those who inspired me.

Contents

About the author

Mohamed Abdallah El-Reedy, PhD, pursued a career in structural engineering. His main area of research is the reliability of concrete and steel structures. He has provided consulting services to different engineering companies and oil and gas industries in Egypt and to international companies including the International Egyptian Oil Company (IEOC) and British Petroleum (BP). Moreover, he provides concrete and steel structure design packages for residential buildings, warehouses, telecommunication towers, and electrical projects of WorleyParsons Egypt. He has participated in liquefied natural gas and natural gas liquid projects with international engineering firms. Currently, he is responsible for reliability, inspection, and maintenance strategies for onshore concrete structures and offshore steel structure platforms. He has managed these tasks for about 100 of these structures in the Gulf of Suez in the Red Sea.

He has consulted with and trained executives at many organizations, including the Arabian American Oil Company (ARAMCO), British Petroleum (BP), Apache, Abu Dhabi Marine Operating Company (ADMA), the Abu Dhabi National Oil Company and King Saudi's Interior Ministry, Qatar Telecom, Egyptian General Petroleum Corporation, Saudi Arabia Basic Industries Corporation, the Kuwait Petroleum Corporation, Qatar Petrochemical Company (QAPCO), PETRONAS Malaysia, and PTT Thailand. He has taught technical courses about offshore structure design and offshore structure integrity management systems worldwide.

He has written numerous publications and presented many papers at local and international conferences sponsored by the American Society of Civil Engineers, the American Society of Mechanical Engineers, the American Concrete Institute, the American Society for Testing and Materials, and the American Petroleum Institute. He has been a member of the technical committee for the Offshore Mechanics and Arctic Engineering (OMAE) conference for 10 years. He has published many research papers in international technical journals and has authored seven books about total quality management, economic management for engineering projects, and the repair and protection of reinforced concrete structures, advance materials, onshore projects in oil and gas offshore structure and concrete structure reliability, and marine structure calculation. He earned a bachelor's degree from Cairo University in 1990, a master's degree in 1995, and a PhD from Cairo University in 2000.

Preface

The first addition of this book was successful in helping many engineers worldwide, based on their positive feedback, which encouraged me to enrich this edition with the addition of new topics. For this new edition I have added up-to-date techniques for most topics and also added a new chapter about the design and installation of subsea pipelines, as this is a very important topic for anyone working on offshore projects. In addition, as decommissioning projects are increasing rapidly due to the existing mature structures, so I try to focus on this in this edition.

When a structural engineer start works in the design, construction, or maintenance of offshore structures, it will be a steep learning experience as most engineering faculties, especially for structural or civil engineering, focus on the design of residential, administration, hospital, and other domestic concrete or steel structure buildings. In contrast, some courses in the faculty are concerned with the design of harbors.

The design of offshore structure platforms combines the steel structure design methods with the loads that are applied to the harbor, such as waves, currents, and other parameters. The design of the platforms is dependent on technical practice which relies on the experience of the engineering company itself.

On the other hand, the construction of steel structures is more familiar to the structure engineer as the construction of new steel buildings is widely seen throughout society, but the construction and installation of offshore structure platforms is very rarely seen, unless the individual has a direct role in the project as the installation will be in the sea or ocean. There are few offshore structures worldwide when compared with the steel structures for normal buildings on land. Therefore the major design guide and roles for offshore structures are dependent on research and development which are growing rapidly to keep pace with the development of related businesses throughout the world.

Therefore all the major oil and gas exploration and production companies are supporting and sponsoring more researches to enhance the design and reliability of offshore structures to grow the revenue from these petroleum projects and their assets.

The aim of this book is to cover the design, construction, and maintenance of platforms deeply, with comprehensive attention focused on the critical issues in design that usually face the designer and to provide the simplest tools for design based on the most popular codes, such as American Petroleum Institute (API), International Standards Organization (ISO), and the other technical standards and practices that are usually used in offshore structure design. In addition, it is also important to focus on the methods of controlling and reviewing the design, which

will face most engineers on the reviewing cycle, and so this book is prepared to cover the whole scope of the offshore structure engineer's activities whatever their role in the big theater.

The offshore structure platform is considered a large asset in oil and gas projects, so another goal of this book is to assist the structural engineer in becoming familiar with decision-making in design and the factors, parameters, and constraints that face the owner and designer and which control the options and alternatives in the engineering studies phase.

Also, the offshore project lifecycle is very important to be identified from an owner, engineering firm, and contractor point of view. Therefore the structural engineer should have an overview of the relation between the structure system and its configuration from economic and engineering points of view.

Most offshore structure platforms were constructed worldwide in the period of growing oil investment between 1970 and 1980, therefore these platforms now have an age of over 40 years. There are also many mature offshore structures worldwide which are going through rehabilitation projects to increase and maintain their structural reliability. The decommissioning of a platform is one of the raised topics due to the age of the existing structures, and so this book presents a case study for platform decommissioning. In addition, the development of an integrity management system with an up-to-date advanced technique for qualitative and quantitative risk assessment is essential these days to develop a risk-based inspection and maintenance plan that enhances the reliability of platforms throughout their life time while providing optimum performance.

Therefore another aim of this book is to provide an advanced technique in topside and underwater inspection and assessment of offshore structure platforms, with the methods to implement a maintenance and rehabilitation plan for a platform that matches with the business requirement.

It is also important to present cases studies for the methods of repair and strengthening of platforms and the methods for decommissioning platforms in the case of required platform demolition.

It is intended for this book to be a guidebook for junior and senior engineers who work in the design, construction, repair, and maintenance of fixed offshore structure platforms.

The book provides an overview and a practical guide for the traditional and advanced techniques in the design, construction, installation, inspection, and rehabilitation of fixed offshore structure platforms with the principles of repairing and strengthening of the fixed offshore structures and the methodology to deliver a maintenance plan for a fleet of platforms. In addition, the book provides the main features of the design, construction, and installation of a subsea pipeline.

Mohamed Abdallah El-Reedy
Cairo, Egypt
Email: elreedyma@gmail.com
www.elreedyman.com

Introduction to offshore structures 1

1.1 Introduction

Offshore structures have special characteristics from economic and technical points of view, where offshore structure platforms are dependent on oil and gas production which directly, through the oil price, affects worldwide investment.

From a practical point of view, increasing oil prices, as happened in 2008, enable many offshore structure projects to be started.

From a technical point of view the offshore structure platform design and construction is a merger between steel structure design and harbor design, and there are a limited number of faculty engineering areas focusing on offshore structural engineering, such as the design of fixed offshore platforms, whether floating or other types. On the other hand, due to the limited number of offshore structural projects with respect to normal steel structure projects, such as residential, factories, and others, these depend on continuous research and studies over a long time period from many countries around the world.

All the major multinational companies working in the oil and gas business are interested in offshore structures research and studies.

Therefore these companies continuously support research and development to enhance the capability of engineering offices and construction contractor companies that they deal with to support their business need.

1.2 History of offshore structures

As early as 1909 or 1910 wells were being drilled in Louisiana. Wooden derricks were erected on hastily built wooden platforms constructed on top of woodpiles.

Over the past 40 years two majors categories of fixed platforms have been developed—the steel template type which was pioneered in the Gulf of Mexico (GoM) and the concrete gravity type first developed in the North Sea.

Recently a third type has been the tension-leg platform which was used due to the need to drill wells in deep water and for the development of gas projects in deep water.

In 1976 Exxon installed a platform in the Santa Barbara channel with water depth of 259 m (850 ft.).

There are three basic requirements in the design of a fixed offshore platform:

1. Withstand all loads expected during fabrication, transportation, and installation;

Offshore Structures. DOI: https://doi.org/10.1016/B978-0-12-816191-3.00001-8

2. Withstand loads resulting from severe storms and earthquakes;
3. Function safely as a combined drilling, production, and housing facility.

Around 1950, while the developments were taking place in the GoM and Santa Barbara channel, BP was engaged in similar exploration on the coast of Abu Dhabi in the Persian Gulf.

The water depth there is less than 30 m (100 ft.) and the operation grew steadily over the years.

In the 1960s hurricanes in the GoM caused serious damage to the platform forcing a reevaluation of platform design criteria. The following hurricane history occurred in the GoM:

- With hurricane Hilda in 1964, wave heights of 13 m and wind gusts up to 89 m/s were experienced, this once-in-100-years storm resulted in 13 platforms being destroyed;
- The next year another storm with a 100-year recurrence probability, hurricane Betsy, destroyed three platforms and damaged many others;
- Subsequently, designers abandoned the 25- and 50-year conditions and began designing for storm recurrence intervals of 100 years.

1.3 Overview of field development

Estimates for future oil reserves in different areas of the world, based on geological and geophysical studies and oil and gas discoveries as of January 1996, forecast that about 53% of these reserves are in the Middle East, which may be a reason for the political troubles in that part of the world. Sixty percent of all reserves are controlled by the Organization of Petroleum Exporting Countries (OPEC). This explains why OPEC and Middle East are so important for the world's current energy needs.

Companies and countries have good assessments of the undiscovered reserves in the Middle East and the former Soviet Republics. Most researchers believe that the major land-based hydrocarbon reserves have been already discovered and most significant future discoveries are expected to be in offshore and arctic regions and other difficult to reach and produce areas of the world.

The geological research depends on studying why North America, northwest Europe, and the coastal areas of West Africa and eastern South America appear to have similar potential for deep water production. At this stage in the geological history, sediments were deposited in basins with restricted circulation, which were later converted to the super source rocks found in the coastal regions of these areas. The presence of these geological formations gives us an initial indication for the discovery of hydrocarbons.

Based on studying the reservoir characteristics, the decision has to be taken whether particular offshore areas have potential economic hydrocarbon reserves or not.

A team of geologists and geophysicists performs an assessment study of the geological formations. Then a feasibility study should be done by preparing the cost,

schedule, and studying the economics by calculating the financial parameters based on the rules, laws, and concession agreements that cover production in that area.

At this stage, there are many unknowns and uncertainties of the available data, as there is no comprehensive information about the reservoir characteristics or the oil and gas prices in the future. The experts need to carry out a study and make recommendations based on their past experience for similar projects, on cost and schedule estimates based on data available to the company from their previous history. The success of the oil and gas companies depends on their expertise in these decisions, and so most of these companies keep their expertise within their company and compete with each other. Sometimes, the available data are insufficient and decisions are made as a result of brainstorming sessions attended by experts and management, and can be greatly affected by the company culture and past experience.

The following factors affecting decisions on field development:

- Reservoir characteristics;
- Production composition (oil, gas, water, H_2S, and others);
- Reservoir uncertainty;
- Environment, such as water depth;
- Regional development status;
- Local technologies available;
- Politics;
- National content;
- Partners;
- Company culture;
- Schedule;
- Equipment availability;
- Construction facilities availability;
- Market availability;
- Economics.

If the preliminary economic studies in the feasibility study phase are positive, the geophysicists start to generate the seismic data and evaluate them. The main information required to estimate the reserve is to obtain its depth, spread, faults, domes, and other factors, then an estimate of the recoverable reserves of hydrocarbons can be made with reasonable accuracy.

The exploratory drilling shall be started after the seismic testing provides positive results and management make the decision to go ahead.

The selection of a suitable exploration scheme depends on the location, water depth, and environmental conditions.

In the case of shallow water the best option is to use a jack-up exploratory unit. In water depths exceeding 120 m (400 ft.), ships or semisubmersible drilling units are utilized. In the case of 300 m (1000 ft.) water depths, floating drilling units are selected and provide special mooring arrangements or a system of dynamic positioning. The floating semisubmersible drilling rig is capable of operating in 900−1200 m (3000−4000 ft.) water depths

Delineation exploratory drilling work follows the discovery well.

In most cases these drilling wells number from three to six wells at the reservoir. These drilling wells carry out a test for production and provide reasonable detailed data about the size, depth, and extent of the reservoir. In addition to reservoir topography such as fault lines, impermeable layers, etc. and recoverable reserves, the viscosity which is presented by the API grade, and the fluid characteristics such as oil−water ratio and other impurities such as sulfur or other critical components, are calculated.

Reservoir information enables the geologists and geophysicists to suggest the best location and number of wells that will provide an economic production volume of oil and gas and this information is mandatory to estimate the required production facilities and the method of transport for the produced oil and gas.

Therefore it is obvious that the accuracy of the reservoir data is very important as the estimated cost for all the production facilities is dependent on these data in the appraisal stage. The challenge in marginal or complex reservoirs, as the accuracy of the reservoir estimation is not high, is that the appraise design should consider flexible production facilities that can be changed to accommodate any changes in reservoir characteristics.

1.3.1 Field development cost

The field development for a new project or to extend existing facilities is performed through many cycles. The first step is to collect the essential data such as the reservoir and environmental data; the proposed best design for the major system such as the production drilling wells and facilities; and to define the economics and other decision criteria. The next important step is to evaluate the different field development alternatives that are a result of the collected data and a ranking system is established between the different options as per the agreed decision criteria.

The next step is to prepare the concept and then the front end engineering design (FEED) for the selected system. These cycles are repeated until all the engineering members from all engineering and operation disciplines are satisfied from a technical point of view. At the end of the detailed engineering the construction activities shall be well defined. Sometimes there are changes to the system or one of its components, however, these changes in most cases are under control and there are no major delays or cost overruns.

After transferring the project to operations, they are responsible for the operation and performance of the required maintenance based on their maintenance plant and they also perform repairs and reassessments for the production facilities and maintain the pipeline for oil and gas transportation.

In the FEED, after defining the required facilities on the topsides of the deck, the geometrical shape of the platform will be defined and a preliminary structure analysis is run through structure analysis software to choose the most suitable section that matches with the loads and the geometrical shape, with suitable deck dimensions that serve the required facilities on the deck. The structure system of the jacket and method of construction based on the water depth are

selected in this phase. The new project management approach is called the select phase.

In practice it is found that the FEED phase selects between the options and provides a preliminary engineering approach, this stage usually costs about 2%−3% of the field development total project cost (TPC), but it has a major impact on the cost, schedule, quality, and success of the project as a whole. If this stage is ignored or there is insufficient time and effort expended, there are likely to be major cost overruns. It is found that for projects that do not perform an adequate FEED the cost is increased by about 50% of the actual TPC compared with if the FEED phase is performed in a professional way.

Fig. 1.1 shows the variation in the value of the total installed cost estimates through different phases of a project.

After finalizing the key stages of the project, an economic study is performed based on the new completion date, and based on that other parameters of the economic study are more accurate, which assist the management in taking decisions based on the economic criteria. For the select phase, which is the concept and start of the FEED, a selection is made between the main alternatives, for example, constructing a platform and installing a pipeline to offshore or using floating, production, storage, and offloading (FPSO) or transporting the oil from one location to another near facilities for another platform or even a platform belonging to a

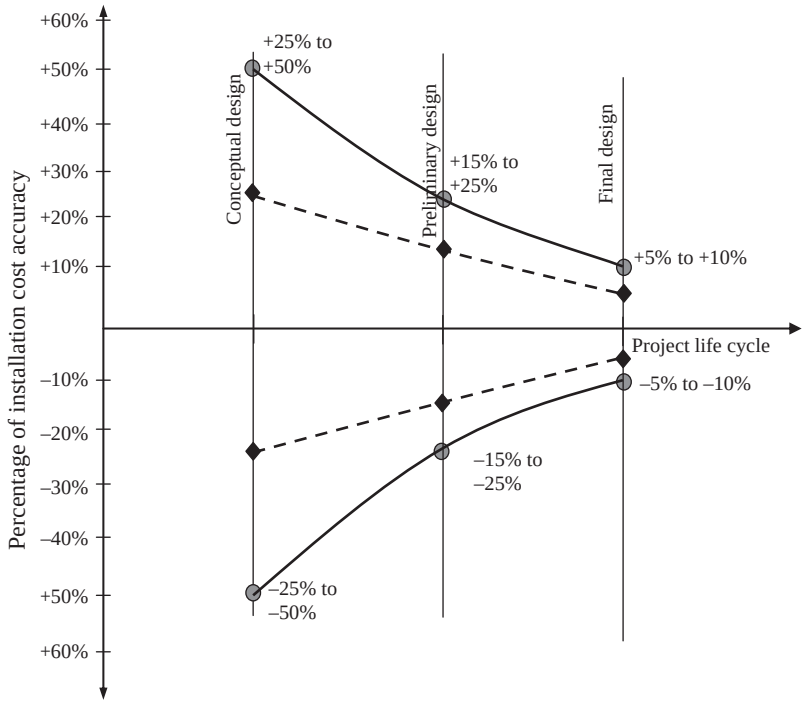

Figure 1.1 Accuracy of the installation cost at every project stage.

different company. This stage also defines the required topside facilities and the living quarters, and the numbers of conductors and risers, all of which affect the project cost and schedule. At this phase, the accuracy of the total installed cost estimates is within a $\pm 15\% - \pm 40\%$ range.

Any technology has risks and it is often found that many projects with new techniques and innovations have major problems during operations compared with those using traditional equipment and facilities.

After finalizing the FEED engineering procedure the process flow diagram (PFD) and the piping and instrumentation diagram (P&IDs) for the platform are available, and the platform plot plan and its structure system are defined with the design of the main element and the major production facilities are known, as are the equipment list and data sheet with specifications; therefore the accuracy of the cost estimate for the project TPC is estimated to be around $\pm 15\% - 25\%$.

Savings made in detailed design and construction phases will generally help in achieving good project controls and execution.

At the end of this stage the detailed engineering package is available, including approved for construction drawings and specifications that will cover all phases from fabrication, transportation, installation, precommissioning, until hook-up and commissioning in the field.

Effective project management in the execution plan, schedule, cost control, quality control, verification, safety assurance, purchasing management, and documentation provides good results on the TPC. As a rule of thumb, at the start of the construction phase the accuracy of the TPC estimates are in the $\pm 10\%$ range.

In most cases these projects are time driven as the owner pushes the project to start production as early as possible, as production is in barrels per day (bpd) so if you have a production of 10,000 bpd, with a 1 month earlier start the gain shall be 300,000 Bl, so assuming the oil price is 50 USD/Bl, the gain is 15,000,000 USD in 1 month.

For the first year from the project start up the cash flow is negative. Until the start of production the negative value decreases until it reaches the value of zero, which is the break-even point. The payout time should be reached as quickly as possible and it depends on the capital cost and the revenue from production; sometimes this point can be reached by the second quarter of the third year from starting production. The Payout method is one of the economic factors that is important to be considered with other decision criteria factors as which are already discussed. The payout method define the break-even point which is mandatory to define it to control the project to remain or decrease the time period until reach this point. whereas after achieve the break even point, the cash flow shall be positive, so when this time period is less, the gain of revenue will be fast.

For field development when constructing a new platform with drilling activities, in most cases the negative cash flow increases from the start of the project, reaching the highest negative cash flow value when production starts, and can take from 1 to 3 years depending on the project duration. From this point the negative cash flow decreases gradually until reaching the break-even point (equal to zero). and then start to become positive. In one project, the zero cumulative cash flow position was

reached within the third quarter of the fourth year—related to the capex, the oil and gas production, and the operating cost value also.

In practice, after constructing the platform, the gas volume may be increased later; in this case the companies will increase the compression facilities by constructing another platform. In some cases, due to a decline in oil, water flood facilities are needed and so it is required to construct another platform, however, time may be a constraint and so a crash schedule may be needed to allow the construction of a satellite platform within 6 months as this will enhance production quickly.

The budget and available cash for investment vary from one oil company to another, depending on its facilities worldwide and also the market status. The decision to accept creating new platforms depends on many factors that should be addressed in the feasibility stage, such as the market situation, taxes, the country's regulation, internal rate of return and the time value of money, the inflation rate, the oil price forecast, and the company cash flow.

1.3.2 Multicriteria concept selection

In the project selection phase there are many factors that affect the concept selection, in addition to economic parameters there are the political situation of the country, the culture(s), the infrastructure of the country in which the project is taking place, and also the technology transfer, in addition to the environmental pollution rules in the relevant country. Other factors include the shareholder and its percentage in the production and the concession agreement terms and conditions which have a major impact on the economic study.

During the selection between different concepts, in addition to the above factors, there are concept criteria that must be established and scores obtained for each item to enable comparisons between the alternatives. These criteria are set by a team of experts and also during the evaluation and assessment phase for each option. Expert judgment is the main factor at this stage.

After finalizing the basic design, the platform structure configurations and the geometric size are obtained for the production facilities. All these data go to the engineering, procurement, and construction (EPC) tender to invite contractors to bid for the project through this project strategy.

In general, the output from the basic design shall be as follow:

- The field development plan;
- Conceptual design drawings for the platform structure, the piles design, the pipeline size and routes, the configurations and number of wells and risers, the long lead items;
- The reservoir maps and production profile shall be delivered in this stage;
- The PFD and the major equipment list;
- At the end of the concept study the cost estimate can be calculated with accuracy ($\pm 15\% - \pm 40\%$), with this range depending on the nature of the project and the associated risk and tentative time schedule for the whole project and based on that the economic parameters can be obtained, such as the capital and operational expenses, cash flow diagrams, and net present value (NPV).

The owner shall prepare the above study by their team or with the assistance of a specialized engineering firm, so that these documents shall be the start point for the next step.

1.4 Front end engineering design requirements

The FEED phase starts after the appraisal stage, during the FEED engineering phase the following deliverables shall be obtained.

- The engineering firm shall deliver a basic engineering package from design drawings for the platform and deck structures and components such as the jacket structure, deck structure, piles, conductors, and risers. This package should provide sufficient detail to allow an accurate cost and schedule estimate. This information is mandatory, particularly if the owner's strategy is to hire an EPC contractor.
- The engineering firm shall deliver a basis of design (BOD) document for the detailed design phase. The objective of the BOD document is to clarify the detailed design requirements including the platform structure system, which is selected from FEED, and this document shall contain the environmental parameters such as metocean, seismic, ice, and others, with the site-specific data such as water depth, temperature, soil characteristics, mud slides, shallow gas pockets, etc.
  - The design load shall be defined, such as the equipment in its dry and empty condition and the associated live loads in addition to the dynamic impact due to rotating equipment and pumps for mud.
  - The accidental design loads shall be defined as, for example, the boat impact, dropped objects, fire and blast, and its effect on the control room.
  - The identification of load combinations considering extreme environmental, operational, transportation, lift, and launch.
  - It will define the design, specifications requirement, technical practice, and codes with the applied regulations.
  - The general appurtenances, such as the escape way and evacuation equipment with the location of boat landing, and barge bumpers, this along with the plot plan shall be approved and reviewed by all disciplines.
  - The cathodic protection (CP) system will be selected by defining the anode type and the impressed current.
  - The construction and installation method will be discussed in this phase considering the country-specific marketing for the available vessel to handle the project by considering the cost as based on that which will define the loadout procedure, lifting, skidding, and launching.
  - It will address also the operational requirements such as the jack-up drilling unit clearances, tender rig sizes, and weights.

The following activities should be carried out in this phase also.

- Prepare detailed PFDs considering that if detailed engineering starts without final PFDs, any process changes in the detailed stage will have a direct impact on the cost and time schedule.
- Deliver the final (P&IDs) drawings.
- Deliver the final drawings for the deck and facility layouts, considering that review by the entire project team of the layout is very important, with the engineering discipline and

also operations representative to agree on the space and clearance for all equipment as being reasonable from an operations point of view.
- Deliver a data sheet with material take off and specifications.
- Deliver the detailed engineering for the load out, sea fastening, and transportation.
- Provide the scope of work for the precommissioning and commissioning activities.
- The in-place structure analyses and associated analysis required to design the platform.

1.5 Types of offshore platforms

There are different types of fixed offshore platforms which are dependent on the function of this platform:

- Drilling/well-protector platforms;
- Tender platforms;
- Self-contained platforms (template and tower);
- Production platforms;
- Flare jacket and flare towers;
- Auxiliary platforms.

Each of these types of platforms has its characteristics from a functionality point of view and these platforms are further described below.

1.5.1 Drilling/well-protected platform

This platform is used to drill the oil and gas well so the rig will approach this platform to drill the new wells or perform the work through the platform life.

Platforms built to protect the risers on producing wells in shallow water are called well-protectors or well jackets.

Usually a well jacket serves from one to four wells.

1.5.2 Tender platforms

The tender platform is not used as commonly now as it was 40 years ago. This platform is functionally used as the drilling platform but in this case the drilling equipment will rest on the platform topside to perform the job, however, now it is normal to use the jack-up rig.

In this type of platform, the derrick and substructure, drilling mud, primary power supply, and mud pumps are placed on the platform.

As mentioned earlier, these types of platform are not seen in new designs or new projects but they can be found in old platforms, and so this information is needed in case an assessment is required for the drilling platform.

Fig. 1.2 presents a tender platform where above the deck are two beams along the platform deck length to be used as a railway to the tender tower above the deck for drilling activity.

Figure 1.2 Tender platform.

1.5.3 Self-contained platforms

The self-contained platform is large, usually multiple decked, and has adequate strength and space to support the entire drilling rig with its auxiliary equipment and crew quarters and enough supplies and materials to last through the longest anticipated period of bad weather when supplies cannot be brought in.

There are two types: the template type and the tower type.

1.5.4 Production platform

Production platforms support control rooms, compressors, storage tanks, treating equipment, and other facilities. Fig. 1.3 shows a production platform carrying the separators and other facilities for production purposes.

1.5.5 Quarters platform

The living accommodation platform for offshore workmen is commonly called the quarters platform.

1.5.6 Flare jacket and flare tower

A flare jacket is a tubular steel truss structure that extends from the mud line to approximately 3−4.2 m (10−13 ft.) above the mean water line.

It is secured to the bottom by driving tubular piles through its three legs.

1.5.7 Auxiliary platform

Sometimes small platforms are built adjacent to larger platforms to increase the available space or to permit the carrying of heavier equipment loads on the principal platforms.

Figure 1.3 Production platform.

Such auxiliary platforms have been used for pumping or compressor stations, oil storage, quarters platforms, or production platforms. Sometimes they are free-standing, other times they are connected by bracing to the older structure.

1.5.8 Bridges

A bridge 30–49 m (100–160 ft.) in length that connects two neighboring offshore structures is called a catwalk.

Catwalks supporting pipelines, pedestrian movement, or a bridge of materials handling and the different geometries of the bridges are shown in Figs. 1.4 and 1.5 presents a photo of a bridge between two platforms.

1.5.9 Heliport

The heliport is the landing area for helicopters, so it must be large enough to handle loading and unloading operations.

A square heliport has side lengths from 1.5 to 2.0 times the length of the largest helicopter expected to use it.

The heliport landing surface should be designed for a concentrated load of 75% from the gross weight.

The impact load is two times the gross weight for the largest helicopter, and this load must be sustained in an area $24'' \times 24''$ anywhere in the heliport surface. Fig. 1.4 shows a heliport platform.

1.6 Different types of offshore structures

There are different types of offshore platforms from a structure system point of view which have been developed over time due to the requirements from owners to obtain oil and gas from locations with greater water depths.

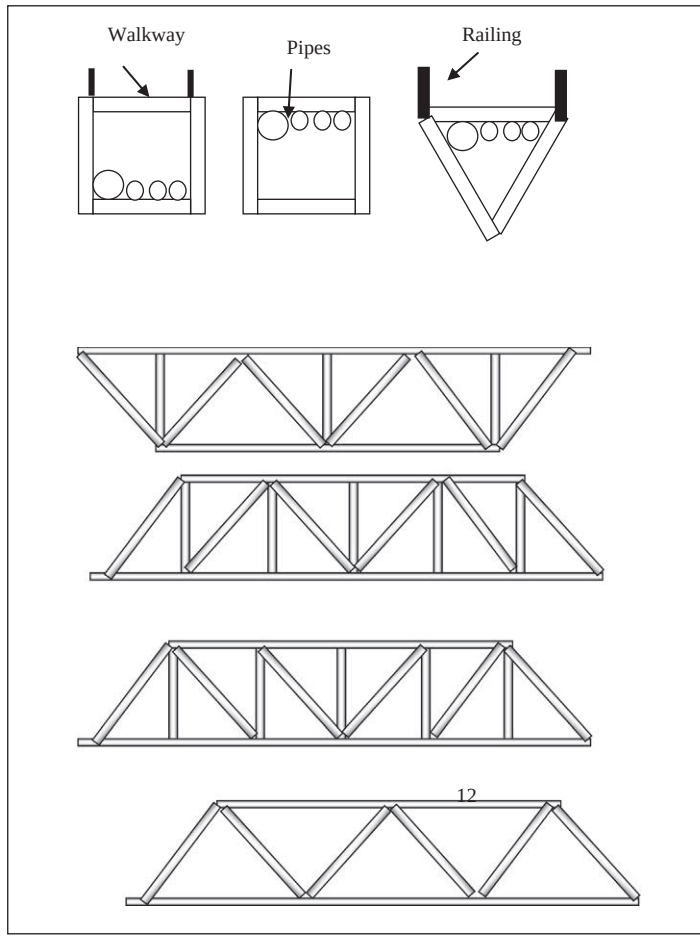

Figure 1.4 Different bridge geometries.

These types of platforms are described here.

1.6.1 Concrete gravity platform

A concrete gravity platform for Shell was constructed in 1997. The concept of concrete gravity is to store the liquid at the seabed. The problem is the corrosion of the steel bars due to the harsh environment and multiple methods are used for protection from corrosion.

Fig. 1.6 presents a photo of a well-protector platform with four legs which is a satellite platform and Fig. 1.7 illustrates a complex platform consisting of a production and drilling platform connected by bridges.

In some areas there will be a low reserve so it is required to drill only one well so many solutions have been developed to solve this situation and to obtain the

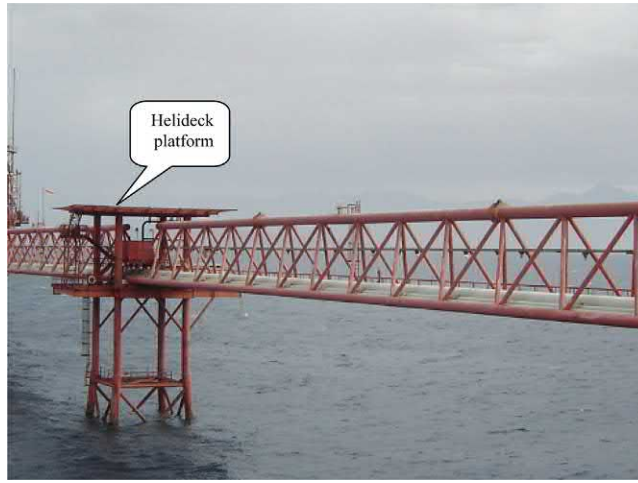

Figure 1.5 Photo of bridges connecting a helideck platform.

Figure 1.6 Satellite platforms.

target. One of these solutions is to have a subsea well and to be connected to the nearest platform by a pipeline, this solution is costly but it is now used widely in the case of deep water.

The other solution is to use a minimal offshore structure as shown in Fig. 1.8A and B (for elevation and plan views, respectively). The concept for this platform is to use the conductor itself as the main support to the small deck as shown in the

Figure 1.7 Complex platforms.

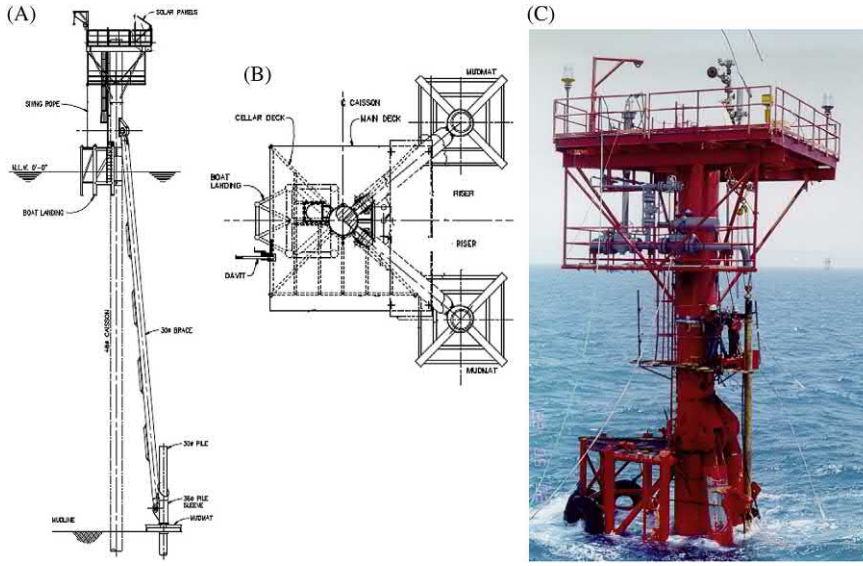

Figure 1.8 (A) Three-leg platform elevation view; (B) three-leg platform plan view; and (C) photo of a three-leg platform.

Figure 1.9 Floating, production, storage, and offloading (FPSO).

figure and there also two diagonal pipes are connected to the soil by two piles as shown in the elevation view. The shape of the topside for this three-leg platform is shown in Fig. 1.8C.

1.6.2 Floating production, storage, and offloading

The first tanker converted to FPSO was done in 1969 and this is the oldest FPSO in the world and is still in existence in Egypt, as shown in Fig. 1.9. In Spain, in 1977, the first FPSO was built. As per the development in gas processing in the last 25 years, in 2007 the first conversion was done for a liquified natural gas (LNG) carrier into an LNG floating storage tanker, this conversion was done in Singapore by the Keppel shipyard.

Due to increase in the locations of marginal fields and the specific gas reserve having a shorter lifetime than oil, many FPSOs have been built and conversions to tankers carried out in the last 15 years. The concept of the oil FPSO and LNG FPSO is the same but the LNG FPSO produces only condensate, natural gas. In 2018 the commissioning with the biggest FPSO in the world in Nigeria.

FPSO vessels are particularly effective in the case of the reserve locations away from the shoreline or far from production facilities, which requires the transport of the fluid to it or the installation of a pipeline being too expensive due to the distance from the shore and the cost related to the reserve volume. It is used also in the case of deep water very successfully as the traditional platform is uneconomical or cannot be used. On the other hand, for a marginal field when the reserve study expects that the lifetime is within 10−15 years, it the most economic solution can be using an FPSO rather than spending a money on an asset that after a time shall not be used, whereas the FPSO can be relocated once the field is depleted.

The deepest water depth operating FPSO is owned by Shell USA and SBM offshore and is called Espirito Santo FPSO.

In Brazil there are FPSOs working at depths of 1800 m (5400 ft.).

1.6.3 Tension-leg platform

A tension-leg platform (TLP) is a floating structure with a vertical special tie wire to the seabed and is used for water deeper than 300 m (1000 ft.), and it is a more economic solution for these water depths.

In the 1980s the first TLP was installed in the North Sea in Cononco's Hutton field. This TLP was constructed by two contractors as the hull was constructed in a dry dock in the north of Scotland at Highland Fabricator's Nigg yard and the deck was constructed at Ardersier at McDermott's yard. The Magnolia TLP was constructed in a water depth of 1425 m (4674 ft.).

Fig. 1.10 presents a brief summary of different types of the platform structures and their range depending on the water depth and function. These ranges change with time as there are many researches and developments involved in the construction of structures in deep water.

Nowadays there is a major trend to use gas, which was not used 40 years ago but was burnt off, therefore there are many projects aiming to discover gas for production and so exploration has been extended to deep water, which is not matched by the conventional steel structure platforms. Due to the requirement to produce from the area in deep water, there are a lot of researches and development have been done, by universities, owner companies and associated with engineering firms to go through using a floating platform on the sea and connected it by a tension wires to the seabed.

On the other hand, there are many platform shapes that have been constructed over the years, such as minimum offshore structures with one pile by using the conductor itself as a support with two inclined members as a support for the pile. In

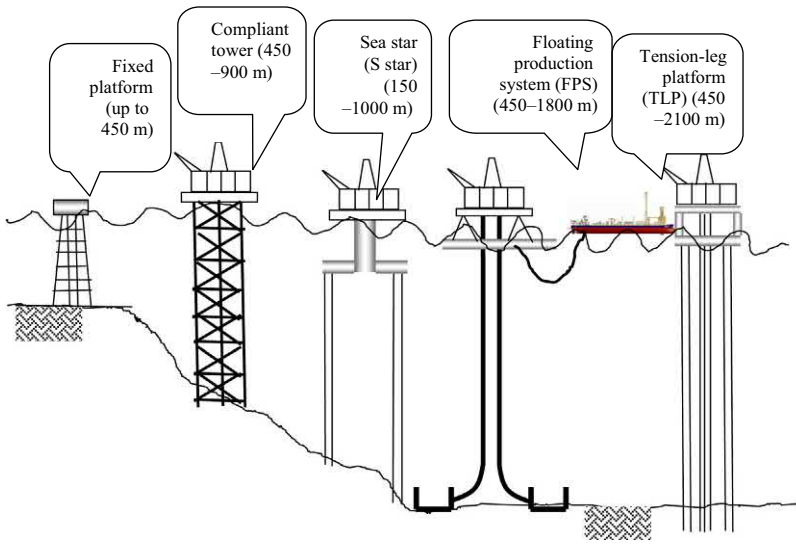

Figure 1.10 Different types of offshore structures.

addition, in the last 20 years many projects have used concrete gravity platforms by making a platform from reinforced concrete structure and there are many researches and structures using these types of platform.

This chapter gives an overview of all types of offshore structures that have been used in oil and gas projects.

The chapter also focuses on the economics and policies that guide and direct these projects.

Worldwide there is a relationship between the multinational petroleum industry companies and the countries which own the oil and gas reserves, and usually there is an agreement to share control between them. It is important to bear in mind that most structural engineers are focused on the stresses, strains, structural analyses and codes, and design standards, which are the main elements of their job, but the creation of a solution and selecting the structure configuration and from the other side matching the engineering office knowledge and capability with the owner expectation are not necessarily part of their job description.

The contractors and the engineering firm, and also the engineering staff in the owner organization, should be on the same page to achieve the owner target and goals.

The organization target and policies are based on the business target and profit, the expected oil and gas reserve, the expected oil and gas prices, and the final important factor the country which owns the land and the reserve. Therefore the terms and conditions and the political situation in this country will direct the investment of the project. Therefore any engineer working on this type of project should have a helicopter view of all the constraints around the project as these constraints will be a guide to the engineering solutions, options, and alternative designs, and this overview is very important knowledge for the senior manager staff down to the junior staff.

The load calculation is the first step in any structural analysis. The loads on platforms are usually defined based on the owner specifications. Therefore there are some studies that govern the loads and other technical practices which are discussed in detail in Chapter 2, Offshore structure loads and strength.

To start the design of a offshore structure platform, it is required mainly to understand the principles of the steel structure design and then understand the effect of the environmental loads which is the major loads affect the offshore structures, all these designs are illustrated within the scope of API, ISO19902, ISO, in Chapter 3, Offshore structure platform design.

The foundation is very a critical element to the structure safety and it has many variations and uncertainties, therefore Chapter 4, Geotechnical data and pile design, presents many researches and studies that have been performed for the pile capacity in offshore structures for sand and clay soil. All the tools and data required to estimate the pile capacity by the different researches will be illustrated.

The construction of an offshore structure platform is very costly. The fabrication, erection, launching, and installing of a platform are discussed in detail in Chapter 5, Fabrication and installation.

The corrosion of offshore structures is very critical and there are different types of CP, and so it is required to choose the most suitable system for existing

structures and retrofitting projects. In addition, the design of the sacrificial anode and CP system is presented in Chapter 6, Corrosion protection. Structural engineers usually have a shortage of information in this area and will have to address corrosion in the integrity system to maintain structural reliability. In this case corrosion is a very important factor that should be understood by the maintenance engineer who should be familiar with different CP systems and the main principles for selecting the optimum corrosion protection system. This information will be very important to ensure harmony in the teamwork with the corrosion engineer, who is responsible for the design of the system and the construction group who carry out the system installation. The maintenance engineer should know what the pitfalls are for each system and from the readings of the CPCP during inspection they should have a sense of the structure condition from a corrosion point of view.

Oil and gas platforms are facing a problem of aging as there are many platforms that were constructed over 40 years ago, noting that API for a fixed offshore structure platform design was started in 1969 and so all the old platforms were designed according to the then-current engineering office experience.

It is worth remembering that companies are not using a reports and drawing from 20 years ago as they were hard copies which have been destroyed over time, and we also need to remember that there was not the management of change policy as is currently applied. Therefore there may not be drawings available which match the actual condition. All these factors affect many rehabilitation projects worldwide, and so this book has a separate chapter (Chapter 7: Assessment of existing structures and repairs) to discuss in depth the assessment and evaluation of offshore structure platforms. The risk-based inspection technique has been used recently as a tool to establish a maintenance plan for platform fleet and the qualitative risk assessment method is discussed in detail in Chapter 8, Risk-based inspection technique, as it is a practical tool that can be used in conjunction with the risk-based inspection technique.

Reference

International Organization for Standardization. Petroleum and Natural Gas Industries, Offshore Structures, Part 1. Fixed Steel Offshore Structures. ISO/DIS 19902:2004.

Further reading

Earthly Issues. Gulf of Mexico Deep Water Horizon Oil Spill. <http://www.earthlyissues.com/gulfspill.htm>.

Karasan, D.I., 2000. General Design of Fixed Offshore Structure. University of Texas at Austin, Short Course.

Shell International Ltd. Oil Rig Photos. <http://www.oilrigphotos.com/picture/number202.asp>.

Offshore structure loads and strength

2

2.1 Introduction

Fixed offshore platforms are unique structures as they are located in the sea or ocean and their main function is to carry industrial equipment that services oil and gas production and drilling.

The robust design of fixed offshore structures is dependent on define all the applied loads. Most loads that affect laterally the platform, such as wind and waves, are variables which depend on the metocean data for the location of the platform.

The structure design depends on the strength of materials used and the applied load.

In general the loads which act on the platform are as follows:

- gravity loads;
- wind loads;
- wave loads;
- current loads;
- earthquake loads;
- installation loads;
- other loads.

2.2 Gravity load

The gravity load consists of the dead load and the live (imposed) load. The dead load is the weight of the platform itself and in addition to that the weight of machines such as pump, compressors, and electrical generators, and static equipment like separators, in addition to piping which is a major item.

2.2.1 Dead load

The dead load is the overall weight of the platform structure in air, including piling, superstructure, jacket, stiffeners, piping and conductors, corrosion anodes, decking, railing, grout, and other appurtenances.

Sealed tubular members are considered either as buoyant or flooded, whichever produces the maximum stress in the structure analysis.

The main function of the topside is to carry the load from the facilities and drilling equipment. The percentage between the weights of the topside component is as

Offshore Structures. DOI: https://doi.org/10.1016/B978-0-12-816191-3.00002-X

Table 2.1 Example for weight and weight percentage for an eight-leg platform drilling/production platform.

1.	Deck	Weight (tons)	Percentage (%)
	Drilling deck		
	Plate	82	11.2
	Production deck		
	Plate	62	8.5
	Grating	5.0	0.6
	Subtotal	**149**	**20.3**
2.	Deck beams		
	Drilling deck	184	25.17
	Production deck	66	9.03
	Subtotal	**250**	**32.2**
3.	Tubular trusses weight	156	21.34
4.	legs	115	15.73
5.	Miscellaneous		
	Vent stack	9	1.23
	Stairs and handrails	20	2.74
	Lifting eyes	3	0.41
	Drains	8	1.09
	Fire wall	6	0.82
	Stiffeners	15	2.05
	Total	**731**	**100**

shown in Table 2.1. From this table one can calculate the self weight of the topside for an eight-leg platform in 90 m water depth.

In calculating the self weight a contingency allowance of 5% should be considered to cover the variables in these loads.

The jacket is mainly used to insert the pile inside its legs, whereas the pile is carrying the topside and transfers the load to the soil underneath the mudline with a specific depth. Another function of the jacket is to carry the boat landing, anodes for corrosion protection, and riser guards (Table 2.2).

The golden rule in design is to minimize the projected area of the member near the water surface in high wave zones to minimize the load on the structure and also reduce the foundation requirements.

2.2.2 Live load

Live loads are the loads imposed on the platform during its use and which may change during a mode of operation or from one mode of operations to another and should include the following:

1. the weight of drilling and production equipment;
2. the weight of living quarters, heliport, and other life support equipment;
3. the weight of liquid in storage tanks; and
4. the forces due to deck crane usage.

Table 2.2 Jacket weight for eight-leg platform drilling/production for 100 m water depth.

ID	Component description	Weight (ton)	% of total weight
1.	Legs		
	Joint can	187	14.52
	Between tubular and others	319	24.77
2.	Braces		
	Diagonal in vertical plan	242	18.79
	Horizontal	168	13.04
	Diagonal in horizontal plan	110	8.54
3	Other framing		
	Conductor framing	45	3.49
	Launch trusses and runners	92	7.14
	Miscellaneous framing	3	0.23
4	Appurtenances		
	Boat landing	32	2.48
	Barge bumpers	29	2.25
	Corrosion anodes	22	1.71
	Walkways	16	1.24
	Mud mats	5	0.43
	Lifting eyes	2	0.19
	Closure plates	2	0.16
	Flooding system	7	0.62
	Miscellaneous	4	0.39
	Total	1288	100

Table 2.3 Guidelines for the live load.

	Uniform load beams and decking kN/m^2 (lbs/ft.^{2})	Concentrated line load on decking (kN/m′ lbs/ft.)	Concentrated load on beams (kN) (kips)
Walkways and stairs	4.79 kN/m^2 (100)	4.378 kN/m′ (300)	4.44 kN (1)
Areas over 400 ft.^{2}	3.11 kN/m^2 (65)		
Areas of unspecified light use	11.97 kN/m^2 (250)	10.95 kN/m′ (750)	267 kN (60)
Areas where specified loads are supported directly by beams		7.3 kN/m′ (500)	

The live load is dependent on the owner as he will define it and normally it will be included in the statement of requirement or basis of design (BOD) documents which will be approved by the owner (Table 2.3).

Table 2.4 presents the live load considered in designing the topside decks in general and considers the imposed load applied in the open area in the deck if the equipment load intensity is less than the imposed load.

Table 2.4 Guidelines for live loads.

Area	Loading (kN/m^2)				Point Load (kN)
	Member category (see below)				
	Deck plate grating and stringers	**Deck beams**	**Main framing**	**Jacket and foundation**	
Laydown areas	12	10	c		30
Open deck areas and access hatches	12	10	c	d	15
Mechanical handling routes	10	5	c	d	30
Stairs and landings	2.5	2.5	b	–	1.5
Walkways and access platforms	5	2.5	c	d	5 a

a. Point load for access platform beam design to be 10 and 5 kN for deck grating and stringers, respectively.
b. Loading for deck plate, grating, and stringers should be combined with structural dead loads and designed for the most onerous of the following:
   - Loading over entire contributory deck area;
   - A point load (applied over a 300 × 300 mm footprint);
   - Functional loads plus design load on clear areas.
c. For the design of the main framing two cases shall be considered:
   - Maximum operating conditions: All equipment, including future items and helicopter, together with 2.5 kN/m^2 on the laydown area;
   - Live load: equipment loads, with 2.5 kN/m^2 applied on the laydown areas, with an additional 50-ton live load. This live load shall be uniformly distributed load.
   - Deck loading on clear areas for extreme storm conditions is ignored in design substructure as in storm cases platforms are not manned. A total live load of 200 kN at the topside center of gravity shall be assumed for the design of the jacket and foundations.
d. For substructure design, deck loading on clear areas in extreme storm conditions may be reduced to zero, in view of the fact that the platform is not normally manned during storm conditions. A total live load of 200 kN at the topside center of gravity should be assumed for the design of the jacket and foundations.

DvV (2008) defines the variable functional loads on deck areas of the topside structure based on the data in Table 2.5. These values are considered as guidelines and should be defined on the BOD or design criteria which must be approved by the owner. If the owner needs to increase the load then this should be mentioned in the code and stated on the BOD and the detail drawings should include the load on the deck. In Table 2.5 loads are identified for the local design which will be considered in the designs of plates, stiffeners, beams, and brackets. The loads in primary design should be used in the design of girders and columns. The loads will be defined for the design deck main structure and substructure, and is called the global design.

From Table 2.5 the wheel loads can be added to distributed loads where relevant (wheel loads can be considered acting on an area of 300 × 300 mm).

The point load shall be applied on an area of 100 × 100 mm for the worst position without considering the distribution or a wheel action.

The design of the lay down area is done by applying a load of 15 kN/m^2 as a minimum. As per Table 2.5, q is to be assumed as per each case. The value of f will be from the following:

$$f = \min\{1.0, (0.5 + 3/\sqrt{A})\} \tag{2.1}$$

where A is the area of loading in m^2.

For the structure global analysis, the global load cases shall consider the most severe condition by using a load combination to achieve cases that provide the worst straining action.

In calculating the dry weight of piping, valves and other structure support and increase 20% for contingency to all estimates of piping weight.

As in most cases there are a changes in piping dimensions and location along the structure life time. In addition to that all the piping and its fittings are calculating in the operating condition by assume it is full of water with specific gravity equal to 1 with 20% contingency.

If calculating the dry weight of all equipment, equipment skid, storage and helicopter, the contingency allowance of 10% shall be included in the equipment.

From a practical point of view Table 2.6 presents the live load values from industrial practice.

Table 2.5 Variable functional loads on deck areas.

	Load design		**Primary design**	**Global design**
	Distributed load (kN/m^2)	**Point load (kN)**	**Applied factor for distributed load**	**Applied factor to primary design load**
Storage areas	q	1.5q	1.0	1.0
Lay down areas	q	1.5q	f	f
Lifeboat platforms	9.0	9.0	1.0	May be ignored
Area between equipment	5.0	5.0	f	May be ignored
Walkways, staircases, and platform crew spaces	4.0	4.0	f	May be ignored
Walkways and staircases for inspection only	3.0	3.0	f	May be ignored
Areas not exposed to other functional loads	2.5	2.5	1.0	May be ignored

Table 2.6 Minimum uniform loads from industrial practice.

Platform deck	Uniform load (kN/m^2) (psf)
Helideck	
W/o helicopter	14 (350)
W/bell 212	2.0 (40)
Mezzanine deck	12 (250)
Production deck	17 (350)
Access platforms	12 (250)
Stairs/walkways	4.7 (100)
Open area used in conjunction with the equipment operating and piping loads for operating and storm conditions	2.4 (50)

2.2.3 Impact load

For structural component-carrying live loads which include impact, the live load must be increased to account for the impact effect as shown in Table 2.7.

2.2.4 Design for serviceability limit state

The serviceability of the topside structures can be affected by excessive relative displacement or vibration in a vertical or horizontal direction.

Limits for either can be dictated by:

1. discomfort to personnel;
2. integrity and operability of equipment or connected pipework
3. limits to control deflection of supported structures as in flare structures
4. damage to architectural finishes.
5. operational requirements for drainage (free surface or piped fluids).

Unless more onerous limits are established by the platform owner company or regulator, the following limits of deflection will apply as presented in Section 2.2.4.2.

Vibrations

All sources of vibration shall be considered in the design of the structure. As a minimum the following shall be reviewed for their effect on the structure:

- operating mechanical equipment, including that used in drilling operations;
- vibrations from variations of fluid flow in piping systems, in particular slugging;
- oscillations from vortex shedding on slender tubular structures;
- global motions from the effect of environmental actions on the total platform structure;
- vibrations due to earthquakes and accidental events.

Table 2.7 Impact load factor.

Structural item	Load direction	
	Vertical	Horizontal
Rated load of cranes	100%	100%
Support of light machinery	20%	0
Support of reciprocating machinery	50%	50%
Boat landings	200 kips (890 kN)	200 kips (890 kN)

Table 2.8 Maximum vertical deflection based on ISO 9001.

Structural element	Δ_{max}	Δ_2
Floor beams	*L*/200	*L*/350
Cantilever beams	*L*/100	*L*/150
Deck plate		2*t* or *b*/150

where *L* is the span; *t* is deck thickness; and *b* is the stiffener spacing.

Design limits for vibration shall be established from operational limits set by equipment suppliers and the requirements of personnel comfort and health and safety.

It is important to be obvious that in the case of design of large cantilevers whether formed by simple beams or trusses forming an integral part of the topsides, but excluding masts or booms, they shall normally be proportioned to have a natural period of less than 1 second in the operating condition.

Deflections

The final deflected shape, Δ_{max}, of any element or structure comprises three components as follows:

$$\Delta_{max} = \Delta_1 + \Delta_2 - \Delta_0 \tag{2.2}$$

where Δ_0 is any precamber of a beam or element in the unloaded state if it exists; Δ_1 is the deflection from the permanent loads (actions) immediately after loading; and Δ_2 is the deflection from the variable loading and any time-dependent deformations from permanent loads.

The maximum values for vertical deflections are given in Table 2.8 based on ISO 9001.

In the case of using load resistance factor design (LRFD) in the design, Table 2.9 provides the limits to vertical deflection.

Lower limits may be necessary to limit ponding of surface fluids and ensure that drainage systems function correctly.

Table 2.9 Limiting values for vertical deflection based on load resistance factor design (LRFD).

Structure member	Δ_{max}	Δ_2
Deck beams	*L*/200	*L*/300
Deck beams supporting plaster or other brittle finish or nonflexible partitions	*L*/250	*L*/350

L is the beam span. For a cantilever *L* is twice the projecting length of the cantilever.

Horizontal deflections shall generally be limited to 0.3% of the height between floors. For multifloor structures the total horizontal deflection shall not exceed 0.2% of the total height of the topside structure. Limits can be defined to limit pipe stresses so as to avoid risers or conductors over tresses, or failures. In most cases designers allow higher deflections for structure elements where serviceability is not compromised by deflection.

2.2.5 Helicopter landing loads

The collapse load of the landing gear shall produce the maximum dynamic load on the helideck in the case of an emergency landing. These data shall be obtained from the manufacturer as they are related to the type of helicopter. In the case of these data not being available from the manufacturer it is appropriate to use a total helicopter impact load as equal to 2.5 times the maximum takeoff weight (MTOW).

It is assumed in design that the land of the two main undercarriages or skid for a single rotor helicopter and the load shall be a concentrated load applied at the center of the helicopter and divided equally between the two main carriages. In the case of a tandem main rotor helicopter it is also assumed in design that all wheels land at the same time and also the load on the helipad is considered a concentrated load divided equally between the main undercarriages corresponding to the carriage which is carrying the maximum static weight. In the case of a wheel we can use a contact tire rather than the concentrated load, which will be according to the manufacturer specifications.

Information on the dimensions and MTOWs of specified helicopters is given in Table 2.10.

The *D* value, as per CAP 437 or International Civil Aviation Organization (ICAO) when rotors are turning, is the largest overall helicopter dimension. This D value is the distance from the main rotor tip path plane in the most forward position to the tail rotor tip in the most rearward position; "*t*" indicates the allowable helicopter weight in tons in a particular helideck.

Based on CAP 437, the helideck shall be designed for the takeoff and landing area for the heaviest and largest helicopter using it and to be used in future, as shown in Table 2.9.

Table 2.10 Helicopter weights, dimensions, and D value for different helicopter types.

Type	*D* value (m)	Perimeter "*D*" marking	Rotor height (m)	Rotor diameter (m)	Maximum weight (ton)	Landing net size
Bolkow bo 105D	11.81	12	3.80	9.90	2.3	Not required
Bolkow 117	13.00	13	3.84	11.00	3.2	Not required
Augusta A109	13.05	13	3.30	11.00	2.6	Small
Dauphin SA365N2	13.68	14	4.01	11.93	4.25	Small
Sikorsky S76B&C	16.0	16	4.41	13.40	5.31	Medium
Bell 212	17.46	17	4.80	14.63	5.08	Not required
Super puma AS 332L2	19.50	20	4.92	16.20	9.3	Medium
Super Puma AS 332L	18.70	19	4.92	15.0	8.6	Medium
Bell 214ST	18.95	19	4.68	15.85	7.94	Medium
SIKORSKY S61N	22.20	22	5.64	18.90	9.3	Large
EH101	22.80	23	6.65	18.60	14.6	Large
Boeing BV234LR Chinook[a]	30.18	30	5.69	18.29	21.32	Large

Note: With skid-fitted helicopters the maximum height may be increased with ground handling wheels fitted.
[a]The BV234 is a tandem rotor helicopter and in accordance with International Civil Aviation Organization (ICAO) the helicopter size is 0.9 of the helicopter *D* value, that is, 27.16 m.

Helideck structures should be designed in accordance with the ICAO requirements for the Heliport Manual, International Standards Organization (ISO) codes for offshore structures. For a floating installation, the relevant International Maritime Organization code is applied. It is worth mentioning that in any vessel the helideck maximum size and weight should be listed in its manual and also in the stated classification papers.

Loads for helicopter landing

The helideck should be designed to withstand all the forces applied on it during landing and takeoff.

1. *Dynamic load*
   The dynamic load is due to the impact that happens during landing. There are two cases:
   a. The heavy normal landing, where the impact load factor is 1.5;
   b. Emergency landing, where the impact load factor is 2.5.
   These load factors shall be multiplied by the maximum takeoff mass. This dynamic load is considered as a live load and should be applied with the action effect of (2) to (3) below. The designer shall inspect many positions on the deck during the structure analysis and these position shall produce the maximum straining action for different members.
2. *Structure response factor*
   A structure response factor equal to 1.3 should be considered in design. This is the maximum value can take as it is related to the natural frequency of the helideck.
3. *Live load on the helideck*
   The live load factor is considered equal to 0.5 kN/m^2 to cover the load of persons, snow, and others but in the case of a helicopter at rest this value increases to 3 kN/m^2.
4. *Helideck lateral load*
   The lateral force shall be 0.5 multiplied by the maximum takeoff force. This load shall be defined in more than one direction that produces the maximum strain to the member.
5. *Dead load of structural members*
6. *Wind loading*
   The wind load is as per the design code you are using for ICAO, 3-second gust speed has been used for 50 years.
7. *Deck design*
   To design the deck it is required to check the punching shear from an undercarriage wheel with a contact area of 65×10^3 mm^2 as per CAP 437 and 64×10^3 mm^2 for ICAO.

Loads for helicopters at rest

The helideck should be designed to withstand all the applied forces that could result from a helicopter at rest; the following should be taken into account.

The helideck components shall be designed to resist the following simultaneous actions in normal landing and at rest situations:

- helicopter static loads (local landing gear local patch loads);
- area load;
- helicopter tie-down loads, including wind loads from a secured helicopter;
- dead loads;

- helideck structure and fixed appurtenances self weight;
- wind loading;
- installation motion.

Helicopter static loads

All parts of the helideck accessible to the helicopter shall be designed to carry an imposed load equal to the MTOW of the helicopter. This shall be distributed at the landing gear locations in relation to the position of the center of gravity (CoG) of the helicopter, taking account of different orientations of the helicopter with respect to the installation.

Area load

To allow for personnel, freight, refueling equipment, and other traffic, snow and ice, rotor downwash, and others, a general area load of 2.0 kN/m^2 shall be included.

Helicopter tie-down loads

For design by ICAO consider the wind speed for a 3 second gust wind speed; in the case of applying API RP2L consider the 100-year storm conditions. The touchdown point shall be designed to ensure the helicopter shall be safe during rest in the case of maximum wind occurring. For the helideck on the vessel the movement of the vessel and its effect on the helicopter at rest should be considered.

Wind loading

In the design process the wind load is considered with its direction in the helideck structure with a combination of the horizontal imposed load to obtain the maximum horizontal forces as one case of loading.

Installation motion

During transportation and installation the acceleration forces or the dynamic amplification factors (DAFs) for lifting analysis consider 100-year storm conditions, where normally the forecast during construction will be known and construction is usually stopped in the case of high wind or waves.

Safety net arms

Most civil aviation requirements request a safety net with a length at least 1.5 m horizontally which it can be above the landing deck by not more than 250 mm with a slope of 10 degrees, with this safety net being considered flexible. The frame that carries the safety net shall withstand a weight of 75 kg dropped in an area of 0.25 m^2 from a 1 m height. The aim of this safety net is to protect persons from falling into the sea.

The values for these overall live loads, dead loads, and wind loads are the same as those discussed and should be considered to act in combination with the dynamic load impact as discussed above. Consideration should also be given to the additional wind loading from any parked or secured helicopter.

Based on API RP2L design for heliports, the flight deck, stiffeners, and supporting structure should be designed to withstand a helicopter landing load encountered

during an exceptionally hard landing after power failure while hovering. Helicopter parameters are given in Table 2.11. It is recommended that helicopter parameters such as those given in Table 2.11 be obtained from the manufacturer for any helicopter considered in the heliport design.

The maximum contact area per landing gear, used to design deck plate bending and shear, should conform to the manufacturer's furnished values given in Table 2.11. For multiwheeled landing gear, the given value of the contact area is the sum of the areas for each wheel. The contact area for float or skid landing gear is that area of the float or skid around each support strut.

The load distribution per landing gear in terms of percentage of gross weight is given in Table 2.11.

The design landing load is the landing gear load based on a percent of the helicopter's gross weight times an impact factor of 1.5. For percentages and helicopter gross weights, refer to Table 2.11.

Design load conditions

The heliport should be designed for at least the following combinations of design loads:

1. dead load plus live load;
2. dead load plus design landing load. If icing conditions are prevalent during normal helicopter operations, superposition of an appropriate live load should be considered;
3. dead load plus live load plus wind load.

The classification society for the North Sea in the United Kingdom considers the helideck specifications, these classifications are focused on mobile offshore units, however Lloyd's Register of Shipping and Det Norske Veritas has issued specifications for helidecks in fixed platforms.

These classification bodies are as follow:

- American Bureau of Shipping (ABS);
- Bureau Veritas (BV);
- Det Norske Veritas (DNV);
- Germanischer Lloyd (GL);
- Lloyd's Register of Shipping (LRS).

Tables 2.11 and 2.12 summarize the loading requirements for the most regular specifications. Table 2.12 presents the loads during helicopter landings and Table 2.13 illustrates the loads for helicopters in the rest position.

As per these two tables there are differences between the specification in the following parameters:

- dynamic factor for emergency landing;
- structure response factor;
- the lateral load;
- wind load.

Table 2.11 Different types of helicopter with their technical parameter data from American Petroleum Institute (API).

								Contact area per					
Manufacturer model	**Common name**	**Gross weight**	**Rotor diameter**	**Overall length**	**Type**	**Number**		**Fore**	**Aft**	**Percentage of gross weight per**		**Distance between fore and aft gears**	**Width between gear**
		ton	**m**	**m**		**Fore**	**Aft**	**cm^2**	**cm^2**	**Fore**	**Aft**	**m**	**m**
Aerospatiable													
316B	Lama	2.21	11.0	12.9	Wheel	1	2	297	594	28	72	3.1	2.4 2.6 2.3
319B	AlouetteIII	2.25	11	12.9	Wheel	1	2	297	594	34	66	4.1	2.6
330J	Puma	7.4	15.1	18.2	Wheel	2	4	1200	2142	36	64	5.3	3.0
332L	Super Puma	8.35	15.6	18.7	Wheel	2	2	465	735	40	60	4.5	3.0 2.0
341G	Gazelle	1.8	10.5	12.0	Skid					51	49		2.1 2.1 2.0
360C	Dauphin	3.0	11.5	13.4	Wheel	2	1	213	123	84	16	3.32	2.4
360C		3.0	11.5	13.4	Skid					84	16	3.32	2.3
365C		3.4	11.5	13.4	Wheel	2	1	213	123	84	16	3.32	2.4 2.3
365N	Dauphin2	3.85	11.9	13.5	Wheel	2	2	245	426	22	78	3.6	2.0
Augusta/Atlantic													
A109	Hirando	2.45	11.0	13.1	Wheel	1	2	129	129			3.5	2.3
A-19A	Mark II	2.6	11.0	13.1	Wheel	1	2	46	284	23	77	3.5	2.5

(*Continued*)

Table 2.11 (Continued)

								Contact area per					
Manufacturer model	**Common name**	**Gross weight**	**Rotor diameter**	**Overall length**	**Type**	**Number**		**Fore**	**Aft**	**Percentage of gross weight per**		**Distance between fore and aft gears**	**Width between gear**
		ton	**m**	**m**		**Fore**	**Aft**	**cm^2**	**cm^2**	**Fore**	**Aft**	**m**	**m**
Bell helicopter													
47G		1.34	11.6	13.3	Skid			174	174			1.6	2.3
205A-1		4.3	14.7	17.4	Skid			310	310			2.3	2.7
206B	Jet ranger	1.45	10.2	12.0	Skid			174	174	19	81	1.4	1.8
206L	Lone ranger	5.1	11.3	13.0	Skid			174	174	29	71	2.1	2.2
212	Twin	5.1	14.6	17.5	Skid			310	310	22	78	2.3	2.5
214B	Big lifter	7.3	15.2	19.0	Skid								2.6
214ST	Super transport	7.94	15.9	19.0	Skid			319	319	22	78	2.3	2.5
214ST	Super transport	7.94	15.9	19.0	Wheel	2	2	247	581	22	78	4.8	2.8
222		3.56	12.1	14.5	Wheel	1	2	122	410	19	81	3.7	2.8
222B		3.74	12.8	15.3	Wheel	1	2	123	413	19	81	3.7	2.8
222UT		3.74	12.8	15.3	Skid			310	310	32	68	2.4	2.4
412		5.3	14.0	17.1	Skid			310	310	20	80	2.4	2.5
Boeing vertol													
BO105C		2.3	9.8	11.8	Skid								2.6
bO105CBS		2.4	9.8	11.9	Skid			181	181	36	64		2.5
BK117		2.85	11.0	13.0	Skid			206	206	34	66		2.5
234		21.9	18.3	30.2	Wheel	4	2	2529	1600	58	42	7.9	3.4
CH47234		22.68	18.3	30.2	Wheel	4	2	1007	503			6.9	3.4
107-11		10.03	5.2	25.3	Wheel	2	4	323	323			2.6	3.9

179		8.48	14.9	18.1	Wheel	2	2	1058	529			4.7	2.7 2.2 2.3 2.3
Hughes													
269C		0.93	8.2	9.4	Skid			71	71	41	59		2.0 2.0 2.1
369D		1.36	8.0	9.3	Skid			194	242	33	67		2.1
Sikorsky													
S55T		3.27	16.2	19.0	Wheel	2	2	258	258			3.2	3.4
S58T		5.9	17.1	20.1	Wheel	2	1	1032	290	88	12	8.6	3.7
S61NL		9.3	18.9	22.3	Wheel	2	1	1497	277	85	15	7.2	4.3
S62		3.58	16.2	19.0	Wheel	2	1	697	348	87	13	5.4	3.7 6.0
S65C		19.05	22.0	26.9	Wheel	2	4	994	994	25	75	8.2	4.0
S76		4.67	13.4	16.0	Wheel	1	2	123	310			5.0	2.4
S78C		9.07	16.4	19.8	Wheel	2	1	471	471			8.8	2.7

Table 2.12 Helicopter landing loading specifications for various authorities.

Authority	International Standards Organization (ISO)	CAP	HSE	American Bureau of Shipping (ABS)	Bureau Veritas (BV)	Det Norske Veritas (DNV)	Germanischer Lloyd (GL)	Lloyd's Register of Shipping (LRS)
Heavy landing	–	1.5 M						
Emergency landing	2.5 M	2.5 M	2.5 M	1.5 M[a]	3.0 M	2.0 M	1.5 M	1.5 M[b] 2.5 M[c]
Deck response factor	1.3	1.3[d]	1.3[d]	–	–	–	–	–
Super imposed load (kN/m^2)	0.5	0.5	0.5	2.0[e]	2.0[e]	As normal class	0.5	–[b] 0.2[c]
Lateral load	0.5 M	0.5 M	0.5 M	–	–	0.4 M	–	0.5 M
Wind load	Max. oper.			Normal design		$V_w = 30$ m/s	$V_w = 25$ m/s	–

CAP, Civil Aviation practice; HSE, Health and Safety Executive; M is the maximum takeoff weight; V_w is the wind velocity.
[a]Or manufacturer's recommend wheel impact loads.
[b]For design of plating.
[c]For design of stiffening and supporting structure.
[d]Additional frequency dependent values given for Chinook helicopter.
[e]Considered independently.

Table 2.13 Loading specifications for a helicopter at rest from various authorities.

Authority	International Standards Organization (ISO)	CAP	HSE	American Bureau of Shipping (ABS)	Bureau Veritas (BV)	Det Norske Veritas (DNV)	Germanischer Lloyd (GL[a])	Lloyd's Register of Shipping (LRS)
Self weight	M	M	M	M	M	M	1.5M	M
Super imposed load (kN/m^2)	2.0	0.5	0.5	0.49	0.5	As normal class	2.0	2.0
Wind load	100 year storm	As HSE	As HSE	Normal design	Normal design	$V_w = 55$ m/s	$V_w = 50$ m/s	–

M is the maximum takeoff weight; V_w is the wind velocity.
[a]Fixed platforms for floating platforms also include a lateral load of 0.6 (M + W) where W is the deck weight in place of the platform motion.

Example of helicopter load

The helicopter loads are presented to the model utilizing the skid loading command in the SACS input loading menu for a helicopter model Bell-212 of MTOW = 50 kN (5.0 ton).

The helicopter has two skids. Each skid geometrical dimensions is assumed to be 3.68 L × 2.856 W m, with the CoG. point of application at the middle of the skid. The height of the helicopter fuselage is taken as 2.00 m.

1. CAP-437 imposed live load = 0.5 kN/m^2;
2. at-rest condition = 1 × MTOW = 50.0 kN;
3. normal operating condition = 1.5 × 1.3 × MTOW = 97.50 kN;
4. emergency landing condition = 2.5 × 1.3 × MTOW = 162.50 kN.

The landing conditions at either normal operating or emergency conditions are combined with lateral horizontal force = 0.5 × MTOW = 25.0 kN applied on both skids.

2.2.6 Crane support structure

The crane support structure comprises the crane pedestal and its connections to the topside primary steelwork. It does not include the slew ring or its equivalent or the connections between the slew ring and the pedestal.

Crane support structures shall, where practical, be attached at the intersection of topside primary trusses and connected at main deck elevations with minimal eccentricities.

The pedestal shall be included in the analytical model of the primary structure as its stiffness can have a significant effect on load distribution. When located in accordance with this guidance their performance will generally be governed by static actions with negligible dynamic amplification. They are, however, subject to fatigue damage and should always be checked to ensure that their fatigue life is satisfactory for the required service conditions.

The maximum rotation at the top of the pedestal or in the plane of the effective point of support shall not exceed the manufacturer's recommended requirements and in no case shall it exceed 1 degree for the most onerous case of loading. Where this criterion cannot be met the dynamic response shall be checked.

A number of separate situations shall be considered for the design of crane support structures as follows.

1. *Crane working in calm conditions*.
2. *Crane working at maximum operating wind conditions*. The maximum operating wind conditions may be different for platform lifts and for sea lifts and lifts to or from an adjacent vessel, and may also vary depending on the weight being lifted.
3. *Crane collapse*. This situation is included to ensure that in the event of a gross overload of the crane, causing collapse of any part of the crane structure (most commonly the boom or frame structure), no damage to the crane support structure is suffered and progressive collapse is avoided.

The cases of loading shall be checked as follows based on ISO 9001:

(1) *Crane working without wind*

$$F_G + f \cdot F_L + F_H \tag{2.3}$$

where F_G is the vertical load due to dead weight of components; F_L is the vertical load due to the suspended load, including sheave blocks, hooks, and others; F_H is the horizontal loads due to off-lead and side-lead; f is a dynamic coefficient and shall be taken as 2.0 for sea lifts and 1.3 for platform lifts

(2) *Crane working with wind*

$$F_G + fF_L + F_H + F_W \tag{2.4}$$

where F_G, F_L, F_H, and f are as above; F_W is the operating wind action; and f shall be taken as 2.0 for sea lifts and 1.3 for platform lifts for a maximum crane operating wind.

(3) *Crane not working, extreme wind*

$$F_G + F_{W,\max} \tag{2.5}$$

where

F_G is as above; $F_{W,\max}$ is the extreme wind action.

The action factors used with each of the above shall be those for normal operating conditions.

For cases (1)and (2), F_L shall be selected to check the lifted load applicable to both maximum and minimum crane radius, for sea and platform lifts.

For cases (2) and (3) the most onerous wind directions shall be checked.

It shall be demonstrated that the crane pedestal and its components are designed to safely resist the forces and moments from the most onerous loading condition applicable to the prevailing sea state together with associated off-lead and side-lead forces. These values shall be obtained from the crane manufacturer, and the angles used shall be not less than the following:

- off-lead angle 6 degrees;
- side-lead angle 3 degrees.

The crane support structure shall be designed such that its failure load exceeds the collapse capacity of the crane.

The crane manufacturer's failure curves, for all crane conditions, shall be used to determine the worst loading on the pedestal. It shall be assumed that the maximum lower bound failure moment of the weakest component will place an upper bound on the forces and moments to which the pedestal can be subjected.

The design moment for the crane failure condition shall be taken as the lower bound failure moment described above, multiplied by a safety factor of 1.3.

It is not normal practice for the support structure of offshore cranes to be subject to dynamic analysis. The process of fatigue design incorporates an average DAF for all lifts and this has been found to provide satisfactory results in practice.

A dynamic analysis is only required where the design is unconventional or the maximum rotation at the plane of support exceeds the limit of 1 degree and experience or engineering judgment indicates that the performance of the crane support structure may be adversely affected by its dynamic response to actions.

Where considered necessary the model employed shall be sufficiently detailed to ensure that the coupled response of the crane and its supports are realistically represented. Any mechanical damping device incorporated within the design of the crane shall be taken into consideration.

Where appropriate the results of the dynamic analysis may be used to modify the fatigue design process.

2.3 Wind load

The owner is responsible for delivering the wind data according to the metocean study which define the prevailing wind direction and the maximum wind speed every 1, 50, and 100 years.

Figs. 2.1 and 2.2 are samples of the wind data that will be in the metocean study report.

The most important design considerations for an offshore platform are the storm wind and storm wave loadings it will be subjected to during its service life.

These data are usually available to the owner and submitted to the engineering firm officially and if these data are not available they should be delivered from an experienced authority in the country or international specific offices.

The wind speed at any elevation above a water surface is presented as:

$$V_z = V_{10}\left(z/10\right)^{1.7} \tag{2.6}$$

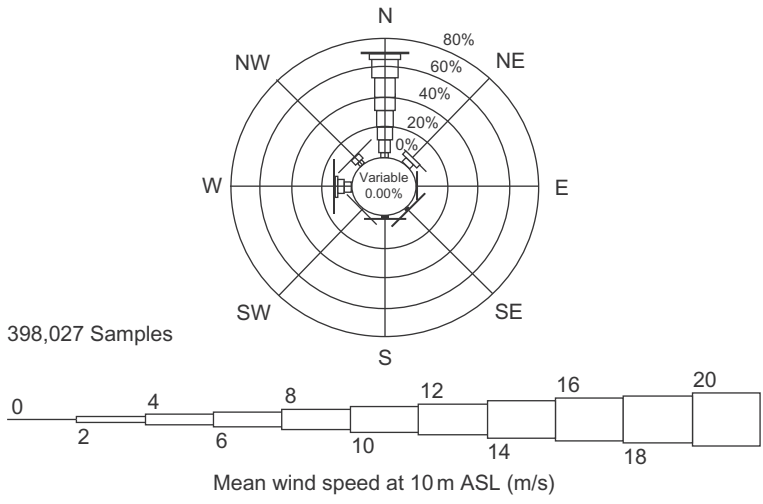

Figure 2.1 Example of wind rose.

Mean wind speed at 10 m ASL (m/s)	N	NE	E	SE	S	SW	W	NW	Total	CFD
0.0	0.34	0.28	0.24	0.24	0.19	0.22	0.39	0.43	2.3	100.0
2.0	1.9	1.2	0.61	0.60	0.32	0.34	2.0	2.9	9.8	97.7
4.0	8.2	1.9	0.16	0.47	0.22	0.31	4.8	3.6	19.8	87.9
6.0	19.3	1.7	0.01	0.35	0.18	0.25	3.6	0.93	26.2	68.1
8.0	21.6	0.74	<0.01	0.23	0.13	0.15	1.4	0.13	24.4	41.8
10.0	12.6	0.18	<0.01	0.11	0.05	0.03	0.62	0.02	13.6	17.4
12.0	3.2	0.02	<0.01	0.03	0.01	<0.01	0.18	<0.01	3.4	3.9
14.0	0.32	<0.01		<0.01	0.01	<0.01	0.04	<0.01	0.38	0.42
16.0	<0.01			<0.01	<0.01	<0.01	0.01		0.03	0.04
18.0	<0.01			<0.01			<0.01	<0.01	<0.01	<0.01
20.0							<0.01		<0.01	<0.01
22.0										
Total	67.4	6.0	1.0	2.0	1.1	1.3	13.0	8.0	100.0	

Figure 2.2 Tabulated data for mean wind speed from different directions.

The wind velocity, vertical wind profile, and time averaging duration in relation to the dimensions and dynamic sensitivity of the structure's components shall be determined. In special cases the dynamic response to wind action can be significant and shall be taken into account.

In addition to that, the following data should be obtained from the meteorology data:

- lowest air temperature;
- highest air temperature;
- average air temperature;
- maximum relative humidity;
- minimum relative humidity;
- average relative humidity;
- annual fog days;
- annual thunderstorm days;
- total annual rainfall;
- maximum rainfall in one day;
- annual rainfall days;
- seawater surface temperature;
- maximum degree of salt;
- minimum degree of salt;
- average degree of salt;
- mud temperature at seabed, 0.0, 1.0, 1.5, and 2.0 m;
- snow maximum and average thicknesses.

The wind load shall be applied in the omni direction, the object normal to the wind shall be considered its area and in the case of an inclined member or wall

Table 2.14 Shape coefficient, C_s, for perpendicular wind approach angles.

Component	Shape coefficients (C_s)
Flat walls of buildings	1.5
Overall projected area of structure	1.0
Beams	1.5
Cylinder	
• Smooth, $R_e > 5 \times 10^5$	0.65
• Smooth, $R_e \leq 5 \times 10^5$	1.2
• Rough, all R_e	1.05
• Covered with ice, all R_e	1.2

with an angle with the wind direction it shall be considered in the calculation. In the case of ice increasing the surface, roughness has an effect on the wind load.

The wind force can be obtained by applying this equation:

$$F = 1/2\rho_a(V_w)^2 C_s A \tag{2.7}$$

where F is the wind force applied on the structure; ρ_a is the air mass density (1.25 kg/m^3); V_w is the wind velocity; C_s is the aerodynamic coefficient for shape; A is the area of structure or object.

Table 2.14 presents the shape factor that can be used in the case that the shape factor is not defined.

Wind loads on downstream components can be reduced due to shielding by upstream components.

The extreme quasistatic global action caused by wind shall be calculated as the vector sum of the above wind loads on all objects.

In the case of a special structure in which the wind load is governing the design, the wind tunnel is a better option to present the effect of the wind on the structure and can do the computational flow model, however it is not used for normal offshore structure platforms.

From the code equation, which is the same for the different codes, the wind force on the structure can be calculated:

V_{10} = wind speed at height 10 m;
10 = reference height, m;
z = desired elevation, m.

Table 2.15 lists some design wind pressures that have been used in conjunction with a 100-year sustained wind velocity of 125 mph.

As per table 2.16 the shielding factor is applied for the first and second series of beams. In case of third beam and more, the wind effect will neglect. However for third and more trusses the wind effect will be consider with sheilding factor. In case of a short object behind a long object, theshort object will not be affect by the wind load.

Table 2.15 Wind pressures values in the case of 125 mph wind velocities.

Structure member	Pressure (kN/m^2) (psf)
I-beams, gusset plates, sides of building, and other flat surfaces	2.9 (60)
Tubular structural members	2.3 (48)
Cylindrical deck equipment ($L = 4D$)	1.4 (30)
Tanks on the deck ($H \leq D$)	1.2 (25)

Table 2.16 Shield factors on American Petroleum Institute (API).

Component	Shielding factor
For trusses, the second one in the series	0.75
For trusses, the third or further in a series	0.50
For beams, the second in a series	0.50
For beams, the third or further in a series	0.00
For tanks, the second in a series	1.00
Short objects behind tall objects	0.00

Based on DNV, the wind pressure acting on the surface of helidecks may be calculated using a pressure coefficient $C_p = 2.0$ at the leading edge of the helideck, linearly reducing to $C_p = 0$ at the trailing edge, taken into account the direction of the wind. The pressure may act both upward and downward.

2.4 Example for stair design

The first bay of the stair which connects the main deck at level 13.525 m to the helideck is the most critical stair bay.

2.4.1 Gravity loads

Uniform gravity loads/one stair channel = (dead load + live load) × ½ stair width + handrail weight/meter + channel own weight/meter:

- Dead load = 0.5 kN/m′;
- Live load = 50 psf = 2.5 kN.m′ (extracted from the next tables as per project specifications)
- Handrail weight/meter = 0.4 kN/m′;
- Channel own weight/meter = 0.379 kN/m′.

Uniform gravity loads (ton/m)/one stair channel = (0.5 + 2.5) × 0.5 × 1.2 + 0.4 + 0.379 = 2.6 kN/m′;

Table 2.17 Live load on the fixed platform from technical practice.

Area	Loadings (kN/m^2)		
	Member category		
	Deck plate, grating, and stringers	Deck beams	Main truss framing, girders, jacket, and foundation
Cellar and main decks	14.4	9.6	9.6
Walkway, stairs, and access decks	4.8	2.4	7.2
Laydown areas	19	14.4	150

Moment = (uniform load/m) × inclined length × projected length/8 = 2.6 × 6.22 × 4.4/8 = 8.9 m kN;

Actual stress = moment/section modulus = 8.9 (10^6)/371 = 24,000 kN/m^2;

Unsupported length = 6.22 m;

Allowable stress (ksi) = 12,000 C_b/(member length × depth/area of flange) = 12,000 × 1/[622 × 26/(9 × 1.4)] = 9.35 ksi = 64,466 kN/m^2 > actual stress (Table 2.17).

2.4.2 Wind loads

Wind loads/one stair channel = C_d × ½ × ρ × v^2 × ½ stair width:

- C_d (drag coefficient) = 2;
- ρ (air intensity) = 1.3 kg/m^3;
- V (wind velocity) = 29 m/s.

Wind loads/one stair channel = 2 × ½ × 1.3 × 29^2 × 0.6 = 655.98 N/m = 0.66 kN/m^2;

Moment = (wind load/m) × inclined length × projected length/8 = 0.66 × 6.22 × 4.4/8 = 0.23 m kN;

Actual stress (gravity + wind) = moment/section modulus = (8.9 + 0.23) (10^6)/371 = 24,609 kN/m^2 < allowable stress × 1.33.

Note that wind loads on the channel in a minor axis direction are neglected since horizontal bracing is provided.

2.5 Offshore loads

The offshore loads are most loads that affect the platforms, such as waves, tide, and current. Terminology related to the water level in the sea and ocean is as follows:

- High high water level;
- Mean high water level;

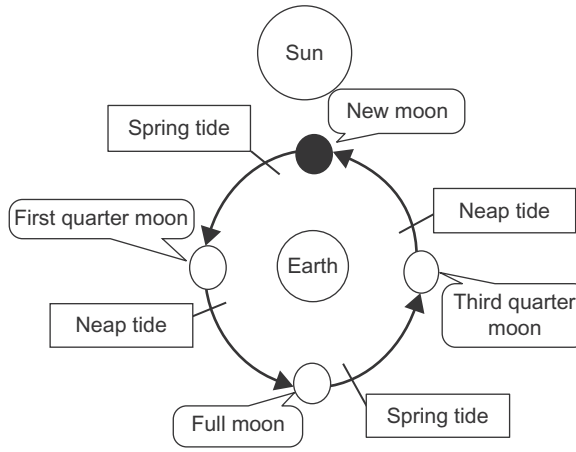

Figure 2.3 Times of neap and spring tides.

- Mean water level, equal to mean sea level, and still water level (SWL);
- Low low water level which is equal to the chart datum;
- Mean low water level.

The main low water lever is less than the mean high water level by 304 mm (1 ft.).

The tides are a function of gravitational force due to moon and sun rotation; all these nature phenomena cause the rise and fall of ocean and sea levels, which are called tides.

In most places in the oceans and seas worldwide each day there are two high and two low tides, called a semidiurnal tide. Diurnal tides occur in some locations, where there is only one high and one low tide per day. Fig. 2.3 presents the movement of the moon and its effect on the tide, and also the near-shore bathometry and coastline shape that affect the tide also.

The rising of water due to storms in addition to the tide is called a storm surge. A storm surge moves the water in the ocean up, and which is associated with low pressure, as happens in tropical cyclones. High wind causes the upward movement of waves in the ocean or sea, so that the water level is higher than normal.

2.5.1 Wave load

Large forces result when waves strike a platform's deck and equipment. Where an insufficient air gap exists, then all actions resulting from waves including buoyancy, inertia, drag, and slam shall be taken into account (see ISO 19901-1 and ISO 19902).

Waves characteristic in the sea or ocean, can be seen easily as constantly changing between wave crests and troughs. The wave direction propagation is defined by means of the directions of individual waves.

The actual wave phenomena are complicated and to define them accurately using a mathematical model is not easy and there are many assumptions. There are three-dimensional effect and also nonlinearities.

For describing simple wave calculation there are two classical theories, which were performed by Airy in 1845 and Stokes in 1880.

The Airy and Stokes theories generally predict wave behavior better where water depth relative to wavelength is not too small. For shallow-water regions, conidial wave theory, originally developed by Korteweg and DeVries in 1895, provides a rather reliable prediction of the waveform and associated motion for some conditions. Recently, work involving conoidal wave theory has been substantially reduced by the introduction of graphical and tubular forms of function by Wiegel in 1960 and by Masc and Wiegel in 1961.

A finite amplitude theory was developed by Stokes in 1880; the second-order Stokes equation was then developed and subsequently there was an approach to use the higher-order approximation in some practical problems.

The other wave theory which is used is stream function theory, which is similar to Stokes' fifth-order theory which uses a nonlinear solution approach. Stokes' fifth law and stream function used the summation of cosine and sin traditional wave forms.

The offshore structure engineer should choose the best theory to apply to his design.

The selection of the best method is defined by curves produced by Atkins (1990) and modified by the API Task Group, where H/gT_{app}^2 is dimensionless wave steepness; d/gT_{app}^2 is dimensionless relative depth; d is mean water depth; T_{app} is the wave period; H is the wave height; g is the acceleration due to gravity; and H_b is breaking wave height.

Metocean data shall be obtained depending on the specific location of the platform, as an example data are illustrated in Table 2.18 and Fig. 2.4.

The sea state (E) is calculated by dividing a waveform into small slides noting that for each slide, the height H_i is squared and added together and averaged. Then E is calculated as:

$$E = 2\frac{\sum_{i=1}^{N} H_i}{N}$$

Fig. 2.5 shows a two-dimensional, simple progressive wave propagation in the positive x-direction, the symbol, η, denotes the displacement of the water surface relative to the SWL which is a function of x and time, t, at the wave crest, η, equal to one half of the wave height.

Water particle displacement is presented in Fig. 2.6 for deep and shallow water. Water particle displacement is an important factor in linear wave mechanics dealing with the displacement of individual water particles within the wave. Water particles generally move in elliptical paths in shallow water or to transitional water and in circular paths shapes in deep water, as clearly presented in Fig. 2.6. If the mean

Table 2.18 Example of metocean data.

Return period (years)	W_s (m/s)	H_s (m)	T_z (s)	T_p (s)	H_{max} (m)	T_{ass} (s)	H_c (m)	U (cm/s)
1	16.1	2.2	4.7	6.2	3.2	6.3	1.9	1
10	17.7	2.8	5.4	7.1	5.3	7.2	3.2	5
50	18.7	3.2	5.9	7.7	6.6	7.7	4.0	11
100	19.2	3.3	6.0	7.9	7.2	8.0	4.3	15
10,000	22.0	4.5	7.1	9.4	10.9	9.4	6.6	51

W_s is 1 h average wind velocity at 10 m above sea level (m/s).
H_s is the significant wave height (m), which is equal to the mean height of the highest third of the waves in a sea state (m) as per Fig. 2.4.
H_{max} is the maximum wave height (m); which is the highest individual zero crossing wave height in a storm for duration 24 h.
T_z is wave period at the average zero crossing (s); wave heights in a sea-state.
T_p is the peak wave period associated with the peak in the wave energy spectrum.
T_{ass} wave period associated with maximum wave height (s).
H_c Crest height is the highest crest to mean-level height of an individual wave in a storm of duration 24 h (m).
U is the horizontal wave orbital velocity at 3 m above seabed estimated from H_{max} and T_{ass} using stream function wave theory (cm/s).

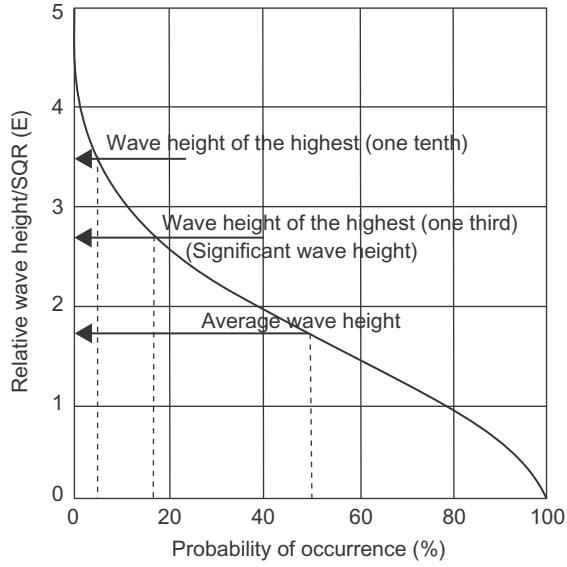

Figure 2.4 Probability of wave height.

particle position is considered to be at the center of the ellipse or circle then vertical particle displacement with respect to the mean position cannot exceed one half the wave height. Therefore the displacement of the fluid particle is small if the wave height is small.

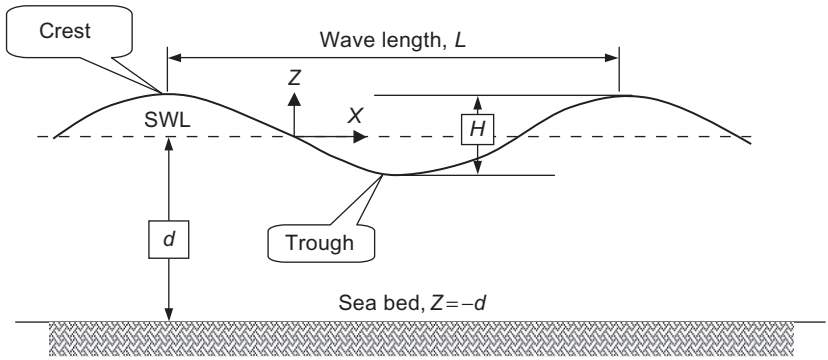

Figure 2.5 A sinusoidal progressive curve.

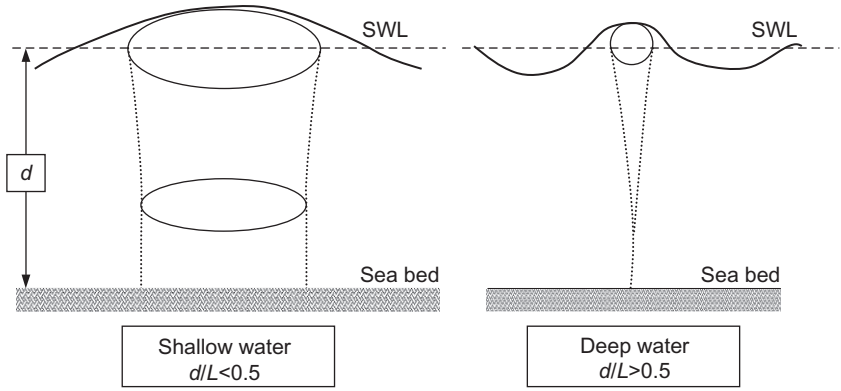

Figure 2.6 Water particle displacement for shallow and deepwater waves.

Fig. 2.7 presents the horizontal and vertical velocities and acceleration for various locations of particles which is very important in calculating the wave forces in any structure member in the subsea as the drag force and inertia force are functions of the particle velocity and acceleration, respectively, and the following equations calculate the wave velocity and acceleration:

$$F1 = \left(2\pi(z+d)/L\right) \tag{2.8}$$

$$F2 = \left(2\pi d/L\right) \tag{2.9}$$

$$F3 = \left(2\pi x/L\right) - \left(2\pi t/T\right) \tag{2.10}$$

- *Velocity*

$$U = \left[(H/2)\ (gT/L)\ \cosh F1/\cosh F2\right] \cos F3 \tag{2.11}$$

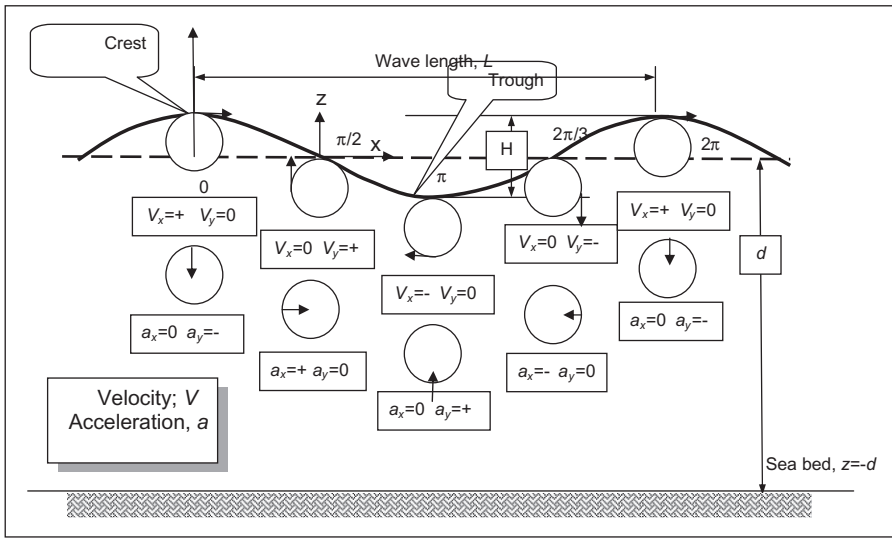

Figure 2.7 Fluid particle velocities and acceleration direction at every location.

$$W = \left[(H/2)(gT/L)\sinh F1/\cosh F2\right] \sin F3 \tag{2.12}$$

- *Acceleration*

$$a_x = \left[+gpH/L \cosh F1/\cosh F2\right] \sin F3 \tag{2.13}$$

$$a_z = \left[-gpH/L \sinh F1/\cosh F2\right] \cos F3 \tag{2.14}$$

In the 19th century, the theories of ocean wave modeling were developed. In 1950, Morison equation wave force theories were presented which are concerned with offshore platforms as presented in Fig. 2.8.

$$F = F_{\mathrm{D}} + F_{\mathrm{I}} \tag{2.15}$$

where F_{D} is the drag force and F_{I} is the inertia force.

- *Drag force*

  The drag force due to a wave acting on an object can be found by:

$$F_D = ½\rho C d V^2 A \tag{2.16}$$

  where F_{D} is the drag force (N); C_{d} is the drag coefficient (no units); V is the velocity of object (m/s); A is the projected area (m^2); ρ is the density of water (kg/m^3).
- *Inertia force*

  The inertia force due to a wave acting on an object can be found by:

$$F_{\mathrm{I}} = \pi\rho \cdot a \cdot C_{\mathrm{m}} \cdot D^2/4 \tag{2.17}$$

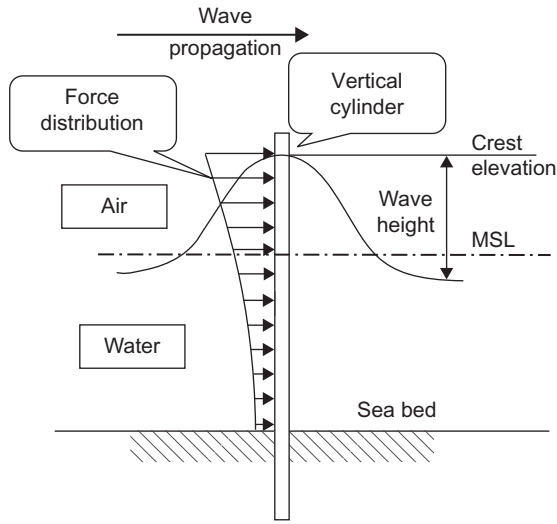

Figure 2.8 Wave forces distribution on a vertical pipe.

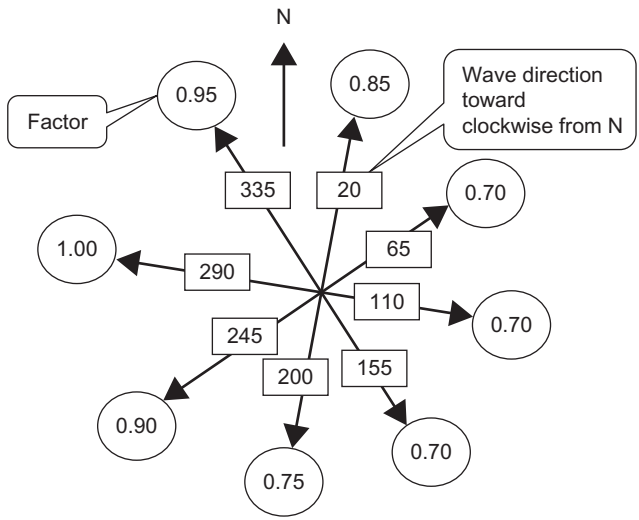

Figure 2.9 Design of wave directions and factors to apply to the omnidirectional wave height in Gulf of Mexico (GoM) based on American Petroleum Institute (API).

where F_I is the inertia force (N); C_m is the mass coefficient (no units); a is the acceleration for water particle in horizontal direction (m^2/s); D is the cylinder diameter (m); and ρ is the water density (kg/m^3) as shown in Fig. 2.9.

Wave load calculation:

- The C_d and C_m are dimensionless and in the Morison equation have values of 0.7 and 2.0, respectively. The API recommend 0.65 and 1.6, respectively, for smooth or 1.05 and 1.2 for rough surfaces as in the case of existing marine growth.

- Water particle velocity and acceleration are functions of wave height, wave period, water depth, distance above the bottom, and time.
- The most elementary wave theory was presented by Airy in 1845.
- Another widely used theory, known as stream function theory, is a nonlinear solution similar to Stokes' fifth-order theory.

The wave direction is omnidirectional (Fig. 2.9).

Fig. 2.9 presents an example of the principal wind direction in the Gulf of Mexico (GoM) which is 290 degrees in a clockwise direction. Therefore the platform will be applied in eight directions by the wave height versus the water depth. Noting that the principal wave direction with the maximum wave height value will be defined in the metocean report based on the location of the platform. Based on API RP2A is applying a reduction factor on the other direction as shown in Fig. 2.9 for water depth higher than 12 m, noting that this direction with 22.5 degrees is regardless of the platform orientation.

Comparison between wind and wave calculations

When we calculate the force affect structure due to wind we take the drag force into consideration and neglect the inertia force, but in the case of waves we should consider drag force and inertia force and the following example provides the reason to neglect the inertia force in the case of wind load.

Example

Pipe dia. = 0.4 m

$$V_{air} = 25\ m/s \quad V_{water} = 1\ m/s$$

$$a_{air} = 1\ m^2/s \quad a_{water} = 1\ m^2/s$$

$$\rho_{air} = 1.3\ kg/m^3 \quad \rho_{water} = 1000\ kg/m^3$$

$$F_d = (1/2) \cdot Cd \cdot \rho \cdot V^2 \cdot A$$

$$F_m = Cm \cdot \rho \cdot \pi \cdot (D^2/4) \cdot a$$

Air

$$F_d = (1/2)(0.8)(1.3)(25)^2(0.4) = 130 \text{ Newton}$$

$$F_m = 2(1.3)(p)(0.4)^2/4(1) = 0.33 \text{ Newton}$$

Water

$$F_d = (1/2)(0.8)(1000)(1)^2(0.4) = 160 \text{ Newton}$$

$$F_m = 2(1000)(\pi)(0.4)^2/4(1) = 251 \text{ Newton}$$

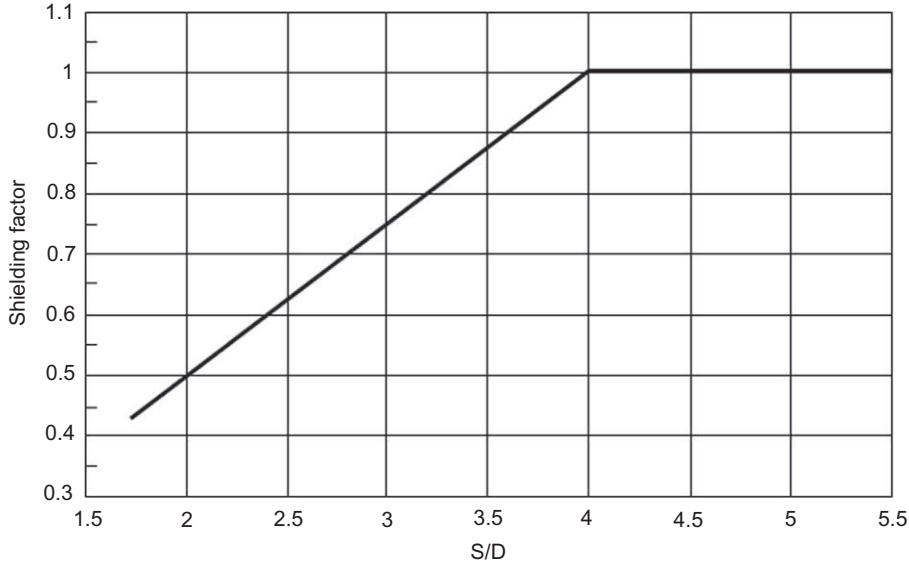

Figure 2.10 Shielding factor for conductors.

Conductor shielding factor

The vertical pipe on the water is the main element of generated force, so the number of well conductors is the one of the main factors that produces a significant portion of the total wave forces that affect the platform.

The spacing between the conductor is a factor of the hydrodynamic shielding as, if the space is smaller, the force will be reduced due to the hydrodynamic shield.

The reduction factor for wave force due to the shield is taken from Fig. 2.10, noting that S is the spacing in wave direction and D is the conductor diameter.

2.5.2 Current force

Based on ISO 9002, the most common categories of ocean currents are:

- wind-generated currents;
- tidal currents;
- circulation currents;
- loop and eddy currents;
- soliton currents;
- longshore currents.

Wind-generated currents are caused by wind stress and atmospheric pressure gradients throughout a storm.

For tides there are two levels, highest astronomical tides (HATs) and lowest astronomical tides (LATs).

In general, current associated with tide is strong near the shoreline and weak in deep water.

Soliton currents are due to internal waves generated by density gradients.

Loop/eddy currents and soliton currents penetrate deeply in the water column.

Longshore currents in coastal regions run parallel to the shore as a result of waves breaking at an angle to the shore, and are also referred to as *littoral* currents.

An earthquake can cause a turbidity current which is considered in offshore pipelines design in Chapter 9, Subsea pipeline design and installation. Stronger earthquakes underwater can produce tsunamis, which produce an extremely high horizontal current as happened in Indonesia in 2018.

The effects of currents should be considered in the designs of ships and offshore structures, their construction, and operation.

The effects of currents require some checks during the design of offshore structures, as follows:

- moored platforms present a slow drift motion;
- The increase in drag and lift forces on submerged structures;
- vortex-induced vibrations affect the slender structural elements;
- vortex-induced motions affect large-volume structures;
- increase of wave height as a combination between currents and wave heights, and also a change in the wave period;
- Scouring around the piles in the seabed occurs mainly due to current.

There are many research studies about the current velocity profile on most ocean and seas around the world using statistical methods. In ISO 19901-1 (2005) "Metocean design and operating considerations," there is general information about currents. At the start of the project at the FEED stage the current speed profile should be determined.

If sufficient joint current−wave data are available, joint distributions of parameters and corresponding contour curves (or surfaces) for given exceedance probability levels can be established. Otherwise conservative values, using combined events, should be applied (NORSOK N-003, DNV-OS-C101).

The presence of current in the water produces some minor effects, the most variable of which is the current velocity which should be added vectorially to the horizontal water particle velocity.

From a practical point of view some designers sometimes increase the maximum wave height by 5%−10% to account for the current effect and the current is neglected from further calculations.

Design current profiles

When detailed field measurements are not available the variation in shallow tidal current velocity water with depth may be modeled as a simple power law, assuming unidirectional current,

$$V_{c,\text{tide}}(Z) = V_{c,\text{tide}}(0)\left(\frac{d+z}{d}\right)^{\alpha} \quad \text{for} \quad Z \le 0 \tag{2.18}$$

The variation in *wind*-generated current can be taken as either a linear profile from $z = -d_0$ to the SWL,

$$V_{c,\text{wind}}(Z) = V_{c,\text{wind}}(0)\left(\frac{d_o + z}{d_o}\right) \quad \text{for} \quad -d_o \le Z \le 0 \tag{2.19}$$

or a slab profile

$$V_{c,\text{wind}}(Z) = V_{c,\text{wind}}(0) \quad \text{for} \quad -d_0 < Z < 0 \tag{2.20}$$

The profile giving the highest loads for the specific application should be applied.

Wind-generated current can be assumed to vanish at a distance below the SWL,

$$V_{c,\text{wind}}(Z) = 0 \quad \text{for} \quad z < -d_0 \tag{2.21}$$

where $v_c(z)$ is the current velocity at level z; and z is the distance from the SWL, positive upwards. At the SWL, $v_{c,\text{tide}}(0)$ is the tidal current velocity and $v_{c,\text{wind}}(0)$ is the wind-generated current velocity where the water depth to the SWL is d; and d_0 is the reference depth for wind-generated current,

$$\alpha = 1/7$$

In the case that the current statistics are not available for an open coast line with deep water the wind that generates the current velocities at the SWL can be calculated from the following equation:

$$V_c, \text{wind}(0) = MU_1 \text{ hour, } 10 \text{ m} \quad \text{where } M = 0.015 - 0.03$$

where U_1 hour, 10 m is at height 10 m above sea level, with 1 hour sustained wind velocity.

The variation in current velocity over depth depends on the local oceanographic climate, the vertical density distribution, and the flow of water into or out of the area. This may vary from season to season. Deep water profiles may be complex. The current direction can change 180 degrees with depth.

The current profile is as shown in Fig. 2.11 based on API RP2A (2007).

However, this profile in present GoM is as shown in Fig. 2.11. API mentions that the minimum speed is 0.31 km/h (0.2 knots) as shown in the current profile figure.

Current profile

The recommended current profile is as given in ISO 19901-1:2005, as follows:

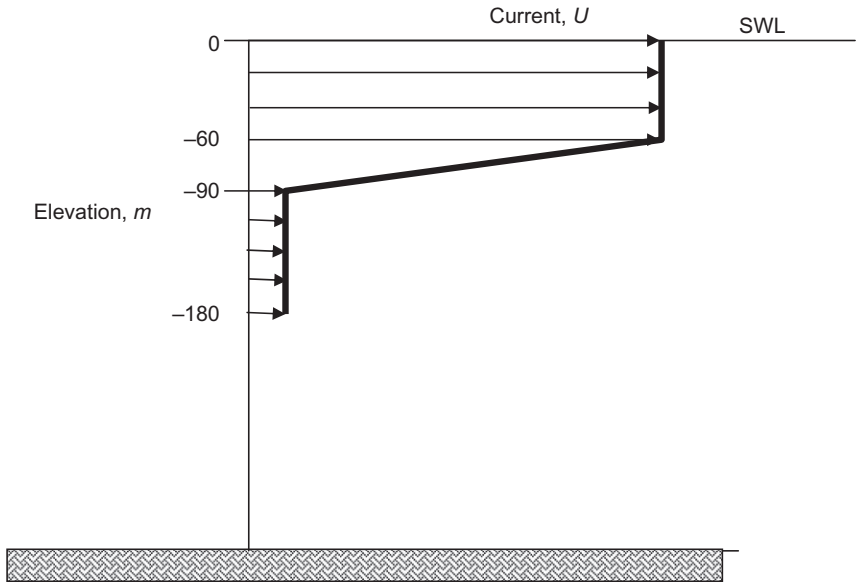

Figure 2.11 The current profile in location at Gulf of Mexico (GoM).

$$U_c(z) = U_{cs}\left(\frac{z+d}{d}\right)^{1/7} \tag{2.22}$$

where $U_c(z)$ is the current speed at elevation z (z less than or equal to 0); $U_{cs}(z)$ is the surface current speed at $z = 0$; d is the still water depth; and z is the vertical coordinate, measured positively upward from the SWL.

The current profile is illustrated in Fig. 2.12, and Table 2.19 gives the factors to be applied to the depth-mean current speed, to give current speeds at different depths.

2.5.3 Earthquake load

Approximately 100 conventional steel pile-supported platforms have been installed in high-activity earthquake regions such as offshore California, Alaska, New Zealand, Japan, China, and Indonesia. New areas in high-activity earthquake regions include offshore structures in Venezuela, Trinidad, and the Caspian Sea.

It is worth mentioning that fixed offshore structures are usually be long-term structures that have a natural period in lateral, flexural, and torsion in the range of 1−5 seconds. The first vertical mode periods are frequently in the range of 0.3−0.5 seconds.

The ductility requirements are intended to ensure that the platform has sufficient reserve capacity to prevent its collapse during rare intense earthquake motion, although structure damage may occur.

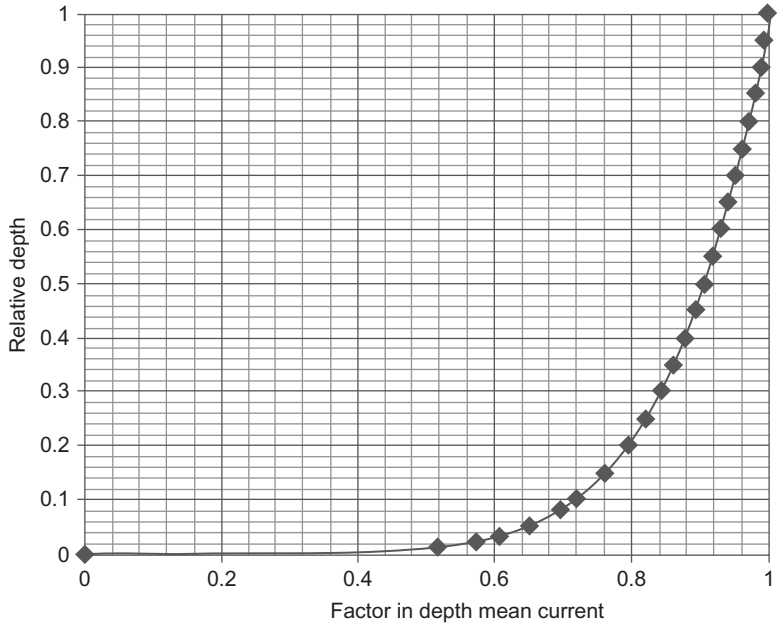

Figure 2.12 Current profile.

In regional areas of low seismic activity less than 0.05 g, the design of environmental loading other than for earthquakes will provide sufficient resistance against earthquakes (Table 2.20).

In the case of seismic activity of 0.05−0.1 g the most important item is the deck appearances such as piping, facilities, and others.

The platform should be checked against earthquakes using a dynamic analysis procedure such as spectrum analysis or time history analysis.

The spectrum analysis method is for a structure with uniform shape and structure system and a structure height between 100 and 150 m, or the ratio between the heights to the horizontal dimension is more than 5 in the earthquake load direction.

The seismic effect on the structure in this item has a static lateral load effect on the floor level of the structure and its values are calculated from the dynamic properties as the natural period and natural mode, that is, calculated by the modal analysis. The calculated lateral force shall be higher than or equal to 80% of the lateral load calculated using the previous method.

The soil types in Fig. 2.13 are A, B, and C, which are classified as follows:

Soil type A is rock crystalline, and similar soil types with wave shear velocity more than 914 m/s (3000 ft./s).

Soil type B is dense soil from strong alluvium or dense sands, silts, and stiff clays with shear strengths more than 72 kPa (1500 psf), and is for depths less than 60 m (200 ft.) and overlying rock strata.

Table 2.19 Relation between relative depth and factors.

Relative depth	Factors
0	0
0.01	0.517947
0.02	0.57186
0.03	0.605963
0.05	0.651836
0.08	0.697106
0.1	0.719686
0.15	0.762603
0.2	0.794597
0.25	0.820335
0.3	0.841982
0.35	0.86073
0.4	0.877307
0.45	0.892193
0.5	0.905724
0.55	0.91814
0.6	0.929624
0.65	0.940315
0.7	0.950323
0.75	0.959736
0.8	0.968625
0.85	0.97705
0.9	0.985061
0.95	0.992699
1	1

Table 2.20 Comparison between the seismic zone factor and horizontal ground acceleration for American Petroleum Institute (API) and uniform building code (UBC).

Seismic zone (relative seismicity) factor, Z[a]	1	2	3	4	5
Horizontal ground acceleration to gravitational acceleration, g in API	0.05	0.10	0.20	0.25	0.40
Horizontal ground acceleration to gravitational acceleration, g in UBC	0.075	0.15	0.20	0.30	0.40

[a]The zones in UBC are 1, 2A, 2B, 3, and 4 which correspond to 1, 2, 3, 4, and 5 in API, respectively.

Soil type C is the same soil as type B but with depth greater than 61 m (200 ft.) and overlying rock soil (Table 2.21).

Earthquake loading shall be determined by the response spectrum analysis in accordance with API RP2A. Both strength level (SLE) and ductility level (DLE)

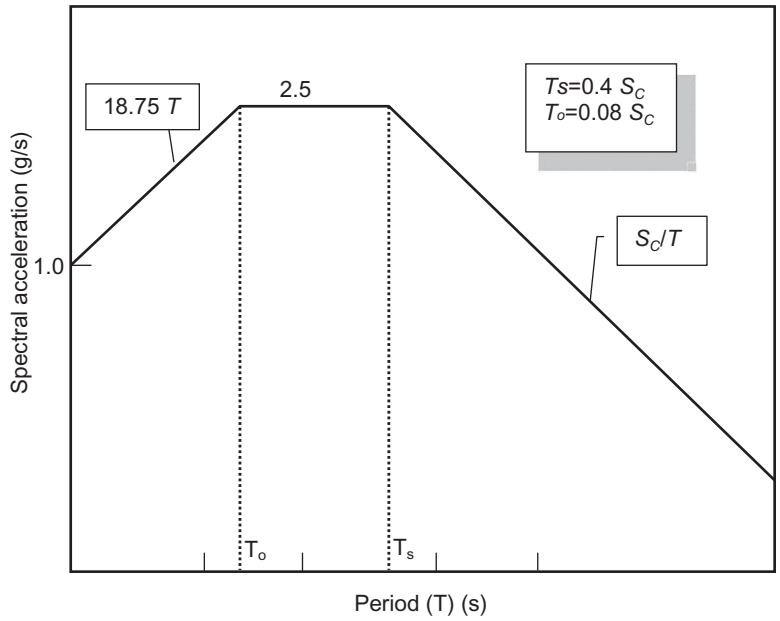

Figure 2.13 Normalized response spectra for design.

Table 2.21 Seismic factor S_C.

Soil type	Seismic zone				
	1	**2**	**3**	**4**	**5**
Soil type A	1.0	1.0	1.0	1.0	1.0
Soil type B	1.44	1.39	1.33	1.36	1.40
Soil type C	1.5	1.45	1.42	1.5	1.45

earthquakes shall be considered in the design. The following return period shall be used in design: SLE for 200 years.

Strength requirements

Twice the SLE peak accelerations shall be used in the DLE analysis.

The design of the platform against earthquake load will depend on the dynamic analysis. In the dynamic analysis process the mass shall consist of the platform mass and the gravity loading, also adding the entrapped mass of water that will be inside the structure such as pile-jacket annulus and other appurtenances. This together can be estimated as the displaced mass due to displaced structures in water in transverse and longitudinal directions of the axis of appearances, such as boat landing, riser guards, and the structure as a whole.

During the in-place structure analysis the structure model shall present the distribution of stiffness and mass of the structure in 3D. If there is no symmetric distribution of stiffness or mass the torsion stress shall be generated and should be considered in the design.

While performing the dynamic analysis the damping ratio is considered as 5% in the case of elastic analysis.

Based on ISO 19002, the square root of the sum of the squares (SRSS) is used for combining the directional response where the complete quadratic combination is used to combine the model responses; this is in the case of applying the spectrum method.

It is worth mentioning that in the case of using SRSS in the modal response, the corner pile loads shall be lower values than in reality. To present the structure well it needs many modes of response in the analysis.

Considering the dynamic analysis output for spectrum methods, there are three main directions, at least two modes for each direction and the torsional modes.

The other dynamic method which can be used is the time history method; the design of the dynamic response depends on calculating the average of the maximum values of the time history response.

The seismic load shall be combined with 75% of the maximum storage load plus the gravity loads which are the platform self weight and the hydrostatic pressure that affects the member under water, and considers buoyancy.

In considering seismic load the American Institute of Steel Construction (AISC) allowable stresses may be increased by 70%. Pile-soil performance and pile design requirements should be determined on the basis of special studies. These studies should consider the design loadings, installation procedures, earthquake effects on soil properties, and characteristics of the soils as appropriate to the axial or lateral capacity algorithm being used. Both the stiffness and capacity of the pile foundation should be addressed in a compatible manner for calculating the axial and lateral response.

Ductility requirements

The purpose of these requirements is to guarantee that an offshore platform located in an active seismic zone has sufficient reserve capacity to have a high displacement without collapsing.

For an area with an active seismic zone with ground motion of 2 or less, a structure with its pile system can withstand this rare load if it is strength designed.

In the case of a platform with eight legs or more there is no ductility analysis required in the case of a seismic zone 2 or less.

As per ISO 19902n, the following precautions are required:

1. Using twice the SLE seismic loads in design of jacket legs, including any enclosed piles, that are designed;
2. The K-bracing system is not preferred for use if it cannot transfer the shear if the buckling occurs in the compression member;
3. For diagonal bracing the vertical face shall be configured to distribute the shear force equally between the horizontal frames and the leg vertical running;

4. if (2) and (3) cannot be applied the portal frame system shall be used between the jacket and deck and it shall be designed using twice the strength-level seismic loads;
5. The horizontal members should have a compression capacity to redistribute the loads resulting from buckling to the adjacent diagonal braces;

The slenderness ratio (Kl/r) is less than or equal to 80% of diagonal bracing in vertical faces and their diameter to thickness ratio (D/t) is limited to 13,100/Fy for Fy in MPa (1900/Fy where Fy is in ksi). In general, the other nontubular members at connections in vertical faces of the jacket are designed as compact sections as per the AISC specifications or using twice the SLE seismic loads.

Structure-pile systems should be modeled and analyzed to guarantee their capacity to withstand the seismic load without collapsing. In some special projects a local seismic study is done, for example, in evaluating the existing structure.

The effect of the seismic level on the soil structure interaction design shall be considered by taking into consideration the P-delta effect for elastic and inelastic deformation. The cyclic loads and their effect on the soil should be taken into consideration as per the discussion in Chapter 4, Geotechnical data and pile design.

Topsides appurtenances and equipment

Topsides design accelerations shall include the effects of the global dynamic response of the structure and, if appropriate, the local dynamic response of the topsides and appurtenance itself.

It is recommended that topsides response spectra or other in-structure response spectra are obtained from time history analyses of the complete structure. The topsides response spectra are recommended to be the average values from at least four time history analyses. Direct spectra-to-spectra generation techniques may also be used, however, such methods should be calibrated against the time history method.

Equipment, piping, and other topsides appurtenances shall be designed and supported such that they can resist extreme-level earthquake loads. On the other hand, the displacements and deformations of the topsides in the case of extreme earthquake load shall be limited or designed to avoid damage to the equipment, piping, appurtenances, and supporting structures.

Safety critical systems and structures on or in the topsides shall be designed such that they are functional during and after the abnormal level of earthquake event. Hazardous systems shall be designed such that they do not fail catastrophically or rupture during the abnormal earthquake level event, which is defined in ISO 19902 and the ductile requirement as in API. In lieu of performing an abnormal level analysis of deck-supported structures, topsides equipment, and equipment tiedowns, they shall be designed with an increased partial action factor on E of 1.15 rather than 0.9.

2.5.4 Ice loads

Ice has an impact force to the offshore structure, especially in the area of the sea pole as in Alaska. To imagine the effect of the ice on the platforms, it is very

important to know that drifting ice travels at a speed of about 1%−7% of the wind speed.

A typical ice island in Alaska is about 1 km diameter with 1 km thickness and has a travel speed of 3 knots.

The thickness of the ice above water to that under water is about 1:2 but in general it is in the range from 1:1 to 1:7.

API has recommended the following formula to calculate the ice impact force:

$$F_i = C_i S_{ci} A_o \tag{2.23}$$

Grouping effects depend on the spacing of individual members. Generally, the following rules are used:

1. *Spacing ≥ 6 diameters*
   Ice will crush against the tubular members and pass through and around the platform if the tubular spacing is greater than six times the tubular diameter. For groups of tubular members of different size, the average tubular diameter should be used to determine the spacing.
2. *Spacing ≤ 4 diameters*
   As the tubular spacing decreases, interference effects may occur which influence both the load on the tubular members and the failure mode of the ice. With a tubular spacing less than four diameters, or with closely spaced conductors between platform legs, ice blocks may wedge inside the structure and the effective contact area becomes the out-to-out dimension across the closely spaced tubular members in the direction of the ice movement. In this case, the total ice load on the structure should be calculated with D taken as the out-to-out dimension across the closely spaced tubular members.
3. *4 < Spacing < 6*
   Ice forces shall be determined by linear interpolation between loads for spacing of 4 and 6.

Noting that, shielding occurs when the tubular members are located in the lee of other structure members. The loads on these piles may be considerably less as the ice may fail in another mode or simply be cleared away under pack ice pressures. These clearing forces are estimated as the product of the pack ice pressure (estimated at 2 ton/m width based on floe area, floe profile, wind speed, and current velocity) and pile diameter.

2.5.5 Other loads

These loads are presented due to the configuration of the platform and the environmental condition as follow:

1. marine growth;
2. scour;
3. materials selection and corrosion, stress analysis, welding, structure analysis, design for fabrication and installation, welding;
4. Marine civil engineering, such as the installation equipment, installation methods, navigation safety instrument;
5. Naval architecture, such as floating and buoyancy, towing, launching, controlled flooding.

Marine growth

Marine growth is an increase in the diameter of the jacket member so that the drag force will increase.

Based on API 1.5″ from MHHW to −150 ft., MHHW is 300 mm (1 ft.) higher than MLLW. A smaller or larger value of thickness may be used from a site-specific study.

A structural member is considered smooth if it is above MHHW or lower than 45 m (150 ft.) where marine growth is light enough to ignore.

The zone between MHHW and 45 m is considered rough.

Scour

Seabed scour affects both lateral and axial pile performance and capacity. Scour prediction remains an uncertain art. Sediment transport studies may assist in defining scour design criteria but local experience is the best guide. It is practical in design to assume the scour is 1.5 pile diameter.

2.6 Design for ultimate limit state

An action factor shall be applied to each of the nominal external actions in the combinations given in Clause 7 in ISO 19902. The action factors are dependent on the national or regional building code in use. This is to ensure that similar levels of reliability for topsides design are achieved to those implied in other ISO 19900 series International Standards.

The combination of factored nominal actions causes amplified internal forces, *S*. A resistance factor is applied to the nominal strength of each component to determine its factored strength. Each component shall be proportioned to have sufficient factored strength to resist *S*. The appropriate strength and stability criteria shall be taken from the appropriate national or international building code. These criteria are the formulas for the nominal strength of the component and the associated resistance factors.

In some conditions, particularly during construction and installation, the internal forces should be computed from unfactored nominal actions and then the action factors applied to the internal forces to arrive at *S*, as discussed in ISO 19902.

Deformation actions can arise from the effects of fabrication tolerance, foundation settlement, and the indeterminate effects of transportation and lift. For the primary structure supported by a multicolumn gravity base structure (GBS) the movement of the column tops can also constitute significant deformation actions. They can also occur from operational or accidental thermal effects. All such actions shall be considered in combination with operating actions to ensure that serviceability and ULSs are not exceeded.

2.6.1 Load factors

The partial action factors to be used when AISC-LRFD, EC 3, NS 3472, BS 5950, or BS 5400 Part 3 is the chosen code are given below. The action factors cover

Table 2.22 Partial actions factors in different international standards and specifications for maximum gravity.

Code	Permanent (γ_G)	Variable (γ_Q)
ISO 19902	1.30	1.50
AISC-LRFD	1.25	1.40
NS 3472	1.25	1.45
EC3	1.30	1.50
BS5950	1.45	1.65
BS 5950 part 3	1.25	1.45

maximum gravity, and extreme environmental and operating environmental combinations. Other relevant codes or standards may be used. In such cases appropriate action factors shall be evaluated to achieve a similar level of reliability to that implied in the International Standard. The procedure should be followed to derive appropriate sets of action factors, as necessary.

The internal force, S, resulting from the design action, F_d, shall be calculated using Eq. (2.24).

$$F_d = \gamma_G(G_1 + G_2) + \gamma_Q(Q_1 + Q_2) \tag{2.24}$$

The partial action factors for selected codes and standards are given in Table 2.22.

2.6.2 Extreme environmental situation for fixed offshore platforms

The internal force, S, resulting from the design action, F_d, shall be calculated using Eq. (2.25).

$$F_d = \gamma_G(G_1 + G_2) + \gamma_Q Q_1 + \gamma_E(E_e + 1.25D_e) \tag{2.25}$$

When the internal forces due to gravity forces oppose those due to wind, wave, and current forces, the internal force, S, resulting from the design action, F_d, shall be calculated using reduced partial action factors as in Eq. (2.26):

$$F_d = \gamma_G \cdot (G_1 + G_2) + \gamma_Q Q_1 + \gamma_E(E_e + 1.25D_e) \tag{2.26}$$

For this combination, G_2 and Q_1 shall exclude any actions that cannot be assured to be present during an extreme storm in order to maximize the difference between the opposing action effects.

The appropriate partial action factors for the environmental load are dependent on the location of the installation.

ISO 19902 allows a value of γ_E of 1.35 where no other information is available. The partial action factors for selected codes and standards are given in Table 2.23.

Table 2.23 Partial action factors in different international standards and specifications in extreme environmental condition.

Code	Partial load factor		
	Permanent (γ_G)	**Variable (γ_Q)**	**Environmental (γ_E)**
ISO 19902	1.10	1.10	1.00 γ_{ELs}
AISC-LRFD	1.05	1.05	0.96 γ_{ELs}
NS 3472	1.05	1.05	0.96 γ_{ELs}
EC3	1.10	1.10	1.00 γ_{ELs}
BS5950	1.20	1.20	1.11 γ_{ELs}
BS 5950 part 3	1.05	1.05	0.96 γ_{ELs}

γ_{ELs} is the appropriate partial factor for the substructure.

2.6.3 Operating environmental situations—fixed platforms

Platform operations are often limited by environmental conditions and differing limits may be set for different operations. Examples of operations that might be limited by environmental conditions include:

- drilling and workover;
- crane transfer to and from supply vessels;
- crane operations on deck;
- deck and over-side working;
- deck access.

Each operating situation that might be restricted by environmental conditions shall be assessed as below where E_o and D_o represent the environmental action limiting the operations. The value of Q_2 shall be that associated with the particular operating situation being considered.

The internal force, S, resulting from the design action, F_d, shall be calculated using Eq. (2.27).

$$F_d = (1/\gamma_G) \cdot (G_1 + G_2) + 1/\gamma_Q Q_1 + g_E(E_o + D_o) \tag{2.27}$$

The action factors for selected codes and standards are given in Table 2.24.

2.6.4 Partial action factors

Each member, joint, and foundation component shall be checked for strength using the internal force due to load effect (S) resulting from the design action F_d calculated by Eqs. (2.28) and (2.29):

$$Q = 1.1\ G_1 + 1.1\ G_2 + 1.1\ Q_1 + 0.9E \tag{2.28}$$

where E is the inertia action induced by the extreme level earthquake (ELE) ground-motion and determined using dynamic analysis procedures such as response

Table 2.24 Partial action factors in different international standards and specifications in operating environmental condition.

Code	Partial load factor		
	Permanent (γ_G)	**Variable (γ_G)**	**Environmental (γ_E)**
ISO 19902	1.30	1.50	1.20
AISC-LRFD	1.25	1.40	1.15
NS 3472	1.25	1.45	1.15
EC3	1.30	1.50	1.20
BS5950	1.45	1.65	1.35
BS 5950 part 3	1.25	1.45	1.15

Table 2.25 Case for 1-year storm conditions.

Load case	Load condition	Combination
1	1	Dead load + buoyancy
2	2	Unmodeled dead load (jacket and deck)
3	3	Blanket live load on main deck
4	4	Blanket live load on helideck
5	11	Wind + wave + current hitting 0.0 degree
6	12	Wind + wave + current hitting 45 degrees
7	13	Wind + wave + current hitting 90 degrees
8	14	Wind + wave + current hitting 135 degrees
9	15	Wind + wave + current hitting 180 degrees
10	16	Wind + wave + current hitting 225 degrees
11	17	Wind + wave + current hitting 270 degrees
12	18	Wind + wave + current hitting 315 degrees

spectrum analysis or time history analysis. G_1, G_2, and Q_1 shall include loads that are likely to be present during an earthquake.

When contributions to the internal forces due to weight oppose the inertia actions due to the earthquake, the partial load factors for permanent and variable actions shall be reduced such that:

$$Q = 0.9\,G_1 + 0.9\,G_2 + 0.8\,Q_1 + 0.9E \tag{2.29}$$

where G_1, G_2, and Q_1 shall include only loads that are reasonably certain to be present during an earthquake.

For global assessment of the offshore structure platform, Tables 2.25 and 2.26 present a matrix for load combination. This is a traditional load combination used in the input for the design or assessment of a fixed offshore platform. Table 2.26 presents the load combination for a 1-year storm condition and Table 2.28 presents the load combination for a 100-year storm condition. Tables 2.27 and 2.28 illustrate

Table 2.26 Case for 100-year storm conditions.

Load case	Load condition	Combination
1	1	Dead load + buoyancy
2	2	Unmodeled dead load (jacket and deck)
3	3	Blanket live load on main deck
4	4	Blanket live load on helideck
5	21	Storm wind + wave + current hitting 0.0 degrees.
6	22	Storm wind + wave + current hitting 45 degrees
7	23	Storm wind + wave + current hitting 90 degrees
8	24	Storm wind + wave + current hitting 135 degrees
9	25	Storm wind + wave + current hitting 180 degrees
10	26	Storm wind + wave + current hitting 225 degrees
11	27	Storm wind + wave + current hitting 270 degrees
12	28	Storm wind + wave + current hitting 315 degrees

Table 2.27 Load combination in 1-year storm condition factors.

Load combination	Load condition											
	1	2	3	4	11	12	13	14	15	16	17	18
30	1.1	1.0	1.0	1.0	1.0							
31	1.1	1.0	1.0	1.0		1.0						
32	1.1	1.0	1.0	1.0			1.0					
33	1.1	1.0	1.0	1.0				1.0				
34	1.1	1.0	1.0	1.0					1.0			
35	1.1	1.0	1.0	1.0						1.0		
36	1.1	1.0	1.0	1.0							1.0	
37	1.1	1.0	1.0	1.0								

Table 2.28 Load combination in 100-year storm condition factors.

Load combination	Load condition											
	1	2	3	4	21	22	23	24	25	26	27	28
40	1.1	1.0	1.0	1.0	1.0							
41	1.1	1.0	1.0	1.0		1.0						
42	1.1	1.0	1.0	1.0			1.0					
43	1.1	1.0	1.0	1.0				1.0				
44	1.1	1.0	1.0	1.0					1.0			
45	1.1	1.0	1.0	1.0						1.0		
46	1.1	1.0	1.0	1.0							1.0	
47	1.1	1.0	1.0	1.0								1.0

Table 2.29 Load combination factors for maximum pile tension conditions.

Load combination	Load condition											
	1	2	3	4	11	12	13	14	15	16	17	18
40	0.9	0.9	0.8		1.0							
41	0.9	0.9	0.8			1.0						
42	0.9	0.9	0.8				1.0					
43	0.9	0.9	0.8					1.0				
44	0.9	0.9	0.8						1.0			
45	0.9	0.9	0.8							1.0		
46	0.9	0.9	0.8								1.0	
47	0.9	0.9	0.8									1.0

a matrix for the load combination versus the applied load in WSD concept for 1- and 100-year storm conditions, respectively.

The load combination for the maximum pile tension condition is illustrated in Table 2.29.

2.7 Collision events

In a rigorous impact analysis, if required, accidental design situations shall be established representing bow, stern, and beam-on impacts on all exposed components.

The collision events can be divided into two categories:

1. The event happens regularly as the supply boat daily approaches the boat landing, the vessel velocity for approaching, leaving, or standing alongside the platform presents a low energy level.
2. The event is rare and happened in the case of an accident due to weather conditions and the vessel operates near the platform, producing a high energy level.

For the case of a low energy level, the design is based on the requirement of the client for the serviceability level as it is a function of practical and economic impact. In the case of a high energy level it shall be designed by the ULS and can assume some damage for the boat landing or riser guard but there is no collapse of the platform as a whole.

For the collision analysis for both cases the type of expected vessel and its mass with the velocity during approach are required. The water depth and the geometric dimensions of the vessel and structure, the tidal range, and vessel drift enable the designer to calculate the vertical height of the impact zone during collision.

2.7.1 Accidental impact energy

Total kinetic energy

The total kinetic energy during collisions can be calculated from the following formula:

$$E = ½\, a \cdot m \cdot V^2$$

where m is vessel mass (kg), a is the coefficient for the vessel which is equal to 1.4 and 1.1 for sides and bow or stern collision, respectively. V is the vessel impact velocity (m/s). In general, the total kinetic energy (E) shall be taken as the lower of 14 and 11 MJ for sideways and bow or stern collisions, respectively, corresponding to a vessel of 5000 tons with an impact speed of 2 m/s. In some cases for operations restriction and practical conditions for the available vessel and its speed, a reduction can be made in the calculation due to a reduction in the vessel mass or its approach speed.

As per OTI (1988), the reduced impact speeding V (m/s) is equal to half the maximum permissible significant wave height (m) for vessel operations near to the platform.

The collision analysis includes denting and damage to the member with elastic and plastic deformation and also presents the elastic and plastic deformation of the structure as a whole so that pushover analysis is essential to this analysis. In addition, the vessel itself shall absorb some energy which should be considered and be defined in the simulation with the time history presenting the energy dissipation.

2.7.2 Dropped objects

When evaluating the impact risk from dropped objects the nature of all crane operations in the platform vicinity shall be taken into account. If the probability of impact is not negligible relevant accidental design situations shall be defined and evaluated following the requirements. As per the structure integrity approach to the company, as will be discussed in Chapter 8, Risk-based inspection technique, the consequence on the platform governs the required assessment of the impact analysis and its required level of accuracy.

2.8 Fires and explosions

Hydrocarbon pool fires on the sea surface can cause heating of and hence degradation of the properties of structural components. Sources of hydrocarbons can include conductor or riser fractures, or spillage from the topsides following a process vessel rupture, while ignition sources can include radiation from oil burners and flares.

If the probability of exposure of the structure to fires is not negligible relevant accidental design situations shall be defined and evaluated. Consequential damage resulting from such accidental design situations should be provided for in the structure design.

In general, for small platforms like satellites without any production facilities there is no need to consider collision. However, in the case of complex platforms or platforms of a larger size and with production facilities and a control room, the explosion scenario shall be studied and in most cases the control rooms shall be design to resist a blast load.

Table 2.30 Present the steel chemical composition based on American Society of Testing materials (ASTM).

C	0.18% max
Mn	1.5% max
Nb	0.10% max
V	0.015% max
S[a]	0.025% max
CEV[b]	0.42% max

[a]For plate designated on the order as Z grade, with through-thickness properties, the sulfur content shall be limited to 0.008% max.
[b]Carbon equivalent (CEV) shall be based on product analysis and shall be calculated using the following equation.

2.9 Material strength

During the design phase the designer shall define the required type of steel and its specification as per their design. The fabricators or the materials suppliers shall issue the mill test report certificate for review and approval, and in some cases the quality control team takes a sample and carries out the mill test to guarantee the steel specification matches the required specifications. The laboratory test shall comply with ASTM A6 or A20, as applicable to the specification listed in Table 2.30, constituting evidence of conformity with the specification. The steel component which is not identified by the supplier shall not be used.

2.9.1 Steel groups

Steel may be grouped according to the SLE and welding characteristics as follows:

- Group I are mild steels with specified minimum yield strengths of 279 MPa or less. These steels may be welded by any of the welding processes described in AWS D1.1.
  Most of the platform's structural members are made from Group I steel, as shown in Table 2.31.
- Group II are intermediate-strength steels with specified minimum yield strengths of over 279 through 360 MPa. These steels require the use of low-hydrogen welding processes.
- Group III are high-strength steels with specified minimum yield strengths in excess of 52 ksi (360 MPa).

Table 2.31 presents the steel groups, their yield strength ranges, and their Charpy toughness.

The selection of steels depends on the following information and if it is applicable to the project, such as:

1. The steel weldability; this means the required welding procedure.
2. Behavior under fatigue stresses, as offshore fatigue is one of the main concerns.
3. Its notch toughness influences fracture control, which is affected by the environmental temperature with applied stresses, inspection procedure, and fabrication process.

Table 2.31 Materials category and selection for structures.

Steel group	Yield strength range (MPa)	Charpy toughness (J)	Structure element
I	220–275	20	• Primary and secondary bracing • Barce end stubs at node • Legs • Piling • Conductor panels • Boat landings and walkways • Stiffener elsewhere
II	280–395	35	• Joint cans • Barce end stubs at node • Legs • Stiffener at nodes • Piling with thick wall at sea floor
III	400–455	45	• Legs • Bracing in area of high collision

The steel should be made by the basic oxygen or basic electric arc furnace process. The minimum rolling reduction ratio of material used for plates should be 4:1.

In most offshore structures using American Society of Testing materials (ASTM) A572 Grade 50 the material should conform to the requirements of ASTM A572 and ASTM A6, except as noted below. All steel should be supplied in the normalized condition.

The chemistry should conform to ASTM A572 (see Table 2.30), with the following additional requirements for product analysis:

$$\text{Carbon equivalent (CE)} = \text{C} + (\text{Mn}/6) + (\text{Ni} + \text{Cu}/15) + (\text{Cr} + \text{Mo} + V/5)$$

The ratio of soluble aluminum to nitrogen should be a minimum of 2:1. The supplier should submit a full chemical analysis, identifying maximum and minimum levels, with their bid.

Product analysis should be determined twice per cast and should be determined on the test sample used for verification of mechanical properties.

For mechanical testing, the tensile samples should be cut with the longitudinal axis of the test samples transverse to the principal direction of rolling. Test specimens should be prepared for testing from material in the delivered condition (i.e., from a plate). A separate piece is not acceptable.

For plate designated on the order as Z Grade, through-thickness testing requirements S4 of ASTM A6 should apply.

Charpy impact testing should be carried out in accordance with the requirements of S5 of ASTM A6. All tests should be carried out at 0°C. Minimum average absorbed energy should be 50 J, with a minimum individual value of 38 J. The frequency of testing should be in accordance with ASTM A673. No impact testing is required for 6 mm thickness or less.

When steel is used for topside offshore structures, the material should conform to the requirements of ASTM A36 and ASTM A6, except as noted below. All steel should be supplied in the normalized condition.

In this grade the carbon equivalent should not exceed 0.42% and the carbon content should not exceed 0.20% by product analysis. Rimming steel should not be permitted.

The testing and tensile testing should be in accordance with ASTM A6 and the Charpy impact tests should be carried out in accordance with the requirements of S5 of ASTM A6. All tests should be carried out as follows:

- Test temperature = 0°C;
- Absorbed energy = 27 J (average); 20 J (minimum individual);
- Frequency of testing should be in accordance with Section 5.1 of ASTM A673;
- No impact testing is required on material of 6 mm thickness or less.

For tubular members, steel-grade API 5L tubular members should be supplied in the following conditions:

- Diameters = 18 inches (457 mm)—seamless;
- Diameters > 18 inches (457 mm)—double-sided submerged arc welded.

Tubular members should be supplied either in the normalized or quenched and tempered condition.

Product analysis should be undertaken and the chemistry should comply with API 5L X52 (see Table 2.32).

The yield and tensile strength of the parent material and the weld metal (where applicable) should comply with Table 2.33.

Charpy impact tests shall be taken in the transverse direction at 0°C and the frequency of testing shall be in accordance with Section 5.1 of ASTM A673.

Tubular members shall be clean and free from such defects as can be established by visual examination.

Surface marks/imperfections such as tears, laps, slivers, gouges, scabs, and seams shall be dressed and the remaining thickness confirmed by UT. MPI shall confirm defect removal. All dressed areas shall blend smoothly into the contour of the tubular.

Tubular members shall not contain any dents greater than 3 mm or 1% × OD, whichever is the lesser. The length of the dent shall not exceed 25% × OD (Table 2.34).

All tubular shall be UT inspected for laminations over the full length in accordance with API 5L except the depth of the reference notch shall be 5% of the thickness. In addition, UT inspection using compression wave techniques shall be carried out for a minimum distance of 50 mm from the end of the tubular to ensure freedom from lamination.

Table 2.32 Chemical composition for steel API 5L X52.

C	0.17% max.
Mn	0.8−1.5% max.
Cr	0.30% max.
Mo	0.12% max.
V	0.06% max.
Nb (cb)	0.02% max.
Ni	0.08% max.
Cu	0.05% max.
s	0.025% max.
p	0.02% max.
si	0.15−0.45% max.
Al (total)[a]	0.06% max.
N[a]	0.014% max.
CEV[b]	0.42% max.
Pcm[c]	0.20 max.

Note: Chemistry for API 5L Grade B shall comply with API 5L.
[a]The minimum soluble aluminum to nitrogen ratio should be 2:1; soluble aluminum content should be defined as the total content (0.005%).
[b]$CE = C + (Mn/6) + (Cr + Mo + V/5) + (Ni + Cu)/15$.
[c]*Pcm*, phase change material, which is used to express weldability, and is obtained from the following equation
$Pcm = C + Si/30 + (Mn + Cu + Cr)/20 + Mo/15 + V/10 + 5B$.

Table 2.33 Steel mechanical properties

Steel type	Yield strength (N/mm^2)	Tensile strength (N/mm^2)
API5LX52	359	455
API 5L 'B'	241	414

UT inspection of welds in welded tubular members shall be subject to 100% UT and shall comply with API 5L.

2.9.2 Steel classes

The steel can be classified depending on the characteristics of its notch toughness which should match with the steel service in the project (Tables 2.35−2.36). These types of steel are as follows.

Class C is used in piles, jacket legs and braces, and deck beams and legs. In the case of high redundancy, as in fractures, there shall be no sudden catastrophic failure, and this type of steel is also good for welding at temperatures above freezing. It is applied to structure members with limited thickness, low restrain, and the load can increase in 1 second or longer, and is called quasistatic loading.

Table 2.34 Pipe dimensions and properties.

Nominal pipe size (in.)	Nominal pipe size (mm)	OD (in.)	OD (mm)	Schedule designations ANSI/ASME	Wall thickness (in.)	Wall thickness (mm)	Weight (lbs/ft.)	Weight (kg/m)
1/2	15	0.84	21.3	STD/40S	0.109	2.77	0.851	1.27
1/2	15	0.84	21.3	XS/80S	0.147	3.73	1.088	1.62
1/2	15	0.84	21.3	XX	0.294	7.47	1.714	2.55
3/4	20	1.05	26.7	STD/40S	0.113	2.87	1.131	1.68
3/4	20	1.05	26.7	XS/80S	0.154	3.91	1.474	2.19
3/4	20	1.05	26.7	XX	0.308	7.82	2.441	3.63
1	25	1.315	33.4	STD/40S	0.133	3.38	1.679	2.5
1	25	1.315	33.4	XS/80S	0.179	4.55	2.172	3.23
1	25	1.315	33.4	XX	0.358	9.09	3.659	5.45
1-1/4	32	1.66	42.2	STD/40S	0.14	3.56	2.273	3.38
1-1/4	32	1.66	42.2	XS/80S	0.191	4.85	2.997	4.46
1-1/4	32	1.66	42.2	XX	0.382	9.7	5.214	7.76
1-1/2	40	1.9	48.3	STD/40S	0.145	3.68	2.718	4.05
1-1/2	40	1.9	48.3	XS/80S	0.2	5.08	3.631	5.4
1-1/2	40	1.9	48.3	XX	0.4	10.16	6.408	9.54
2	50	2.375	60.3	STD/40S	0.154	3.91	3.653	5.44
2	50	2.375	60.3	XS/80S	0.218	5.54	5.022	7.47
2	50	2.375	60.3	XX	0.436	11.07	9.029	13.44
2-1/2	65	2.875	73	STD/40S	0.203	5.16	5.793	8.62
2-1/2	65	2.875	73	XS/80S	0.276	7.01	7.661	11.4
2-1/2	65	2.875	73	XX	0.552	14.02	13.69	20.37
3	80	3.5	88.9	STD/40S	0.216	5.49	7.576	11.27
3	80	3.5	88.9	XS/80S	0.3	7.62	10.25	15.25
3	80	3.5	88.9	XX	0.6	15.24	18.58	27.65
3-1/2	90	4	101.6	STD 40S	0.226	5.74	9.109	13.56
3-1/2	90	4	101.6	XS/80S	0.318	8.08	12.5	18.6
3-1/2	90	4	101.6	XX	0.636	16.15	22.85	34.01
4	100	4.5	114.3	STD/40S	0.237	6.02	10.79	16.06
4	100	4.5	114.3	XS/80S	0.337	8.56	14.98	22.29
4	100	4.5	114.3	XX	0.674	17.12	27.54	40.99

(*Continued*)

Table 2.34 (Continued)

Nominal pipe size (in.)	Nominal pipe size (mm)	OD (in.)	OD (mm)	Schedule designations ANSI/ASME	Wall thickness (in.)	Wall thickness (mm)	Weight (lbs/ft.)	Weight (kg/m)
5	125	5.563	141.3	STD/40S	0.258	6.55	14.62	21.76
5	125	5.563	141.3	XS/80S	0.375	9.53	20.78	30.93
5	125	5.563	141.3	XX	0.75	19.05	38.55	57.37
6	150	6.625	168.3	STD/40S	0.28	7.11	18.97	28.23
6	150	6.625	168.3	XS/80S	0.432	10.97	28.57	42.52
6	150	6.625	168.3	XX	0.864	21.95	53.16	79.12
8	200	8.625	219.1	STD/40S	0.322	8.18	28.55	42.49
8	200	8.625	219.1	XS/80S	0.5	12.7	43.39	64.58
8	200	8.625	219.1	XX	0.875	22.23	72.42	107.78
10	250	10.75	273.1	STD/40S	0.365	9.27	40.48	60.24
10	250	10.75	273.1	XS/80S	0.5	12.7	54.74	81.47
10	250	10.75	273.1	XX	1	25.4	104.13	154.97
12	300	12.75	323.9	STD/40S	0.375	9.53	49.56	73.76
12	300	12.75	323.9	XS/80S	0.5	12.7	65.42	97.36
12	300	12.75	323.9	XX	1	25.4	125.49	186.76
14	350	14	355.6	40	0.438	11.13	63.44	94.41
14	350	14	355.6	XS/80S	0.5	12.7	72.09	107.29
16	400	16	406.4	STD/40S	0.375	9.53	62.58	93.13
16	400	16	406.4	XS/80S	0.5	12.7	82.77	123.18
18	450	18	457.2	STD/40S	0.375	9.53	70.59	105.06
18	450	18	457.2	XS/80S	0.5	12.7	93.45	139.08
20	500	20	508	STD/40S	0.375	9.53	78.6	116.98
20	500	20	508	XS/80S	0.5	12.7	104.13	154.97
24	600	24	609.6	STD/40S	0.375	9.53	94.62	140.82
24	600	24	609.6	XS/80S	0.5	12.7	125.49	186.76
30	750	30	762	STD/40S	0.375	9.53	118.65	176.58
30	750	30	762	XS/80S	0.5	12.7	157.53	234.44
36	900	36	914.4	STD/40S	0.375	9.53	142.68	212.34
36	900	36	914.4	XS/80S	0.5	12.7	189.57	282.13

40S, schedule 40; *STD*, standards; *80S*, Schedule 80; XS, extra strong; *XX*, double extra strong.

Table 2.35 Mechanical properties for structural steel plates American Society of Testing material (ASTM).

Group	Class	Specifications and grade	Yield strength (MPa)	Tensile strength (MPa)
I	H	A36 (to 50 mm thickness)	250	400–550
		A131 Grade A (to 12 mm thick)	235	400–490
		A285 Grade C (to 19 mm)	205	380–515
I	N	A131 Grades B, D	235	400–490
		A516 Grade 65	240	450–585
		A573 Grade 65	240	450–530
		A709 Grade 36T2	250	400–550
I	C	A131 Grades CS, E	235	400–490
II	H	A572 Grade 42 (to 50 mm thick)	290	415 min
		A572 Grade 50 (to 50 mm thick; S91 required over 12 mm)	345	450 min
II	N	API Spec 2 MT1	345	483–620
		A709 Grades 50T2, 50T3	345	450 min
		A131 Grade AH32	315	470–585
		Grade AH36	350	490–620
II	C	API spec 2H Grade 42	290	430–550
		Grade 50 (to 62 mm thick)	345	483–620
		Grade 50 (over 62 mm thick)	325	483–620
		API Spec 2 W Grade 50 (to 25 mm thick)	345–517	448 min
		API Spec 2 W Grade 50 (over 25 mm thick)	345–483	448 min
		API Spec 2Y Grade 50 (to 25 mm thick)	345–517	448 min
		(over 25 mm thick)	345–483	448 min
		A131 Grades DH32, EH32	315	470–585
		Grades DH36, EH36	350	490–620
		A537 class I (to 62 mm thick)	345	485–620
	A	A633	290	435–570
	C, D		345	485–620
		A678 Grade A	345	485–620
III	A	A537 Class II (to 62 mm thick)	415	550–690
		A678 Grade B	415	550–690
		API Spec 2 W Grade 60 (to 25 mm thick)	414–621	517 min
		API Spec 2 W Grade 60 (over 25 mm thick)	414–586	517 min
		API Spec2Y Grade 60 (to 25 mm thick)	414–621	517 min
		API Spec2Y Grade 60 (over 25 mm thick)	414–586	517 min
		ASTM A710 Grade A Class 3 (quenched and precipitation heat treated)		
		To 50 mm	515	585
		50–100 mm	450	515
		Over 100 mm	415	485

Table 2.36 Mechanical properties for structural steel shapes.

Group	Class	Specifications and grade American Society of Testing material (ASTM)	Yield strength (MPa)	Minimum tensile strength (MPa)
I	C	A36 (<50 mm thickness)	250	400–550
		A131 Grade A (<12 mm thick)	235	400–550
I	B	A709 Grade 36T2	250	400–550
II	C	API Spec 2 MT2 class C	345	450–620
		A572 Grade 42 (to 50 mm thick)	290	415
		A572 Grade 50 (to 50 mm thick; S91 required over 12 mm)	345	450
		A992	345–450	450
II	B	API Spec 2 MT2 class B	345	450–620
		A709 Grades 50T2, 50T3	345	450
		A131 Grade AH32	315	470–585
		Grade AH36	350	490–620
II	A	API spec 2MT2 Class A	345	450–620
		A913 Grade 50	345	450

Class B is used if there is a stress concentration, restrain, and cold work, or there is a low redundancy for the member and higher notch toughness is needed. The impact test for this type of steel for Charp-V notch energy is 20 J for Group I and for Group II is 34 J at the lowest service temperature. It can comply with a Charpy test requirement at temperatures from 0°C to 10°C; the Charpy test follows ASTM A 673.

Class A steel can be used as the lowest temperatures as it can comply with the Charpy test at temperature from −20°C to −40°C. This type of steel, due to its notch toughness, prevents brittle fracture propagation from large flaws. The impact test is important to be done for this type of steel and to comply with its standard.

Structural shape specifications are listed in Table 2.37. Steels above the thickness limits stated may be used and should be considered by the designer.

Structural steel pipe

Unless otherwise specified, seamless or welded pipe should conform to one of the specifications listed in Table 2.37. Table 2.37 presents the mechanical properties of the pipe. The pipe should be of prime quality unless it has limited service, or structural grade or reject pipe is specifically approved by the designer.

Structural pipe should be fabricated in accordance with API Spec. 2B, ASTM A139**, ASTM A252**, ASTM A381, or ASTM A671 using grades of structural plate as listed in Table 2.37 except that hydrostatic testing may be omitted.

Selection for conditions of service

In the case of pipes which are cold formed and with diameter to thickness ratios of less than 30 and that are not heat treated, notch toughness degradation may happen

Table 2.37 Mechanical properties for structural steel pipes.

Group	Class	Specifications and grade, as American Society of Testing material (ASTM)	Yield strength (MPa) (ksi)	Minimum tensile strength (MPa) (ksi)
I	C	API 5L Grade B A53 Grade B A135 Grade B A 139 Grade B	240 (35)	415 (60)
		A500 Grade A (round)	230 (33)	310 (45)
		(shaped)	270 (39)	310 (45)
		A501	250 (36)	400 (58)
I	B	A106 Grade B (normalized)	240 (35)	415 (60)
		A524 Grade I (to 10 mm thick)	240 (35)	415 (60)
		Grade II (over 10 mm thick)	205 (30)	380−550 (55−80)
I	A	A333 Grade 6	240 (35)	415 (60)
		A334 Grade 6	240 (35)	415 (60)
II	C	API 5L Grade X42, 2% max. cold expansion	290 (42)	415 (60)
		API 5L Grade X52, 2% max. cold expansion	360 (52)	455 (66)
		A500 Grade B (round)	290 (42)	400 (58)
		A500 Grade B (shaped)	320 (46)	400 (58)
		A618	345 (50)	485 (70)
II	B	API 5L Grade X52 with SR5 or SR6	360 (52)	455 (66)

so it is important to select a higher class of steel or otherwise define the notch toughness test at low temperature.

Specific for the tubular joints it needs a special precaution as there is a stress concentration and this joint can be applied to yielding and plastic restrains in addition to that affected by the cycling loading which initiates fatigue cracks. This joint also is responsible for structure ductility under dynamic loading. Therefore in platform design since 1970, joints have been designed to increase ductility and overcome punching shear.

For the under water part of the platform structure, such as the jacket, and its bracing and the joints cans which is design for overlapping labing; the notch toughness shall meet the following criteria as per the temperature conditions in Table 2.38:

1. No break performance for a drop weight test;
2. Charpy V-notch energy is 20 J for Group I steels, 34 J Group II steels, and 47 J for Group III steels.

Table 2.38 Input testing conditions

D/t	Test temperature	Test condition
Over 30	36°F (20°C) LAST	Flat plate
20−30	54°F (30°C) LAST	Flat plate
Under 20	18°F (10°C) LAST	As fabricated

LAST, Lowest anticipated service temperature.

These criteria can be achieved at a water temperature of 40°F (4°C) or higher for Class A steels as per Table 2.37.

Class A steels shall be used as API 2H, Grade 42, or Grade 50 in the case of joints above water and if impact is possible, as in the case of boat landing. In the case of using steel 345 MPa (50 ksi) yield strength or higher, the welding procedure shall be taken into consideration.

For critical connections involving high restraint (including adverse geometry, high yield strength, and/or thick sections), through-thickness shrinkage strains, and subsequent through-thickness tensile loads in service, consideration should be given to the use of steel with improved through-thickness (Z-direction) properties, such as API Spec 2H.

There is a high concentration on the end of the bracing which is welded to the joint can a brittle fracture would be more severe, therefore stub-ends can be used which have the same class of steel as the joint can.

Cement grout

Cement grout is required to fill the annulus between the jacket and the pile, in some cases as a method of strengthening the platform if it is not in the original design. The mix design should be carried out and tested before pouring it and also the laboratory specification shall be taken for the applied grouting as per ASTM C109. The curing for the test laboratory should be with water with the same salinity as the sea water. The cement grout used in the platform should have a compressive strength not less than 20 MPa after 28 days. The designer shall define the required grouting compressive strength as the test shall be done during the performing of the grouting and the precautions and recommendations for performing and the required quality control shall follow ACI214-77, BS8110, or equivalent based on the project specification and standard.

References

American Petroleum Institute, 2007. Working Stress Design, API RP2A-WSD, 21th Ed.

Atkins Engineering Services, 1990. Fluid Loading on Fixed Offshore Structures, OTH 90 322.

Further reading

American Institute of Steel Construction, Load and Resistance Factor Design Specification for Structural.

American Petroleum Institute, 1993. Recommended Practice for Planning, Designing, and Constructing.

British Standard BS5400 Part 3, Steel, Concrete and Composite Bridges, Code of Practice for Design of Steel Bridges.

British Standard BS 5950, Structural Use of Steelwork in Buildings, Code of Practice for Design.

Design and Plastic Design, June 1989.

DNV (Det Norske Veritas), Offshore Standard DNV-OS-C101: Design of Offshore Steel Structures, General (LRFD Method), October 2008. http://dc140.4shared.com/doc/Pflypj7r/preview.html

ENV 1993-1-1:1992, Eurocode 3, Design of Steel Structures, General Rules and Rules for Buildings.

Fixed Offshore Platforms, Load and Resistance Factor Design, API RP2A-LRFD, first ed.

Fixed Offshore Platforms, 1999.Working Stress Design, API RP2A-WSD, twelfth ed. American Institute of Steel Construction, Specification for Structural Steel Buildings, Allowable Stress.

NS 3472, Norwegian Standard NS 3472, Steel Structures, Design Rules.

Steel Buildings, December 1999, AISC LRFD.

Offshore structure platform design

3

3.1 Introduction

Offshore fixed platform design has three main phases, the first of which is design of the deck that carries the topside facility. The dimensions of the deck depend on the function of the platform and the facilities that will be located on it.

The second part is design of the jacket, which depends on the water depth, the wave and current loads, and the other loads described in Chapter 2, Offshore structure loads and strength. The configuration of the jacket structural system is chosen based on the water depth and the designer's experience.

The third phase of design is to assess the robustness of the deck and jacket design for lifting, pullout, transportation, launching, and installation.

The topside facilities (decks), the jacket, and the piles are the main components of the offshore structure platform.

Topside decks in most cases are a drilling deck, a well head, and production deck, a cellar deck, and in some cases a mezzanine deck. The decks are supported by a structure system consisting of girders, trusses, and columns. Figs. 3.1 and 3.2 show a plan of the main deck and two elevation views, including the three common levels on all platforms (the main deck, cellar deck, and spider deck or mezzanine deck in some cases).

The main function of the topside is to carry the load from the facilities and drilling equipment. The function of the jacket is to surround the piles and to hold the pile extensions in position all the way from the mud line to the deck substructure. Moreover, the jacket provides support for boat landings, mooring bits, barge bumpers, the corrosion protection system, and many other platform components. Examples of jacket drawings are presented in Fig. 3.3. Plan views at different levels are presented in Fig. 3.4 for the highest jacket level, in Fig. 3.5 for the mud-mat level, and Fig. 3.6 for the horizontal frames at different levels.

3.2 Preliminary dimensions

The topside deck structure is regularly designed by the American Institute of Steel Construction (AISC), with Allowable Stress Design (ASD) or load resistance factor design (LRFD) according to the project basis of design (BOD). The main supporting element may be the plate girder or tubular truss, but it is preferred to be a tubular member to reduce the wind load effect.

Offshore Structures. DOI: https://doi.org/10.1016/B978-0-12-816191-3.00003-1

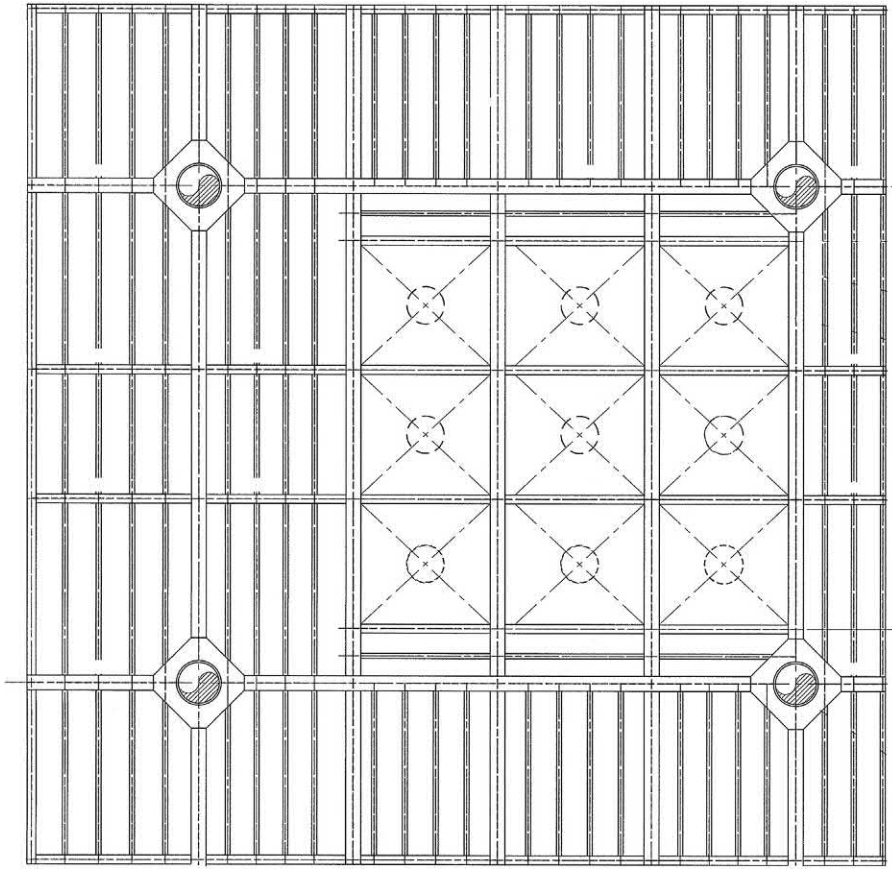

Figure 3.1 Plan of the main deck.

The steel plate thickness around 38 mm (1½ inches) thick shall be the main cover with its thickness depending on the spacing between the secondary beam and the load effect, in some cases it will be a grating.

Fig. 3.7 is a platform elevation view showing the main parts of the offshore platform and affected load.

3.2.1 Approximate dimensions

- Large forces result when waves strike a platform's deck and equipment.
- There should be an air gap between maximum wave crest height and first deck. This air gap will be considered at least 1.5 m (5 ft.) added to the crest wave height, which is obtained from 100-year omnidirectional wave, as shown in Fig. 3.7.
- From a practical point of view, sea deck levels are usually considered to be at an elevation of 10−14 ft. (3−4 m) above the mean water level (MWL).

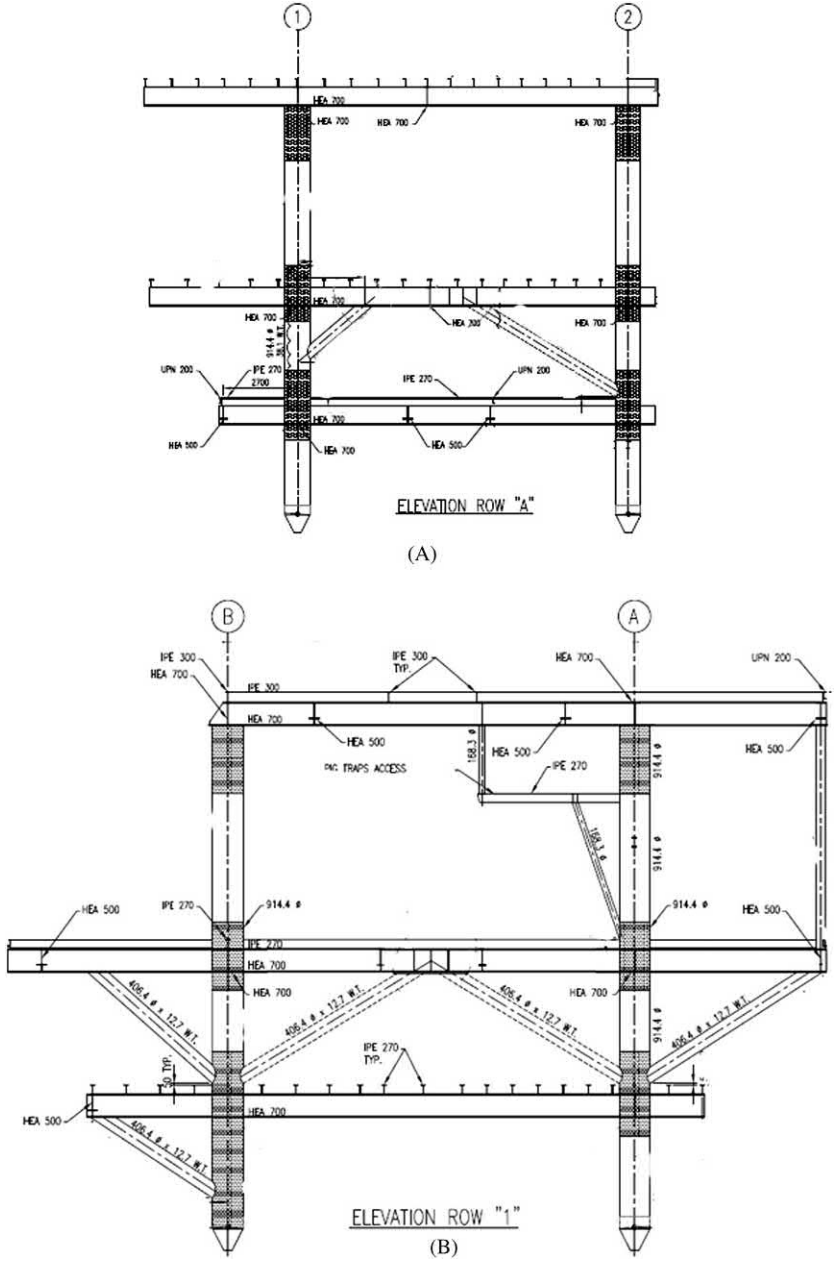

Figure 3.2 (A) Elevation at row A; (B) elevation at row 1.

- The jacket walkway is above the normal everyday waves that pass through the jacket.
- In the case of an eight-legged platform, the spacing between the legs is about 11−19 m (35−65 ft.) and it is defined based on the spacing of launch runners for the barge which is proposed to use in installation.

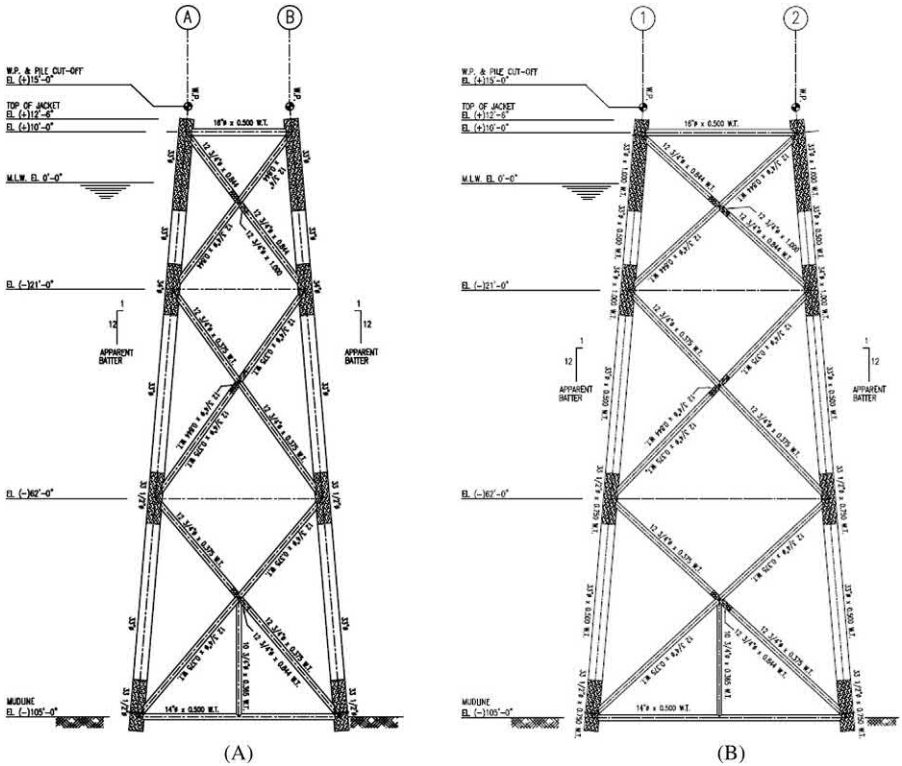

Figure 3.3 (A) Jacket view; (B) another view of the jacket.

- In the short direction, the leg spacing is approximately 14 m (45 ft.). The drilling and production packages that will be placed on the deck govern this dimension.
- The length of the cantilever overhang is usually about 3.5−4.5 m (12−15 ft.).
- Allowing 25 mm (1 inch) annular clearance between the pile and the inside of leg, for a pile of 60 and 48 inches OD, the legs will have internal diameters of 62 inches and 50 inches, respectively.
- Jacket legs are battered with slopes of 1:8 or 1:7 to provide a larger base for the jacket at the mud line and thus assist in resisting the horizontal load from waves and wind.
- The pipeline engineer, with process engineers, shall define the conductor and riser numbers and sizes; the conductor is always 18, 20, 24, or 30 inches and the risers are always from 14 to 20 inches.

3.3 Bracing system

The bracing system is mainly vertical, horizontal, and diagonal tubular members connected to jacket legs. This system transfers mainly the wave load or seismic acting on the platforms to the piles. The designer can choose the best structure bracing

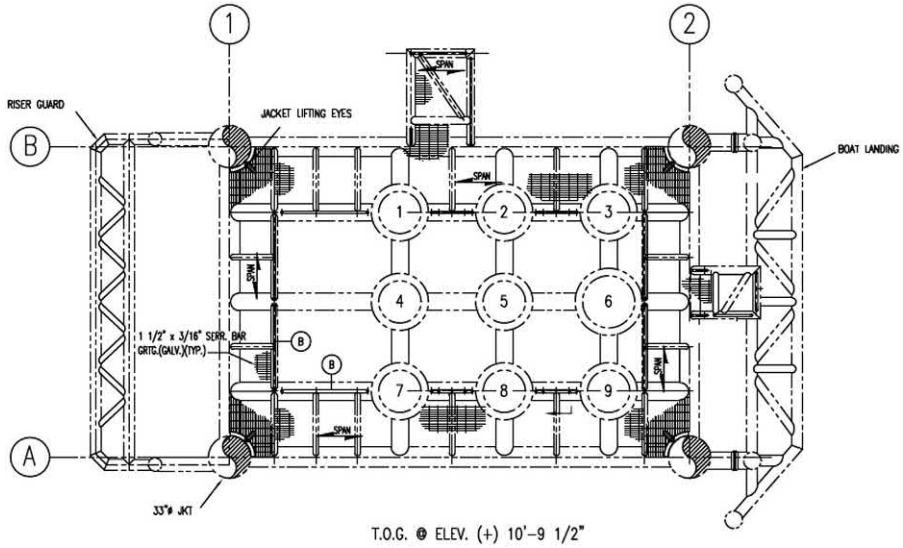

Figure 3.4 Plan view at the highest jacket level.

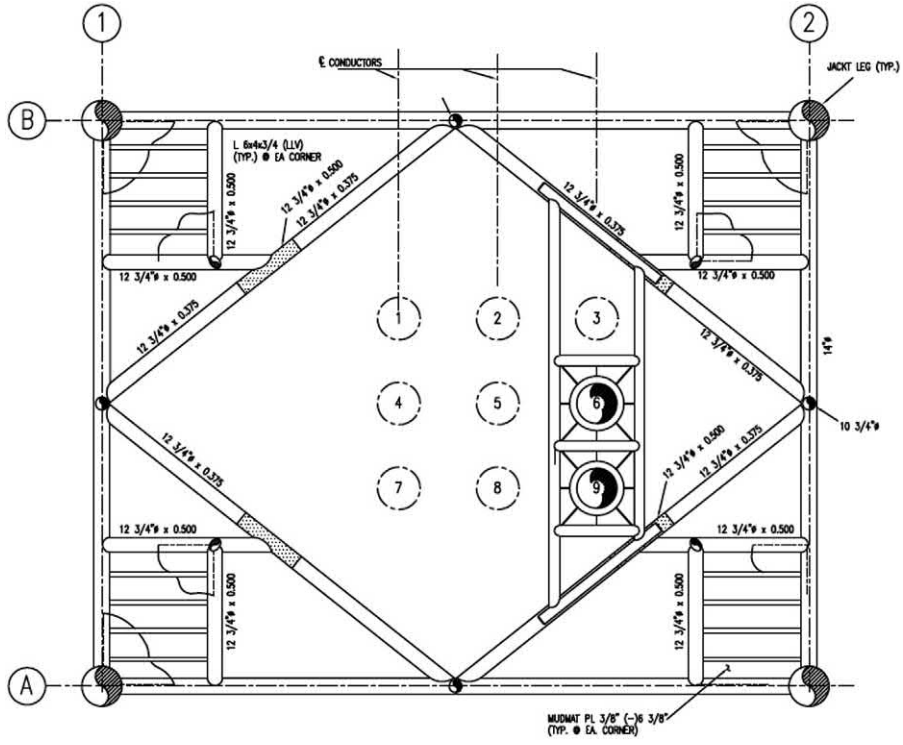

Figure 3.5 Plan view at the mudmat.

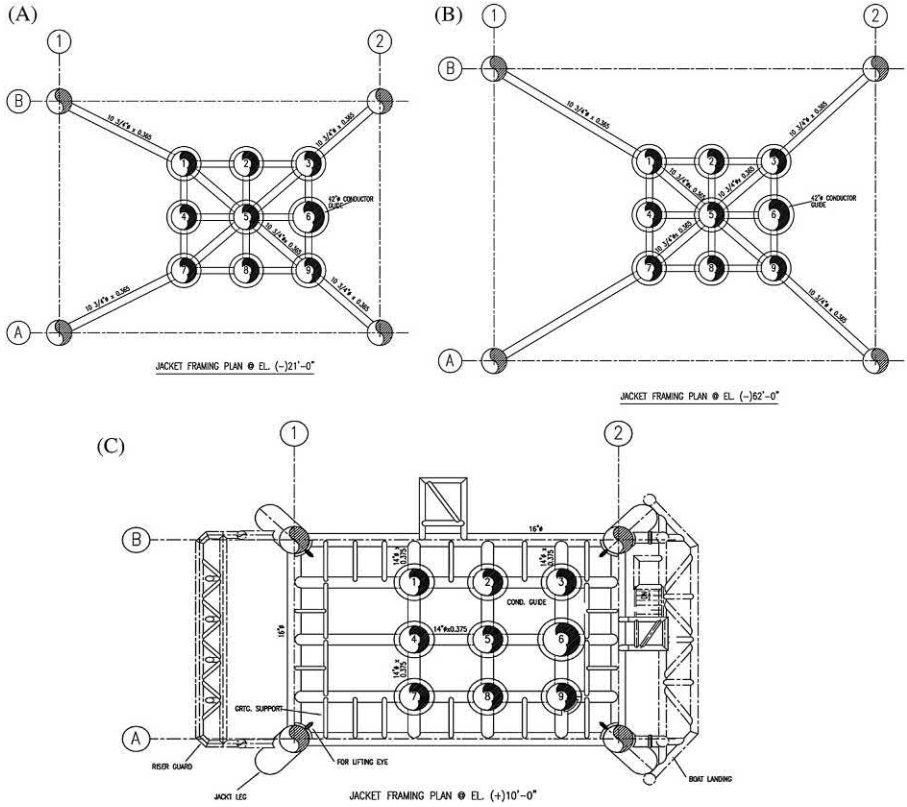

Figure 3.6 (A) Plan view of the jacket at an elevation of 21 ft.; (B) plan view of the jacket at an elevation of 62 ft.; (C) plan view of the jacket at an elevation of 10 ft.

system as each type has it pros and cons. The *K* brace has fewer members intersecting at joints, so it has reduced welding and assembly costs. However, its disadvantage is that *K* bracing has less redundancy than *X* bracing. This is based on the results of a BOMEL study in 1999 performed jointly by different oil and gas companies.

Fig. 3.8 presents a frame of a jacket that was subjected to lateral load in the test workshop. The load applied was increased gradually until complete failure. The figure shows the buckling of the bracing member.

It is recommended to choose a brace member diameter that has a slenderness ratio (*KL*/*r*) in the range of 70−90. Limiting the ratio to the 70−90 range is an industry-accepted practice. As the slenderness of a brace increases, its allowable axial stress (F_a) decreases. At *KL*/*r* equal to 80, the allowable axial stress (F_a) for A-36 steel (248 MPa) is 71% of that allowable for a nonslender member, that is, that with a *KL*/*r* equal to zero. In the case of steel of 345 MPa (50 KSI) at a *KL*/*r* equal to 80, F_a is reduced to about 63% of that of a nonslender member.

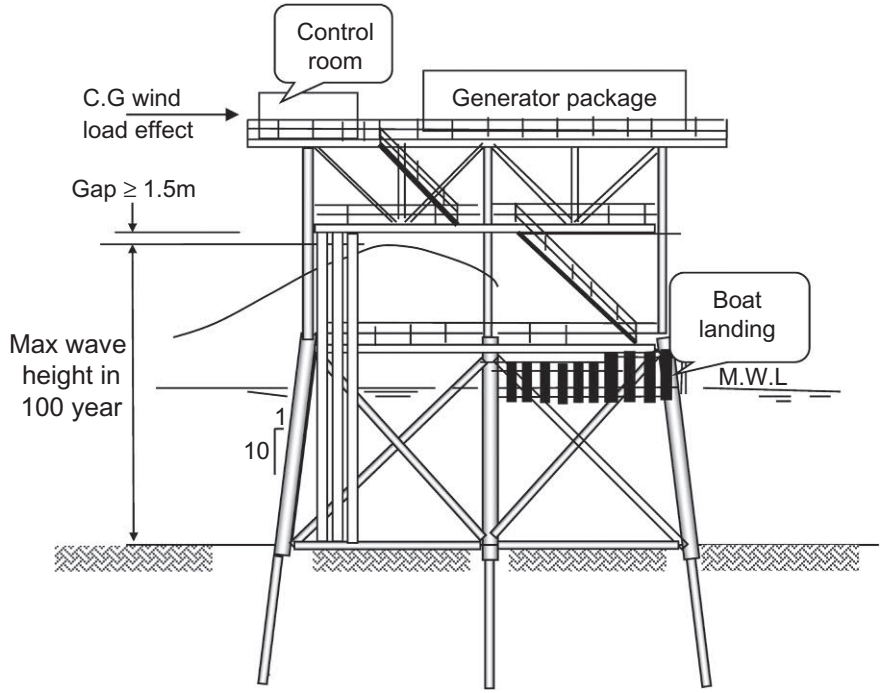

Figure 3.7 Platform elevation view.

At a high *KL*/*r* ratio, the high-yield pipe is less efficient than at lower values. Note that lower slenderness ratios also encourage higher *D*/*t* ratios for tubular members which may compound local buckling problems.

For sizes up to and including 0.45 m (18 inches), use the wall thickness for a standard pipe to start. For sizes up to and including 0.7 m (27 inches), try 12 mm. For 0.75−0.90 m, start with 16 mm.

Engineering practice is to have the *D*/*t* ratio of the members between 20 and 60. In the case of a pipe less than 20 inches it will be not available in the market and complicated in fabrication. For A-36 steel, a *D*/*t* higher than 60 may be limited by local buckling. From engineering practice in the case of water depth *h* (ft.), begin to check the hydrostatic problems in the case that *D*/*t* is $>250/(h)^{0.3333}$.

In general, the legs of the jacket are interconnected and rigidly held by diagonal bracing in vertical planes and horizontal and diagonal bracing in horizontal planes. In most design cases, the plan of horizontal bracing spaced (12−16 m) and near to the water surface the span is approximately 12 m.

The benefits and general functions of the bracing system are:

- Transmission of the horizontal load to the soil through the pile foundation;
- Provision of structural integrity during fabrication and installation;
- Resistance to the wrenching motion of the installed jacket-pile system;
- Support for the corrosion anodes and well conductors.

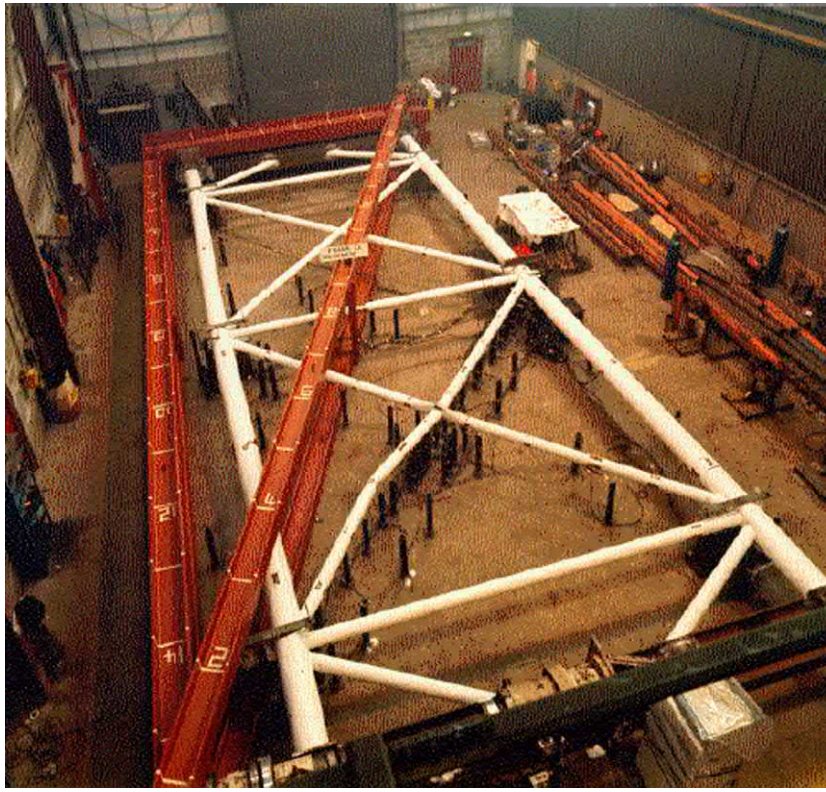

Figure 3.8 Buckling of a beam in the jacket.

3.4 Jacket design

Virtually all of the decisions about design depend on the jacket leg. The soil conditions and foundation requirements often control the leg size.

The golden rule in jacket design is to minimize the projected area of the member near the water surface (high wave zone), to minimize the load on the structure and to reduce the foundation requirements.

From a joint industrial project study (Report for Joint Industry Typical Frame Projects, 1999), Figs. 3.9 and 3.10 present the prototype in two dimensions and the buckling of the K bracing member, respectively.

The results of the study are presented in Fig. 3.11. The relationship between the applied load and displacement for X bracing with horizontal bracing and without a joint-can is presented in Fig. 3.11A. Fig. 3.11B presents the relation between load and displacement in the case of existing horizontal bracing and with a joint-can. It can be seen that, in the case of a joint-can, the jacket can carry more load than specified for the design based on American Petroleum Institute (API). In addition, ductility is higher with a joint-can.

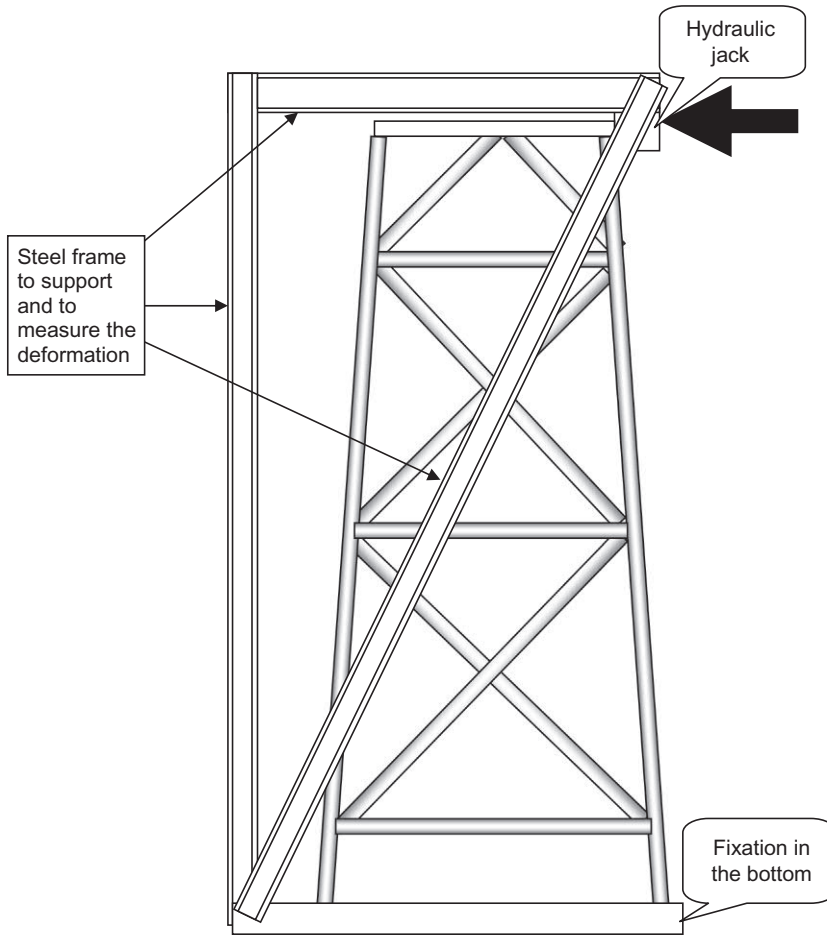

Figure 3.9 Shape of the jacket model in two dimensions for the load test.

If there is no horizontal bracing and without a joint-can, as in Fig. 3.11C, the jacket will carry less load than in the case with a horizontal member.

The test was performed for *K* bracing with different β, which is the relation between the bracing diameter and the chord diameter (d/D), and with a different gap between the bracing (the gap is denoted by g).

Fig. 3.12 presents the relation between the applied load and the frame displacement for designs according to the API and Det Norske Veritas (DNV). With decreasing β values, the redundancy will increase. Also, with an increased gap between the braces, the ductility will increase, as shown in Fig. 3.12 with different dimension parameters values.

Comparison of *X* bracing with horizontal bracing can carry more lateral load than the design load higher than the *K* bracing system, so in general the redundancy of *X* bracing is higher than that in *K* bracing.

Figure 3.10 Buckling in the member for *K* bracing.

3.5 Structure analysis

For environmental and gravitational loads, all the necessary parameters required for automatic load generation by the software program are input by the engineer. Most software programs on the market use default values for many of these parameters.

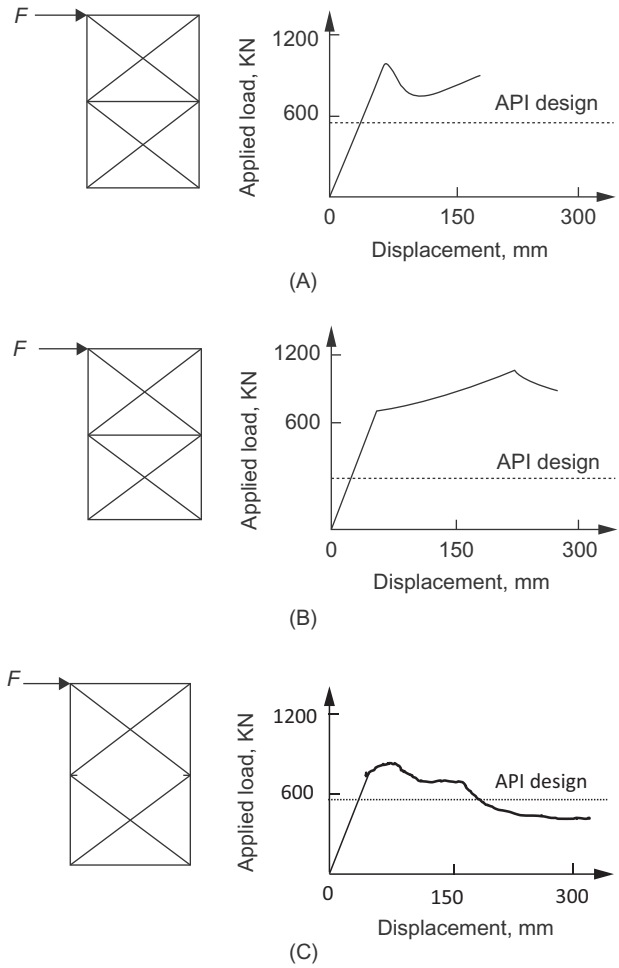

Figure 3.11 (A) *X* bracing with horizontal bracing and without a joint-can; (B) *X* bracing with horizontal bracing and with a joint-can; (C) *X* bracing without horizontal bracing and without a joint-can.

Usually, the engineer must override the defaults and input project-specific values. The following should be defined in the program:

- Self weight;
- Buoyancy for flooded and unflooded members;
- Wind (direction, terrain category, gust duration, drag coefficients, etc.);
- Waves [wave theory, direction, height, period, drag and inertia coefficient (C_D, C_M), wave kinematics, etc.];
- Current direction, speed variation with depth, current blockage factor, etc.;
- Marine growth (thickness variation with depth, roughness, etc.).

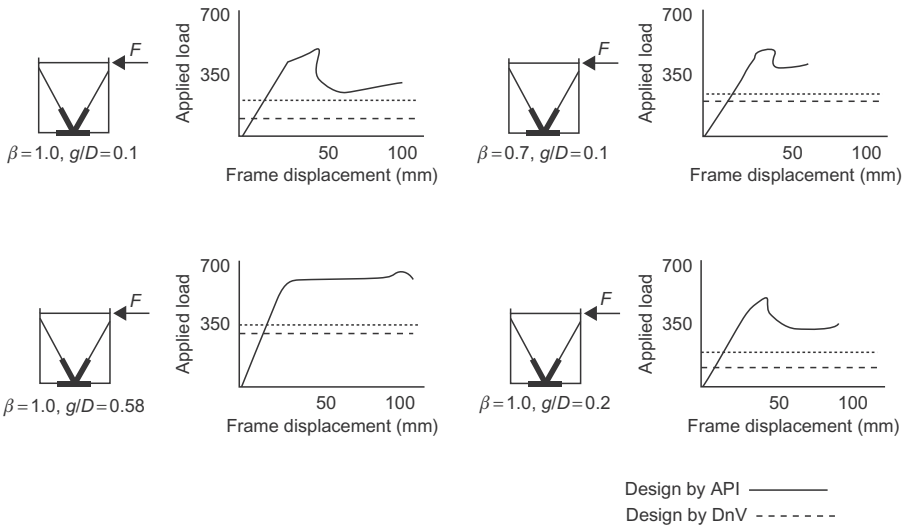

Figure 3.12 Relation between applied load and displacement for different *K*-bracing geometries.

In most cases, the software does not use the correct default coefficients so it should be reviewed carefully.

The structure's pile foundations should be modeled sufficiently to reflect the actual stiffness of the foundation:

- Simple (fixed, pinned, sliding, etc.);
- Linear springs;
- Nonlinear stiffness.

3.5.1 Global structure analysis

The steps for using software in design are:

1. The physical dimensions, member size, and materials properties shall be defined by the structural designer.
2. The structural engineer shall input the soil conditions as obtained from the soil specialist or from the geotechnical report, a $P-y$ curve is also required.
3. All loads must be entered into the program.
4. The wave load is applied through the structure at several angle directions and the direction defined that produces higher base shear, and overturning moment at the pile head (mudline) and the current load is as presented in Fig. 3.13.
5. For each load condition, the computer analysis provides the total base shear and overturning moment, the member-end forces and moments, joint rotation and deflection, and External support reaction
6. After calculating the stresses, the computer compares them with the allowable stresses as defined by the AISC.

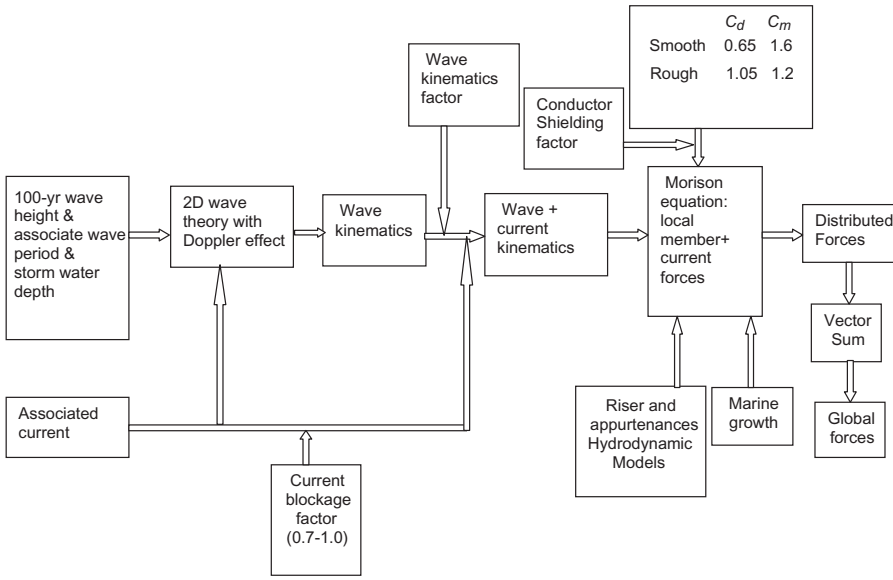

Figure 3.13 Applied environmental loads.

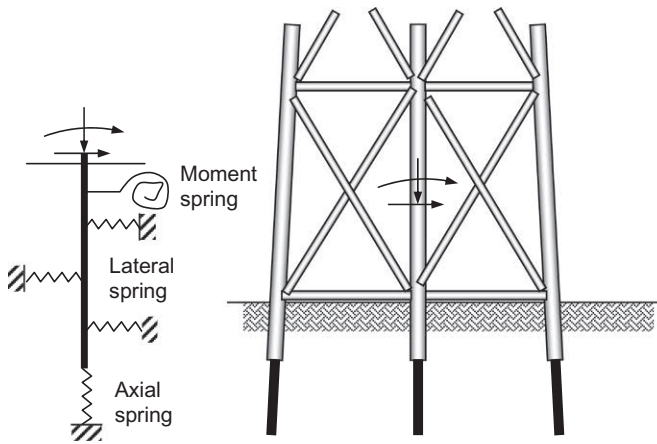

Figure 3.14 Foundation piling model.

7. The pile is presented with lateral springs in two directions, with an axial spring and a moment spring. The piling interacts with the surrounding soil in an inelastic manner, but the software linearizes its response to produce the equivalent elastic spring, as shown in Fig. 3.14.
8. In the case of sea ice abrasion, an allowance of 0.1 mm/year is to be considered for all steel between the elevations of −1.3 to 3.0 m and usually results in a minimum decrease in thickness of 2.5 mm over the life of the platform.

The process of applying the wave load and current to the offshore structure is illustrated in Fig. 3.13, as described in API RP2A.

The horizontal members in the wave zone should be designed for wave slam forces, in accordance with API RP2A. Bending stresses due to both horizontal and vertical slam forces should be investigated. However, the current velocity components should not be included in the wave kinematics when calculating wave slam loading. For X braces, members are assumed to span the full length. Member lengths are reduced to account for the jacket leg ratio. Wave slam calculations are carried out during detailed design, not basic design.

The static structure analysis for the offshore structure is the same as in normal structures, because the software uses the stiffness matrix to calculate the deflection and then the internal forces and stresses on each member. However, for offshore structures, the problem is the interaction between the structure and the piles, as the structure will be elastic and the piles will be inelastic. Therefore the structure analysis steps are:

1. Set-up of the geometrics of the jacket with material specifications and preliminary member sections with the dimensions. The software calculates the stiffness matrix for the jacket excluding the piles.
2. Apply the loads on the structure jacket with different load cases, but the software cannot be run because there are no supports applied to the structure system
3. Order the nodes that reflect the degree of freedom in K, F so that the nodes p that will connect the piles are together at the end of the stiffness matrix and follow the nodes j that are slowly connected to jacket members. The stiffness matrix and force vector can be:

$$\begin{bmatrix} j_1 & j_2 & p_1 & p_2 \\ & & & \\ & & & \\ k_{jj} & & k_{jp} & \\ k_{pj} & & k_{pp} & \end{bmatrix} \begin{Bmatrix} \delta_j \\ \\ \\ \delta_p \end{Bmatrix} = \begin{Bmatrix} F_j \\ \\ \\ F_p \end{Bmatrix} \tag{3.1}$$

4. In order to analyze foundation behavior, the stiffness of the jacket and loading on the jacket as felt by the piles are required. Detailed behavior of the jacket is not required at this stage, as an equation of form $K_s\delta_p = F_s$ is wanted, where K_s and F_s represent the stiffness and applied forces on the structure as seen at the pile connecting nodes p.
5. Form the model of the foundation by developing the stiffness matrix for the foundation at zero deflection.
6. Assume no load is applied directly to the piles and the only load is applied through the structure. The foundation forcing vector contains the element from the forces on the structure but located in the appropriate positions for the same degree of freedom in the foundation stiffness matrix.
7. Add the foundation and the jacket substructure and solve, then recalculate the piles foundation stiffness and displacement, as the first nodal displacement along the pile and at connection to the jacket is only the first estimate because it has been based on step 5 in which the stiffness of $p-y$ and $t-z$ curves at zero deflection. Note that once the pile deflections have been estimated, a better estimate of $p-y$ and $t-z$ stiffness can be made. The model of the foundation is shown in Fig. 3.14. The stiffness may be represented by

either a secant or tangent stiffness. Note that the secant stiffness method is generally slower but more stable than the tangent stiffness approach.

8. Repeat the sequence from step 5 until the stiffnesses have converged; then the nodal deflections can be used to determine the forces, shears, and moment in the piles.
9. The deflections at the link to the jacket are also known now. They can be applied as prescribed deflection to the pile nodes on the original jacket model for step 2.
10. Given the jacket deflections, the jacket member forces are calculated from separate member stiffness properties.

Fig. 3.15 illustrates the global structure analysis procedure in a flowchart.

3.5.2 The loads on piles

The loads on the piles are calculated by the software but preliminary calculation can be done by hand. The method shown in Fig. 3.16 presents the calculation parameters.

Another way to obtain the pile load is by obtaining the overturning moment value at the mud line.

The calculation of the reaction force at each pile in the jacket plan at the mudline is as shown in Fig. 3.17, where M is the total overturning moment, d_x and d_y are the distances in x and y directions from the natural axis, respectively, and θ is the axis wave angle.

It is assumed that the base is rigid. The resultant force at each pile is calculated by assuming that M is constant with different wave angle θ.

$$R = \frac{M_x d_y}{\sum A d_y^2} + \frac{M_y d_x}{\sum A d_x^2}$$

where R = vertical pile reaction; M = total overturning moment; A = relative axial pile stiffness; D_{xy} = distance from neutral; θ = axis wave angle.

3.5.3 Modeling techniques

The following is a guideline and recommendations for using software in modeling any steel structure and specifically an offshore platform structure.

As a guide, the global axis system should be orientated as noted below. The origin should be at the center of the platform or structure at chart datum, mean sea level (MSL) or mud line, as determined by the project.

- x-axis points toward platform east;
- y-axis points toward platform north;
- z-axis points vertically upward.

Note that the axes conventions may differ for each project.

Joint numbers are assigned by the engineer. Allowing the program to automatically assign joint numbers should not be permitted. It is important to follow a strict

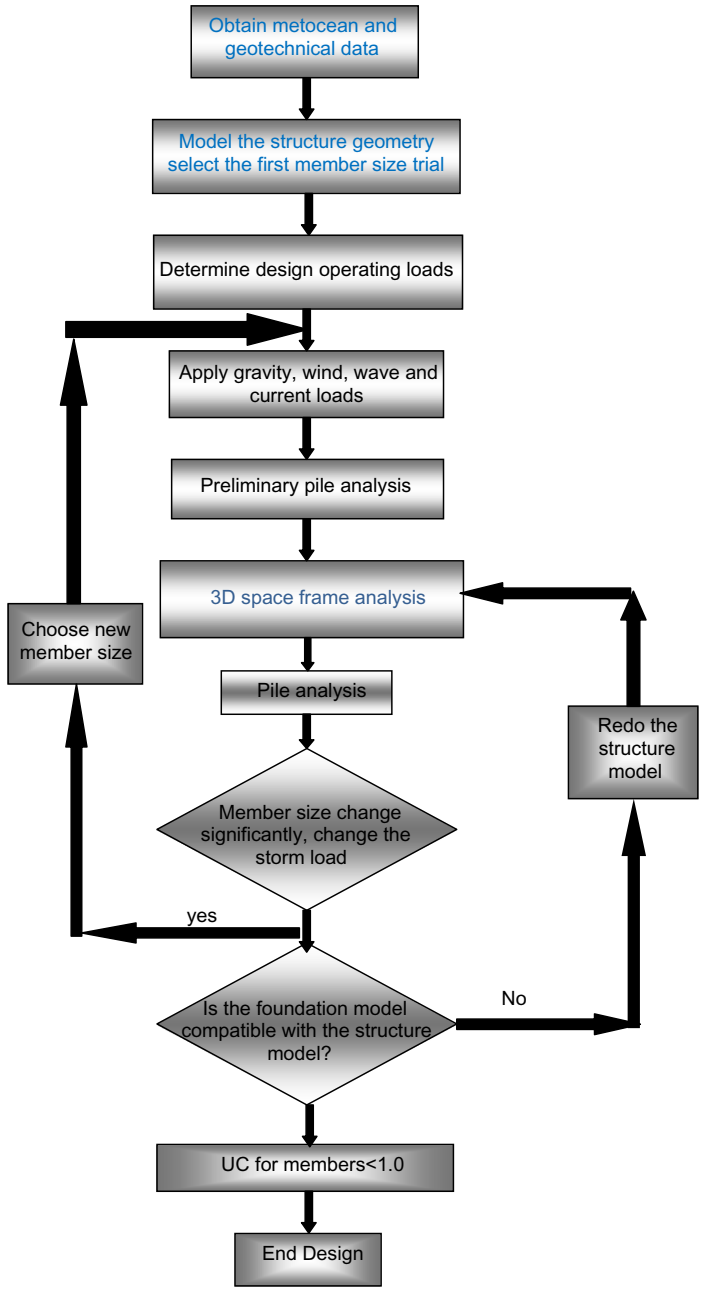

Figure 3.15 Fixed offshore platform design procedure.

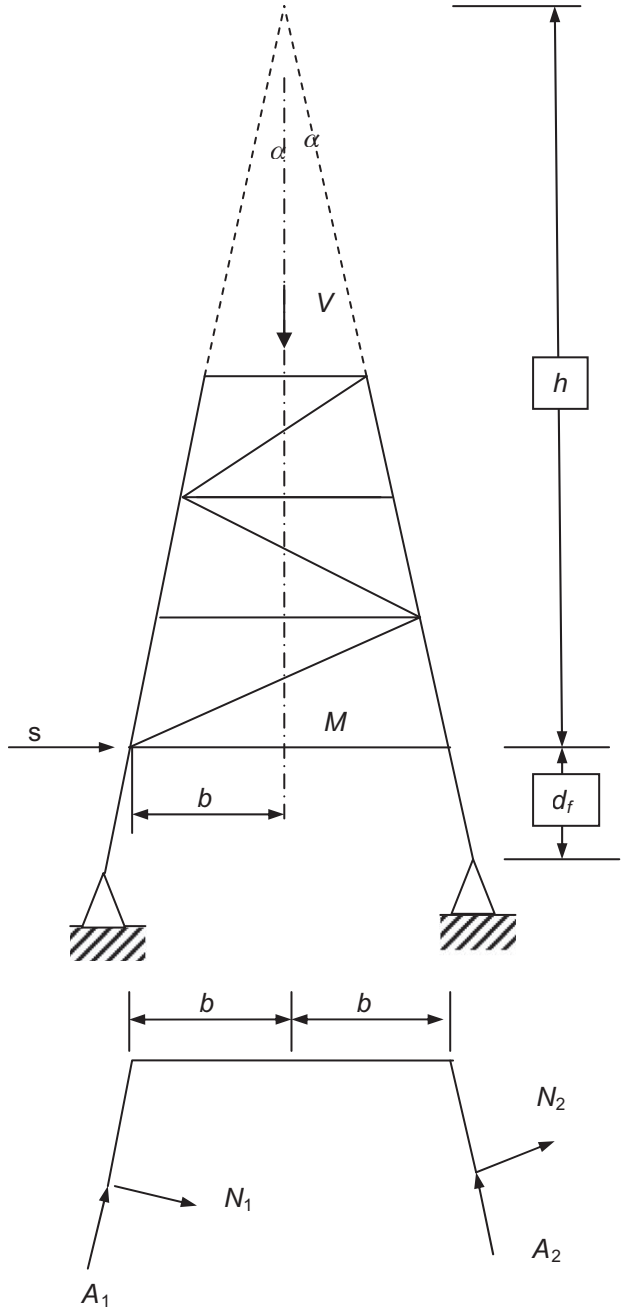

Figure 3.16 Calculation of loads on piles.

numbering system when creating or editing a model. This allows easier interpretation and use of the analysis results. An example of modeling is shown in Fig. 3.18.

Joint coordinates

To facilitate the checking process when using software, the joint coordinates are always input and presented using a single set of units (i.e., m or ft.). Take care to avoid using dual units (m/cm or ft./in), which is the usual mistake. Fig. 3.19 presents the structure geometry with node, tubular element, and pile modeling.

Offshore structure fixed platforms usually have a sliding connection between the structure element that should be considered in the modeling, and the two most common cases are:

- Jacket piles are welded off at the top of the jacket and guided within the legs by spacers, as shown in Fig. 3.20;
- Conductors are restrained horizontally but not vertically by conductor frames, as shown in Fig. 3.21.

The boundary conditions should be clearly defined and should reflect the actual support conditions for the structure.

Any model should generally consist of all primary framing members. Secondary members need not be explicitly modeled unless they facilitate the input of loads or contribute to the structural action of a primary member.

Primary and secondary steelwork is defined as:

- Topside primary steel includes all truss members, girders, and horizontal bracing;
- Jacket primary steel includes legs, diagonal bracing, horizontal bracing, and piles;
- Topside major secondary steel includes deck plate, grating, deck beams, walkways, stairs, and the crane pedestal;
- Jacket major secondary steel includes cathodic protection, boat landing, barge bumpers, walkways, appurtenance supports, and mudmats.

◀

$$N = \frac{(M - sh)\cos\alpha}{2(h + d_f)}$$

$$A_1 = \frac{1}{2}\left(\frac{V}{\cos\alpha} - \left(s + \frac{(M - sh)\cos^2\alpha}{h + d_f}\right)\frac{1}{\sin\alpha}\right) \tag{3.2}$$

$$A_2 = \frac{1}{2}\left(\frac{V}{\cos\alpha} + \left(s + \frac{(M - sh)\cos^2\alpha}{h + d_f}\right)\frac{1}{\sin\alpha}\right) \tag{3.3}$$

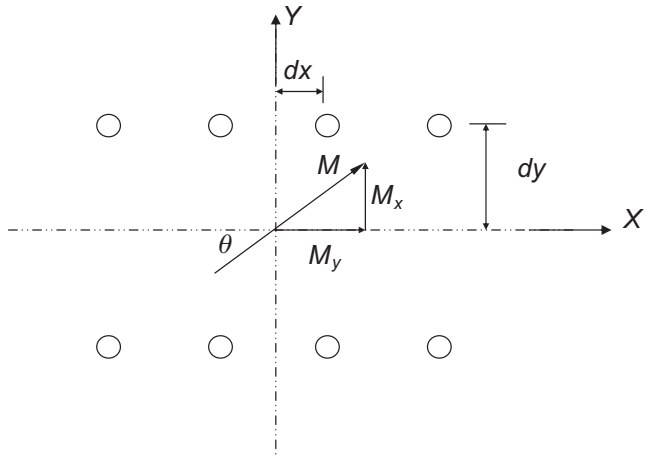

Figure 3.17 Jacket plan at mud line.

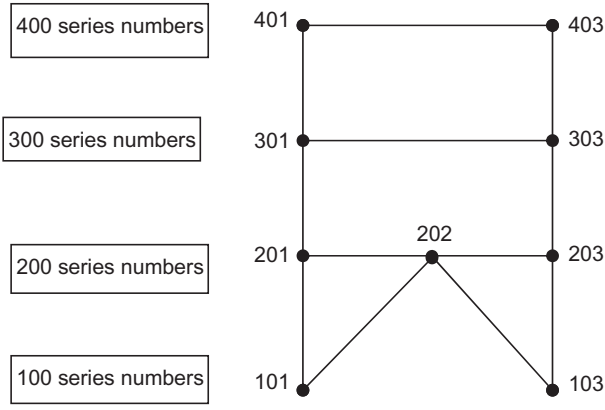

Figure 3.18 Nodes modeling consequence to enhance quality assurance.

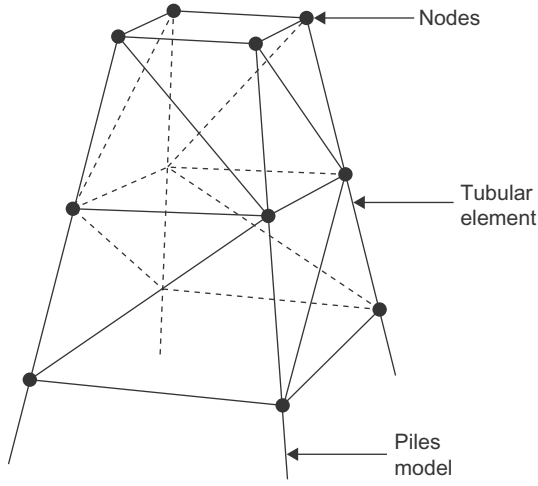

Figure 3.19 Modeling for the jacket structure.

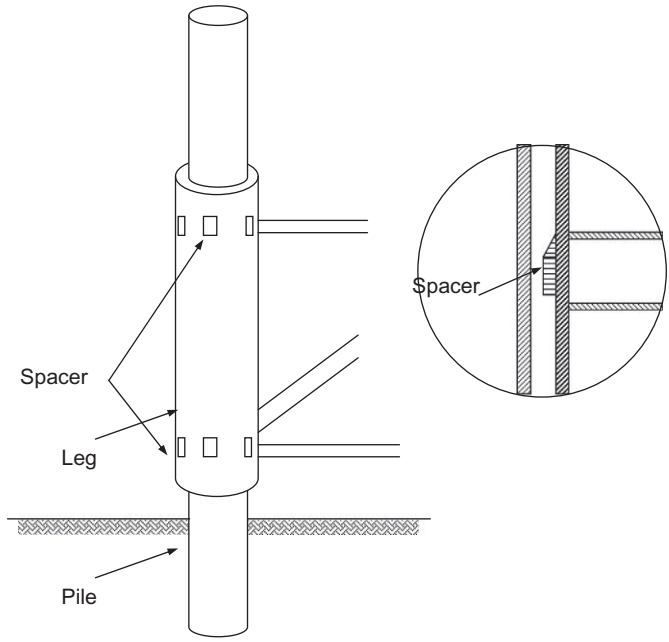

Figure 3.20 Spacer between legs and piles.

Figure 3.21 Conductor guides.

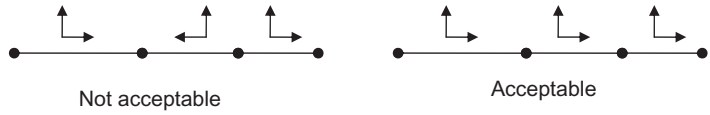

Figure 3.22 Local axis technique.

Local member axes

When constructing the model and running the software, the engineer should review and appreciate the program's default member axis system and adopt this system where possible. In addition, the default local member axis system should be taken into consideration with vertical members (especially I-beams and channels), because it will affect the orientation of the flanges.

The orientation of the members should follow a consistent format, as shown in Fig. 3.22. That is, all like members should be oriented in the same direction.

Member-end releases should be clearly defined and should reflect the actual connection constraints for the member.

In most cases, the member-end offsets may be used where there are large joint thicknesses. The offset should extend only to the face of the joint.

Member effective lengths

The effective length of a member under axial compression should reflect the relative joint stiffnesses at the end of the member. The appropriate effective length factor K should be selected from the recommended values in the design codes. Consideration should be given to the constraining effect provided by intermediate members along the length of the member; the effective length of a member buckling about its $y-y$-axis is often different from the effective length about the $z-z$-axis.

The compression flange (or critical flange) of a member may buckle under bending lateral torsional buckling. The effective length of a member under bending should reflect the degree of torsional restraint offered by the end connections of the member and by intermediate members along the length of the member. The bending effective length of a member should be calculated using the appropriate factors given in the design codes.

Joint eccentricities

Eccentric joints in jacket structures should be modeled using member-end offsets. For topside type structures, joint eccentricities should be modeled using discrete elements, thereby allowing easy extraction of joint forces from the output.

When required, the deck plate should be modeled as a structural element using it as a membrane plate. Note that the plate elements need not be offset.

Alternatively, pinned-end axial brace members may used in lieu of plate elements.

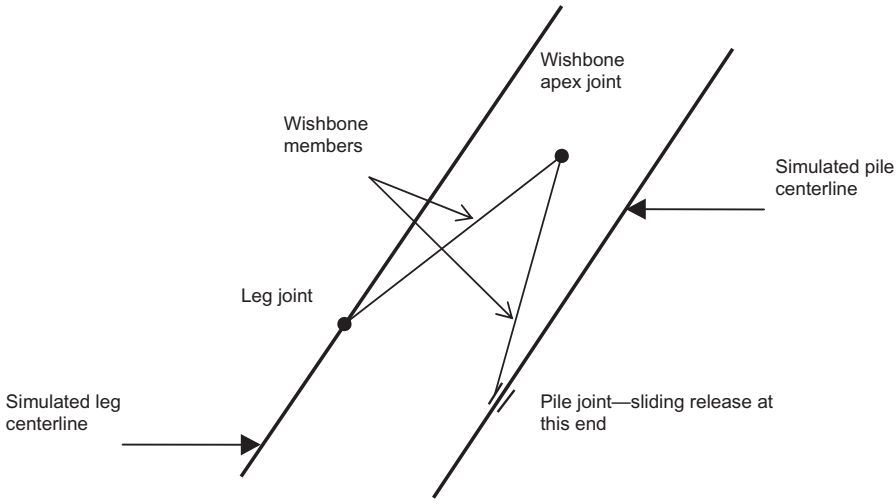

Figure 3.23 Pile-to-leg annulus modeling.

A problem the structural engineer always faces is how to model the pile inside the leg. Most software provides a wishbone member that should be modeled at all horizontal bracing levels of the jacket to account for pile-to-jacket leg interaction, as shown in Fig. 3.23. If the pile-to-jacket leg annulus is to be grouted, then a rigid connection between the pile and leg should be modeled.

Generally, appurtenances do not contribute to the structural stiffness of the primary structure. Appurtenances may be modeled to facilitate automatic load generation by the program and are sometimes referred to as nonstructural members. Appurtenances may be modeled by assigning a small modulus of elasticity or small stiffness properties to these members. It is important to ensure any member-end releases, etc., accurately reflect the actual support conditions for the appurtenance and that no spurious forces enter the structure due to poor modeling techniques. When using this modeling method, the engineer should verify the analysis and ensure there are no compatibility problems caused by the small stiffnesses.

3.5.4 Dynamic structure analysis

As the platform is a unique and high cost structure so dynamic analysis is important to be done and also for harsh environmental conditions at many deep-water sites that cannot be adequately modeled by static analysis. Software for dynamic analysis is now available so the process has become easier. The equation of motion is:

$$M\ddot{x} + C\dot{x} + kx = P(\dot{x}, \ddot{x}) \tag{3.4}$$

where M is the diagonal matrix of virtual mass; C is the matrix for structural and viscous damping; K is the square linear structure stiffness matrix; $P(\dot{x}, \ddot{x})$ is the load vector where $\dot{x}$ and $\ddot{x}$ are the water velocity and acceleration, respectively; and $\ddot{x}$ is the structural acceleration; $\dot{x}$ is the velocity; and x is the displacement.

Natural frequency

The first step in the dynamic analysis is to calculate the natural frequency of the structure.

In general, there are two methods for calculating the natural frequency of linear single-degree-of-freedom structural models: the Rayleigh method, which is based on the energy principle, and the direct method, which is based on the equation of motion, and the latter method is illustrated here.

The direct method of obtaining the natural frequency of a single-degree-of-freedom structure is to use its equation of motion. The structure's natural frequency, ω_o, is defined as the frequency compatible with an undamped structure of constant mass, with a restraint force that varies linearly with the displacement coordinate, and with no external excitation force. Under these conditions, the governing equation of motion, written in terms of the displacement coordinate x, is:

$$m\ddot{x} + kx = 0 \tag{3.5}$$

A special case of Eq. (3.5) occurs when the applied force is zero and there is no damping; this is called a simple harmonic motion.

$$x = x_o \sin\omega_n t \tag{3.6}$$

Substituting Eq. (3.2) and its second derivative into Eq. (3.5) results in:

$$(-m\omega_n{}^2 + k)x_o \sin\omega_n t = 0$$

However, the term sin $\omega_n t$ is not zero for all time t and thus the term in brackets must be zero. This leads to the following equation for the natural frequency of the structure:

$$\omega_n = \sqrt{\frac{k}{m}} \tag{3.7}$$

where ω_n is the natural frequency in rad/s.

The natural period T and the natural frequency f are calculated from:

$$T = 2\pi/\omega = 2\pi\sqrt{\frac{M}{k}}\ \text{s} \tag{3.8}$$

$$f = 1/T = 1/2\pi\sqrt{\frac{k}{M}}\ \text{cycle}/s\ (\text{Hz}) \tag{3.9}$$

In multiple-degree-of-freedom systems, as in the case of the structure in general and the fixed offshore structure shown in Fig. 3.24, every level of the structure has

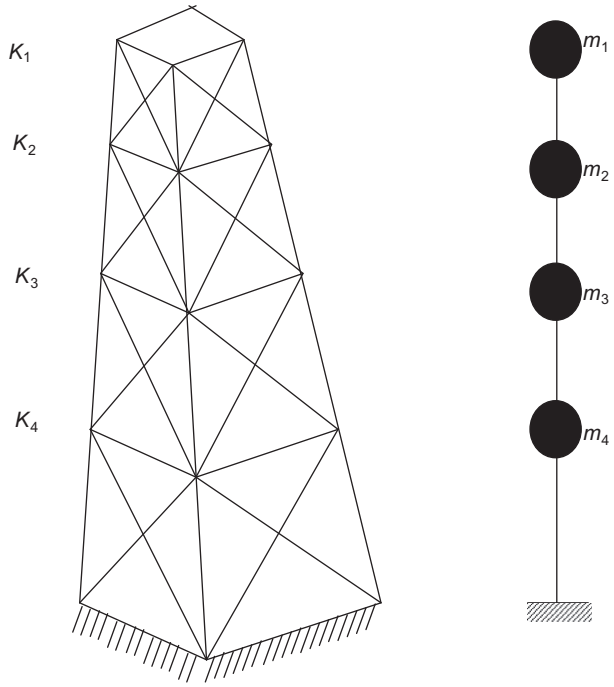

Figure 3.24 Mass distribution for the jacket.

its own mass and stiffness. So the values of the mass, stiffness, displacement, and acceleration will be represented in matrix form as:

$$[M]\{\ddot{X}\} + [k]\{x\} = 0 \tag{3.10}$$

$$\{x\} = (A\sin\omega t + B\cos\omega t)\{\phi\} \tag{3.11}$$

where ϕ is the vibration shape.

$$\{\ddot{x}\} = -\omega^2(A\sin\omega t + B\cos\omega t)\{\phi\} \tag{3.12}$$

$$[k]\{x\} = \omega^2[M]\{x\} \tag{3.13}$$

Eq. (3.10) is the standard eigenvalue problem, which may be solved by the natural frequency and natural modes.

The dynamic analysis will provide the time history for the following:

1. member-end forces;
2. joint displacement;
3. maximum values of joint displacement;
4. base shear time;

5. overturning moment time;
6. axial pile loads.

The simple harmonic motion with mass and stiffness is shown in Fig. 3.24.

$$\begin{bmatrix} m_1 & 0 & 0 & 0 \\ 0 & m_2 & 0 & 0 \\ 0 & 0 & m_3 & 0 \\ 0 & 0 & 0 & m_4 \end{bmatrix} \begin{Bmatrix} \ddot{x}_1 \\ \ddot{x}_2 \\ \ddot{x}_3 \\ \ddot{x}_4 \end{Bmatrix} + \begin{bmatrix} K_{11} & K_{12} & K_{13} & K_{14} \\ K_{21} & K_{22} & K_{23} & K_{24} \\ K_{31} & K_{32} & K_{33} & K_{34} \\ K_{41} & K_{42} & K_{43} & K_{44} \end{bmatrix} \begin{Bmatrix} x_1 \\ x_2 \\ x_3 \\ x_4 \end{Bmatrix} = \begin{Bmatrix} 0 \\ 0 \\ 0 \\ 0 \end{Bmatrix} \tag{3.14}$$

Fig. 3.25 presents the movement of point X_1 at applied unit load at this point and its effect at all nodes.

The modes will be as shown above, but in the space structure as in the jacket structure analysis there are modes of direction of displacement, as shown in Fig. 3.26.

The analysis can be done by mode supposition: the total response can be obtained by adding the individual modes, as presented for the four-level structure shown in Fig. 3.27.

The total procedure may be summarized as:

1. Calculate the natural frequency (ω_n) and mode shapes (ϕ_n);
2. Calculate generalized masses for each mode

$$M_m = \{\phi_m\}^T [M] \{\phi_m\} \tag{3.16}$$

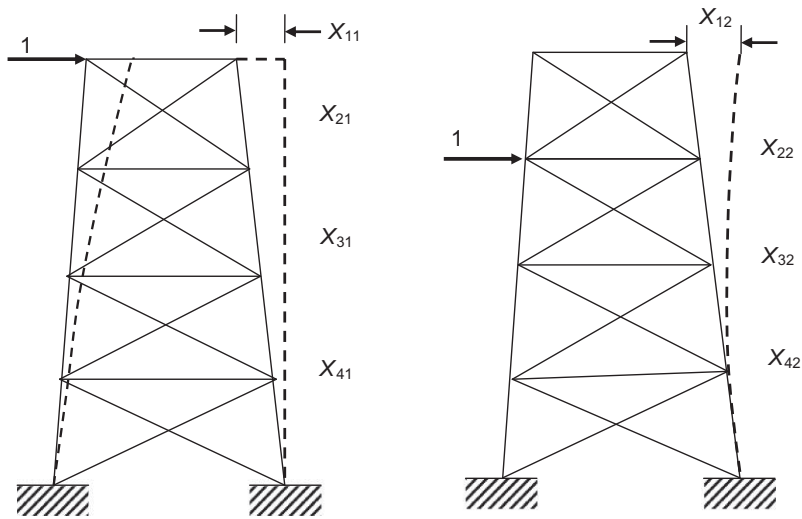

Figure 3.25 Relation between applied unit load at each level and deflection.

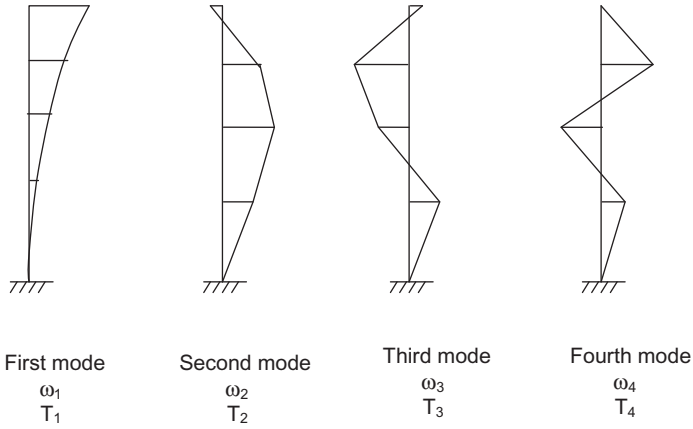

Figure 3.26 Modes of deformation.

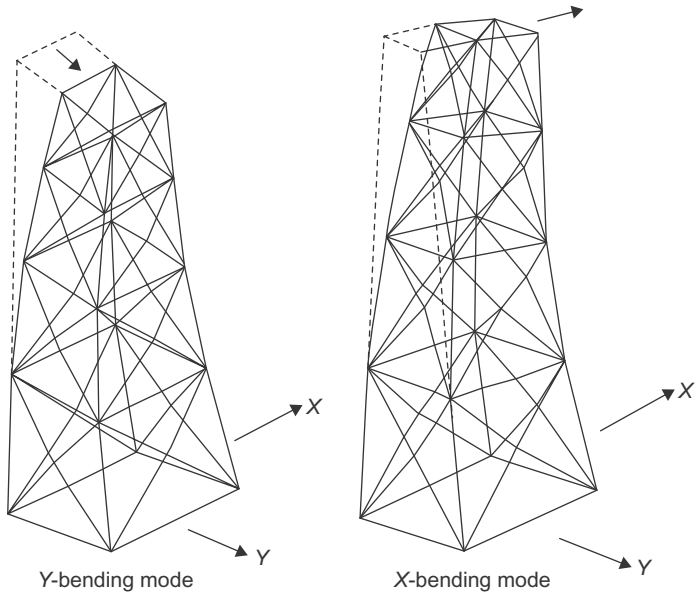

Figure 3.27 Modes of deflection.

$$\begin{Bmatrix} X_1 \\ X_2 \\ X_3 \\ X_4 \end{Bmatrix} = \{\phi_1\}x_1 + \{\phi_2\}x_2 + \{\phi_3\}x_3 \tag{3.15}$$

3. Calculate generalized stiffness for each mode

$$K_m = \{\phi_m\}^T [K] \{\phi_m\} \tag{3.17}$$

4. Calculate generalized force for each mode

$$P_m = \{\phi_m\}^T \{P(t)\} \tag{3.18}$$

5. Calculate the response for each mode from the following equation:

$$M_m \ddot{X} + K_m = P_m(t) \tag{3.19}$$

6. The equations for step 5 are:

$$\ddot{X}_1 + \omega_1^2 X_1 = P_m/M_m \quad X_1(t) = \frac{P_m}{M_m \omega^2}(1 - \cos\omega_1 t) \tag{3.20}$$

$$\ddot{X}2 + \omega_2^2 X_2 = P_m/M_m \quad X_2(t) = \frac{P_m}{M_m \omega^2}(1 - \cos\omega_2 t) \tag{3.21}$$

$$\ddot{X}_3 + \omega_3^2 X_3 = P_m/M_m \quad X_3(t) = \frac{P_m}{M_m \omega^2}(1 - \cos\omega_3 t) \tag{3.22}$$

$$\ddot{X}_4 + \omega_4^2 X_4 = P_m/M_m \quad X_4(t) = \frac{P_m}{M_m \omega^2}(1 - \cos\omega_4 t) \tag{3.23}$$

$$\begin{Bmatrix} X_1 \\ X_2 \\ X_3 \\ X_4 \end{Bmatrix} = \{\phi_1\} X_1(t) + \{\phi_2\} X_2(t) + \{\phi_3\} X_3(t) + \{\phi_4\} X_4(t) \tag{3.24}$$

Using the above equation, we can define the values of drift with time for each floor.

3.5.5 In-place analysis according to ISO 19902

To perform in-place analysis of the LRFD according to ISO 19902, the general equation for determining the design load (action) (F_d) for in-place situations is:

$$\begin{aligned} F_\mathrm{d} = {} & g_{f,G_1} G_1 + g_{f,G_2} G_2 + g_{f,Q_1} Q_1 + g_{f,Q_2} Q_2 + g_{f,E_\mathrm{o}}(E_\mathrm{o} + g_{f,D} D_\mathrm{o}) \\ & + g_{f,E_\mathrm{e}}(E_\mathrm{e} + g_{f,D} D_\mathrm{e}) \end{aligned} \tag{3.25}$$

where G_1 and G_2 are the permanent loads; Q_1 and Q_2 are the variable loads; E_o is the environmental load, which is defined by the owner as the operating wind, wave,

Table 3.1 Partial load factors for in-place situations.

Design situation	Partial load factors[a]					
	$\gamma_{f,G1}$	$\gamma_{f,G2}$	γ_{f,Q_1}	γ_{f,Q_2}	γ_{f,E_o}	γ_{f,E_e}
Permanent and variable actions only	1.3	1.3	1.5		0.0	0.0
Operating situation with corresponding wind, wave, and/or current conditions[b]	1.3	1.3	1.5	1.5	$0.9\gamma_{f,E}$	0.0
Extreme conditions when the action effects due to permanent and variable actions are additive[c]	1.1	1.1	1.1		0.0	
Extreme conditions when the action effects due to permanent and variable actions are opposed[d]	0.9	0.9	0.8	0.0	0.0	$\gamma_{f,E}$

[a]A value of 0 for a partial action factor means that the action is not applicable to the design situation.
[b]For this check G_2, Q_1, and Q_2 are the maximum values for each mode of operation.
[c]For this check G_1, G_2, and Q_1 include those parts of each mode of operation that can reasonably be present during extreme conditions.
[d]For this check G_2 and Q_1 exclude any parts associated with the mode of operation considered that cannot be guaranteed to be present during extreme conditions.

and current parameters; D_o is the equivalent quasi-static action representing dynamic response, but caused by the wave condition that corresponds with that for E_o; E_e is the extreme quasi-static action due to wind, waves, and current; D_e is the equivalent quasi-static action representing dynamic response; and $\gamma_{f,G_1}, \gamma_{f,G_2}, \gamma_{f,Q_1}$, and γ_{f,Q_2} are the partial load (action) factors for the various permanent and variable actions and for which values for different design situations are given in Table 3.1.

On the other hand, $\gamma_{f,E}$ and $\gamma_{f,D}$ are the partial action factors for the environmental actions and for which appropriate values should be defined by the owner through the statement of requirement document (SOR), γ_{f,E_o} and γ_{f,E_e} are partial action factors applied to the total quasi-static environmental action plus equivalent quasi-static action representing dynamic response for operating and extreme environmental conditions, respectively, and for which values for different design situations are given in Table 3.1.

3.6 Cylinder member strength

Traditionally, the member in the jacket and in some cases for the topside is a cylinder member, so this section focuses on design of the tubular member according to ISO 19902, which is principally concerned with the LRFD approach as in the

AISC. In addition, the strength of the cylinder member is also presented according to API RP2A, which focuses on the working stress design.

3.6.1 Cylinder member strength calculation according to ISO 19902

According to ISO 19902, tubular members subjected independently to axial tension, axial compression, bending, shear, or hydrostatic pressure should be designed to satisfy certain strength and stability requirements.

Axial tension

Tubular members subjected to axial tensile forces should be designed to satisfy the condition:

$$f_t \leq \frac{F_t}{\gamma_{R,t}}$$

where f_t is the axial tensile stress due to forces from factored actions; F_t is the representative axial tensile strength, $F_t = F_y$, and F_y is the representative yield strength, in stress units; and $\gamma_{R,t}$ is the partial resistance factor for axial tensile strength, $\gamma_{R,t} = 1.05$.

The member unity check UC under axial tension is calculated from:

$$UC = \frac{f_t}{F_t/\gamma_{R,t}} \tag{3.26}$$

Axial compression

Tubular members subjected to axial compressive forces should be designed to satisfy the following condition:

$$f_c \leq \frac{F_c}{\gamma_{R,c}} \tag{3.27}$$

where f_c is the axial compressive stress due to forces from factored actions; F_c is the representative axial compressive strength, in stress units; and $\gamma_{R,c}$ is the partial resistance factor for axial compressive strength, $\gamma_{R,c} = 1.18$.

The member unity check UC under axial compression should be calculated from Eq. (3.28):

$$UC = \frac{f_c}{F_C/\gamma_{R,c}} \tag{3.28}$$

Column buckling

In the absence of hydrostatic pressure, the representative axial compressive strength for tubular members should be the smaller of the in-plane and out-of-plane buckling strengths determined from the following equations:

$$F_c = \left[1.0 - 0.278\lambda^2\right] F_{yc} \quad \text{for} \quad \lambda \leq 1.34 \tag{3.29}$$

$$F_c = \frac{0.9}{\lambda^2} F_{yc} \quad \text{for} \quad \lambda > 1.34 \tag{3.30}$$

where

$$\lambda = \sqrt{\frac{F_{yc}}{F_e}} = \frac{KL}{\pi r}\sqrt{\frac{F_{yc}}{E}} \tag{3.31}$$

where F_c is the representative axial compressive strength, in stress units; F_{yc} is the representative local buckling strength, in stress units; λ is the column slenderness parameter; F_e is the smaller of the Euler buckling strengths in the y- and z-direction, in stress units; E is Young's modulus of elasticity; K is the effective length factor; L is the unbraced length in the y- or z-direction; r is the radius of gyration $r = \sqrt{\frac{I}{A}}$; I is the moment of inertia of the cross-section; and A is the cross-sectional area.

Local buckling

The representative local buckling strength, F_{yc}, should be calculated from the following equations:

$$F_{yc} = F_y \quad \text{for } F_y/F_{xe} \leq 0.170 \tag{3.32}$$

$$F_{yc} = \left[1.047 - 0.274\frac{F_y}{F_{xe}}\right] F_y \quad \text{for } F_y/F_{xe} > 0.170 \tag{3.33}$$

$$F_{xe} = 2C_x Et/D \tag{3.34}$$

where F_y is the yield strength; F_{xe} is elastic local buckling strength; C_x is the critical elastic buckling coefficient; E is Young's modulus of elasticity; D is the outside diameter; and t is the wall thickness.

The value of C_x is equal to 0.6 in the case of an ideal tubular member; but from a practical point of view during fabrication and erecting as per Chapter 5, Fabrication and installation, there are geometric imperfections within the tolerance limit, the value of C_x shall be equal to 0.3. This reduce value of C_x is also applied in the limits for F_y/F_{xe} given in Eqs. (3.32) and (3.33).

Bending

Tubular members subjected to bending moments should be designed to satisfy the following condition:

$$f_b = \frac{M}{Z_e} \leq \frac{F_b}{\gamma_{R,b}} \tag{3.35}$$

where f_b is the bending stress due to forces from factored actions (when $M > M_y$, f_b is to be considered an equivalent elastic bending stress, M/Z_e); F_b is the representative bending strength, in stress units (see below); $\gamma_{R,b}$ is the partial resistance factor for bending strength, $\gamma_{R,b} = 1.05$; M is the bending moment due to factored actions; M_y is the elastic yield moment; and Z_e is the elastic section modulus:

$$Z_e = \frac{\pi}{64}\left[D^4 - (D-2t)^4\right] / \left(\frac{D}{2}\right)$$

The utilization of a member as described in International Standards Organization (ISO) or unity check U_c, as described in most software, under bending moments should be calculated from:

$$U_c = \frac{f_b}{F_b/\gamma_{R,b}} = \frac{M/Z_e}{F_b/\gamma_{R,b}} \tag{3.36}$$

The representative bending strength for tubular members should be determined from:

$$F_b = \left(\frac{Z_p}{Z_e}\right) F_y \quad \text{for } F_y D/Et \leq 0.0517 \tag{3.37}$$

$$F_b = \left[1.13 - 2.58\left(\frac{F_y D}{Et}\right)\right]\left(\frac{Z_p}{Z_e}\right) F_y \quad \text{for } 0.0517 < F_y D/Et \leq 0.1034 \tag{3.38}$$

$$F_b = \left[0.94 - 0.76\left(\frac{F_y D}{Et}\right)\right]\left(\frac{Z_p}{Z_e}\right) F_y \quad \text{for } 0.1034 < F_y D/Et \leq 120 F_y/E \tag{3.39}$$

where, additionally, F_y is the representative yield strength, in stress units; D is the outside diameter of the member; t is the wall thickness of the member; Z_p is the plastic section modulus, and, calculating from the following equation,

$$Z_p = \frac{1}{6}\left[D^3 - (D-2t)^3\right]$$

Shear

Tubular members subjected to beam shear forces should be designed to satisfy the following condition:

$$f_{v,b} = \frac{2V}{A} \leq \frac{F_v}{\gamma_{R,v}} \tag{3.40}$$

where

$$F_v = F_y/\sqrt{3}$$

and where $f_{v,b}$ is the maximum beam shear stress due to forces from factored actions; F_v is the representative shear strength, in stress units; $\gamma_{R,v}$ is the partial resistance factor for shear strength, $\gamma_{R,v} = 1.05$; V is the beam shear due to factored actions, in force units; and A is the cross-sectional area.

The member unity check U_c under beam shear is calculated from:

$$U_c = \frac{f_{v,b}}{F_v/\gamma_{R,v}} = \frac{2V/A}{F_v/\gamma_{R,v}} \tag{3.41}$$

Torsional shear

Tubular members subjected to torsional shear forces should be designed to satisfy the following condition:

$$f_{v,t} = \frac{M_{v,t}D}{2I_p} \leq \frac{F_v}{\gamma_{R,v}} \tag{3.42}$$

where $f_{v,t}$ is the torsional shear stress due to forces from factored actions; $M_{v,t}$ is the torsional moment due to factored actions; and

$$I_p = \frac{\pi}{32}\left[D^4 - (D-2t)^4\right]$$

where I_p is the polar moment of inertia.

The partial resistance factor for shear, $\gamma_{R,v}$, is the same for both torsional shear and beam shear.

The member unity check U_c under torsional shear should be calculated from:

$$U_C = \frac{M_{v,t}D/2I_p}{F_v/\gamma_{R,v}} \tag{3.43}$$

Hydrostatic pressure

The effective depth at the location being checked should be calculated taking into account the depth of the member below still water level (SWL) and the effect of passing waves. The factored water pressure (p) is calculated from:

$$p = \gamma_{f,G1}\rho H_z \tag{3.44}$$

where $\gamma_{f,G1}$ is the partial action factor for permanent loads, as shown in Table 3.1; ρ is the density of seawater, which may be taken as 1.025 kg/m^3; H_z is the effective hydrostatic head (m)

$$H_z = -z + \frac{H_w}{2}\frac{\cosh[k(d+z)]}{\cosh(kd)} \tag{3.45}$$

where z is the depth of the member relative to SWL which is measured positively upward; d is the water depth from SWL to mudline; H_w is the wave height; k is the wave number = 2 π/λ, and λ is the wave length.

In case of installation, the z value shall be the maximum submergence during launching or it can be considered during the design for an upending case, and $\gamma_{f,G1}$ in Eq. (3.44) should be replaced by $\gamma_{f,T}$, which is equal to 1.1 when permanent and variable actions predominate and equal to 1.35 when the environmental load is predominate, as in transportation and installation calculations.

Hoop buckling

Tubular members subjected to external pressure should be designed to satisfy the following condition:

$$f_h = \frac{pD}{2t} \le \frac{F_h}{\gamma_{R,h}} \tag{3.46}$$

where f_h is the hoop stress due to forces from factored hydrostatic pressure; p is the factored hydrostatic pressure, as calculated from Eq. (3.44); D is the outside diameter of the member; t is the wall thickness of the member; F_h is the representative hoop buckling strength, in stress units; $\gamma_{R,h}$ is the partial resistance factor for hoop buckling strength and $\gamma_{R,h} = 1.25$.

For tubular members satisfying out-of-roundness tolerances, as presented in Chapter 5, Fabrication and installation, F_h should be determined from:

$$F_h = F_y \quad \text{for } F_{he} > 2.44F_y \tag{3.47}$$

$$F_h = 0.7\left(F_{he}/F_y\right)^{0.4}F_y \le F_y \quad \text{for } 0.55\,F_y < F_{he} \le 2.44F_y \tag{3.48}$$

$$F_h = F_{he} \quad \text{for } F_{he} \leq 0.55F_y \tag{3.49}$$

where F_y is the representative yield strength, in stress units, and F_{he} is the elastic hoop buckling strength, in stress units.

The elastic hoop buckling strength (F_{he}) is determined from:

$$F_{he} = 2C_hEt/D \tag{3.50}$$

where the critical elastic hoop buckling coefficient C_h is:

$$C_h = 0.44t/D \quad \text{for } \mu \geq 1.6D/t$$
$$C_h = 0.44t/D + 0.21\left(D/t\right)^3/\text{m}^4 \quad \text{for } 0.825D/t \leq \mu < 1.6D/t$$
$$C_h = 0.737/(\mu - 0.579) \quad \text{for } 1.5 \leq \mu < 0.825D/t$$
$$C_h = 0.80 \quad \text{for } \mu < 1.5$$

where μ is a geometric parameter,

$$\mu = \frac{L_r}{D}\sqrt{\frac{2D}{t}} \tag{3.51}$$

and where L_r is the length of tubular between stiffening rings, diaphragms, or end connections.

For members that violate the allowable tolerance and have out-of-roundness greater than 1% and less than 3%, the reduced value of F_{he} will be:

$$F'_{he} = F_{he}\left(1 - 0.2\sqrt{\frac{D_{\max} - D_{\min}}{0.01D_n}}\right)/0.8 \tag{3.52}$$

where $D_{\max}$ and $D_{\min}$ are the maximum and minimum values of any measured outside diameter at a cross-section and D_n is the nominal diameter.

The unit check UC of a member under external pressure should be calculated from:

$$UC = \frac{pD/2t}{F_h/\gamma_{R,h}} \tag{3.53}$$

Tubular members subjected to combined forces without hydrostatic pressure

In the case of structure members with axial forces and bending moment without hydrostatic pressure special considerations are required.

The $P-\Delta$ effects shall produce a secondary moment effect that is considered in the case of high axial load or in the case that the axial load is applied in a flexible member should be considered but the secondary moment effect can be neglected if it accumulates due to global cations with the bending stresses.

Axial tension and bending

Tubular members subjected to combined axial tension and bending forces should be designed to satisfy the following condition at all cross-sections along their length:

$$\frac{\gamma_{R,t} f_t}{F_t} + \frac{\gamma_{R,b}\sqrt{f_{by}^2 + f_{bz}^2}}{F_b} \leq 1.0 \tag{3.54}$$

where f_{by} is the bending stress about the member's y-axis (in-plane) due to forces from factored actions and f_{bz} is the bending stress about the member's z-axis (out-of-plane) due to forces from factored actions.

Axial compression and bending

Tubular members subjected to combined axial compression and bending forces should be designed to satisfy the following conditions at all cross-sections along their length:

$$\frac{\gamma_{R,c} f_c}{F_c} + \frac{\gamma_{R,b}}{F_b}\sqrt{\left[\left(\frac{C_{m,y} f_{by}}{1-f_c/F_{ey}}\right)^2 + \left(\frac{C_{m,z} f_{bz}}{1-f_c/F_{ez}}\right)^2\right]^2} \leq 1.0 \tag{3.55}$$

and

$$\frac{\gamma_{R,c} f_c}{F_c} + \frac{\gamma_{R,b}\sqrt{f_{by}^2 + f_{bz}^2}}{F_b} \leq 1.0 \tag{3.56}$$

where $C_{m,y}$ and $C_{m,z}$ are the moment reduction factors corresponding to the y- and z-axes, respectively; F_{ey} and F_{ez} are the Euler buckling strengths corresponding to the y- and z-axes respectively, in stress units, such that:

$$F_{e,y} = \frac{\pi^2 E}{(K_y L_y / r_y)^2} \tag{3.57}$$

$$F_{e,z} = \frac{\pi^2 E}{(K_z L_z / r_z)^2} \tag{3.58}$$

where K_y and K_z are the effective length factors for the y- and z-directions, respectively; and L_y and L_z are the unbraced lengths in the y- and z-directions, respectively.

Tubular members subjected to combined forces with hydrostatic pressure

A tubular member below the water line is subjected to hydrostatic pressure unless it has been flooded due to installation procedure requirements. Platform legs are normally flooded in order to assist in their upending and placement and for pile installation. Even where members are flooded in the in-place condition, they can be subjected to hydrostatic pressures during launch and installation. The analysis of the structure can take the axial components of hydrostatic pressure on each member (capped-end actions) into account, or these effects can be included subsequently.

The requirements are presented in terms of axial stresses, which include capped-end forces f_{ac}.

For analyses using factored actions that include capped-end actions, f_{ac} is the axial stress resulting from the analysis. For analyses using factored actions that do not include the capped-end actions:

$$f_{ac} = \left| f_a \pm \gamma_{f,G1} f_q \right| \tag{3.59}$$

where f_a is the axial stress resulting from the analysis without capped-end actions and f_q is the compressive axial stress due to the capped-end hydrostatic actions. f_q should be added to f_a if f_a is compressive and subtracted from f_a if f_a is tensile. Note that the condition for which f_a is tensile and $f_a < \gamma_{f,G1} f_q$ is one of axial compression.

The capped-end stresses (f_q) may be approximated as half the hoop stress due to forces from factored hydrostatic pressure:

$$f_q = \left| 0.5 f_h \right| \tag{3.60}$$

In reality, the magnitude of these stresses depends on the restraint on the member provided by the rest of the structure and its value can be more or less than the value in Eq. (3.60). The approximation $|0.5\ f_h|$ may be replaced by a stress computed from a more rigorous analysis.

In all cases, Eq. (3.46) should be satisfied in addition to the requirements below.

Axial tension, bending, and hydrostatic pressure

Tubular members subjected to combined axial tension, bending, and hydrostatic pressure should be designed to satisfy the following requirements at all cross-sections along their length.

$$\frac{\gamma_{R,t} f_{ac}}{F_{th}} + \frac{\gamma_{R,b} \sqrt{f_{by}^2 + f_{bz}^2}}{F_{b,h}} \leq 1.0 \tag{3.61}$$

where f_{ac} is the tensile axial stress due to forces from factored actions that include capped-end actions ($f_{ac} > 0$) and $F_{t,h}$ is the representative axial tensile strength in the presence of external hydrostatic pressure, in stress units, such that:

$$F_{th} = F_y\left[\sqrt{1 + 0.09B^2 - B^{2\eta}} - 0.3B\right] \tag{3.62}$$

$F_{b,h}$ is the representative bending strength in the presence of external hydrostatic pressure, in stress units, and

$$B = \frac{\gamma_{R,h} f_h}{F_h} \quad B \le 1.0$$

$$\eta = 5 - 4\frac{F_h}{F_y}$$

Axial compression, bending, and hydrostatic pressure

Tubular members subjected to combined axial compression, bending, and hydrostatic pressure should be designed to satisfy the following requirements at all cross-sections along their length.

$$\frac{\gamma_{R,c} f_{ac}}{F_{yc}} + \frac{\gamma_{R,b}\sqrt{f_{by}^2 + f_{bz}^2}}{F_{bh}} \le 1.0 \tag{3.63}$$

If $f_a < 0$, that is, the member is in compression regardless of the capped-end stresses, Eq. (3.64) should also be satisfied.

$$\frac{\gamma_{R,c} f_c}{F_{c,h}} + \frac{\gamma_{R,b}}{F_{bh}}\sqrt{\left[\left(\frac{C_{m,y} f_{by}}{1 - f_c/F_{ey}}\right)^2 + \left(\frac{C_{m,z} f_{bz}}{1 - f_c/F_{ez}}\right)^2\right]} \le 1.0 \tag{3.64}$$

where, additionally, $F_{c,h}$ is the representative axial compressive strength in the presence of external hydrostatic pressure, in stress units.

$$F_{c,h} = 0.5F_{yc}\left[\left(1.0 - 0.278\lambda^2\right) - \frac{2f_q}{F_{yc}} + \sqrt{\left(1.0 - 0.278\lambda^2\right)^2 + 1.12\lambda^2\frac{f_q}{F_{yc}}}\right]$$
$$\text{for } \lambda \le 1.34\sqrt{\left(1 - \frac{2f_q}{F_{yc}}\right)^{-1}} \tag{3.65}$$

$$F_{c,h} = \frac{0.9}{\lambda^2} F_{yc} \quad \text{for } \lambda > 1.34\sqrt{\left(1 - \frac{2f_q}{F_{yc}}\right)^{-1}} \tag{3.66}$$

If the maximum combined compressive stress $f_x = f_b + f_{ac}$ (if $f_{ac} \leq 0$) or $f_x = f_b - f_{ac}$ (if $f_{ac} < 0$) and the elastic local buckling strength F_{xe} exceeds the limits given below, then Eq. (3.68) should also be satisfied.

$$f_x > 0.5\frac{F_{he}}{\gamma_{R,h}} \text{ and } \frac{F_{xe}}{\gamma_{R,c}} > 0.5\frac{F_{he}}{\gamma_{R,h}} \tag{3.67}$$

$$\frac{f_x - 0.5\frac{F_{he}}{\gamma_{R,h}}}{\frac{F_{xe}}{\gamma_{R,c}} - 0.5\frac{F_{he}}{\gamma_{R,h}}} + \left[\frac{\gamma_{R,h} f_h}{F_{he}}\right]^2 \leq 1.0 \tag{3.68}$$

where F_{he} is the elastic hoop buckling strength and F_{xe} is the representative elastic local buckling strength from Eq. (3.34).

Effective lengths and moment reduction factors

The effective lengths and moment reduction factors may be determined using a rational analysis that includes joint flexibility and side-sway. In lieu of such a rational analysis, values of effective length factors (K) and moment reduction factors (C_m) may be taken from Table 3.2. Table 3.2 does not apply to cantilever members, and it is assumed that both member ends are rotationally restrained in both planes of bending (Table 3.3).

From a theoretical point of view the effective length to apply the factor K on it is from centerline to centerline of the joints ends. In the case of the jacket, the leg size is large with respect to the bracing size, so the length shall be taken to the face of the leg and not to the leg centerline. Based on that for diagonal braces the length shall measure from the face of the leg to the other face of the leg. But in the case of a K bracing system it shall be from the leg face to the centerline of end joints of the K bracing.

You can perform more comprehensive analysis when the lower K factors than those of Table 3.2 are utilized. In the case of connecting by more than one member, the buckling factor K can be obtained from the chart alignment in Fig. 3.28.

The subscripts A and R in Fig. 3.28 refer to the joints at the two ends of the column section being considered. G is defined as

$$G = \frac{\sum \frac{I_c}{L_c}}{\sum \frac{I_G}{L_G}} \tag{3.69}$$

in which G is the joint rigidity; I_c is the column moment of inertia; L_c is the column unsupported length; I_G is the girder the moment of inertia; and L_G is the unsupported length of a girder or other restraining member.

Table 3.2 Effective length and moment reduction factors for member strength checking.

Structural component	K	C_m
Topside legs		
Braced	1.0	0.85
Portal (unbraced)	K[b]	0.85
Structure legs and piling		
Grouted composite section	1.0	$C_m = 1.0-0.4 \cdot (f_c/F_e)$, or 0.85, whichever is less
Ungrouted jacket legs	1.0	$C_m = 1.0-0.4 \cdot (f_c/F_e)$, or 0.85, whichever is less
Ungrouted piling between shim points	1.0	$C_m = 0.6-0.4 \cdot M1/M2$
Structure brace members		$C_m = 0.6-0.4 \cdot M1/M2$[a] or $C_m = 1.0 - 0.4 \cdot (f_c/F_e)$, or 0.85, whichever is less
Primary diagonals and horizontals	0.7	$C_m = 1.0 - 0.4 \cdot (f_c/F_e)$, or 0.85, whichever is less
K braces[c]	0.7	
X braces	0.7	
Longer segment length[c]	0.8	
Full length[d]	0.7	
Secondary horizontals	0.7	

[a] $M1/M2$ is the ratio of smaller to larger moments at the ends of the unfaced portion of the member in the plane of bending under consideration. $M1/M2$ is positive when the member is bent in reverse curvature, negative when bent in single curvature. $F_e = F_{ey}$ or F_{ez} as appropriate.
[b] Use effective length alignment chart as in Fig. 3.28.
[c] For either in-plane or out-of-plane effective lengths, at least one pair of members framing into a K or X joint should be in tension, if the joint is not braced out of plane.
[d] When all members are in compression and the joint is not braced out of plane.

Considering this, I_c and L_G are calculated about axes perpendicular to the plane of buckling.

3.6.2 Cylinder member strength calculation

The design of the cylinder member in accordance with API is based on AISC ASD.

Axial tension

The allowable tensile stress, F_t, for cylindrical members subjected to axial tensile loads should be determined from:

$$F_t = 0.6F_y \tag{3.70}$$

where F_y is the yield strength, in ksi (MPa).

Table 3.3 K and C_m values based on API RP2A.

Structure element	Effective length factor K	Reduction factor C_m
Superstructure legs		
Braced	1.0	0.85
Portal (unbraced)	K[a]	0.85
Jacket legs and piling		
Grouted composite section	1.0	Min of $\{1 - 0.4(f_a/F_e)\}$ or 0.85
Ungrouted jacket legs	1.0	Min of $\{1 - 0.4(f_a/F_e)\}$ or 0.85
Ungrouted piling between shim points	1.0	$0.6 - 0.4(M1/M2)$, $0.4 < C_m < 0.85$
Deck truss web members		$0.6 - 0.4(M1/M2)$, $0.4 < C_m < 0.85$
In-plane action	0.8	$0.6 - 0.4(M1/M2)$, $0.4 < C_m < 0.85$ or 0.85
Out-of-plane action	1.0	0.85
Jacket braces		$0.6 - 0.4(M1/M2)$, $0.4 < C_m < 0.85$ or Min of $\{1 - 0.4(f_a/F_e)\}$ or 0.85
Face-to-face length of main diagonals	0.8	
Face-of-leg to centerline of joint length of K braces[b]	0.8	Min of $\{1 - 0.4(f_a/F_e)\}$ or 0.85
Longer segment length of X braces[b]	0.9	Min of $\{1 - 0.4(f_a/F_e)\}$ or 0.85
Secondary horizontals	0.7	Min of $\{1 - 0.4(f_a/F_e)\}$ or 0.85
Deck truss chord members	1.0	0.85 or $6 - 0.4(M1/M2)$, $0.4 < C_m < 0.85$ or Min of $\{1 - 0.4(f_a/F_e)\}$ or 0.85

[a]As in Fig. 3.28.
[b]At least one pair of members framing into a joint must be in tension if the joint is not braced out of plane.

Axial compression

The allowable axial compressive stress, F_a, should be determined from the following AISC formulas for members with a D/t ratio equal to or less than 60:

$$F_a = \frac{\left[1 - \frac{(kl/r)^2}{2C_c^2}\right]F_y}{5/3 + \frac{3(kl/r)}{8C_c} - \frac{(kl/r)^3}{8C_c^3}} \quad \text{for } kl/r < C_c \tag{3.71}$$

$$F_a = \frac{12\pi^2 E}{23(kl/r)^2} \quad \text{for } kl/r \geq C_c \tag{3.72}$$

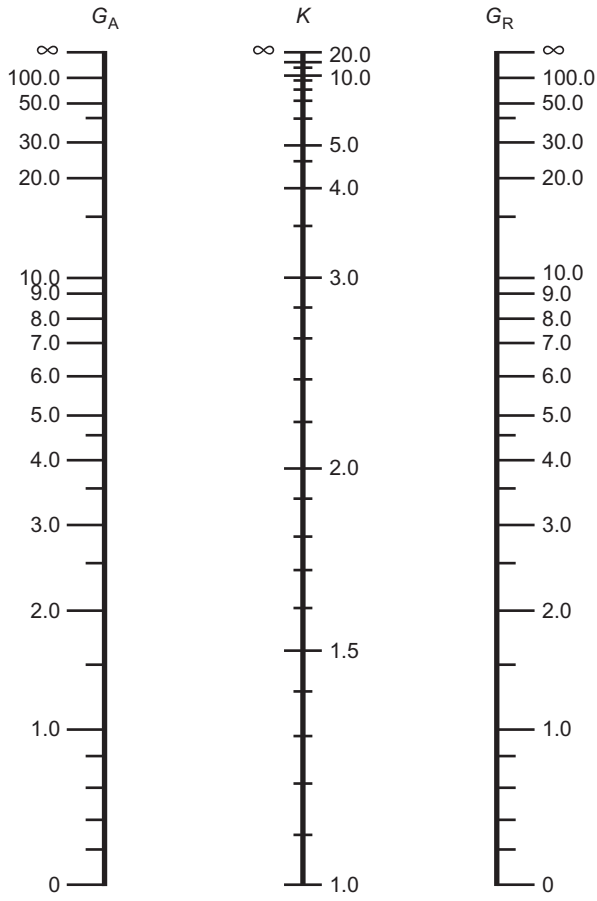

Figure 3.28 Chart alignment.

In this case K and C_m values can be obtained from Table 3.3 for different structural members, where

$$C_c = \sqrt{\frac{2\pi^2 E}{F_y}}$$

E is the Young's modulus of elasticity, in ksi (MPa); K is the effective length factor; l is the unbraced length, m (in); and r is the radius of gyration, m (in).

For members with a D/t ratio greater than 60, substitute the critical local buckling stress (F_{xe} or F_{xc}, whichever is smaller) for F_y in determining C_c and F_a.

Local buckling

If D/t in the range >60 and <300, and wall thickness, t, is more than 6 mm (0.25 inch), then the elastic (F_{xe}) and inelastic local buckling stress (F_{xc}) as a result of

axial compression should be calculated from Eq. (3.83). Overall column buckling should be determined by substituting the critical local buckling stress (F_{xe} or F_{xc}, whichever is smaller) for F_y in Eq. (3.81) and in the equation for C_c.

Elastic local buckling stress

The elastic local buckling stress, F_{xe}, should be determined from Eq. (3.34).

Inelastic local buckling stress

The inelastic local buckling stress, F_{xc}, should be determined from:

$$\begin{aligned} F_{xc} &= F_y\left[1.64 - 0.23\left(D/t\right)^{0.25}\right] \le F_{xe} \\ F_{xc} &= F_y \ \text{ for } \ \left(D/t\right) \le 60 \end{aligned} \tag{3.73}$$

Bending

The allowable bending stress, F_b, should be determined from the following equations:

$$F_b = 0.75\,F_y \ \text{ for } D/t \le 10,340/F_y \text{(SI units)}$$

$$F_b = \left[0.84 - 1.74\frac{F_y D}{Et}\right]F_y \quad \text{for } 10,340/F_y < D/t \le 20,680/F_y \text{ in SI units} \tag{3.74}$$

$$F_b = \left[0.72 - 0.58\frac{F_y D}{Et}\right]F_y \quad \text{for } 20,680/F_y < D/t \le 300 \text{ in SI units} \tag{3.75}$$

For *D/t* ratios greater than 300, refer to API Bulletin 2U.

Shear

The maximum beam shear stress, f_v, for cylindrical members is:

$$f_v = \frac{V}{0.5A} \tag{3.76}$$

where f_v is the maximum shear stress, in MPa (ksi); V is the transverse shear force, MN (kips); and A is the cross-sectional area, m^2 ($inches^2$).

The allowable beam shear stress, F_v, should be determined from:

$$F_v = 0.4F_y \tag{3.77}$$

Torsional shear

The maximum torsional shear stress, f_{vt}, for cylindrical members is:

$$f_{vt} = \frac{M_t(D/2)}{I_p} \tag{3.78}$$

where f_{vt} is the maximum torsional shear stress (in MPa); M_t is the torsional moment, MN-m; and I_p is the polar moment of inertia, in m^4.

The allowable torsional shear stress, F_{vt}, should be determined from Eq. (3.77).

Pressure on stiffened and unstiffened cylinders

For tubular platform members satisfying API Spec 2B out-of-roundness tolerances, the acting membrane stress, f_h, in ksi (MPa), should not exceed the critical hoop buckling stress, F_{hc}, divided by the appropriate safety factor:

$$f_h \leq F_{hc}/SF_h \tag{3.79}$$

$$f_h = pD/2t \tag{3.80}$$

where f_h is the hoop stress due to hydrostatic pressure, in ksi (MPa); p is the hydrostatic pressure, in ksi (MPa); and SF_h is the safety factor against hydrostatic collapse.

Design hydrostatic head

The hydrostatic pressure calculation in API is the same as presented in Eq. (3.55) considering the water depth is measure downward from the SWL with in ft. (m), z.

For considering the installation phase, the z shall be a maximum submerged member during launching and also consider the upending position of the jacket, it is important to consider some increase on the head to overcome the structural tolerance in its weight. Seawater density is equal to 0.01005 MN/m^3 (64 $lbs/ft.^3$).

Hoop buckling stress

The elastic hoop buckling stress, F_{he}, and the critical hoop buckling stress, F_{hc}, are determined from the following formulas.

Elastic hoop buckling stress

The elastic hoop buckling stress determination is based on a linear stress−strain relationship from:

$$F_{he} = 2C_hEt/D \tag{3.81}$$

where the critical hoop buckling coefficient C_h includes the effect of initial geometric imperfections within API Spec 2B tolerance limits.

$$
\begin{aligned}
&C_h = 0.44t/D \quad \text{for } M \geq 1.6D/t \\
&C_h = 0.44t/D + 0.21(D/t)^3/M^4 \quad 0.825D/t \leq M < 1.6D/t \\
&C_h = 0.736/(M - 0.636) \quad 3.5 \leq M < 0.825D/t \\
&C_h = 0.736/(M - 0.559) \quad 1.5 \leq M < 3.5 \\
&C_h = 0.8 \quad M < 1.5
\end{aligned}
$$

The geometric parameter M is defined as:

$$M = \frac{L}{D}\sqrt{\frac{2D}{t}} \tag{3.82}$$

where L is the length between stiffening rings, diaphragms, or end connections, inch (m).

It is worth mentioning that in the case of M being greater than $1.6D/t$, the elastic buckling stress is approximately equal to that for a long unstiffened cylinder. Based on that, stiffening rings spacing shall have a value of M less than $1.6D/t$ to have an effect.

Critical hoop buckling stress

The steel yield strength shall be checked against the hoop buckling stress calculated for elastic or inelastic hoop buckling. The critical hoop buckling stress, F_{hc}, in ksi (MPa), is defined by the following equation:

Elastic buckling:

$$F_{hc} = F_{he} \quad \text{for } F_{he} \leq 0.55F_y$$

Inelastic buckling:

$$
\begin{aligned}
&F_{hc} = 0.45F_y + 0.18 + F_{he} \quad \text{for } 0.55F_y < F_{he} \leq 1.6F_y \\
&F_{hc} = \frac{1.31F_y}{1.15 + (F_y/F_{he})} \quad \text{for } 1.6\,F_y < F_{he} < 6.2F_y \\
&F_{hc} = F_y \quad \text{for } F_{he} > 6.2F_y
\end{aligned}
\tag{3.83}
$$

Combined stresses for cylindrical members

The method of calculating the applied combined stress between bending with compression and tensile stress in addition to the hydrostatic stress is discussed in the following section based on AISC.

Combined axial compression and bending

Cylindrical members subjected to combined compression and flexure should be proportioned to satisfy both the following requirements at all points along their length.

$$\frac{f_a}{F_a} + \frac{C_m\sqrt{f_{bx}^2 + f_{by}^2}}{\left(1 - \frac{f_a}{F_e'}\right)F_b} \leq 1.0 \tag{3.84}$$

$$\frac{f_a}{0.6F_y} + \frac{\sqrt{f_{bx}^2 + f_{by}^2}}{F_b} \leq 1.0 \tag{3.85}$$

where the undefined terms used are as defined by the AISC *Specification for the Design, Fabrication, and Erection of Structural Steel for Buildings.*

When $f_a/F_a \leq 0.15$, the following formula may be used in lieu of the above two formulas.

$$\frac{f_a}{F_y} + \frac{\sqrt{f_{bx}^2 + f_{by}^2}}{F_b} \leq 1.0 \tag{3.86}$$

Eq. (3.84) assumes that the same values of C_m and Fe' are appropriate for f_{bx} and f_{by}. If different values are applicable, the following general formula should be used instead of Eq. (3.84):

$$\frac{f_a}{F_a} + \frac{\sqrt{\left(\frac{C_{mx}f_{bx}}{1-\frac{f_a}{F_{ex}'}}\right)^2 + \left(\frac{C_{my}f_{by}}{1-\frac{f_a}{F_{ey}'}}\right)^2}}{F_b} \leq 1.0 \tag{3.87}$$

Member slenderness

The slenderness of the steel section is defined by (Kl/r) where l is the member length, k is the buckling factor, and r is the radius of gyration which is applied also for cylindrical compression members, and should be in accordance with the AISC. To obtain the buckling factor, the joint on its end should be defined from its fixity and the joint movement. Moreover, a rational definition of the reduction factor should consider the character of the cross-section and the loads acting on the member. In lieu of such an analysis, the following values may be used.

Combined axial tension and bending

Cylindrical members subjected to combined tension and bending should be proportioned to satisfy Eq. (3.85) at all points along their length, where f_{bx} and f_{by} are the computed bending tensile stresses.

Axial tension and hydrostatic pressure

The hydrostatic pressure is usually apply on the member and the sea mean level. Therefore the following interaction equation applies in the case of the member being under longitudinal tensile stresses and hoop compressive stresses at the same time:

$$A^2 + B^2 + 2\nu|A|B \leq 1.0 \tag{3.88}$$

where

$$A = \frac{f_a + f_b - (0.5f_h)}{F_y}(SF_x) \tag{3.89}$$

The term A should reflect the maximum tensile stress combination

$$B = f_h / F_{hc}(SF_h) \tag{3.90}$$

ν is the Poisson's ratio = 0.3; F_y is the yield strength, in ksi (MPa); f_a is the absolute value of acting axial stress, in ksi (MPa); f_b is the absolute value of acting resultant bending stress, in ksi (MPa); f_h is the absolute value of hoop compression stress, in ksi (MPa); F_{hc} is the critical hoop stress; SF_x is the safety factor for axial tension; and SF_h is the safety factor for hoop compression.

Axial compression and hydrostatic pressure

The following interaction equation applies in the case of the member being under longitudinal compression tensile stresses and hoop compressive stresses at the same time:

$$\frac{f_a + (0.5f_h)}{F_{xc}}(SF_x) + \frac{f_b}{F_y}(SF_b) \leq 1.0 \tag{3.91}$$

$$SF_h \frac{f_h}{F_{hc}} \leq 1.0 \tag{3.92}$$

Eq. (3.91) should reflect the maximum compressive stress combination.
The following equation should also be satisfied when $f_x > 0.5F_{ha}$.

$$\frac{f_x - 0.5F_{ha}}{F_{aa} - 0.5F_{ha}} + \left(\frac{f_h}{F_{ha}}\right)^2 \leq 1.0 \tag{3.93}$$

where F_{aa} is the F_{xe}/SF_x; F_{ha} is the F_{he}/SF_h; SF_x is the safety factor for axial compression; and SF_b is the safety factor for bending. f_x is the $f_a + f_b + (0.5\ f_h)$ and f_x

Table 3.4 Safety factor based on API RP2A.

Design condition	Loading			
	Axial tension	**Bending**	**Axial compression**	**Hoop compression**
Where the basic allowable stresses would be used (e.g., pressures that will definitely be encountered during the installation or life of the structure)	1.67	F_y/F_b	1.67−2.0	2.0
Where the one-third increase in allowable stresses is appropriate (e.g., when considering interaction with storm loads)	1.25	$F_y/1.33F_b$	1.25−1.5	1.5

should reflect the maximum compressive stress combination, where F_{xe}, F_{xc}, F_{he}, and F_{hc} are given by Eqs. (3.34), (3.73), (3.82), and (3.84), respectively.

Note that if $f_b > f_a + 0.5\, f_h$, both Eqs. (3.88) and(3.91) must be satisfied.

Safety factors

To compute allowable stresses, the required safety factors should be used with the local buckling interaction equations presented in Table 3.4.

3.7 Tubular joint design

In older versions of API RP2A, punching shear governed the design of the tubular joints. The historical development of the API RP2A-WSD provisions clarifies the background of the most recent major updates. According to Marshall and Toprac (1974), the third edition of API RP2A-WSD, issued in 1972, presents just a principal's recommendations about the punching shear. The API 4th edition presents some factors to calculate the load in the chord with respect to the ratio (β), which is the brace diameter divided by the chord diameter. In 1977 API published the 9th edition, in this book they present *T/Y*, *X*, and *K* load configuration for the tubular joint and illustrate the corresponding allowable stress equations.

Between 1977 and 1983, much work was done, including large-scale load tests to failure, to improve the understanding and prediction of joint behavior. This work culminated in the 14th edition of API RP2A-WSD, in which the punching shear

stress formulations were considerably modified and included a more realistic expression to account for the effect of chord loads, as well as providing an interaction equation for the combined effect of brace axial and bending stresses. The 14th edition also introduced the alternative nominal load approach, which gives equivalent results to the punching shear method. It is worth mentioning that the guidance remained unchanged for all editions until the 21st, considering that the other recommendation was added for transfer load through the chord in the 20th edition in 1993.

Since the 14th edition of API RP2A-WSD was issued, much further knowledge has been gained on the behavior of joints, including both experimental data and the results of numerical researches. Over the period 1994−1996, MSL Engineering, under the auspices of a joint industry project, undertook an update to the tubular joint database [see the MSL report (1996) and Dier and Lalani (1995)]. The ISO drafting committee started their work from the 1st edition of API RP2A−LRFD, which is similar to the API RP2A−WSD 20th edition. The ISO approach in design is LRFD. However, it is worth mentioning that API provisions have a major modification in the time of issue of ISO drafting as it incorporates the recent researches about tubular joints.

There was a supplement to the 21st edition of API RP2A-WSD, and the updates in this supplement over the principal 21st edition include the relaxation of the {2/3} limit on tensile strength, additional guidance on detailing practice, removal of the punching shear approach, new Q_u and Q_f formulations, and a change in the form of the brace load interaction equation.

The old method for calculating the tubular joint capacity, based on the punching shear that was removed from the new API RP2A (2007), is presented here.

3.7.1 Simple joint calculation API RP2A (2007)

Joint classification and detailing

The first step is to define the joint classification under axial load: the K, X, and Y components of the load correspond to the three joint types for which capacity equations exist. Such a subdivision normally considers all of the members *in one plane* at a joint.

Based on API RP2A (2007), the brace planes within ± 15 degrees of each other may be considered as being in a common plane. Each brace in the plane can have a unique classification that could vary with load condition. Note that the classification can be a mix of the three main joint types, which are *X*, *T* and *K*.

Some simple examples of joint classification are presented in Fig. 3.29.

For a brace to be considered as X joint, the normal force on the brace shall be transferred through the chord member to the opposite side such as the launch rails and padeyes, etc.

In the case of a *K* joint, the normal force applied on the brace will be balanced within 10% by loads from other braces in the same plane. For a *Y* joint, the normal force on the brace members shall be transferred like a beam shear in the chord.

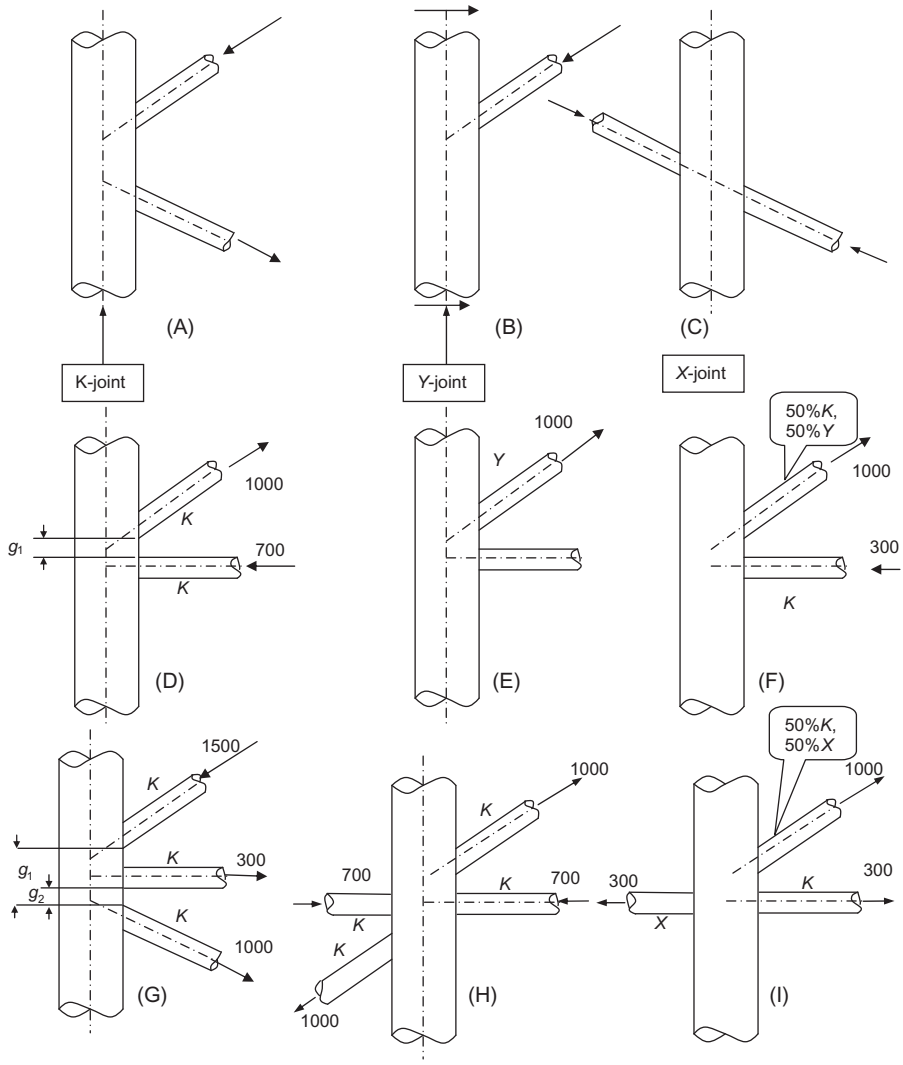

Figure 3.29 Joint classification.

Fig. 3.29 presents the first three cases (A), (B), and (C), which present the main joint classifications *K*, *Y*, and *X*, respectively.

Cases (*d*) and (*g*) present the gap between the adjacent braces, and case (*g*) illustrates the intermediate brace. The gap (g_2) is the gap between the outer loaded braces.

Case (*f*) presents a combination of *K* and *Y* joints and case (*i*) presents a combination of *K* and *X* joints by 50% and the other 50% of the *X* joint will be with the *X* joint for the brace on the left-hand side. For case (*h*), as the forces on the member opposite and the values are equal, all the members are considered a *K* joint.

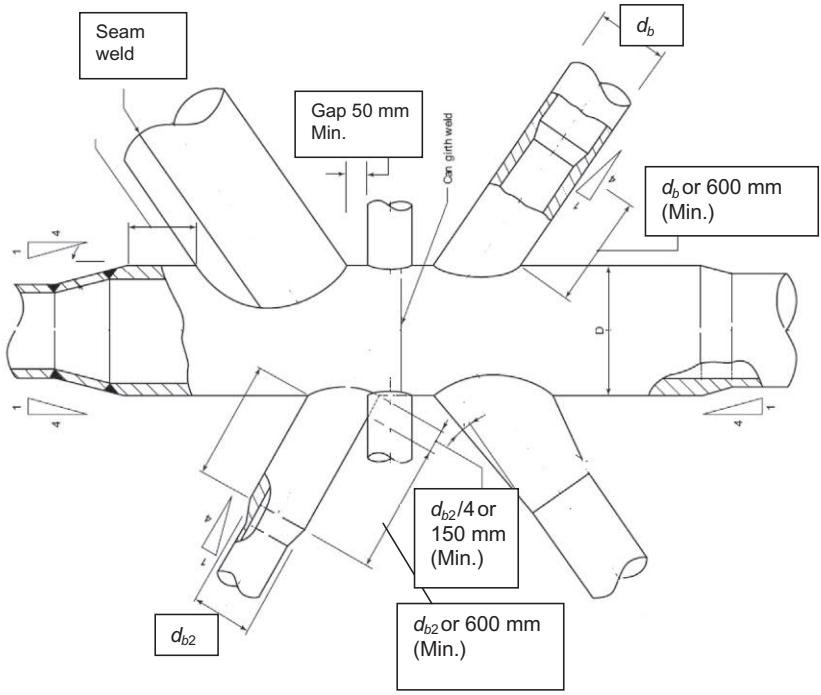

Figure 3.30 In-plane joint detailing.

Joint detailing is an essential element of joint design. For unreinforced joints, the recommended detailing nomenclature and dimensions are shown in Figs. 3.30 and 3.31. It is illustrated that the chord wall thickness may increase, in this case it will extend after the outside edge of the bracing equal or greater than one-fourth of the chord diameter or 300 mm (12 inches). In some cases it can use a special steel type. If increased wall thickness for a brace or special steel is required, it should extend a minimum of one brace diameter or 24 inches (600 mm), whichever is greater. Neither the cited chord can nor the brace stub dimension includes the length over which the 1:4 thicknesses taper occurs. In situations where fatigue has a major effect, tapering on the inside may have the undesirable consequence of fatigue cracking originating on the inside surface, which is difficult to inspect.

The gap between the adjacent bracing has a minimum value of 50 mm (2 inch) in the case of in-plane or out-of-plane and it is important to avoid welds overlapping at the joint toes.

If the welds overlapping cannot be avoided then the overlap length should be greater than a quarter of the bracing diameter (d/4) or 150 mm (6 inches). This dimension shall be measured along the axis of the main member.

In a case of overlapping, the bracing which has the larger wall thickness should be the main member and have a full penetration weld to the chord. The differences

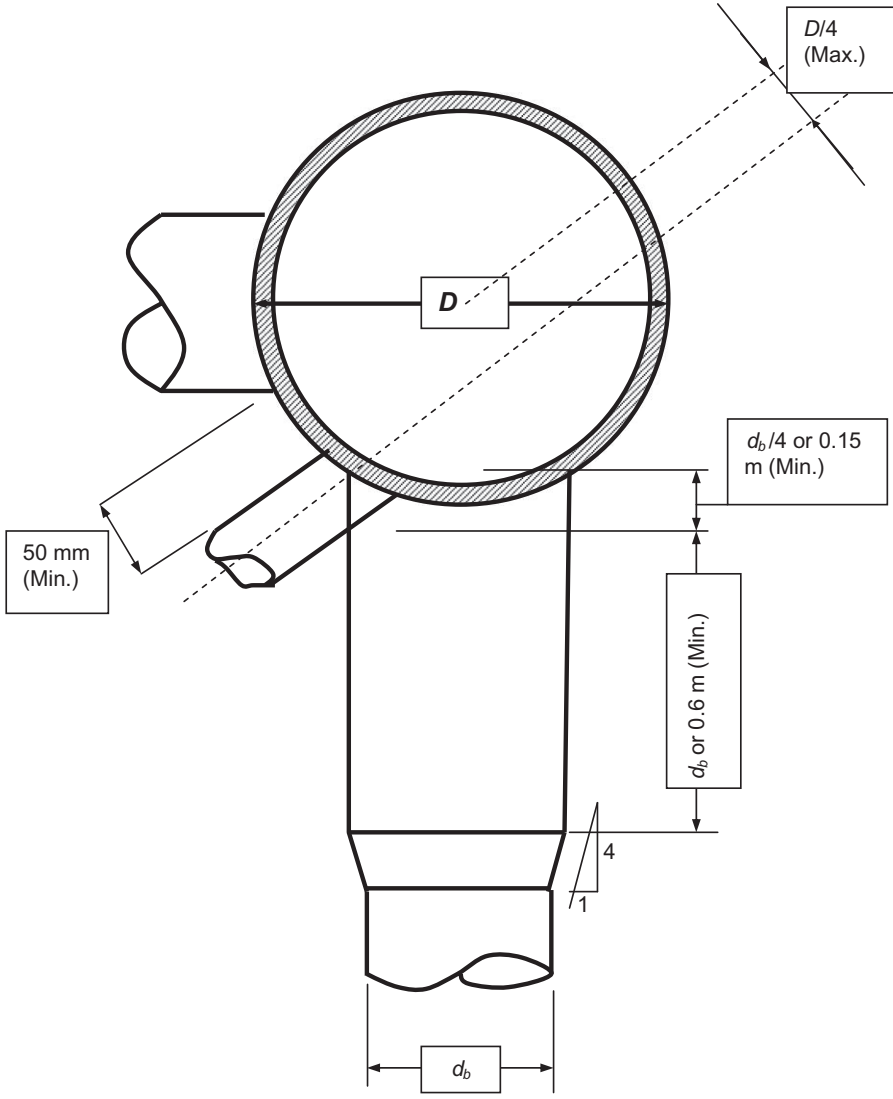

Figure 3.31 Out-of-plane joint detailing.

in the thicknesses between the braces shall be more than 10%. From a practical point of view the main brace member shall have an end stub.

Fig. 3.31 presents the longitudinal weld of the chord away from the near braces by 300 mm (12 inches), on the other hand this weld shall be welded close to the joint crown heel. The girth weld shall be applied for long chord cans. Fig. 3.30 illustrates the weld between the saddle and crown locations to be welded at the brace intersection under higher loads.

Simple tubular joint calculation

The simple joint calculation is valid based on the following criteria:

$0.2 \le \beta \le 1.0$
$10 \le \gamma \le 50$
$30 \le \theta \le 90^{\circ}$
$F_y \le 72$ ksi(500 MPa)
$g/D > -0.6$(for K joints)

Tubular joints without overlap of principal braces and having no gussets, diaphragms, grout, or stiffeners should be designed using the following guidelines (plus a one-third increase in both cases where applicable).

$$P_a = Q_u Q_f \frac{F_{yc} T^2}{FS \sin\theta} \tag{3.94}$$

$$M_a = Q_u Q_f \frac{F_{yc} T^2 d}{FS \sin\theta} \tag{3.95}$$

where P_a is the allowable capacity for brace axial load; M_a is the allowable capacity for brace bending moment; F_{yc} is the yield stress of the chord member at the joint (or 0.8 of the tensile strength, if less), ksi (MPa); FS is the safety factor = 1.60.

For joints with thickened cans, P_a should not exceed the capacity limits defined in Eq. (3.99).

For axially loaded braces with a classification that is a mixture of K, Y, and X joints, a weighted average of P_a based on the portion of each in the total load is taken.

Strength factor Q_u

The strength factor Q_u varies with the joint and load type, as shown in Table 3.5. Note that at the gap connection, the working point has a distance from the chord centerline by more than $D/4$ and is also applicable when the branch members are loaded in more than one plane. Therefore, the connection is considered a multiplanar connection.

Q_β is a geometric factor defined by:

$$Q_\beta = \frac{0.3}{\beta(1 - 0.833\beta)} \quad \text{for } \beta > 0.6 \tag{3.96}$$

$Q_\beta = 1.0$ for $\beta \le 0.6$. Q_g is the gap factor defined by $Q_g = 1 + 0.2\ [1-2.8\ g/D]3$ for $g/D \ge 0.05$ and $Q_g = 0.13 + 0.65\ \phi\ \gamma^{0.5}$ for $g/D \le -0.05$ where $\phi = t\ F_{yb}/(TF_y)$.

It is recommended that the overlap be equal to or greater than $0.25\beta D$. For calculations it is permitted to use a linear interpolation between the limiting values of

Table 3.5 Values for Q_u.

Joint classification	Brace load			
	Axial tension	**Axial compression**	**In-plane bending**	**Out-of-plane bending**
K	$(16 + 1.2\gamma)\beta^{1.2}\ Q_g$ but $\leq 40\ \beta^{1.2}\ Q_g$		$(5 + 0.7\gamma)\beta^{1.2}$	$2.5 + (4.5 + 0.2\gamma)\beta^{2.6}$
T/*Y*	30β	$2.8 + (20 + 0.8\gamma)\beta^{1.6}$ but $\leq 2.8 + 36\beta^{1.6}$		
X	23β for $\beta \leq 0.9$ $20.7 + (\beta - 0.9)$ $(17\gamma - 220)$ for $\beta > 90$	$[2.8 + (12 + 0.1\gamma)\beta]Q_\beta$		

the above two Q_g expressions for $-0.05 < g/D < 0.05$ when this is otherwise permissible or unavoidable.

F_{yb} is equal to the minimum of the brace or brace stub material yield strength, or 0.8 steel tensile strength, in ksi (MPa).

Q_u presents the joint capacity at first crack in the case of tension loading. The Q_u as per APIRP2A presents the joint ultimate capacity in the case of the applied tension force for *Y* and *X* joints.

The coaxial braces are achieved if $e/D \leq 0.2$ where e, is the two braces' eccentricity, in this case the *X* joint with axial tension force, the Q_u term for $\beta > 0.9$ shall be applied in this case. Otherwise, when not coaxial, 23 shall be used for all values of β.

Chord load factor Q_f

The chord load factor Q_f accounts for the presence of nominal loads in the chord and is calculated from the following equation.

$$Q_f = \left[1 + F_1\left(\frac{FSP_c}{P_y}\right) - F_2\left(\frac{FSM_{ipb}}{M_p}\right) - F_3A^2\right] \tag{3.97}$$

The parameter *A* is defined as:

$$A = \sqrt{\left[\left(\frac{FSP_c}{P_y}\right)^2 + \left(\frac{FSM_c}{M_p}\right)^2\right]} \tag{3.98}$$

where P_c and M_c are the nominal axial load and bending resultant in the chord; P_y is the yield axial capacity of the chord; and M_p is the plastic moment capacity of the chord. [Where a one-third increase is applicable, $FS = 1.20$ in Eqs. (3.97) and (3.98).]

Table 3.6 presents the coefficients F_1, F_2, and F_3, which depend on the joint and load type.

When applying Eqs. (3.97) and (3.98), consider the average straining action for normal force and bending for the brace interception for both sides.

Table 3.6 Values of F_1, F_2, and F_3.

Joint type	F_1	F_2	F_3
T/Y joints under brace axial loading	0.3	0	0.8
K joints under brace axial loading	0.2	0.2	0.3
X joints under brace axial loading[a]			
$\beta \leq 0.9$	0.2	0	0.5
$\beta = 1.0$	−0.2	0	0.2
All joints under brace moment loading	0.2	0	0.4

[a]Linearly interpolated values between $\beta = 0.9$ and $\beta = 1.0$ for *X* joints under brace axial loading.

In the equations the thickness of the chord shall be used. The bending moment that affects the compression in the footprint is considered the positive in the plane bending moment and the tension normal force is considered positive also.

Joints with thickened cans

Simply put, for axially loaded *Y* and *X* joints where a thickened joint-can is specified, the joint allowable capacity may be calculated as:

$$P_a = \left[r + (1 - r)(T_n/T_c)^2\right](P_a)_c \tag{3.99}$$

where $(P_a)_c = P_a$ from Eq. (3.94) based on chord can geometric and material properties, including Q_f calculated with respect to chord can; $T_n$is the nominal chord member thickness; T_c is the chord can thickness; $r = L_c/(2.5D)$ for joints with $\beta \leq 0.9$ and $r = (4\beta - 3)L_c/(1.5D)$ for joints with $\beta > 0.9$; and L_c = effective total length as in Fig. 3.30, in which r cannot have a value greater than unity.

Alternatively, an approximate closed-ring analysis is used in the calculation including plastic analysis with a suitable factor of safety (FoS) that covers the approximation in the calculation and using an effective chord length up to $1.25D$, where D is the chord diameter, on either side of the line of action of the branch loads at the chord face, but not more than the actual distance to the end of the joint-can. The finite element (FE) method can be used in the case of more complex joints. For multiple branches in the same plane, dominantly loaded in the same sense, the relevant crushing load is $\Sigma_t P_i \sin_t$. A reinforcement can be used, such as diaphragms, rings, gussets or the stiffening effect of out-of-plane members, and is included in the analysis, noting that its effectiveness decreases with distance from the branch footprint.

Strength check

The interaction ratio J_{IR} for the joint in the case of applied axial loads and bending moments in the brace should be calculated using the expression:

$$J_{IR} = \left|\frac{P}{P_a}\right| + \left(\frac{M}{M_a}\right)^2_{ipb} + \left|\frac{M}{M_a}\right|_{opb} \leq 1.0 \tag{3.100}$$

Overlapping joints

Braces that have in-plane or out-of-plane overlap at the chord member form overlapping joints.

Regarding the joints that have in-plane overlap involving two or more braces in a single plane such as *K* and *KT* joints may be designed using the simple joint equation, using negative gap in Q_g, with exceptions that the shear stresses parallel to the chord face are a potential failure mode and should be checked. Joints with the joint-can equation will not apply to overlapping joints with balanced loads.

During calculation, the thicker brace will be considered the through brace if the nominal thicknesses of the overlapping and through braces differ by more than 10%.

To consider the joint simple equation care should be taken that the combined moment of the overlapping from in-plane or out-of-plane bending moments and through braces should be checked by through-brace intersection capacity. This combined moment is considered the sign of the moments. Where there are combined nominal axial and bending stresses in the overlapping brace, the overlapping brace should also be checked, taking into account that Q_g is equal to 1.0. The through-brace capacity should be checked for combined axial and moment loading in the overlapping brace. In this instance, the Q_f is calculated based on the through brace.

Joints having out-of-plane overlap may be assessed on the same general basis as in-plane overlapping joints, with the exception that axial load capacity may be calculated as for multiplanar joints.

Grouted joints

The two traditional types of grouted joints are a fully grouted chord and the double-skin type, where grout is placed in the annulus between a chord member and an internal member. In both cases, the grout is unreinforced and, as far as joint behavior is concerned, benefit because shear keys that may be present are not permitted.

The value of Q_u for grouted joints is calculated from the following.

In the case of axial tension:

$$Q_u = 2.5\gamma\beta \, \mathrm{K_a} \tag{3.101}$$

where $K_a = 0.5(1 + 1/\sin)$.

In the case of bending:

$$Q_u = 1.5\gamma\beta \tag{3.102}$$

It is worth mentioning that the grouted joints cannot fail under compression load and the compression capacity is limited by the brace to carry this compression load. Therefore there is no calculation presented to the axial compression.

In the case of a complex joint, for fully grouted and double-skin joints, the Q_u values may be replaced with the values pertinent to grouted joints given in Eqs. (3.101) and (3.102) in the case of axial tension and bending, respectively. By any means the value of Q_u should not be less than those calculated for simple joints.

For double-skin joints, failure may also occur by chord ovalization. The ovalization capacity can be estimated by substituting the following effective thickness into the simple joint equations.

$$T_e = \sqrt{\left(T^2 + T_p^2\right)} \tag{3.103}$$

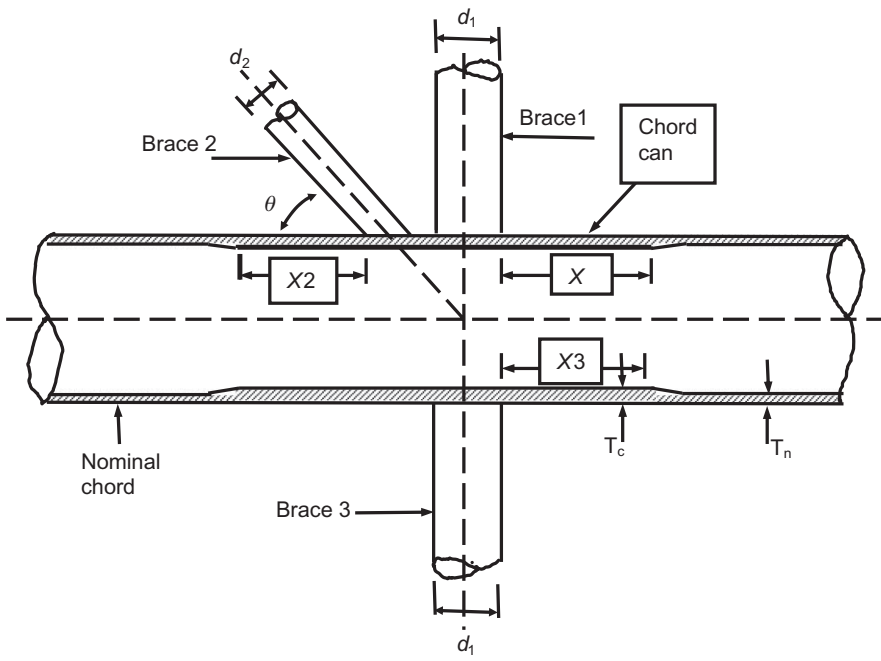

Figure 3.32 Chord length, L_c.

Fig. 3.32 presents an example of calculating the chord length (L_{ch}). For different braces, the chord length will be calculated as:

Brace 1: $L_{ch} = 2x_1 + d_1$;
Brace 2: $L_{ch} = 2x_2 + d_2/\sin$;
Brace 3: $L_{ch} = 2x_3 + d_3$.

where x_1, x_2, and x_3 are obtained as shown in Fig. 3.32, $T_e$is the effective thickness (inches or mm), T is the wall thickness of chord (inches or mm), and T_p is the wall thickness of inner member (inches or mm). T_e should be used in place of T in the simple joint equations, including the γ term.

The Q_f calculation for fully grouted and double-skinned joints should be based on the wall thickness of the chord, the Q_f has considered the distribution of load sharing between the inner member and chord based on that using this term in grouting joint has no influence.

For fully grouted joints, Q_f is equal to 1.0, except in the following cases: (1) high β ($\geq$0.9), (2) X joints with brace tension and out of plan bending (OPB), and (3) chord axial compression with OPB.

3.7.2 Joint calculation according to API RP2A (2000)

Geometrics and parameters for a tubular joint are as shown in Fig. 3.33: t is the brace thickness; g is the gap between braces; T is the chord thickness; d is the brace

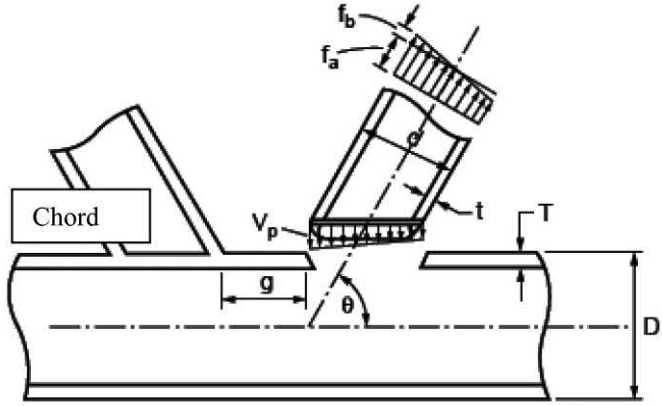

Figure 3.33 Geometrics and parameters for a tubular joint.

diameter; D is the chord diameter; θ is the brace angle measured from the chord; $\tau = t/T$; $\beta = d/D$; $\gamma = D/2T$.

Punching shear

$$V_p = \tau f \sin\theta \tag{3.104}$$

where f is the nominal axial, in-plane bending, or out-of-plane bending stressing the brace.

The allowable punching shear stress in the chord wall is the lesser of AISC shear allowable or

$$V_{pa} = Q_q Q_f \left(F_{yc}/0.6\ \mathrm{g}\right)$$

$$Q_f = 1.0 - \lambda\gamma A^2$$

where $\lambda = 0.030$ for brace axial stress; $\lambda = 0.045$ for brace in-plane bending stress, and $\lambda = 0.021$ for brace out-of-plane bending stress. $A = [(f_{AX})^2 + (f_{IPB})^2 + (f_{OPB})^2]^{0.5}/0.6F_{ye}$. $Q_f = 1.0$ when all extreme fiber stresses in the chord are tensile.

The value of Q_q can be obtained from Table 3.7.

$$Q_\beta = 0.3/(\beta(1 - 0.833\beta)) \text{ for } \beta > 0.6$$
$$Q_\beta = 1.0 \text{ for } \beta \le 0.6$$
$$Q_g = 1.8 - 0.1\left(g/T\right) \text{ for } \gamma \le 20$$
$$Q_g = 1.8 - 4\left(g/D\right) \text{ for } \gamma > 20$$

In any case, Q_g should be ≥ 1.0.

Table 3.7 Values of Q_q.

Joint	Axial compression	Axial tension	In-plane bending	Out-of-plane bending (OPB)
K (gap)	$(1.10 + 0.2/\beta)Q_g$		$(3.27 + 0.67/\beta)$	$(1.37 + 0.67/\beta)Q_\beta$
T and Y	$(1.10 + 0.2/\beta)$			
Cross without diaphragm	$(1.10 + 0.20/\beta)$	$(0.75 + 0.20/\beta)Q_\beta$		
Cross with diaphragm	$(1.10 + 0.20/\beta)$			

Table 3.8 Values of Q_u.

Joint	Axial compression	Axial tension	In-plane bending	Out-of-plane bending (OPB)
K (gap)	$(3.4 + 19\beta)Q_g$		$(3.4 + 19\beta)$	$(3.4 + 7\beta)Q_\beta$
T and Y	$(3.4 + 19\beta)$			
Cross without diaphragm	$(3.4 + 19\beta)$	$(3.4 + 13\beta)Q_\beta$		
Cross with diaphragm	$(3.4 + 19\beta)$			

The joint classification has the following classifications, K, T, Y, or cross-joints, which depend on the load pattern for each load case during the analysis. The criteria for these classifications are as follow:

1. For a K joint, the punching load in a brace shall be balanced by loads on other braces in the same plane and the same side of the joint.
2. In T or Y joints if the punching load reaches the same as a beam shear in the chord.
3. In cross-joints, the punching load is applied from the chord to braces on the opposite side.

Allowable joint capacity

The allowable joint capacity will be calculated as:

$$P_a = Q_u Q_f F_{yc} T^2 / 1.7 \sin\theta \tag{3.105}$$

$$M_a = Q_u Q_f F_{yc} T^2 / 1.7 \sin\theta (0.8d) \tag{3.106}$$

P_a and M_a are the allowable capacity for brace axial load and bending moment, respectively. The values of Q_u are shown in Table 3.8.

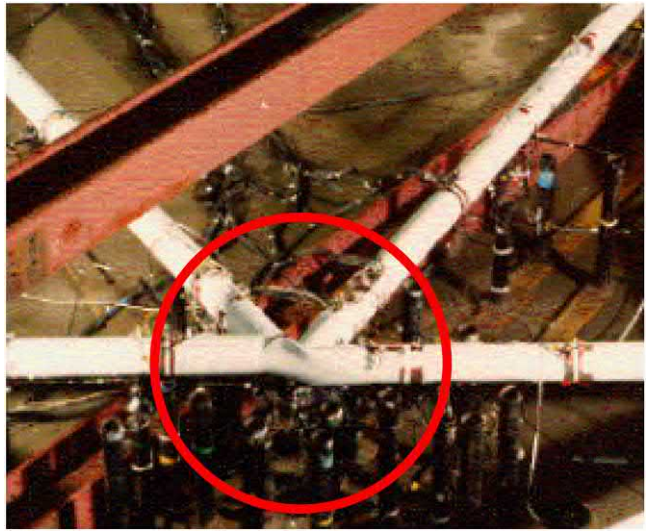

Figure 3.34 Failure in the *K* joint.

Tubular joint punching failure

The experimental test for a frame structure jacket as per a joint industrial study (1999) with *K* bracing is as shown in Fig. 3.34.

The potential for punch through of compression *K* joint member into chord due to plastic deformations around an intersection under cyclic loads is as shown in the following figures, where punching shear is obvious in Fig. 3.35 and the buckling of the tubular joint is illustrated in Fig. 3.36.

Limited deformation at $\beta = 1.0$ for *X* joint under compression at maximum load is repeatable under cyclic-affected loads as the wave load.

Fig. 3.37 presents tearing in the tubular joint due to a direct tensile force.

Flattening of $\beta = 1.0$ tension *X* joint as chord yields is shown in Fig. 3.37 with splitting of paint but no cracks in the steel member itself, which indicates that with more load the cracks will propagate to the steel member.

Therefore it should be a guideline for tubular joint detailing that joint-can precautions and detailing are as shown in Fig. 3.30.

3.7.3 Fatigue analysis

In the last 60 years, many laboratories tests have proven that in the case of a repeated load the metal may fracture by applying a low stress if that stress is repeated a great number of times. The offshore structure, particularly its tubular joints, must resist progressive damage due to fatigue that results from continuous wave action during the 20- to 30-year design life of the structure. Over the years,

Figure 3.35 Punching shear.

Figure 3.36 Buckling for the tubular joint.

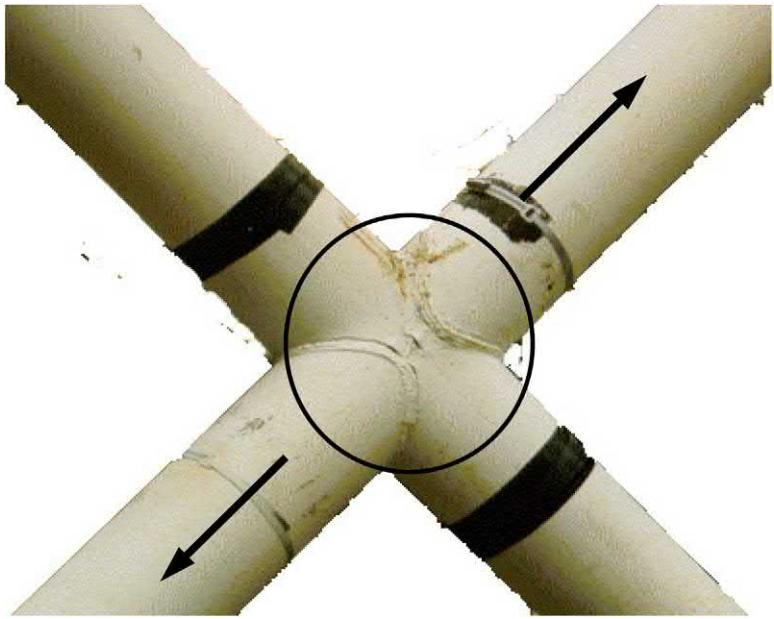

Figure 3.37 Tearing in the tubular joint.

platforms are subjected to a wide variety of sea states and, within each sea state, the structure experiences many cycles of stress at various levels.

The purpose of fatigue analysis is to account for the fact that the number of cycles of stress that a structural component can withstand varies with the magnitude of the cyclic stress.

Dynamic analysis is used in fatigue evaluation to predict the number of cycles and magnitude of stresses that occur in various sea states. As in the extreme wave analysis, dynamic effects become increasingly important for deep-water structures with a heavy deck load.

Fatigue cracks grow because of tensile stresses; corrosion of a metal is accelerated if the metal is subjected to tensile stress. Thus, the effects of corrosion and fatigue are combined in the case of an offshore platform.

Kuang et al. (1975) described the design of tubular joints for offshore structures as an iterative procedure. The process begins with the sizing of the jacket piles according to the requirements of the specific soil and foundation needs of the platform. Sizing determines the diameter of the jacket legs and allows clearance for the piles to go through them. Once the truss work geometry is selected, the column buckling characteristics determine the diameters of the various jacket braces. The initial wall thicknesses of chords and braces are determined by structural analysis. The next cycle of calculation involves increasing the chord wall thicknesses with heavy joint-cans to ensure sufficient static strength to meet code or specification requirements. The next iteration involves calculating the fatigue strength of the joint

to determine if it is compatible with the service life requirement of the platform. Depending on the method of fatigue analysis used, allowable stress concentration factors (SCFs) must be either specified for each joint or built into the method of analysis.

For each intersection member on the jacket, the stress response about this intersection shall be calculated for each sea state condition considering the stresses in global structure and local joints. This calculated stress response considers the cumulative fatigue damage ratio D, where

$$D = \sum(n/N) \tag{3.107}$$

where n is the number of cycles applied at a certain stress range and N is the allowable number of cycles corresponding to this stress range as per the $S-N$ curve.

The damage ratio shall be calculated at each sea state and then the summation to calculate the cumulative damage ratio is performed.

Based on that the expected fatigue life shall be calculated and should be higher than the platform structure lifetime multiplied by a safety factor.

Critical elements are those whose sole failure could be catastrophic. In lieu of a more detailed safety assessment of Category L-1 structures, which are manned and nonevacuated, a safety factor of 2.0 is recommended for inspectable, nonfailure-critical, connections. For failure-critical and/or noninspectable connections, increased safety factors are recommended, as shown in Table 3.9. A reduced safety factor is recommended for Categories L-2 and L-3, which are manned evacuated or unmanned structures, respectively. For conventional steel jacket structures, on the basis of in-service performance data, $SF = 1.0$ for redundant diver or remotely operating vehicle inspectable framing, with safety factors for other cases being half those in the table.

When fatigue damage can occur due to other cyclic loadings, such as transportation, the following equation should be satisfied.

$$\sum_i SF_i D_i < 1.0 \tag{3.108}$$

where D_i is the fatigue damage ratio for each type of loading and SF_i is the associated safety factor.

For transportation where long-term wave distributions are used to predict short-term damage, a larger safety factor should be considered.

Table 3.9 Safety factor for fatigue life.

Failure criticality	Inspectable	Not inspectable
No	2	5
Yes	5	10

Stress concentration factors

The SCF differs from one joint geometry to another. It is known that the applied loads on tubular joints cause stresses at certain points along the intersection weld to be many times the nominal stress acting in the members. The SCF is a multiplier applied to the nominal stress to reach the peak or maximum stress at the hot spot.

The hot spot is the location in the tubular joint where the maximum applied tensile stress occurs. To carry out a fatigue analysis of certain selected tubular joints in an offshore structure, the stress history of the hot spots in those joints must first be determined. Three basic types of stress contribute to the development of a hot spot. Primary stresses are caused by axial forces and moments resulting from the combined truss and frame action of the jacket. As shown for the in-plane tubular joint in Fig. 3.38, hot spots in locations 1, 2, 3, 4, and 6 are most affected by axial forces and in-plane bending moments, while locations 2 and 5 are most affected by the axial forces and circumferential moments in braces.

Secondary stresses are caused by structural details of the connection, such as poor joint geometry, poor fit-up, local variation within the joint due to rigid reinforcement or restraint of the braces by circumferential weld, and these secondary stresses will amplify the primary stresses. Secondary stresses are also caused by metallurgical factors, such as faulty welding practice, insufficient weld penetration, heavy beading, weld porosity, or varying cooling rates. These stresses mainly affect location 1, but their effect is also significant at locations 3, 4, and 6. Because metallurgical factors are essential in fatigue stresses on tubular joints, the quality control (QC) procedure for constructing this connection should be given more attention, as described in Chapter 5, Fabrication and installation.

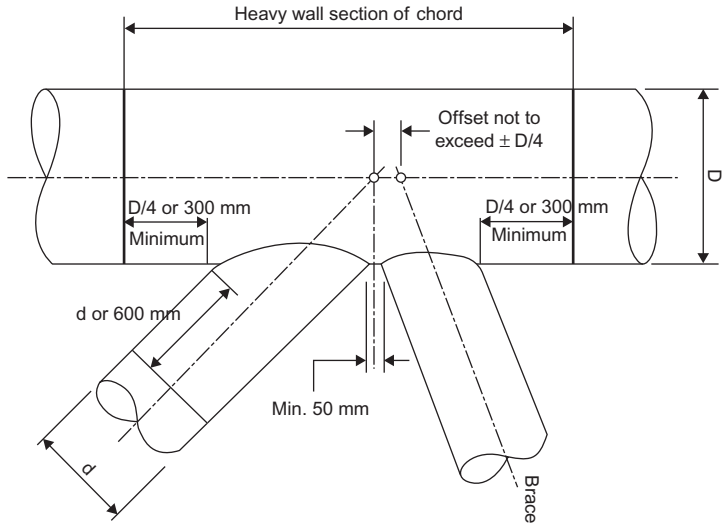

Figure 3.38 Detail of a tubular joint.

The most fatigue-sensitive areas in offshore platforms are the welds at tubular joints, because of the high local stress concentrations. Fatigue lives at these locations should be estimated by evaluating the hot-spot stress range (HSSR) and using it as input into the appropriate $S-N$ curve.

The SCF can be obtained using a FE technique. In the case of applying a FE, it is recommend to use thick shell elements to present the weld area. By using this method the stress concentration can be obtained by performing an extrapolation for stress components to the weld toes and the maximum principal stress can be calculated.

According to Healy and Buitrago (1994) and Niemi et al. (1995), if thin shell elements are used, the results should be interpreted carefully, considering that there is no single method i available to provide the accurate stresses.

It is worth mentioning that while applying the FE it can overpredict the SCF if the extrapolation is done on the middle of the surface intersection and underpredict if the calculation is done at the end of the weld toe. A higher stresses value is also obtained if the calculation is done on the average stresses of the nodes at the middle of the surface interstation.

The general definition for the SCF for any tubular joint configuration and each type of brace loading is presented by the following formula:

$$\text{SCF} = \text{HSSR}/\text{nominal brace stress range}.$$

The nominal brace stress range should be based on the section properties of the brace-end under consideration, taking due account of the brace-stub, or a flared member end, if present. Similarly, the SCF evaluation should be based on the same section dimensions.

The SCF presents the increase in stresses as a result of the geometry of the joint and the load types. The SCF can be obtained also by different methods such as a model test in a laboratory which is associated with empirical equations. HSSR is affected by the nominal cyclic stresses that are applied on the chord. Based on that, SCF is affected by the cyclic loaded applied on the brace members and the axial forced which is applied to the bracing is out-of-plane or in-plane bending and the joint details with its geometry.

In general, for all welded tubular joints under all three types of loading, a minimum value of SCF equal to 1.5 should be used.

For unstiffened welded tubular joints, SCFs should be evaluated using the Efthymiou equations, as discussed later, in the thickness effect on the SCF.

The linearly extrapolated hot-spot stress from Efthymiou may be adjusted to account for the actual weld toe position, where this systematically differs from the assumed American Welding Society (AWS) basic profiles.

The SCF applies also to internally ring-stiffened joints, including the stresses in the stiffeners and the stiffener-to-chord weld. Special consideration should be given to these locations. SCFs for internally ring-stiffened joints can be determined by applying the Lloyd's reduction factors based on the Lloyd's Report (1988) to the SCFs for the equivalent unstiffened joint. For ring-stiffened joints analyzed by such

means, the minimum SCF for the brace side under axial or OPB loading should be taken as 2.0.

SCFs in grouted joints

Grouted joints are usually used in repairing or strengthening the platform. Grouting joints tend to reduce the SCF of the joint since the grout reduces the chord deformations. In general, the larger the ungrouted SCF, the greater the reduction in SCF with grouting. Hence, the reductions are typically greater for *X* and *T* joints than for *Y* and *K* joints. More discussion of the effect of grouting on strengthening is presented in Chapter 7, Assessment of existing structures and repairs.

S−N *curves for all members and connections*

Nontubular members and connections in deck structures, appurtenances, and equipment and tubular members and attachments to them, including ring stiffeners, may be subject to variations of stress due to wave, wind, and other environmental loads or operational loads. Operational loads include loads associated with machine vibration, crane usage, and filling and emptying of tanks. Where variations of stress are applied to conventional weld details, presented in Figs. 2.11 and 2.13 in ANSI/AWS D1.1-2002, the *S−N* curve for Fig. 2.11 can be used for nontubular members. In the case of tubular members, Fig. 2.13 presents a tubular joint in stress categories which are ET, DT, FT, K1, and K2.

Where the hot-spot SCF can be determined, the exposed different factors on the joints are taken into consideration, such as the variable loads and the corrosion effect which are related to the cathodic protection system.

It is worth mentioning that the *S−N* curve in the above reference considers the combination of stress concentration due to geometrical and notch.

ET is a simple T-, Y-, and K-connection with groove welds or fillet welds; and for complex tubular connections if the punching shear capacity of the main member, cannot carry the entire load. In addition, the load transfer is accomplished by overlap (negative eccentricity), gusset plates, and ring stiffeners. The main stresses are due to tension and compression failure.

FT is a simple *T*-, *Y*-, or *K*-connection loaded in tension or bending, with fillet or PJP groove welds and the main stress is due to shear in the weld.

DT is a connection designed as a simple *T*-, *Y*-, or *K*-connection with CJP groove welds, including overlapping connections in which the main member at each intersection meets punching shear requirements. The main stresses are due to tension, compression, and bending with reversal action.

K2 is a simple *T*-, *Y*-, or *K*-connection in which the gamma ratio *R/tc* of the main member does not exceed 24 and the main stresses are due to punching.

Reference may alternatively be made to the *S−N* criteria similar to the other joint (OJ) curves contained within ISO DIS.

The ISO 19902:2004 code proposal uses a weld detail classification system whereby the OJ curves include an allowance for notch stress and a modest geometrical stress concentration.

Table 3.10 Basic design $S-N$ curves.

Curve	$\text{Log}_{10}(k_1)$ with S in ksi	$\text{Log}_{10}(k_1)$ with S in MPa	m
Welded joints (WJ)	9.95	12.48	3 for $N < 10^7$
	11.92	16.13	5 for $N > 10^7$
Cast joints (CJ)	11.80	15.17	4 for $N < 10^7$
	13.00	17.21	5 for $N > 10^7$

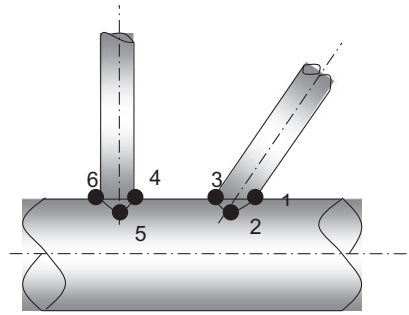

Figure 3.39 Hot spots at in-plane tubular joint.

S−N *curves for tubular connections*

Design $S-N$ curves are given below for welded tubular and cast joints. The basic design $S-N$ curve is of the form:

$$\text{Log}_{10}(N) = \text{Log}_{10}(k_1) - m\text{Log}_{10}(S) \tag{3.109}$$

where N is the predicted number of cycles to failure under stress range S, k_1 is a constant, and m is the inverse slope of the $S-N$ curve.

Table 3.10 illustrates the basic welded joint (WJ) and cast joint (CJ) curves. In the case of a brace to chord tubular joint the WJ curve is used, considering that these curves are used only for steel yield strengths less than 500 MPa (72 ksi). These curves are applicable for environmental and operational variable loads.

The basic allowable cyclic stress should be corrected empirically for seawater effects, the apparent thickness effect, with the exponent, depending on the profile, and the weld improvement factor on S. (An example of $S-N$ curve construction is given in Fig. 3.39.)

The basic design $S-N$ curves given in Table 3.8 are applicable for joints in air and submerged coated joints. In case of welded joints in seawater with adequate cathodic protection, the value of m is equal to 3 branch of the $S-N$ curve should be reduced by a factor of 2.0 on life, with the m is equal to 5 branch remaining unchanged and the position of the slope change adjusted accordingly.

Fabrication of WJs should be in accordance with the QC procedure. The curve for CJs is applicable only to castings having an adequate fabrication inspection plan.

Thickness effect

The WJ curve is based on a five-eighths of an inch (16 mm) reference thickness. The following equation will be applied for material thickness above the reference thickness:

$$S = S_o(t_{ref}/t)^{0.25} \tag{3.110}$$

where t_{ref} is the reference thickness, five-eighths inch (16 mm); $S$is the allowable stress range; S_o is the the allowable stress range from the $S-N$ curve; and t is the member thickness for which the fatigue life is predicted.

If the weld has profile control, the exponent in the above equation may be taken as 0.20 instead of 0.25. On the other hand, the exponent can be taken equal to 0.15, if the weld toe has been ground or peened.

The material thickness effect for castings is given by:

$$S = S_o(t_{ref}/t)^{0.15} \tag{3.111}$$

where the reference thickness t_{ref} is 1.5 inches (38 mm).

For the next equations the thickness of the chord and brace are used for the chord and brace side, respectively.

The allowable fatigue $S-N$ range for a tubular structure is as in Fig. 3.40.

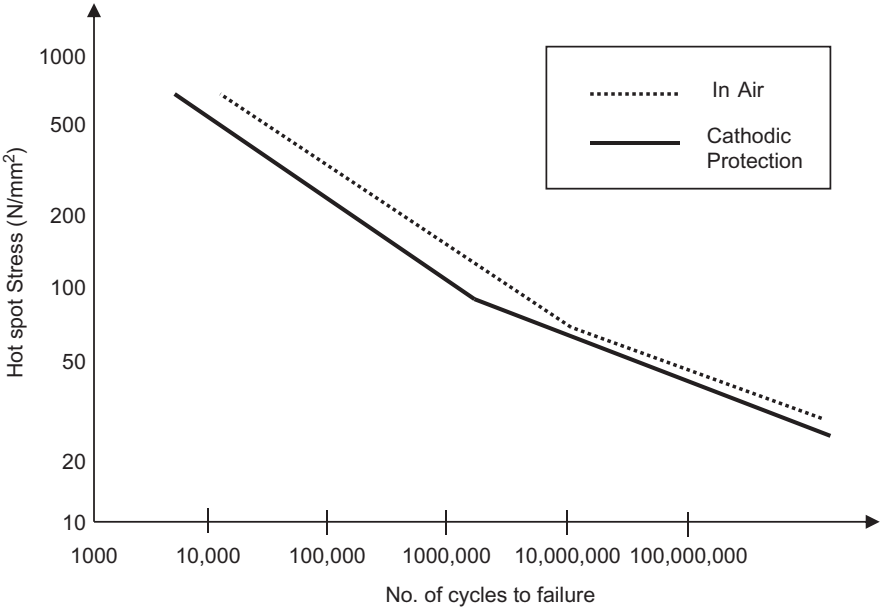

Figure 3.40 Allowable fatigue $S-N$ ranges for stress categories for tubular structures in atmospheric service (adopted from AWSD1.1).

Use of the Efthymiou SCF equations is recommended because these equations cover all joints and load types and are also used for *K* and *KT* joints when they are overlapped.

These equations are also recommended by Eurocode 3 and ISO DIS 14347 in addition to the International Institute of Welding. Therefore a combination of equations is not preferred.

It is worth mentioning that Efthymiou equations for SCF are valid under these conditions:

1. β from 0.2 to 1.0;
2. τ from 0.2 to 1.0;
3. γ from 8 to 32;
4. α (length) from 4 to 40;
5. from 20 to 90 degrees; and
6. ζ (gap) from -0.6β/sin to 1.0.

In some times one or two conditions of geometric factors are not in the range, in this case the following steps can be follow:

1. Using the actual values of geometric parameters and obtain the SCF value;
2. Using the limit values of geometric parameters and obtain the SCF value;
3. Use the maximum of the above steps (1) or (2).

(A) *Axial load − chord ends fixed*
Chord saddle

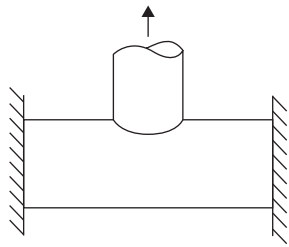

$$\mathrm{SCF} = \gamma\tau^{1.1}[1.11 - 3(\beta - 0.52)^2]\sin^{1.6}\Theta \tag{3.112}$$

For a short chord there is a correction factor F1.
Short chord correction factors ($\alpha < 12$):

$$F1 = 1 - (0.83\beta - 0.56\beta^2 - 0.02)\gamma^{0.23}\exp[-0.21\gamma^{-1.16}\alpha^{2.5}] \tag{3.113}$$

where $\exp(x) = e^x$.
Chord crown

$$\text{SCF} = \gamma^{0.2}\tau[2.65 + 5(\beta - 0.65)^2] + \tau\beta(0.25\alpha - 3)\sin\theta \tag{3.114}$$

Brace saddle

$$\text{SCF} = 1.3 + \gamma\tau^{0.52}\alpha 0.1[0.187 - 1.25\beta 1.1(\beta - 0.96)]\sin(2.7 - 0.01\alpha)\theta \tag{3.115}$$

For short chord there is a correction factor F1.
Brace crown

$$\text{SCF} = 3 + \gamma^{1.2}[0.12\exp(-4\beta) + 0.011\beta^2 - 0.045] + \beta\tau(0.1\alpha - 1.2) \tag{3.116}$$

(B) *Axial load − general fixity conditions*

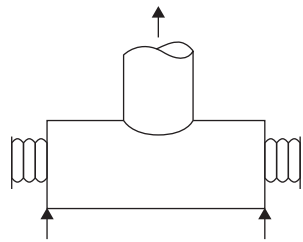

1. *Chord saddle*

$$\text{SCF} = [\text{Eq. (3.112)}]C_1(0.8\alpha - 6)\tau\beta^2(1 - \beta^2)^{0.5} + \sin^2 2\theta \tag{3.117}$$

For short chord there is a correction factor F2:

$$F2 = 1 - (1.43\beta - 0.97\beta^2 - 0.03)\gamma^{0.04}\exp[-0.71\gamma^{-1.38}\alpha_{2.5}] \tag{3.118}$$

Chord crown

$$\text{SCF} = \gamma^{0.2}\tau[2.65 + 5(\beta - 0.65)^2] + \tau\beta(C_2\alpha - 3)\sin\theta \tag{3.119}$$

Brace saddle: Eq. (3.115)
Brace crown

$$\text{SCF} = 3 + \gamma^{1.2}[0.12\exp(-4\beta) + 0.011\beta^2 - 0.045] + \beta\tau(C_3\alpha - 1.2) \tag{3.120}$$

Note that, for chord-end fixity parameter C, $0.5 \le C \le 1.0$, and typically $C = 0.7$, $C_1 = 2(C - 0.5)$, $C_2 = C/2$, and $C_3 = C/5$.

(C) *In-plane bending*

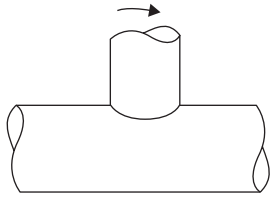

1. *Chord crown*

$$\text{SCF} = 1.45\beta\tau^{0.85}\gamma(1 - 0.68\beta)\sin^{0.7}\theta \tag{3.121}$$

For short chord there is a correction factor F, where

$$F3 = 1 - 0.55\beta^{1.8}\gamma 0.16\exp[-0.49\gamma^{-0.89}\alpha^{1.8}] \tag{3.122}$$

2. *Brace crown*

$$\text{SCF} = 1 + 0.65\beta\tau^{0.4}\gamma(1.09 - 0.77\beta) + \sin_{(0.06\gamma - 1.16)}\theta \tag{3.123}$$

(D) *Out-of-plane bending*

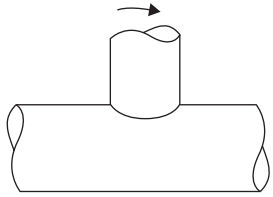

Chord saddle

$$\text{SCF} = \gamma\tau\beta(1.7 - 1.05\beta^3)\sin^{1.6}\theta \tag{3.124}$$

Brace saddle

$$\text{SCF} = \tau^{-0.54}\gamma^{-0.05}(0.99 - 0.47\beta + 0.08\beta^4) \times [\text{Eq. (3.124)}] \tag{3.125}$$

Chord-end fixity parameter C

(E) *Axial load (balanced)*

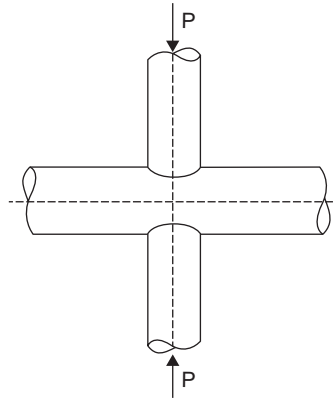

Chord saddle

$$\text{SCF} = 3.87\gamma\tau\beta(1.10 - \beta^{1.8})\sin^{1.7}\theta \tag{3.126}$$

Chord crown

$$\text{SCF} = \gamma^{0.2}\tau[2.65 + 5(\beta - 0.65)^2] + 3\tau\beta\sin\theta \tag{3.127}$$

Brace saddle

$$\text{SCF} = 1 + 1.9\gamma\tau^{0.5}\beta^{0.9}(1.09 - \beta^{1.7})\sin^{2.5}\theta \tag{3.128}$$

Brace crown

$$\text{SCF} = 3 + \gamma^{1.2}[0.12\exp(-4\beta) + 0.011\beta^2 - 0.045] \tag{3.129}$$

In joints with short chords ($\alpha < 12$) and closed ends, the saddle SCFs can be reduced by the short chord factors F1 or F2, where:

$$F1 = 1 - (0.83\beta - 0.56\beta^2 - 0.02)\gamma^{0.23}\exp[-0.21\gamma^{-1.16}\alpha^{2.5}] \tag{3.130}$$

$$F2 = 1 - (1.43\beta - 0.97\beta^2 - 0.03)\gamma^{0.04}\exp[-0.71\gamma^{-1.38}\alpha^{2.5}] \tag{3.131}$$

(F) *In-plane bending*

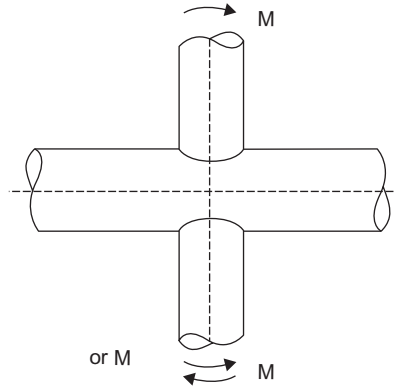

Chord crown: Eq. (3.121)
Brace crown: Eq. (3.123)
(G) *Out-of-plane bending (balanced)*

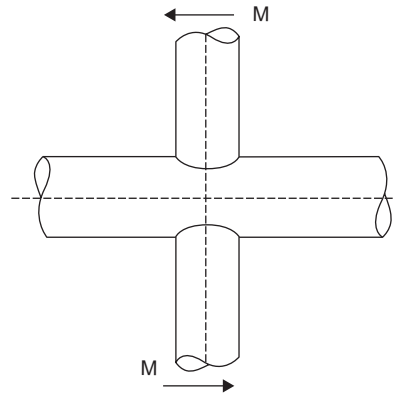

Chord saddle

$$\text{SCF} = \gamma\tau\beta(1.56 - 1.34\beta^4)\sin^{1.6}\theta \tag{3.132}$$

Brace saddle

$$\text{SCF} = \tau^{-0.54}\gamma^{-0.05}(0.99 - 0.47\beta + 0.08\beta^4) \times [\text{Eq. (3.132)}] \tag{3.133}$$

In joints with short chords ($\alpha < 12$) and closed ends, Eqs. (3.132) and (3.133) can be reduced by the short chord factor F3, where:

$$F3 = 1 - 0.55\beta^{1.8}\gamma^{0.16}\exp[-0.49\gamma^{-0.89}\alpha^{1.8}] \tag{3.134}$$

(H) *Balanced axial load*

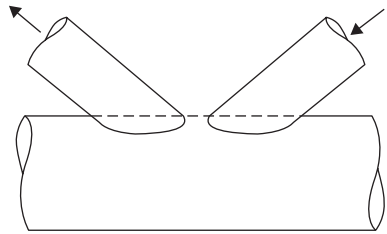

Chord SCF

$$\mathrm{SCF} = \tau^{0.9}\gamma^{0.5}\left(0.67 - \beta^2 + 1.16\beta\right)\sin\theta\left[\frac{\sin\theta_{\max}}{\sin\theta_{\min}}\right]^{0.30}\left[\frac{\beta_{\max}}{\beta_{\min}}\right]^{0.30} \left[1.64 + 0.29\beta^{-0.38}\mathrm{ATAN}(8\zeta)\right] \tag{3.135}$$

Brace SCF

$$\mathrm{SCF} = 1 + [\text{Eq. (3.135)}](1.97 - 1.57\beta^{0.25})\tau^{-0.14}\sin^{0.7}\theta +$$
$$\mathrm{SCF} = C\beta^{1.5}\gamma^{0.5}\tau^{-1.22}\sin^{1.8}(\theta_{\max} + \theta_{\min}) \times [0.131 - 0.084\mathrm{ATAN}(14\zeta + 4.2\beta)] \tag{3.136}$$

where $C = 0$ for gap joints, $C = 1$ for the through brace and $C = 0.5$ for the overlapping brace. Note that τ, β, θ, and the nominal stress relate to the brace under consideration and ATAN is arctangent evaluated in radians.

(I) *Unbalanced IPB*

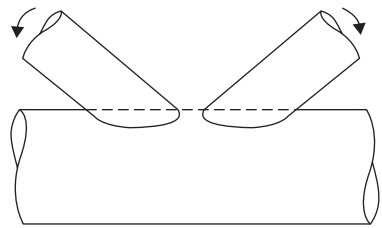

Chord crown SCF: Eq. (3.114). (For overlaps exceeding 30% of contact length, use 1.2 × [Eq. (3.121).]

Gap joint−brace crown SCF: Eq. (3.123)

Overlap joint−brace crown SCF: [Eq. (3.123)] × (0.9 + 0.4)

(J) *Unbalanced OPB*

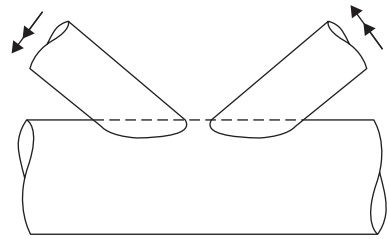

Chord saddle SCF adjacent to brace A:

$$\begin{aligned}\text{SCF} = &[\text{Eq. (3.124)}]_A[1 - 0.08(\beta_{B\gamma})^{0.5}\exp(-0.8x)] + \\ &[\text{Eq. (3.124)}]_B[1 - 0.08(\beta_{A\gamma})^{0.5}\exp(-0.8x)][2.05(\beta_{\max})^{0.5}\exp(-1.3x)]\end{aligned} \tag{3.137}$$

where

$$x = 1 + \frac{\zeta \sin\theta_A}{\beta_A}$$

Brace A saddle SCF:

$$\text{SCF} = \tau^{-0.54}\gamma^{-0.05}(0.99 - 0.47\beta + 0.08\beta^4) \times [\text{Eq. (3.137)}] \tag{3.138}$$

$$F4 = 1 - 1.07\beta^{1.88}\exp[-0.16\gamma^{-1.06}\alpha^{2.4}] \tag{3.139}$$

Note that $[\text{Eq. (3.124)}]_A$ is the chord SCF adjacent to brace A as estimated from Eq. (3.124).

The designation of braces A and B is not geometry dependent. It is nominated by the user.

(K) *Balanced axial load for 3 bracing*

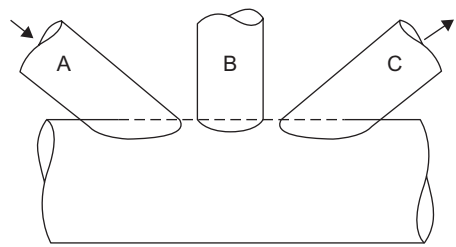

Chord SCF: Eq. (3.135)
Brace SCF: Eq. (3.136)
For the diagonal braces A and C, use $\zeta = \zeta_{AB} + \zeta_{\text{BC}} + \beta_B$
For the central brace B, use ζ = maximum of ζ_{AB}, ζ_{BC}
(L) *In-plane bending for 3 bracing*

Chord crown SCF: Eq. (3.121)
Brace crown SCF: Eq. (3.123)
(M) *Unbalanced out-of-plane bending for 3 bracing*

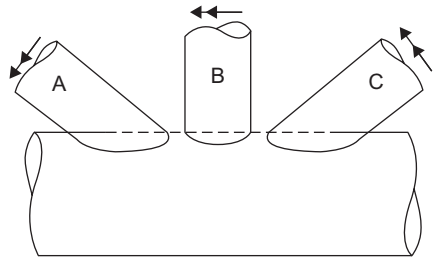

Chord saddle SCF adjacent to diagonal brace A:

$$\begin{aligned}\text{SCF} = {} & [\text{Eq. (3.124)}]_A\,[1 - 0.08(\beta_{B\gamma})^{0.5}\exp(-0.8x_{AB})]\cdot[1 - 0.08(\beta_{C\gamma})0.5\exp(-0.8x_{AC})] \\ & + [\text{Eq. (3.124)}]_B[1 - 0.08(\beta_{A\gamma})^{0.5}\exp(-0.8x_{AB})][2.05(\beta_{\max})^{0.5}\exp(-1.3x_{AB})] \\ & + [\text{Eq. (3.124)}]_C\,\left[1 - 0.08(\beta_{A\gamma})^{0.5}\exp(-0.8x_{AC})\right][2.05(\beta_{\max})^{0.5}\exp(-1.3x_{AC})]\end{aligned} \tag{3.140}$$

where

$$x_{AB} = 1 + \frac{\zeta_{AB}\sin\theta_A}{\beta_A} \tag{3.141}$$

$$x_{AC} = 1 + \frac{(\zeta_{AB} + \zeta_{BC} + \beta_B)\sin\theta_A}{\beta_A} \tag{3.142}$$

Chord saddle SCF adjacent to central brace A:

$$\begin{aligned}\text{SCF} = {} & [\text{Eq. (3.124)}]_B[1 - 0.08(\beta_{A\gamma})^{0.5}\exp(-0.8x_{AB})]^m \\ & \cdot[1 - 0.08(\beta C_\gamma)^{0.5}\exp(-0.8x_{BC})]^{\text{m}} \\ & + [\text{Eq. (3.124)}]_A\cdot[1 - 0.08(\beta_{B\gamma})^{0.5}\exp(-0.8x_{AB})][2.05(\beta_{\max})^{0.5}\exp(-1.3x_{AB})] \\ & + [\text{Eq. (3.124)}]_C\cdot[1 - 0.08(\beta_{B\gamma})^{0.5}\exp(-0.8x_{BC})][2.05(\beta_{\max})^{0.5}\exp(-1.3x_{BC})]\end{aligned} \tag{3.143}$$

where

$$m = (\beta_A/\beta_B)^2$$
$$x_{AB} = 1 + \frac{\zeta_{AB}\sin\theta_A}{\beta_B} \text{ and } x_{BC} = 1 + \frac{\zeta_{BC}\sin\theta_B}{\beta_B}.$$

Brace saddle SCFs under OPB: obtained from the adjacent chord SCFs using

$$\mathrm{SCF} = \tau^{-0.54}\gamma^{-0.05}(0.99 - 0.47\beta + 0.08\beta^4) \times \mathrm{SCFchord} \tag{3.144}$$

where SCFchord = Eq. (3.140) KT1 or Eq. (3.143)

In joints with short chords ($\alpha < 12$), Eqs. (3.140), (3.143), and (3.144) can be reduced by the short chord factor F4, where $\mathrm{F4} = 1 - 1.07\beta^{1.88}$ exp $[-0.16\gamma^{-1.06}\alpha^{2.4}]$.

Effect of weld toe position. Ideally, the SCF should be invariant, given the tubular connection's geometry (γ, τ, β, θ, and ζ). This is how the Efthymiou and all the other SCF equations are formulated.

One method used to correct analytical SCF based on weld toe position was discussed in Marshall (1989). Based on Marshall et al. (2005), a more robust formulation is now proposed:

$$\mathrm{SCF}_{corr} = 1 - (L_a - L)/L_{mp} \tag{3.145}$$

where $\mathrm{SCF}_{corr}$is the correction factor applied to Efthymiou SCF; $L_a$is the actual weld toe position for typical yard practice; $L$is the nominal weld toe position; and $L_{mp}$is the moment persistence length (distance from nominal toe to reversal of shell bending stress).

Various expressions for L_{mp} are shown in Table 3.11 as a function of joint and load type with the orientation of the hot spot.

For the joint-can, R is the radius and T is the thickness. There should be compatibility with the strain gauge rules as per its location at the crown and saddle.

The relation between the hot spot stress and the cycles of load until failure is presented in Fig. 3.41 in the case of the thickness of the chord being equal to 16 mm.

Failure is expressed as damage or life fatigue damage, so fatigue life damage is the particular stress range number of the cycle divided by the allowable number of the cycle from the $S-N$ curve corresponding to the stress range.

Table 3.11 Expressions for L_{mp}.

Circumferential stress at saddle	
All loading modes	$L_{mp} = (0.42 - 0.28\beta)R$ Angle $= (24 - 16\beta)$ degrees
Longitudinal stress at crown	
Axis symmetric	$L_{mp} = 0.6(RT)^{0.5}$
Gap (g) of K joint	L_{mp} = lesser of 0.6 $(RT)^{0.5}$ or g/2
Outer heel/toe, axial	$L_{mp} = 1.5(RT)^{0.5}$
In-plane bending	$L_{mp} = 0.9(RT)^{0.5}$

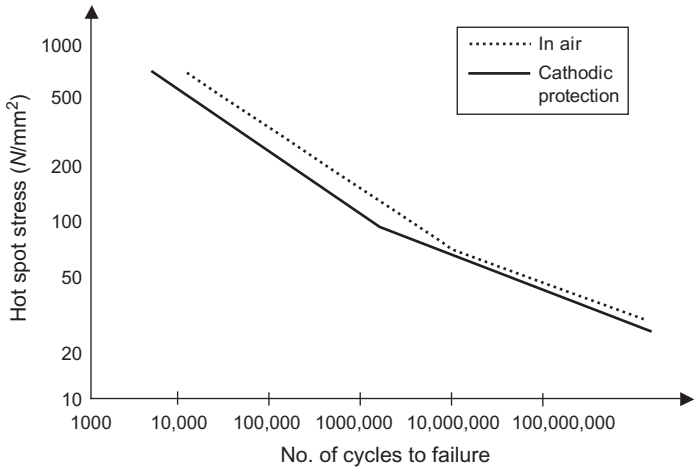

Figure 3.41 Tubular joint $S-N$ curve for $T = 16$ mm (from API RP2A).

Table 3.12 Fatigue analysis.

Stress range	Number of cycles of stress occurrence	Number of cycles allowable
5	10×10^6	50×10^6
10	4×10^5	4×10^6
20	6×10^4	3×10^5
50	5×10^2	1×10^4
90	25	1×10^3

Table 3.12 is an example of a fatigue analysis, with the stress range and the corresponding number of cycles of stress occurrence and the allowable number of cycles based on the $S-N$ curve. Assuming a point is subject to five cyclic stress ranges (due to wave), $D_5 = 10 \times 10^6/50 \times 10^6 = 0.2$, $D_{10} = 0.1$, $D_{20} = 0.2$, $D_{50} = 0.055$, and $D_{90} = 0.025$. Total damage = 0.58.

Therefore if these waves occurred over 10 years, then the fatigue life = 10/0.58 = 17.24 years.

Fatigue design for a jacket

The first step is to perform dynamic analysis to define the structure natural frequency, then identify the wave that caused excitation to the structure. The corresponding structure time period to obtain the dynamic amplification factor (DAF) is included in the in-place analysis.

The spectral method is applicable in the case of a platform time period less than 3 seconds. It is very important to choose a fatigue method that is matched with the nature of the platform structure dynamic excitation.

From a practical point of view, the in-service fatigue design life of the joints should be at least twice the service life of the platform (i.e., 50 years).

Fatigue analysis using software will include:

- The environmental loads parameters;
- A sufficient number of wave directions. For each direction, a minimum of four wave heights should be used to compute the stress range versus wave height relationship. The directions, wave heights, and exceedances selected should be those closest to the directions indicated in the metocean data. A sufficient number of wave crest positions should also be considered;
- If the natural period of the structure exceeds 3 seconds, dynamic amplification effects should be taken into account in calculation of the cycle loading;
- Where significant cyclic stresses may be induced by the action of wind, wave slamming, changes in member buoyancy, etc., such stresses should be combined with those due to wave action to obtain the total effective stress spectrum for a particular member or joint. Fatigue damage accumulated during fabrication and transportation should also be considered.

The analysis procedure should then take the following steps:

- For each joint and type of failure under consideration, the stress range spectra should be computed at a minimum of eight positions around the joint periphery;
- Two types of failure should be considered, using the appropriate SCFs (e.g., brace-to-weld failure and chord-to-weld failure);
- For joints other than those between tubular members, individual detailed consideration should be given, with due regard paid to published, reliable experimental data.

SCFs should be determined for tubular to tubular joints that are ungrouted and unstiffened. SCF should be calculated using Efthymiou equations as discussed earlier.

In lieu of a more accurate procedure for analysis, ring-stiffened joints may be checked using the same procedure as for simple joints, but using modified chord thickness.

3.8 Topside design

In general, major rolled shapes for offshore structure design should be compact sections, as defined by AISC. The minimum thickness of a structural plate or section should be 6 mm. The minimum diameter to thickness ratio of tubular members should not be less than 20, where the diameter is based on the average of the tubular outside and inside diameters.

For connections designed to comply with the codes, they must fulfill the following minimum requirements:

- The minimum fillet weld should be 6 mm;
- Wherever possible, joints should be designed as simple joints with no overlap;
- Tubular joints should be designed in accordance with API RP2A.

The deflection (discussed in Chapter 2, Offshore structure loads and strength) should be matched with the codes and defined in the owner's specification.

- Deflections should be checked for the actual equipment live loads and casual area live loads. Pattern loading should be considered.
- Deflection of members supporting deflection-sensitive equipment should be no greater than L/500 for beams and L/250 for cantilevers under live loads.
- Deflection of beams in the workrooms and living quarters should be no greater than L/360 for beams and L/180 for cantilevers under live loads.
- Deflection limits for other structures should be L/250 for beams and L/125 for cantilevers under live loads.

In performing structural analysis using software (such as SACS, for example), it is better to define the direction of the model. In most cases, the directions can be:

- + x-axis aligned with platform east;
- + y-axis aligned with platform north;
- + z-axis aligned vertically upward;
- The datum for the axes should be at the chart datum.

In general, only the primary structural steel should be modeled. However, secondary members should be modeled where they are necessary for the structural integrity or to facilitate load input. Deck plates should be modeled as shear panel elements. Joint eccentricities should be modeled using discrete elements rather than using the "offset" facility of SACS. When individual elements are used, joint forces can be more easily extracted from the output.

All the differing analyses (in-place, lift, loadout, etc.) should utilize the same base model. That is, the in-place model should form the basis for all the other analyses to be performed.

The in-service analyses should include a basic model of the jacket structure to ensure the correct stiffness interaction between the jacket and the topside structures. Pile foundations to the jackets need not be considered for topside analysis and design—simple supports are sufficient.

3.8.1 Grating design

The grating is the traditional member used in covering the platform floor (as well as in onshore facilities). The checklist in Table 3.13 should be filled in, to make certain that the design of the grating matches the client's requirements for its function.

Grating should have a 1-inch (25-mm) minimum bearing on supporting steel. Where grating areas are shown as removable on the drawings, the weight of fabricated grating sections for such areas should not exceed 160 kg (350 lb).

The direction in which the load bars run is important to ensure that it rests on the secondary beam support. This short direction is consider the grating span. The span is the smallest length and is the main panel size reference used in specification for procurement. In most cases, the grating has to be supported in the span direction only and does not require support on all four sides, unlike the floor plate.

Table 3.13 Grating design checklist.

Item to be checked	Yes/no
Grating to be removable	
Vibration performance required	
Corrosive environment	
Grating over stainless steel grating or piping	
Panels to be sized to facilitate fabrication	
Weight and size limitation defined	
Impact or high local load	
Loads meet the design requirement	
Special operating loads to be considered	
Grating match with the required strength	
Grating within the allowable deflection limit	
Suitable corrosion protection specified	
Antislip surface specified	
For fiber reinforced polymer (FRP) the fire performance requirements were specified	
For FRP the smoke and toxicity requirements were defined	
Grating slope is acceptable	
Adequate lateral restraint was provided	
Tolerance was checked	
Support arrangements provide adequate support at penetrations and cut-outs	
There is an isolation between different materials	

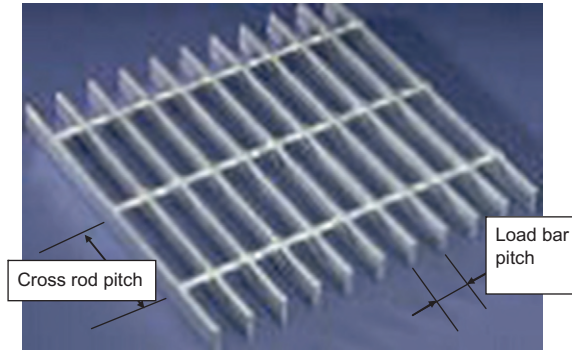

Figure 3.42 Grating dimensions.

The different grating dimensions are shown in Fig. 3.42 and the different types of grating are shown in Fig. 3.43.

There is a relation between the span and the deflection. When the grating is selected from the manufacturer, their type and calculation should be referred to. To illustrate a grating sheet based on its type and loads, Table 3.14 has been arranged

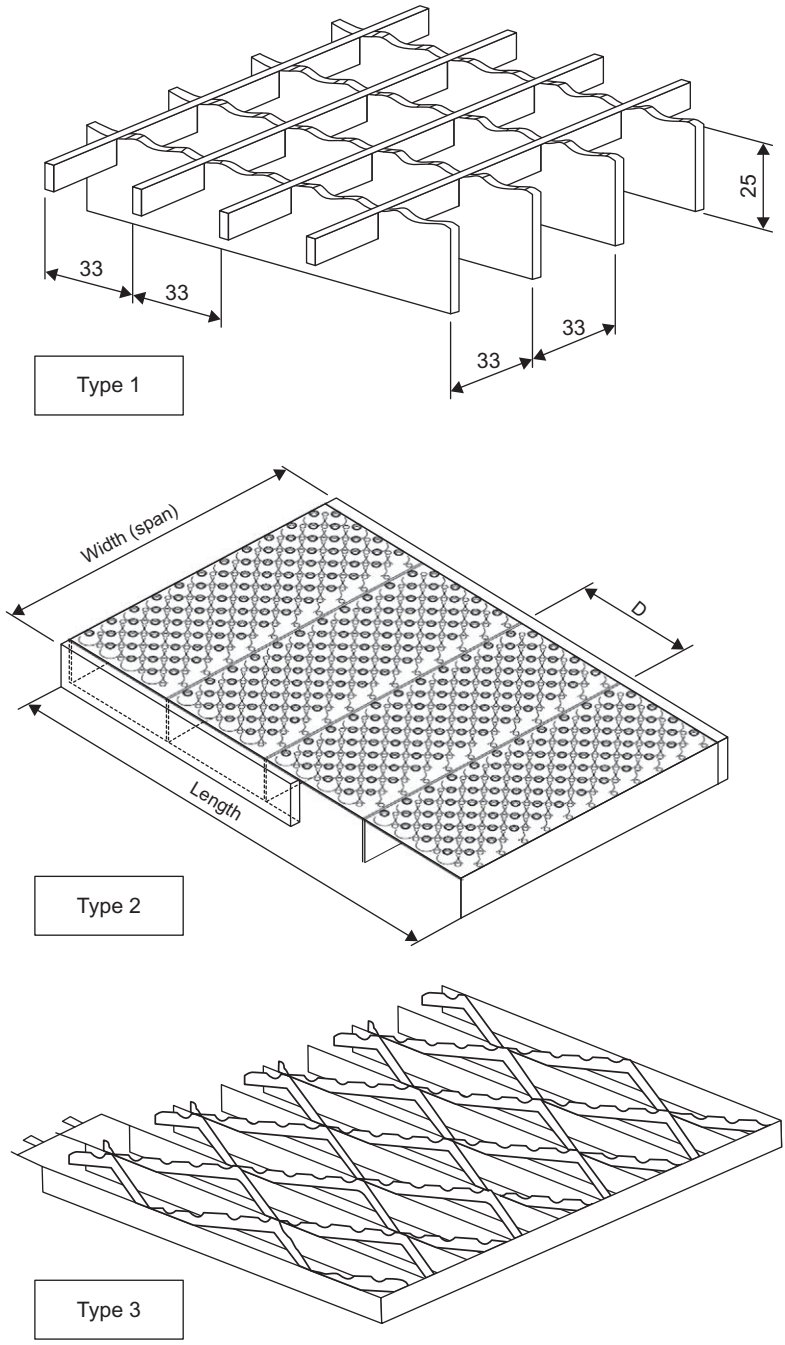

Figure 3.43 Types of grating.

Table 3.14 Relation between grating dimensions, maximum span, and maximum load.

Type	Load bar spacing (mm)	Cross bar pitch	Weight (kg/m^2)	Bar size	Load (Kpa)	Spacing between supports (mm)								
						450	600	750	900	1050	1200	1500	1800	2100
	40	100	17.5	25 × 3	L	53	30	19	13	10	7	5	3	2
					D	1.4	2.6	4	5.8	7.8	10.2	16	23.1	31.5
	60	50	22.3	25 × 5	L	56	32	20	14	10	8	5	3	2
					D	1.4	2.6	4	5.8	7.8	10.2	16	23.1	31.
	40	100	26.9	25 × 5	L	70	39	24	17	13	9	6	4	3
					D	1.6	2.9	4.5	6.5	8.8	11.5	18.0	25.9	35.3
	30	100	22.8	25 × 3	L	70	39	25	17	13	10	6	4	3
					D	1.4	2.6	4	5.8	7.8	10.3	16.0	23.1	31.5
	60	50	26.4	32 × 5	L	76	43	27	19	14	11	7	5	3
					D	1.2	2.2	3.4	4.9	6.7	8.7	13.6	19.7	26.8
	30	100	34.7	25 × 5	L	91	51	33	23	17	13	8	6	4
					D	1.6	2.9	4.5	6.5	8.8	11.5	18.0	25.9	35.3
	40	100	34	32 × 5	L	120	67	43	30	22	17	11	7	5
					D	1.2	2.2	3.4	4.9	6.7	8.7	13.6	19.7	26.8
	30	100	28.4	32 × 3	L	114	64	41	28	21	16	10	7	5
					D	1.1	2	3.1	4.5	6.1	8.0	12.5	18.1	24.6
	40	100	42.1	40 × 5	L	226	127	81	56	41	31	20	14	10
					D	0.9	1.6	2.5	3.6	4.9	6.4	10.0	14.4	19.7
	30	100	62.9	45 × 5	L	377	212	135	94	67	52	33	23	17
					D	0.8	1.4	2.2	3.2	4.3	5.7	8.9	12.8	17.5

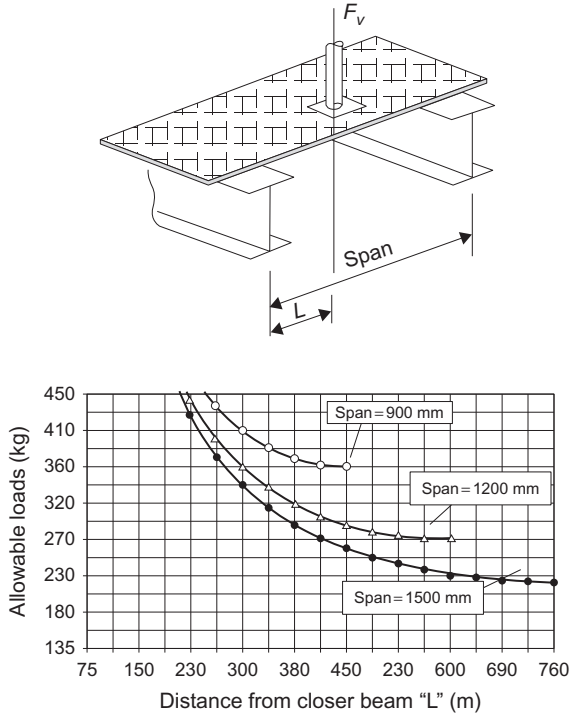

Figure 3.44 Relation between allowable loads and location of pipe support for different spans.

in increasing strength order. The load, L, is a safe superimposed uniformly distributed load in kPa (100 kg/m^2 = 0.98 kPa), where D is the deflection (in mm) for L. Loads are calculated in accordance with an allowable bending stress of 171.6 MPa. Note that the load bars are assumed to be simply supported.

Sometimes pipe support will form a concentrated load on the grating, as shown in Fig. 3.44; in this situation, the pipe support is usually a base plate resting directly on the grating, and there is no steel under the support.

3.8.2 Handrails, walkways, stairways, and ladders

Handrails, walkways, stairways, and ladders should be designed in accordance with OSHA 3124.

Handrails should be provided around the perimeter of all open decks and on both sides of stairways. All handrails should be 1.10 m high and made removable in panels no more than 4.5 m long. Handrail posts should be spaced 1.5 m apart. The gap between panels should not exceed 51 mm. Handrails shall be designed for the extreme maximum wave if located in the wave zone.

The load combination that shall be used in designing the walkways, stairways, and landings is as follow:

1. Dead load + live loads;
2. Greater of (dead loads + wind) or (dead load + maximum wave at storm).

It is important to use a double runner with serrated bar grating treads and handrails for the stairs.

3.9 Boat landing design

The boat landing is designed for the impact load from a vessel or boat to the offshore structure. To absorb the impact load, there is usually a fender attached to the boat landing; the fender can be a car tire or a special tire. The connection between the boat landing frame structure and the platform jacket will be through a shock absorber, such as a piston. Fig. 3.45 shows the general configuration for a boat landing and its main component.

Fig. 3.46 shows the boat landing connection to the offshore structure leg as this mechanism is traditionally used to absorb the impact load.

Fig. 3.47 shows the shock cell.

The barge bumpers and their associated connections to the jacket should be designed for the loading incurred by vessel impact directly in the middle third of the height of the post. Energy to be absorbed in the system should be 560 kJ.

Barge bumpers should be designed to be easily replaced in case of damage. During the detailed design phase, the details considered will include the jacket elevation tolerances. In lieu of specific data, a minimum installation tolerance on a jacket elevation of ± 0.3 m will be adopted.

For stab-in guides and bumpers, the following should be considered:

- The aids should be designed so that they fail prior to permanent deformation of any part of the permanent structure. The permanent structural members should be designed so that they can withstand significantly more load than the aids;
- Any deflections must be within the elastic limit of the material;
- A 33% overstress increase in allowable member stresses is permitted.

3.9.1 Boat landing calculation

The calculation of collision force is based on a 1000-ton boat impacting at a velocity of 0.5 m/s using Regal shock cell model SC1830.

Note that the forced applied to the boat landing frame has to be defined and then the stresses calculated on the frame by the software to start the design.

$$m = (1000 \times 9810) \times 2200/2000(9.81 \times 1000) = 1100 \text{ kN} \cdot \text{s}^2/\text{m}$$
$$\nu = \text{approach velocity} = 500 \text{ mm/s}$$
$$E = \tfrac{1}{2} \times 1100 \times (500)^2 = 13.75 \times 10^7 \, N/\text{mm} = 13.75 \text{ kN}/m$$

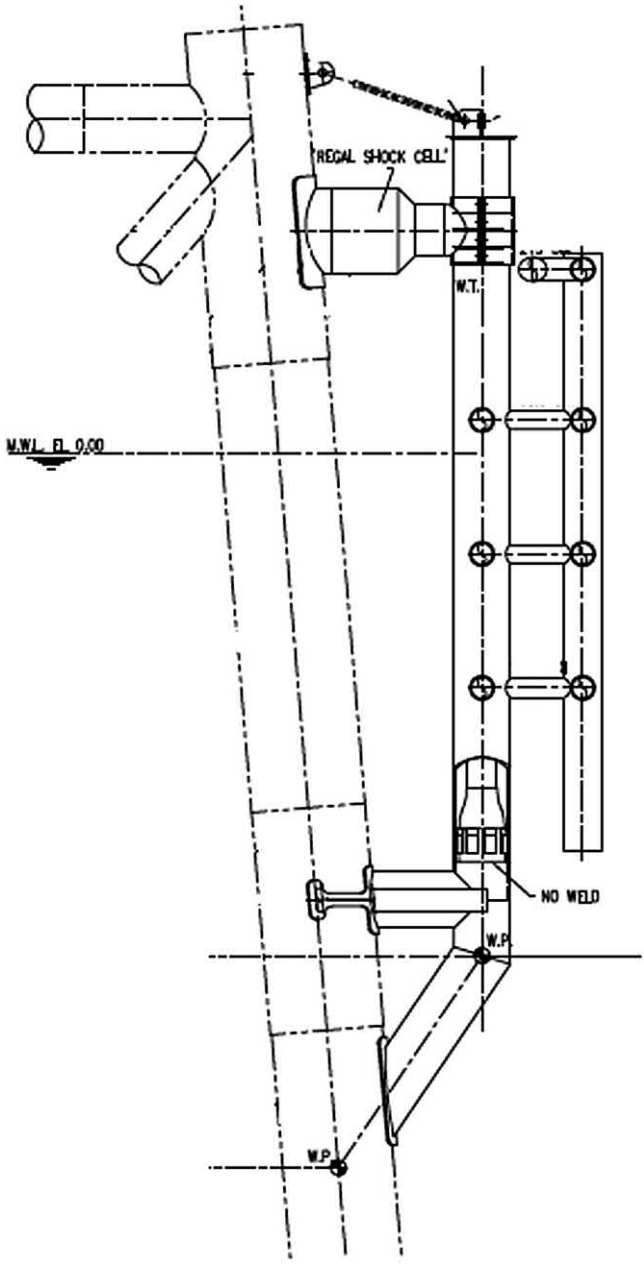

Figure 3.45 Boat landing support.

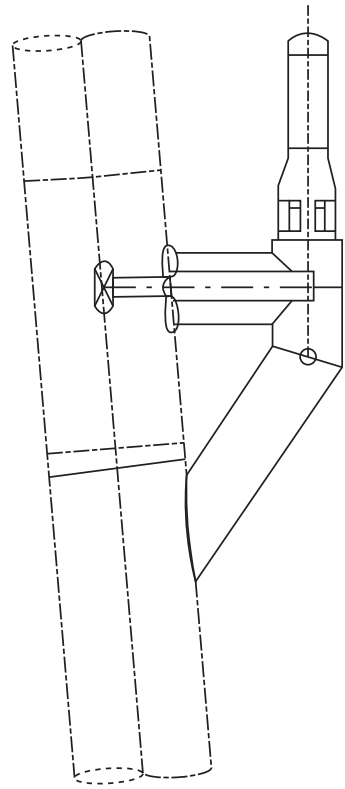

Figure 3.46 Connection between the leg and the boat landing.

Figure 3.47 Photograph of a shock cell.

From the shock cell type, choose the suitable curve for the relation between the energy versus deflection curve, as shown in Fig. 3.48.

$\delta = 360$ mm for $E = 13.75 \times 10^7$ kN/m

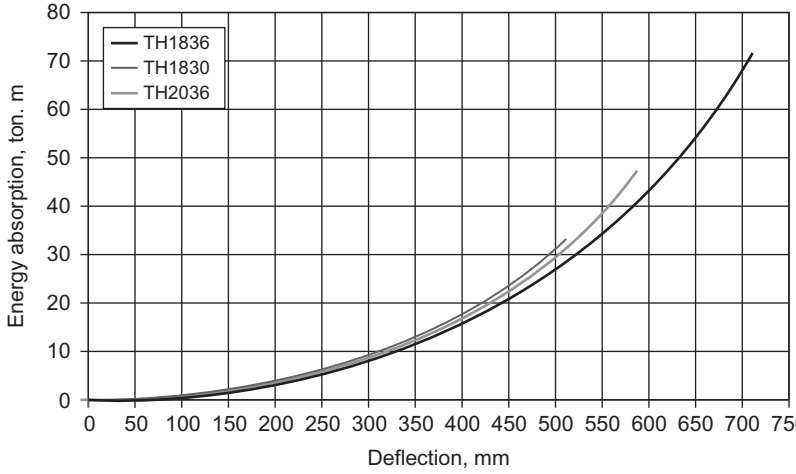

Figure 3.48 Energy absorption versus deflection.

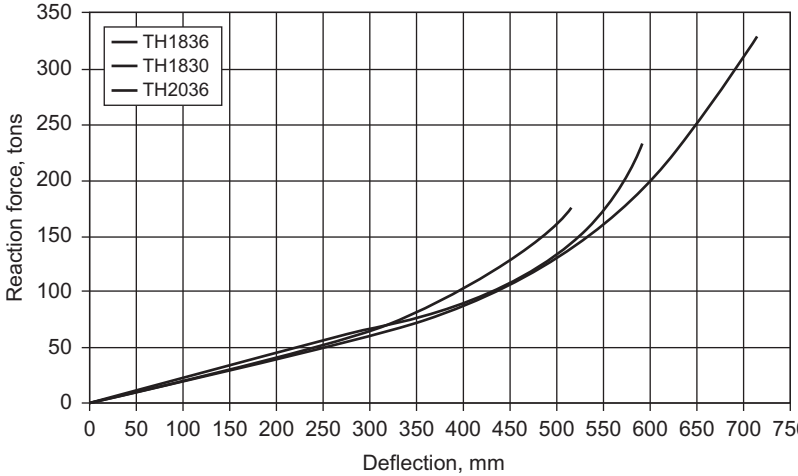

Figure 3.49 Reaction force versus deflection.

The force versus deflection is based on the model curve shown in Fig. 3.49.

$F = 70$ tons $= 686.6$ kN

Some of the energy is absorbed by the vessel (assume 30% absorbed by the vessel and 70% absorbed by the structure).

$E = 13.75 \times 10^7 \times 0.7 = 9.63 \times 10^7$ kN/m
$\delta = 300$ mm
$F = 510$ kN

This force will not be concentrated at one point because collision occurs across a considerable area, depending on the dimensions of the vessel and its position during impact and also because the fender system distributes the load.

Cases of impact load

Fig. 3.49A and B presents the configuration of the structure of the boat landing and the boat impact length is L, and defined in a certain level in Fig. 3.49A and assumed affect in two level as in Fig. 3.49B.

$F = 9.81 \times 10^5$ N
$L = 5560$ mm (assumed)

Case 1: Uniform load at mid-span at elevation (+) 300 mm, where uniform load = $F/L = 510/6000 = 85$ kN/mm (see Fig. 3.50a).

Case 2: Uniform load at mid-span at elevation (−) 900 mm, with the same values as in case 1 but applied at level −900 mm.

Case 3: Uniform load at mid-span at elevation (+) 0.3 m and elevation (−) 0.9 m, where uniform load = 0.5 $F/L = 42.5$ kN/mm (see Fig. 3.50b).

Case 4: Assume impact load distributed as a concentrated load at the mid-span at elevation (+) 300 and elevation (−) 900 (six concentrated loads), where force at each joint = $F/6 = 510/6 = 85$ kN.

3.9.2 Riser guard design

The riser guard design will be the same as that for the boat landing, but a shock cell is not required because boats rarely accidentally collide with the riser guard. Therefore the design is based on plasticity, and the member of the riser guard is designed to reach the plasticity limit in case of accidents, to have a minimum cross-section to reduce the lateral load effect, and on the other hand the design should consider that maximum deformation of the riser guard should not affect the risers in the case of an accident.

Using a tubular member 12.5 inch × 0.5 inch (323.9 × 12.7 mm), $F_y = 240$ N/mm^2 (mild steel).

Fig. 3.51 presents the situation of the plasticity as all the pipe cross-section will be under yield stress.

The plastic modulus = 70.2 inch^3 = 1,150,371.9 mm^3 and $M_p = 240 \times 1{,}150{,}371.9/1000 \times 1000 = 276.09 \times 10^6$ kN/m.

The deformation of the riser guard is presented in Fig. 3.52.

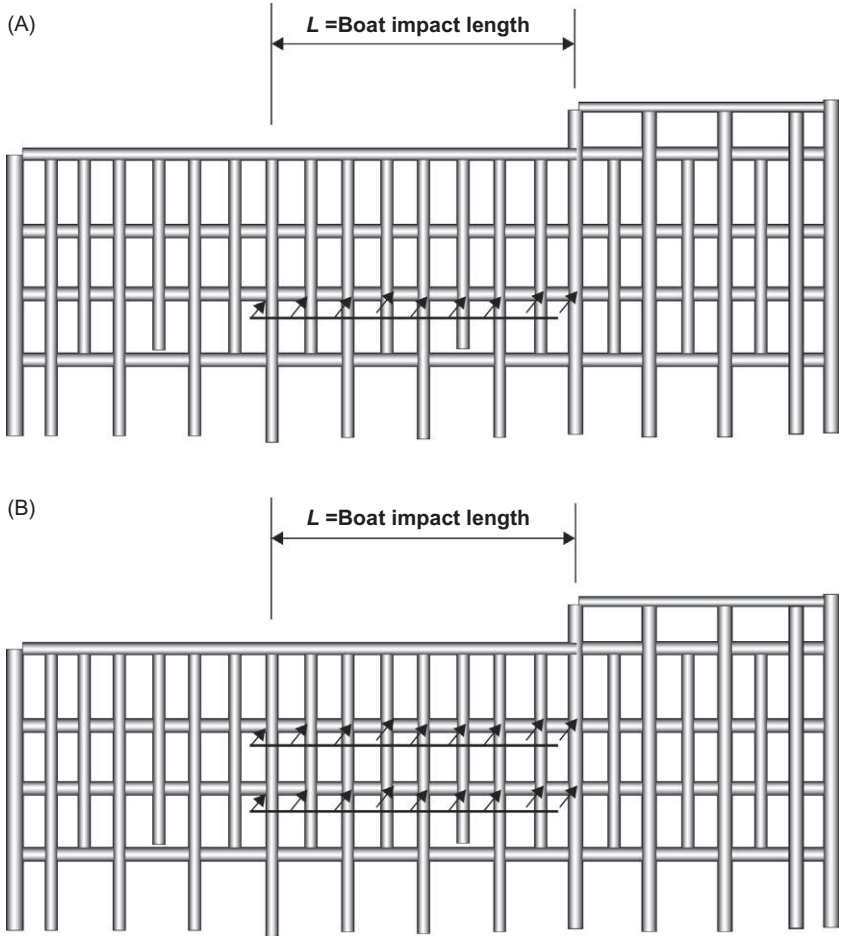

Figure 3.50 (A) Boat impact length (force in one level); (B) boat impact length (force in two levels).

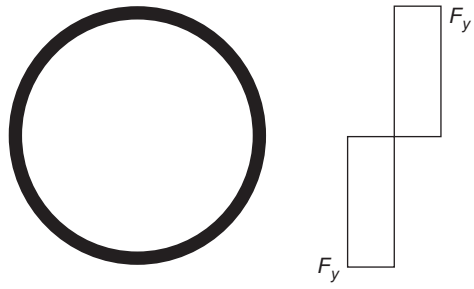

Figure 3.51 Member at plastic moment.

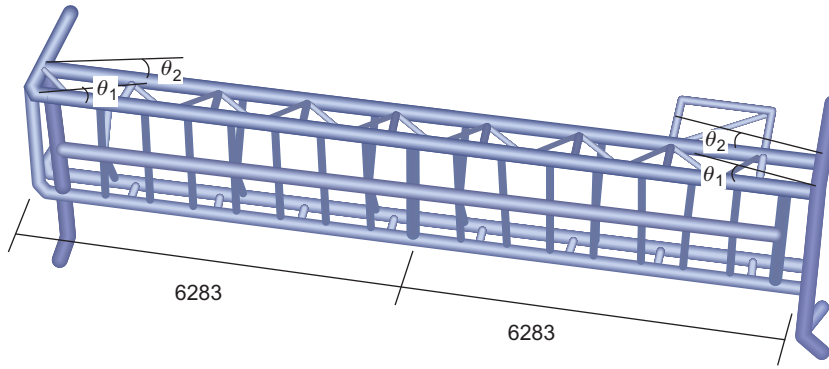

Figure 3.52 Proposed deformation of riser guard.

$$P \times \delta = 5 \times M_p \times (\theta_1 + \theta_2)$$
$$\theta_1 = \theta_2 = \delta/6283$$
$$P \times \delta = 5 \times 276.09 \times 10^6 \times 2 \times \delta/6000$$
$$P = 4.6 \times 10^5$$
$$E = 0.9 \times 4.6 \times 10^5 \times \delta = 0.5\, mv^2 \times 0.7$$
$$V = 500 \text{ mm}/s$$
$$m = 1100 \text{ N} \cdot \text{s}^2/\text{mm}$$
$$E = 0.7\ (1/2)\ 1100\ (500)^2 = 0.9 \times 4.7 \times 10^5 \times \delta$$

The 232 mm deflection is less than the distance between the outside diameter of the risers and the rear face of the riser guard.

Cases of impact load

Load case A: Uniform load at mid-span elevation 0.0 (MWL), with $L = 7$ m (assumed), uniform load = 65.7 N/mm.

Load case B: Uniform load at mid-span at elevation (+) 1.2 m and elevation (−) 1.2 m, so the total load will be distributed to two levels, such that the applied uniform load will be uniform load = 32.9 N/mm (for each elevation).

3.9.3 Boat landing design using the nonlinear analysis method

In some studies, boat landing and riser guard design is done by the nonlinear analysis method, which depends on the strain and denting that will occur on the boat landing member. This analysis is usually performed by special nonlinear analysis software and the member size is reduced as much as possible to reduce the wave load effect on the platform.

A nonlinear analysis is normally used to study the behavior of the platform due to the impact of a 3500-MT vessel at a velocity of 1 knot. The impact energy is calculated and the model analyzed using software. Resizing the boat landing members

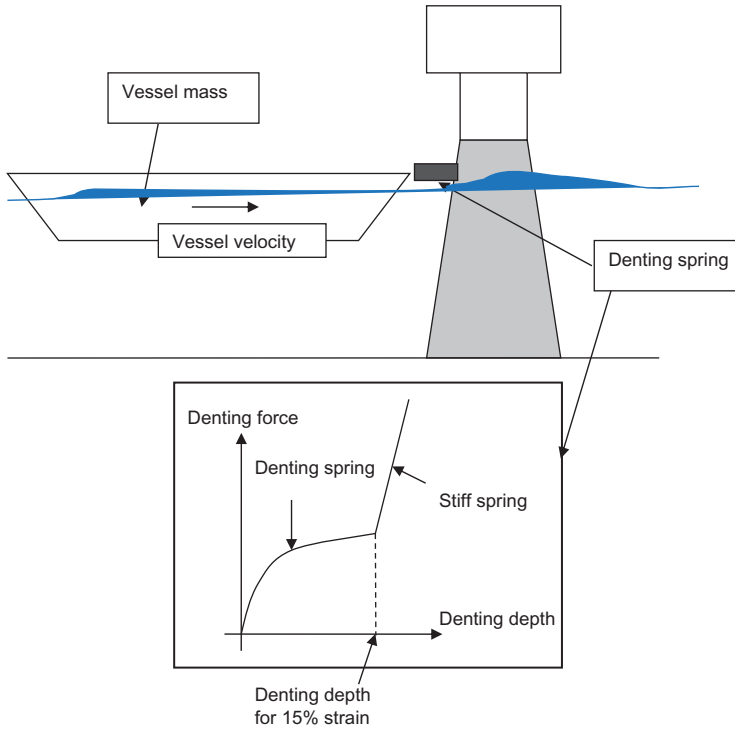

Figure 3.53 Denting of the member of a riser guard.

allows the impact energy to be absorbed and the results show the impact force and formulation of the plastic hinges on the members.

Comparison of the two methods by applying dynamic boat impact analysis shows that dynamic and static (energy) boat impact analyses give a similar impact force for a fixed offshore jacket, and a static boat impact analysis is sufficient for the jacket boat impact analysis. Denting of the member is presented in Fig. 3.53.

3.9.4 Boat impact methods

The static boat impact method utilizes the impact energy to calculate an impact load that is incremented until the impact energy has been dissipated. The fracture control is used in the software to monitor the strain in the members as energy is progressively applied. When the specified strain of 15% is reached in a member, that member is removed and the loading is redirected to other members. If no other load path can be found, the analysis is terminated.

In the dynamic method, the ship is modeled as a mass point connected to the platform through a nonlinear spring. The mass representing the ship is given an initial velocity corresponding to the impact speed and the analysis is carried out as a free vibration problem. The ship force unloads once the spring starts to elongate,

that is, the ship and platform move away from each other. When the contact force has vanished, the ship's mass is disconnected from the model. The dynamic impact analysis is a nonlinear, step-by-step analysis.

For dynamic analysis, the vessel mass and velocity were modeled; at first, the results show a higher (20%−30%) impact load in dynamic impact analysis than in the static impact condition. Referring to the static impact results reveals that a major portion of the impact energy is absorbed by the denting of the tubular member and the software usually automatically models the denting progress of a pipe during a static impact. The effect of denting is also very important in a dynamic boat impact analysis: in impact between two bodies, the duration of the impact directly affects the impact load. A softer surface in the impact increases the impact time and reduces the impact force. Denting behavior is like a soft spring and makes the impact condition a "soft impact," so it reduces the impact load.

We can use the API formula for modeling a denting spring. According to API RP2A-WSD (21st edition):

$$P_d = 40F_Y t^2 \left(X/D\right)^{0.5} \tag{3.146}$$

where P_d is the denting force and X is the denting depth. F_y, t, and D are the yield stress, wall thickness, and diameter of the denting member, respectively.

This formula gives us the relation between denting depth and denting force, and it can be modeled in the software as a nonlinear spring.

After modeling the denting springs, the impact load in the dynamic analysis is reduced and is around 5% less than the static impact load. In some cases, the impact analysis has been done for 12 and 55 m water depth jackets, and after modeling of the denting, the dynamic impact analysis gave an impact load similar to that in the static impact analysis.

The dynamic impact simplified model is shown below.

3.9.5 Tubular member denting analysis

Denting of a tubular member has a complicated behavior and there are few formulas to describe the relation between denting force, denting depth, and denting energy, some of which are presented in the API RP2A standard. The important question is that, in order to define how much a dent can progress in a tubular member, we need to define the maximum allowable strain in a tubular member; usually this value is 15% in an impact analysis. Therefore the question becomes, how much is the maximum denting depth that causes 15% strain in a tubular member?

The first solution is to model the tubular member in a finite element method (FEM) and to check the strain in the dented tubular member; this was done for a 20-inch tubular member. The relation between denting load and denting depth in the FEM analysis is very close to the API formula. This solution requires extensive time for modeling the tube in FEM, so a simplified solution is needed, such as the one described below.

Referring to FEM deformed shapes, we can conclude that denting deforms a circular shape to approximately an oval shape as shown in Fig. 3.54, and the maximum stress and strain happens at the sides of the deformed tubular as shown in Fig. 3.54, where the radius is minimal.

For simplified calculation of the strain at the critical zone of the oval, we need to find the geometry and minimum radius of the oval. The main assumption is "the circumference of the circle tubular and deformed elliptic is similar." After finding the oval's minimum radius, the strain can be checked against 15% strain to calculate the denting limit. A simplified method for the denting limit calculation is presented in the following section.

This method is valid only for boat landing members with bending behavior. For checking accidental impact on the jacket members (e.g., legs) with axial loads, the simplified method is not valid and more detail analysis needs to be done.

Simplified method for denting limit calculation

The denting calculation will be calculated based on converting the circle shape of the member to an oval after impact load as shown in Fig. 3.55.

The circle's perimeter is

$$P_c = 2\pi R \tag{3.147}$$

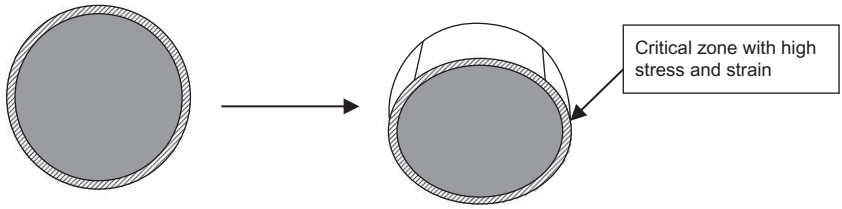

Figure 3.54 Critical zone for a denting member.

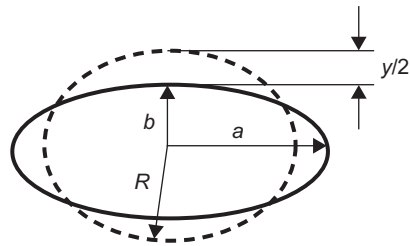

Figure 3.55 Calculation parameter.

The ellipse's perimeter has a different equation and the following equation has a higher accuracy.

$$P_e \cong 2\pi\left(\frac{a^{1.5}+b^{1.5}}{2}\right)^{2/3} \tag{3.148}$$

Note that in the case of denting of the cylinder section, the perimeter of the circle will be the same after denting and will be like the ellipse.

$$\begin{aligned} &2\pi R = 2\pi\left(\frac{a^{1.5}+b^{1.5}}{2}\right)^{2/3} \\ &a = (2R^{1.5}-b^{1.5})^{2/3} \end{aligned} \tag{3.149}$$

where y is the dent distance

$$b = R - y/2 \tag{3.150}$$

Knowing the dent distance y and the radius of the section R, we can obtain b from Eqs. (3.149) and (3.150).

By assuming that the coordinate system has the origin at ellipse's center

$$\frac{x^2}{a^2} + \frac{y^2}{b^2} = 1$$

We need the radius of curvature at $(x,y) = (a,0)$, which is actually found using calculus. Radius of curvature R is:

$$R = \frac{[(x')^2+(y')^2]^{1.5}}{x'y'' - y'x''} \tag{3.151}$$

where the x and y coordinates can be parameterized as

$$\begin{aligned} &x(\tau) = a\cos(\tau), y(\tau) = b\sin(\tau) \\ &x'(\tau) = -a\sin(\tau), y'(\tau) = b\cos(\tau) \\ &x''(\tau) = -a\cos(\tau), y''(\tau) = -\mathbf{b}\sin(\tau) \end{aligned}$$

Plugging these into the expression for R gives us

$$R = \frac{[a^2\sin^2\tau + b^2\cos^2\tau]^{1.5}}{ab[\sin^2\tau + \cos^2\tau]}$$

at $\tau = 0$, $R_{\min} = b^2/a$.

Fig. 3.56 presents the strain ε in the tubular section due to denting.

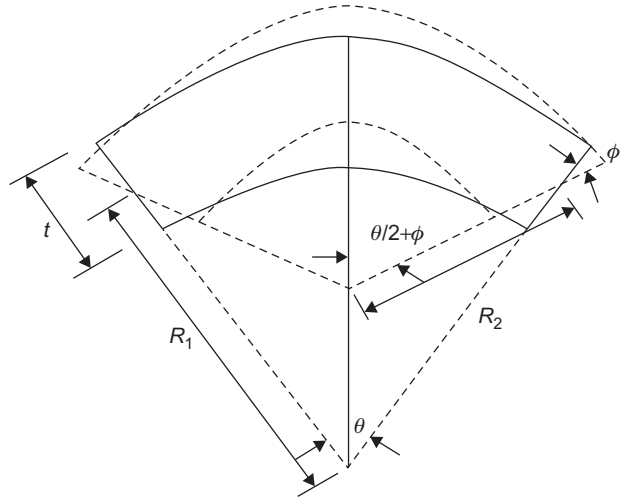

Figure 3.56 Strain to the denting member.

$$\varepsilon = \frac{\phi \cdot t/2}{R_1 \cdot \theta/2} = \frac{t}{R_1} \cdot \frac{\phi}{\theta}$$
$$R_1\theta = 2(\theta/2 + \phi)R_2$$
$$\phi = \theta/2\left(\frac{R_1}{R_2} - 1\right) \tag{3.152}$$
$$\varepsilon = \frac{t}{2R_1}\left(\frac{R_1}{R_2} - 1\right)$$

Nonlinear finite element method analysis

Figs. 3.57 and 3.58 present the FE analysis for a pipe 20 inches in diameter with a 0.625 inch thickness. The figures show the effect of a collision of a plate and the pipe by using FE analysis. The stress and strain contour is presented in the figures and the location of higher stresses. From the figures the final stage of failure was caused at a strain value of about 0.15.

3.10 Riser guard

The riser guard consists of a tubular steel space frame that provides the jacket face between elevations +2.5 m lowest astronomical tide (LAT) and −2.5 m (LAT) to protect the riser from boat collisions or any accidents that may occur. The riser guard should be designed to resist a collision of an equivalent static force acting

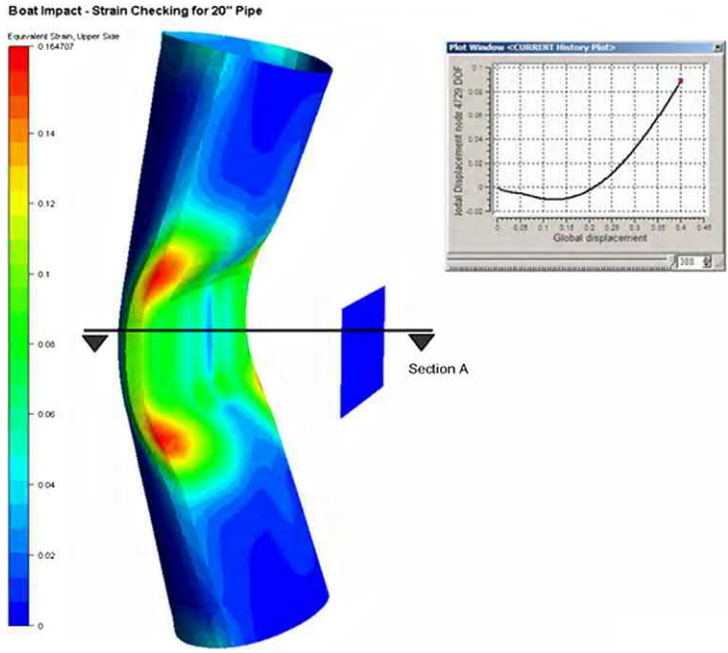

Figure 3.57 Strain contour for 400 mm displacement with maximum strain of 16%.

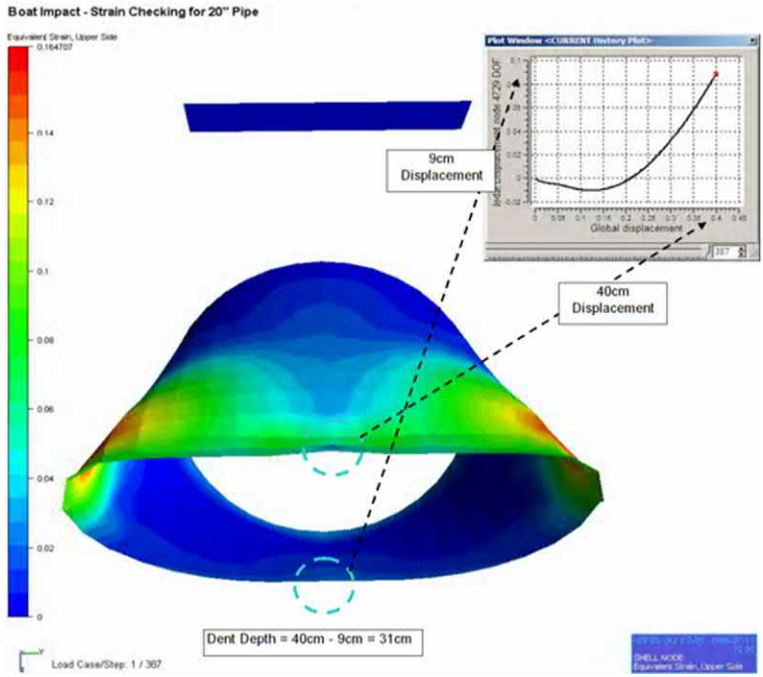

Figure 3.58 Strain contour in transverse direction.

anywhere on the frame. The said equivalent static force has to be defined by the client or by engineering and approved by the client. This force has to be mentioned in the project premises specification.

A static in-place analysis of the riser guard should be performed using a structural computer program. The model geometry should include all the structural members of the riser guard.

The structural dead loads should be generated by the computer program based on geometry and member properties.

Several load cases should be investigated in the analysis for the equivalent static force. For each case, the program should calculate reactions, deformations, and member forces and should check all members for compliance with AISC Code. A 33% stress increase is allowed for all load cases.

3.11 On-bottom stability

During the installation phase the jacket shall be set on the seabed until driving the pile. Therefore it needs some sort of on-bottom stability study and this stability is the main challenge to define the dimensions and the system of the mudmat to withstand the wave load until driving the pile. Fig. 3.5 presents the horizontal bracing and the mudmat at the lowest level.

The design of the mudmat depends mainly on the geotechnical investigation as described in Chapter 4, Geotechnical data and pile design. The design of the mudmat depends on these data to obtain an economic design and to maintain the safety of the structure during the installation phase.

Soil boring shall be achieved in this location for depths of around 10−20 m from the sea bed.

The bearing capacity of the soil shall be obtained and the structural engineer shall do a trial between the leg extension and the size of mudmat considering that the dimension of the mudmat is affected by the data of the bearing capacity, so in this case the scope of the geotechnical study includes different scenarios of mudmat size to be considered to cover later the alternative designs to reach an optimum solution. The main driver for designing the mudmat is it shall resist the weight of the jacket in addition to sliding and overturning.

According to the API code, the bearing capacity analysis should take into account the combined effect of vertical, horizontal, and moment loading. More heavily loaded mudmats may experience a lowering of soil stiffness, which can allow load to be transferred to other mudmats.

The safety factors against bearing-capacity failure recommended herein are 2.0 for on-bottom gravity loads alone and 1.5 for the design environmental condition applicable for the installation period.

It is important to consider that sometimes there are delays in the piling process for a number of reasons so the design should be adequate to resist overturning, sliding, or soil failure, on the other hand, the steel allowable stresses are permitted to increase about 33%.

In the case of weak top soil it is very important to study the settlement as a simple method comparing between the ultimate bearing capacity of the soil and the applied pressure so if there is an adequate FoS it will be sufficient but for a critical case a specific settlement study is needed.

A check list for on-bottom stability analysis is given in Table 3.15.

3.12 Bridges

In cases where two or more platforms are forming a complex or in the case where separate installations are built to support a helideck or a flair, bridges may be required to connect the different structures.

The bridge should be designed to resist the following loads:

- Self weight of the bridge;
- Uniformly distributed live load equal to 250 kg/m^2 of the walkway area;
- All piping loads carried by the bridge, if any;
- Wind loads acting directly on the bridge;
- Maximum imposed relative displacement between the bridge ends due to the environmental level loads acting on the two structures connected by the bridge;
- Thermal effect due to temperature changes.

The bearings of the bridge should be designed to allow for the expected displacements and rotations. Normally, the bearings at one end should be hinged, allowing only for rotation. The bearings at the other end should be free for sliding and rotation. Flurogold slide bearings should be adequate to specify the slide bearing.

The design of the bridge should account for a span tolerance of ± 1.0 m liable to result from possible mislocation of the supporting structures. Span length rectification should in this case be accounted for by a possible increase or decrease in the theoretical bridge span or by relocation of the bearings on the structure deck.

The bridge should have an upward camber equal to the deflection supposed to happen under dead loads.

Fig. 3.59 presents the hinge support for the bridge, where it can be seen that axial movement is prevented, which is opposite to the situation in Fig. 3.60, which shows the roller support that permits axial movement.

3.13 Crane loads

Normally, the deck crane is installed over a cylindrical pedestal extending to the required level of its fixation. The cylindrical pedestal may contain an inverted, truncated conical transition part in order to reduce the large diameter of the pedestal to the size of the deck leg where the pedestal should be connected.

The cylindrical pedestal, including the conical transition, should be checked for all crane loading conditions. The design engineer should verify that the loads

Table 3.15 Checklist for jacket on-bottom stability analysis.

Project:		
Client:		
Items	**Check point**	**Check (yes/no)**
I	Computer model	
1	It is assumed that the model is checked for dimensions, elevations, member group, and section properties in the in-service analysis and is upgraded to suit the current analysis. Check for LDOPT, OPTIONS, UCPART in the input file Model modifications to suit the current analysis (a) remove pile, appurtenances (b) revise C_d, C_m with member and group overrides as for clean members in the entire structure (c) Remove marine growth card from the input file (d) Check for flooded members and support conditions	
II	Loads	
1	It is assumed that the load calculations are verified in the in-service analysis and only relevant load cases are picked for the current analysis	
2	Wave parameters – installation wave conditions and directions	
3	Weight of lead and add-on pile sections (before driving in)	
4	Load contingencies	
5	Load combinations	
6	(a) Load combination without contingencies + environmental forces (b) Load combinations with lead piles in (1) Each leg, one at a time + environmental forces (2) All legs at the same time + environmental forces (c) Load combination with lead + add-on pile in (1) Each leg, one at a time + environmental forces (2) Two diagonally opposite legs at the same time + environmental forces (3) Two opposite legs at a time + environmental forces	
III	Analysis results	
1	Analyze for factor of safety (FoS) determination for sliding and overturning [translate model origin to match load center of gravity (CoG); basic load case summary is calculated]	
2	Analyze for FoS determination for bearing (translate model origin to match the mudmat CoG: combined load case summary is considered)	
3	Analyze for bearing pressure check on the jacket structure and mudmat	
4	Enclose sea-state summary (basic/combined load case summary)	
5	Enclose member check report; review overstressed members	

(*Continued*)

Table 3.15 (Continued)

Project:		
Client:		
Items	**Check point**	**Check (yes/no)**
6	Enclose joint check summary: review overstressed joints (check $F_y = \{2/3\}F_u$ for chords of high-strength members)	
7	Enclose member unity check ratio plot	
8	Enclose FoS calculations	
IV	Factor of safety and mudmat design	
1	FoS against sliding (>1.50)	
2	FoS against overturning (>1.50)	
3	FoS against bearing (>1.50 without environmental forces)	
4	FoS against bearing (>2.00 with environmental forces)	

Figure 3.59 Hinge support for the bridge.

supplied by the crane supplier are rated loads (i.e., including the dynamic amplification) according to the API 2C or Lloyd's Register rules for lifting appliances and that the wind load is considered in the load combinations.

In addition to the static analysis of stresses, a check for fatigue should be considered.

Stress analysis should be carried out according to API RP2A.

The static and dynamic crane loads should be based on data provided by the crane manufacturer.

Figure 3.60 Roller support for the bridge.

3.14 Lift installation loads

The lifting force calculation is mainly dependent on the weight of the lifting structure, the location and number of the padeyes which is related to the lifted structure configuration in addition to the angle between the vertical axis and the sling plus the angle between each sling, and the condition and environment condition during lifting.

In general, as a result of the static equilibrium between the lifting structure and tension force in the sling all the attached structures shall be checked in design based on that. API RP2A recommend adding a horizontal force equal to 5% of the static sling load which shall be applied perpendicular to the center of the hole at the padeye. This horizontal force is to cover any side movement effect during lifting on the padeye and lifting structure.

It is worth mentioning that all these design forces are applied as static loads if the lifts are performed in the fabrication yard.

In the case of doing the lifting by vessel offshore then the dynamic load factor shall be applied on the static calculated lifting forces. As per API RP2A a dynamic factor equal to 2.0 is considered in the case of doing the design of the padeye and all the members and any structure attached to the padeye. This factor is equal to 1.35 for all members transmitting the lifting forces. For shelter location and doing loadout these factors shall be 1.5 and 1.15.

Jacket, topside, and living quarters lift analyses (onshore and offshore) should be performed based on the requirements of DNV rules. All members and connections should be checked to API RP2A or AISC basic allowable stresses.

Table 3.16 Dynamic amplification factors.

	Gross weight (tons)			
	0–100	**100–1000**	**1000–2500**	**>2500**
Offshore lift	1.3	1.2	1.15	1.10
Onshore lift	1.15	1.10	1.05	1.05

It is worth mentioning that the weight contingency factor is a factor that allows for lift weight inaccuracies. For jacket structures, a minimum factor of 1.1 should be used unless the jacket is weighed at the end of the construction using load cells, in which case this factor may be reduced to 1.03. The weight contingency factor should be applied to the "net weight" and "rigging weight."

Dynamic amplification factors allow for the dynamic effects experienced during the lift. For typical jacket structures, the DAFs are as presented in Table 3.16.

Note that the DAFs for the offshore lift presented in Table 3.16 should be used for calm sea conditions ($H_s < 2.5$ m). If, for any reason, the lift is carried out in adverse conditions, the factor should be recalculated based on the expected accelerations associated with the sea state.

3.15 Vortex-induced vibrations

In fluid dynamics, vortex-induced vibrations (VIVs) are motions induced on bodies interacting with an external fluid flow and are produced by periodical irregularities in the flow.

A classical example is the VIVs of an underwater cylinder. If you put a pipe into the water and move it through the water in a direction perpendicular to its axis you can see this vortex.

During the movement there is a boundary layer formulated due to fluid viscosity and this slows down the fluid movement.

Due to excessive curvature the boundary layer shall be isolated from the body of the object.

As per the pressure distribution change along the surface, the vortex shall be formulated.

Due to the vortices formed nonsymmetrically around the body, different lift forces develop on each side of the body, thus leading to motion transverse to the flow. This motion changes the nature of the vortex formation in a way that leads to a limited motion amplitude.

The tubular members of the flare/vent booms should be checked for VIVs. If the members and booms are found to be dynamically sensitive, they should be checked for fatigue during detailed design.

The risers and conductors in the offshore platforms are affected by vortex as it is the main source of fatigue damage. These slender members are affected by the flow

of current and the top end vessel motions, these produce relative motion between the structure and the flow that cause VIV. It is important to mention that the vessel motion shall produce oscillation to the risers and as a result the flow profile appears unsteady.

The possibility of VIVs due to the design current velocity profiles should be considered for all appurtenances, including risers, sump pipes, caissons, and any individual members considered potentially susceptible.

One of the classical open-flow problems in fluid mechanics concerns the flow around a circular cylinder, or, more generally, a bluff body. At very low Reynolds numbers, according to the diameter of the circular member, the streamlines of the resulting flow are perfectly symmetrical, as is expected from potential theory.

The Strouhal number, named after Čeněk (Vincent) Strouhal, a Czech scientist, provides the relation between the shedding frequency, flow velocity, and the diameter in the case of a cylinder member.

The Strouhal number is defined as

$$\mathrm{St} = f_{st} D / U,$$

where f_{st} is the vortex shedding frequency or the Strouhal frequency of a body at rest; D is the diameter of a cylinder member; U is the ambient flow velocity.

The Strouhal number for a cylinder is 0.2 over a wide range of flow velocities. When the vortex shedding frequency comes close to the natural frequency of vibration of the structure, large and damaging vibrations can occur.

Unsteady flow patterns occur due to vortex shedding which is the result of passing the fluid flow, wind, and current to the structure member. This unsteady flow produces oscillations to the cylinder elements perpendicular to their longitudinal axis. These vortex-induced oscillations should be address.

Important parameters governing vortex-induced oscillations (VIOs) are geometry (L/D), damping ratio (ζ), mass ratio [$m^* = m/(¼\pi\rho D^2)$], Reynolds number ($\mathrm{Re} = uD/\nu$), reduced velocity ($VR = u/f_n D$), and flow characteristics [flow profile, steady/oscillatory flow, turbulence intensity (σ_u/u), etc.], where L is the member length (m); D is the member diameter (m); m is mass per unit length (kg/m); ζ is the ratio between damping and critical damping; ρ is fluid density (kg/m^3); ν is fluid kinematic viscosity (m^2/s); u is the average flow velocity (m/s); f_n is natural frequency of the member (Hz); and σ_u is standard deviation of the flow velocity (m/s).

The relation between type of shedding and Re is shown in Table 3.17.

Table 3.17 Relation between type of shedding and Reynolds number.

Periodic shedding	$10^2 < \mathrm{Re} < 0.6 \times 10^6$
Wide-band random shedding	$0.6 \times 10^6 < \mathrm{Re} < 3.0 \times 10^6$
Narrow-band random shedding	$3.0 \times 10^6 < \mathrm{Re} < 6.0 \times 10^6$
Quasi-periodic shedding	$\mathrm{Re} > 6.0 \times 10^6$

3.16 Helideck design

The loads affecting the helideck are discussed in Chapter 2, Offshore structure loads and strength.

- Helidecks are designed in accordance with API RP2A and API RP2L.
- The layout of the helideck should be sufficient for one helicopter.
- One stair for primary access and a ladder for secondary access are required.
- Safety netting should surround the helideck completely, at a minimum width of 1500 mm.
- Paint markings, sizes, and colors are in accordance with API RP2L.

The helideck may have a separate platform, in some cases in old designs this is on the bridge direct but in this case, it shall have special consideration in maintenance and for any change on load.

According to CAP437, the following dimensions should be considered.

The safety net's main function is for personnel protection. Based on that the safety net is located around the helicopter landing area. The safety net is designed to be flexible and should be from nonflammable materials and its edge below the edge of the helideck or at the same level and it should follow advice of the civil aviation authority that governs the rules of aviation in the country of the project. The safety net length is equal to 1.5 m in the horizontal plane, with an inclination upward of at least 10 degrees.

For the helicopter it should be a clear distance without any obstacles, and there are some limits from CAP437 as shown in Fig. 3.61

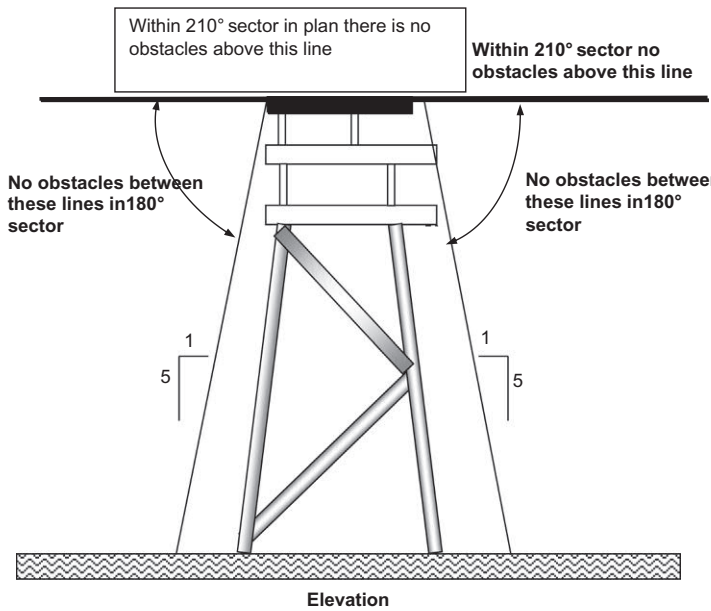

Figure 3.61 Limits of free obstacles below landing area level.

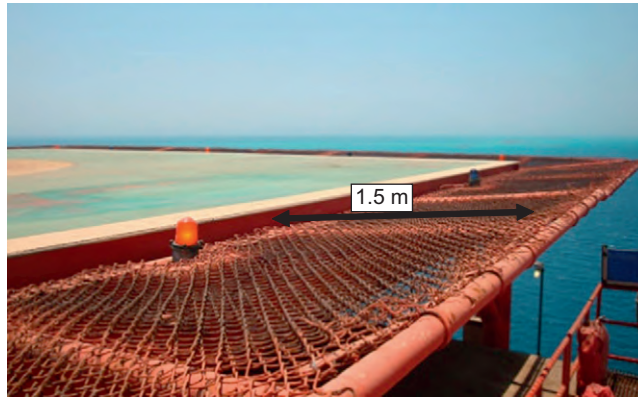

Figure 3.62 The main configuration of a traditional safety net.

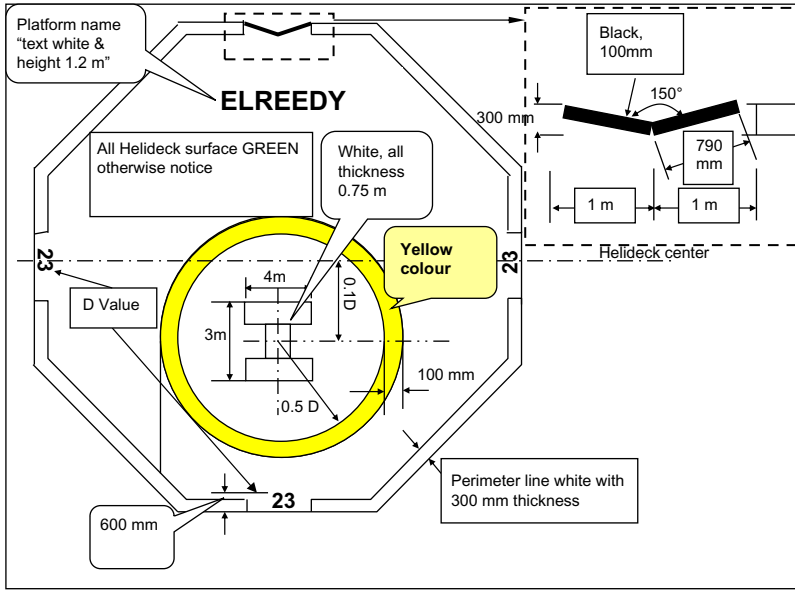

Figure 3.63 Helideck marking specifications and dimensions.

As per International Civil Aviation Organization (ICAO) and CAP437 the acceptance test for the safety net is by a falling object weighing 100 kg from a height of 1 m without any damage to the safety net. Fig. 3.62 presents a photo of a safety net.

For the helideck markings, the color of the helideck should be dark green or gray, as shown in Fig. 3.63. In addition, the perimeter should be clearly marked with a white painted line 300 mm wide.

Table 3.18 Helicopter weights, dimensions, and *D* value for different types as per CAP437.

Type	*D* value (m)	Max weight (ton)	Landing net size	Landing minimum size (m)
Augusta A109	13.05	2. 600	small	9 m × 9 m
Dauphin SA365N2	13.68	4.250	small	9 m × 9 m
Sikorsky S76B&C	16	5.307	Medium	–
Bell 212	17.46	5.080	Not required	–
Super puma AS 332L2	19.50	9.300	Medium	12 m × 12 m
Super Puma AS 332 L	18.70	8.599	Medium	12 m × 12 m
Bell 214ST	18.95	7.936	Medium	12 m × 12 m
SIKORSKY S61N	22.20	9.298	Large	15 m × 15 m
EH101	22.80	14.600	Large	15 m × 15 m
Boeing BV234LR Chinook**	30.18	21.315	Large	15 m × 15 m

Note: With a skid fitted helicopter the maximum height may be increased with ground handling wheels fitted.
Note:**The BV234 is a tandem rotor helicopter and in accordance with International Civil Aviation Organization (ICAO) the helicopter size is 0.9 of the helicopter *D* value, that is, 27.16 m.

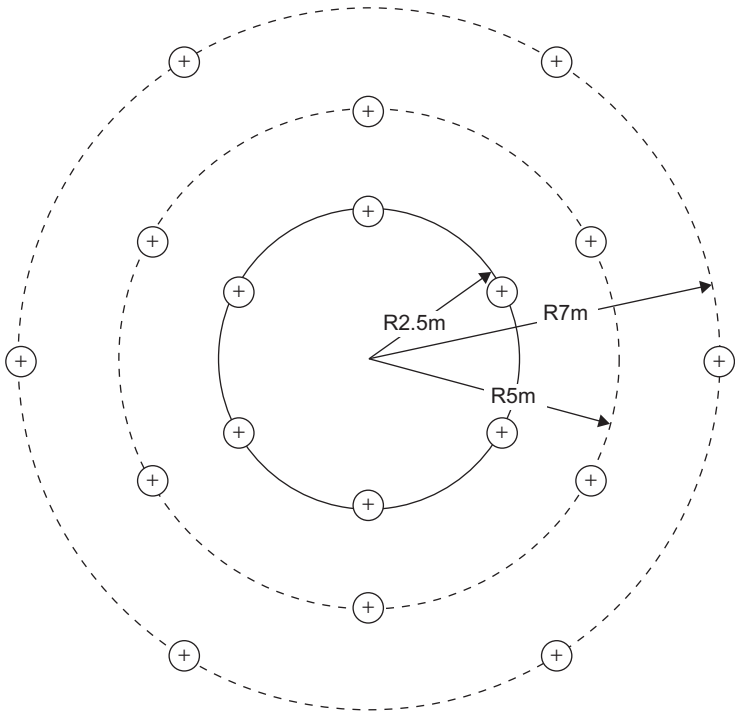

Figure 3.64 Suitable tie-down configuration.

Table 3.19 Checklist for jacket in-place analysis.

Items	Check point	Check (yes/no)
	Computer model	
1	Framing dimensions according to the drawings or sketches	
2	Framing elevations according to the drawings or sketches	
3	Water depth and mud line elevation match the basis of design (BOD)	
4	Member group properties: E, G, density match the BOD	
	(a) Section details, segment lengths, member offsets	
	(b) Corrosion allowance in splash zone	
	(c) Zero density for wishbone elements in ungrouted jackets	
	(d) Grout density corrections for grouted leg and pile	
5	Member properties: K_x, K_y, L_x, L_y	
6	Member end releases where applicable	
7	Flooded members (legs, risers, J tubes, caissons, etc.)	
8	Dummy members (relevant joints kept, rest deleted)	
9	Plate/membranes modeled correctly	
10	Boundary conditions	
11	Drag and inertia coefficients (smooth, rough members)	
12	Marine growth data as per BOD	
13	Member and group overrides	
	(a) No wave load and marine growth on piles and wish bones in jacket legs	
	(b) Enhancement of C_d, C_m for anode-supported members	
	(c) Enhancement of C_d, C_m for jacket walkway members	
	(d) Enhancement of C_d, C_m	
14	Hydrostatic collapse check selected with redesign option	
15	Allowable stress modifiers for extreme storm load cases	
16	Unity check ranges in the analysis input file	
	Loads	
17	Load description, calculations, and distribution	
18	Wave theory, wave, current, and wind directions (nonlinear current stretch with apparent wave period calculation)	
19	Equivalent C_d, C_m calculations for items mentioned above	
20	Load contingencies match the BOD	
21	Load combinations for operating and extreme cases	
22	Load summations	
23	Load summation verification against weight control data	
	PSI data and input file	
24	Units for T-Z, Q-Z, and P-Y data from the geotechnical data.	
25	Pile segmentation data, end-bearing area	
26	With reference to the input format, check T, Q, and P factors	
	Analysis results	
27	Enclose sea-state summary to be checked against load summation	
28	Enclose member check summary: review for overstressed members	

(*Continued*)

Table 3.19 (Continued)

Items	Check point	Check (yes/no)
29	Enclose joint check summary: review overstressed joints (check $F_y = 2/3F_u$ for chords of high-strength members)	
30	Check maximum pile compression and tension	
31	Enclose model plots: joints/group/section names, K_x, K_y, L_x, L_y, and loading	
32	Enclose deflection plots, member unity check ratio plots	
33	Enclose hydrostatic collapse check reports and check for need of rings	
34	Review pile factor of safety (FoS) calculations	
35	Review permissible deflection calculations	
36	Review plot plan and latest structural drawings	
37	Review relevant sections of weight control report	
	Dynamic in-place analysis (if required)	
38	Determine dynamic amplification factor (DAF) based on single degree of freedom (DoF) concept and apply on wave load cards	
39	Determine DAF based on inertia load distribution and apply on total structure	
	General	
40	Joint name range identified for each framing level and sequential	
41	Member group name specific to each framing level and sequential	
42	Check for future loads and loads due to specific requirement, such as rigless interventions	

BOD, basis of design; *DAF*, dynamic amplification factor.

Fig. 3.63 presents also the dimensions of the yellow circle and the *H* marking on the helideck.

The letter H on the helideck has standard dimensions, as shown in Fig. 3.63, and it is painted white.

Based on Cap437 the helideck netting dimension is dependent on the landing net size which is dependent on the helicopter type and the *D* value and maximum weight as shown in Table 3.18.

The helicopter should be tied to the helideck. This tie-down point should be located and be of such strength and construction as to secure the helicopter when subjected to weather conditions pertinent to the installation design considerations. The tie-down rings should match the tie-down strop attachments. Noting that, the maximum bar diameter of the tie-down ring should be 22 mm in order to match the strop hook dimension of the tie-down strops in most helicopters. Advice on the recommended safe working load should be obtained from the helicopter operator. Fig. 3.64 presents the suitable tie-down configuration noting that the outer circle is not required if the *D* value is less than 22.2 m. All the circle centers coincide with the centers of the marking circle which is shown in Fig. 3.64.

Table 3.20 Checklist for topside in-place analysis.

Items	Check points	Check (yes/no)
	Computer model	
1	Framing dimensions match with the drawings	
2	Framing elevations match with the drawings	
3	Member properties: K_x, K_y, L_x, L_y	
4	Member end releases where applicable	
5	Plate and membranes modeled correctly	
6	Boundary conditions	
7	Review the loads in the analysis input file	
8	Allowable stress modifiers for extreme storm load cases	
9	Unity check ranges in the analysis input file	
	Loads	
10	Load description and calculations	
11	Secondary structural item dead load calculations	
12	Equipment, piping operating, and dry load, E&I bulk load calculations	
13	Wind load calculations, wind area considered	
14	Earthquake load calculation	
15	Load contingencies	
16	Load combinations for operating and extreme cases	
17	Load combinations for local checks	
18	Load summations	
	Installation and preservice loads may be applied as a separate load case	
	Crane load cases may be magnified and applied for local checks	
19	Check for future loads and loads due to specific requirement, such as rigless interventions	
	Analysis results	
20	Enclose sea-state summary and check against load summation	
21	Enclose member check summary: review for overstressed members	
22	Enclose joint check summary: review overstressed joints (check $F_y = 2/3F_u$ for chords of high-strength members)	
23	Enclose model plots: joint/group/section names, K_x, K_y, L_x, L_y, F_y	
24	Enclose deflection plots, member unity check ratio plots	

3.17 Structure analysis and design quality control

An offshore structure is complicated and not an easy structure to design, so it requires many quality checks. One method is to use checklists to ensure that all factors are taken into account in the design.

Table 3.19 is a checklist for a jacket in-place analysis and Table 3.20 is a checklist for a topside in-place analysis.

Table 3.21 Report checklist.

Task		LE	AE	CE
Model set-up	Latest data/information used			
	Unique model/run name used			
	Geometry			
	Support conditions			
	Member effective lengths			
	Loads			
	Load combinations[a]			
	Line by line check of input file			
Self-checking	Review model geometry plots			
	Check load sums against load combination matrix			
	Program-generated loads reasonable (e.g., dead, wave, wind, etc.)			
Post-run verification	Review errors and warning messages			
	Check reaction totals match load combination matrix			
	Check deflections are consistent with expected loadings, storm directions, etc.			
	Check pile convergence, stresses, and safety factors			
	[b]Review member stresses			
	Review tubular joint stresses			
	Model and results saved on the server			
	All checks complete and satisfactory			

LE, lead engineer; *AE*, analyst engineer; *CE*, checking engineer.
[a]The combination between different loads to be every case of combination is one case of loading.
[b]For local design, hydrostatic test weights should be considered where applicable.

The calculation report delivered to the client should include, as a minimum, the following data:

- Calculation cover sheet;
- Contents page;
- Description of the analysis methodology and techniques;
- Explanation of the model geometry and axis system;
- Explanation of boundary conditions;
- Explanation of the input loads and any supporting calculations showing the development of the loads;
- Load combination matrix;
- Explanation of the stress analysis assumptions, including member effective length philosophy;
- Discussion of the results, including deflections, member stresses, joint stresses, reactions, pile capacities, etc.;
- Additional calculations supporting the results, including calculations showing the justification of overstressed members, etc.;

Attachments should contain the following:

- Any reference information used for the model;
- Drawings;
- Input files (including the model, pile soil interaction (PSI) input file, joint-can input, etc.);
- Model plots showing joint numbers and member groups. Member effective lengths, etc., may also be presented if required;
- Selected results, including reactions, summary of maximum member U_c, summary of maximum joint U_c, summary of maximum joint deflections, pile and safety factors, and other relevant results;
- Calculation checklist and any other checklist that ought to be included.

A summary report check list to be used by the lead engineer, analyst engineer, and checking engineer is given in Table 3.21.

References

American Petroleum Institute, 2007. Working Stress Design, API RP2A-WSD, 21 st Ed.

Dier, A.F., Lalani, M., 1995. Strength and stiffness of tubular joints for assessment/design purposes. In: Offshore Technology Conference. Paper OTC 7799, Houston.

Healy, R.E., Buitrago, J., 1994. Extrapolation procedures for determining SCFs in mid-surface tubular joint models. In: Sixth International Symposium on Tubular Structures, Monash University, Melbourne, Australia.

Kuang, J.G., Potvin, A.B., Leick, R.D., 1975. Stress concentration in tubular joints. In: Paper Offshore Technology Conference. OTC Paper No. 2205, Houston, TX.

Lloyd's Register of Shipping, 1988. Stress Concentration Factors for Tubular Complex Joints, Complex Joints JIP. Final Report No. 3 of 5 of Simple Unstiffened Joint SCFs.

Marshall, P.W., 1989. Recent Developments in Fatigue Design Rules in the U.S.A. Fatigue Aspects in Structural Design. Delft University Press.

Marshall, P.W., Toprac, A.A., 1974. Basis for tubular joint design. Weld. J. 53 (5), 192–201.

Marshall, P.W., Bucknell, J., Mohr, W.C., 2005. Background to new RP2A-WSD fatigue provision. In: Proceedings Offshore Technology Conference. Paper OTC 17295, Houston, May 2005.

MSL Engineering Limited, 1996. Assessment Criteria, Reliability and Reserve Strength of Tubular Joints. Doc. Ref. C14200R018, Ascot, England.

Niemi, E., et al., 1995. Stress Determination for Fatigue Analysis of Welded Components. IIW-1221-93. Abington Publishing, Cambridge.

Report for Joint Industry Typical Frame Projects, 1999. Bomel Engineering Consultants. Maidenhead, Berkshire, England.

Further Reading

EDI, 2003. SACS IV, User's Manual, Release 5.1. Published by SACS-Bentely, Exton.

International Organization for Standardization, 2004. Petroleum and Natural Gas Industries – Offshore Structures – Part 2: Fixed Steel Structures. ISO/DIS 19902:2004.

Yettram, A., Husain, H., 1966. Plane framework methods for plates in extension. J. Eng. Mech. Div. (ASCE) 91 (EM3), 53–64.

Geotechnical data and pile design

4

4.1 Introduction

The foundation design is the main part in the design of any structure system. The foundation design depends on the soil characteristics and type. The geotechnical investigation starts in early stage of the front end engineering design (FEED) or at the basic engineering as the structure system configuration depends mainly on the pile size. The offshore soil investigation is a different technique than the onshore soil investigation, and it also higher cost and takes a longer time as there are few companies worldwide that have the experience to carry out the offshore geotechnical investigation, which is not like the onshore soil investigation.

A fixed offshore platform consists of a topside and jacket structure, which is higher than seawater level and supported by relatively long piles, and this type of structure has been an industry standard for many years. Nowadays other types of structures are being built and many different designs are being proposed, as presented in Chapter 1, Introduction to offshore structures, and the soil investigation requirements and its depth depend on the type of structure, since they can vary considerably for different types of structures.

In traditional fixed offshore platforms, the soil investigation usually consists of a single boring sampled to a penetration below the expected pile-tip penetration depth.

4.2 Investigation procedure

The final design of a fixed offshore platform is based on the best soil field test data that can be obtained at the exact structure location. Therefore an accurate survey should be implemented with the soil investigation. In general, the soil data are usually needed well in advance of any construction at a site.

The marine vessel and drilling equipment that must be provided for conducting and supporting the soil investigation should have a mooring or positioning system and should be capable of drilling and sampling well below the maximum expected penetration of the piles. Furthermore, offshore soil investigation is characteristically more costly than similar work onshore, due to the cost of the marine vessel itself, as its fee is calculated per day, which is expensive.

Provision should be made for on-site determinations of pile capacity versus depth for the pile size proposed to be used in the structure. Thus, an adequate but not excessive depth of investigation can be ensured for the pile load anticipated.

Offshore Structures. DOI: https://doi.org/10.1016/B978-0-12-816191-3.00004-3

There is a main difference that should be kept in mind between onshore and offshore soil investigation as in the case of offshore the soil investigation depends on the vessel which is very costly.

Therefore the objectives of an investigation should always be kept in mind and the planning effort and selection of equipment and techniques should be aimed at achieving the objectives at the lowest cost. If there is leeway in scheduling of the work, the work can be undertaken in suitable weather; if there is no leeway, larger equipment may be needed to cope with more severe conditions. The drilling and sampling techniques must be adapted to the marine environment in order to produce the desired results within a reasonable time.

Once the desired field investigation has been completed, further investigation is needed in the laboratory to evaluate and obtain soil properties and to apply the field and laboratory results to the design problem.

It is appropriate to mention at this point that a fairly wide range of results can be obtained, particularly in the field, depending upon several factors. It is essential that the factors influencing the results be evaluated in interpreting the data and in applying the results to the design.

Offshore soil investigation provides useful information in connection with platform installation as well as design. An accurate water-depth determination, made in connection with obtaining a sample exactly at the seabed, gives the engineering office the required information, and high-quality samples and data near the seabed provide very useful information relative to jacket support before piles are driven, jacket leg penetration below the seabed and soil−pile interaction under lateral load.

The observations made during drilling and sampling should be recorded, because they can also provide some indication of potential problems in pile installation. The scope of work and execution of an investigation should encompass all possible elements important to design and construction.

4.2.1 Performing an offshore investigation

An investigation at sea must begin by identifying the location, which is ordinarily done by a survey boat. After the correct location has been established, a buoy may be dropped to mark the location for drilling. The survey vessel also assists in running the anchors for the drilling vessel. In most cases, while drilling and sampling are in progress, the survey vessel remains in the area to serve as an emergency stand.

Most offshore investigations done at the present time utilize self-propelled vessels, usually of the oilfield-supply class. Such vessels have adequate deck space and can easily be outfitted for drilling. A typical vessel length is in the range of 40−70 m. The vessel is equipped with winches, cables, and anchors for four-point mooring. Anchor lines usually approach about eight times water depth.

Anchors may weigh as much as, or more than, 2.5 tons, to give reasonable assurance of maintaining station in adverse conditions of wind, wave, current, and mudline soils. As much as possible, the bow of the vessel is oriented into the prevailing

surface sea and wind to minimize vessel roll, pitch, and heave. Satisfactory drilling and sampling can be done in seas of 1.8−2.4 m (6−8 ft.) height.

The supply vessel should have sufficient quarters for both the vessel and drilling crews, and two drilling crews are provided so that work can be conducted on a 24-hour basis once boring has started.

Many vessels have been modified to include a centrally located drilling well through the hull. The central location minimizes the amount of vessel motion and provides ample work space around the drilling rig. If such a well is not available, drilling can be done from a temporary deck cantilevered over the side. The best location for the platform, from the standpoint of vessel motion, is at the mid-point of the side.

4.2.2 Drilling equipment and method

Nowadays, the offshore industry has moved to using deep-water platforms designed and built for depths approaching 150 m (500 ft.); one has even been designed for a water depth of about 300 m. Pile foundations frequently penetrate 90−120 m into the sea bottom. The combination of water depth and bottom penetration means that drilling equipment for soil borings should have a depth capability of 300 m or more.

A convenient rig has utilities that include hoisting drums and a rotary pump.

A drilling operation may be improvised from power swivel or tongs to provide rotation, a crane to provide hoisting capacity, and a pump for circulation.

Weight on the bit must be provided through drill collars. Telescoping bumper subs are sometimes used to keep the bit on the bottom as the vessel heaves, or a motion compensator can be used for the same purpose. A weight indicator on the drilling line permits the driller to observe and control the bit weight and prevent damage to the drill pipe.

In the early days of offshore soil exploration, it was customary to set a casing or conductor from the drilling deck into the sea floor. This provided a means of recirculating drilling fluid and allowed repeated entry into the hole to drill and sample by conventional land methods. However, as work moved into deeper water, this procedure became quite slow and costly. The longer time on site invited more weather interference. Therefore it became desirable to develop new and faster drilling and sampling techniques; the so-called “wire-line” methods were the result.

4.2.3 Wire-line sampling technique

In the wire-line method, the drill pipe itself serves as the conductor; no other pipe is used. An open-center drill bit is used on the lower end. A boring is advanced by ordinary rotary methods; drilling fluid pumped through the drill pipe prevents soil from entering the open-center bit. Since there is no provision for recirculation of drilling fluid, all fluid pumped is expended as it emerges from the boring at the sea floor; thus a continuous supply of new fluid is required. As discussed below, a fluid

of controlled weight and viscosity is used to counteract formation pressures and to stabilize the drilled hole.

The wire-line sampler consists of a thin-walled tube attached to the lower end of a device incorporating a down-hole hammer or set of mechanical parts. The device is run through the bore of the drill pipe, so its size is limited by the inside diameter.

The driving operation results in some disturbance to clay samples. Shear strengths measured on driven samples will be generally lower than on pushed samples. Comparative borings and tests have been made to evaluate this effect.

The wire-line procedure for sampling sand is obviously the same as the standard penetration test (SPT), in that drill rods attached to the sampler are eliminated and driving is by means of the down-hole hammer, which imparts a fairly uniform driving energy at any depth. Correlations have been made between driving resistances and soil strength; it is doubtful that the SPT method has any validity at the great sampling depths offshore. The wire-line procedure provides a qualitative indication of density and permits close observations of variations with depth.

The advantages of using the wire-line procedure are: (1) the sampler is completely independent of the drill pipe, and thus from vessel-imparted motion, and (2) sampling can be done rapidly, in that a boring that might take 4−5 days to complete using conventional methods can be finished in about one day with wire-line techniques. This results in reduced weather exposure and, obviously, reduced cost.

4.2.4 Offshore soil investigation problems

The effects of weather upon marine operations are well known. The smaller equipment used in soil-boring operations is considerably more vulnerable than the large equipment used for offshore well drilling and construction.

Boring sites are frequently 100 miles or more from land or safe anchorage. It is therefore necessary that marine equipment used for soil-boring operations be able to endure sea conditions much worse than those in which drilling can be conducted. If adverse conditions are encountered after a boring is started, it may be necessary to suspend drilling temporarily or even to withdraw the drill pipe, reposition anchors, and redrill the boring to continue sampling at greater depth.

As stated above, it is important to define the water depth, as the design of the jacket is based on this value. The matter of determining water depth may appear simple, but it can be very difficult because of currents, tide, and very soft seabed soils, yet an exact water depth is essential, so that sampling can be begun at the seabed.

Probably the best way to determine water depth is to use a sounding weight on the small wire line used for sampling and to use a wire-line counter to measure the length of line. The weight must be adequate to minimize current effects but must be designed so that it defines the seabed and does not sink into a very soft bottom. The water depth can be confirmed on the first sampling attempt.

Worldwide predictions of seasonal weather conditions and sea states are available from several sources. Short-term forecasts are also available in most offshore

areas. Predicted tide and current tables can be obtained for almost any area. All of this information is useful in design planning and jacket installation.

If the platform is located in an area where significant tide changes occur, it is necessary to make frequent observations to define the tide cycle and thereby control the sampling depth.

A plot of time versus water depth can be used to reduce water depth to any desired datum. The time, date, and measured water depth should be recorded at the start of a boring. Tide variations can sometimes be recorded by a suitable fathometer.

In areas of very soft, underconsolidated soils, it is necessary to exercise very careful control of drilling fluid weight to counteract the tendency of the material to squeeze into the drilled hole and up into the drill pipe. Failure to do so can result in very severe sample disturbance. Furthermore, in such areas, the problem of handling disturbance on recovered samples is also quite severe.

Once a boring has penetrated a granular soil formation, it is essential that drilling mud having suitable viscosity and gel properties be used to stabilize the drilled hole and to prevent caving; commercial saltwater gel is excellent for this purpose. Particularly in glacial deposits, coarse granular material such as cobbles or boulders may be encountered and may make drilling extremely difficult. The presence of rock formations within the depth of investigation requires that special tools and procedures be used.

In most cases, gas present within formations penetrated by soil borings and flows of water may also be encountered. The normal procedure of using a blowout preventer on cased holes is not easily applied to the wire-line method.

Sometimes a large mobile rig may be used to drill at a location where a platform may be installed later, and it may be desirable to make a soil boring from the mobile rig. If space is available, the boring can be made without interference with the normal rig activity by placing a soil-boring rig on board. The drilling and sampling procedures are identical to those used from a floating vessel. The large rigs, either jack-ups or floaters, provide a relatively stable base for soil-boring operations.

Sometimes the soil boring is performed using a large oilfield rig. If the soil-boring rig cannot be accommodated, it is possible to use the large drilling rig and its crews, working under technical supervision, to make the soil boring. The large mobile rig and its support equipment may cost $25,000–$50,000 per day; therefore the soil boring may be quite expensive. This approach should generally be avoided if other means are available for making a boring. If the large rig must be used, wire-line procedures will minimize the rig time devoted to soil-boring operations.

Existing diver-operated equipment consists of fairly conventional drilling equipment adapted to work on the sea floor and there is a support from a surface vessel. The diver-operated approach to drilling and sampling may become more competitive with other traditional methods, but the diver training must also include experience in soil sampling.

Several pieces of equipment have been developed to operate on the sea floor by remote control from a surface vessel. To date, this equipment, known as a remotely

operating vehicle (ROV), does not have the capability to sample at the depths required to investigate deep-pile foundations. As development continues, the use of such equipment may become more feasible.

Much attention has been given to use of small manned submersibles to perform various underwater tasks without exposing personnel to the pressures associated with diving. These devices have been equipped with manipulators of various kinds, and they have been used to perform in situ tests at shallow penetrations while resting on the ocean bottom. A logical extension of this technology would be to equip a submersible to drill and sample at significant depth; no such equipment has yet been built, although a design has existed since 1996.

4.3 Soil tests

The wet rotary process which is commonly used to advance an onshore soil boring is used also for offshore soil tests; in this respect, there is little difference between onshore and offshore practice except in some details in the way the objective is accomplished. However, the different offshore environmental conditions have necessitated changes in soil-sampling procedures. An understanding of onshore sampling techniques, tools, and results will aid in understanding the required alterations, the concessions made, and the advantages of the offshore procedures.

Most onshore sampling is done by what is termed a conventional means which is used also in offshore sampling. At the desired sampling depth, the drill pipe is pulled from the hole and the drill bit is replaced by a soil sampler. The sampler is run to the bottom on the drill pipe. After the sample has been taken, the drill pipe is again pulled to retrieve the sample, then the soil sampler is replaced by the bit and the drill pipe is run back into the hole to advance the boring to the next sampling interval.

Due to the high cost of offshore soil investigation, therefore, during the preliminary engineering, there are many sources of useful information and data about soil characteristic that can be discovered by the geologic information to the platform location, drilling records, acoustic data, or weather and sea state.

The most common method of sampling cohesive soils (clay) is to push a thin-walled tube into undisturbed material below the bottom of the drilled hole; this procedure is standardized in ASTM D-1587. Penetration of the tube is normally achieved by a rapid, continuous push from a pull-down system on the drilling rig. The sampling tube is vented to permit escape of fluid as soil enters.

The tube wall must be clean and smooth to minimize friction. The tube diameter may range from 50 to100 mm and the wall thickness may be 1.5−3 mm. The lower end of the tube is sharpened and is swaged to give a slight inside clearance. The tube length to diameter ratio is usually between about 10 and 15. The length of sample as compared to the length of push is ideally near 100%. All of these factors have a bearing on obtaining an undisturbed sample and, therefore upon certain soil parameters that may be determined from tests on samples.

As mentioned above, for granular soils (sands), the SPT has been widely used in onshore projects; this procedure is described in ASTM D-1586.

In the 1920s the SPT was created in the United States as an easy applicable method to understand the soil parameters. Its equipment and test procedure are simple. Based on that it was used worldwide using different procedures. With time it was found that it was mandatory to standardize the test to allow easy comparison with different investigation results. This method is simple and not expensive, but its results depends on the experience of the engineer and staff who are carrying out the test.

In general, the test depends on carrying out a prebored hole with a diameter range from 60 to 200 mm. Then a split barrel sampler is driven from the bottom of the hole by a hammer with a weight of 63.5 kg that falls from a distance of 760 mm. If the hole cannot stay open, the casing can be used for drilling mud. The sampler hammers to drill down for a distance 150 mm from the bottom of the prebored hole and counts the number of blows, and then repeats the process and counts the number of blows to push the sampler down another 300 mm inside the soil, this number is called the N30. The rod that is used for sampler hammering should be rigid enough to withstand the hammer load.

There are many factors that affect the result accuracy. The SPT depends on dissipating the energy to the soil which is affected by the drill rod dynamic properties and the method of drilling, from a practical point of view the energy varies from 50% to 80%. Seed and De Alba (1986) research was recommended to use a correction factor to compensate for a rode energy of 60%. It is worth mentioning that in SPT it is difficult to obtain accurate data or do the test in a proper way in the case of silty or loose sand under the water level due to collapsing of the bore hole and the soil being disturbed. Other factors may provide variations in the data, such as the frequency of hammering, the drilling fluid type, and the borehole diameter.

The *N* value, which is the number of blows every 300 mm, is called the standard penetration to the soil which depends on its strength, and so the strength of the soil can be defined by this method at different soil layers.

Based on settlement observations of footings, Peck et al. (1974) proposed the following relationship for correction of confinement pressure. The measured *N*-value is multiplied by a correction factor C_N to obtain a reference value, N_1, corresponding to an effective overburden stress of 1 t/ft.^{2} (approximately 107 kPa)

$$N_1 = N \cdot C_N \tag{4.1}$$

where C_N is a stress correction factor or SPT and p' is the effective vertical overburden pressure (see Eq. (4.2)).

$$C_N = 0.77 \cdot \log 10 \left(20/p'\right) \tag{4.2}$$

Preliminary knowledge of the geologic conditions in an offshore area will aid in selection of exploration tools best suited to the job. However, at the present time, sub-bottom profiles are the main source of information about soils and rocks that may be encountered.

In many areas of offshore oilfield activity, previous investigations have been made. Although information may be for a location miles away from the desired location, it can provide an insight into the foundation conditions. Furthermore, general information about the character of materials within the probable depth of a soil boring may sometimes be obtained from well records.

Geophysical exploration precedes drilling activity in offshore areas. The depth of a geologic structure important from a production standpoint is generally well below the zone of interest for foundations; records from seismic exploration are probably of very limited value for foundation purposes. However, shallow-penetration surveys are frequently available and do provide useful data on soil stratigraphy.

Many in situ testing devices have been developed and are in use to determine soil properties and conditions in the ground. Among them are the cone penetrometer, commonly known as the "Dutch" cone, the pressure meter, and the vane shear device. None of these provides a sample for other tests; if samples are required, sampling must be done between the in situ tests or in a companion boring.

The Dutch cone was developed principally to define granular soil strata that would serve to support point-bearing piles. The cone is modified to measure both side friction and point-bearing resistance. Experienced operators claim to be able to identify soil types by the ratios of these resistances. Modern cone equipment has been used successfully only to shallow penetrations at sea. Remotely operated sea floor equipment presently being developed in Europe may have a substantially greater depth capability.

The pressure meter is designed to determine soil behavior by using an expanding pressure cell to measure load–deformation characteristics. The pressure cell is either driven or pushed into undisturbed soil to begin testing or is installed in the bottom of a drilled hole of carefully controlled dimensions. Readings, interpreted in terms of modulus of deformation and limit pressure, are used to determine bearing capacity, settlement, and other data. This tool has seen little success in connection with deep exploration for pile foundations at sea.

The remote vane, which is the vane shear device, has been used for years to measure in-place shear strengths of soils; however, soil shear failure was produced through torque applied to rods extending to the surface.

Remotely operated vane equipment has been developed in recent years and has been used successfully in a number of offshore investigations in conjunction with wire-line sampling operations.

Tests can be conducted fairly quickly and economically in material having a shear strength up to about 192 kN/m^2. The present vane probe is powered electrically through a conductor cable extending to the surface but has no connection to the drill pipe. Continuous torque readings throughout a test are monitored on a readout at the surface. Development is under way on another device that has no electrical connection to the surface; readings will be stored in the down-hole device and will be read when it is brought to the surface after a test.

Results of the remote vane tests show strengths consistently higher than can be measured on samples recovered. This is to be expected because of disturbance

created by sampling and by sample handling and because of the pressure relief experienced by samples brought to the surface. The vane shear device probably better measures the true in situ shear strength of a cohesive soil than any other device.

Until the principal emphasis shifts from pile-supported platforms, which is not expected any time soon, and until offshore activity extends into much deeper water, the present methods and techniques of offshore soil investigation will continue to be employed. Boat drilling and wire-line sampling methods offer the most versatile and economical means of investigation. Use of remote devices, such as the vane probe and cone penetrometer, in drilled holes will increase and will add much to our knowledge of in situ soil properties. Dynamic positioning of surface drilling vessels or support vessels for other operations will become more important as operations move into deeper waters beyond the continental shelf. There will be much more activity in the development of remotely operated sea floor drilling and sampling devices. Manned submersibles should also play an increasingly important role with further development.

4.4 In situ testing

As mentioned earlier, offshore soil investigation is much more expensive than onshore investigation. Therefore the Nosrok (2004) report recommend to check and calibrate the investigation tools and guarantee that they are working in an accurate manner before mobilizing the equipment with the survey vessel. In addition, before mobilization it should be assured that all procedures and equipment specification are available.

Any professional company should have a checklist to identify the items that need to be checked, for example, the sensors' signal response, acquisition system that transfers the data, and the subsea equipment that is mandatory to be checked in a wet condition.

All the equipment that is used on the subsea should be capable of working under a high water pressure and its reliability high under these environmental conditions. Before and after the test for all sensors a zero reading will be recorded.

Records of experience with the use of the equipment, routines, and procedures for interpretation of measurements for assessment of soil parameters should be documented and be made available upon request.

In most cases, the in situ test tool can be inserted into the soils from the sea bed until it reaches the target depth or until failure to penetrate the soil further due to the load sensor capacity or reaching the maximum pushing force. This is called the *sea-bed mode*.

The following recommendations should be considered to reduce the effect of the rig footprint on the soil test data.

- The footprint should be with an open space to push the tools into the seabed for any shape of foot print, ring, rectangle, or square;
- If there are skirts to transfer the rig load to the stiff soil layer;

- There is an equilibrium between the rig weight and the reaction force in the footprint and there is no overweight.

There will be a TV camera mounted on the rig to monitor the penetration into the sea bed, and to assess the effects of the rig on the in situ test result. The other method is to use a ROV to perform shallow testing, depending on the soil type and the required penetration depth.

The drilling of the borehole should be carried out in such a way that the disturbance to the soil below the drill bit is minimized. In order to avoid any disturbed zone below the drill bit, the in situ test tool should penetrate at least 1 m if soil strength and density allow. The disturbed zone can be assessed by continuous CPT/Cone Penetration Test with Pore Pressure (CPTU) (see Section 4.4.1) penetrated to approximately 3 m below the drill bit.

4.4.1 Cone penetration test

The cone penetration test (CPT) (Dutch cone) is modified to piezocone penetration depth. The piezocone test (CPT testing that also gathers piezometer data, called CPTU testing) is a CPT with additional measurement of the pore water pressure at one or more locations (U_1, U_2, and U_3) on the penetrometer surface, as shown in Fig. 4.1.

The CPT is an in situ testing method for determining the geotechnical engineering properties of soils and for delineating soil stratigraphy. It was initially developed in the 1950s at the Dutch Laboratory for Soil Mechanics in Delft to investigate soft soils, therefore in some textbooks it is called the Dutch cone test. Nowadays, CPT is the most popular tool used worldwide for soil investigation.

The CPT test is based on pushing a cone with an attached instrument system into the soil layer at a rate of 20 mm/s. The cone size is related to the soil layer and in most cases has a diameter of 36 or 44 mm with a cross-sectional area of 1000 or 1500 mm^2.

The American Society of Testing Materials (ASTM) presents the apparatus and test procedure for the CPT and the measurement of q_c. In particular, ISO (2005) prescribes cones with a base area in the range of 500−2000 mm^2 and a penetration rate of 20 ± 5 mm/s.

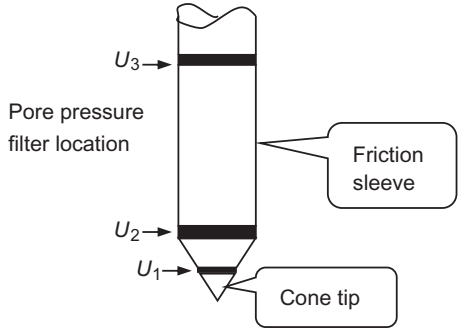

Figure 4.1 Sketch of a cone penetration test (CPT).

It is noted that the CPT-based design methods were established for cone resistance values up to 100 MPa. Caution should be used when applying the methods to sands with higher resistances.

The early target for CPT is to define the soil-bearing capacity as a function of the penetration resistance of the conical tip. After that there are many upgrades to the test to separate the measurement of resistance due to the friction on the conical tip and also the friction resistance due to rod string.

Measurement of the friction resistance on the sleeve started in the 1960s and as per Begemann (1965) the measuring of cohesive soil strength was added to the tools. In 1948, electronic measurement started and there was an improvement made in the 1970s as per De Reister (1971).

The new CPT which is used has another important function, which is to measure the pore water pressure using a pressure transducer with filters. The filters are mainly located in three positions, $U1$, $U2$ and $U3$, which are in the following positions at the cone tip, directly behind the cone tip and behind the friction sleeve, respectively. The measurement of pore water pressure is important to correct the friction values at the tips and to know the type of soil layers.

CPT and CPTU testing equipment generally advance the cone using hydraulic rams mounted on a heavily ballasted vehicle or using screwed-in anchors as a counterforce. One advantage of CPT over SPT is a more continuous profile of soil parameters, with CPTU data recorded typically at 20 mm intervals.

In 1986, CPT for geotechnical investigation was standardized by ASTM Standard D-3441 (ASTM, 2004). ISSMGE provides international standards for CPT and CPTU. Later ASTM standards recommend using CPT for environmental site characterization and groundwater monitoring.

Specific for soil investigations, CPT is a more recommended method over SPT because of its greater accuracy and quick results, in addition it presents a continuous soil profile and reduced cost compared with other methods. The arrangement for the CPT on the drilling vessel is shown in Fig. 4.2.

In general, after performing the geotechnical investigations as there will be several vertical CPT profiles made, for example, one per platform leg, therefore it is recommended that at least two approaches should be calculated and the capacity should be first based on the combined averaged resistance capacity q_c profile and then based on individual q_c profiles. After that, experience is important in providing judgment for selecting the most appropriate resistance capacity profile and associated final axial capacity.

Equipment requirements

Until now the International Reference Test procedure (IRTP 1999/2001) has been considered one of the main references for the CPT equipment requirement, which is as follows:

1. The penetrometer tip and its rods have the same diameter size, equal to or higher than 400 mm;

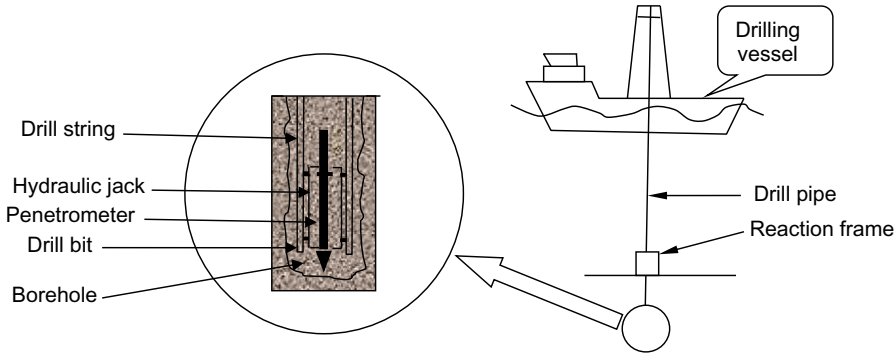

Figure 4.2 Arrangement for cone penetrometer tests.

2. The cross-sectional area of the cone is 1000 m^2 with a diameter of 35.3−36.0 mm and conical height in the range 24−31.2 mm.

According to the IRTP (1999) cone penetrometers with a diameter between 25 mm with the cross-sectional area of the cone equal to 500 mm^2 and 50 mm with cone a cross-sectional area equal to 2000 mm^2 are allowed in some special cases, with no need to apply the correction factors.

CPT testing procedure

As per IRTP 1999/2001 The testing procedure is as follows:

- The nominal penetration rate is 20 mm/s and its accuracy is ± 5 mm/s.
- The continuous penetration is preferred so each stroke length should be as long as practical.
- The readings shall be at least once per second (for every 20 mm of penetration).
- Zero readings should be recorded before and after each test.

For CPTU testing, the filter stones should be fully saturated and the pore pressure measurement system should give an instantaneous response to changes in pressure. A documented procedure for saturation of filter stones should be available.

At 50% consolidation or more, the pore pressure dissipation tests should be carried out. The client and contractor, based on the importance of the test, should define the maximum test duration.

The following is the minimum sample rate during a dissipation test:

- During the first minute, twice a second;
- Between the first minute and tenth minute, once a second;
- Between the 10th and 100th minutes, once every 2 seconds;
- After 100 minutes, once every 5 seconds.

The resolution of the measured results should be within 2% of the measured value. The real-time inspection shall be obtained through a data-acquisition system in the form of digital data and a graph. These data should be stored for further study.

Calibration requirements

Accurate calibration based on IRTP (1999) should be done for the cone and the friction sleeve. This calibration shall be performed once per year. It is worth mentioning that the calibration should be performed for each sensor to every project as a minimum of every 20 days or after about 100 soundings. In the case that the load cells are loaded approaching maximum capacity, new calibrations should be carried out.

During field work, regular function checks of the cone penetrometer and measuring system should be carried out. As discussed above, offshore soil investigation is very expensive, so it is important to follow the calibration procedure for any tools before use. The owner's representative should check this with the contractor.

Before mobilization, one of the main documents that should be ready to be final checked by the client is the calibration certificate for every cone penetrometer.

The temperature calibration should be done for every CPTU and cone at least once as follows:

- For temperatures varying from 0°C to 40°C measure the response variation under zero load.
- At temperature +5°C for each sensor the calibration factor should be obtained and the method described that is used to obtain this factor.

The use of accuracy classes, as required in IRTP (1999), should be adopted. Equipment and procedures to be used should be selected according to the required accuracy class given in Table 4.1. These precautions are very critical and important to be considered and monitoring by the project quality team.

If all possible sources of errors are included, the accuracy of the recordings should be better than the largest of the values given in Table 4.1. The soil parameter calculations and profile for soft or loose soil will be class 1, but class 3 is specific for stiff or dense soil and class 2 for stiff clays and sand.

For the sounding, zero readings should be taken with the probe temperature in the same way as the ground temperature, and temperature stabilization achieved for all sensors and other electronic components in the data-acquisition system.

CPT results

IRTP 1999/2001 also provide a guideline for the minimum data to be in the CPT report which can be shown in the CPT profile results or in a tabulated form.

- CPT location;
- test date;
- number of tests;

Table 4.1 Accuracy classes.

Class	Measured parameter	Minimum allowable accuracy	Maximum length between measurements (mm)
1	Cone resistance Sleeve friction Pore pressure Inclination Penetration	50 kPa or 3% 10 kPa or 10% 5 kPa or 2% 2 degrees 0.1 m or 1%	20
2	Cone resistance Sleeve friction Pore pressure Inclination Penetration	200 kPa or 3% 25 kPa or 15% 25 kPa or 3% 2 degrees 0.2 m or 2%	20
3	Cone resistance Sleeve friction Pore pressure Inclination Penetration	400 kPa or 5% 50 kPa or 15% 50 kPa or 5% 5 degrees 0.2 m or 2%	50

- test location shall be defined by coordinates system;
- water depth;
- state serial number of the cone;
- the dimensions and geometry of the cone;
- the dimensions and the position of the filter stone;
- tip, sleeve friction, pore pressures, sensor capacity;
- calibration factors used;
- mention in the report for all sensors the readings for zero level at the sea bed or bore hole bottom before and after the test;
- if there is wear or damage to the tip or sleeve this should be stated;
- the rate of penetration;
- any irregularities during testing;
- the friction ratio between the tip and sleeve;
- water depth variation due to tide effect;
- the frame sinking observation;
- In the case of sea bed tests, for 1 m maximum penetration depth, record if there is cone penetrometer inclination to the vertical axis.

The engineering units that are used for measured results should be presented as:

- depth of penetration (in m);
- cone tip resistance (in MPa);
- pore pressure(s) (in MPa);
- sleeve friction (in kPa);
- total thrust during test (in kN).

The graphical representation of the results from CPTs in the field (offshore) should be presented. If not otherwise agreed upon, the depth scale should be 1 m (field) = 10 mm (plot).

The zero reference for sea-bed CPTs should be the sea bottom, and for down-hole CPT, the bottom of the borehole. The selection of the scale for presenting the measured cone resistance, pore pressure, and friction should be reasonable to suit the soil conditions.

In addition to the measured CPT/CPTU values, the following correction measurement formula should be stated in the geotechnical report:

- The corrected cone penetration resistance, $q_t = q_c + (1 - a)\ u$; whereas u is measured behind the cone;
- The correction of the sleeve friction, f_t, only if pore pressures have been measured at both ends of the friction sleeve; friction ratio is $R_f = (f_t/q_t) \times 100\%$, where f_t is the sleeve friction corrected for pore pressure effects, noting that the measurement of the pore pressure should be done at both ends of the friction sleeve

The output data are presented in a graph, as shown in Fig. 4.3.

4.4.2 Field vane test

Vane blades should be rectangular, as defined in ASTM D-2573-01 or BS 5930:1999.

Shear strengths are given in Table 4.2, based on the geometrical dimensions of the vane blades. The vane test in the borehole offshore is presented in Fig. 4.4.

Testing procedure

As a normal procedure before a vane test is started, the vane blade should be pushed at least 0.5 m below the bottom of the borehole. The pushing rate should be less than 25 mm/s.

The waiting time, which is the time from starting the push until reaching the required depth, should be from 2 to 5 minutes.

The vane shall be rotated smoothly and for the start of the test it shall rotate from 6 to 12 degrees per minute.

The vane should be rotated 10 times as a minimum with a rate equal to or higher than 4 RPM until reaching continuous rotation with a constant torque over 45 degrees to measure the soil shear strength. If a fast rotation happens the shear strength shall be measured and recommended without delay. In the seabed the intervals between the tests shall be about 500 mm.

The result report should include the test procedure and illustrate the method of vane penetration below the bottom of the borehole, the torque and rotation data, and also the rotation rates.

The data-recording system should be able to obtain the required accuracy. Taking into account all sources of error, including the data-acquisition system, the uncertainty in the measured torque should not exceed the smaller of 5% of

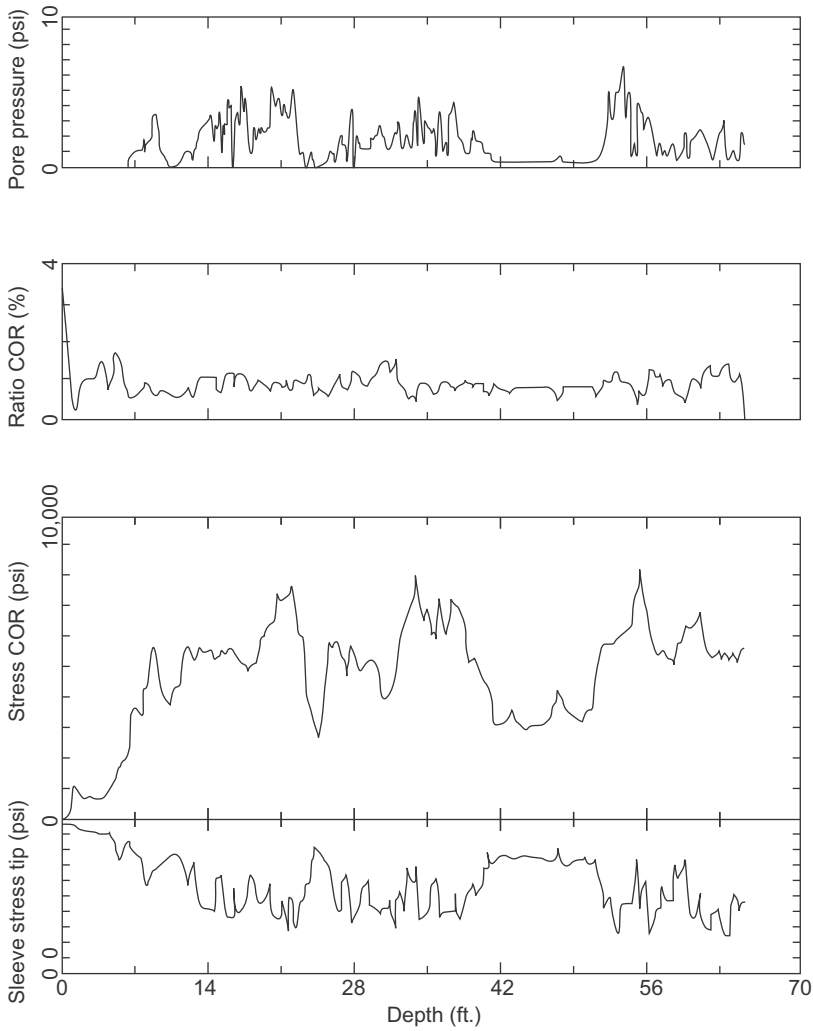

Figure 4.3 Cone Penetration Test with Pore Pressure (CPTU) output results.

Table 4.2 Measuring range with different vane blade dimensions.

Measuring range of s_u	**Vane height (mm)**	**Vane width (mm)**	**Vane blade thickness (mm)**
0−50	130	65	2
30−100	110	55	2
80−250	80	40	2

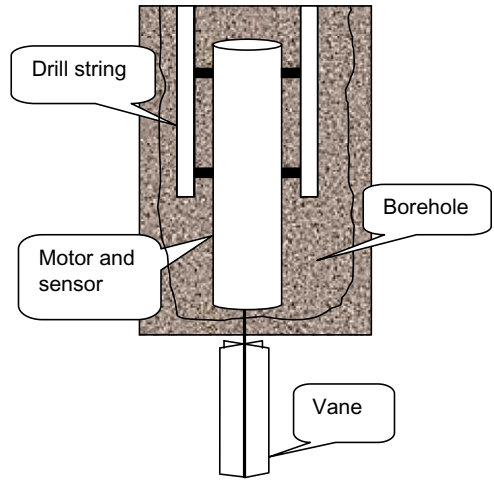

Figure 4.4 Sketch of a vane test.

measured value or 2% of the maximum value of the measured torque of the layer under consideration.

The resolution of the measured result should be within 2% of the measured value.

During testing, the data-acquisition system should allow for real-time inspection of measured results in both digital and graphical form.

It is very important that, at least every year and before each project, the sensor for measuring the torque during vane testing should be calibrated. If the sensor is loaded close to its maximum or any damage is suspected, it should be checked and recalibrated. In addition, function checks should be carried out in the field.

For each vane test, the following information should be given:

- the test location preferably with a coordinate system;
- test date;
- test identification number or bore number;
- water depth;
- the vane dimensions;
- depth below sea bottom to vane tip;
- rotation rate;
- provide the curve that presents the relation between torque versus rotation (degrees);
- time to failure;
- record any obstacles during testing;
- The equation which is used to obtain the vane undrained shear strength, s_{uv}, presenting shear stress distribution on the ends of the vane and explain the justification for the assumption.

4.5 Soil properties

The soil in general is natural material formulated due to weather conditions on the upper layer of the Earth's crust for a distance from 20 up to 100 m, this material varies from hard rock, gravel, sand, clay, silt, to very fine and loose materials.

Therefore the behavior of soil is different than artificial materials like concrete and steel, and in soil there is a lot of uncertainty and variation in its characteristics.

The soil mechanical behavior is different than other materials as it is nonlinear and also it has a plastic behavior in the case of loading and unloading, whatever the stress, as there may be low stresses and they may show anisotropic behavior and creep and volume change can happen associated with a shear effect. In general, soil is inhomogeneous in its nature. Therefore by carrying out field tests and laboratory tests, the behavior of the soil should be included and reasonable safety measures taken. It is worth highlighting that soil behavior is complicated due to the presence of water in the pores, as the existence of fluid in the pores may resist or delay volume deformations.

There are many theories that define a correlation between the properties of soil and its behavior but until now the best method is to carry out the required laboratory test and the in situ test, and then the required parameters can be obtained to allow the design of the foundation in a safe manner. In seabeds there is a layer of carbonate in some locations.

In the case of carbonate soil, the following information should be obtained as a minimum:

1. soil composition, and the carbonate content defined;
2. skeletal and nonskeletal sediments differentiated between;
3. particle angularity, porosity, and initial void ratio;
4. soil compressibility;
5. soil strength parameters, such as the angle of internal friction;
6. formation cementation, at least in a qualitative sense.

4.5.1 Strength

Soils usually cannot transfer stresses beyond a certain limit. This is called the strength of the soil. The shear strength of soils is usually expressed by Coulomb's relation between the maximum shear stress and the effective normal stress:

$$\tau_{\max} = c + \sigma' \tan\phi \tag{4.3}$$

where c is the cohesion and ϕ is the friction angle. For sands, c is usually negligible, so that ϕ is the only strength parameter.

For clay the main laboratory test is triaxial testing which is used to obtain the shear strength parameters. In the case of clay the effective stress remains constant in the undrained condition so it is optimum to obtain the undrained shear strength s_u for clay.

CPT, as described in Section 4.2.4, gives a very good presentation of the soil in the case of using pile in the foundation as per our case in an offshore structure, as by hydraulically pushing the cone tip shall measure the bearing stress on the cone tip and the friction by the sleeve along the profile for the whole depth.

By using correlation equations the soil strength can be calculated from the CPT data results. As per Brinch Hansen's formula the cone-bearing capacity, q_c, can be obtained for sand based on the CPT penetration test.

$$q_c = s_q N_q \sigma_v^{'} = s_q N_q \gamma^{'} z \tag{4.4}$$

where s_q is a shape factor to express the effective weight of the overburden, for which one may use the formula:

$$s_q = 1 + \sin\phi \tag{4.5}$$

z is the depth, and N_q is a dimensionless constant for which theoretical analysis has given the value as in Eq. (4.6):

$$N_q = \frac{1 + \sin\phi}{1 - \sin\phi} \exp(\pi \tan\phi) \tag{4.6}$$

The predicted cone resistances q_c for various types of sand at depths of 10 and 20 m are shown in Table 4.3, assuming that $\gamma = 10\ \text{kN/m}^3$. The values in the table are often observed for sand layers at these depths. They may also be used inversely: if a certain cone resistance is observed, it is indicative of a certain type of material.

For a CPT in clay soil, the Brinch Hansen formula can be used to correlate the CPT result for the undrained shear strength.

The general Brinch Hansen formula is

$$q_c = s_c N_c c + s_q N_q \sigma_v^{'} \tag{4.7}$$

Because the test is performed very quickly, the soil behavior can be considered to be undrained. The above coefficient values can be taken as $N_c = 5.14$, $N_q = 1$, $s_c = 1.3$, and $s_q = 1$. Eq. (4.7) shall be as follows:

$$q_C = 6.7 s_u + \sigma_v^{'} \tag{4.8}$$

where the cohesion parameter, c, has been presented by the undrained shear strength s_u.

For normally consolidated clays, the undrained shear strength has a direct relation with the vertical stress $\sigma_{v'}$. Ladd provides a correlation to obtain the undrained shear strength by knowing the vertical stresses as follows:

Table 4.3 Guidance for cone resistance in sand.

Soil type	**ϕ (degrees)**	**N_q**	**q_c ($z = 10$ m) (MPa)**	**q_c ($z = 20$ m)**
Loose sand	30	18.4	2.8	5.5
Medium dense sand	35	33.3	5.2	10.5
Very dense sand	40	64.2	10.5	21.1

$$s_u = 0.22\sigma_v' \tag{4.9}$$

Substitution of this result into Eq. (4.8) gives

$$q_c \approx 11 s_u \tag{4.10}$$

American Petroleum Institute (API) values for q_c are presented in Eq. (4.16)

For a soft clay, with $s_u = 20$ kPa, the order of magnitude of the cone resistance would be 220 kPa $\approx$ 0.2 MPa. Such values are often observed. Again, they may also be used to estimate the undrained shear strength from CPT data.

Table 4.4 provides guidance to cohesive soil characteristics based on the rule of thumb.

The relative density for cohesionless soil can be predicted using Table 4.5 as a guideline.

Tables 4.6 and 4.7 present terminology for soil structure and characteristics and the common names of various soil types.

Table 4.4 Consistency of cohesive soil.

Consistency	**Unconfined compressive strength (KPa)$_t$**	**Rule-of-thumb test**
Very soft	(0−27)	Core (height twice diameter) sags under own weight
Soft	(27−54)	Can be pinched in two by pressing between thumb and finger
Firm	(54−107)	Can be imprinted easily with finger
Stiff	(107−215)	Can be imprinted with considerable pressure from fingers
Very stiff	(215−429)	Barely can be imprinted by pressure from fingers
Hard	>429	Cannot be imprinted by fingers

Table 4.5 Degree of compactness for cohesionless soil.

Degree of compactness	**Relative density (%)**
Very loose	0−15
Loose	15−35
Medium dense	35−65
Dense	65−85
Very dense	85−100

Table 4.6 Terminology for soil structure characteristics.

Slicken-sided	Cut by old fracture planes that are slick and glossy in appearance and constitute planes of weakness; generally of random orientation
Fissured	Containing old shrinkage cracks that are frequently filled with fine sand or silt; generally predominantly vertical
Laminated	Composed of thin layers of varying color and texture
Interbedded	Composed of alternate layers of different soil types
Calcareous	Containing appreciable quantities of calcium carbonate
Well graded	Having a wide range of particle sizes and substantial amounts of all intermediate particle sizes
Poorly graded	Predominantly of one particle size, or having a range of sizes with some intermediate sizes missing

Table 4.7 Common soil types.

Topsoil	Surface formation, generally black or gray due to organic content or degree of weathering; the top portion of the soil profile that supports vegetation
Hard pan	Hard, cemented conglomerate that will not soften when wet
Fill	Any manmade soil deposit
Caliche	Layers of soil cemented together by calcium carbonate deposited by evaporation of ascending or descending ground waters
Adobe	Heavy-textured, light-colored, alluvial clay soils occurring in the southwestern part of the United States
Gumbo	Fat clays with little sand that, when saturated with water, are impervious and have a waxy or soapy appearance and feel
Muck	Highly organic soil of very soft consistency

The approximate soil parameters for different types of soil are illustrated in Table 4.8.

4.5.2 Soil characteristics

The first important step is to know the soil characteristics to allow us to present it well in the analytical model for soil pile interaction under the cycling loading and its behavior.

As discussed in previous sections, the accuracy of the in situ test and laboratory test are very important as they can affect dramatically the pile design. Some special projects do a prototype model for the pile and test to measure its behavior.

Table 4.8 Approximate property values for different soil types.

Soil type	Undrained shear strength (S_u, in kPa)	Effective cohesion (c', in kPa)	Friction angle (f', in degrees)	Saturated density (D_s, in t/m^3)	Voids ratio
Soft to firm clay	10–50	5–10	19–24	1.4–1.8	
Stiff clay	50–100	10–20	22–29	1.8–1.9	
Very stiff to hard clay	100–400	20–50	27–31	1.9–2.2	
Silt	10–50	–	27–35	1.7–2.3	1.1–0.3
Loose sand	–	–	29–30	1.7–1.8	1.1–0.8
Medium dense sand	–	–	30–40	1.8–2.0	0.8–0.5
Dense sand	–	–	35–45	2.0–2.3	0.5–0.2
Gravel	–	–	35–55	1.7–2.4	1.1–2.2

According to McClelland and Ehlers (1986), an in situ test, such as the vane test and CPTU and other tests, provides the required information about the soil behavior with its stress–strain behavior.

The in situ test can also obtain the behavior of soil in the long term, such as the creep loading and also the soil behavior under cyclic loading.

Carrying out the laboratory test from the extracted sample can provide the stress–strain characteristics for the soil in different layers, in addition, laboratory tests can study the in situ stresses under remodeling and reconsolidating, which result from pile installations.

The soil samples during tests shall be done under different boundary conditions, such as triaxial, simple shear, and interface shear, and to different levels of sustained and cyclic shear time histories to simulate in-place loading conditions.

Another important source of data to develop soil characterizations for cyclic loading analyses is tests on model and prototype piles. Based on Bogard et al. (1985) and Karlsrud and Haugen (1985), model piles can be highly instrumented, and repeated tests can be performed in soils and for a variety of loadings.

Geometric scale, time scale, and other modeling effects should be carefully considered in applying results from model tests to prototype behavior analyses. As discussed by Pelletier, and Doyle (1982) and Arup et al. (1986), the data from load tests on prototype piles are useful for calibrating analytical models.

Such tests, even if not highly instrumented, can provide data to guide the development of analytical models. These tests can also provide data to verify the results of soil characterizations and analytical models.

Prototype pile-load testing, coupled with in situ and laboratory soil testing and realistic analytical models, can provide an essential framework for making realistic evaluations of the responses of piles to cyclic axial loadings.

The foundation should be designed to carry static, cyclic, and transient loads without excessive deformations or vibrations in the platform. Special attention should be given to the effects of cyclic and transient loading on the strength of the supporting soils as well as on the structural response of piles.

It is very important to consider the possibility of movement of the sea floor against the foundation members, and the forces caused by such movements, if anticipated, should be considered in the design.

4.6 Pile foundations

Offshore structure platforms commonly use open driven piles. These piles are usually driven into the sea bed with impact hammers, which use steam, diesel fuel, or hydraulic power as the source of energy. Therefore the pile wall thickness should be adequate to resist axial and lateral loads as well as the stresses during pile driving.

According to Smith (1962), it is possible to predict approximately the stresses during pile driving using the principles of one-dimensional elastic stress wave transmission by carefully selecting the parameters that govern the behavior of soil, pile, cushions, capblock, and hammer.

The above approach may also be used to optimize the pile hammer cushion and capblock using the computer analysis commonly known as wave equation analyses. The design penetration of driven piles should be determined, rather than correlation of pile capacity with the number of blows required to drive the pile a certain distance into the sea bed.

If a pile stops before it reaches the design penetration, one or more of the following actions can be taken:

1. Hammer and the pile head instrumentations performance shall be reviewed to identify the problem and as a solution a more powerful hammer can be used or the operation and maintenance for the hammer improved.
2. By reviewing and studying the driving records with the hammer instrumentation data, this can allow another look at the soil parameters which can be rechecked and revised enabling an increase in the pile capacity by redoing the calculations.
3. The last action is to modify the piling procedures, such as using jetting and air lifting or by drilling to remove the plugged soil inside the pile, but in the case of removing the plug the pile capacity shall be reduced so that the removed plugged soil can be replaced by gravel with grout that have a sufficient load-bearing capacity.

Note that plug removal may not be effective in some circumstances, particularly in cohesive soils.

Soil below the pile tip is removed by drilling an undersized hole or by lowering jetting equipment through the pile, which acts as the casing pipe for the operation. The effect on pile capacity of drilling an undersized hole is unpredictable unless there has been previous experience under similar conditions.

According to API RP2A (2007), jetting below the pile tip should be avoided because of the unpredictability of the results.

A first stage or outer pile is driven to a predetermined depth, the soil plug is removed, and a second stage or inner pile is driven inside the first-stage pile. In this case, the grouting will be inserted in the annulus between the two piles to provide load transfer between the two piles and to develop composite action.

The piles of the offshore structures are exposed to static and cyclic loading, and the loads will be axial and lateral. Therefore all of these load effects should be considered in the pile design.

4.6.1 Pile capacity for axial loads

On the basis of API RP2A (2007), the ultimate static axial capacity (*QI*) of an open-ended pipe pile in compression is given by the equation:

$$Q_t = Q_f + Q_s + \{\text{small values from } Q_{fi} \text{ or } Q_{sp}\} \tag{4.11}$$

$$Q_t = f \cdot A_s + A_a \cdot Q + A_p \cdot q \tag{4.12}$$

where A_p is the area of the pile or

$$Q_t = f \cdot A_s + A_a \cdot Q + fA_{si} \tag{4.13}$$

where Q_t is the total pile resistance, Q_f is the total outside shaft resistance, $Q_s$is the end-bearing capacity of the annulus, Q_{fi} is the total inside shaft resistance, Q_{sp} is the bearing capacity of the soil beneath the plug, f is the unit skin friction capacity (in kPa), A_s is the outside surface area of pile (in m^2), q is the unit end-bearing capacity (in kPa), A_a is the area of the pile annulus (in m^2), and A_{si} is the inside surface area of pile (in m^2).

In calculating the pile capacity, the weight of the soil plug weight and hydrostatic uplift shall be considered, and also the deformation and compressibility between the pile and the soil.

Coyle and Reese (1966), Murff (1980), and Randolph (1983) discussed skin friction and assumed that the skin friction is considered the maximum value along the pile length.

They mentioned that the capacity may be less than the value obtained from Eq. (4.11) due to the increments of ultimate skin friction along the pile that are not directly added and also the ultimate bearing capacity added to the skin friction.

In such cases, a more explicit consideration of axial pile performance effects on pile capacity may be warranted. There are many factors governing the pile size in addition to the soil parameters, which are the practical and economic solution to the selected size as it depends on the available construction equipment to drive the piles.

For the pile design, the pile capacity factor of safety is defined in Table 4.9 according to API RP2A (2007). The allowable skin friction values on the pile

Table 4.9 Design parameter guide for cohesionless siliceous soil (based on API RP2A).

Soil description	Soil condition	Shaft friction factor	Limited shaft friction values (MPa)	End-bearing factor N_q	Limited unit end-bearing values (MPa)
Sand-silt	Medium dense	0.29	(0.067)	12	3
Sand	Medium dense	0.37	(0.081)	20	5
Sand-silt	Dense	0.37	0.081	20	5
Sand	Dense	0.46	0.096	40	10
Sand-silt	Very dense	0.46	0.096	40	10
Sand	Very dense	0.56	0.115	50	12

section on the upper surface on the pile should be discounted in computing skin friction resistance, Q_f. The end-bearing area of a pilot hole, if drilled, should be discounted in computing the total bearing area.

Skin friction and end bearing in cohesive soils

In the case of traditional piles are used in offshore structure platforms which are steel open pipes. If this pipe piles is penetrated in cohesive soils, the shaft friction, f (in kPa), at any point along the pile may be calculated by the following equation:

$$f = \alpha c \tag{4.14}$$

where α is a dimensionless factor and c is the undrained shear strength of the soil at the point in question.

The factor α can be computed by:

$$\begin{aligned} \alpha &= 0.5\psi - 0.5\psi \leq 1.0 \\ \alpha &= 0.5\psi - 0.25\psi > 1.0 \end{aligned} \tag{4.15}$$

with the constraint that $\alpha \leq 1.0$, where $\psi = c/p'$ for the point in question and p' is the effective overburden pressure at the point in question (in kPa). For underconsolidated clays, clays with excess pore pressures undergoing active consolidation, α can usually be taken as 1.0.

The appropriate methods for determining the undrained shear strength, c, and effective overburden pressure, p', including the effects of various sampling and testing procedures, are important. As the number of pile-load tests is not enough in soils with c/p' ratios greater than 3, Eq. (4.15) should be applied with some engineering judgment for high c/p' values. The same engineering judgment should be

applied for deep-penetrating piles in soils with high undrained shear strength c, where the computed shaft frictions, f, using Eq. (4.14), are generally higher than previously specified in API RP2A. In the case of very long piles, some reduction in pile capacity would happen, because the shaft friction may reduce to some lesser residual value on continued displacement.

For pile end bearings in cohesive soils, the unit end bearing, q (in kPa), may be computed by:

$$q = 9c \tag{4.16}$$

For pile calculation there are two assumptions calculated and the minimum is taken:

1. Assume it is unplugged, so the skin friction is calculated internally and externally with the end bearing calculated at the annulus of the pipe;
2. Assume it is plugged, so calculate the external skin friction and the end-bearing capacity for the pile cross-sectional area.

A static calculation can illustrate if it is plugged or unplugged. A pile could be driven in an unplugged condition, but act plugged under static loading.

In some cases the piles are driven in undersized drilled holes, jetted in place, or in some minor projects, they are drilled and grouted in place. In this situation, the soil disturbance resulting from installation will affect the shaft friction values.

In general, the skin friction, f, should not exceed its calculated values in the case of driven piles which are more traditional in offshore platforms; however, in some cases of overconsolidated clay and using drilled and grouted piles, f may exceed these values.

In determining the skin friction, f, for drilled and grouted piles, the strength of the soil−grout interface, including the potential effects of drilling mud, should be considered. As discussed by Kraft and Lyons (1974), further investigation and checking should be made of the allowable bond stress between the pile steel and the grout.

The shaft friction values, f, in the cohesive layers should be as given in Eq. (4.14). End-bearing values for piles tipped in cohesive layers with adjacent weaker layers may be as given in Eq. (4.16), assuming that the pile achieves penetration of two to three pile diameters or more into the layer in question and the tip is approximately three pile diameters above the bottom of the layer, to avoid punching through.

Some modification in the end-bearing resistance may be necessary if these distances are not achieved.

Shaft friction and end bearing in cohesionless soils

A simple method for assessing pile capacity in cohesionless soils will be discussed. There are reliable methods for predicting pile capacity that are based on direct correlations of pile unit friction and end-bearing data with cone penetration test (CPT)

results. The CPT-based methods have been discussed in depth recently in many researches and it was found that it provided good results from a statistical point of view as the results almost coincide with pile-load test results and, although they are not required, they are, in principle, the preferred methods. CPT-based methods also cover a wider range of cohesionless soils. As the experience of CPT in offshore structures is limited and increases only in the last 30 years, it should be applied only by competent engineers who are experienced in the interpretation of CPT data and understand the limitations and reliability of the methods. It also may require putting pile-driving instrumentation data systems to use to provide greater confidence in our calculating capacities.

For pipe piles in cohesionless soils, the unit shaft friction at a given depth, f, may be calculated by:

$$f = \beta p' \tag{4.17}$$

where β is a shaft friction factor and p' is the effective overburden pressure.

In the case of open-ended piles driven unplugged, Table 4.10 may be used for selection of β if there are no available data. In the case of plugged piles, values of β can be obtained also from Table 4.10 but its values are increased by 25%.

From q practical point of view in the case of long piles, the skin friction cannot increase linearly with the overburden pressure, as per Eq. (4.17) for infinity, so the limit of the skin friction value, f, should be as stated in Table 4.10.

From the following equation the end-bearing capacity for piles in cohesionless soils can be calculated:

$$q = Nq\, p' \tag{4.18}$$

where Nq = a dimensionless bearing capacity factor and p' = effective overburden pressure at the depth in question.

Recommended Nq values are also presented in Table 4.9.

In the case of long piles, q may not increase linearly with the overburden pressure, which is different to that the stated in Eq. (4.18). In such cases, it may be appropriate to limit q to the values given in Table 4.9. For plugged piles, the unit end bearing q acts over the whole cross-section of the pile. For unplugged piles, q

Table 4.10 Pile-capacity factor of safety in API RP2A (2007).

Load condition	**Factor of safety**
Design environmental conditions with appropriate drilling loads	1.5
Operating environmental conditions during drilling operations	2.0
Design environmental conditions with appropriate producing loads	1.5
Operating environmental conditions during producing operations	2. 0
Design environmental conditions with minimum loads (for pullout)	1.5

is calculated by considering the area of annulus of the pile only. Based on that the pile internal skin friction shall be considered in pile capacity calculation.

The design parameters in Table 4.9 are just a guide from API RP2A, and detailed information must be obtained from the CPT results, strength tests, and other soil and pile response tests.

The soil condition is identified based on the relative density, as shown in Table 4.5.

Olson (1987) compared the load test data for piles in sand (obtained by measuring the axial load capacities for open steel piles) and the calculated capacity from API RP2A. Studies done in 2005 by Lehane indicate that variability in capacity predictions using the API calculation method may exceed those for piles in clay. These researches also indicated that the calculation method is conservative for short offshore piles [short = piles less than 45 m (150 ft.) long] in dense to very dense sands loaded in compression and may be unconservative in all other conditions. In unfamiliar situations, the designer may want to account for this uncertainty through a selection of conservative design parameters or by going toward higher factors of safety.

In the case of soil types that do not have characteristic values that fall within the ranges of soil density and the description given in Table 4.9, or for materials with unusually weak grains or compressible structure, Table 4.9 will be not suitable to consider in selecting design parameters. A special laboratory or field tests are required to obtain the design parameters as in the case of very loose silts or soils containing large amounts of mica or volcanic grains, or sands containing calcium carbonate, which are found extensively in many areas of the oceans. From a practical point of view, it suggests that driven piles in these types of soils may provide lower design strength parameters than those described in Table 4.9.

On the other hand, drilled and grouted piles in carbonate sand may have significantly higher capacities than driven piles and have been used successfully in many areas with carbonate soils. The characteristics of carbonate sands are highly variable and the experience of the behavior of this type of soil in the location of the platform will be the main factor in obtaining the design parameters which will be used.

It is worth mentioning that for carbonate soils with higher quartz content and higher densities the pile capacity can be improved.

However, the cementation may increase the pile end-bearing capacity but there are losses in lateral pressure which reduce the pile skin friction capacity.

Except the unusual soil types, which are discussed above, the f and q values given in Table 4.9 may be used for drilled and grouted piles, with consideration given to the strength of the soil−grout interface.

The unit shaft friction values in cohesionless layers and the end-bearing values for cohesionless layers are presented in Table 4.9, provided that the pile penetrates into the cohesionless soil layer more than 2−3D, in which D is the pile diameter, and the tip is at least 3D above the bottom of the layer, to avoid punching this layer.

4.6.2 Foundation size

In most cases, in the FEED engineering phase, the pile configuration will be defined based on past experience. During selection of the size of the pile

foundation, the following items should be considered: diameter, penetration, wall thickness, type of tip, spacing, number of piles, geometry, location, seabed restraint, material strength, installation method, and other parameters as may be considered appropriate.

A number of different analysis procedures may be utilized to determine the requirements of a foundation. At a minimum, the procedure used should properly simulate the nonlinear response behavior of the soil and ensure load−deflection compatibility between the structure and the pile−soil system.

During the pile design the rotation and deflection of the single pile and the whole structure system shall be addressed during the design stage, specifically at the pile head. In any case the deflection and rotation should be within the allowable serviceability limit.

Pile penetration

During design, select a reasonable pile penetration that provides the required pile capacity as per the soil report and resists the maximum axial bearing and pullout loads as well with an appropriate factor of safety as per the design code.

The ultimate pile capacities can be computed in accordance with previous sections, or by other methods that are supported by reliable comprehensive data. API RP2A (2007) defined the minimum factor of safety by dividing the ultimate pile capacity into the actual load, as shown in Table 4.10.

There are two safety factors in APIRP2A depending on the design environmental condition with a 100-year storm wave effect and the operating environmental conditions which are considered as the maximum wave height per year.

The provisions of API RP2A (2007) for sizing the foundation pile are based on an allowable stress (working stress) method, except for pile penetration. In this method, the foundation piles should conform to the requirements of the specification and design. Any alternative method supported by sound engineering methods and empirical evidence may also be utilized. Such alternative methods include the limit state design approach or ultimate strength design of the total foundation system.

4.6.3 Axial pile performance

Static load-deflection behavior

The static pile axial deflection should be compatible with the structural forces and deflection, therefore it should be within the service limit. An analytical method for determining axial pile performance is provided in Meyer et al. (1975). This method depends on the ($t-z$) curves which present the relation between the axial pile shear transition and the pile penetration. The other ($Q-z$) curve presents the relation between the pile bearing capacity and the deflection. The pile behavior and response depend on the load type, directional sequence, and soil type, in addition to the installation technique and the pile stiffness.

Some of these effects for cohesive soils have been observed in both laboratory and field tests.

In the case of axially flexible piles or soil that is soft, the actual pile capacity may be less than the obtained value from Eq. (4.11).

Note that other factors, such as increased axial capacity under loading rates associated with storm waves, may counteract the above effects, as discussed by Dunnavant et al. (1990).

Cyclic response

The definition of cyclic loading, as the load which includes inertial loadings developed by environmental conditions such as storm waves and earthquakes, can have two opposite effects on the static axial capacity as it can be the pile under compression and sometimes less compression or under tension. On the other side, the repetitive loadings can cause a temporary or permanent decrease in load-carrying resistance and may cause an accumulation of deformation. In addition, in the case of cyclic loading, rapidly applied loadings may happen and cause an increase in load-carrying resistance and stiffness of the pile, and inversely in the case of very slowly applied loadings can cause a decrease in the load-carrying resistance and stiffness of the pile. The cyclic loading is a load with magnitudes, cycles, and rates combined together to the applied pile loads, the structural characteristics of the pile, the types of soils, and the factors of safety used in the design of the piles.

The design pile penetration should be selected to be sufficient to develop an effective pile capacity to resist the design static and cyclic loadings.

The design pile penetration can be confirmed by performing pile response analyses of the pile−soil system subjected to static and cyclic loadings. The pile−soil resistance−displacement $t-z$ and $Q-z$ characterizations are discussed below.

The static and cyclic loading will be considered in pile analysis and design and apply the load at the top of the pile and calculate the displacement related to the load. At the end of the pile design procedure the maximum pile resistance and displacement shall be obtained considering that the pile deformation shall comply with the structural serviceability allowable limits.

Axial load-deflection (t−z and Q−z) data

The fixed offshore platform pile foundation should be designed to resist static and cyclic axial loads. The axial resistance of the soil is provided by a combination of axial soil−pile unit skin friction or load transfer along the sides of the pile and end-bearing resistance at the pile tip. The plotted relationship between mobilized soil−pile shear transfer and local pile deflection at any depth is described using a $t-z$ curve. Similarly, the relationship between mobilized end-bearing resistance and axial tip deflection is described using a $Q-z$ curve.

Axial deformation of piles may be modeled in a similar way to the lateral case, to permit stress transfer to be computed and axial pile stiffness to be assessed. For axial loading, $t-z$ curves are used to represent the resistance along the pile shaft, and $Q-z$ curves are introduced to model the end bearing. Characteristic shapes of the curves for sand and clay are shown in Fig. 4.5A and B for clay and sand soil, respectively.

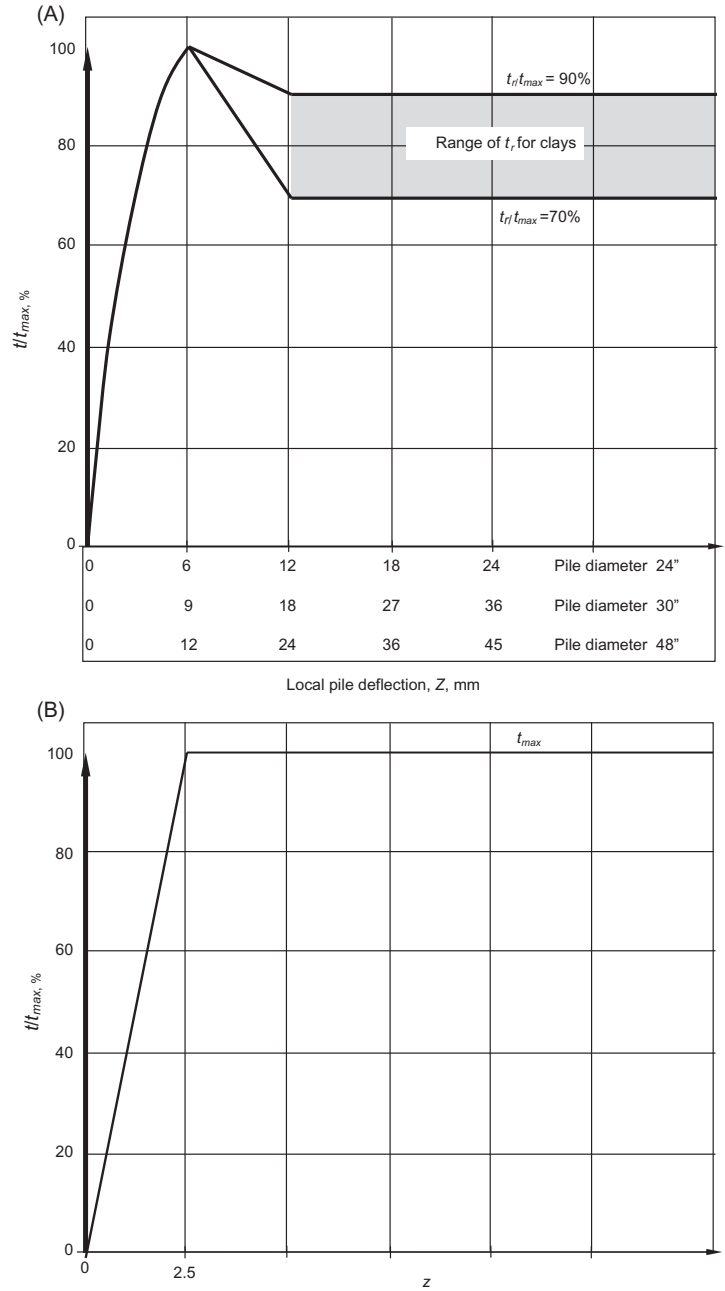

Figure 4.5 (A)Sketch of the shape of a $t-z$ curve for clay soil for different pile diameters. (B) Sketch of the shape of a $t-z$ curve for sand soil for different pile diameters. (C) $t-z$ curves recommended for noncarbonate soils, according to API RP2A.

Axial support to a pile is provided by surrounding soil, and axial pile deformation at the end of pile depth may be considered to consist of four components: elastic pile deformation, elastic soil deformation, plastic soil deformation, and plastic soil−pile slip deformation. The purpose of the $t-z$ curves is to model the latter three components. $Q-z$ curves model elastic and plastic soil deformation around the pile tip. Elastic pile deformation is not directly related to soil characteristics and is modeled in the beam−column representation of the pile.

In the past, $t-z$ curves were based directly on experimental evidence from Coyle and Reese (1966). This led to an adopted standard that peak shaft resistance was mobilized at a vertical relative pile−soil movement (Zc) of 2.54 mm (0.1 inch) in sands. For clays, the value is 1% of the pile diameter. It has been shown theoretically and experimentally that the form of the $t-z$ curve will be a function of the pile length and diameter, soil stiffness, and shaft resistance as discussed by Kraft et al. (1981a,b). However, to account for these characteristics, the average shear modulus of the soil must be known. In sand, the appropriate strain-level shear modulus is only known within an order of magnitude, and thus $t-z$ curves generated by this method will contain considerable uncertainty. However, a parametric study by Meyer et al. (1975) showed that a sixfold variation in soil yield displacement had only a small effect on the predicted pile head displacement.

The data include a peak−residual behavior for $t-z$ curves in clay, the governing parameter of which is the ratio of peak to residual unit skin friction. The recommended range for this parameter is 70%−90%. Vijayvergiya (1977) indicates that this parameter decreases with increasing overconsolidation ratio. The peak residual behavior in sand has been adopted as per Wiltsie et al. (1982).

For some projects, in the absence of more definitive criteria, the recommended $t-z$ curves for noncarbonate soils, according to API RP2A, are shown in Fig. 4.5C.

Table 4.11 presents the relation between the vertical displacement of the pile to the pile diameter and the skin friction between the pile and the soil as a percentage of the total friction capacity. The shape of the $t-z$ curve at displacements greater than z_{max}, as shown in Fig. 4.5C, should be carefully considered, where, z is the pile displacement axially, D is the pile diameter, t is the soil pile unit friction, and t_{max} is the maximum unit skin friction capacity.

The ratio between the residual unit skin friction to the maximum skin friction between pile and soil t_r/t_{max} at the axial pile displacement at which it occurs (z_r) are affected by the soil stress−strain behavior, stress history, pipe installation method, pile load sequence, and other factors.

The value of t_r/t_{max} can range from 70% to 90%. Laboratory, in situ, or model pile tests can provide valuable information for determining values of t_r/t_{max} and z_r for various soils.

The end-bearing or tip-load capacity should be determined. However, relatively large pile tip movements are required to mobilize the full end-bearing resistance. A pile-tip displacement of up to 10% of the pile diameter may be required for full mobilization in both sand and clay soils. In the absence of more definitive criteria, the curve in Fig. 4.6 is recommended for both sands and clays.

Table 4.11 Relation between the ratio of pile deflection to the diameter and the skin friction capacity.

Soil type	***z/D***	**Pile axial deflection for different pile diameter (mm)**			t/t_{max}
		24″	**36″**	**48″**	
Clays	0.0016	0.98	1.46	2.0	0.30
	0.0031	1.89	2.83	3.8	0.50
	0.0057	3.5	5.21	7.0	0.75
	0.0080	4.9	7.32	9.8	0.90
	0.0100	6.1	9.14	12.2	1.00
	0.0200	12.2	18.3	24.4	0.70−0.90
	∞				0.70−0.90
Sands	z (mm)				t/t_{max}
	0.000	0	0	0	0.00
	2.5	2.5	2.5	2.5	1.00
	∞				1.00

z is the local pile deflection (in mm), D is the pile diameter (in mm), t is the mobilized soil pile unit skin friction (in lb/ft.^{2} or kPa), and t_{max} is the maximum soil pile unit skin friction capacity computed (in lb/ft.^{2} or kPa).

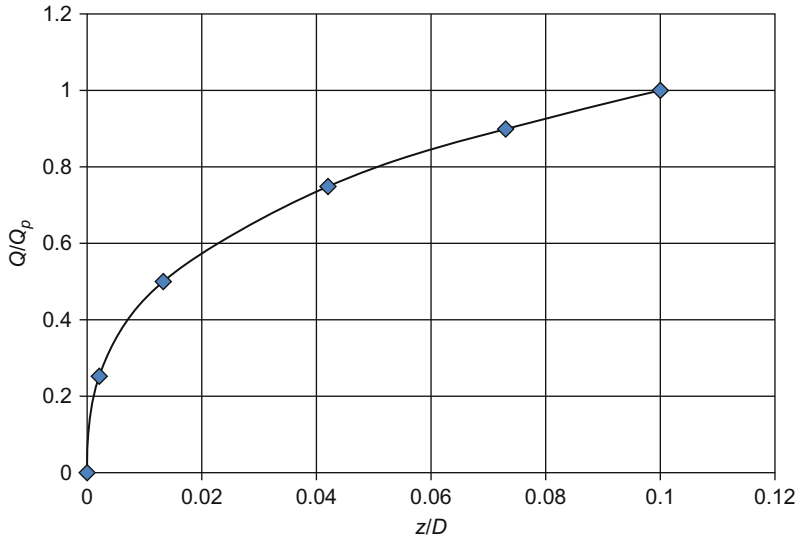

Figure 4.6 Pile-tip load displacement ($Q-z$) curve.

Table 4.12 Relation between the axial deflection to pile diameter ratio and percentage of end-bearing capacity.

z/D	**Pile axial deflection for different pile diameter (mm)**			*Q/Q_p*
	24″	**36″**	**48″**	
0.002	1.2	1.8	2.4	0.25
0.013	7.9	11.9	15.8	0.50
0.042	25.6	38.4	51.2	0.75
0.073	44.5	66.8	89	0.90
0.100	61	91.4	121.9	1.00

z is the axial tip deflection (in mm), D is the pile diameter (in mm), Q is the mobilized end-bearing capacity (in lb or kN), and Q_p is the total end bearing (in lb or kN).

Table 4.12 presents the relation between the axial displacement of the pile relative to the pile diameter and the end-bearing capacity as a percentage of the total end-bearing capacity.

The recommended curve is shown in Fig. 4.6.

Axial pile capacity

There have been several studies that have compared the axial pile capacity with pile load test by using the available data and comparing them with the offshore pile design procedure. These studies are very important to evaluate the design procedure, as a result there is a scatter diagram presenting the relation between the pile load test measurement and the predicted value from the calculation model. Based on this some important limitations should be considered, such as:

1. It is found that there are uncertainties in measurement and also in calculation, as the measured pile capacities are affected by the uncertainty in measurement error. On the other hand, the predicted pile capacity from the equation is very sensitive to the undrained shear strength values which also have an uncertainty in their values.
2. It is found that the pile load test results are affected by the design loads and the field conditions. In addition, there are a limited number of tests for the large pile diameters, with high deep length with high capacities. Generally, pile load tests have capacities that are 10% or less of the prototype capacities. Briaud et al. (1984) mentioned that another factor is the rate of loading and the cyclic load history not usually being well represented in load tests. According to Clarke (1993), pile load tests are often conducted before full set-up occurs, for practical reasons. Furthermore, for offshore pile tips the pile is open ended, which provides different results to the closed end.
3. In most studies, there are trials to eliminate factors which are significantly affected by extraneous conditions in load testing, such as protrusions on the exterior of the pile shaft from the weld beads, cover plates, or others, and also installation procedure effects if using jetting, drilled-out plugs, or other methods.

In the United States and Europe most researches into pile tests are related to offshore applications.

It is worth mentioning that the geology and operating experience in the project region are very important in pile design, so when applying exercise or case studies or research results from other regions these factors should be considered.

In addition, the designer should consider that testing the pile in tests in low plasticity silty clay soils provides an overestimate of frictional resistance by using Eqs. (4.14) and (4.15). There are a lot of researches about this point as there is no clear reason for the overestimation, therefore the designer should take care in cases with this type of soil.

Additional considerations that apply to drilled and grouted piles are discussed by Kraft and Lyons (1974) and O'Neill and Hassan (1994).

Pile load tests are commonly used as the basis for determining pile load–movement characteristics. In clay, the ultimate capacity of the pile, as shown in Fig. 4.7, reaches a maximum value at some movement, beyond which there is a gradual drop to a residual value.

The frictional resistance increases rapidly and reaches a maximum value at a very small displacement, referred to as the *critical movement*. However, the point resistance continues to increase beyond this critical movement and tends to reach a maximum value at a relatively larger movement. This maximum value is referred to as the *end-bearing capacity*.

In sand, as presented in Fig. 4.7, the ultimate capacity seems to increase and reach a constant value. The point resistance in sand continues to increase gradually. This is probably why a pile in sand does not usually reach a plunging failure during a load test. The difference between pile behavior in sand and that in clay is attributed to the different point and frictional resistances as a function of pile movement.

The relation between the lateral resistance and displacement for a 36-inch diameter pile in clay and sand is shown in Fig. 4.8.

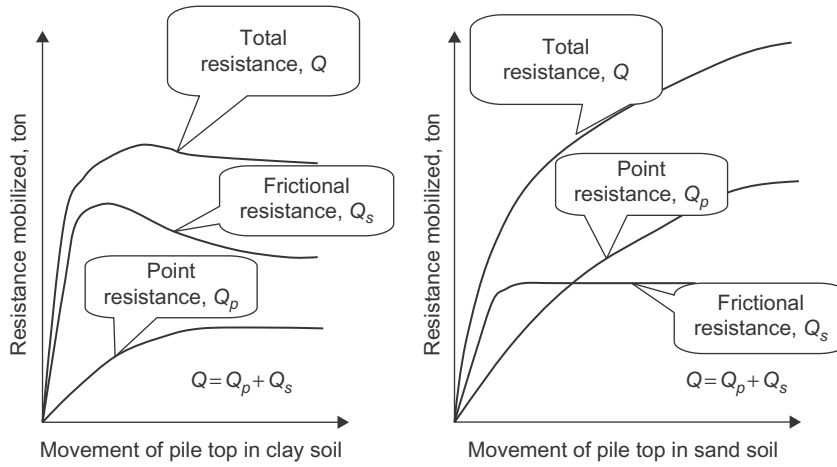

Figure 4.7 Typical load–movement characteristics of an axial-loaded pile.

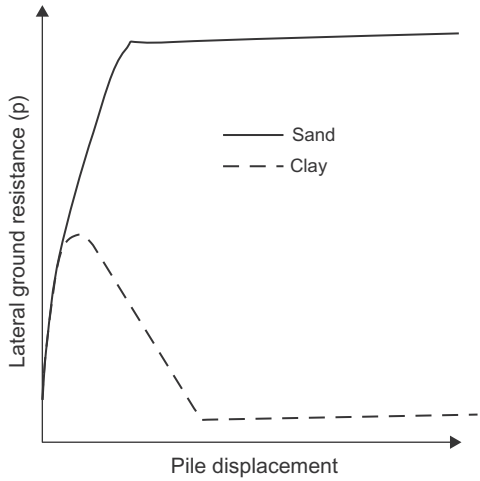

Figure 4.8 Example of a typical $p-y$ curve for a 36-inch pile.

Laterally loaded pile reactions

In the case of an offshore structure platform, the pile is designed to resist the axial load and the lateral load also in static and cyclic conditions. The pile design capacity to resist the overload lateral action should be within the factor of safety. In general, the design target is that the overall structure foundation shall not fail under overloading.

The soil lateral resistance near the sea bed influences the pile design which is also affected by the scour phenomena. In addition, soil disturbance that happens during pile installation should be considered during the design.

Clay soils behave as a plastic material under lateral loading, which makes it necessary to relate pile and corresponding soil deformation to soil resistance. Therefore lateral soil resistance deflection ($p-y$) curves should be obtained using stress−strain data from laboratory soil samples and these should be one of the deliverables in the geotechnical report. The ordinate for these curves is soil resistance, p, and the abscissa is soil deflection, y. By iterative procedures, a compatible set of load−deflection values for the pile−soil system can be developed.

Matlock (1970) performed a comprehensive study of the design of laterally loaded piles in soft clay, and Reese and Cox (1975) performed a study of laterally loaded piles in stiff clay.

In the absence of more definitive criteria, Fig. 4.11 and Table 4.14 may be used for constructing ultimate lateral-bearing−capacity curves and $p-y$ curves.

The $p-y$ curves are very important to obtain bending moment, displacement, and rotation for the pile in the case of static and cyclic loads.

Lateral bearing capacity for soft clay

According to API RP2A (2007), in the case of soft clay, the ultimate unit lateral bearing capacity under static loads, p_u, has a value that varies from $8c$ to $12c$. These values are not valid for shallow depths, because the failure occurs in a

different mode due to minimum overburden pressure. Therefore cyclic loads cause deterioration of lateral bearing capacity below that for static loads.

If there are no available accurate data, the following is recommended: p_u increases from $3c$ to $9c$ as X increases from 0 to X_R as per the following:

$$p_u = 3c + \gamma X + J\left(cX/D\right) \tag{4.19}$$

and

$$p_u = 9c \quad \text{for } X \geq X_R \tag{4.20}$$

For a condition of constant strength with depth, Eqs. (4.19)and (4.20) are solved simultaneously to have the following equation:

$$X_R = 6D/[(\gamma D/c) + J] \tag{4.21}$$

where p_u is the ultimate resistance (in kPa); c is theundrained shear strength for undisturbed clay soil samples (in kPa); D is the pile diameter (in mm); γ is the effective unit weight of soil (in MN/m^3); J is an empirical constant with values from 0.25 to 0.5; it shall be obtained by field testing; it is equal to 0.5 in Gulf of Mexico clays; X is the depth below soil surface (in mm), and X_R = depth below the soil surface to the bottom of the reduced resistance zone (in mm).

Where the strength varies with depth, Eqs. (4.19)and (4.20) may be solved by plotting the two equations, that is, p_u versus depth, where, X_R is the first intersection point of the two equations.

If the strength variation is very high, these empirical relationships may not apply. In general, minimum values of $X_R = 2.5\ D$; where D is the pile diameter.

On the other hand, in soft clay, the load−deflection ($p-y$) curves for lateral soil resistance−deflection relationships for piles are generally nonlinear. The $p-y$ curves for the short-term static load case may be generated from Table 4.13, where p = actual lateral resistance (in kPa), y = actual lateral deflection (in m),

$$y_c = 2.5\varepsilon_c D \tag{4.22}$$

and ε_c is the strain that occurs at one-half the maximum stress on laboratory unconsolidated, undrained, compression tests of undisturbed soil samples.

For the case where equilibrium has been reached under cyclic loading, the $p-y$ curves may be generated from Table 4.14.

Lateral bearing capacity for stiff clay

For static lateral loads, the ultimate bearing capacity p_u of stiff clay ($c >$ 96 kPa), as for soft clay, would vary between $8c$ and $12c$. In the case of cyclic loading, there is a rapid deterioration, therefore the ultimate resistance will be reduced to something considerably less than should be considered in cyclic design.

Table 4.13 Relation between pile lateral load and lateral deflection.

p/p_u	y/y_c
0.00	0.00
0.23	0.1
0.33	0.3
0.5	1.0
0.72	3.0
1.00	8.00
1.00	∞

Table 4.14 Relation between pile load and lateral displacement.

$X > X_R$		$X < X_R$	
p/p_u	y/y_c	p/p_u	y/y_c
0.00	0.00	0.00	0.0
0.23	0.1	0.23	0.1
0.33	0.3	0.33	0.3
0.50	1.0	0.50	1.0
0.72	3.0	0.72	3.1
0.72	∞	0.72 X/X_R	15.0
		0.72 X/X_R	∞

There is a rapid deterioration of load capacity at large deflection in the case of stiff clay, as this soil type has nonlinear stress−strain relationships and has a more brittle behavior than soft clay. Therefore its stress−strain curves and subsequent $p-y$ curves for cyclic loads should reflect this behavior with good judgment.

For a more detailed study of the construction of $p-y$ curves, see Matlock (1970) for soft clay, Reese and Cox (1975) for stiff clay, O'Neill and Murchison (1983) for sand, and Georgiadis (1983) for layered soils.

Lateral bearing capacity for sand

A series of studies have verified the theoretical studies with the field-test results during lateral loading of a 24-inch diameter test pile installed at sites with clean, fine sand and silty sand. (The studies were funded by Amoco's production

company, Chevron oil field research, Esso's production research company, Mobil Oil Corporation, and Shell's development company.) The results suggest a shape for the $p-y$ curve as shown in Fig. 4.9, where the initial part is a straight line representing the elastic behavior and the horizontal straight line represents the plastic behavior, with the straight lines connected by a parabola.

The values of *Pm* and *pc* are a function of the ultimate soil resistance. A difference between the ultimate resistance from theory and that from experiments was observed that was covered by empirical factors. Another study was performed by O'Neill and Murchison (1983), who evaluated $p-y$ relationships in sands. API RP2A (2007) recommends that the $p-y$ curve be calculated using the information from that study.

In the case of sand soil, the ultimate lateral bearing capacity is calculated in shallow depths by Eq. (4.21) and for deep depths by Eq. (4.23). Therefore at the target depth, the equation that provides the smallest value of p_u should be used as the ultimate bearing capacity.

$$p_{us} = (C_1 H + C_2 D)\gamma H \tag{4.23}$$

$$p_{ud} = C_3 D \gamma H \tag{4.24}$$

where p_u = ultimate resistance (force/unit length) (in kN/m) (s = shallow, d = deep); γ = effective soil weight (in kN/m^3); H = depth (in m); φ' = angle of internal friction of sand (in degrees); C_1, C_2, C_3 = coefficients determined from Table 4.15 as function of φ'; and D = average pile diameter from surface to depth (in m).

The relationship between lateral soil resistance and deflection ($p-y$ curve) for sand is nonlinear. If there is no definitive information available, the curve may be approximated at any specific depth H, according to API RP2A, by the following equations:

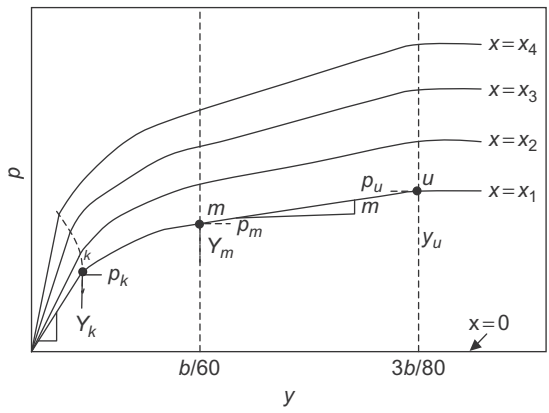

Figure 4.9 Typical family of $p-y$ curves for the proposed criteria.

Table 4.15 Coefficient C_1, C_2, C_3.

Angle of internal friction, ϕ	C_1	C_2	C_3
20	0.6	1.5	8.5
21	0.7	1.6	9.6
22	0.8	1.7	10.8
23	0.9	1.8	12.2
24	1.0	1.9	13.8
25	1.1	2.0	15.6
26	1.2	2.1	17.6
27	1.3	2.2	19.9
28	1.4	2.3	22.5
29	1.6	2.5	25.4
30	1.7	2.6	28.7
31	1.9	2.7	32.4
32	2.1	2.9	36.6
33	2.3	3.0	41.4
34	2.5	3.2	46.7
35	2.8	3.4	52.8
36	3.1	3.6	59.6
37	3.4	3.8	67.4
38	3.8	4.0	76.1
39	4.2	4.2	86.0
40	4.6	4.4	101.5

$$P = Ap_u \tanh\left[\frac{kH}{Ap_u} y\right] \tag{4.25}$$

where A is a factor to account for the cyclic or static loading condition, evaluated by $A = 0.9$ for cyclic loading and by $A \geq 0.9$ for static loading, so that:

$$A = [3.0 - 0.8(H/D)] \tag{4.26}$$

where p_u = ultimate bearing capacity at depth H (in kN/m); k = initial modulus of subgrade reaction (in kN/m^3), as determined from Table 4.16 as a function of the angle of internal friction, φ', and the relative density for sand under the water table; y = lateral deflection (in inches or m); and H = depth (in m).

Alternative methods for determining pile capacity

In clay soil, there are alternative methods described by APIRP2A (2007) for determining pile capacity that comply with industry experience. One such method is described briefly here.

For piles driven in clay soil, the skin friction, f, as from the principal is equal to or less than the undrained shear strength of the clay, c_u, as obtained from unconsolidated-undrained (UU) triaxial tests and vane shear tests.

Unless test data indicate otherwise, f should not exceed c_u or the following limits:

1. For highly plastic clays, f may be equal to c_u for underconsolidated and normally consolidated clays.

   For overconsolidated clays, $f \leq 48$ kPa for shallow penetrations or the equivalent value of c_u for a normally consolidated clay for deeper penetrations, whichever is greater.

Table 4.16 Relation between subgrade reaction, angle of internal friction, and relative density for sand below the water table.

Soil type	Angle of internal friction, ϕ	Relative density (%)	Subgrade reaction (K, t/m^3)
Very loose	<29	20	265.7
Loose sand	29–30	25	426.3
		30	553.6
		35	744.6
		40	996.4
Medium dense	30–36	45	1356.3
		50	1716.1
		55	2026.1
		60	2491.1
Dense	36–40	65	2850.9
		70	3293.8
		75	3792.0
		80	4262.6

2. For other types of clay:

$$f = c_u \text{for } c_u < 24 \text{ kPa} \tag{4.27}$$

$$f = c_u/2 \text{ for } c_u < 72 \text{ kPa} \tag{4.28}$$

f varies linearly for values of c_u between the above limits.

It has been shown that the above method provides, on average, reasonable accuracy with the pile load test database results as discussed by Olson (1984). Any method used should depend on the engineering judgment which considers the previous experience on the soil for this specific site and the industrial experience in similar soil types.

Establishing design strength and effective overburden stress profiles

The undrained shear strength and effective overburden stress profiles are the two factors that most affect the pile axial capacity calculation. The wide variety of sampling techniques and the potentially large scatter in the strength data from the various types of laboratory tests complicate appropriate selection. Therefore the undrained unconsolidated triaxial compression tests should be done carefully with a full-quality control system from the field sample and the laboratory tests as described previously.

The following factors can be a reason for the capacity degradation of long piles driven in clay soils:

1. During the pile installation, there is continuous shearing of a specific soil horizon during pile installation.
2. There is soil away from the pile due to "pile whip" during driving, causing soil lateral movement.
3. Softening phenomenon, which is a soil strength reduction with continuous displacement, and is considered a soil progressive failure. This behavior depends on the soil behavior and installation conditions.

Time affects changes in the axial capacity in clay soil

The pile capacity which is calculated from the previous equation, is not consider the effect of time aging on the pile capacity, noting that in an old platform that was constructed 40 years previously and more if the calculation is reviewed you can find that it is away from API factor of safety in addition to the environmental condition the effect of time sure affect the pile capacity as by normal phenomena with time the pile work with the surrounded soil as one unit so there are an additional adhesion is not considered in the calculation. Therefore there was a study recently performed to define the behavior of the axial capacity in clay soil with time.

Clarke (1993) and Bogard and Matlock (1990) conducted field measurement studies in which it was shown that the time required for driven piles to reach ultimate capacity in a cohesive soil can be relatively long—as much as 2−3 years.

It is worth mentioning that there is a significant strength increase in a short period after installation and this happens due to the strength rate gained rapidly after driving directly, and this rate decreases during the dissipation process.

During pile driving in normal to light overconsolidated clays, the soil surrounding a pile is significantly disturbed, the stress state is altered, and this also generates a large excess of pore pressures. After pile installation, these excess pore pressures start to dissipate meaning the surrounding soil around the piles starts to consolidate and, based on that, the pile capacity increases with time in clay soil. This process is called "*set-up*." The excess pore pressure dissipation rate is a function of the radial consolidation coefficient, pile diameter, and soil layering.

In the most popular case, where the driven pipe piles supporting a structure have design loads applied to the piles shortly after installation, the time−consolidation characteristics should be considered in the pile design. In traditional fixed offshore structure installations, the time between the pile installation and the platform being fully loaded is in the range of 1−3 months, but in some cases the commissioning and start up come early, and in this case this information should be transferred to the engineering office as the expected increase in capacity with time are important design variables that can affect the safety of the foundation system during the early stages of the consolidation process.

The pile behaviors under significant axial loads in highly plastic, normally consolidated clays were studied using a large number of model pile tests and some full-scale pile load tests.

As a result of this study of pore−pressure dissipation with load test data at different times after pile driving, empirical correlations were obtained between the degree of consolidation, plugging conditions, and pile shaft shear capacity. This study revealed that test results for closed-ended steel piles in heavily overconsolidated clay indicate that there is no significant change in capacity with time. This is contrary to tests on 0.273 m (10.75 inches) diameter closed-ended steel piles in overconsolidated clay, where considerable and rapid set-up in 4 days was found, so the pile capacity at the end of installation never fully recovered.

Therefore it is very important to highlight that the axial capacity of the pile with time is under research and development and there is no solid formula or equation to follow, but it should be a focus on the research that is done on the specific site location and also depends on the previous history of the location.

4.6.4 Pile capacity calculation methods

API RP2A (2007) presents new methods for calculating pile capacity based on the CPT.

As it is presented as a simple method for assessing pile capacity in cohesionless soils, this method is recommended in previous editions of API RP2A-working stress design (WSD). Changes were made to previous editions. The CPT is the most reliable test to calculate pile capacity. The methods of calculation depend on direct correlations between pile unit friction and end-bearing data with cone tip resistance (q_c) values and caisson friction from CPT. These CPT methods provide a pile

capacity prediction for a wider range of cohesionless soils, and have shown to be statistically closer to the pile load test results.

The new CPT-based methods for assessing pile capacity in sand are preferred to the previous method. However, more experience is required with all these new methods before any single one can be recommended for routine design instead of the previously presented method. API stated clearly that due to the sensitivity of new CPT methods, it needs a qualified engineer with enough experience to interpret the CPT data and to know the limitations and reliability of these methods.

The assumption is based on the friction and end-bearing being uncoupled. According to that, for all CPT methods, the ultimate bearing capacity in compression (Q_d) and tensile capacity (Q_t) of plugged open-ended piles are calculated by:

$$Q_t = Q_f + Q_p = P_o \int f_{c,z} dz + A_q q_p \tag{4.29}$$

$$Q_f = P_o \int f_{t,z} dz \tag{4.30}$$

As the friction component, Q_f, is calculated by the numerical integration, so the results are sensitive to the depth increment used, especially in the case of CPT-based methods. The depth increments for CPT-based methods should be in the order of one hundredth of 1% of the pile length (or smaller), this is incremental as a guide only and in any case, the depth increment should not exceed 250 mm.

There are four recommended CPT-based methods mentioned in API RP2A:

1. Simplified ICP-2005;
2. UWA-05 for offshore (Lehane et al., 2005a,b);
3. Fugro-05 (Lehane et al., 2005a; Kolk et al., 2005);
4. NGI-05 (Lehane et al., 2005a; Clausen et al., 2005).

ICP-05 method is a simplified form of the Jardine et al. (2005) design method, whereas the second is a simplified a form of the UWA-05 method, which is applicable to offshore piles. The other three methods are summarized by Lehane et al. (2005a). It is important to avoid calculating friction and end-bearing components from different methods.

The unit skin friction formulae for open-ended steel pipe piles for the first three recommended CPT-based methods (Simplified ICP-05, Offshore UWA-05, and Fugro-05) can all be considered as special cases of the general formula:

$$f_z = u\prime\, q_{cz} \left(\frac{\sigma'_{vo}}{P_a}\right) A_r^b \left[\max\left(\frac{L-z}{D}, v\right)\right]^{-c} [\tan \delta_{cv}]^d \left[\min\left(\frac{L-z}{D}\frac{1}{v}, 1\right)\right] \tag{4.31}$$

where f_z is the unit skin friction, δ_{cv} is pile−soil constant−volume interface friction angle, L *is* the pile length underneath the seabed, $A_r = 1 - (D_i/D)^2$, D_i is the pile inner diameter ($D_i = D - 2t$), z is the depth under the seabed, q_{cz} is the CPT tip resistance at depth z, D is the outer diameter, t is the wall thickness, and P_a is the atmospheric pressure equal to 100 kPa.

Table 4.17 provides the recommended values for parameters a, b, c, d, e, u, and v for compression and tension, which are the unit skin friction parameter values for driven open-ended steel piles for the Simplified ICP-05, Offshore UWA-05, and Fugro-05 methods.

Additional recommendations for computing unit friction and end bearing for all four CPT-based methods are presented in the following subsections.

Simplified ICP-05

A comprehensive overview of research work performed at Imperial College on axial pile design criteria of open- and closed-ended piles in clay and sand is presented by Jardine et al. (2005). The design equations for unit friction in sand in this publication include that unit friction is favorably influenced by soil dilatancy. This influence reduces with increasing pile diameter.

The Simplified ICP-05 method as presented by API RP2A for unit skin friction of open-ended pipe piles and the parameter values in Table 4.17 are a conservative approximation of the full ICP-05 method, since dilatancy is ignored and some parameter values were conservatively rounded up and down.

Use of the original design equations in Jardine et al. (2005) may be considered, particularly for small-diameter piles ($D < 0.76$ m), provided that larger factors of safety are considered in the WSD design.

The ultimate unit end bearing for open-ended pipe piles, Q_p, follows the recommendations of Jardine et al. (2005), which specify an ultimate unit end bearing for plugged piles given by:

$$q_p = q_{ca}\{[0.5 - 0.25 \log 10(D/D_{CPT})] \geq 0.15 q_{c,av,1.5D}\} \tag{4.32}$$

where q_{ca} is the average q_{cz} value between 1.5 D_o above the oil tip to 1.5 D_o below the pile tip level, and D_{CPT} is the CPT tool diameter (about 36 mm for a standard 1000 mm^2 base net cone).

Table 4.17 Unit skin friction parameter values for driven open-ended steel pipes (simplified ICP-05 and Fugro-05 methods).

Method	**Load direction**	***a***	***b***	***c***	***d***	***e***	***u***	***ν***
Simplified ICP-05	Compression	0.1	0.2	0.4	1	0	0.023	$4\sqrt{A_r}$
	Tension	0.1	0.2	0.4	1	0	0.016	$4\sqrt{A_r}$
Fugro-05	Compression	0.05	0.45	0.90	0	1	0.043	$2\sqrt{A_r}$
	Tension	0.15	0.42	0.85	0	0	0.025	$2\sqrt{A_r}$

Jardine et al. (2005) specify that plugged pile end-bearing capacity applies; that is, the unit end-bearing q_p acts across the entire tip cross-section, only if both the following conditions are met:

$$D_i < 2(D_r - 0.3)$$

(Note: D_i units are inches or m and D_r units are not percentages, but fractions.) and

$$D_i/D_{CPT} < 0.083 q_{c,z} < p_a \tag{4.33}$$

Should either of the above conditions not be met, then the pile will behave as unplugged and the following equation should be used for computing the end-bearing capacity:

$$Q_p = \pi\, t(D - t) q_{c,z} \tag{4.34}$$

The full pile end bearing calculated using Eq. (4.32) for a plugged pile should not be less than the end-bearing capacity of an unplugged pile calculated using Eq. (4.34).

Offshore UWA-05

For friction, Lehane et al. (2005a) summarize the results of recent research work at the University of Western Australia on the development of axial pile design criteria of open- and closed-ended piles driven into silica sands. The full design method, which was presented by Lehane et al. (2005a,b) for unit friction on pipe piles, includes a term allowing for favorable effects of soil dilatancy being similar to ICP-05 and an empirical term allowing for partial soil plugging during pile driving. Lehane et al. recommend for offshore pile design to ignore these two favorable effects, which are dilatancy and partial plugging. Use of the original full design equations in Lehane et al. (2005a) can be confidently used for small-diameter piles, $D < 750$ mm (30 inches), provided that larger factors of safety are considered in the WSD design.

For end bearing, Lehane et al. (2005a,b) present design criteria for ultimate unit end bearing of plugged open-ended pipe piles. Their full design method for pipe piles includes an empirical term allowing for the favorable effect of partial plugging during pile driving. For offshore pile design, Lehane et al. (2005a,b) recommend this effect be ignored, resulting in the recommended design equation for plugged piles in the Offshore UWA-05 method:

$$Q_p = q_{ca}(0.15 + 0.45 A_r) \tag{4.35}$$

Since the UWA-05 method considers nonplugging under static loading to be exceptional for typical offshore piles, the method does not provide criteria for unplugged piles.

The unit end-bearing q_p calculated in Eq. (4.35) is therefore acting across the entire tip cross-section. The use of $q_{c,av15D}$ in Eq. (4.35) is not recommended in sand profiles, where the CPT q_c values show significant variations in the vicinity of the pile tip or when penetration into a founding stratum is less than five pile diameters. For these situations, Lehane et al. (2005a) provide guidance on the selection of an appropriate average q_c value for use in place of q_c.

The unit skin friction in compression and tension will be obtained as follow:

Compression:

$$f_{zc} = 0.03.q_{cz}\left(\frac{\sigma'_{vo}}{P_a}\right)A_r^{0.3}\left[\max\left(\frac{L-z}{D},2\right)\right]^{-0.5}[\tan c\delta_{cv}]\left[\min\left(\frac{L-z}{2D},1\right)\right] \tag{4.36}$$

Tension:

$$f_{zt} = 0.022.q_{cz}\left(\frac{\sigma'_{vo}}{P_a}\right)A_r^{0.3}\left[\max\left(\frac{L-z}{D},2\right)\right]^{-0.5}[\tan \delta_{cv}]\left[\min\left(\frac{L-z}{2D},1\right)\right] \tag{4.37}$$

Fugro-05

For friction, the Fugro-05 method is a modification of the ICP-05 method. This method was studied by Fugro (2004) and Kolk et al.(2005), and also by Lehane et al. (2005a) and in Eq. (4.31) and the parameter values in Table 4.17. In the case of using ICP-05 and the UWA-05 or Fugro-05 methods, it is recommended to consider larger factors of safety when using as discussed by CUR (2001) in the reliability of design using these methods.

For end bearing, the basis for the ultimate unit end bearing on pipe piles according to Fugro-05 is presented in the research report to API (Fugro, 2004) and is summarized by Kolk et al. (2005). The recommended design criterion for plugged piles is given by the following equation:

$$Q_p = 8.5\sqrt{p_a q_{ca}}A^{0.25}r \tag{4.38}$$

Note that the UWA-05 and Fugro-05 methods do not specify unplugged end-bearing capacity because in traditional fixed offshore platforms, piles behave in a plugged end mode during static loading as discussed by CUR (2001). It can be shown that plugged behavior applies in the following cases:

1. If the cumulative thickness of sand layers within a soil plug is in excess of 8D, or;
2. The total end bearing (Q_p) is limited, as follows:

$$Q_p \leq Q_{f,I,clay}e^{\mathrm{Ls/D}} \tag{4.39}$$

The value of the friction capacity ($Q_{f,i,clay}$) inside the pile in plugged soil can be calculated using the same methods in calculating the pile friction in clay.

The above criteria apply for fully drained behavior of sand within the pile plug. Criteria for undrained and partially drained sand plug behavior are presented by Randolph et al. (1991).

For the exceptional case of unplugged end-bearing behavior in fully drained conditions, reference is made to CUR (2001) and Lehane and Randolph (2002) for estimating end-bearing capacity.

NGI-05

For friction calculation in NGI-05, Clausen et al. (2005) provided the ultimate unit skin friction values for tension ($f_{t,z}$) and compression ($f_{c,z}$) for driven open-ended steel pipe piles:

$$f_{tz} = (z/L)p_a(\sigma'_{vo}/p_a)^{0.25}F_{D_r} > 0.1\sigma'_{vo} \tag{4.40}$$

$$f_{cz} = 1.3(z/L)p_a(\sigma'_{vo}/p_a)^{0.25}F_{D_r} > 0.1\sigma'_{vo} \tag{4.41}$$

where:

$$F_{D_r} = 2.1(D_r - 0.1)^{1.7} \tag{4.42}$$

$$D_r = 0.4\ln\left(\frac{q_{c,z}}{22(\sigma'_{vo}p_a)^{0.5}}\right) > 0.1 \tag{4.43}$$

Note: $D_r > 1$ should be accepted and used.

As for the "full" ICP-05, "full" UWA-05, and Fugro-05 methods, higher factors of safety are recommended when using the NGI-05 method.

For end bearing, the recommended design equation for ultimate unit end bearing of plugged open-ended steel pipe piles in the NGI-05 method, according to Clausen et al. (2005), is:

$$Q_p = \frac{0.7q_{ca}}{1 + 3D_r^2} \tag{4.44}$$

where;

$$D_r = 0.4\ln\left(\left[q_{ca}/(22(\sigma'_{vo}p_a)^{0.5})\right] > 0.1\right) \tag{4.45}$$

Note that $D_r > 1$ should be accepted and used.

The resistance of nonplugging piles should be computed using an ultimate unit wall end-bearing value (q_{wz}) given by:

$$q_{wz} = q_{cz} \tag{4.46}$$

and an ultimate unit friction (f_{pz}) between the soil plug and inner pile wall given by:

$$f_{pz} = 3f_{cz} \tag{4.47}$$

The lower value of the plugged resistance by Eq. (4.46) and unplugged resistance by Eqs. (4.46) and (4.47) should be used in design.

Application of CPT

By using CPT measurement as the basis for the previous methods to calculate the unit skin friction and end bearing for the pile there are some precautions and information that should be considered as in obtaining $t-z$ data for axial load–deformation response, the peak unit skin friction in compression and tension at a given depth, f_{cz} and f_{tz}, are not unique and are both dependent on pile geometry. In general, the axial load and deformation response are affected by the pile penetration depth, the pile diameter, and its wall thickness. Noting that, an increased pile penetration will decrease these ultimate values at a given depth.

In the case of doing the test to obtain the $q-z$ data for axial load–deformation response, the end bearing (Q_p) is assumed to be fully mobilized at a pile tip-displacement value of $0.1D$.

Soil types such as carbonate sands, micaceous sands, glauconitic sands, volcanic sands, silts, and clayey sands have unusually weak structures with compressible grains. These require special consideration in situ and in laboratory tests for the selection of an appropriate design method and design parameters according to Thompson and Jardine (1998) and Kolk (2000) for pile design in carbonate sand, and Jardine et al. (2005).

It is worth mentioning that in the case of using CPT in cohesionless soil, such as gravel, when particle sizes are in excess of 10% of the CPT cone diameter, they are misleading, and one possible approach could be to use the lower-bound q_c profile. In this case, one can estimate the end-bearing capacity profile from the adjacent sand layers.

In the case of using CPT in weaker clay layers near the pile tip, it is recommend that obtaining q_c data averaged between $1.5D$ above the pile tip to $1.5D$ below the pile tip level should generally be satisfactory, provided q_c does not vary significantly. The UWA method should be used, if there is significant q_c variations occur, to compute $q_{c,av}$.

The case of a thin clay layer, which is less than around $0.1D$ thick, is a problem, especially when CPT data are discontinuous vertically or not all pile locations have

been investigated. From a practical point of view, the offshore piles usually develop only a small percentage of q_p under extreme loading conditions. Therefore the finite element method can be used in calculating the pile capacity and settlement of a pile tip on sand containing weaker layers, and may be considered to assess the axial pile response under such conditions.

It is recommended that the end-bearing component be reduced in the case that the pile tip is within a zone up to $\pm 3D$ from such layers. When q_c data averaging is also applied to this $\pm 3D$ zone, the combined effects may be unduly cautious and such results should be critically reviewed; this rule is applied also in the case of large pile diameter ($D > 2$ m).

4.6.5 Pile capacity under cyclic loadings

Environmental loadings are developed by winds, waves, currents, earthquakes, and ice floes. These loadings are considered the source of cyclic loading as they can have both low- and high-frequency cyclic components in which the rates of load application and duration are measured in seconds. Storm and ice loadings can have several thousand cycles of applied forces, while earthquakes can induce several tens of cycles of forces.

For most fixed offshore platforms supported on piles, experience has proven the adequacy of determining pile penetration based on static capacity evaluations, static ultimate design loads, and commonly accepted factors of safety that, in part, account for the cyclic loading effects.

Cyclic loading effects

A study by Briaud et al. (1984) on the axial capacity and performance of piles showed that, as compared with long-term, static loadings, cyclic loading may have the following important influence on pile axial capacity and stiffness: it may decrease capacity and stiffness due to repeated loading. On the other hand, it may increase capacity and stiffness due to the high rates of loading.

The cyclic loading effect on pile capacity comes from resistance from the pile and soil and the load itself. The primary influences of the pile properties include stiffness, length, diameter, material, soil characteristics (type, stress history, strain rate, and cyclic degradation), and the loadings, such as the numbers and magnitudes of repeated loadings.

Cyclic loading can provide a positive effect by stiffening and strengthening, or on the contrary, may be a reason for softening and weakening of the soils around the pile and also may cause accumulation of pile displacements.

For earthquakes, free-field ground motions, which are natural phenomena, are not affected by the existence of the piles and structure but develops due to vibrations and cyclic straining effects in the soils; these effects may influence pile capacity and stiffness. The soil will dampen the earthquake vibration and absorb the loading energy.

Analytical models

A primary objective of these analyses is to ensure that the pile and its penetration under static and cyclic loading are adequate to meet the structure's serviceability and capacity based on the ultimate limit state requirements.

There are different analytical models that have been developed and applied to determine the cyclic axial response of piles, as presented in API RP2A. In general, these models can be categorized into two model types—discrete element models and continuum models—noting that these two models use the finite difference method or finite element method. These two types of analytical model are described next.

Discrete element models

The soil around the pile is modeled by a series of uncoupled springs or elements attached between the pile and the far field soil, and in most cases it is assumed to be rigid. The material behavior of these elements may vary from linearly elastic to nonlinear, hysteretic, and rate dependent. According to Bea and Audibert (1979) and Karlsrud et al (1986), the soil elements are commonly referred to as shaft resistance−displacement ($t-z$) and tip resistance−displacement ($Q-z$) elements.

Linear or nonlinear dashpots as the velocity and dependent resistances can be placed in parallel and in series with the discrete elements to model radiation damping and rate of loading effects, as per Bea (1982) and Bea et al. (1984). The pile can also be modeled as a series of discrete elements, for example, rigid masses interconnected by springs, or it can be modeled as a continuous element (rod), either linear or nonlinear. In these models, the material properties for soil and pile can vary along the pile.

This type of model is the most popular in fixed offshore structure analysis.

The primary steps in performing an analysis of cyclic axial loading effects on a pile using discrete element models are summarized in the following:

1. The characteristic of pile loadings during hammering such as the magnitudes, durations, and numbers of cycles. This includes both long-term loadings and short-term cyclic loadings. The design shall be done for static and cyclic loadings that are expected.
2. The pile properties must be defined such as its diameter, wall thickness, stiffness properties, weight, and length. Therefore this will need an initial estimate of the pile penetration that is expected to be enough to withstand the design loadings. For pile length estimation, an empirical, pseudostatic method based on pile load tests or soil tests can be used.
3. Soil properties should be defined, as any analytical approaches will require different soil parameters.

For practical reasons, discrete element models solved numerically have seen the most used in the evaluation of piles subjected to high-intensity cyclic loadings. Based on Poulos (1983) and Karlsrud et al. (1986), the results from these models are used to develop information on pile accumulated displacements and pile capacity following high-intensity cyclic loadings.

Continuum models

The soil around the pile is idealized as a continuum attached continuously to the pile.

The pile is typically modeled as a continuous rod, either linear or nonlinear. According to Novak and Sharnouby (1983) and Desai and Holloway (1972), the model material properties can vary in any direction. A wide range of assumptions can be used regarding boundary conditions, solution characteristics, and others that lead to an unlimited number of variations for either of the two approaches.

The main key for establish the model is to define the soil elastic properties of E, G, ν, D. In addition, the discrete element model, relation between soil resistance and corresponding displacement along the pile shaft ($t-z$) and at its tip ($Q-Z$) should be defined. These factors can be defined by in situ and laboratory soil tests, and also model and prototype pile load tests. These tests should at least cover the effects of pile installation, loading, and time. Another important key to the model is to establish the boundary condition of the model.

The finite element models have been used for specialized analyses of piles subject to monotonic axial loadings, as discussed by Novak and Sharnouby (1983).

As the elastic continuum models solved analytically are similar to machine vibration analyses, it is found that this model is useful in evaluating piles subjected to low-intensity, high-frequency cyclic loadings at or below design working loadings. In the case of higher-intensity loading, Lysmer (1978) suggested that, where material behavior is likely to be nonlinear, the continuum model solved analytically can still be used by employing equivalent linear properties that approximate the nonlinear, hysteretic effects.

4.7 Scour

Sea-bed scour affects both lateral and axial pile performance and capacity. Scour prediction remains an uncertain art. Sediment transport studies may assist in defining scour design criteria but local experience, from ROV inspection of the existing platform, is the best guide. The uncertainty in design criteria should be handled by robust design, or by an operating and maintenance strategy of monitoring the scour and performing a proper remedy maintenance action. Typical remediation experience as documented in scour design criteria will usually be a combination of local and global scour.

Scour (sea-bed erosion due to wave and current action) can occur around offshore piles. Common types of scour are:

- General or global scour, which affects the area of the piles and is usually twice the area that is covered by the platform;
- Local scour, which occurs around specific areas of the structure, such as the piles.

Scour occurs if the water velocity is high enough to lift and carry the sea-bed sediments in suspension from the area. Turbulence assists this process by breaking

up consolidated sediments. Scour is a particular problem in the southern end of the North Sea, which has high tidal currents and a loose sand sea bed. Significant scour may occur during a single storm.

Bijaker (1980) defines three mechanisms that cause scour to occur:

- An increase in water velocity around the object;
- A vortex trail shed on the downstream side of the object;
- A vertical component of the water velocity caused by the presence of the object.

Niedoroda et al. (1981) discussed the process of scour formation in more detail, and Chow and Herbich (1978) have studied scour patterns around pile groups.

In general, in the design of the offshore jacket structure it is assumed that local scour is 1.5 times the leg diameter, and depth of global scour is assumed to be 1 m.

There is no generally accepted method to account for scour in axial capacity for offshore piles. Whitehouse (1998) gave techniques for scour depth assessment. In addition, general scour data may be obtained from national authorities.

Scour decreases the axial pile capacity in sand. Both friction and end-bearing components may be affected. This is because scour reduces both q_c and σ'_v (vertical effective stress) whereas q_c is simply proportional to σ'_v

$$q_{cf} = \phi q_{co} \tag{4.48}$$

where $q_{c,f}$ is the final q_c value after general scour, q_{co} is the original q_c value before general scour, ϕ a dimensionless scour reduction factor is the $\sigma'_{vf}/\sigma'_{vo}$, where σ'_{vf} is the final vertical effective stress value, and σ'_{vo} is the original vertical effective stress value.

The scour reduction factor is presented by the following equation based on a conservative approach (Fugro, 1995) for normally consolidated sands.

$$\phi = \left(\frac{1}{1 + 2k_o} \sqrt{\frac{H' + 2k_o\sqrt{H_{GS}H' + H^2 H_{GS}}}{H_{GS} + H'}} \right) \tag{4.49}$$

where H' is the depth below final sea-bed level $= H - H_{GS}$ and $H_{GS}$is the general scour depth.

Scour reduces lateral soil support (Fig. 4.10), which leads to an increase in pile maximum bending stress. Scour is generally not a problem for cohesive soils, but should be considered for cohesionless soils.

As shown in Fig. 4.10, H_{GS} is the general scour depth. H_O is the overburden reduction depth ($6.0 \times D$ is typical), H_{LS} is the local scour depth ($1.5 \times D$ is typical), p' is the vertical effective stress, H is the depth below the original sea floor, and H' is the depth below the final general sea floor.

E_S is the initial modulus of subgrade reaction and is calculated from the following equation:

$$E_S = kH$$

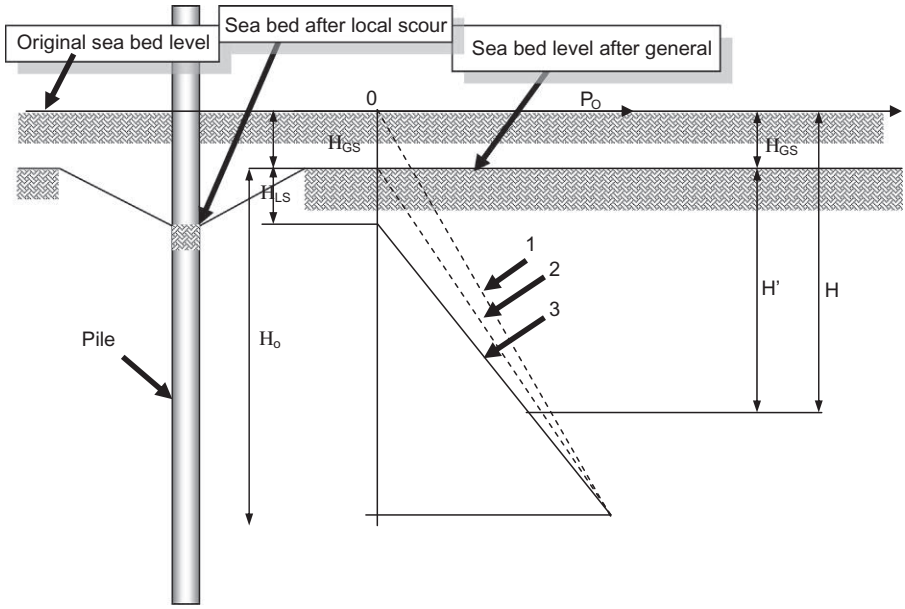

Figure 4.10 Relation between scour and lateral soil support.

Therefore the scour will decrease the modulus of the subgrade which is the lateral soil support as the scour will decrease the value of H which is the soil depth around the pile as shown in Fig. 4.10, so the triangle of calculating the lateral soil support will decrease from 1 to 2 after general scour and reduce to 3 after local scour.

In the absence of project-specific data, for an isolated pile, a local scour depth equal to $1.5D$ and an overburden reduction depth equal to $6D$ may be adopted, where D *is* the pile outside diameter.

A reduction in lateral soil support is due to:

1. A lower ultimate lateral pressure caused by decreased vertical effective stress p_0, and
2. A decreased initial modulus of subgrade reaction (E_S).

There is no generally accepted method to allow for scour in the $p-y$ curves for offshore piles. There is a method for evaluating p_0 and E_S dependent on scour depths. In this method, general scour reduces the p_0 profile uniformly with depth, on the other hand the local scour reduces p linearly with depth to a certain depth below the base of the scour pit.

The subgrade modulus reaction (E_S) can be calculated assuming the general scour condition only. Other methods can be used depending on the local practice and previous experience in the same location.

Another area of concern in installing piles for offshore structures is the adequacy of existing hammers to produce the required pile penetration to support the applied load on the platform. Wave theory is based on the fact that each hammer blow

produces a stress wave that moves along the length of the pile at the speed of sound. That the entire length of the pile is not stressed simultaneously is assumed in conventional dynamic formulas.

4.8 Pile wall thickness

The wall thickness of the pile may vary along its length and may be controlled at a particular point by any one of several loading conditions or requirements.

The allowable pile stresses should be the same as those permitted by the American Institute of Steel Construction (AISC) specification for a compact hot-rolled section. The in-place structure analysis considers the restraints placed upon the pile by the soil structure interaction should be used to determine the allowable stresses for the portion of the pile that is not laterally restrained by the soil.

General buckling of the pile underneath the soil bed will not be considered unless the pile is expected to be laterally unsupported in the case of extremely low soil shear strengths, large computed lateral deflections, or another specific reason.

4.8.1 Pile stresses

The higher pile stresses close to the seabed, and possibly at other points, are normally controlled by the combined axial load and bending moment due to the design loading applied to the platform.

The bending moment on the pile may be calculated with the calculated soil reactions taking into consideration the scour effect. It may be assumed that the axial load is removed from the pile by the soil at a rate equal to the ultimate soil−pile unit skin friction divided by the appropriate pile safety factor, as specified in Table 4.11. When lateral deflections associated with cyclic loads at or near the seabed are relatively large, exceeding y_c for soft clay, consideration should be given to reducing or neglecting the soil−pile adhesion by friction through this zone.

4.8.2 Stresses due to the hammer effect

Each pile head on which a pile hammer will be hammered should be checked for stresses due to impact load and the weight of the auxiliary equipment. These loads may be the limiting factors in establishing the maximum length of add-on sections. This is particularly true in cases where piling will be driven or drilled on a batter which is common in fixed offshore platforms, as shown in Chapter 3, Offshore structure platform design. The most traditional effects include: static bending, axial loads, and the lateral loads generated during initial hammer placement.

The following recommendations should be followed in calculating static stresses to avoid failure of the pile wall due to hammering loads.

1. The pile is considered as a freestanding column. The effective buckling length factor = 2.1 as a minimum and a reduction factor C_m = 1.0 as a minimum.

2. Bending moments and axial loads calculation based on the full weight of the pile hammer, cap, and leads acting through the center of gravity of their combined masses, and the pile weight considering the pile batter eccentricities.

The calculated bending moment should be higher or equal to a value that corresponds to a load equal to 2% of the sum of the weight of the hammer, cap, and leads applied at the pile head and perpendicular to its centerline.

Allowable stresses in the pile shall comply with the allowable stress design by AISC. Note that the one-third increase in allowable strength should not be considered.

More attention should be paid to the stresses that occur in the freestanding pile section during driving, as shown in Figs. 4.11 and 4.12. Generally, stresses are checked based on the conservative criterion that the sum of the stresses due to the dynamic stresses caused by the impact from the hammer and the stresses due to axial load and bending (the static stresses) should not exceed the minimum yield stress of the steel.

The engineering office should clearly define in the calculation notes, drawings, and specification the required pile hammers that will be used.

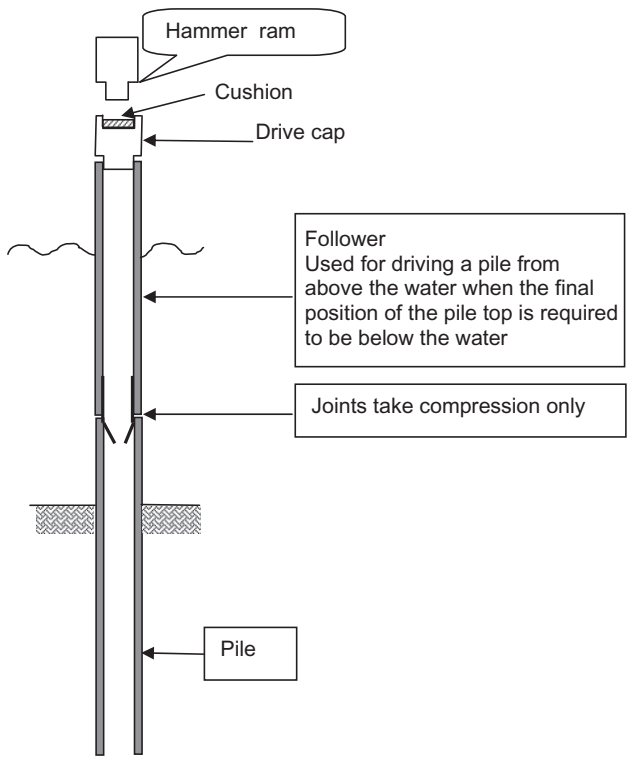

Figure 4.11 Typical arrangement for pile driving.

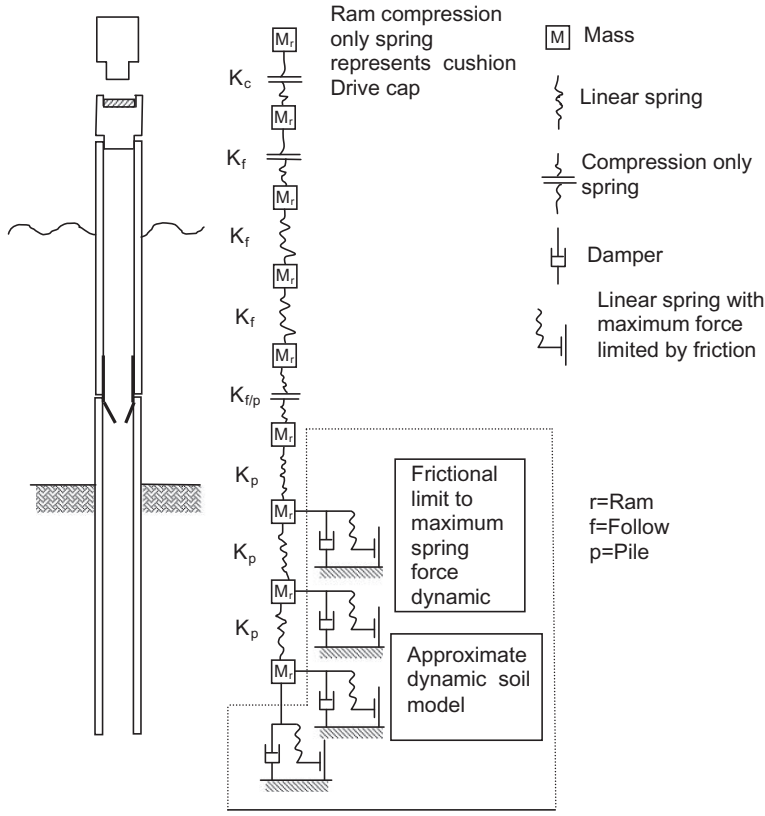

Figure 4.12 Dynamic analysis model of pile driving.

A method of analysis based on wave propagation theory should be used to determine the dynamic stresses.

In general, it is assumed that pile buckling will not occur as a result of the dynamic portion of the driving stresses. The dynamic stresses $\leq 0.8-0.9\ F_y$, depending on specific factors, for example, the maximum stresses location, the number of blows, previous experience with the pile−hammer combination, and the confidence level in the analyses. In most cases special considerations apply to avoid damage to the appurtenances when significant driving stresses may be transmitted into the structure.

The static stress during driving may be taken to be the stress resulting from the weight of the pile above the point of calculation plus the pile hammer components actually supported by the pile during the hammer blows, including any bending stresses resulting therefrom. The responsibility of the contractor to control hydraulic hammers, that the driving energy should not exceed the rated energy as there is a limited deviation is only usually considered in engineering studies. It is important to calculate carefully the static stresses which are present due to the hydraulic

hammers as there are possible variations in driving configurations, for example, in the case of installing and driving the piles without lateral restraint and at the same time being exposed to wave and wind forces during driving.

In the past, many case studies were reported that describe some of the unusual characteristics of piles on carbonate soils and their often poor performance. In the Gulf of Mexico, it has been observed from numerous pile load tests data that piles driven into carbonate soils with weak cemented and compressible mobilize only a fraction of the capacity, as low as 15%, predicted by conventional design methods for siliceous material.

On the other side, in the case of dense, strongly cemented carbonate deposits, they can provide higher capacity values than the equation.

The energy is determined primarily by the mass of the ram and its impact velocity:

$$E = \{1/2\}mV^2 \tag{4.50}$$

Note that only 60%−70% of the energy is typically transferred to the drive cap from the ram, as shown in Fig. 4.16. It is obvious that the greater the energy, the greater will be the penetration; on the other hand, the greater will be the risk of damaging the pile. The maximum stress in the stress wave is largely determined by the velocity of the ram. It is worth mentioning that, for easy driving conditions, long duration, and a low stress waveform are the best, and this could be achieved by a heavier and slower ram and a soft cushion.

Using the finite difference method, the ram is represented by a concentrated mass, and the required information about the ram is available from the hammer manufacturer. The efficiency of the hammer depends on the conditions as well as the operating procedures, as shown in Table 4.18 for various hammer types.

4.8.3 Minimum wall thickness

API RP2A defines that the minimum wall thickness of the pile based on the diameter to thickness ratio (D/t) ratio of the entire length of a pile should be small to avoid local buckling when the stresses reach the yield strength of the pile material. It is very important to consider the installation process when choosing the pile

Table 4.18 Efficiency for different hammer types.

Hammer	Efficiency
Single-acting steam or air	0.75−0.85
Double-acting steam or air	0.70−0.80
Diesel	0.85−1.0
Hydraulic	0.85−0.95

thickness and also the service life of the piling as it should consider a corrosion allowance to cover the corrosion effect during the platform life time.

For piles that are to be installed by driving, where sustained hard driving 820 blows per meter with the largest size hammer to be used is anticipated, the minimum piling wall thickness used should be more than

$$t = 6.35 + D/100 \tag{4.51}$$

where t is the wall thickness (in inches or mm) and $D$is thediameter (in inches or mm).

Minimum wall thickness for normally used pile sizes should be as listed in Table 4.19.

The preceding requirement for a smaller D/t ratio when hard driving is expected may be relaxed when it can be shown by past experience or by detailed analysis that the pile will not be damaged during its installation. A typical example of pile thickness at different depths is shown in Fig. 4.13.

4.8.4 Driving shoe and head

The driving shoe and head is usually the responsibility of the contractor with approval from the engineering office. The objective of the driving shoes is to assist piles to penetrate through hard layers and also to reduce driving resistances as it can enable easy installation. Noting that, different design considerations apply for each use.

Table 4.19 Minimum pile wall thickness.

Pile diameter, in mm (inches)	Nominal wall thickness, in mm (inches)
610 (24)	13 (½)
762 (30)	14 ({9/16})
914 (36)	16({5/8})
1067 (42)	17({11/16})
1219 (48)	19({3/4})
1524 (60)	22({7/8})
1829 (72)	25(1)
2134 (84)	28 (1{1/8})
2438 (96)	31(1{1/4})
2743 (108)	34 (1{3/8})
3048 (120)	37 (1{1/2})

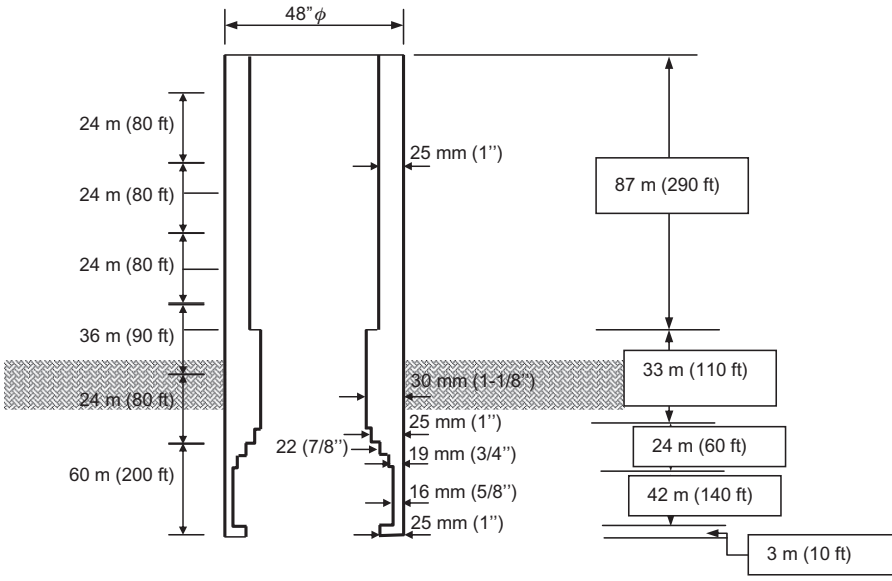

Figure 4.13 Example of design and assembly for offshore pile.

From the soil report, if there is a hard layer the driving shoe should be designed to avoid high driving stresses from occurring at and above the transition point between the normal and the thickened section at the pile tip.

On the other hand, the design of the pile shoe should be checked to guarantee that the piling shoe will not reduce the end-bearing capacity of the soil plug below the value assumed in the design. As the external shoes tend to reduce the skin friction along the length of pile above them, they are not used.

The installation contractor is responsible for designing the driving head at the top of the pile, which should be designed to ensure that it is fully compatible with the proposed installation procedures and equipment.

In comparing pile driving onshore with offshore pile driving (as shown in Fig. 4.14), one can see that the ultimate capacity of the pile onshore is 200 tons and the hammer needs to produce 2.7 tons, while for the offshore pile, the capacity can reach 200 tons with three times higher energy, for about 8.3 tons with the same pile diameter (48 inches).

4.8.5 Pile section lengths

To select suitable pile section lengths, the following constraints should be considered:

1. The lifting equipment capability to raise, lower, and stab the sections;
2. The lifting equipment capability to place the pile-driving hammer on the sections to be driven;

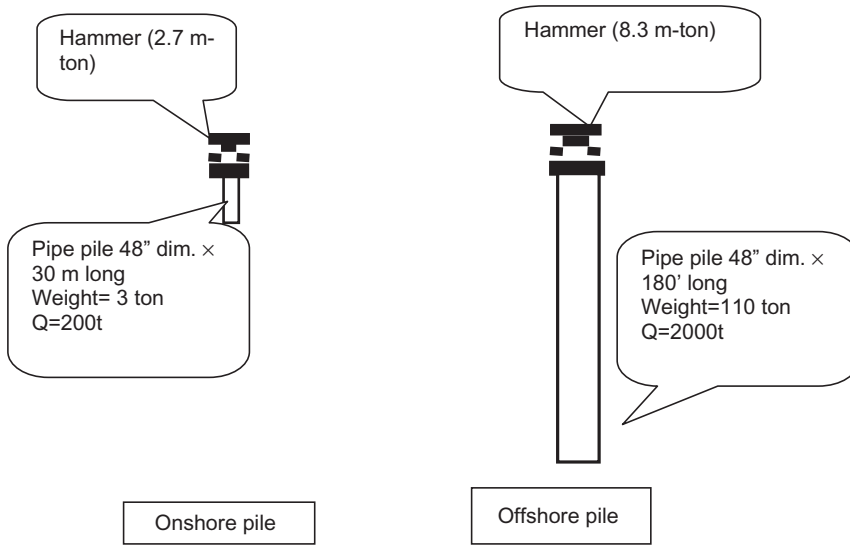

Figure 4.14 Comparison of pile driving onshore and offshore.

3. The possible occurrence of a large amount of downward pile movement;
4. The amount of stresses which will be developed in the pile section while lifting;
5. The pile wall thickness and material properties at field welds;
6. Avoiding interference with the planned concurrent driving of neighboring piles;
7. The type of soil in which the pile tip is positioned. In addition, static and dynamic stresses due to the hammer weight and operation should be considered. Each pile section on which driving is required should contain a cutoff allowance to permit the removal of material damaged by the impact of the pile-driving hammer. The normal allowance is 2−5 ft. (0.5−1.5 m) per section. This cutoff allowance should be made at a conveniently accessible elevation.

4.9 Pile drivability analysis

The pile drivability analysis has three stages:

1. evaluation of soil resistance to driving (SRD);
2. wave equation analysis;
3. estimate of blowcount versus pile penetration.

The procedures used to evaluate the SRD are empirical and have been developed from the back-analysis of pile-driving records. Their use is therefore limited to pile drivability assessment by wave equation analysis and they are not intended to provide an estimate of the ultimate axial capacity of foundation piles.

In the present case, as is often true, some of the parameters required for the wave equation analysis (step 2) depend on the maximum achievable penetration, which is calculated in step 3. Thus, to ensure consistency between the steps, an iterative analysis has been carried out.

4.9.1 Evaluation of soil resistance drive

There are different procedures for evaluating SRD in cohesionless and cohesive soils. These are discussed below. As is the case for static pile capacity analysis, the components of shaft resistance and end bearing in SRD are evaluated separately, then combined to give the total driving resistance (Toolan and Fox, 1977).

The variability of the soil conditions across the site and some anticipated variation in hammer performance are likely to influence the apparent driving resistance. Furthermore, the driving resistance during continuous driving is known to be considerably lower than when driving is restarted after an interruption long enough to allow soil set-up. To account for these factors, upper-bound and lower-bound SRD profiles have been formulated for a given design soil profile, based on the recommendations of Stevens et al. (1982).

4.9.2 Unit shaft resistance and unit end bearing for uncemented materials

In cohesive soil, the unit skin friction has been assessed based on the method proposed by Semple and Gemeinhardt (1981). This method was developed from back-analysis of pile installations in normally consolidated to heavily overconsolidated clays from many areas.

The unit shaft resistance component of SRD is derived using the APIRP (1984) procedure for static pile capacity, modified by a pile capacity factor F_p, which is a function of the overconsolidation ratio (OCR), as follows:

$$F_p = 0.5(\mathrm{OCR})^{0.3} \tag{4.52}$$

The unit end-bearing component of SRD is taken as $9S_u$.

The OCR is defined as the ratio of the maximum past effective consolidation stress and the present effective overburden stress. OCR is a function for undrain shear strength ratio (S_u/p'), which is equal to 0.22 in the case of normally consolidated clay with a shear stress angle equal to 26 degrees. In general OCR shall be obtained by CPT.

In cohesionless (granular) soil, shaft resistance and end-bearing components of SRD can be derived using the API (1984) procedure for static pile capacity together

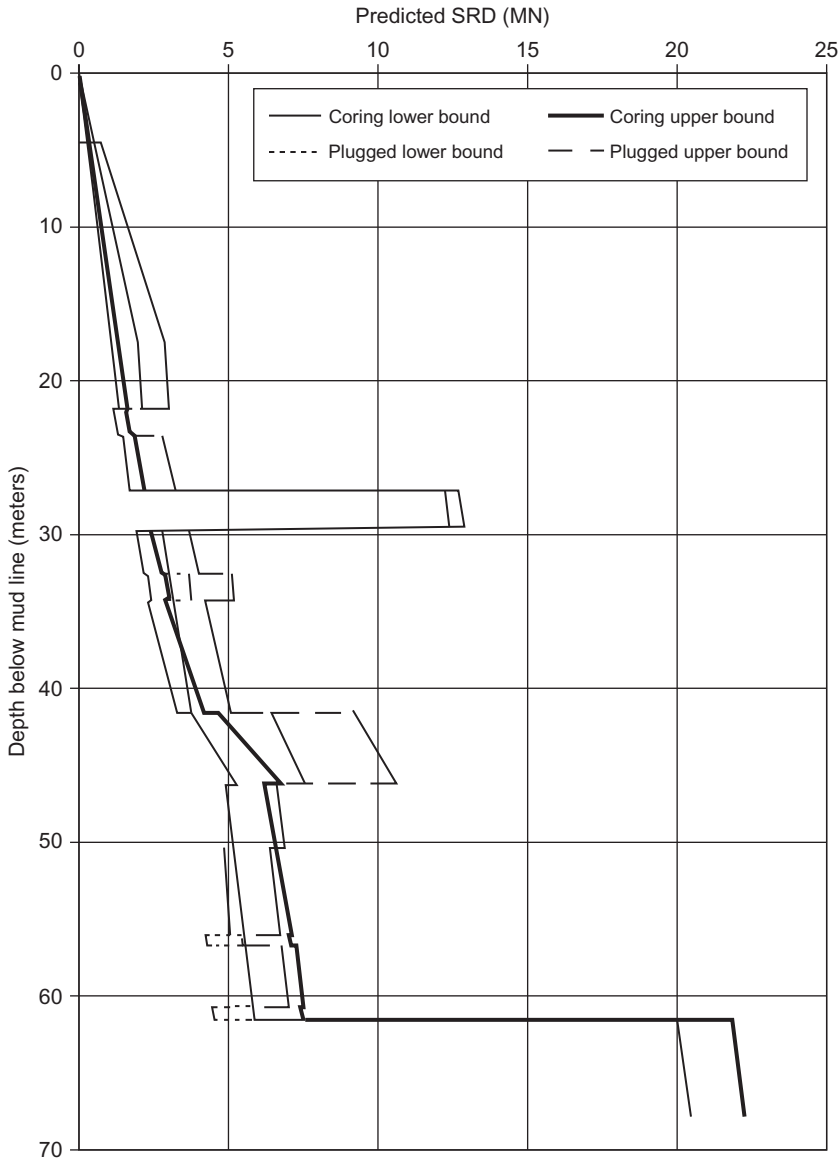

Figure 4.15 Example of soil resistance to driving (SRD) for 30-inch pipe pile with 1¼-inch thickness.

with the soil parameters specified by Stevens et al. (1982) for the particular soil type. A limiting skin friction of 15 kPa has been taken for the calcareous and carbonate sand layers.

4.9.3 Upper- and lower-bound soil resistance drive

Based on Stevens et al. (1982), four cases have been assessed to obtain upper- and lower-bound SRD values in uncemented and weakly cemented soil layers:

1. SRD for lower-bound, coring pile is the outside shaft friction in addition to the inside shaft friction as half the outside. End bearing is unit end bearing multiplied by steel annulus area.
2. SRD for upper-bound, coring pile is similar to the previous case but with the full shaft friction on the inside of the pile.
3. SRD for lower-bound, plugged pile is the outside shaft friction in addition to the end bearing multiplied by full cross-section area.
4. SRD for upper-bound, plugged pile for cohesionless soil layers is with outside shaft friction from case 3 increased by 30% and end bearing from case 3 increased by 50%. For cohesive layers, outside shaft friction is as in case 3, and end bearing from case 3 is increased by 67%.

For the sandstone and limestone layers, plugged conditions are unrealistic, and only the coring cases are considered.

SRD calculations have been made to cover the range in unit values set out above. Sample results are shown in Fig. 4.15. As shown in the figure, a range in SRD is provided, reflecting the various combinations in unit values given above. The lower bounds are likely to be applicable to the minimum resistances during continuous driving, with upper bounds indicative of local variations in soil conditions and resistances expected immediately on restarting a drive (i.e., soil set-up condition)

4.9.4 Results of wave equation analyses

Blowcount versus SRD curves have been developed for the hammers listed in Table 4.20, using a software program.

The input parameters for the wave equation analyses differed for each hammer, pile, and SRD bound, primarily in terms of the percentage of SRD that was due to skin friction. This has an effect on the amount of energy lost through damping, because of differences in damping values for skin friction and end bearing. The following damping values were used:

Table 4.20 Summary of drivability analysis for pile 30 inches in diameter.

Hammer	Pile penetration depth (m)	Maximum driving stresses (MPa)
Delmag D-80	27.2	202
MRBS 3000	27.2	220
MRBS 3900	61.5	252
Achievable penetration is based on refusal criteria of 15 blows/0.25 m		

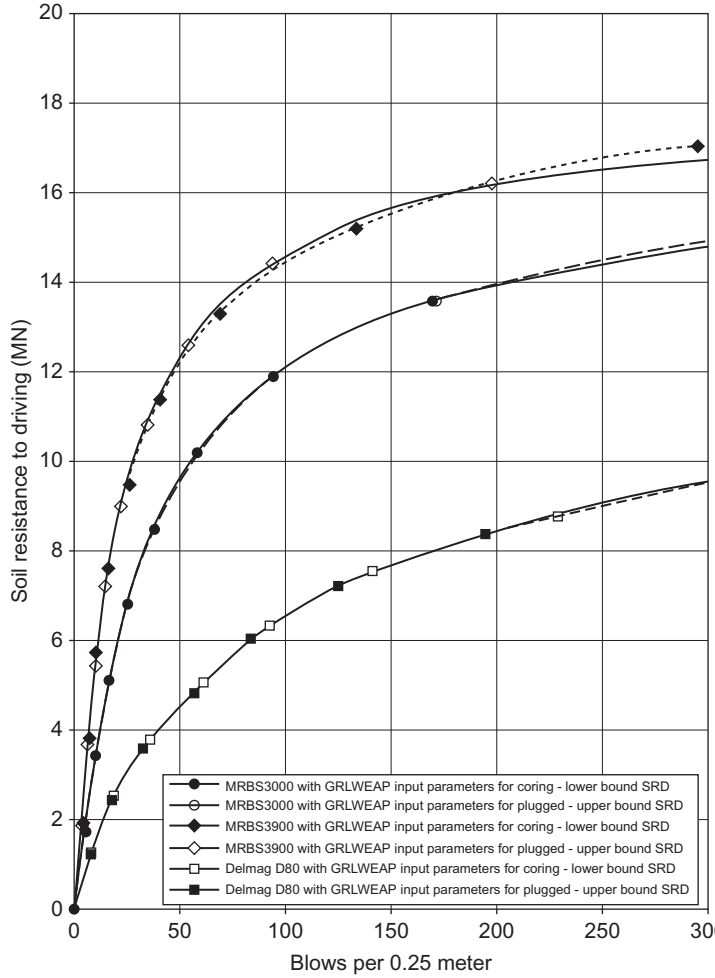

Figure 4.16 Blowcount versus soil resistance to driving (SRD) curves for three hammer types (MRBS 3000 and 3900, and Delmag) for 30-inch pipe pile with 1¼-inch wall thickness.

skin damping for purely cohesive soil, 0.65 s/m;
skin damping for cohesionless soil, 0.15 s/m;
tip damping, all soils, 0.50 s/m.

Skin damping for a combination of soil types was assessed by taking account of the fraction of total skin resistance due to each type and linearly interpolating between the purely cohesive and purely cohesionless values. Quakes of 0.1 inch were taken in all calculations.

The results are shown in Fig. 4.16. There are two curves for each hammer analyzed, corresponding to input parameters associated with the relevant lower- and upper-bound SRD cases.

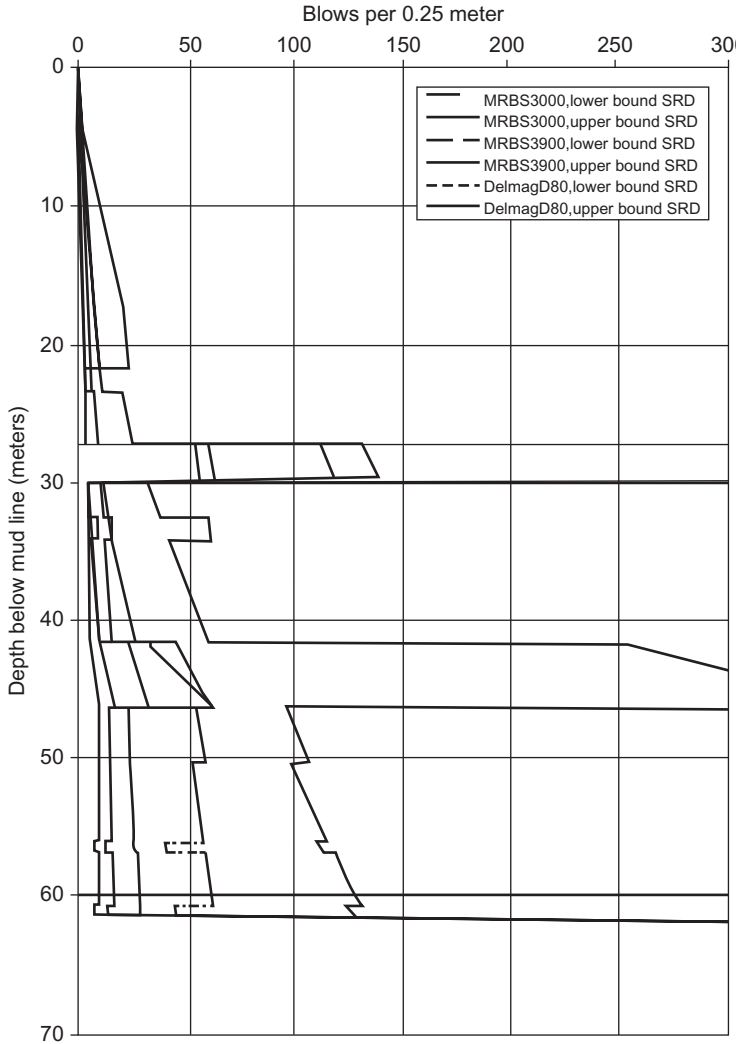

Figure 4.17 Blowcount versus depth for three types of hammers and 30-inch pile with 1¼-inch wall thickness.

4.9.5 Results of drivability calculations

By combining the SRD versus depth curves and the wave equation results, one obtains predicted blowcount versus depth. The results are shown in Fig. 4.17 and summarized in Table 4.20.

According to a case study carried out in the Red Sea, refusal will occur at 27.2 m penetration if the Delmag 080 hammer is used. For the Menck MRBS 3000, high blowcounts will be experienced during penetration. and refusal may occur

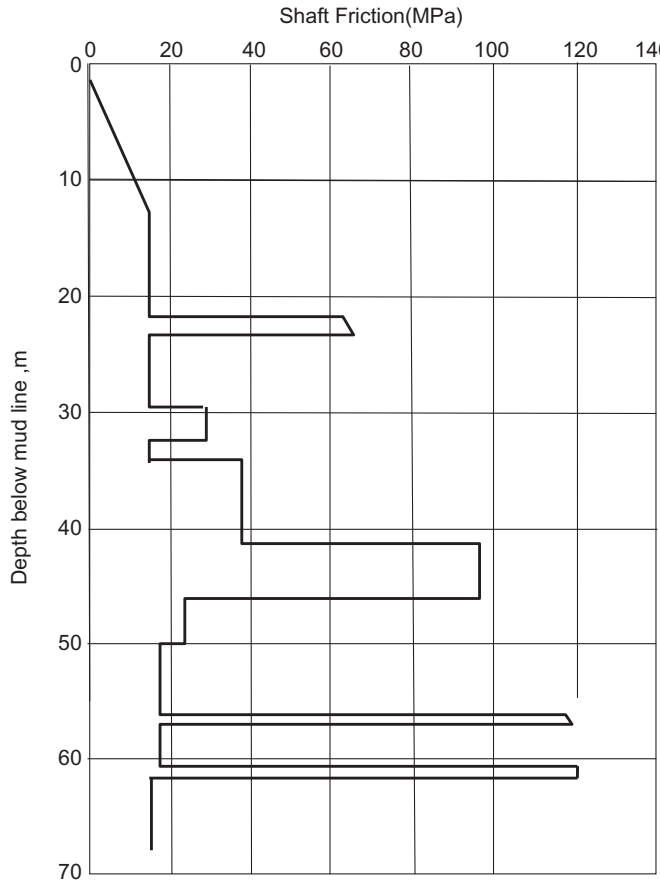

Figure 4.18 Relation between the shaft friction capacity and the depth below the seabed.

should, for example, the thickness or strength of cemented material at 27.2 m increase significantly from that identified in the borehole. For the Menck MRBS 3900, and indeed for all the hammers analyzed, refusal is indicated at 61.5 m penetration.

4.9.6 Recommendations for pile installation

The lower-bound curve of blowcounts versus depth in Fig. 4.21 applies if there is no interruption during driving. The upper-bound curves represent estimates of effects of delays during driving. To ensure an efficient offshore pile-driving operation, it is recommended that delays during driving be avoided if possible. Attention should be paid to ensure that the blowcount does not become excessive and that no pile-tip damage occurs, for all hammers analyzed. Depending on the pile-driving plant finally selected, it may be advisable to have equipment readily available

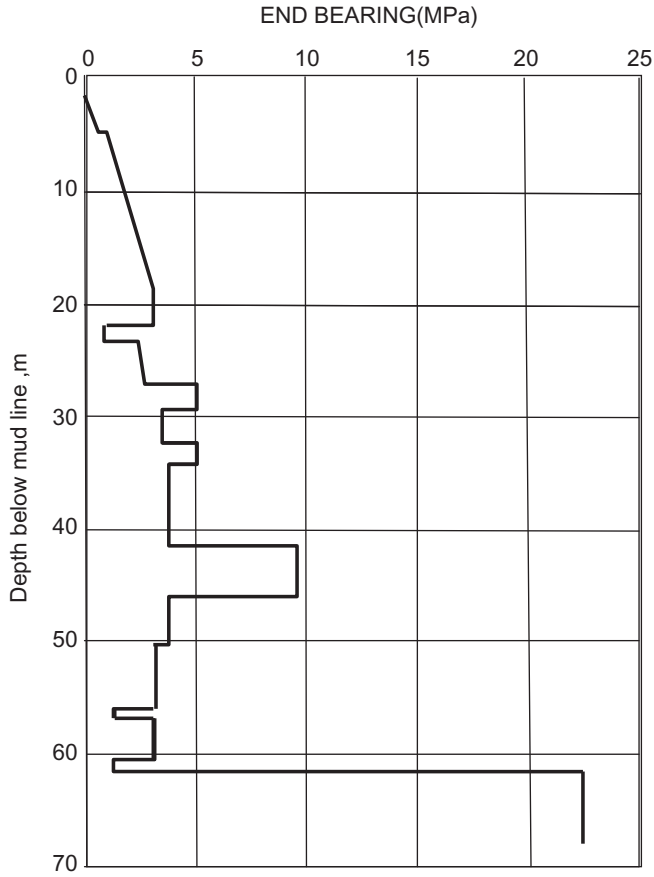

Figure 4.19 Relation between the end-bearing capacity and the depth below the seabed.

during piling operations in case refusal or particularly high blowcounts occur at 27.2 m below sea bed. If refusal occurs, an assessment may be needed of the effect on ultimate pile capacity and therefore on target penetration.

The pile analysis usually assumes uniform wall thickness over the entire pile length. Should the wall thicknesses of the piles finally selected differ from this, then the drivability analyses should be repeated to assess the effect on blowcounts and achievable penetration. It is recommended that consideration be given to the incorporation of a pile shoe to prevent undue distress to the pile during driving through the cemented layers.

The shoe should be externally flush, should have an appropriate outer bevel profile at the tip, and should have an increased wall thickness over a suitable length. As with an overall increase in pile wall thickness requiring some additional drivability assessment, the incorporation of a pile shoe will also need to be re-addressed with regard to its effect on pile-driving behavior.

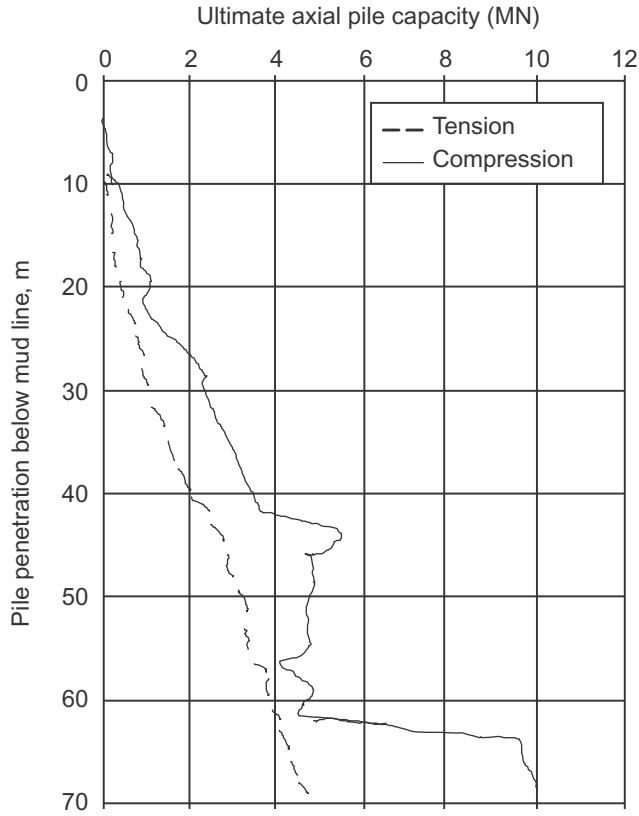

Figure 4.20 Relation between the ultimate axial pile capacity in tension and compression.

4.10 Soil investigation report

After all soil investigation tests on site and in the laboratory are completed, the following curves, which assist in pile design, should be presented in the soil investigation report: the curve for the relationship between the depth below the seabed and the unit skin friction (Fig. 4.18) and the curve for the relationship between the pile depth below the seabed and the unit of end bearing (Figs. 4.19 and 4.20).

If the pile diameter is not identified, the study should include the pile capacity in compression for different pile diameters, as presented in Fig. 4.21, and the pile capacity in tension for different pile diameters, as shown in Fig. 4.22

4.11 Conductor support platform

There is another approach in constructing the platform that uses the conductor as the pile support for the offshore structure platform. Therefore the four or three piles

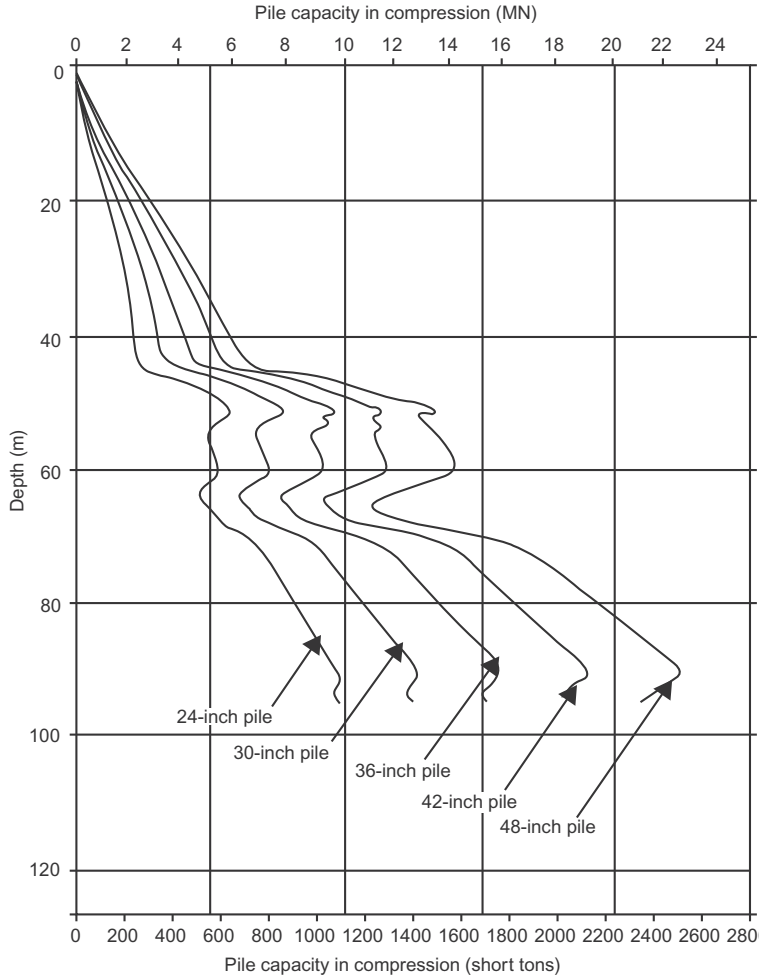

Figure 4.21 Pile capacity in compression with depth for different pile diameters.

will be used also as conductor in the same time and as piles to resist the lateral load as its function as describes above. This type of platform is more cost effective for offshore platforms and was performed by Apache Energy in the Carnarvon Basin. This type of structure is used in the case of small facilities and in most cases is in a water depth from 40 to 60 m with a boat landing. It can be installed by a drilling rig so it will be easy to install and at a lower cost. A recent conductor support platform was 26 m water depths, with five slots. The conductors were 30″ and they had minimal facilities on deck topsides. There is only a riser for the pipeline to onshore and a power cable from onshore; the substructure weighed 120 tons and the topside weight (structure and facilities) was 220 tons (Larnder, 2018). A recent project in Egypt was at a water depth of 23 m with four wells conductors at 30″ and was

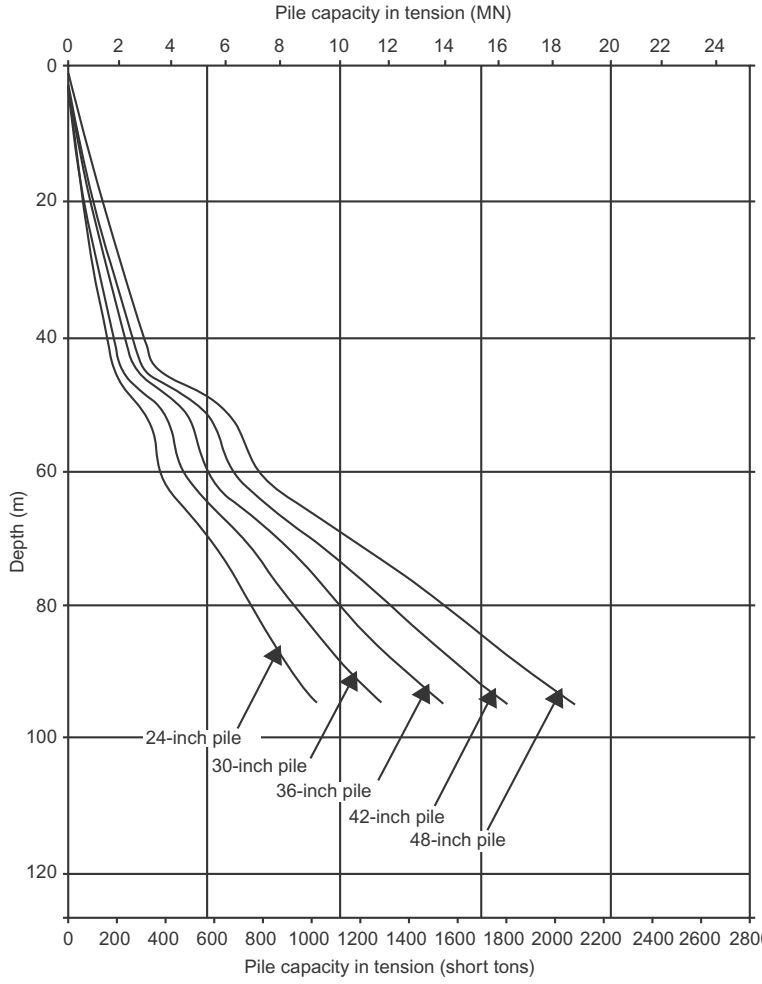

Figure 4.22 Pile capacity in tension for different pile diameters.

installed by barge. The substructure with pile sleeves weighed 330 tons and the topsides with a helideck weighed 420 tons. In Trinidad, a substructure with water depth 27 m with four wells with 36 and 30″ conductors was installed with the conductors jacked up and a crane installed the topsides. The substructure weighed 125 tons and the topside weight was 170 tons. However, this type is limited by the soil type and environmental conditions.

References

American Society for Testing Materials (ASTM), 2004. Standard Method of Deep Quasi-Static Cone and Friction-Cone Penetration Tests of Soil. ASTM Standard D 3441, ASTM International, West Conshohocken, PA.

Arup, O., et al., 1986. Research on the Behavior of Piles as Anchors for Buoyant Structures —Summary Report. Offshore Technology Report OTH 86 215, Department of Energy, London, England, March 1986.

Bea, R.G., 1982. Soil strain rate effects on axial pile capacity. In: Proceedings of the 2nd International Conference on Numerical Methods in Offshore Piling, Austin TX, 29−30 April 1982.

Bea, R.G., Audibert, J.M.E., 1979. Performance of dynamically loaded pile foundations. In: Proceedings of the Second International Conference on Behavior of Offshore Structures, BOSS '79, Imperial College, London, England, 28−31 August 1979.

Bea, R.G., Litton, R.W., Nour-Omid, S., Chang, J.Y., Vaish, A.K., 1984. A specialized design and research tool for the modeling of near-field pile-soil interactions. In: Proceedings of the Offshore Technology Conference, OTC 4806, Houston TX, May 1984, pp. 249−262.

Begemann, H.K.S., 1965. The friction jacket cone as an aid in determining the soil profile. In: Proceedings of the 6th ICSMFE, Montreal, Quebec, vol. I, pp. 17−20.

Bijaker, E.W., 1980. Physical causes of scour. Paper presented at a seminar on scour held by Society of Underwater Technology, London, England.

Bogard, J.D., Matlock, H., 1990. Applications of model pile tests to axial pile design. In: Proceedings of the 22nd Annual Offshore Technology Conference, OTC 6376, Houston TX, May 1990.

Bogard, J.D., Matlock, H., Audibert, J.M.E., Bamford, S.R., 1985. Three years' experience with model pile segment tool tests. In: Proceedings of the Offshore Technology Conference, OTC 4848, Houston TX, 6−9 May 1985.

Briaud, J.L., Garland, E.E., Felio, G.Y., 1984. Loading rate parameters for piles in clay. In: Offshore Technology Conference, Hiuston, TX, May 1984.

Chow, W.Y., Herbich, J.B., 1978. Scour around a group of piles. In: Proceedings of the 10th Annual Offshore Technology Conference (OTC 3308), Houston TX, pp. 2243−2254.

Clarke, J. (Ed.), 1993. Large-Scale Pile Tests in Clay. Thomas Telford, London.

Clausen, C.J.F., Aas, P.M, Karlsrud, K., 2005. Bearing capacity of driven piles in sand, the NGI approach. In: Proceedings of the International Symposium on Frontiers in Offshore Geotechnics [ISFOG—05], Perth, September. A.A. Balkema, Rotterdam, pp. 677−682.

Coyle, H.M., Reese, L.C., 1966. Load transfer for axially loaded piles in clay. ASCE J. Soil Mech. Found. Div. 92 (1052), 1−26.

CUR Centre for Civil Engineering Research and Codes, 2001. Bearing Capacity of Steel Pipe Piles. CUR-Report. CUR, Gouda, 2001-8.

De Reister, J., 1971. Electric penetrometer for site investigations. ASCE J. SMFE Div. 97 (SM-2), 457−472.

Desai, C.S., Holloway, D.M., 1972. Load-deformation analysis of deep pile foundation. In: Proceedings of the Symposium on Applications of the Finite Element Method in Geotechnical Engineering, U.S. Army Engineers Waterways Experiment Station, Vicksburg, MS, 1972, pp. 629−656.

Dunnavant, T.W., Clukey, E.C., Murff, J.D., 1990. Effects of cyclic loading and pile flexibility on axial pile capacities in clay. In: Offshore Technology Reference, OTC 6374, Houston.

Fugro, 1995. Final Report, Foundation Design—Bridge Piles, Jamuna Bridge, Bangladesh. Fugro Engineers BV Confidential Report No. K-2380/120 to HDEC, June 1995.

Fugro, 2004. Axial Pile Capacity Design Method for Offshore Driven Piles in Sand. Fugro Engineers BV Report No. P1003 to API, Issue 3, August 2004.

Georgiadis, M., 1983. Development of p−y curves for layered soils. In: Proceedings of the Conference on Geotechnical Practice in Offshore Engineering, Austin TX. American Society of Civil Engineers, New York, pp. 536−545.

IRTP, 1999. ISSMGE International Society of Soil Mechanics and Geotechnical Engineering (1999). International Reference Test Procedure for the Cone Penetration Test (CPT) and the Cone Penetration Test with Pore Pressure (CPTU). Report of the ISSMGE Technical Committee 16 on Ground Property Characterisation from In-situ Testing. In: Proceedings of the Twelfth European Conference on Soil Mechanics and Geotechnical Engineering, Amsterdam. Balkema, pp. 2195−2222.

ISO (International Organization for Standardization), 2005. ISO 22476-1 (DIS 2005), Geotechnical Investigation and Testing—Field Testing—Electrical Cone and Piezocone Penetration Tests, International Standard ISO 22476-1.

Jardine, R., Chow, F., Overy, R., Standing, J., 2005. ICP Design Methods for Driven Piles in Sands and Clays, Imperial College, Thomas Telford, London.

Karlsrud, K., Haugen, T., 1985. Behavior of piles in clay under cyclic axial loading—results of field model tests. In: Proceedings of the 4th International Conference on Behavior of Offshore Structures, BOSS '85, Delft, The Netherlands, 1−5 July 1985.

Karlsrud, K., Nadim, F., Haugen, T., 1986. Pile in clay under cyclic axial loading field tests and computational modeling. In: Proceedings of the 3rd International Conference on Numerical Methods in Offshore Piling, Nantes, France, 21−22 May 1986.

Kolk, H.J., 2000. Deep foundations in calcareous sediments. In: Al-Shafei, K.A. (Ed.), Engineering for Calcareous Sediments: Proceedings of the Second International Conference on Engineering for Calcareous Sediments, vol. 2, Bahrain, 21−24 February, 1999. A.A. Balkema, Rotterdam, pp. 313−344.

Kolk, H.J., Baaijens, A.E., Senders, M., 2005. Design criteria for pipe piles in silica sands. In: Gourvenec, S., Cassidy, M. (Eds.), Frontiers in Offshore Geotechnics ISFOG 2005: Proceedings of the First International Symposium on Frontiers in Offshore Geotechnics, 19−21 September 2005, University of Western Australia, Perth. Taylor & Francis, London, pp. 711−716.

Kraft, L.M., Lyons, C.G., 1974. State of the art: Ultimate axial capacity of grouted piles. In: Proceedings of the 6th Annual Offshore Technology Conference, OTC 2081, Houston, TX, May 1974.

Kraft, L.M., Focht, J.A., Amarasinghe, S.F., 1981a. Friction capacity of piles driven into clay. ASCE J. Geotech. Eng. Div. 107 (GT11), 1521−1541.

Kraft Jr., L.M., Cox, W.R., Verner, E.A., 1981b. Pile load tests: cyclic loads and varying load rates. ASCE J. Geotech. Eng. Div. 107 (GT1), 11−19.

Larnder, J., 2018. Conductor supported platforms. In: OTO 1994, Egyps Conference, Cairo, Egypt.

Lehane, B.M., Randolph, M.F., 2002. Evaluation of a minimum base resistance for driven pipe piles in siliceous sand. ASCE J. Geotech. Geoenviron. Eng. 128 (3), 198−205.

Lehane, B.M., Schneider, J.A., Xu, X., 2005a. A review of design methods for offshore driven piles in siliceous sand. University of Western Australia Geomechanics Group. Report No. GEO: 05358, September 2005.

Lehane, B.M., Schneider, J.A., Xu, X., 2005b. The UWA-05 method for prediction of axial capacity of driven piles in sand. In: Gourvenec, S., Cassidy, M. (Eds.), Frontiers in Offshore Geotechnics ISFOG 2005: Proceedings of the First International Symposium on Frontiers in Offshore Geotechnics, University of Western Australia, Perth, 19−21 September 2005. Taylor & Francis, London, pp. 683−689.

Lysmer, J., 1978. Analytical procedures in soil dynamics. Report No. UCB/EERC-78/29. In: Presented at the ASCE Geotechnical Engineering Division Specialty Conference on Earthquake Engineering and Soil Dynamics, Pasadena CA, December 1978.

Matlock, H., 1970. Correlations for design of laterally loaded piles in soft clay. In: Proceedings of the 2nd Annual Offshore Technology Conference, OTC 1204, Houston TX, April 1970.

McClelland, B., Ehlers, C.J., 1986. Offshore geotechnical site investigations. In: McClelland, B., Reifel, M.D. (Eds.), Planning and Design of Fixed Offshore Platforms. Van Nostrand Reinhold, New York.

Meyer, P.C., Holmquist D.V., Matlock, H.T.l., 1975. Computer predictions of axially loaded piles with non-linear supports. In: Proceeding for Offshore Technology Conference, OTC 2186, Houston TX, May 1975.

Murff, J.D., 1980. Pile capacity in a softening soil. Int. J. Numer. Anal. Methods Geomech. 4 (2), 185–189.

Niedoroda, A.W., Dalton, C., Bea, R.G., 1981. The descriptive physics of scour in the ocean environment. In: Proceedings of the 13th Annual Offshore Technology Conference, OTC 4145, Houston TX, pp. 297–304.

NORSOK Standard G-001 Rev. 2, October 2004. Marine soil investigations

Novak, M., Sharnouby, B.E., 1983. Stiffness constants of single piles. J. Geotech. Eng. ASCE 109 (7), 961–974.

O'Neill, M.W., Hassan, K.M., 1994. Drilled shafts: Effects of construction on performance and design criteria. In: Proceedings of the International Conference on Design and Construction of Deep Foundations. U.S. Federal Highway Administration (FHWA), vol. 1, pp. 137–187.

O'Neill, M.W., Murchison, J.M., 1983. An evaluation of $p-y$ $r$elationships in sands. Prepared for the American Petroleum Institute Report PRAC 82-41-1. University of Houston, Houston, March 1983.

Olson, R.E., 1984. Analysis of Pile Response Under Axial Loads. Report to API, USA, December 1984.

Peck, R.B., Hanson, W.E., Thornburn, T.H., 1974. Foundation Engineering. John Wiley & Sons, New York, p. 312.

Pelletier, J.H., Doyle, E.H., 1982. Tension capacity in silty clays—beta pile test. In: Proceedings of the 2nd International Conference on Numerical Methods of Offshore Piling, Austin TX, 29–30 April 1982.

Poulos, H.G., 1983. Cyclic axial pile response—alternative analyses. In: Proceedings of the Conference on Geotechnical Practice in Offshore Engineering, ASCE, Austin, TX, 27–29 April 1983.

Randolph, M.F., 1983. Design considerations for offshore piles. In: Proceedings of the Conference on Geotechnical Practice in Offshore Engineering, Austin, TX. American Society of Civil Engineers, New York, pp. 422–439.

Randolph, M.F., Leong, E.C., Houlsby, G.T., 1991. One-dimensional analysis of soil plugs in pipe piles. Géotechnique 61 (4), 587–598.

Reese, L.C., Cox, W.R., 1975. Field testing and analysis of laterally loaded piles in stiff clay. In: Proceedings of the 5th Annual Offshore Technology Conference, OTC 2312, Houston TX, April 1975.

Semple, R.M., Gemeinhardt, J.P., 1981. Stress history approach to analysis of soil resistance to pile driving. In: Offshore Technology Conference, Houston, TX, vol. 1, pp. 165–172.

Smith, E.A.L., 1962. Pile driving analysis by the wave equation, Part 1, Paper No. 3306. Trans. ASCE 127, 1145–1193.

Stevens, R.S. Wiltsie, E.A, Turton, H., 1982. Evaluating pile drivability for hard clay, very dense sand and rock. In: Proceedings of the 14th Offshore Technology Conference, Houston, TX, vol.1, pp. 465–482.

Thompson, G.W.L., Jardine, R.J., 1998. The applicability of the new Imperial College design method to calcareous sands. In: Proceedings of the Conference on Offshore Site Investigations and Foundation Behavior, Society for Underwater Technology, London, pp. 383–400.

Toolan, F.E., Fox, D.A., 1977. Geotechnical planning of piled foundations for offshore well-head jacket centers. In: Proceedings of the Institute of Civil Engineers, vol. 62 (Part 1), pp. 221–244.

Vijayvergiya, V.N., 1977. Load movement characteristics of piles. In: Proceedings of the Ports '77 Conference, vol. II. American Society of Civil Engineers, pp. 269–284.

Whitehouse, R., 1998. Scour at Marine Structures. Thomas Telford, London.

Further Reading

American Society for Testing Materials (ASTM), 1968. Standards, Part II. ASTM, West Conshohocken, PA.

American Society for Testing Materials (ASTM), 1972. Underwater soil sampling, testing, and construction control. ASTM Special Technical Publication SOl, March 1972. ASTM, West Conshohocken, PA.

American Society for Testing Materials (ASTM), 2000. ASTM D-5778 Standard Test Method for Performing Electronic Friction Cone and Piezocone Penetration Testing of Soils. ASTM, West Conshohocken, PA.

Angus, N.M., Moore, R.L., 1982. Scour repair methods in the southern North Sea. Paper OTC 4410. In: Proceeding of 14th OTC, pp. 385–395.

API RP2A, 1984. Recommended Practice for Planning, Designing, and Constructing Fixed Offshore Platforms, 15th ed. American Petroleum Institute, Washington, DC.

ASTM International, 1996. Standard Test Method for Performing Electronic Friction Cone and Piezocone Penetration Testing of Soils, ASTM D 5778-95 (Reapproved 2000), ASTM Standards on Disc Volume 04. 09: Soil and Rock (II): D 5714 – Latest. ASTM, West Conshohocken.

Audibert, J.M.E., Dover, A.R., 1982. Pile load test: cyclic loads and varying load rates. J. Geotech. Eng. Div. ASCE 108 (GT3), 501–505.

Bailey, E., Davis, G.L., Henderson, H.O., 1971. Design of an automatic marine corer. In: Third Annual Offshore Technology Conference. Preprint, vol. 1, Paper No. 1365, pp. 397–416.

Baldi, G., Bellotti, R., Ghionna, N., Jamiolkowski, M., Pasqualini, E., 1986. Interpretation of CPTs and CPTUs, 2nd Part: drained penetration of sands. In: Field Instrumentation and In-Situ Measurements. In: Proceedings of the 4th International Geotechnical Seminar, Singapore, 25–27 November 1986. Nanyang Technological Institute, Singapore, pp. 143–156.

Bea, R.G., 1980. Dynamic response of piles in offshore platforms. In: Proceeding of the Speciality Conference One on Dynamic Response of Pile Foundations—Analytical Aspects. ASCE, Geotechnical Engineering Division, 30 October 1980, pp. 80–109.

Bea, R.G., 1984. Dynamic response of marine foundations. In: Proceedings of the Ocean Structural Dynamics Symposium '84. Oregon State University, Corvallis, OR, 11–13 September 1984.

Bea, R.G., Vahdani, S., Guttman, S.I., Meith, R.M., Paulson, S.F., 1986. Analysis of the performance of piles in silica sands and carbonate formations. In: Proceedings of the18th Annual Offshore Technology Conference, OTC 5145, Houston, TX, 5–8 May 1986.

Bond, A.J., Jardine, R.J., 1995. Shaft capacity of displacement piles in a high OCR clay. Geótechnique 45 (1), 3–23.

Doyle, E.H., McClelland, B., Ferguson, G.B., 1971. Wire-line vane probe for deep penetration measurements of ocean sediment strength. In: Third Annual Offshore Technology Conference, Preprint, vol. 1, Paper No. 1327, pp. 21–32.

Focht Jr, J.A., Kraft Jr, L.M., 1986. Axial performance and capacity of piles. In: McClelland, B., Reifel, M.D. (Eds.), Planning and Design of Fixed Offshore Platforms. Van Nostrand Reinhold Company, New York.

Gallagher, K.A., St. John, H.D., 1980. Field scale model studies of piles as anchorages for buoyant platforms. In: European Offshore Petroleum Conference, Paper EUR 135, London, England, 1980.

Hironka, M.C., Green, W.C., 1971. A remote controlled seafloor incremental corer. In: Third Annual Offshore Technology Conference, Preprint, vol. 1, Paper No. 1325, pp. 13–20.

Hvorslev, M.J., 1949. Subsurface Exploration and Sampling of Soils for Civil Engineering Purposes. Waterways Experiment Station, Vicksburg, MS, November 1949. (Reprinted by Engineering Foundation, New York, 1962.)

Jamiolkowski, M., Ghionna, V.N., Lancellotta, R., Pasqualini, E., 1988. New correlations of penetration tests for design practice. In: De Ruiter, J. (Ed.), PenetrationTesting 1988: Proceedings of the First International Symposium on Penetration Testing, ISOPT-1, vol. 1, Orlando FL, 20–24 March 1988. A.A. Balkema, Rotterdam, pp. 263–296.

Kolk, H.J., Van Der Velde, E., 1996. A reliable method to determine friction capacity of piles driven into clays. In: Proceedings of the 28th Annual Offshore Technology Conference, OTC 7993, Houston, TX, May 1996.

Ladd, C.C., Foott, R., 1974. New design procedure for stability of soft clays. ASCE J. Geotech. Eng. Div. 100 (GT7), 763–786.

Lehane, B.M., Jardine, R.J., 1994. Displacement pile behavor in glacial clay. Can. Geotech. J. 31 (1), 79–90.

Matlock, H., Foo, S.H.C., 1979. Axial analysis of piles using a hysteretic and degrading soil model. In: Proceedings of the Conference on Numerical Methods in Offshore Piling. Institution of Civil Engineers, London, England, 22–23 May 1979.

McAnoy, R.P.L., Cashman, A.C., Purvis, O., 1982. Cyclic tensile testing of a pile in glacial till. In: Proceedings of the 2nd International Conference on Numerical Methods in Offshore Piling, Austin, TX, 29–30 April 1982.

McClelland, B., 1972. Techniques Used in Soil Sampling at Sea. Offshore Magazine, March 1972, p. 51.

Meyerholf, G.G., 1956. Penetration tests and bearing capacity of cohesionless soils. J. ASCE 82 (SMI), 1–19.

Miller, T.W., Murff, J.D., Kraft, L.M., 1978. Critical state soil mechanics model of soil consolidation stresses around a driven pile. In: Proceedings of the 10th Annual Offshore Technology Conference, OTC 3307, Houston, TX, May 1978.

O'Neill, M.W., Hawkins, R.A., Audibert, J.M.E., 1982. Installation of pile group in overconsolidated clay. ASCE J. Geotech. Eng. Div. 108 (GT11), 1369–1386.

Panel on Offshore Platforms, 1978. Engineering fixed offshore platforms to resist earthquakes. In: ASCE Specialty Conference on Earthquake Engineering and Soil Dynamics. ASCE Geotechnical Engineering Division, 19−21 June 1978.

Pelletier, J.H., Sgouros, G.E., 1987. Shear transfer behavior of a 30-inch pile in silty clay. In: Proceedings of the 19th Annual Offshore Technology Conference, OTC 5407, Houston, TX, 27−30 April 1987.

Pelletier, J.H., Murff, J.D., Young, A.C., 1995. Historical development and assessment of current API design methods for axially loaded piles. In: Proceedings of the 27th Annual Offshore Technology Conference, OTC 7157, Houston, TX, May 1995.

Randolph, M.F., Murphy, B.S., 1985. Shaft capacity of driven piles in clay. In: Proceeding of the 17th Annual Offshore Technology Conference, OTC 4883, Houston, TX, May 1985.

Randolph, M.F., Wroth, C.P., 1979. An analytical solution for the consolidation around a driven pile. Int. J. Numer. Anal. Methods Geomech. 3 (3), 217−230.

Roesset, J.M., Angelides, C., 1979. Dynamic stiffness of piles. In: Proceedings of the Conference on Numerical Methods in Offshore Piling, London, England, May 1979, pp. 75−81.

Semple, R.M., Rigden, W.J., 1984. Shaft capacity of driven pipe piles in clay. In: Proceedings of the Symposium on Analysis and Design of Pile Foundations, San Francisco. American Society of Civil Engineers, New York.

Tomlinson, M.J., 1994. Pile Design and Construction Practice, fourth ed. E. and F.N. Spon, London.

Vermeiden, J., 1948. Improved sounding apparatus, as developed in Holland since 1936. In: Proceedings of the 2nd International Conference on Soil Mechanics, Rotterdam, 1948.

Wood, D.M., 1982. Laboratory investigations of the behavior of soils under cyclic loading: a review. In: Pande, G.N., Zienkiewicz, O.C. (Eds.), Soil Mechanics—Transient and Cyclic Loads. John Wiley & Sons.

Youd, T.L., Idriss, I.M., 2001. Liquefaction resistance of soils: Summary report from the 1996 NCEER and 1998 NCEER/NSF workshops on evaluation of liquefaction resistance of soils. ASCE J. Geotech. Geoenviron. Eng. 127 (4), 297−313.

Fabrication and installation

5

5.1 Introduction

The construction of a fixed offshore platform is very specific to this type of structure. Therefore the contractor company, that is, responsible for fabrication and installation should be a specialist in this type of structure, and have a competent staff and reasonable facilities to carry out the construction project. The design of the platform should be checked against transportation, lifting, and installation in this phase. It will require interface management between engineering and construction as, for example, in some cases the sea fastening or lifting will be done by the contractor but it will be checked by the engineering company. The launching and lifting of the platform component will be designed by the engineering company but the input data for the analysis will be delivered to the engineering company based on the available barge, cranes, and other equipment, and the capability for launching, transportation, and installation.

5.2 Construction procedure

The engineering firm, that is, performing the design of the jacket should take into consideration the lifting, launching, or self-floating, which depend primarily on the available offshore installation equipment and also the water depth. In general, the preference is to lift the jacket in place. The size of such jackets has being increasing as offshore lifting capacity has grown. Nowadays, the lifting capacity can reach up to 14,000 tons.

In the case of jackets in shallow water, in most cases the height of the jacket is of the same order as the plan dimensions, so the erection is usually carried out vertically in the same direction as the final installation. Therefore in this case, the jacket may be lifted or skidded onto the barge.

In the case of jackets that will be installed in deep water, installation will be by the launching method. This installation method should be accompanied by floating tanks, pipework, and valving to enable the legs to be flooded for ballasting the jacket into the vertical position on its location. This installation method can be used for jackets up to 25,000 tons. Very large jackets have been constructed as self-floaters in a graving dock and towed offshore subsequent to flooding the dock.

The key fundamental elements are the contract strategy, the quality plan, and requirement during construction until commissioning and start up.

Offshore Structures. DOI: https://doi.org/10.1016/B978-0-12-816191-3.00005-5

In considering the construction philosophy and contract strategy, the objectives of achieving quality requirements and efficiency are of fundamental importance.

The construction of the offshore structure jacket is in a series of very distinct stages starting with fabrication until the loadout. These stages start with obtaining the steel section which will be delivered under full quality control (QC) from the manufacturer and then starting the fabrication will be manual with less QC. Thus decreasing efficiency occurs as progress through these operations advances. A third basic consideration is that risk increases with each progressive stage.

Some of the actions which can reduce the time and cost during the construction phase are as follows:

- Subdivision into as large components and modules as is possible to fabricate and assemble.
- Define a good location to fabricate the major components.
- The plan for delivering the critical materials by early planning of the flow of components to their assembly site. Providing adequate facilities and equipment for assembly, including such items as synchro lifts and heavy-lift cranes.
- Try to simplify the configurations and standardization of details, grades, and sizes. Avoidance of excessively tight tolerances.
- In general structural systems should be selected that utilize skills and trades on a relatively continuous and uniform basis. Avoidance of procedures that are overly sensitive to weather conditions; ensuring that processes which are weather sensitive are completed during shop fabrication, for example, applying the protective coating.

The quality management system is a vital and integral component of all aspects of offshore fabrication as a small mistake can affect the integrity of the structure with time.

As a rule of thumb, to ensure that what is produced is what is needed the quality assurance process is applied, including that the required documents are available, hold point, audits, reviews, and corrective actions and other quality system are applied.

The inspection test plan should be available and approved from the client which defines the inspection and testing procedure during all phases of construction to ensure that the required specification is achieved.

5.3 Engineering of execution

In practice, the engineering firm which performed the design should follow the execution during each phase to ensure that the design requirements are fulfilled and be online in case of any change request or for clarification. A general method of execution is envisaged at the jacket design stage. The shape of the jacket, its form, and properties require quite specific methods of loadout, offshore transportation, and installation.

The construction phase is under contractor responsibility, but there is an interface with the engineering firm if there are any site queries or other engineering

assistance required. The contractor has freedom to choose any suitable construction method, but it should not contradict with the project requirement and specifications. The contractor is requested to provide a method statement and a presentation describing their method of execution and shows that it matches with the project specification requirement and has no effect on structure integrity.

The project engineering team during construction is responsible for following and reviewing the shop drawings, the method statement, and the materials take off and cutting plans. The assembly, erection, and lifting during these activities shall be reviewed as per the procedure with the engineering firm to guarantee it does not affect the structure integrity.

It is worth mentioning that in the case of a large jacket around 130,000 to 150,000 man hours are required during construction. In the case of a large structure it should be ensured that the subsystem component can be easily assembled without welding or dimension problems.

The most critical and complicated phase of the execution is the tubular joint fabrication, as there are many fitting and welding requirements, and nondestructive testing (NDT) is required. Sometimes automatic welding is used between the joint and the tubular member. The number of fitting and welding and associated NDT depends on the use of ring stiffeners and the numbers and locations of the stubs. From a fabrication point of view, it is preferable to install the ring stiffeners first and then perform the fitting and welding of the stubs to allow for applying automatic welding and to avoid welding distortion. Therefore it will be easier in fabrication if there are no ring stiffeners, which should be avoided or be used in critical joints only.

The nod stubs can be simple or overlapping, where overlapping requires double the effort, and so should be avoided as this also benefits the structure integrity and fabrication The minimum spacing between the weld toes is 50 mm, noting that this distance is not sufficient to do welding of adjacent stubs simultaneously, with the minimum distance to do so is 150 mm.

5.4 Fabrication

The main elements in fabrication and erection are the welding and its QC. Welding procedures should be prepared, detailing steel grades, joint design, thickness range, welding process, welding consumables, welding parameters, principal welding position, preheating/working temperature, and postweld heat treatment (PWHT).

It is also worth mentioning that stress relief is normally not required for the range of wall thickness used in the jackets and piles of offshore jackets in moderate environments such as the Gulf of Mexico (GoM), on the other hand, it is frequently required for the thicker members of large deck structures and for the joints (nodes) of the thicker-walled jackets of North Sea platforms.

NDT and mechanical testing shall be done to provide the welding qualification procedure. The mechanical tests include hardness tests, Charpy V-notch tests, and

bending and tensile tests. NDT for inspection shall include a gamma-ray test, which is called radiographic, ultrasonic test (UT), and magnetic particle inspection (MPI). The notch test shall be applied to the heat-affected zone and the weld and toughness properties limits shall be equal to the members itself. By carrying out these tests with a visual inspection test, the weld shall be free from cracks and cold laps, and no porosity or slag inclusion and, that is, matches with the code limit. The crack opening tests may be done for fracture mechanics toughness for heavy weld joints.

The selection of the welder is very important as the welder should have had continuous work for the previous 3 months. In addition, all welders should be qualified for the type of work assigned to them and be certified accordingly.

Manual welding of all higher strength steels and of normal-strength steel with a carbon equivalent greater than 0.41 should be carried out with low hydrogen electrodes.

For "special structural steels" and for all repair welding, Det Norske Veritas (DNV) requires the use of extralow hydrogen electrodes. It is recommended by Gerwick (2007) that the piles are under impact load so they are welded using electrodes with low hydrogen types to prevent fracture.

The welding electrodes should be stored in sealed moisture-proof containers at a temperature range of 20°C−30°C, but in any event at least 58°C above ambient. If the stored containers are open they should be stored at 70°C−150°C, as per the electrode type. Before starting using the electrodes, they should be kept in heated containers and used within 2 hours. As per the QC procedure, welding electrodes that have been contaminated by moisture, rust, oil, grease, or dirt should not be used.

It should be ensured that the surface does not have any rust, slag, rust, grease, oil, or paint before welding, and the edges should have a smooth and uniform surface.

In case of rain or windy weather the required protection should be arranged before starting the welding process.

Before starting the welding process, the groove should be dry and if there is any moisture it should be removed by preheating. The joint should be at a temperature of at least 5°C.

Before welding, a check on the dimensions should be performed. Misalignment between parallel members should not exceed 10% of the thickness or 3 mm. If the thickness of abutting members differs by more than 3 mm, the thicker member should be tapered by grinding or machining to a slope of 1:4 or flatter, as shown in Fig. 5.1.

In the case of welding which shall be affected by fatigue stresses, it is required to be ground to a smooth curve as this also reduces the occurrence of brittle failure.

The weld of the offshore structure shall be a full-penetration type and it is preferred to be welded from both sides, especially in the case of welds perpendicular to the direction of the applied stresses. Therefore this type of weld is very important in offshore structures to maintain the structure integrity.

In the case of intersecting members for which the welding details have not been specified in the design, they should be joined by complete-penetration groove welds.

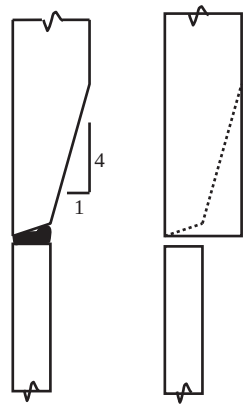

Figure 5.1 Grinding or machine tapering of the steel plate for welding penetration.

The construction contractor should detail all lifting plates, padeyes, and others that are subject to dynamic impact stress, so that welds are not perpendicular to the principal tension. It should be taken into consideration that welds acting in shear are much less sensitive to cracking than welds in tension.

The full-penetration welds must be used and fillet welds avoided if possible. All temporary plates and fittings should be subjected to the same requirements for welding procedures and testing as the material of the member to which they are affixed.

Permanent steel backing strips are especially useful for field welds, and piles or any other members shall be welded in the field when they are not accessible to welding from both sides.

In order to reduce the stress concentration, the corner should be rounded.

As per DNV fillet welds for sealing purposes are required to have a minimum leg length of 5 mm, but API-RP2A requires only 3 mm. Avoid undercutting in welding if the welds are perpendicular to the principal tension of a member under dynamic impact.

As per the QC procedure and after the NDT, a defective weld should be repaired by grinding, machining, or welding as required. In addition, if the welds have insufficient strength, ductility, or notch toughness they should be completely removed prior to carrying out the repair.

In the case of removing the welds by arc-air gouging, this should be followed by grinding. Whenever a discontinuity is removed, a magnetic particle test (MPT) or other NDT should be undertaken to be sure the removal was complete.

The welding shall be repaired by using more electrodes of the low hydrogen type and an appropriate preheating temperature as per the welding procedure, usually 25°C above the level used for production welding and at least 100°C.

As usual, all welds should be subjected to visual inspection and NDT as required by the project specifications for the fabrication and construction process.

As part of the quality assurance, all destructive testing should be properly documented and identified so that the tested areas are ready to be a reference for any

audit during fabrication and construction and after completed installation of the structure.

Accurate cutting and beveling take more care and consequently more time, as it can take a longer time than welding and its QC checks.

It is useful to perform the cutting through controlling with a computerized technique which can fit properly all the intersecting tubular members. In addition, to enhance quality, the welding can be done using semiautomatic welding equipment.

As during construction, documentation is very important as this is a complicated procedure for most offshore structures, and the contractor should make a special effort to set up a quality assurance system that will ensure proper records of all testing during this phase and be ready for any audit from the client or an internal audit.

Welding machines must be properly grounded to prevent underwater corrosion damage. Since welding machines are normally DC, the discharge to ground may otherwise occur underwater at piping penetrations or other similar points of concentration.

All the techniques for NDTs, such as visual inspection, UT, MPT, radiography test, and liquid penetration should be stated clearly in the project specification with relevant American Petroleum Institute (API), DNV, ISO, or other standard.

The fabrication of offshore steel structures should follow applicable provisions of codes, such as the American Institute of Steel Construction (AISC) specification for the design, fabrication, and erection of structural steel for buildings, for example, for the fabrication and erection of structural steel for buildings. The QC for the nondestructive evaluation five-methods tests are presented in Elreedy (2013).

The offshore tubular piles are fabricated with longitudinal seam welds and circumferential butt welds based on the API-RP2A requirement. This states that spiral-welded pipe cannot be recommended.

There are limitations to wall thickness and diameter, which generally preclude their application to offshore structures and deep-water marine projects, especially where heavy hammers will be employed.

However, advances in the control and reliability of the technology are continually being made. In China, for Hangzhou Bay Bridge, spiral-welded piles of 2.0 m diameter and 28 mm wall thickness have been successfully installed.

Additional requirements are given in API-RP2A, such as steel beams from rolled shapes, tubulars, plate, or box girders, may be spliced. In cantilever beams, there should be no splice located closer to the point of support than one-half the cantilevered length. For continuous beams there should be no splice in the middle one-fourth of the span, or in the eighth of the span nearest a support, or over a support.

The most difficult joint is the X-joint of two or more tubulars that connect in the same node.

As a traditional case, the member with the largest diameter and greatest thickness shall continue through the joint and the smaller member will connect on it. Recently, in a large jacket, all the intersecting members were continuous, in this case this special joint shall be fabricated separately and the member shall be framed to it using full-penetration butt welds as shown in Figs. 5.2 and 5.3.

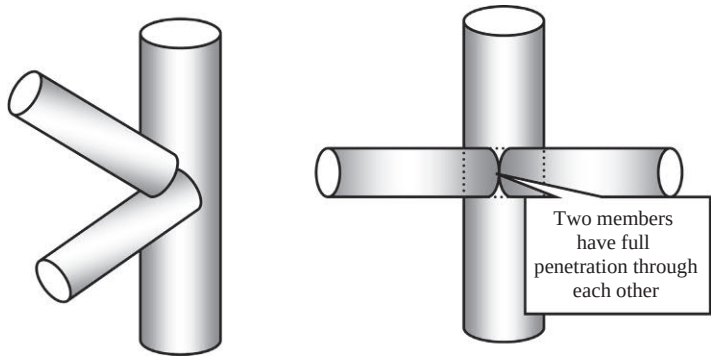

Figure 5.2 F abrication of different nodes.

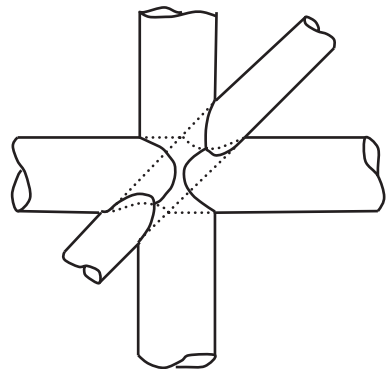

Figure 5.3 Intersecting joint with full sections carried through the joint.

In some cases, the joint shall be fabricated away and then transferred to the jacket fabrication yard so the procedure of QC can be restricted and effective.

The butt weld can be used to join the main legs and braces. To eliminate the welding details there is increasing use of casting the joint.

Fig. 5.3 illustrates the typical details for the proper bevel and weld of tubular members framing into or overlapping another member. To improve the fatigue endurance, perform grinding to the welding on the external profile.

In most cases, the welding between the web and flange for a built-up section is fillet welds from both sides of the web. Welds should have a concave profile and a smooth transition into the flange and web. The welding between flanges and the stiffener plates should be a full-penetration butt weld made from both sides.

The welding between the stiffener plate and web may be continuous fillet welds from both sides. Weld metal and notch toughness of the heat-affected zone should not be less than the minimum toughness requirements for the girder.

High-strength bolts are not usually used in the connection for offshore structures, but may be used in the case of temporary structures. They can be used if welding on site is difficult for any reason.

In special cases choose the best method of ensuring that adequate torque has been applied. In a large joint, with multiple bolts, either the abutting plates should be premilled or shims should be employed to ensure a tight fit.

The fabrication specification of offshore jackets is defined explicitly by the designer. In most cases, it is based on one or more of well-known codes, with additional requirements dictated by the specific design, client standards, statutory rules etc.

In general, the design and fabrication of offshore structure platforms are mainly based on two codes which are used in most projects worldwide; API-RP2A for platform design recommendation and AISC Specification for the Design, Fabrication and Erection of Structural Steel for Buildings.

For larger jackets, the joints tend to be fabricated separately under highly controlled shop conditions. Alternatively, cast steel nodes may be used in order to eliminate critical welding details.

In general, during fabrication in all the construction phases, focusing and paying great attention to the welding process and it QC, are required. The NDT and QC should focus on joint penetration groove welds, by eliminating "notch effects" at the root and especially the cap of joint welds, and achieving the required weld profile as per the specifications and American Welding Society requirement.

The welds which are critical for fatigue stresses should be ground to a smooth curve as this can prevent brittle failure. Typical welding details from API-RP2A are shown in Fig. 5.4, showing tubular members framing into or overlapping another member with access from one side only. Fig. 5.4 presents the welding procedure on the tubular joint based on the thickness of the brace "t" and the chord "T" noting that "α" is the angle formed by the exterior surfaces of the brace and chord at any point on their joint line. However, a lot of emphasis is placed on designing stubs which can be welded from both sides.

Table 5.1 presents the relation between the groove angle and the opening distance. The relation between the angle of inclination and the minimum welding thickness is illustrated in Table 5.2.

Welds are usually subject to 100% visual, MPI, and UT inspection. The weld acceptance criteria, as the maximum weld undercut length (t/2 or 10 mm), and maximum depth (t/20 or 0.25 mm), imply an exceptionally high quality of welding.

The very critical items in welding are the pile sleeve, launch runners, and mud mat, as it is required to minimize the distance between circumferential welds during construction.

Where welds are found to be defective, they should be rectified by grinding, machining, or welding as required. If there are weak welds, from ductility or toughness, the weld should be removed before starting the repair process.

In general, subassemblies are constructed, so that at least one of the two edges has a cutoff allowance which will join during subsequent assembly and erection processes. Based on that, it will have sufficient flexibility during construction to enable the subassemblies to be sent to the field with the cutoff allowance in place and cut to fit on location. Another construction methodology option is that they can

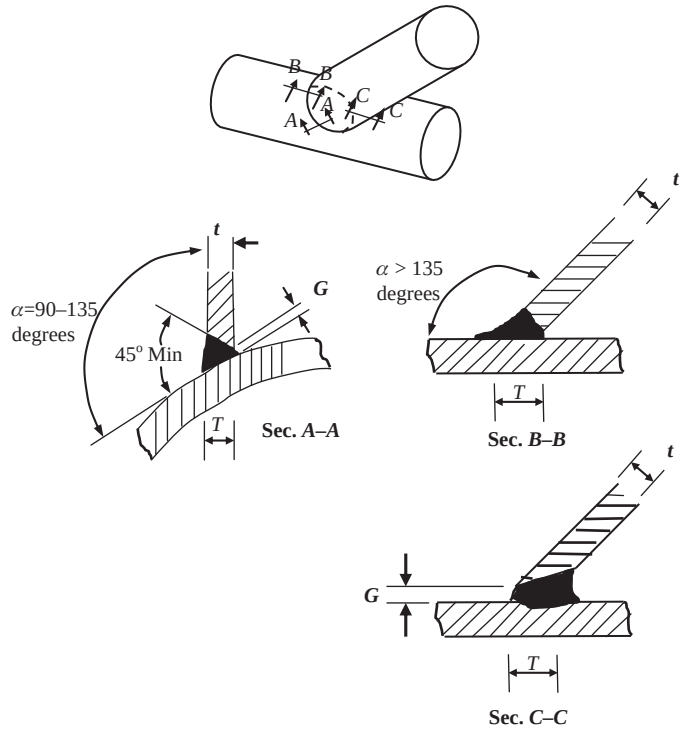

Figure 5.4 Welded tubular connection.

Table 5.1 Relation between groove angle and opening distance.

Groove angle (degrees)	Opening distance *G* (mm)
> 90	0–4.8
45–90	1.6–4.8
< 45	3.2–6.4

Table 5.2 Relation between angle of inclination and minimum welding thickness.

α (degrees)	Min "*T*"
> 135	< 1.75*t*
50–135	1.25*t*
35–50	1.50*t*
< 35	1.75*t*

be cut to exact dimensions during subassembly, where the as-built dimension has already been determined.

5.4.1 Joint fabrication

The main element of the structure is the joints which are frequently geometrically complex. Accordingly the joint fabrication presents a challenge to the construction team, for welding and dimensional control.

On a complex jacket the designer may specify the joint cans, or the whole joint including stubs and ring stiffeners, in material with specified through-thickness properties. This requirement is specified by the designer to overcome the tearing or punching effects likely to be sustained by these elements during their design life.

The designer may also increase the thickness or reinforce the cans to withstand local stresses. Finally, it is important that tubular joint welds have a minimum residual stress as a result of the fabrication, thermal stress relieving, or PWHT. North Sea jackets with thicker walls are frequently required to have a minimum residual stress as a precaution.

API-RP2A and ISO provide tolerance requirements and allowable limitations for final fabrication. The contractor with the QC team must work within the allowable tolerances and also monitor the weight control requirements at each phase of construction. In general, fabrication tolerances of joints are tight, as for a typical working points within 6 mm and, stub angle within 1 minute, all braces within 12 mm of the design dimension.

As a conventional process, the tubular joint fabrication has already been fabricated, and after doing PWHT, start to perform UT to guarantee the welding profile. The tubular joint can be fabricated in different ways depending on its geometry and mainly on the fabricator experience. Most fabricators prefer to fit the stubs to a can placed on horizontal rollers. However, some fabricators perform it by making the can upright, maintaining that this enables more stubs to be fitted simultaneously.

The typical joint fabrication sequence shall be as follows:

- Define working points on the can.
- The technical office on site provides the profile to cut stubs on it. Touch up bevels and trace generators onto the stubs. Trace node locations onto the can surface and grind or blast areas.
- To guarantee that there is no lamination on the steel apply UT. It is important to highlight that, due to shrinkage, strains in the through-thickness direction may cause lamellar tearing in the case of highly restrained joints.
- On the can in the same plane, assemble one or two adjacent stubs.
- Then, apply a tack weld and perform dimensional control checks and weld preparations around the stub.
- The welding processes used are usually shielded metal arc welding (SMAW) or flux-cored arc welding.
- If the weld is double-sided, after three or four passes, back-grind and clean the weld roots from the opposite side.
- Perform an MPI test on ground roots and deposit a weld bead for cap profiling and then perform the grinding.

- Visually inspect finished welds by MPI and UT.
- Repeat previous steps for successive stubs.
- After fitting and welding, perform PWHT as required, blast or grind welds, and perform NDT for all welds.
- At the end cut any extensions on cans or stubs then implement the final dimensional control check for the joint.

5.4.2 Fabrication based on international standards organization

ISO contains the fabrication requirements and tolerances for fixed steel offshore structures. All materials, welding, weld preparations, and inspection shall be in accordance with ISO requirements. Welding and assembly sequences shall be designed to minimize distortion.

Tubular members and joints

According to ISO, in general, circumferential welds are not allowed for cones and node stubs unless it is specified on the design or approved shop drawings.

In a tubular joint, the distance between circumferential welds shall be as a minimum the smaller of 915 mm (36″) or one diameter of the tubular. The ring stiffeners in tubular members shall have a spacing from circumferential welds 100 mm (4″) as a minimum except in some cases in which it is practically impossible, ISO recommend the welds be overlapped by at least 10 mm (3/8″) to avoid coincident location of weld toes.

Ring stiffeners shall not be offset if used for cone−cylinder junctions.

Fig. 5.5 presents longitudinal and circumferential welds in tubular joints that avoid the most critical areas of a joint.

In a tubular joint, the distance between longitudinal seams in adjacent cans shall be maximized, considering the end connections of each member, and in any case this shall be not less than 90 degrees, except when the location of a longitudinal seam is adjusted by no more than 300 mm (12″) to avoid prohibited locations.

All fabrication work shall be performed based on the procedure of safe practices, using equipment which complies with all applicable regulatory requirements, local standards, the requirements of this clause, and any appropriate regional requirements.

Construction staff should be chosen who are competent and qualified to perform their task. All fabrication, assembly, and erection shall be in accordance with approved procedures.

Unless detailed otherwise on the design drawings, the “default” layout rules and fabrication will be based on API or ISO or another standard mentioned in the project specification.

Slotted members

In any members to be slotted to receive gusset plates, the slot shall be the greater of 305 mm (12″) or 12t from any circumferential weld, where t is the member wall

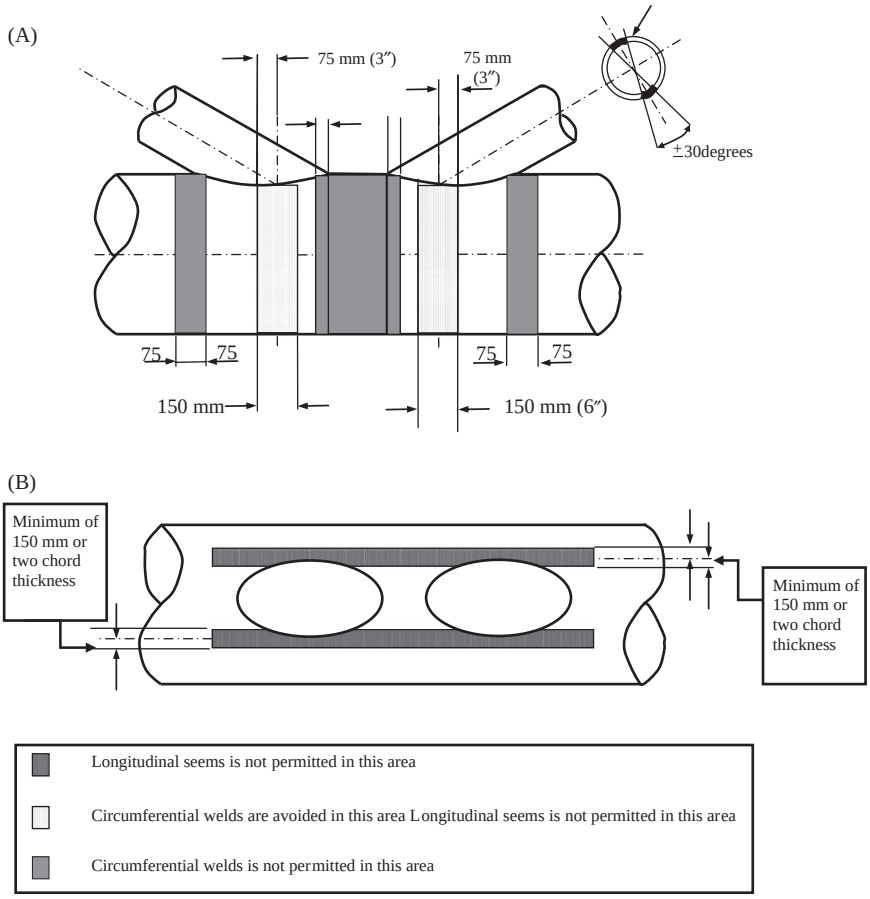

Figure 5.5 Longitudinal and circumferential welds: (A) prohibited locations for circumferential welds on chords and longitudinal seams on stubs and (B) prohibited locations for longitudinal seams on chords.

thickness. The slotted member should be drilled or cut and ground smooth at the slot end with a diameter of at least 3 mm (1/8″) greater than the width of the slot and avoid notches. To have a better fit-up and welding condition, the edge of the gusset plate passes through the slot, and should be ground to an approximately half-round shape.

Grouted pile to sleeve connections

When pouring a grout in the annulus between the pile and leg, the steel surfaces in contact with the interface develop shear, and there must be no loose material, rusting, grease, or any other material that can affect the friction between the grouting and the steel.

During and after the installation of the grouting it is very important to prevent damage from handling, high temperatures, and splatter from welding and debris. Any debris that could cause damage to the grouting during the installation process shall be removed.

For piles, it is important to be sure that the pile surface is untreated bare metal, free from mill varnish, oil, and paint, except for any specified markings. For markings, the surface area should be the minimum requirement with adequate identification.

Fabrication aids and temporary attachments are any members, such as erection braces, sling stops, scaffolding supports, padeyes, walkways, and others used for fabrication purposes. Materials used for fabrication aids and temporary attachments should comply with the project specification.

Fabrication aids and temporary attachments used for lifts during fabrication shall be designed in accordance with this document and shall be shown on the shop drawings and detailed in the fabrication procedures.

Welding procedure specifications and welder and tracker qualifications used to perform welding on fabrication aids and temporary attachments must be qualified.

If the fabrication aids and temporary attachments occur in areas that become part of the welding and are within 300 mm (12″) of an intersecting weld, or in areas that require coating, then the attachment shall be cut using oxy-fuel a minimum of 3 mm (1/8″) above the structural member surface. After that, the remainder is ground to make it flush with the member surface. The surface shall be inspected using MPI after grinding and before performing the weld.

However, if this occurs in areas that do not require coating and that are located more than 300 mm (12″) from an intersecting weld, they shall be seal-welded and cut to within 6 mm (1/4″) of the member surface, with sharp edges removed by grinding. Oxy-fuel cutting shall not be used within 3 mm (1/8″) of the surface of the underlying component.

Heat straightening

Based on a written heating procedure, straightening of members distorted by welding may be undertaken using localized heating. The maximum temperature of the heated areas shall be checked with heat-indicating equipment and shall not exceed the stated limit unless qualified in advance by mechanical testing.

Steel plate complying with the specification requirements may be rolled down to a diameter to thickness ratio of 20:1 with no additional treatment. If a diameter to thickness ratio of less than 20:1 is required mechanical tests should be carried out to demonstrate that the steel retains its mechanical properties. Postforming heat treatments, or hot forming, may be necessary to ensure the properties are maintained.

Mechanical tests will be performed in the case of T-sections or similar hot-rolled sections are formed into flanged ring stiffeners of any diameter to demonstrate that the mechanical properties are maintained after forming and welding.

The visual acceptability and also acceptable mechanical test results on test specimens taken from regions of maximum strain are the two main factors in accepting the wedges or other techniques in assisting rolling.

Based on ISO recommendations, any materials to be fabricated within the allowable tolerance are required to be straightened before use, and they can be cold straightened if the strain does not exceed 5%. The same principle applies in tubular cans for members or joints that can be rerolled after welding to comply with the dimensional tolerances requirement under condition the strain during rerolling is less than 5%.

Rat-holes, penetrations, and cut-outs

Rat-holes, penetrations, and other cut-outs should be avoided where possible. Rat-holes may be included provided they are approved by the owner, marked on shop drawings, and subject to the following requirements:

- If permanent rat-holes exist they shall be ground smooth and have a radius larger than 50 mm (2″) or twice the plate thickness. Rat-holes affect the structural integrity, and rat-holes less than this radius may be considered. Fillet welds shall be returned through the rat-holes.
- Temporary rat-holes shall have a radius higher than twice the plate thickness and shall be reinstated to an approved welding procedure. Use of weld metal is not permitted for filling.
- The radius of any approved cut-outs other than rat-holes shall be higher than 100 mm (4″). Before cutting, it is preferred that the area be checked using UT to ensure that no cut is made within 300 mm (12″) of internal stiffeners.

Movement, erection, and roll-up of subassemblies

To ensure good-quality construction it is recommended that the subassembly be welded at ground level or under cover. When such subassemblies are moved and installed into position in larger subassemblies or within the structure, care should be exercised to ensure that no members or joints within the subassemblies are overstressed or distorted.

Suitable supports may include webbing slings, wire slings when the components are protected from damage, and temporary lifting attachments welded to the subassemblies.

Subassemblies may be rolled into the correct orientation in the structure or to allow lifting at the correct orientation in the structure. Roll-up saddles shall be designed and positioned to ensure that the structure is not overstressed during roll-up and shall be well greased or otherwise lubricated.

Fabrication tolerances

As per the contract, the contractor should provide qualified persons approved by the owner's representative and also deliver suitable equipment and the necessary instrumentation to perform, monitor, and control dimensions within the allowable tolerance. At the end of each stage the tolerances should be checked as per the

fabrication procedures and at the end of the fabrication the final tolerance should match the allowable limits.

Fitters should carry out their own checking during the work progresses and their tape measures and straight edges should be calibrated. The final dimensions checks shall be on complete subassemblies and also after finalizing the structure, after PWHT if applicable.

Based on ISO, the final survey responsible personnel should be either qualified surveyors or have had at least 5 years' experience of similar work. Instruments used shall be accurately adjusted and have current valid calibration certificates.

Based on ISO the tolerances are guided by the following:

- Local tolerances shall be controlled for structural components and subassemblies so that the accumulation of such tolerances does not affect the specified global tolerances. The specified tolerances shall apply at all stages of fabrication and assembly.
- Allowance shall be made for weld gap tolerances and weld shrinkage in all component, subassembly, and global tolerance calculations.
- Where tolerances have to be derived from a formula as tolerances expressed in terms of the component dimension, such as wall thickness, the results shall be taken to the nearest mm (0.04″).
- Tolerances shall be based on theoretical setting-out points and centerlines of the structure referenced to permanent approved datum points (e.g., coordinated survey stations) and corrected to a temperature of +20°C (68°F).
- Fabrication and assembly of the supports in the fabrication yard shall be located with tolerances of ± 5 mm (1/4″) from the position shown on the approved workshop drawings. Where no such drawings exist, fabrication shall be carried out from a level plane to within ± 5 mm (1/4″).
- For the launcher structure, the dimensional tolerance of its centerlines shall be within ± 20 mm (3/4″) of the workshop drawings and shall also be within ± 6 mm (1/4″) of its reference elevation. The variation in elevation between any two points on a launcher shall not exceed 3 mm (1/8″) within any 3 m (10 ft.).

Legs spacing tolerance

The global tolerances for leg spacing at plan bracing levels are as shown in Fig. 5.6 and detailed below:

- The horizontal distance and the diagonal distance center-to-center between adjacent legs at the top of a structure where a deck or other structure is to be placed, that is, stab in nodes, shall be within 10 mm (3/8 in) tolerance from the construction drawings.
- The horizontal distance center-to-center between legs at other locations shall be within 20 mm (3/4″) of the construction drawing values.
- The horizontal diagonal distance center-to-center between legs at other locations shall be within 20 mm (3/4″) of the construction drawings values.

Vertical level tolerance

The global tolerances for vertical levels of plan bracing are as shown in Fig. 5.7 and detailed below:

- The elevation of plan bracing levels shall be within ± 13 mm (± 1/2″) of the construction drawings.

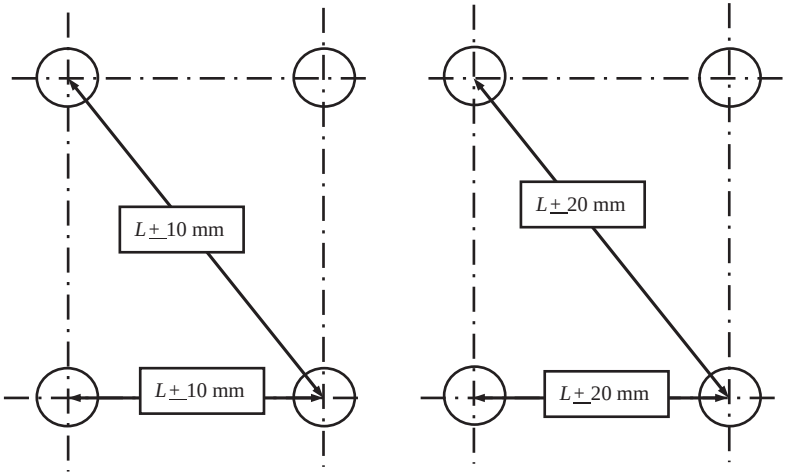

Figure 5.6 Horizontal tolerance: (A) top elevation for deck and (B) other elevation.

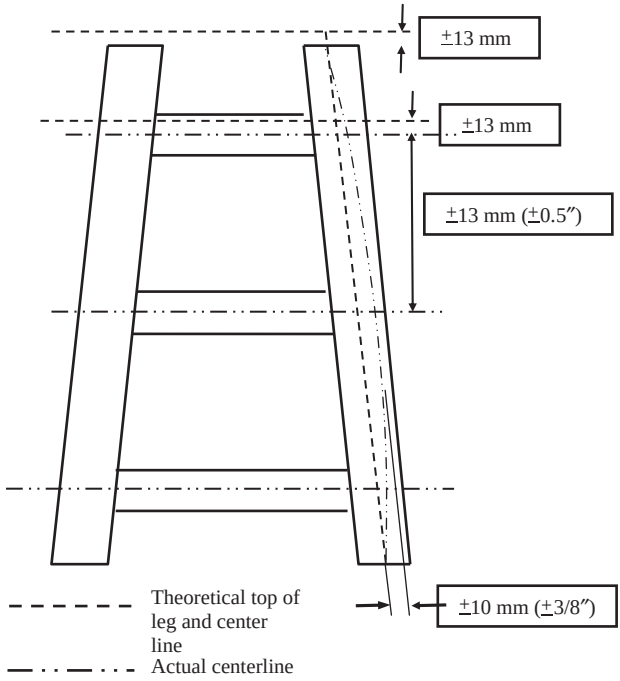

Figure 5.7 Vertical tolerance based on ISO.

- The vertical level of braces within a horizontal plane shall be within ± 13 mm (± 1/2″) of the construction drawings.
- The vertical distance between plan bracing elevations shall be within than ± 13 mm (± 1/2″) of the construction drawings.

Tubular member tolerance

For tubular members with thicknesses up to 50 mm (2″) at any point of a tubular member, the out-of-roundness, which is the difference between the major and the minor outside diameters, shall not exceed the smaller of 1% of the diameter or 6 mm (1/4″).

In the case of tubular members with thicknesses $\geq$ 50 mm (2″) at any point of a tubular member, the difference between the major and minor outside diameters shall be less than 12.5% of the wall thickness.

For tubular members with a diameter of 1200 mm or more, and a thickness of 100 mm or less, the difference between the major and minor outside diameters at any point of a tubular member may increase to 13 mm (1/2″) provided the tolerance on the circumference is less than 6 mm (1/4″).

The difference between the actual and nominal outside circumferences at any point of a tubular member shall not exceed the smaller of 1% of the nominal circumference or 13 mm (1/2″).

Fig. 5.8 presents the tolerances for the straightness of tubular members and beams, based on ISO, as follows:

- straight to be within $\pm$ 10 mm ($\pm$ 3/8″) for length $\leq$ 12 m and
- straight to be within $\pm$ 13 mm ($\pm$ 1/2″) for length $>$12 m.

In addition, the tolerances for the tubular member straightness and beams when assembled into the structure are:

- Braces between the joint stubs ends shall be straight to within 0.12% of the length.
- Braces between the joint chords ends shall be straight to within 0.10% of the length.

The tolerances for the location of cans with different wall thicknesses within a tubular are as shown in Fig. 5.8 and as detailed below:

- for joint cans, within 25 mm (1″) from the construction drawings and
- for other changes of wall thickness, within 50 mm (2″) of the construction drawings.

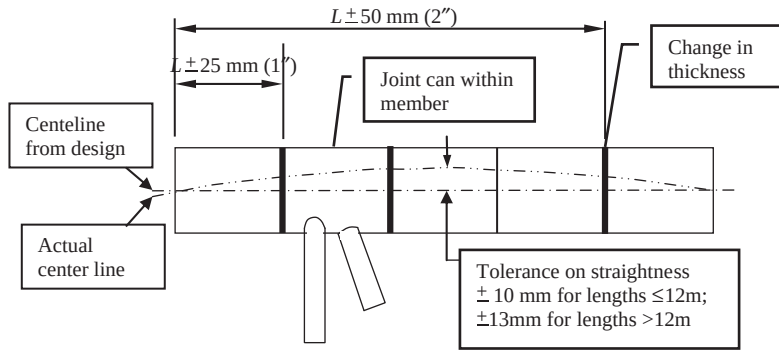

Figure 5.8 Tolerances on positioning of cans within members and straightness of members.

Fig. 5.9 illustrates the tolerances for the mismatch at circumferential welds and longitudinal seams in tubular members:

- for double-sided welds: the smaller of 10% of the thicker tubular, and 6 mm (1/4″) and
- for single-sided welds: the smaller of 10% of the thicker tubular, and 3 mm (1/8″).

Where these tolerances are exceeded the transitions shall be made by weld profiling to a maximum slope of 1:4.

Tolerance of leg alignment and straightness

In addition to the tolerances for all tubular members, the tolerances for the alignment and straightness of legs are as shown in Fig. 5.10 and detailed below:

- For structures with more than four legs, at each plan bracing level the legs will be aligned within 10 mm (3/8″) of a straight line.
- Between horizontal bracing plans, legs shall be straight to within 10 mm (3/8″).
- Between nodes legs shall be straight to within 10 mm (3/8″).

Tubular joint tolerance

For tubular joint tolerances, a best-fit work point shall be determined taking into account all the design and as-built dimensions of the complete tubular joint. The best-fit work point shall be within 15 mm (5/8″) of the design position.

The alignment of a brace stub best-fit centerline or, for point-to-point construction, the brace centerline, shall be within 13 mm (1/2″) of the design work point, as in Fig. 5.11.

The lengths of cans within the chord of a tubular joint shall be within the range of design length +10 mm to design length −5 mm and the location of the circumferential weld between chord cans shall be within 5 mm of design location (see Fig. 5.12).

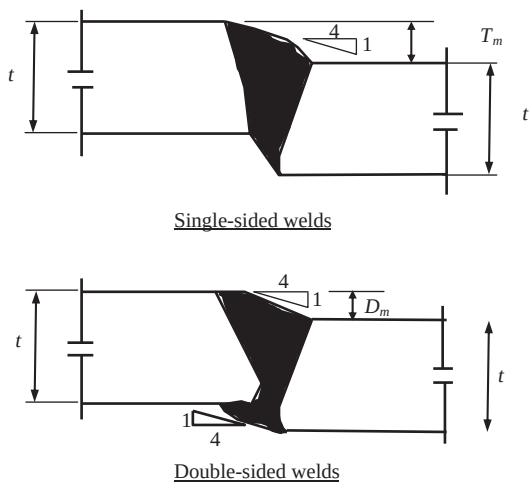

Figure 5.9 Joint mismatch tolerance.

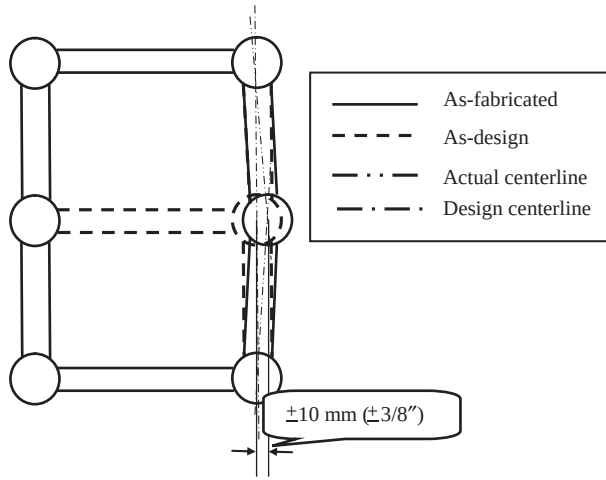

Figure 5.10 Allowable tolerance in the leg alignment.

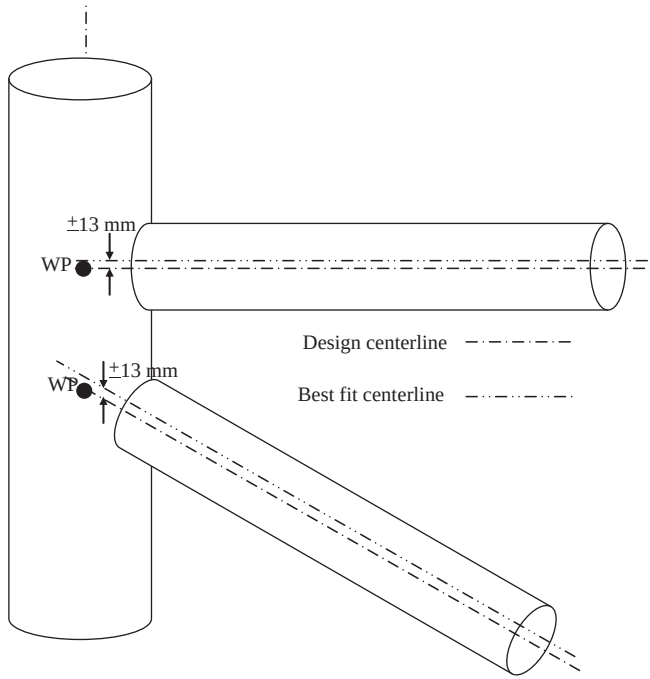

Figure 5.11 Allowable tolerance on brace stubs at tubular joints.

The lengths of the brace stub of a tubular joint shall be within the range of design length +50 mm to design length −5 mm.

The tolerances on the positioning and alignment of stubs on tubular joints are as shown in Fig. 5.11.

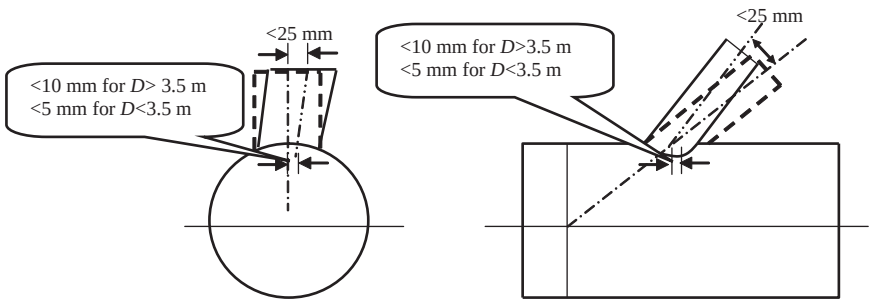

Figure 5.12 Allowable tolerance for tubular joints by ISO.

- The centerline of the brace at the intersection with the chord wall shall be within 5 mm of the construction drawing in case of chord diameter <3.5 m.
- The centerline of the brace at the intersection with the chord wall shall be within 10 mm of the design position where chord diameter >3.5 m.
- The angular orientation of the brace stub shall be within 10 degrees of the design orientation.
- The position of the centerline of the brace end of the stub shall be within 5 mm of the design position.

Where plates carrying in-plane faces are arranged to form a cruciform, the misalignment shall be less than 50% of the thickness of the thinnest noncontinuous member or 10 mm, whichever is smaller.

Stiffener tolerances

The stiffener tolerance from the construction drawings will be as follows:

- At or within 150 mm of a conical transition, to within 3 mm (1/8″).
- In the case of launch legs, the tolerance is within 3 mm (1/8″).
- In the case of tubular joints other than at conical transitions of launch leg nodes, to be within 5 mm (1/4″).
- At all other locations, to within 10 mm (3/8″).

The tolerances on ring stiffener cross sections in case of the web of the stiffener shall be perpendicular to the centerline of the tubular and within 2.5% of the web height, as shown in Fig. 5.13. On the other hand, the stiffener flange shall be parallel to the centerline of the tubular and within 1.5% of the flange width and the stiffener web shall be flat over its height to within 1.0% of the web height.

The longitudinal or diaphragm stiffeners, out-of-straightness for tubular shall be limited to 0.15% of the length or 3 mm, whichever is larger, as shown in Fig. 5.14.

Conductor guides and piles tolerances

The tolerance on conductors are the same as for pile guides, sleeves, and appurtenance supports and is related to a best-fit line through the centers of the guides, sleeves, and supports, as illustrated in Fig. 5.15. The tolerance between the center of each guide or sleeve and the best-fit line shall be within $+10$ mm ($\pm 3/8''$) at the top guide and where the vertical spacing between guides is less than 12 m

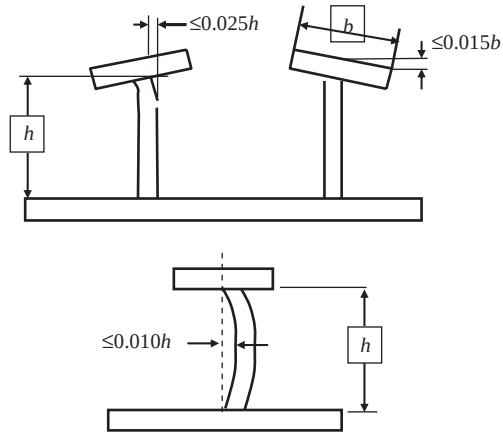

Figure 5.13 Tolerances for ring stiffener cross section based on ISO.

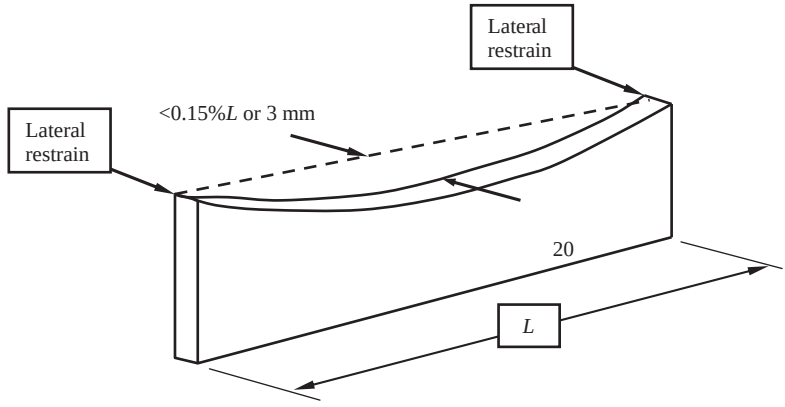

Figure 5.14 Tolerance for ring stiffener straightness.

(40 ft.). The tolerance of the center of each guide and the construction drawing line shall not exceed 13 mm (1/2″) in other cases. The tolerance check is done to the pile sleeves at the mid height of each set of centralizers.

The tolerance of the center of each support and the best-fit line shall be less than 10 mm (3/8″) at the top and less than ± 25 mm (± 1″) elsewhere.

In addition to the tolerances for other dimensions for tubular members, the tolerances of the straightness of a pile shall be:

- In any 3 m (10 ft.) length, piles shall be straight to within 3 mm (1/8″).
- In any 12 m (40 ft.) length, piles shall be straight to within 10 mm (3/8″).
- In any length over 12 m (40 ft.), piles shall be straight to within 0.1% of the length considered.

The design of anodes will be discussed in detail in Chapter 6, Corrosion protection, but, during construction, the tolerance of the locations of anodes shall be less

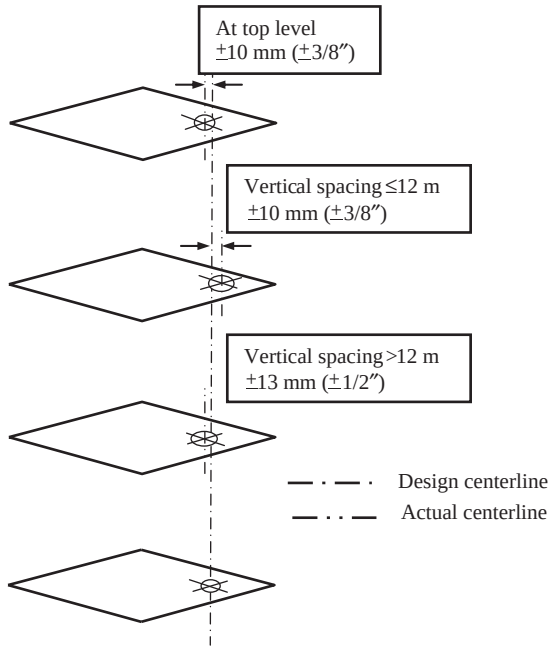

Figure 5.15 Tolerance for conductor guide alignment.

than 300 mm (12″) and less than 10 degrees circumferentially of the design position.

Dimensional control

The QC should be within the overall quality plan that was established before starting the fabrication. The owner should verify that all persons and required equipment to control the quality are available.

All the areas of QC which require attention, such as that of dimensional control, are emphasized in the code and specifications, especially for offshore structures. As previous sections have made clear, a restricted QC procedure is required for the dimension checks which have structural significance, such as the straightness of elements, ovality of tubular members, eccentricities at node joints, etc.

It is also obvious that on a jacket the global alignment or verticality of pile sleeves, conductor guides, launch runners, etc. is very important. Finally, dimensional control of items which shall be removed during installation, for example, buoyancy tank or supports, and others are critical to the efficiency of offshore installation. Based on that, there are many aspects which require close attention to dimensional control.

Surveys shall be performed using survey techniques and technology which enables the achievement of a survey accuracy better than the specified tolerances.

The methods and equipment used shall enable verification of the survey accuracy. All instruments used shall be in accurate permanent adjustment, have current valid control certificates, and be subject to a program of periodic checking.

The principal reason for requiring such accurate dimensional control of joints and tubular members during fabrication is not because of the structural consequences of being out-of-tolerance but rather because the parts may not fit together in the yard. In the case of the tubular steel jacket, the theoretical tolerances on node stub eccentricity are matched from the structural viewpoint, while the actual tolerances are very tight because of considerations regarding the fitting together of components during the later phases of construction.

There are approved construction drawings, so during fabrication any measurement verification must be within the allowable tolerance that will be based on ISO, API, AISC, or any other standard within the project specification document.

The dimensional control of node fabrication, in particular, involves potentially intricate calculations in the shop. However, the most successful systems simply involve the inclusion on the shop drawings of several additional "checking" measurements and the correct marking of the node can and stub generators and offsets.

Fabrication for all jackets and topsides structures shall be checked for loads applied during fabrication. These loads shall be based on the proposed fabrication methodology. Consideration shall be given to structure support points used for weighing and loadout. Site wind loads shall be included as part of this load condition. These checks will be carried out during detailed design and not basic design.

5.5 Jacket assembly and erection

Subassembly can be considered as an intermediate stage between standard shop fabrication as joints, tubular members, beams, and assembly or erection. The work should be managed such that the maximum number of welds is done in the shop. As the shops have the highest weld quality many node and tubular welds can be double-sided and/or automatic when performed in the fabrication shop.

When defining subassemblies, the principal factors to be considered are the following:

- Dimension, size, and weight are the main factors governing the available methods of transportation.
- Subassemblies should not need a difficult welding sequence that can induce stresses during the subassembly welding or erection or avoid causing distortion to any members.
- Certain subassemblies may have specific construction difficulties associated with them, such as short, large-diameter infillings that are difficult to erect vertically and are best included in subassemblies, if possible.

The erection sequence shall plan the lift procedure for the fabricated subassemblies and loose items. In most cases, for a large jacket, there are four types of assembly as follows:

- jacket levels with their conductor guide frames;

- top frames;
- jacket rows, such as bents or partial bents; and
- pile sleeve clusters.

The assembly and erection phases are based on the following objectives:

- Increase the opportunity for access around the jacket during execution and increase the ground assembly.
- Decrease the number of main structural element erection joints, such as jacket legs, launch runners, rows, and levels. During erection maintain the alignment for critical elements, such as conductor guides, pile sleeves, and launch runners.
- Subassemble the structural elements of the jacket, such as jacket legs, rows, and levels. Subassemble, and pretest the subsystems, such as grouting and ballasting if possible. Include the maximum quantity of secondary items such as anodes, risers, J-tubes, and caissons. Coat or paint required areas prior to erection.
- Reduce the use of temporary structures such as scaffolding, walkways, and lifting aids which require subsequent removal, where possible. and preinstall such aids where they are necessary.

The assembly of a jacket frame, often having a spread at the base of 50 m or more, places severe demands on field layout and survey, and on temporary support and adjustment bracing, as shown in Fig. 5.17. Such large dimensions mean that the thermal changes can be significant. Temperature differences may be as great as 30°C between dawn and afternoon, and as much as 15°C between various parts of the structure, resulting in several centimeters distortion. In the case of high temperature it will tend to induce residual stresses in the structure. Because of the difficulty associated with thermal distortion, it is normal to "correct" all measurements to a standard temperature, at 20°C.

Noting that, for a joint the elastic deflections are also a source of difficulty in maintaining tolerances. Foundation settlement or displacements under the skid beams and temporary erection skids must be carefully calculated and monitored.

In the construction plan each assembly should be completed before starting the lifting process, so it is required to define the location, orientation, and whether it is face-up or face-down, of each assembly to match the lifting procedure.

Central coordinates for each assembly are usually shown in the layout drawings. The central coordinates are then used as local benchmarks for erection of the assembly, subassemblies, loose items, appurtenances, and temporary attachments which comprise field welds, overall dimensions, weight, reference drawings, etc.

The QC check on dimensions should be performed before and after welding to verify the measurements by checking through the measurements of the structure.

It should take into consideration that the assembly is located in position to theoretical dimensions using allowable positive tolerances to compensate for weld shrinkage. Perhaps the most fundamental rule in fitting is the avoidance of applying excess force on the member during fitting prior to welding or to force stresses into unwelded members through the welding sequence since such conditions cannot have been foreseen by the designer and will account for more stresses that were not considered in the design calculations.

The following assembly sequence applies in most cases:

- Perform the assembly support preparation.
- Perform a dimensional control check for the main structure assembly and do position tacking.
- Perform a dimensional control check for the secondary structure assembly and do position tacking.
- Perform NDT before welding. Welding shall be accepted as per the continuous inspection and according to the approved sequence.
- All appurtenances such as anodes, supports, walkways, risers, J-tubes, caissons, grouting and ballasting and scaffolding, lifting, aids, erection guides, and temporary attachments shall be installed.
- Overall NDT, dimensional control.
- Blasting and painting or touch up. Removal of temporary assembly supports and staging.
- Preparation for transport, lift and erection.

In this phase, assembled, subassembled, and fabricated structures, together with loose items, are incorporated into the final structure according to the sequence of erection as shown in Fig. 5.16A–E.

Jacket frames are typically laid out flat and then lifted upward by more than one crawler crane. Coordinating such a rigging and lifting operation requires thoroughly developed three-dimensional layouts, firm and level foundations for the cranes, and competent operators.

The structural analysis should be performed to check the structure member stresses during the erection process for a given assembly, usually using a computer model with all relevant structural characteristics. The assembly is analyzed for a number of load cases which correspond approximately to the support conditions of the assembly with the assumption of the locations of the cranes, bogies, saddles, etc. when the panel is being transported and is in a horizontal and vertical position. The structural analysis for lifting and transportation identifies the worst cases from a structural stresses perspective. These cases are then analyzed to determine the maximum stresses and displacements. The calculations should show that global and local stresses are within allowable limits according to API/AISC codes.

In general, the erection for the major components will be as follows:

- Obtain a certificate for lifting with the lifting analysis calculations for crane configuration, rigging accessories.
- The cranes shall be prepared for lifting activity and also perform preparation for rigging and transport assembly to the lift location. The roll-up into position may be done with scaffolding and staging in position in some cases.
- The wind bracing and other fixing system is performed using guy wires and turnbuckles. The crane access and release should be addressed.
- Crane release. Removal of rigging and temporary attachments.

Fig. 5.17 presents the fabrication of one face of the jacket frame on the ground; however, the erection of the other face side is shown in Fig. 5.18A and B.

The erection of the additional steel framing to strength the jacket structure during launching is presented in Fig. 5.19.

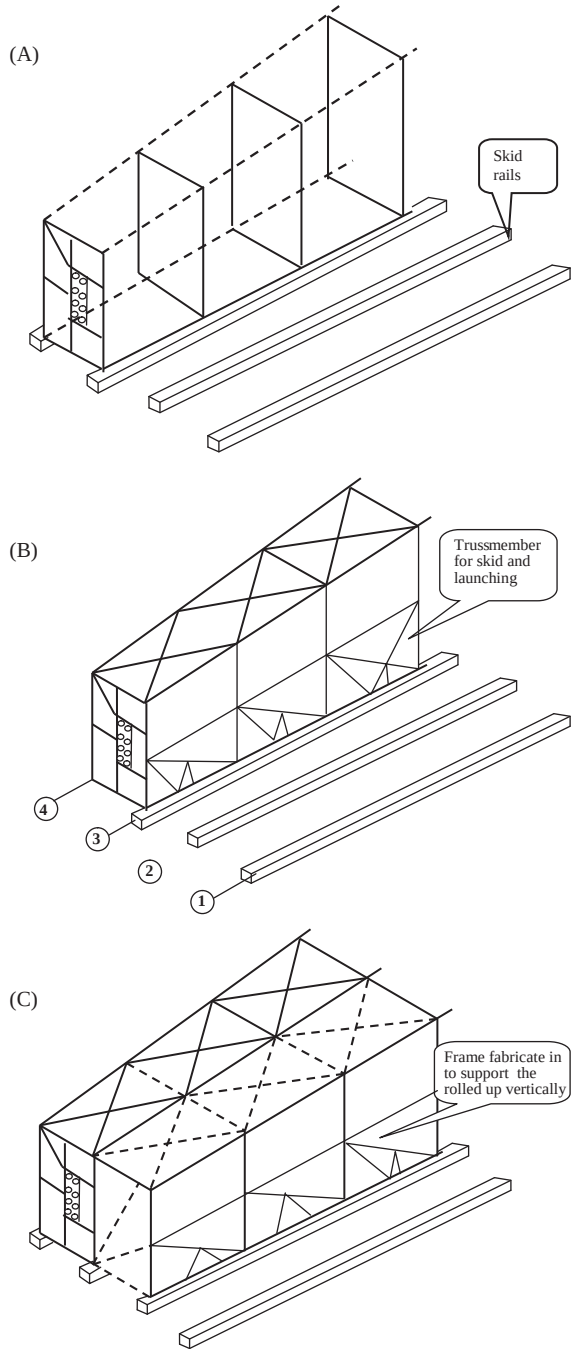

Figure 5.16 (A) Step 1, erection of plan frames; (B) step 2, erection of bay 1; (C) frame roll-up; (D) roll up the last frame and fill in between; and (E) jacket is ready for loadout and launching.

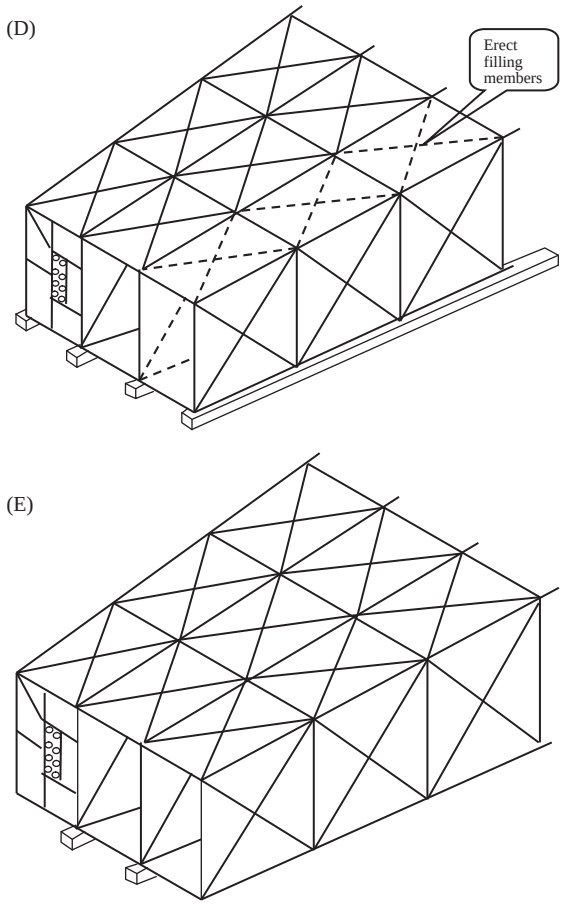

Figure 5.16 Continued.

After constructing the first frame, start to put a temporary and permanent horizontal plan as shown in Fig. 5.20 and at the same time start to construct the diagonal bracing as shown in Fig. 5.21.

Fig. 5.22 illustrates the erection of the last plan in the first level of the jacket, whereas Fig. 5.23 presents the fabrication of the plan on the ground.

The last face on the jacket will be fabricated on the ground as shown in Fig. 5.24 and one can see the exterior conductor guide and then this face will be lifted as shown in Fig. 5.25 to complete constructing the jacket.

The fabrication of the topside is shown in Fig. 5.26, erecting the topside and the helideck is shown in Fig. 5.27 and 5.28 shows the last stage of the fabrication which is the painting. The topside includes the vessels which were installed on it.

The accessories, such as the flare tip, riser guard, and boat landing will be fabricated on site and attached to the jacket after its installation. The boat landing fabrication on the yard is shown in Fig. 5.29.

Figure 5.17 Frame jacket located horizontally.

5.6 Weight control

The weight control report monitors removal of weight and ensures that through all stages throughout the life of a project weight assessments are up-to-date and traceable through back-up documentation.

The objective of weight control is as follows:

1. Topsides: module support frame, modules, helideck, and bridges as appropriate, and; substructure: steel space frame with all attachments and piles throughout the life of the project. In this context, the project life shall commence at the start of the conceptual design and cease at the time of platform abandonment.
2. To properly report and record all appropriate weight and center of gravity (CoG) data associated with the platform in a suitable form.

From the beginning of front end engineering design up to final platform construction the weights and centers of gravity of topsides and substructures are critical factors upon which major decisions are made. Such decisions typically cover the selection of the construction pad at the fabrication yard; the means for and route of loadout and the need or otherwise for civil works; the selection of transportation barge, associated ballasting requirements, and associated quay clearance requirements; the selection of crane barge and preferred lifting arrangement to facilitate installation; the direction of topsides inventory changes during the platform operating phase to accommodate production changes; and the selection of the optimum solution for platform abandonment should this be necessary at the end of the platform's useful life.

Notwithstanding the above, the progress of initial topsides, substructure, and foundation design is contingent upon the timely provision of reliable topsides weight and CoG data.

(A)

(B)

Figure 5.18 (A and B) Erecting the side frame.

5.6.1 Weight calculation

In addition to drilling loads and other temporary operating loads, the topside weight includes essentially permanent contributions from all associated engineering disciplines including as structural; mechanical; electrical; instrument; communication; HVAC; safety; and architectural. It is useful to categorize the weight elements associated with all disciplines other than structural and architectural as follows:

Figure 5.19 Erecting strength framing for the launching process.

Figure 5.20 Starting erecting the horizontal bracing.

1. main equipment and
2. bulk materials.

Therefore topside weights may be deemed to comprise the following six elements:

1. *Structural steel*

Figure 5.21 Erecting the *X* bracing with the horizontal bracing.

Figure 5.22 Erecting the last horizontal level for the jacket.

This typically includes modules, decks, and all main framing, deck plating and stiffening, all equipment supports integrated in deck structure, major facility supports such as pipe racks, walkways, service platforms, stairs, ladders, handrails, crane pedestals, and bridge supports.

In general, structural steel consists of three main categories which are:

a. primary steel;
b. secondary steel; and

Figure 5.23 Fabricating the conductor guide with the horizontal frame.

Figure 5.24 Fabricating the last face frame for the jacket.

c. temporary steel items, which typically include sea fastenings bumpers, guides, lifting and rigging gear (i.e., slings, shackles, spreader beams, etc.), secondary padeyes.

2. *Architectural*

This typically includes fire walls, ceilings, doors, windows, flooring and floor finishes, furniture, partitions, kitchen fixtures, fittings and utensils, appliances, toilet fixtures and accessories, acoustic, insulation, windshield cladding, weather louvers, heat shields, etc. in the living quarters modules and emergency shelter.

3. *Main equipment*

This typically includes all tagged mechanical, electrical, and instrument equipment; and shall be deemed to include the skid weight, drip pan, and all other items shown in the vendor package identification, on P&IDs, if applicable.

4. *Bulk materials*

Figure 5.25 Erecting the last face of the jacket.

Figure 5.26 Fabrication of the topside.

These typically include all mechanical, piping, and associated fittings and supports, electrical, communication, heating, ventilation and air-conditioning (HVAC), and safety items that have not been listed under equipment.

Piping bulk shall typically include all process and utility piping, piping valves, pipe supports, trace heating, insulation, protective coatings, and all associated accessories which have not been included in the equipment skids. Electrical bulk shall typically include all electrical cables, cable trays, cable ladders, metal-clad interlocking, supports, light fixtures, junction boxes, and instrumentation. Bulk shall typically include all instrument cables and all instruments shown on the instrument diagram legends and all

Figure 5.27 Erecting the deck and the helideck.

Figure 5.28 Painting the topside after assembly.

instrument piping (tubing) and associated supports (including control valves); it also includes instrument workshop equipment, all untagged control room auxiliary equipment, and all instrument equipment not listed under "Equipment."

HVAC bulk shall typically include all ducts, duct supports, insulation, flow dampers, grills, etc. for ventilation and air-conditioning.

Safety bulk shall typically include fire monitors, hose reels, deluge valves, fire and gas detectors, halon and CO_2 systems, portable fire extinguishers, life buoys, life jackets, life rafts, survival suits, and fire equipment.

Figure 5.29 Fabricating the boat landing and coating.

5. *Live loads*
   These are the temporary operating loads on the topsides. They typically include bulk stores, laydown area loads, crane loads, helicopter, emergency shelter, luggage, consumable and personnel effects, and all these loads defined in Chapter 2, Offshore structures loads and strength.
6. *Drilling loads*
   Although drilling loads, from the drilling required equipment and tools which are essentially temporary operating loads, they are treated separately and are not covered by the live load allowance.

Classification of weight accuracy

There are three basic classifications of weight accuracy in which the allowance in weight for each project stage is proposed in Table 5.3.

- *Conceptual*: This is based on initial estimates, possibly obtained from past projects. At the end of conceptual design, the structural weight estimates shall be based on the preliminary structure design by weight takeoff.
- *Detailed*: This is based on weight takeoff and vendor information.
- *Fabrication*: This is based on approved drawings and final takeoff.

Weight information for all items on the platform shall be recorded in a manner consistent with the following definition.

Functional weight conditions are defined as follows:

Dry is that condition in which a single weight item or a collection of items is characterized by its dead weight alone. This condition shall typically exclude any operating fluids/supplies, spares, maintenance, tools, packing, and temporary transportation materials. However, the recorded dry weight of that equipment delivered

Table 5.3 The allowance in weight.

Project stage	Available data	Allowance percentage for topside (%)	Allowance percentage for topside (%)
Conceptual design	Historic volumetric	15	10
	Vendor catalogue	15	10
	Vendor data/quotation	12	10
	Calculated from material take off (MTO)	10	10
	Historical weighted	5	10
	Design change allowance (DA)	5	5
	Fabrication change allowance (FA)	5	5
Detailed design	Vendor catalogue	15	5
	Vendor data/quotation	10	5
	Calculated MTO from (approved for construction, AFC drawings)	5	5
	DA	5	5
	FA	5	5
Fabrication	Vendor data/quotation	5	3
	DA	0	0
	FA	5	2

with lubricants or coolants or the like, that is, preinstalled shall be deemed to include such additional weights.

- Operating is that condition which exists when all equipment and bulks contain all relevant fluids and supply weights which occur under normal operating conditions.
- Hydrotest is that condition which generally occurs during topsides hook-up and commissioning and includes weight contributions from all permanent and temporary facilities together with all weight elements associated with hydrotesting.
- Loadout is that condition which exists during the activity of loading the platform (topsides, substructure) out from the fabrication facility into the transportation barge.
- Lift weight is that condition which exists during lifting of the structure. The lift weight shall be deemed to include the weight of the structure together with the weight of all

equipment and bulks actually being lifted. It shall include all temporary lifting accessories such as lifting slings, shackles, and support frames, including tie-down and support beams and, any shipped-loose items temporarily placed on the structure during lifting, but excluding hook-up spools, infill steel, or other items, which are to be lifted separately.

Allowances and contingencies

The allowance and contingencies of weight are usually based on the engineering firm experience. These contingency allowances are as follows, where the definition of allowance and contingency is stated in Table 5.4.

1. *Item accuracy allowance (IA)*
   This allowance represents the anticipated weight growth of each individual item, or collection of items, as a result of inaccuracies associated with the method of calculating the base weight. The value of the IA is dependent on the degree of definition of each individual item, or collection of items and the level of confidence in the weight estimate at any particular time. Three categories apply:
   a. conceptual design allowance (CA);
   b. detailed design allowance (DA); and
   c. fabrication design allowance (FA).
   The IA appropriate to the beginning of each design phase is stipulated. The average level of AA should reduce with time through each design phase as a function of design maturity.
2. *Design change allowance (DA)*
   This allowance provides for design changes during the detailed design phase. These design changes are a normal part of the design activity and represent the optimization of the design in satisfying the preferred approach defined during the conceptual design of the project.
3. *Fabrication change allowance (FA)*
   This allowance provides for changes to design during the fabrication phase. These changes are a normal part of the fabrication activity and represent the optimization of the design in satisfying previously unidentified constraints arising during the fabrication phase. Examples are steel section substitutes and pipework, cable work or ductwork rerouting, overrolling of plates, weld metal, and paint.
   The fabrication change allowance is applied on a modular basis, and has the same value for each functional weight condition.
   The factored weight of an item or collection of items is obtained as:

$$\text{Base weight of item} \times (1 + A_A) \times (1 + D_A) \times (1 + F_A)$$

Management contingency

This contingency provides for initially unidentified changes in topsides functional requirements that should be checked by the management during the conceptual design and then realistically spread over appropriate regions of the topsides for recording purposes. This contingency may optionally be agreed to be zero. At the end of conceptual design, the management contingency (MC) will have either been

Table 5.4 Offshore lifting terminology.

Term	Definition
Allowance	An amount, expressed in terms of a percentage of base weight, which experience of past projects has shown to be consumed during the various phases of project execution
Barge	The floating vessel, normally nonpropelled, on which the "structure" is transported. A ship or vessel
Base weight	The base weight of any individual item or collection of items is specified to a functional weight condition and is, at the time of estimating, the best available estimate of weight for that item or collection of items exclusive of all allowances and contingency
Bending reduction factor	The factor by which the breaking load of a rope or cable is reduced to take account of the reduction in strength caused by bending round a shackle, trunnion, or crane hook
Breaking load	The load at which a rope or sling will break, calculated in accordance with one of the methods. The breaking load for a sling takes into account the "termination efficiency factor"
Cable-laid sling	A cable made up of six ropes laid up over a core rope, with suitable terminations at each end
Certificate of approval	The formal document issued by the inspection company when, in its judgment and opinion, all reasonable checks, preparations, and precautions have been taken, and an operation may proceed
Consequence factor	A factor to ensure that main structural members have an increased factor of safety related to the consequence of their failure
Contingency	An amount in tons to accommodate future changes in topsides functional requirements instigated by management or by unexpected production changes
Crane vessel	The vessel or barge on which lifting equipment is mounted. It is considered to include crane barges, derrick barges, floating shear-legs, heavy-lift vessels, and semisubmersible crane vessels (SSCVs)
Determinate lift	The slinging arrangement that the sling loads that are statically determinate, so it is not significantly affected by minor differences in sling length or elasticity
Dynamic amplification factor (DAF)	The gross lift weight is multiplied by this factor, to account for dynamic loads and impacts during lifting

(*Continued*)

Table 5.4 (Continued)

Term	Definition
Grommet	A grommet is a single length of unit rope laid up six times over a core to form an endless loop
Factored weight	The factored weight of any individual item is characterized by its base weight multiplied by the product of all relevant allowances
Gross weight	The calculated weight of the structure to be lifted including contingencies, or the weighed weight including weighing allowance
Hook load	The hook load is the summation of the lift weight and the "rigging weight"
Indeterminate lift	Any lift where the sling loads are not statically determinate
Lift point	The connection between the "rigging" and the "structure" to be lifted. May include "padear," "padeye," or "trunnion"
Lift weight	The lift weight is the gross weight in addition to the allowance for dynamic effects
Loadout	The transfer of topside or jacket from land onto a barge by horizontal movement or by lifting
Loadout, lifted	A "loadout" performed by crane
Minimum required breaking load	The minimum allowable value of "breaking load" for a particular lifting operation
Net weight	The calculated or weighed weight of a structure, with no contingency or weighing allowance
Padear	A lift point from a tubular or flat plate form, with horizontal trunnions round which a sling or grommet may be passed on it
Padeye	A lift point from steel plate, reinforced by cheek plates if necessary, with a hole for shackle connection
Rigging	The slings, shackles, and other devices including spreaders used to connect the lifting object to the crane
Rigging weight	The total weight of rigging such as slings, shackles, and spreaders
Rope	The unit rope from which a cable-laid sling or grommet may be constructed, made from either six or eight strands around a steel core

(*Continued*)

Table 5.4 (Continued)

Term	Definition
Safe working load (SWL)	The safe working load of a sling, shackle, or lift point is the maximum load that the sling may raise, lower, or suspend under specific service conditions
Sea fastenings	The structure members which are used to connect the structure to a barge or vessel during transportation
Skew load factor (SKL)	This is a factor used to multiply to the load on any lift point or pair of lift points to account for sling mismatch in a statically indeterminate lift
Sling breaking load	The breaking load of a "sling," being the calculated breaking load reduced by "termination efficiency factor" or "bending reduction factor" as appropriate.
Sling eye	This is formed by an eye splice or mechanical termination to be a loop at each end of a sling
Splice	This is a sling length where the rope is rolled back into itself by tucking the tails of the unit ropes back through the main body of the rope, after forming the sling eye
Spreader bar (frame)	A spreader bar or frame is a structure designed to resist the compression forces induced by angled slings, by altering the line of action of the force on a lift point into a vertical plane
Termination efficiency factor	This factor is multiplied by the breaking load of a wire or cable to account for the reduction of breaking load caused by a splice or other end termination
Trunnion	This is a horizontal tubular cantilever, round which a sling or grommet may be passed on it. An upending trunnion is used to rotate a structure from horizontal to vertical, or vice versa. It forms a bearing round which the sling or grommet will rotate around it

consumed and hence be represented by identifiable weight elements, or be added to the then-existing level of operating contingency (OC).

Operating contingency

During the operation phase usually there are many changes due to change in the mode of operation. The OC provides built-in reserve topsides capacity to facilitate these of operational changes in functional requirements which may arise during the operating phase of the platform. The value of OC, in tons, is to be agreed at the outset of conceptual regions of the topsides for recording purposes. This contingency may optionally be agreed to be zero.

The not-to-exceed-weight of the platform, for example, for topsides or substructures is obtained as:

Factored weights + MC + OC

Weight engineering procedures

Throughout the duration of the project, the lead structural engineer is responsible for gathering and recording the weight and CoG information from all disciplines and for generating the weight report. He is additionally responsible for reporting the status of the weight and CoG of the platform components such as topsides modules, decks, bridge, and other substructures to each discipline and to the project manager/engineer on an agreed regular basis.

On the other side, each discipline is responsible for furnishing all the necessary weight and CoG information of items associated with their discipline to the lead structural engineer. Each discipline is also responsible for updating such information at previously agreed regular intervals or when deemed necessary by the lead structural engineer.

Define the limit of responsibility for the supply of weight information between disciplines as every discipline is responsible for furnishing information about the weight and CoG.

The realistic weight and weight allowances can be obtained from vendors by specifying in the request for quotations packages a requirement that vendors shall guarantee, within agreed limits, their quoted weights and CoG when submitting their quotations.

The discipline should follow up the weight by recording their weight estimates, which shall be kept in a tidy and proper manner. The records may be quotations from vendors and marked-up drawings of weight takeoffs with piece mark numbers.

At the start of the project and as soon as the preliminary equipment layout drawings are established, each discipline shall use the weight and center of gravity control form to furnish all the initial weight and CoG information to the structural engineer. The structural engineer is then responsible for generating the weight report. This shall ordinarily be done using appropriate computer software. He will issue this report to each discipline and the project manager or engineering manager for their review and information. All assumptions, qualifications, and exclusions shall be included in the weight report.

At regular intervals, at least monthly, during the project, each discipline will furnish updated weights and centers of gravity information to the lead structural engineer, who is responsible for generating an updated weight report.

The responsible structural engineer is responsible for gathering any and all information required for his weight control report and shall draw management attention to any undesirable weight trends or problems and shall suggest corrective actions as appropriate

5.7 Loads from transportation, launch, and lifting operations

During the construction phase in the fabrication yard or during offshore installation, the topside and jacker shall be under critical loading condition.

During jacket assembly in the fabrication yard, the jacket members and joints may be affected by higher stresses due to high bending moment or punching loads. Therefore it is required that a structure analysis is done to check under these loading conditions considering the jacket assembly plan and procedures.

During the transportation of the jacket to the site on the barge, the jacket and tie-down braces, their connections, and the transportation barge are subjected to significant dynamic accelerations and inclined self-weight loads. These motions from transportation shall be simulated by software structure analysis package for the incremental load sequences to define the highest stresses under the dynamic load.

In most cases the transportation study shall be revealed to add bracing for the jacket due to the transportation effect. These braces can be removed before installation directly to reduce the amount of wave load.

The very critical analysis is launched, as in this phase the jacket will be affected by significant inertia and drag loadings. In general, as the jacket starts tilting around the launch beam and quickly down to sea, at this moment the jacket shall be under the most critical loading. At this position, the titling beams affect the stiff bracing level with the highest concentrated load value, therefore it is important to strengthen it by a launch bracing system to withstand this high loading condition.

In this case another critical case of loading is a crane lift of the deck or jacket from the transportation barge.

It is important to perform lifting structure analysis as during lifting operations, deck and jacket members and connections may have a straining action in directions different to their in-place structure analysis.

During the lifting analysis the structure deck CoG should be defined as it can cause a shorter or longer lifting sling than planned causing substantially different loads than those calculated for idealized conditions, noting that in the case of a four-sling lift, if one sling is shorter than planned, three instead of four slings will carry the whole deck loads. Lifting padeyes and lugs are components with high consequences of failure. Failure of only one padeye can cause the loss of the deck, jacket, and the crane. Due to its criticality, and connections to the structures lifted, it must be designed for safety factors equal to four or higher against the ultimate capacity. This is common for padeyes, their connections to the structure, and the associated lifting gear.

5.8 Lifting procedure and calculation

The lifting force values depend on the weight of the lifting structure, its geometry, the conditions surrounding it, the location of the padeye, and the angle between each sling and the vertical axis.

The lifting structure analysis is based on the equilibrium between the lifting structure weight and the tension force in the slings. As per this analysis the generated forces on all lifting points and the attached lifting structures with the padeyes shall be designed to resist these forces.

Moreover, API-RP2A recommends that due to the side movement that may be occur during lifting, the padeye and the connection to the supporting structure should be designed for the combined action of the static sling load and a horizontal force equal to 5% of this load, applied perpendicular to the padeye at the pinhole center. If lifting in the fabrication yard, these design forces are due to static loads.

On the other hand, if the lifting derrick or the structure to be lifted is on a floating vessel, then dynamic load factors should be applied to the static lifting forces.

Specifically for offshore lifting, API-RP2A recommends two minimum values of dynamic load factors—2.0 and 1.35. Factor 2.0 is used in designing the padeyes as well as all members and their end connections framing the joint where the padeye is attached, while factor 1.35 is used in designing all other members transmitting lifting forces.

In the case of the loadout at sheltered locations, the corresponding minimum load factors for the two groups of structural components become, according to API-RP2A, 1.5 and 1.15, respectively.

Fig. 5.30 shows the lifting of the deck to put on the skid to start pullout into the barge.

The lifting of the flare stack to be attached to the topside is shown in Fig. 5.31.

The lifting terminology is summarized in Table 5.4.

5.8.1 Lifting calculation

For any lifting requirement, the calculations carried out shall include the following allowances, factors, and loads, or equivalent weight contingency factors as discussed earlier.

Figure 5.30 Presenting the topside to the barge.

Figure 5.31 Lifting the flare stack to fix to the topside offshore.

Weight control shall be performed by means of a well-defined, documented system, in accordance with current good practice, such as ISO Draft International Standard ISO/DIS 19901-5—Petroleum and natural gas industries—specific requirements for offshore structures—Part 5: Weight control during engineering and construction.

Where a limiting design sea state is derived by calculation or model tests, the limiting operational sea state shall not exceed 0.7 × the limiting design sea state.

Calculated weight

- Class A weight control will be needed if the project is weight or CoG sensitive for lifting and marine operations, or "have (sic) many contractors to interface."
- Class B weight control applies in the case that weight and CoG are less critical for lifting and marine operations.
- Class C weight control applies in the case that weight and CoG data are not critical.

Unless it is not stated clearly that the structure and the lift operation are not weight or CoG sensitive, then Class A weight control will be considered. If there is a 50/50 weight estimate, then a reserve of not less than 5% shall be applied. The extremes of the CoG envelope shall be used.

A reserve of not less than 3% shall be applied to the final weighed weight.

$$\text{Gross weight} = \text{calculated or weighed weight} \times \text{reserve} \tag{5.1}$$

Unless operation-specific calculations show otherwise, for lifts by a single vessel the following dynamic amplification factors (DAFs) shall be applied (Table 5.5).

Alternatively, the DAF may be derived from a suitable calculation or model test.

Where the lift is from a barge or vessel alongside the crane vessel or barge, motion must be taken into account as well as the crane boom tip motion

$$\text{Lift weight} = \text{gross weight} \times \text{DAF} \tag{5.2}$$

Table 5.5 Dynamic amplification factors (DAFs) in different locations

Gross weight, *W*	**Offshore**	**Inshore**	**Onshore**	
(tons)			**Moving**	**Static**
$W \leq 100$	1.30	1.15	1.15	1.0
$100 < W \leq 1000$	1.20	1.10	1.10	1.0
$1000 < W \leq 2500$	1.15	1.05	1.05	1.0
$W > 2500$	1.10	1.05	1.05	1.0

Where a limiting design sea state is calculated or from model tests, the limiting operational sea state shall be equal to or less than 70% of the limiting design sea state.

For offshore lifts by two or more vessels, the lift weight shall be multiplied by DAF equal to 1.1.

Hook load

The hook load is calculated in case of the loading on a padeye or the structure, with the lift weight as defined before used. Loads in slings, and the total loading on the crane, should be based on hook load, where

$$\text{Hook load} = \text{lift weight} + \text{rigging weight} \tag{5.3}$$

Rigging weight includes all items between the padeyes and the crane hook, including slings, shackles, and spreaders as appropriate.

The definition of "padeye" here is taken to include any type of lift point, including padear, trunnion, or other type.

Skew load factor

For indeterminate four-sling lifts using matched slings, a skew load factor (SKL) of 1.25 shall be applied to each diagonally opposite pair of lift points in turn. For determinate lifts the SKL may be taken to be 1.0.

$$\text{Vertical padeye load} = \text{padeye resolved lift weight} \times \text{SKL} \tag{5.4}$$

where the padeye resolved lift weight is equal to the vertical load at each padeye, taking into account lift weight and CoG only.

If the allowable location of the CoG is specified as per the geometric shape, then the most conservative CoG location within the allowable area should be considered, until the CoG location can be determined accurately.

Resolved padeye load

The resolved padeye load is the vertical padeye load divided by the sine of the sling angle:

$$\text{Resolved padeye load} = \frac{\text{vertical padeye load}}{\sin\theta} \tag{5.5}$$

where θ is the sling angle which is the angle between the sling and the horizontal plane.

If the lifting point is correctly orientated with the sling orientation, then a horizontal force equal to 5% of the resolved padeye load shall be applied, through the centerline and along the axis of the pinhole or trunnion.

If the lifting point is not correctly orientated with the sling orientation, the calculated force acting along the axis of the pinhole or trunnion and adding 5% of the resolved padeye load should be applied.

Sling force

The sling force is the vertical padeye load plus the sling weight (per sling) divided by the sine of the sling angle

$$\text{Sling force} = \frac{\text{vertical padeye load} + \text{sling weight}}{\sin\theta} \tag{5.6}$$

The minimum safety factor on sling or grommet breaking load after resolution of the load based on the CoG position and sling angle, and consideration of the factors, shall be not less than 2.25.

Crane lift factors

For a two-crane lift, the resolved load at each crane shall be multiplied by the following factors based on the DNV report:

$$\text{Center of gravity factor} = 1.03 \text{ tilt factor} = 1.03$$

$$\begin{aligned}\text{Crane resolved lift weight} = {} & (\text{statically resolved lift weight into each crane}) \\ & \times (\text{center of gravity factor}) \times (\text{tilt factor})\end{aligned} \tag{5.7}$$

For a two-crane lift, with two slings to each hook, the load resolved to each padeye shall be multiplied by a yaw factor:

$$\text{Yaw factor} = 1.05$$

$$\begin{aligned}&\text{Padeye resolved lift weight} \\ &\quad = (\text{crane resolved lift weight, resolved to each padeye}) \times (\text{yaw factor})\end{aligned} \tag{5.8}$$

Two-crane lifts with other rigging arrangements will require special consideration.

Part sling factor

Where a two-part sling passes over, round, or through a shackle, trunnion, padear, or crane hook, other than at a termination, the total sling force shall be distributed into each part in the ratio 45:55.

Sling load = sling force × 0.55 (for two-part slings)

Termination efficiency factor

The breaking load of a sling ending in an eye splice shall be assumed to be the calculated rope-breaking load multiplied by a factor as follows:

For hand splices 0.75.
For resin sockets 1. 00.
Swage fittings, for example, "Superloop" 1.00.
Other methods of termination will require special consideration.

$$\text{Sling breaking load} = \text{rope breaking load} \times \text{termination efficiency factor} \quad (5.9)$$

Bending efficiency factor

Where any rope is bent round a shackle, trunnion, padear, or crane hook, the breaking load shall be assumed to be the calculated rope-breaking load multiplied by a bending efficiency factor

$$\text{Bending efficiency factor} = 1 - \frac{0.5}{\sqrt{(P_d/r_d)}} \quad (5.10)$$

where P_d is the pin diameter and r_d is the rope diameter.
This results in the bending efficiency factors listed in Table 5.6.

Grommets

Grommets require special consideration, to ensure that the rope-breaking load and bending efficiency have been correctly taken into account.

The grommet core should be discounted when computing breaking load. The grommet or any part of it breaking load is equal to six times the unit rope-breaking load, with a factor to account for the spinning losses in cabling. This factor is normally taken as 0.85.

$$\text{Grommet breaking load (each part)} = 0.85 \times 6 \times \text{breaking load of unit rope} \quad (5.11)$$

Table 5.6 Bending efficiency factor.

P_d/r_d	<0.8	0.8	0.9	1.0	1.5	2.0	3.0	4.0	5.0
Factor	Not advanced	0.44	0.47	0.50	0.59	0.65	0.71	0.75	0.78

A grommet is used with one end over the crane hook, and the other end connected to a padeye by a shackle. The bending efficiency factors at each end may differ, therefore the more severe value should be taken. Bending efficiency is derived as before, where rope diameter is the single part grommet diameter. The total breaking load of the grommet used in this manner is

$$2 \times (\text{single part grommet BL}) \times (\text{more severe bending efficiency factor})$$

Shackle safety factors

The minimum shackle breaking load, where this can be reliably determined, shall be not less than the minimum required sling breaking load.

$$\text{The minimum shackle SWL} > \frac{\text{Sling force}}{\text{DAF}}$$

whichever results in the larger required shackle size.

As the shackle is at the lower end of the rigging, the weight of the rigging components above the shackle including its DAF and considering the sling angle may be deducted from the sling force.

Consequence factors

The consequence factors in Table 5.7 shall be considered during the structure design for the lift points and their attachments to the structure.

The above consequence factors shall be applied based on the calculated lift point loads after consideration of all factors. If a limit state analysis is used then the additional factors shall also be applied. A lifting calculations flowchart with the various factors and their applications are illustrated in Figs. 5.32–5.35.

5.8.2 Structural calculation for lifting

Structural calculations are performed considering the factors discussed in the previous sections and considering the different load cases. As an example, for an indeterminate, four-point lift the following load cases should be considered:

Table 5.7 Consequence factors.

Lift points including spreaders	1.35
Attachments of lift points to structure	1.35
Members directly supporting or framing into the lift points	1.15
Other structural members	1.00

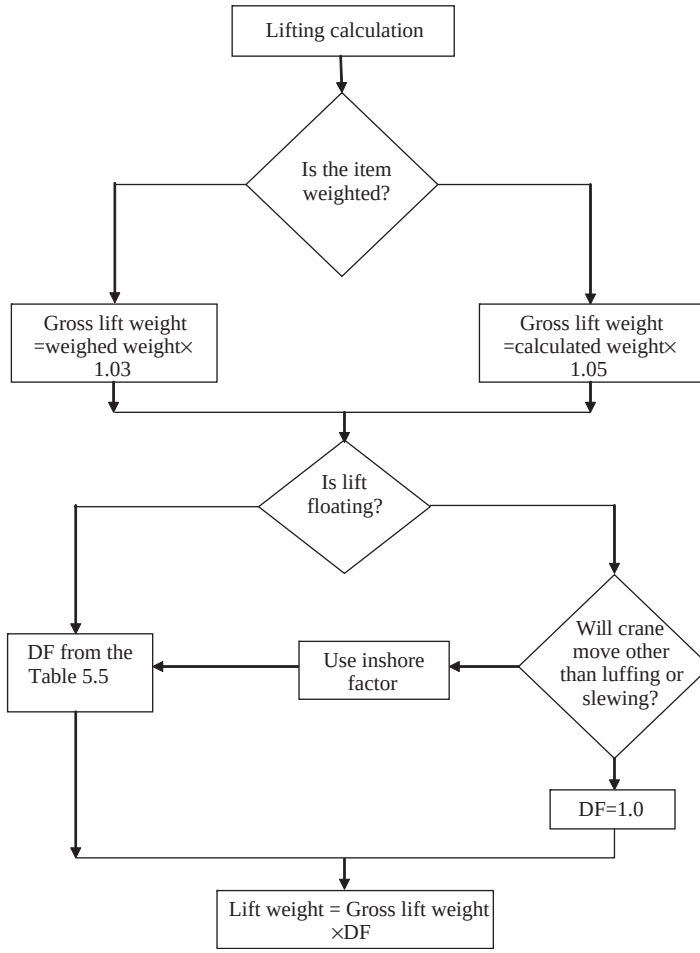

Figure 5.32 Procedure for calculating lifting weight.

1. base case, using lift weight, resolved to the lift points, but without the skew load factor;
2. lift weight, with skew load factor applied to one diagonal; and
3. lift weight, with skew load factor applied to the other diagonal.

For all cases the correct sling angle and point of load, and any offset or torsional loading due to the slings shall be considered.

The overall structure shall be analyzed for the loadings. The primary supporting members shall be analyzed using the most severe loading, with a consequence factor of 1.15 applied as in Table 5.4.

An analysis of the lift points and attachments to the structure shall be performed, using the most severe load resulting, and a consequence factor of 1.35. The 5% side load should also be applied, as should any torsional load resulting from the 45:55 two-part sling loading, if applicable.

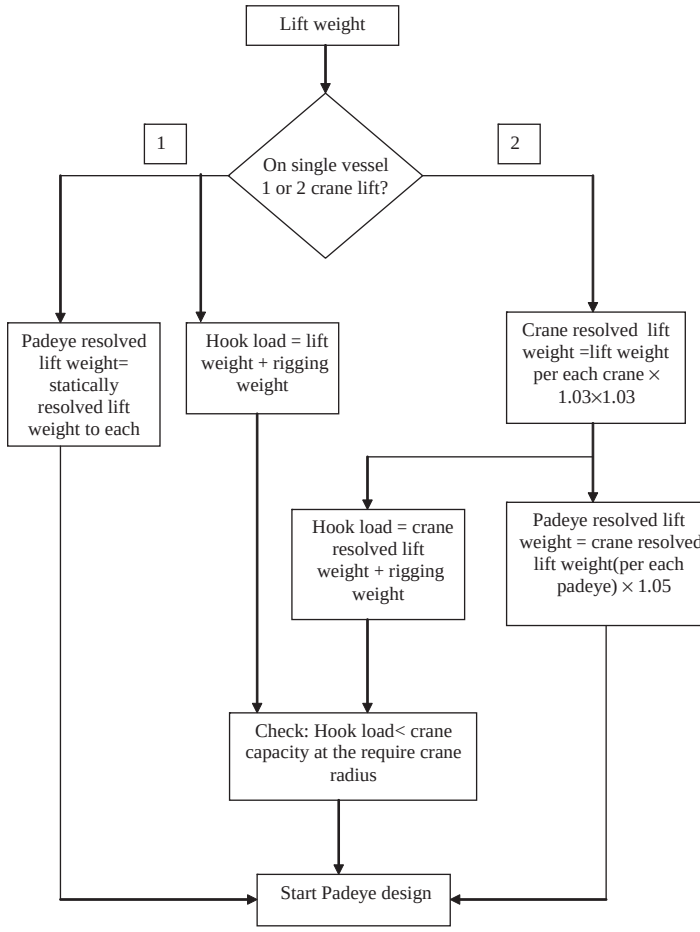

Figure 5.33 Procedure for calculation of loads on the padeye.

Where the lift point forms a structural node, the calculations also include the loads imposed by the members framing into it (Figs. 5.32−5.35).

Spreader bars or frames, if used, should be similarly treated, with load cases as above. A consequence factor of 1.35 shall be applied to lift points, and 1.15 applied to members directly supporting the lift points, as presented in Table 5.8.

Stress levels shall be within those permitted by the latest edition of a recognized and applicable offshore structures code. The loading shall be treated as a normal serviceability level functional load with associated load and resistance or safety factors in case of using an allowable stress design code, the one-third increase for environmental loadings shall not be allowed here; similarly, for an load resistance factor design with partial factor code, the load factor would be greater than that used for ultimate conditions.

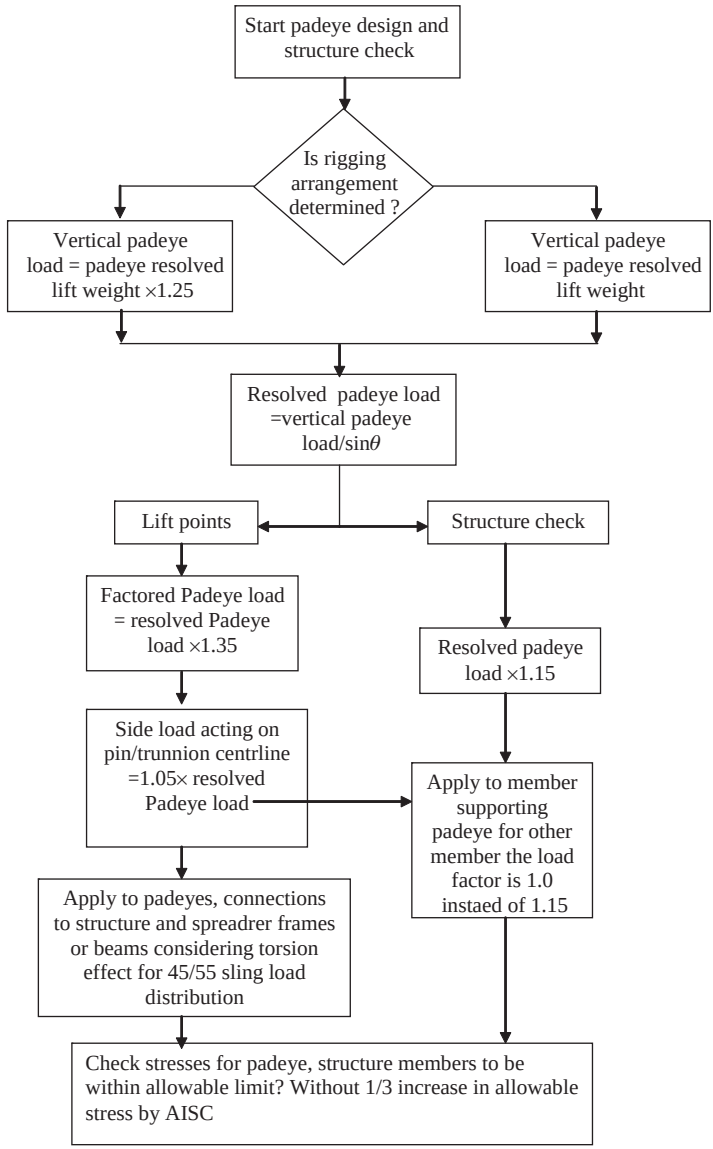

Figure 5.34 Checking the structure member and padeye.

In the case of limit state analysis or load resistance factor, the design approach may be applied according to a recognized code, provided that the total load factor shall not be less than the product of all the required factors, multiplied by a further factor of 1.30.

The material reduction factor shall be not less than:

elastic design of steel structures; 1.15 and
plastic design of steel structures; 1.30.

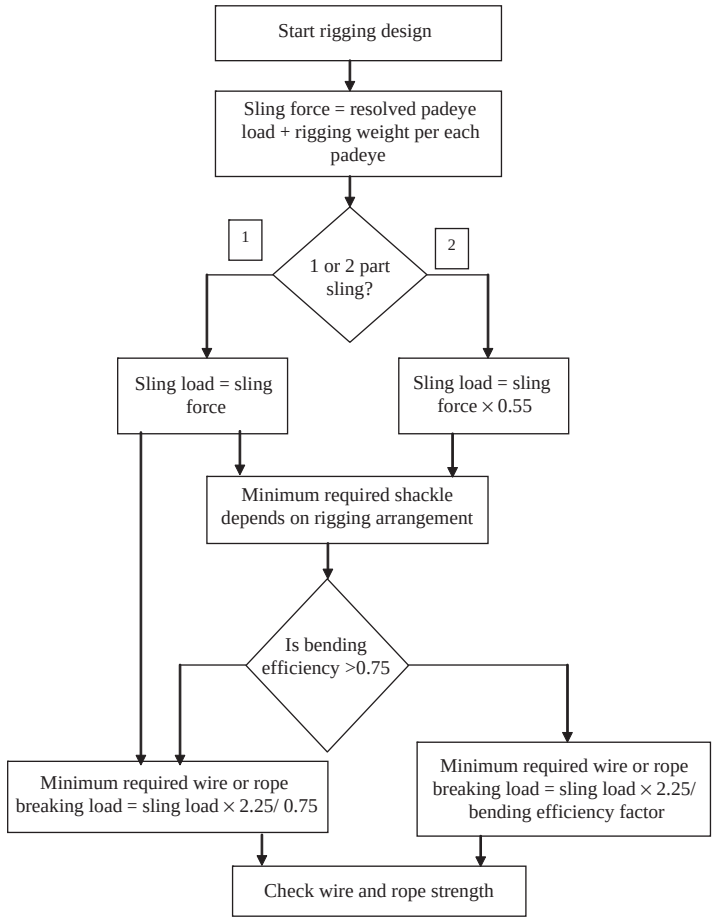

Figure 5.35 Check rigging facilities.

5.8.3 Lift point design

In addition to the structural requirements as described in the previous section, the following should be taken into account in the lift point design.

It is required to connect the sling between cheek plates, or inside trunnion keeper plates, to allow for ovalization under load. In general, the width available for the sling shall be equal to or more than $1.25D + 25$ mm, where D is the nominal sling diameter. From a practical point of view, the rigging and derigging operations may demand a greater clearance than this value.

In general, during fabrication of the lift points, it is important to consider the direction of loading, which should be in the same direction as the plate rolling.

Through-thickness loading of lift points and their attachments to the structure should be avoided if possible. If such loading cannot be avoided, the material used shall be check by UT to guarantee that it is free from laminations.

Table 5.8 Checklist for jacket/topsides transportation analysis.

S/N	Items to check	Check (yes/no)
	Computer model	
	It is assumed that the model is checked for dimensions, elevations, member group and section properties in the in-place/loadout analysis and is upgraded to suit the current analysis	
1	Member end releases for sea fastening	
2	Sea fastening material yield strength	
3	Boundary conditions for dead load case	
4	Boundary conditions for tow load case	
	Loads	
	It is assumed that the load calculations are verified in the in-service as loadout analysis and relevant load cases only are picked for the current analysis	
5	Remove future loads, operating weights, and live loads, add rigging loads	
6	Load contingencies in static and tow analysis	
7	Load combinations in static analysis	
8	Center of rotation data	
9	Roll and pitch direction representation	
10	Consideration of self-weight during inertia load generation	
11	Roll and pitch acceleration data	
12	Coefficients for the lateral load components due to combinations	
13	Primary and secondary load case identification	
14	Load combinations	
15	Chord strength reduction in the joint can input file (check $F_y = 2/3F_u$ for chords of high-strength members)	
16	Allowable stress modifiers	
	Analysis of results	
17	Enclose load case summary for dead load case	
18	Enclose reaction summary from combined analysis	

(*Continued*)

Table 5.8 (Continued)

S/N	Items to check	Check (yes/no)
19	Crosscheck reaction summary values from basic motion equations	
20	Enclose member check report: review overstressed members	
21	Enclose joint check summary: review overstressed joints	
22	Enclose model plots: joint/group/section names, K_x, K_y, L_x, L_y, F_y	
23	Enclose deflection plots, member unity check ratio plots	
	Sea fastening design	
24	Check for adequacy of base plate connections for sea fastenings (weld size less than the barge deck plate thickness, gusset connections for uplift forces preferred)	
25	Check for adequacy of doubler plate connection (weld, doubler plate) on the topside members	
	Barge deck strength check	
26	Check for barge deck transverse girder adequacy	
27	Check for adequacy of weld between barge deck plate/girder for uplift	
28	Check for buckling strength of bulkheads for sea fastening reactions	
29	Check for combined vertical/lateral loads on end bulkheads	
30	Check for combined vertical/lateral loads on internal bulkheads	
31	Check for barge flexibility effect of sea fastening forces	

Pinholes should be bored or reamed, and should be designed to suit the proposed shackle. Adequate spacer plates should be provided to centralize shackles.

Cast padears shall be designed taking into account the geometrical considerations, the stress analysis process, and the manufacturing process and QC.

The extent of NDT shall be submitted for review. Where repeated use is to be made of a lift point, a procedure should be presented for reinspection after each lift.

5.8.4 Clearances

The clearance around the lifting object and crane vessel should be studied in the lifting procedure. It is important to define the clearance during lifting operations,

there are many factors affecting it such as weather condition limitations, the motion and size characteristics of the crane vessel and the transportation barge, and also the bumpers arrangements.

Based on that, offshore lifts, which are consider risky operations, need more specific focus on the following section which presents the required clearances that must be maintained during the lifting operation.

Clearances around the lifted object

The clearance between any part of the lifted object (including spreaders and lift points) and crane boom is not less than 3 m.

The vertical clearance between the underside of the lifted object and any other previously installed structure, except in the immediate vicinity of the proposed landing area, is not less than 3 m.

The distance between the lifted object and other structures on the same transport barge should not be less than 3 m.

The horizontal clearance between the lifted object and any other previously installed structure, unless purpose-built guides or bumpers are fitted, is more than or equal 3 m. Three meters is also reasonable between the traveling block and fixed block at maximum load elevations.

Clearances around the crane vessel

Nobel Delton (2009) recommended, in the case of mooring the crane vessel adjacent to an existing platform, 3 m between any part of the crane vessel and the platform, and 10 m between any anchor line and the platform.

Where the crane vessel is dynamically positioned, 5 m nominal between any part of the crane vessel and the platform is recommended.

The clearance between the crane vessel and seabed, after taking account of tidal conditions, vessel motions, increased draft, and changed heel or trim during the lift, is 3 m.

These clearances around mooring lines and anchors are stated as guidelines in cases of specific clearance requirements as per the project and operations requirements which supersede these guidelines and the following surrounding conditions should also be taken into account:

- water depth;
- proximity of subsea assets;
- the accuracy of the survey;
- the ability to control the anchor handling by the vessel;
- the condition of the seabed;
- estimated anchor drag during embedment; and
- the weather forecast during the anchor installation.

Operators and contractors may have their own requirements which may differ from those stated below, and should be applied if more conservative.

Clearances should take into account the possible working and stand-off positions of the crane vessel and the moorings should never be laid in such a way that they could come into contact with any subsea asset. This may be relaxed when the subsea asset is a trenched pipeline, provided it can be demonstrated that the mooring will not cause frictional damage or abrasion.

The vertical clearance between any anchor line and any subsea asset should be not less than 20 m in water depths exceeding 40 m, and 50% of water in depths of less than 40 m.

The clearance between any mooring line and any structure other than a subsea asset should be more than 10 m.

When an anchor is placed on the same side of a subsea asset as the crane vessel, it should not be placed closer to the subsea asset than 100 m.

If a subsea asset lies between the anchor and the crane vessel, the final anchor location should be more than 200 m from the subsea asset.

The crossed mooring situations should be avoided during lifting operations, if applicable. Where crossed moorings cannot be avoided, the separation between active catenaries should be more than 30 m in water depths greater than 100 m, and 30% of water depth in water depths < 100 m.

If any of the clearances are impractical because of the mooring configuration or seabed layout, a risk assessment shall be carried out and special precautions taken as necessary.

Fig. 5.36 presents a chart of the lifting capacity for the crane on a barge, which is the relation between boom radius, hook height, and lifting capacity. This chart should be included in the lifting procedure which is usually delivered from the construction company and reviewed by the engineering firm and the company representative.

5.8.5 Lifting calculation report

Calculations shall be presented for the structure to be lifted, demonstrating its capacity to withstand, without overstress, the loads imposed by the lift operation, with the load and safety factors, and the load cases.

The lifting study package should contain the following as minimum requirements:

1. plans, elevations, and sections showing main structural members;
2. the structural model, this should present the proposed lifting geometry, including any offset of the lift points;
3. the lifting weight and center of gravity location;
4. the steel grades and properties;
5. the load cases imposed;
6. the design codes and standard;
7. a member unity checks table, or a statement that unity checks are less than 0.8; and
8. justification, or proposal for redesign, for any members with a unity check in excess of 1.0.

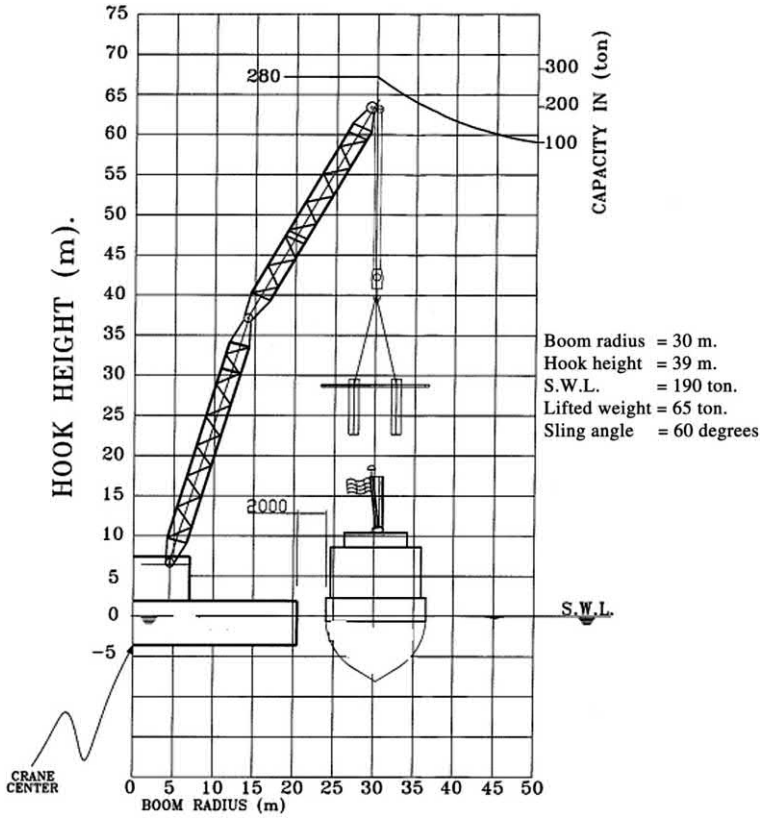

Figure 5.36 Lifting capacity of the crane.

A similar analysis shall be presented for spreader bars, beams, and frames. An analysis or equivalent justification shall be presented for all lift points, including padeyes, padears, and trunnions, to demonstrate that each lift point, and its attachment into the structure, is adequate for the loads and factors set out.

A lifting proposal shall present the following as a minimum:

1. The proposed rigging geometry showing dimensions of the structure, center of gravity position, lift points, crane hook, sling lengths and angles, including shackle dimensions and "lost" length around the hook and trunnions.
2. A computation of the sling and shackle loads and required breaking loads, taking into account the safety factors.
3. A list of actual slings and shackles proposed such as:
   - **a.** position on structure;
   - **b.** sling and shackle identification number;
   - **c.** sling length and diameter with the minimum breaking load (MBL) for slings, SWL and MBL for shackles; and
   - **d.** direction of lay.

4. Copies of inspection and test certificates for all rigging components.

Shackles manufactured should deliver a test certificate which should not be over 5 years old, and if not new, a report of an inspection by a competent person since the last lift.

For each sling and shackle a detailed record of all previous lifts shall be presented including the date and calculated load for each lift.

The crane vessel

The main requested information about the crane vessel and the crane shall be as follows as a minimum:

- general arrangement drawings and specification for the vessel;
- the vessel registration and its class;
- the vessel mooring system and its anchors;
- operating and survival drafts;
- the detailed crane specification and operating charts; and
- details of any ballasting operations procedure during the lift.

A document containing the mooring arrangement for the operation and stand-off position should be submitted. This contains all mooring wires, anchors, lengths, and specifications, and also a mooring plan presenting adequate horizontal clearances from all platforms, pipelines, and any other seabed obstructions. In addition, the elevation of the catenary for each mooring line, with upper and lower tension limits, shall demonstrate adequate vertical clearance over pipelines.

Table 5.9 presents a checklist to verify the topside lifting analysis as the quality assurance to the engineering process in this phase.

5.8.6 Bumpers and guides

The following guidelines based on DnV are to be considered in the design philosophy and installation of bumpers. The following sections present the main parameters that affect the bumpers and guides design and installation.

Module movement

The maximum module movement during installation should be defined. In general the module motions should be limited to:

- movement in a vertical direction: ± 0.75 m;
- movement in a horizontal direction: ± 1.50 m;
- longitudinal tilt: 2 degrees; and
- transverse tilt: 2 degrees.

The plan rotation limit is only applicable in the case that the module is close to its final position.

The position of bumpers and guides shall be determined taking into account acceptable support points on the module.

Table 5.9 Checklist for topsides lift analysis.

Items	Check point	Check (yes/no)
Computer model		
1	It is assumed that the model is checked for dimensions, elevations, member group and section properties in the in-service analysis and is upgraded to suit the current analysis	
1	Check the input file and focus on the member group properties for slings as E, G, and density	
2	Member end releases for slings	
3	Member end offsets for slings at padeye locations	
4	Member properties: K_x, K_y, L_x, L_y for changed support conditions	
5	Support conditions for hook point(s)	
6	Adequate analytical springs are provided	
7	Modeling of sling and hook for 75%:25% sling load distribution (sling mismatch)	
Loads		
1	It is assumed that the load calculations are verified in the in-service analysis and relevant load cases only are picked for the current analysis	
	Remove future loads, post installed items, operating weights, and live loads	
2	Load contingencies	
3	Dynamic amplification factor (DAF), skew load factors, and consequence factors	
4	Proportionate distribution of sling loads (75%:25%)	
5	Calculations for COG shift	
6	Check load combinations, include rigging loads	
Analysis of results		
1	Enclose sea state summary	
2	Enclose member check report: review overstressed members	
3	Enclose joint check summary: review overstressed joints (check $F_y = 2/3F_u$ for chords of high-strength members)	

(*Continued*)

Table 5.9 (Continued)

Items	Check point	Check (yes/no)
4	Enclose spring reactions equal to zero for correct hook location in the model	
5	Enclose sling forces to be zero moment and shear and only axial forces	
6	Enclose deflection plots, member unity check ratio plots	
7	Weight control report extract enclosed and the weight comparison carried out	
Padeye design		
1	Appropriate selection of padeye plates, sling, and shackle size	
2	Padeye design force as per the latest lift analysis	
3	Padeye stresses checked at the attachment to the main structure	
4	Stresses in the member supporting padeye	
Miscellaneous		
1	Design of spreader beam or frame	
2	Design of padeyes on the spreader beam or frame if it exists	
3	Lift drawing enclosed and reviewed, and the derrick barge main block and auxiliary block load-carrying capacity checked	
	Check the requirement for load shedding if the hook load is greater than the load-carrying capacity of the derrick barge	

Bumpers and guides should be designed to the following forces (where W = bumper lift weight).

- *Vertical sliding bumpers*
  - In-plane horizontal force = 0.10 W.
  - Out-of-plane horizontal friction force = 0.05 W.
  - Vertical friction force = 0.01 W.
  - The forces in all three directions will be combined in calculations to provide the worst design case.
- *For pin and bucket guides*
  - On cone or end of pin horizontal force = 0.05 (W).
  - On cone or end of pin vertical force = 0.1 (W).
  - To design for the worst case, the horizontal force in any direction will be added to the vertical force.

- *Horizontal bumpers with a vertical guide are called "cow-horn" type*
  - In any direction horizontal force = 0.1 (W).
  - Friction force in vertical direction = 0.01 (W).
  - Horizontal force in any direction will be combined with vertical force to establish the worst design case.
- *Vertical "cow-horn" type bumper with horizontal guide*
  - Horizontal force in any direction = 0.05 (W).
  - Vertical force on inclined guide face = 0.10 (W).
  - Horizontal force in any direction will be combined with vertical force to establish the worst design case.
  - The main precaution is that there will be an acute angle between the sloping and vertical members; the ledges and sharp corners should be avoided in case of possible contact, in addition the weld beads shall be ground flush. In design it is allowed for the guides and bumpers to be deflected without the member yielding, so the stiffness will be as low as possible for the bumpers and guide members.

5.9 Loadout process

After finishing the erection of the jacket and the topside, the process of the loadout is started, which applies loadout forces to the structure to move from the fabrication yard to the barge.

The loadout forces are generated when the jacket is skidded from the fabrication yard onto the barge. If the loadout is carried out by lifting the structure, and if the lifting arrangement is different from that to be used during installation, the lifting analysis should be done to calculate the forces, because lifting in the open sea has higher dynamic load factors, as described earlier.

If loadout is done by structure skidding onto the barge as shown in Figs. 5.30 and 5.37, a number of static loading conditions must be considered, with the jacket structure supported on its side. In the case of a loadout jacket, the loading conditions affect the structure from a different location in the jacket during the loadout movement, as shown in Fig. 5.37, so the structure analysis for the jacket during loadout should be done considering the barge movement due to tidal fluctuations, or change of draft, and also the possibility of support settlements.

The loading conditions shall be considered static during loadout structure analysis. The friction coefficients that should be considered in the calculation of the skidding forces are the following:

- steel on steel without lubrication 0.25;
- steel on steel with lubrication 0.15;
- steel on teflon 0.10; and
- teflon on teflon 0.08.

All structures shall be checked for the loads applied during loadout. The proposed method of loadout shall be defined explicitly by the contractor and could be skidded, trolleyed, or lifted. The following should be considered:

1. Dry loads only should be used, together with weights for lifting gear, sea fastenings, and others. The loads should be based on the weight control report.

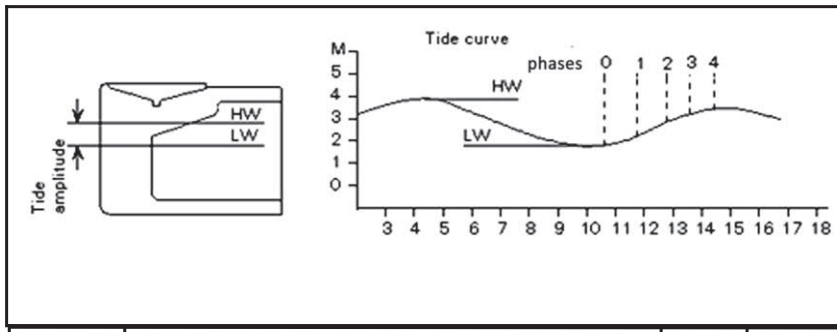

Draft		Progress of jacket	Weight transfered on the barge
5.54 m	Stage (0)	0	0
6.14 m	Stage (1)	65 m	8.5 t
6.59 m	Stage (2)	95 m	12.8 t
7.20 m	Stage (3)	125 m	17.0 t
7.54 m	Stage (4)	142 m	17.0 t

Figure 5.37 Jacket loadout stages.

2. For skidded or trolleyed loadout:
   a. A horizontal load of 15% of the vertical reaction on one skid rail shall be applied.
   b. Total loss of vertical support at one gridline with the structure being supported by the remaining gridlines only.
   c. Supports shall be assumed to be hinged supports.

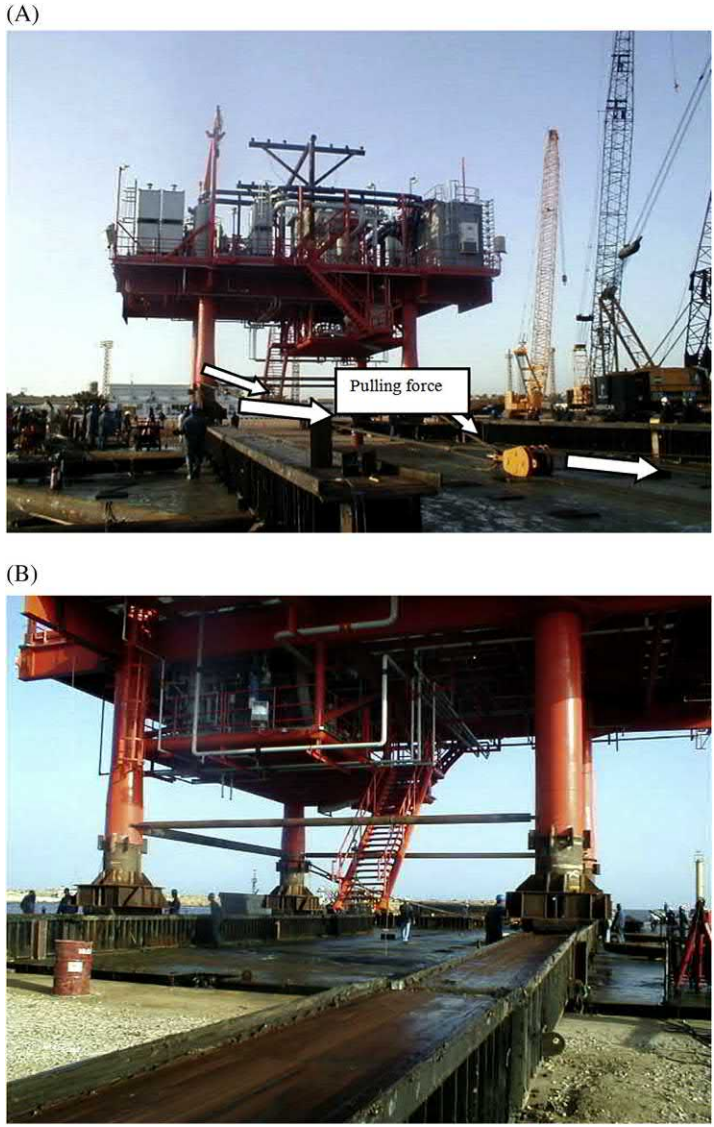

Figure 5.38 (A) Loadout to the topside on another view and (B) moving the topside on the barge.

d. Wind loads for a return period of 1 year shall be included with this load condition in the structure analysis check.
e. A total of 15 support points for the loadout shall be adopted.
f. A total of six support points for the loadout shall be adopted.

The direction of the pullout force is shown in Fig. 5.38A and B.

5.10 Transportation process

During transportation of the deck or jacket structure from the fabrication yard to its location there are forces that will affect the structure during this process. These forces depend upon the weight, geometry, and support conditions of the structure (by barge or buoyancy) and also on the environmental conditions that are predicted during the transportation period.

The main part in the offshore structure project during construction and operation is the vessel that transfers people and equipment from onshore to the platform, and that performs construction. There are different types of vessels which are described next.

5.10.1 Supply boats

A supply boat is a vessel that has a large open bay, to enable the boat to transport cargo, persons, equipment, and other supplies. The open bay is preferred to have sufficient length to transport the pipes, as the pipe length is about 12 m and so the required length of 15−20 m of the bay is traditionally used. Supply boats have a displacement weight of more than 1000 tons and can reach 3500 tons in North Sea activities.

While this boat is designed primarily to transport cargo, it must have maneuvering ability for close-in work alongside other vessels. Therefore it is equipped with reinforced gunwales and heavy fenders to absorb the impact of contact with other vessels.

5.10.2 Anchor-handling boats

This boat is specifically designed to pick up and move anchors, even in a harsh sea environment. Therefore it is a short, highly maneuverable vessel.

The stern of this boat is open and armored, to enable the wires or buoys to be dragged in over the stern if required. It is equipped with a crane at the forward end of the well, as the wire line pendant or buoy will be rapidly dragged on board. In addition, this boat has readily available hydraulic-assistance equipment.

5.10.3 Towboats

The main function of the towboat is to push the barge. There are many types of towboats. The largest towboat is the long-distance towboat which can operate without refueling for 20−30 days. This towboat has a length of more than 80 m and can carry a crew of around 16−20 persons. They can run when light at speeds of up to 15 knots.

Towboats are often described in terms of horsepower, in most cases this is in range from 4000 to 22,000 HP, but this can be misleading. Indicated horsepower (IHP) measures the work done at the cylinders of the engine. Bollard pull, a much

more meaningful measure, is the force exerted by the boat running full ahead while secured by a long line to a stationary bollard; that is, the boat is making no headway through the water.

As a guideline, for example, a 10,000 IHP boat can provide around 100−140 tons of static bollard pull. In reality there are other factors at play, such as the propeller(s) type, whether it is single or double screw, and the towboat draft.

As a rule of thumb, for safe and efficient operations the boat length should be not less than 11 times the expected maximum significant wave height.

Up to eight large boats have been used in tandem to tow a platform displacing 600,000 tons.

5.10.4 Towing

The first main principle in towing is that the attachments to the structure or barge must always be sufficiently strong that they do not fail or damage the structure under a force that breaks the towline.

In selecting the wire, the actual wire rope-breaking strength is more than the guaranteed minimum breaking strength typically by about 10%−15%. In most cases the rope breaks under a dynamic load. It should be ensured that during overload there is no damage to the structure or vessel which is being towed.

For design check the towline attachment can withstand equal to or greater than four times the static bollard pull and 1.25 times the breaking strength. In the case of an emergency for towing ahead, one spare attachment point should be available, with a pennant.

A second principle is that the towing force must be able to be resisted through a significant range of horizontal and vertical angles, thus imparting shear and bending, as well as tension, on the towing attachment(Fig. 5.39).

Fig. 5.40 presents a typical arrangement when a single boat is towing a barge. During passage through restricted waters and during final positioning, the towline

Figure 5.39 Towing boat.

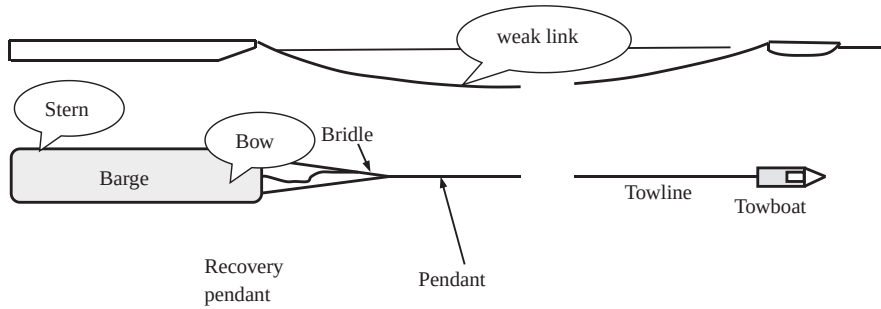

Figure 5.40 Typical towing arrangement for a barge.

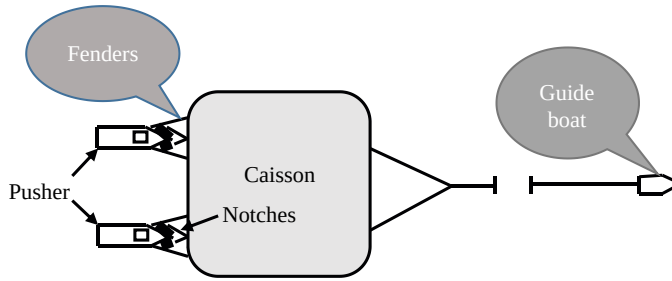

Figure 5.41 Moving massive caisson by pusher tugs.

may be shortened in scope to permit better control. In some cases, due to the structure configuration such as the structure shown in Fig. 5.41, the movement of the structure will be by using a push tug boat that pushes the structure through a fender in the boat and attaches to the structure.

Further, due to the inertia of the towed structure, it is difficult to slow it or change direction. In a narrow channel therefore additional boats may be used alongside and also astern.

Fig. 5.42 presents the types of motion that affect the floating structure.

One of the high risk operations during construction is moving the jacket or topside from the fabrication yard to the installation location, and so it needs to be managed very precisely. There are some precautions that should be considered during this phase as per API-RP2A (2007):

- The tow route shall be defined later.
- Reliability on the data of predicted "weather windows" during transportation.
- The easy route to the platform location.
- Seasonal weather system.
- During the design phase the characteristics of the tow such as size, structure, sensitivity, and cost are very important to define and select the most appropriate return period for design wind, wave, and current conditions.

Transportation forces are generated by the motion of the tow, and the structure and supporting barge. These loads are generated due to the effect of winds, waves,

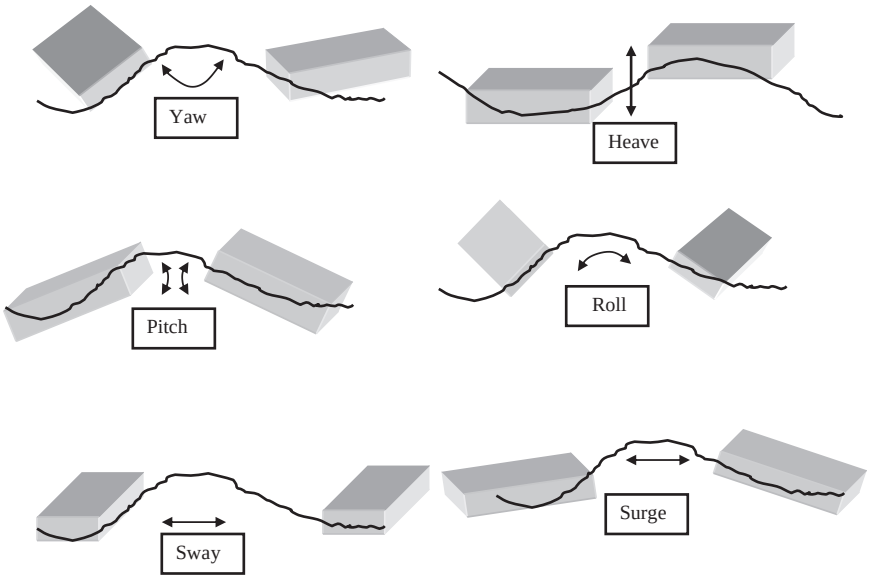

Figure 5.42 Types of motion of any boat.

and currents. As per API-RP2A, the towing analyses must be done from appropriate model tests by performing an accurate analysis of up-to-date software and considering the wind and waves in three directions: parallel, perpendicular, and at 45 degrees to the tow axis. The inertial loads are calculated by carrying out a rigid body analysis of the tow adding roll and pitch with heave motions. The assumptions on the design should match with the size of the tow, magnitude of the sea state, and experience. The following may be considered as typical design values for open sea conditions:

single-amplitude roll: 20 degrees;
single-amplitude pitch: 10 degrees;
period of roll or pitch: 10 second; and
heave acceleration: 0.2 g.

When using a barge to transport a large jacket, the main challenge in design is to maintain stability against the high CoG value of the jacket. In addition, the relative stiffness of the jacket and barge may need to be taken into account together with the wave forces that could result during a heavy roll motion of the tow, as in Fig. 5.43 when structural analyses are carried out for designing the tie-down braces and the jacket members affected by the induced loads. There are a special computer programs or modules in software for structure analysis that are available to compute the transportation loads in the structure−barge system and the resulting stresses for any specified environmental condition.

Based on Gerwick (2007), when towing a very large structure a single lead boat may run ahead to verify the route, confirm depths by forward-looking sonar, and

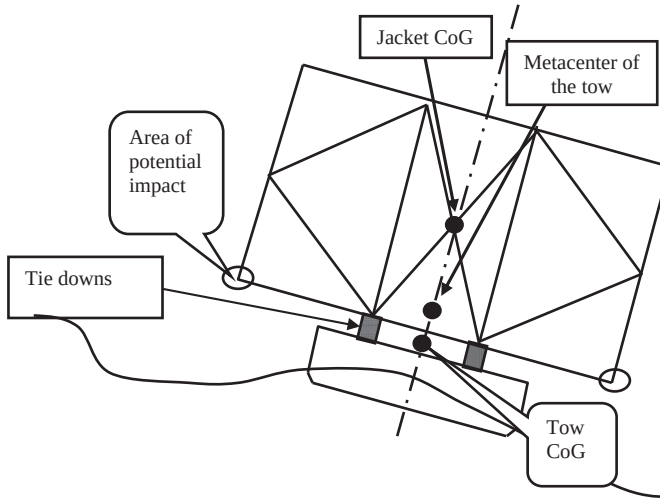

Figure 5.43 Center of gravity for the barge launching a jacket.

pick its way through underwater obstructions or ice. In addition, another function of this boat is to warn other shipping.

To towed structure considering that in some cases of offshore platforms, as for example in the North Sea have drawn around 120 m, therefore it will be towed by a deep-draft vessel.

In an area, that is, not normally used by shipping and it is required to tow structure, a precise and careful survey should be performed using sonar, side-scan, and profiler acoustic equipment, so that both the route and its full swath, including sway excursions, are thoroughly scanned.

Required channel widths in sheltered areas are usually twice the beam, but this must be considered in relation to the environmental conditions and navigational accuracy.

Based on Gerwick (2007) for exposed areas, the required width will depend on the currents and navigational accuracy and thus may vary from about from 600 to 1500 m for relatively short distances of 12 km, unlike the case of a towed ship or barge with a draft of around 8−10 m and width in the range from 30 to 40 m. An offshore structure, such as a deep-water caisson, may have a draft of over 100 m and a width of 100−150 m. Therefore it is not enough to plot only the position of the area of crossing but the extremities must also be considered. For the restricted area, the current speed and direction should be surveyed on the surface and at a reasonable depth.

A structure under tow will experience sway and wander somewhat along its course. In confined waters, a band may be plotted, shaded in color, within which the structure is safe.

The usual requirement for the distance clearance between maximum static draft and minimum water depth should not be less than 2 m or 10% of the maximum

static draft, whichever is lower, plus an allowance for motion. These values can best be determined by model tests. In practice, most of the structures under consideration, which are the fixed offshore platform structures, will be governed by the 2 m minimum clearance.

To obviate these, a carefully agreed set of common procedures should be reviewed and applied so that there will be a clear understanding of all commands between all the crew and care taken as some captains may not speak English fluently. If there are one or more captains who are not fluent in English, it may be desirable to have an interpreter available.

There should be a procedure to handle any instance of a broken towline. The dynamic accelerations of the towed structure should generally be limited to 0.2 g, to minimize forces acting on the tie-downs and to minimize adverse effects on personnel.

When large and valuable structures are towed, the insurance surveyors require full manning, with adequate pumping capacity, power generation, and firefighting capabilities. Manning of large and important structures under tow may require a crew of 10 or more. The crew should have different skills, such as meteorologists, sonar specialists, and navigators, in addition to marine and ballasting skills.

When towing in thin or broken ice, an icebreaking vessel will usually open a clear channel. An offshore platform for the Arctic may have a beam width of 100 m. Somehow the broken ice must be forced to clear from around the sides so as not to jam the tow. Boats at the sides, can clear ice. The vessels shall be equipped with radar to overcome any visibility problems due to fog. In the case of ice its masses on the sides may ride up, and so its effect needs special model test studies.

When locating the structure at an offshore site, the tugs shall fan out in a star shape.

The towing horsepower selected should be sufficient to hold the towed structure against a significant wave height, 40-knot sustained wind speed, and the current speed for the region of work. Obviously, these arbitrary parameters have to be adjusted to the region involved.

Limitations and requirements are placed on stability under tow by the marine surveyor and the typical requirements are as follows:

1. For large offshore structures, the metacentric height must have a positive value about 1−2 m.
2. The maximum inclination of the towed structure under conditions of wind 16 m/s, and full towline pull should not exceed 5 degrees.
3. In the case of a 10-year storm, the maximum inclination of the towed structure should be less than 5 degrees without towline pull.
4. For 50% of towline pull, the static inclination in still water should be less than 2 degrees.
5. Wind speed for a 10-year operation sustained for 60 seconds should be planned for to insure dynamic stability.
6. In some cases with regular or irregular seas, model tests shall be done to define the motion of the towed structure. This test model will determine the directional stability and

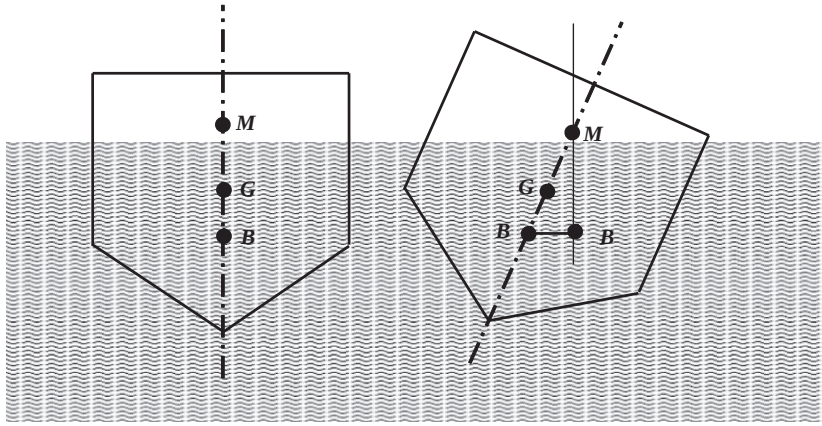

Figure 5.44 Presentation of the metacentric height.

any tendency for excessive yaw. It can predict the effect of motion on the towed structure under damaged (flooded) conditions, and calculate the towing resistance.

7. The metacentric height must be calculated before the tow, after loading all the structures that are required to be transported.

In September 1975, two tugs with a combined horsepower of 15,200 IHP were used to tow a slightly smaller self-floating tower from Tsu, near Nagoya, Japan, to the Maui field off New Zealand. This is a positive case study in which the structure survived a typhoon in the Pacific with only minor damage.

As a case study, there were four platforms with weights between 7000 and 8000 tons which were towed 4250 nautical miles from Cherbourg, France, to a field offshore from the Congo. The draft of each was 16−19 m; towing speed averaged 3.2 knots, using two boats for each platform, developing 30,000 IHP. There were several 5-ton polyurethane foam-filled "floaters" inserted in each towline.

The metacentric height from point G to point M (GM) as presented in Fig. 5.44 is the distance between the vessel center of gravity (G) and its metacenter (M). Before sailing the vessel its metacentric height is calculated as the vessel stability depends on this value. The GM distance must equal or exceed the minimum required GM for that vessel during its complete trip.

As per Fig. 5.45, in the case that the vessel is heeled, the center of buoyancy (B) of the vessel shall move laterally. Therefore the vertical line from the buoyancy point (B) shall intersect with the vessel axis of symmetry at the metacentric point.

5.10.5 Drilling vessels

The drilling vessel is usually available during drilling activity in the case of exploration or normal drilling activity during operations, and in some cases the same rig can be used in installing the platform, especially if it is a smaller size. These are large offshore vessels, fully equipped, including appropriate mooring gear and

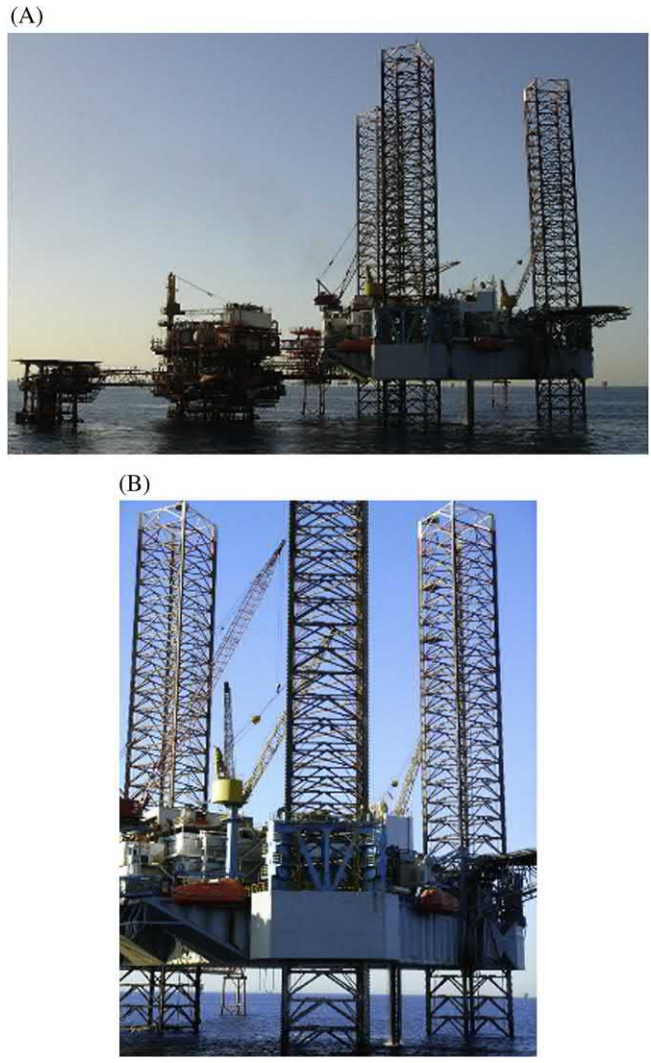

Figure 5.45 (A) Jack-up barge near platform and (B) jack-up barge configuration.

heavy-lift equipment for direct vertical pulls on the drill string, and they have a central moon pool (open well) which provides direct and partially protected access to the sea below with minimal wave action at the interface.

This vessel can work at greater depths, so they have been used for many offshore construction tasks, from setting subsea templates to pipeline repairs and seafloor modifications.

In some cases, the offshore drilling vessel may be a semisubmersible, or a large ship hull especially configured to minimize roll. Nevertheless, such a ship-shaped

vessel does have an inherently greater roll response than a semisubmersible. The drilling derrick is equipped with a large hoist that can reach 500 tons or greater direct lift.

5.10.6 Crew boats

Any company with a fleet of offshore structure platforms needs boats to transfer staff and operators to the platforms from onshore on a daily basis. These crew boats are used also for small constructions or minor modifications on the platform, and so they are used to transfer teams of workers with their tools. Therefore this crew boat must be able to work during any sea conditions, so long as this is carried out in a reasonable and practical manner. Special crew boats are used in the North Sea, as this sea has unpredictable weather conditions and there is a great distance between land and the platforms. Crew boats are used in the GoM and offshore southern California, and also in the Gulf of Suez. Economics dictate that the boat should have as high a speed as practicable. The rule of thumb for selecting a boat is that the required horsepower be proportional to the square of the velocity.

In general, the governing factor in boat safety is the metacentric height (GM) as discussed later. In the case of high metacentric (GM), the roll response shall be quick and this will be reflected in discomfort to passengers, and so the boat acceleration should be minimized for boats with low metacentric height for safety.

In the GoM and Gulf of Suez or similar conditions, in the case that the boat's length exceeds the wavelength, the pitch response is reduced; however, this is not practical in the Pacific or North Atlantic, due to their larger waves.

In relatively low sea states, direct transfer can be made to a large derrick barge or pipe-laying barge by coming alongside the leeside or stern while heading into the sea, thus using the derrick barge as a floating breakwater.

5.10.7 Barges

The barge is considered a floating workshop. As per its function, there are workshop activity will be done on it, so it should have a special characteristics, as to be long enough to minimize the wave effect in pitch and surge response, to have a wide beam to minimize the rolling response due to wave, and deep enough to have adequate bending strength against hog, sag, and torsion, and in general to have an adequate freeboard for work shop activities.

Due to the wave load, the deck plate should be sufficiently continuous to resist membrane compression, tension, and torsion stresses. Side plates are usually under high shear, therefore, the sides have stiffeners to reduce the buckling effect.

If other barges hit its side, an ice effect or wave slam on the bow can generate an impact load.

Unequal load distribution of the deck due to cargo loading will generate bending stress on the hull bottom plates, and should be considered in barge design, also corrosion will reduce the hull thickness plates which is the main factor in evaluating existing barges and during vessel class renewal.

Typical offshore barges run from 80 to 160 m in length and the barge width should be one-third to one-half of the barge length and the depth will typically run from one-fifteenth of the length.

Offshore barges typically have natural periods in roll of 5−7 seconds, which matches the wave period and so resonance is expected to occur, but due to very high damping this dynamic effect is reduced.

Barge corners are usually having a higher rigidity as they are usually subjected to heavy impacts during operations. In addition, there is a fender on each corner and distributed along both sides of the barge to protect it from collision with other vessels during operation.

Consideration should be given to temporarily welding padeyes to the deck in order to secure cargo for sea, these padeyes will distribute their load into the hull. They will be subjected to fatigue and impact loads in both tension and shear, therefore a better design should have special double plates fixed over the internal bulkheads so that padeyes may be attached along them. For welding, low hydrogen electrodes should be used. Alternatively, posts may be installed, running through the deck to be welded in shear to the internal bulkheads to absorb the local impact and abrasion from the load. This is especially needed for barges that carry rock, that is, removed by clamshell or dragline bucket, or upon which a tracked crane or loader will operate.

When heavy loads are skidded to or from the barge, a soft material like a timber is temporarily bolted to the deck edge to skid the load along. The barge will be structurally evaluated considering each stage of loading to ensure that a side or bulkhead will not buckle or fail under the temporary overload.

During transportation there is a combined force between static and dynamic loading. The dynamic forces generated from the acceleration in six degrees of fundamental of barge motions include rolling, pitching, heave, yawing, sway, and surge, so the design of the sea fastening shall include this combination of forces.

The rolling accelerations are therefore directly proportional to the barge stiffness in the transverse direction, which is measured by its metacentric height. The metacentric height is the distance between the CoG of the ship and its metacenter. In the case of a barge, the center of buoyancy of the barge moves laterally, as shown in Figs. 5.46 and 5.47. The metacenter is defined as the point at which a vertical line through the heeled center of buoyancy crosses the line through the original center of buoyancy.

In general, barges have large metacentric heights, so the accelerations are severe. Conversely, if due to high cargo, the metacentric height is low, the period and amplitude of roll and the static force as a result from the load are greater, but the dynamic stress is less.

During transportation, the applied loads are cyclic, therefore, based on the sea fastenings trying to work loose as the wire rope stretches, wedges and blocking may fall out. Care should be taken as the repeated loads generate fatigue stresses, specifically at the welds. Weld quality needs specific attention as the surfaces may be wet or cold, therefore using low hydrogen electrodes is important in this case. Chains are the most preferred method for securing cargo for sea, as they cannot be stretched.

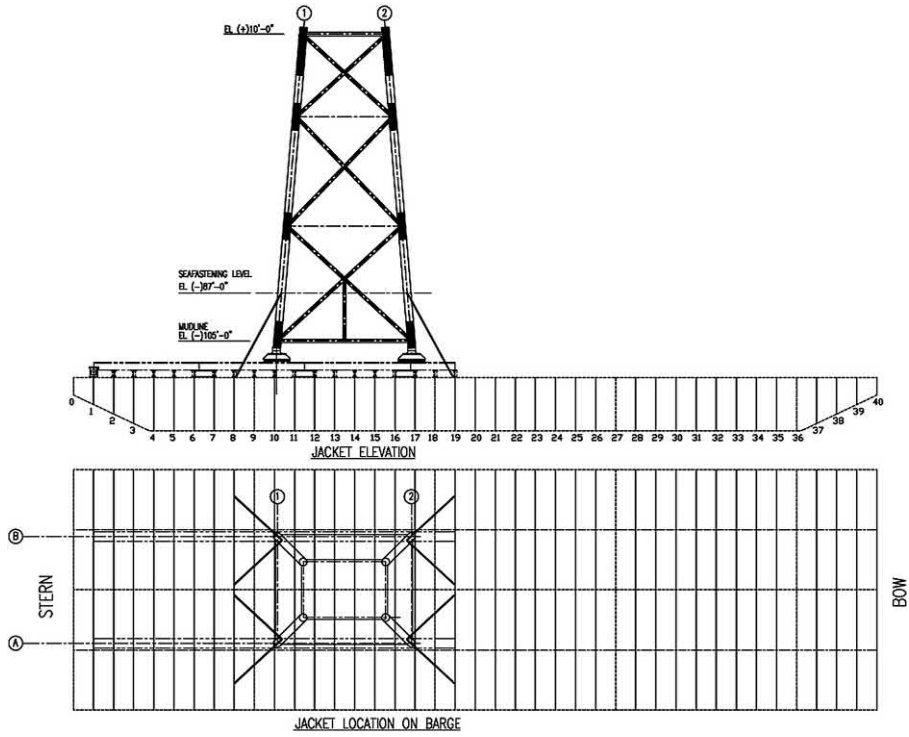

Figure 5.46 Jacket sea fastening during transportation.

Figure 5.47 Material barge.

In the case of deck or jackets which are valuable a sufficient freeboard should be provided to ensure stability, even if one side compartment or end compartment of the barge has been flooded.

These criteria are usually based on submergence of the hull to the deck line, plus an arbitrary load of 3 m of water on deck.

Proposals are often made to build a structure on a barge and then submerge the barge by ballasting and float the new structure off.

However, the following key items should be taken into consideration in the case of submerging a barge by partially filling compartments with ballast, as the external pressures are the same as if the barge were empty and submerged to that depth. Therefore it is important to consider that the hull must be designed for the deepest submergence condition. In order to launch the structure the support barge will be neutrally or negatively buoyant, so the depth control is the main challenge in this case. The marine operating staff tools shall be used to control the depth (Fig. 5.47).

5.10.8 Crane barges

The crane barge is an offshore barge that has a sheer-legs crane or fully rotating crane. A sheer-legs crane can pick loads and luff but cannot swing, as shown in Fig. 5.48. The sheer legs consist of an A-frame made up of two heavy tubulars or trussed columns held back by heavy stays to the bow.

The sheer-legs barge is maneuvered by deck engines, tugs, or mounted outboard engine propellers. The crane barge positions its stern at the side of the cargo barge, picks the load, and then moves as necessary to set the load in the exact position.

The sheer-leg crane has a lower capital cost and maintenance cost than a fully revolving crane. Because of the need to move the entire barge to the proper position to set the load, its operations are slower than those of a fully revolving derrick barge.

Figure 5.48 Crane barge near the platform.

The sheer legs are usually fixed at the appropriate orientation to pick loads from a barge at sea and then set them on a platform.

Any crane or sheer-leg crane on the barge has a chart as shown in Fig. 5.35. Based on this chart the object weight that will be lifted, it can be decided whether the barge is capable or not of doing the job or if another larger crane barge is needed.

The deck engines of a sheer-legs crane barge must be adequate to control the barge's motion in yaw, sway, and surge to a very close tolerance whatever the sea conditions. Sheer-leg crane barges can be utilized for up to 3000-ton crane capacity.

A crane barge has been successfully used in many cases to put jackets into preinstalled frames with a tolerance of only 50 mm. Sheer-leg crane barge have been used in many cases, as shown in Fig. 5.48.

5.10.9 Offshore derrick barges (fully revolving)

Fully revolving derrick barges are the traditional barge used in constructing a new platform or to perform a major modification to a platform. It is very costly, but is capable of carrying out a huge amount of work. As with the sheer-legs crane barges, they are fitted with deck engines and full mooring capability. Fig. 5.49 presents a derrick barge with its sheer-leg cranes.

The marine derrick barge in general has a capacity in the range of 50−400 tons, but the offshore derrick barge has a higher crane capacity in the range of 500−1500 tons. Recently, there higher capacities have become available to accommodate the installation of larger decks and jackets. As a case study, an offshore derrick barge with two cranes, each rated at 6500 tons each, had a total capacity of 13,000 tons.

On the other hand, the effective crane reach and its load capacity are reduced due to the distance from the boom seat to the barge stern or side. The only way to achieve the ideal location is by using a large swing circle that moves the boom seat closer to the barge end while maintaining the center of rotation and support well back.

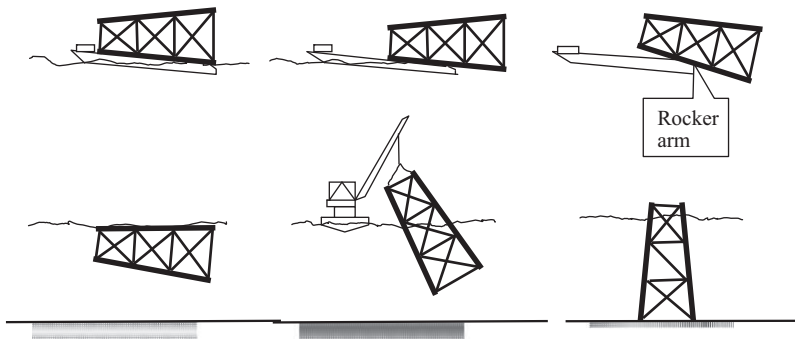

Figure 5.49 Launching and installing the jacket.

The counterweight is usually designed to limit the list under a half load, hence under no-load the barge may list opposite to the boom. This list can be reduced during operations by booming down while swinging under no-load. The swinging is carried out by swing engines. Offshore cranes are therefore provided with two and sometimes three swing engines. The list also places heavy structural loads on the crane tub, which forms the structural connection to the barge. Hence its design must provide proper structural reinforcement for bending and to prevent buckling under inclined compression loads.

The main advantages of the derrick barge are that it has good close control of positioning, so it can quickly reach any point in three-dimensional space, and in addition it has the capability to orient the derrick barge in the most favorable direction to minimize boom tip displacements and accelerations.

The crane load capacity ratings are based on 28 rolls at a period range 10−12 seconds, which is equivalent to an acceleration of 0.07 g. The load swinging generates lateral forces on the boom. Based on that, offshore crane booms are designed with a wide spread at the heel in most cases more than one-fifteenth of the boom length.

The boom lacing (bracing) members are subject to buckling, and must be properly designed to prevent this mode of failure. Booms today are made of high-strength steel, usually round or square tubular members. This makes them lighter and hence increases the effective load capacity of the crane and reduces the inertia in swing.

From a safety point of view, the potential hazard of an offshore derrick barge operation is that, although the lifts have been carefully engineered for load and reach, in a real situation, the derrick barge surges farther away from the platform and moves laterally. In addition, the derrick barge cranes are fitted with automatic warnings to alert the operator when allowable load−radii combinations are being exceeded, but swing control is normally a matter of judgment.

Raising a heavy load from a barge is more difficult since there may be 24 or more parts in the line and the barge will rise as the load is lifted, increasing the risk of impact of the load and boat deck.

Noting that, when setting on a platform, the deck will usually be above the sight lines of the crane operator, and so the operator is working blind, dependent on signals. Hence, one or more guiding devices are needed.

On the platform, the structural guides will be preinstalled, these function so that once the load is within 500 mm or so of the correct location, it will be automatically guided down to the correct location. Taut guidelines can be employed to help pull the load to the correct position.

Noting that the cost of the barge is a major cost in any project and that in many projects the costs will be over budget due to delays in the barge work, as in the case of changing weather conditions which require work to be stopped due to the limit of barge lifting equipment, the owner will pay a daily rate for the standby cost, so choosing the time for using the construction is very critical, depending on the region of the construction and on the weather forecast for the area.

In the barge, tag lines and cranes are installed on the platform to help in guiding the load into place, and another method is to set the load only in an approximate

location, laying it on softeners such as timber or rubber fender units. After it has been set in the approximate location, it can be skidded to the final exact location using hydraulic jacking equipment. This procedure is often used when setting trusses, for example.

5.10.10 Jack-up construction barges

When there is high wind speed and higher wave height or in turbulent sea areas, or breaking waves such as shoal or coastal water, the jack-up barge is a suitable vessel to use in construction.

It is more expensive than the other construction barges, but there will be no standby time as the crew can work all the time, which is one of the main advantages for this type of construction barge.

The barge moves to the site with its legs raised and then after arrival at the required location the legs are lowered to the seabed and allowed to penetrate under their own weight.

Construction jack-ups can operate only in relatively shallow water (30−60 m) and the maximum depth is, rarely, about 150 m.

Once the barge legs are well embedded, the barge is jacked up into clear space above the maximum wave height. If waves strike on the underside of the barge they will produce impact loads on the jacks and this load can deflect the barge laterally and bend the legs. To overcome this impact load, special hydraulic cushioning may be connected to nitrogen-filled cylinders, or neoprene cushioning as an option can be used. A barge jack-up is illustrated in Fig. 5.45A and B.

It is possible that uneven settlements take place due to time, operations, and wave energy input into the legs, and the jacks therefore have to be periodically reactivated to equalize the load.

This is very important during the first few days at a site. The mooring lines are reattached slack, and the barge is then jacked down until it is afloat.

Once again, the critical period is when the waves are hitting the underside. The mooring lines are tightened and then the legs are jacked free, one at a time.

The stability of the rig depends mainly on the soil, so at least one boring takes place on the rig location and the soil studied to define any precautions and the stability of the rig.

A general rule of thumb is to plot the previous leg positions and to space the new leg locations four to five diameters away.

In general, construction barge jack-up rigs are equipped with an even number of legs (six or eight).

The main advantage of the jack-ups is that they provide a fixed platform, and there is no motion response due to sea waves, as illustrated by the configuration in Fig. 5.45A and B.

Based on Gerwick (2007), the statistical studies covering jack-up drilling rigs and jack-up construction rigs show that they are six times more likely to suffer serious damage or loss during relocation and transit than they are when on location.

This is primarily due to the barge having its legs fully raised, thus creating a very high CoG.

5.11 Transportation loads

All structures shall be checked for the inertia loads applied during sea transportation. Consideration shall be given to the support points used for sea fastening. The following should be considered:

- Structure self-weight.
- Equipment and bulk self-weight.
- Transportation inertia loads.
- Roll: 20 degrees; Period: 10 seconds.
- Pitch: 10 degrees; Period: 10 seconds.
- Heave: ± 0.2 g.
- The center of rotation is 60% above the barge keel at longitudinal midship of the transport barge.
- The transportation inertia loads shall be combined as roll ± heave and pitch ± heave.
- Wind loads for a return period of 10 years (1 minute mean) shall be included with this load condition.
- The support points shall reflect the support points adopted during loadout.

Sea fastening is fixing the jacket or the topside to the cargo barge to transport it from the fabrication yard to its location. The module requires fixing to the barge to withstand barge motions in rough seas, so the jacket and the deck are structurally rechecked to see if they need some strengthening due to extra stresses during transportation.

As shown in Fig. 5.46, the jacket rests vertically on the barge as it has low height. Fig. 5.50A presents the transportation of the jacket lying horizontally on the barge. After finishing the structure analysis as discussed previously, the structure analysis will run again taking into consideration the new fixation point and the movement of the barge. This phase will require cooperation between the installation company and the engineering firm that performs the design. After the engineering firm receives the data from the installation contractor, they will run the structure analysis model again to check if some members have critical stresses or will be damage, so they will be resized in this stage to withstand the transportation load. Therefore the cooperation between the installation company and the engineering company should start early to avoid any change to the structure configuration, as discussed in Section 5.8.

The SKL accounts for the sling fabrication tolerance or any other inaccuracies in the sling length. The SKL is calculated based on the recommendations of the DNV rules. In the absence of exact information this factor is set to 1.25 for a typical indeterminate four-point single-hook lift.

As an alternative to the SKL, the lift weight (hook weight) may be distributed on a 75%:25% split between each pair of slings in turn. All structural members, padeyes, shackles, and rigging components are designed or checked for both load distributions.

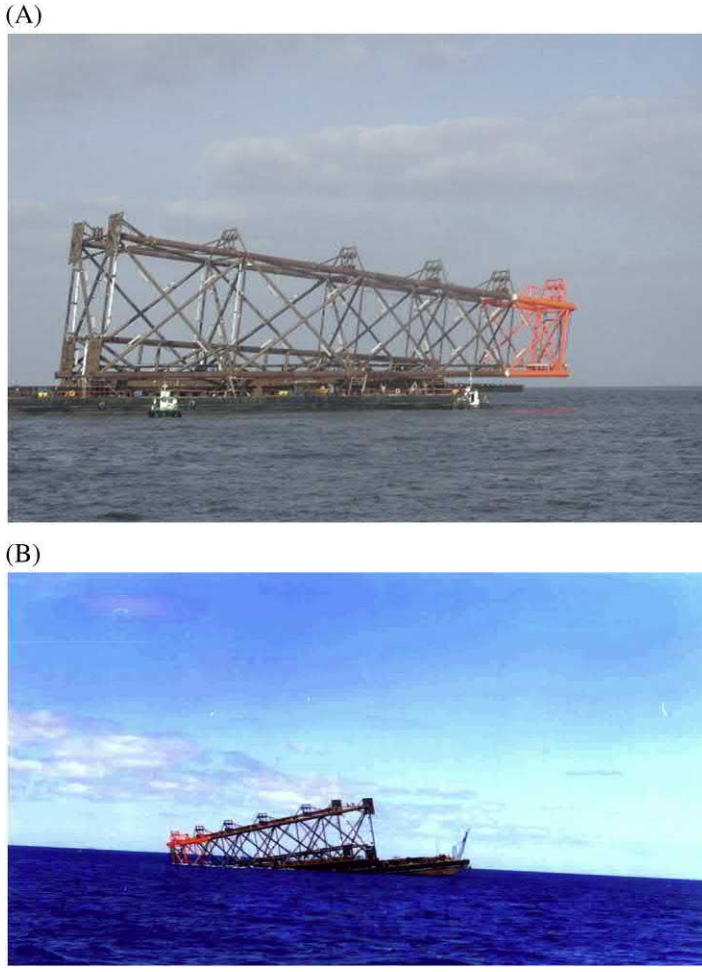

Figure 5.50 (A) Start of launching the jacket; (B) launching the jacket.

For the padeye design, an additional lateral force equivalent to 5% of the sling force is applied to the padeye. The force is applied at the eye of the padeye in conjunction with the design sling load.

The criteria of a 75%:25% split or SKL of 1.25 is based on the variation in fabrication tolerance ± 0.25%. If, for any reason, this cannot be achieved, then the SKL must be modified.

5.12 Launching and upending forces

The launching is a very critical process in constructing a platform as in this process the jacket is affected by different stresses due to transfer from the barge to the sea

and during the subsequent upending into its proper vertical position to rest on the seabed. A schematic view of these operations can be seen in Fig. 5.49.

There are six stages in a launch-upending operation:

- stability position on the barge;
- jacket slides along the skid beams;
- jacket rotates on the rocker arms;
- jacket rotates and slides simultaneously;
- jacket detaches completely and comes to its floating equilibrium position; and
- jacket is upended by a combination of controlled flooding and simultaneous lifting by a derrick barge.

These stages are presented step by step in Fig. 5.51.

The loads, static as well as dynamic, induced will be included in the structure analysis and consider the load of wind, waves, and currents expected during the installation.

The barge shall be ballasted before starting the launching process until it reaches the required draft and trim angle which was calculated previously, and then the crane will pull the jacket toward the barge stern. When the crane is pulling, at the same time the down force load increases due to gravity until its force exceeds the friction force and then the jacket will slide. At this moment, all the jacket load is carried by the launching trusses. The support length keeps decreasing, until it reaches a minimum distance, equal to the rocker beam length, and then rotation starts. At this moment, the jacket is under the maximum severe load due to launching force reactions.

After the jacket falls in the water, the buoyancy calculations are required for every stage of the operation to ensure fully controlled, stable motion and to ensure the jacket floats and does not sink. There are specific software programs to perform the

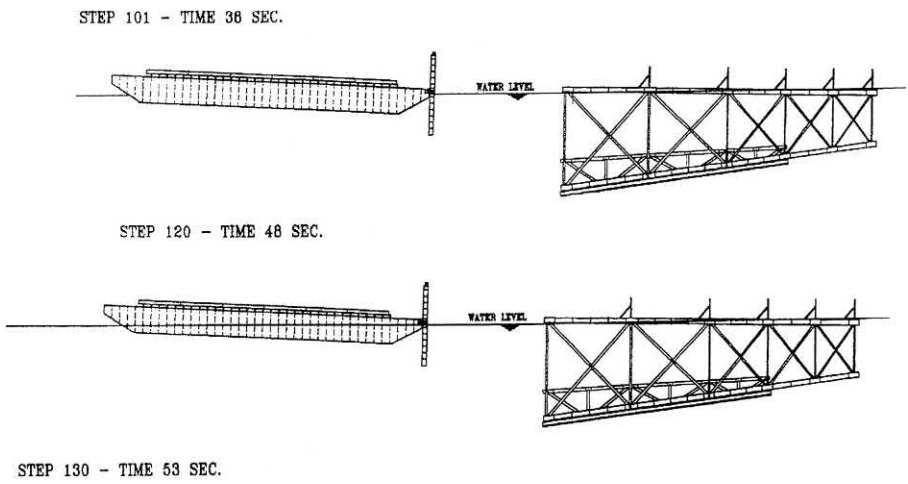

Figure 5.51 Steps of launching by time.

stress analyses required for launching and upending and these are presented graphically in Fig. 5.51. Fig. 5.50A and B illustrates the launching steps for a project.

The typical launch barge is very large and strongly built, long and wide, and subdivided internally into numerous ballast compartments. It must support a progressively moving jacket weighing thousands of tons. The launching barge must be equipped with heavy runner beams or skid beams that extend the length of the barge (Fig. 5.22). It should be borne in mind that the stern will have to support the full weight of the jacket for a short period of time.

The jacket will be sliding on its specially launching trusses as shown in Fig. 5.19; even so, they need a distributed rather than a point reaction. Hence, the stern of the barge is fitted with a rocker section that rotates with the jacket as it slides off.

For loading out the jacket at the fabrication yard, the usual method is to ground the launch barge by a sand pad at the appropriate depth, so that the barge deck matches the yard level.

Then the jacket can be moved by skidding into the deck of the barge with no differences in elevation between the barge deck and the ground. Based on this the transportation barge bottom hull shall be under high local stresses and the stiffeners should be design adequately to avoid any buckling when skidding the jacket into the barge.

While skidding the jacket into the barge, at the same time the barge crew adjusts the ballast quickly to maintain the relative elevation of the jacket during skidding. This adjustment of elevation should be done by an expert and nowadays is control by a computer. In the launch barge there are adequate cranes and jackets on the bow of the barge to assist in pulling the jacket during skidding and to pull off the jacket during launching.

There are available in the market launch barges that can be used for jacket weights of 40,000 tons. It is important to highlight that there should be enough space on the barge to avoid the external jacket leg being affected by waves during barge rolling. In general, the impact load shall be considered during transportation of the jacket and topside, and a sea fastening analysis should be done to check the structure during its movement on the sea (Fig. 5.52).

5.13 Installation and pile handling

After launching the jacket, the crane barge is used to uplift the jacket as shown in Fig.5.52 to its location, and after that it starts driving the piles into the legs. The deck installation is presented in Fig. 5.53.

Fig. 5.54A shows the different methods of providing lifting points for positioning pile sections. Padeyes are welded in the fabrication yard; their design should take into consideration the changes in load direction during lifting. Padeyes are then carefully cut before lowering the next pile section.

Fig. 5.54A and B presents the two different configurations for stabbing guide internal and external types, as shown in Fig. 5.55A an internal stabbing guide was used in this project.

Figure 5.52 Lifting the jacket for installing.

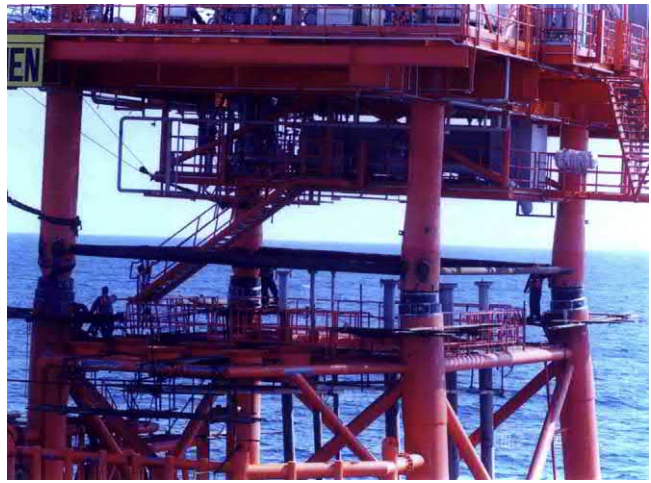

Figure 5.53 Presenting the installation of the deck on the pile.

Fig. 5.56 presents the steps of pile positioning and hammer positioning and actions. The sequence of the pile installation is as described next.

Different solutions for connecting pile segments back-to-back are used either by welding, SMAW, or flux-cored segments held temporarily in place by internal or external stabbing guides. Welding time depends upon the pile wall thickness as it takes 3 hours for 1″ thick (25.4 mm) and 16 hours for 3″ thick (76.2 mm) (typical), and also depends on the number and qualifications of the welders and the

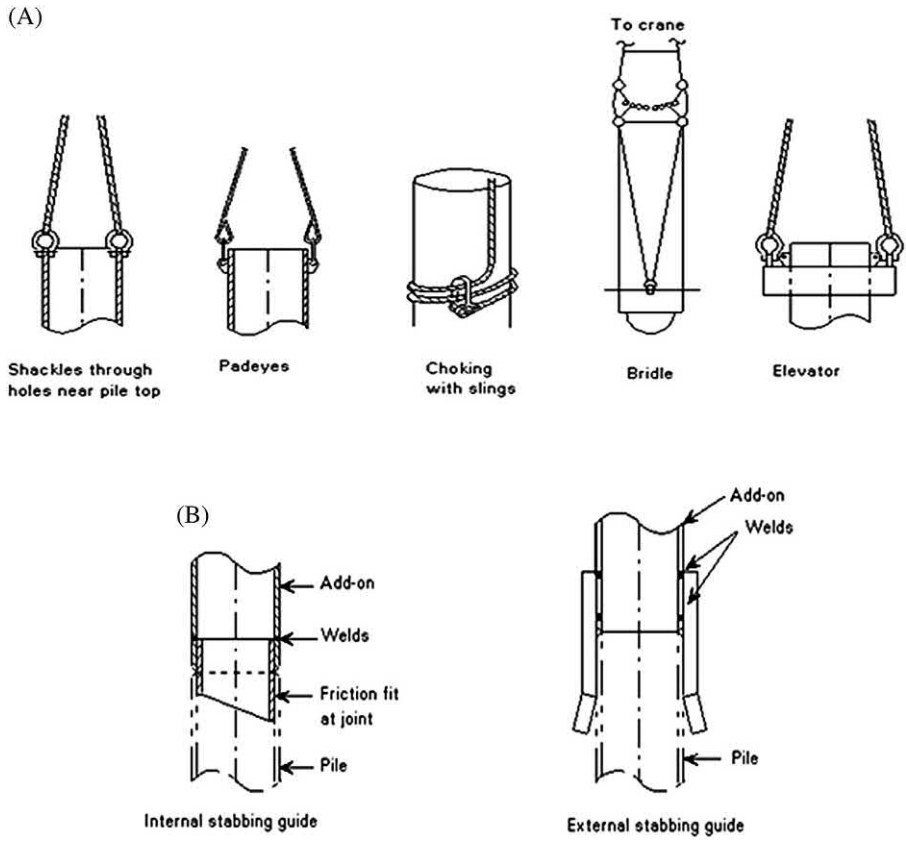

Figure 5.54 (A) Pile lifting method and (B) configuration for different stabbing guide.

environmental conditions, or by mechanical connectors, breech block (twisting method), and lug type (hydraulic method).

Fig. 5.56 shows the different steps of this usual operation in driving the pile:

- lifting from the barge deck;
- hammer to be positioned over the pile by booming out or in, noting that the hammer bell acts as a stabling guide;
- the pile cap alignment; and
- lowering leads after hammer positioning.

For piling activity, each step shall be designed carefully to avoid any bending or buckling failure during installation and in-place conditions.

The lifting pile is as shown in Fig. 5.55A–D, where one can see that there is a white marker along the pile length to define the distance of penetration of the pile exactly.

It is very important to take care with pile penetration under its own weight, and this case is traditional in soft soil so it is very important to avoid uncontrolled run of the pile inside the leg.

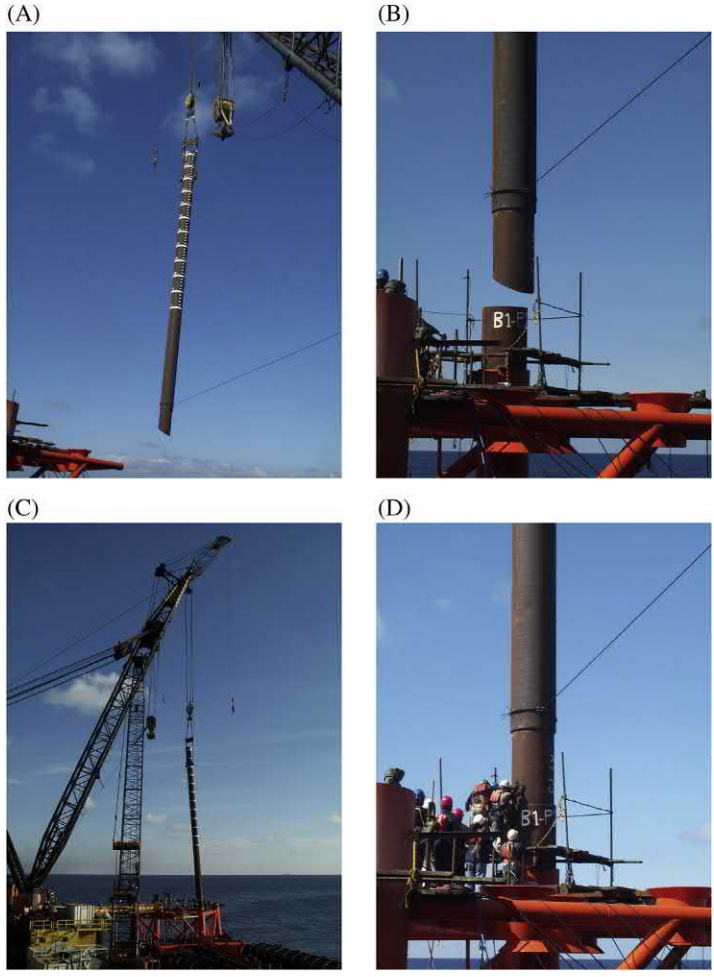

Figure 5.55 (A) Pile lifting; (B) inserting pile into previous one; (C) pile lifting to insert; and (D) connection between piles.

Piling is a continuous activity until the target depth is reached or pile refusal. The definition of pile refusal is the minimum rate of penetration beyond which further displacement of the pile is no longer achievable because of the time required and possible damage to the pile or the hammer. A widely accepted rate for defining refusal is 300 blows/ft. (980 blows/m).

Fig. 5.57A and B presents the erection of the pile to another one, by resting the pile on the jacket leg.

The shims are inserted at the top of the pile within the annulus between the pile and jacket leg and welded afterward.

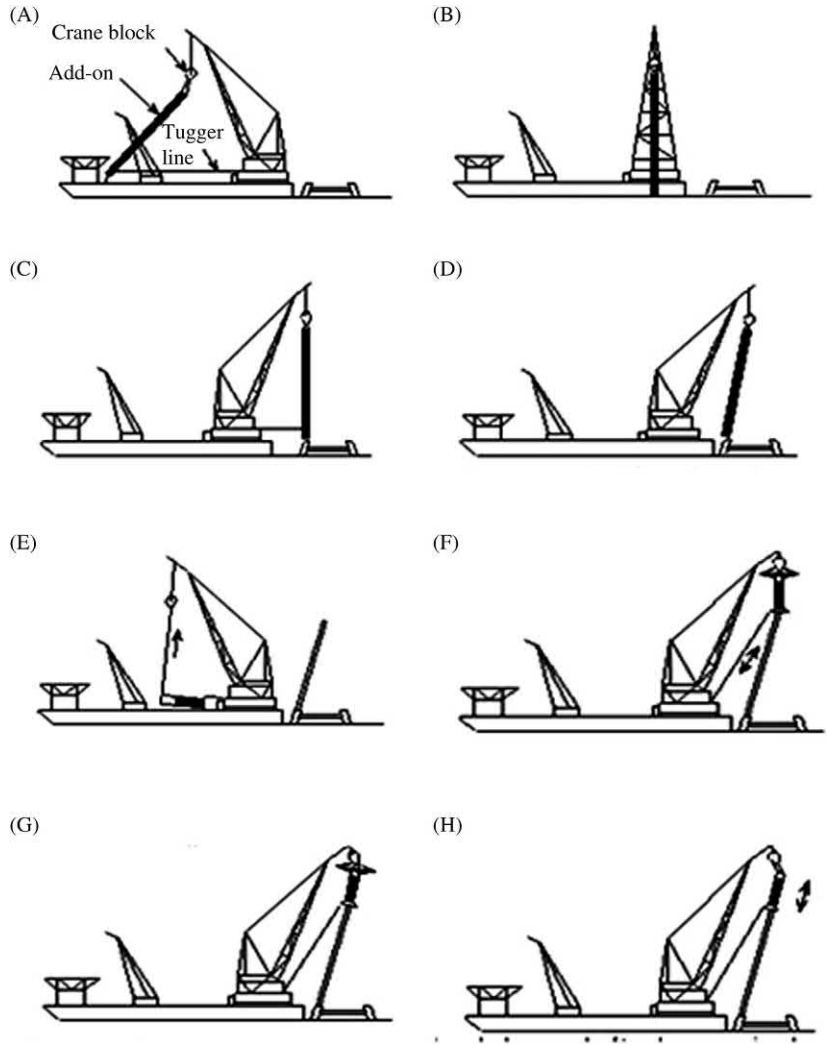

Figure 5.56 Pile installation process: (A) lift pile from barge deck; (B) rotate crane with the pile; (C) rotate pile to the jacket leg; (D) incline the pile to insert in the leg; (E) lift hammer from barge deck; (F) position the hammer over the pile; (G) inclined the hammer to the pile; and (H) start hammering the pile.

Grout is extensively used to "cement" the annulus between the pile leg and jacket sleeve. An annular gap of 50−100 mm is usually selected. The grout should flow from the bottom-up.

The mix is generally cement plus water. Fly ash may be used to replace part of the cement in order to reduce heat of cement dehydration. Silica fume may be

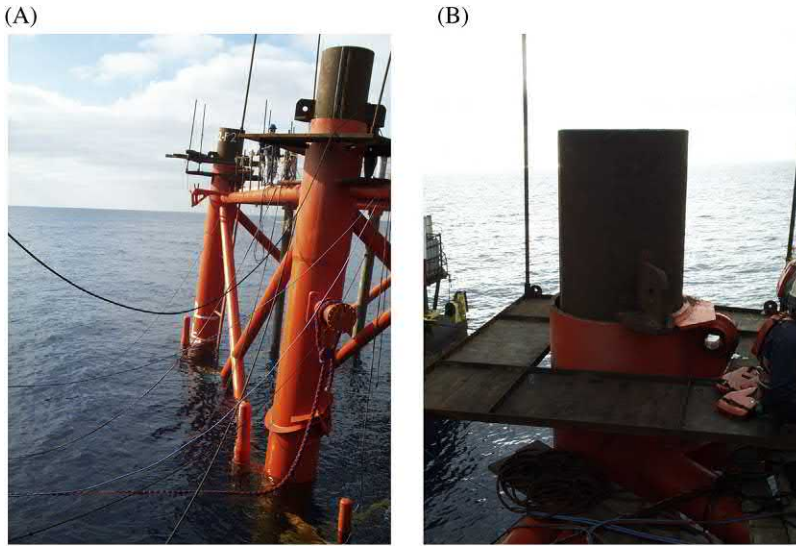

Figure 5.57 (A) Resting the pile to the jacket. (B) Pile padeye for lifting.

added to promote thixotropic behavior, increase strength, and reduce bleeding. Admixtures may be used to provide water reduction, retardation, and expansion characteristics. It is important that trial batches be made to ensure that the grout has the proper flow characteristics as well as strength. The flow rate should be kept low to avoid entrapment of voids. Grout should be overflowed to ensure that the initial mixture of cement and seawater is cleared. Pressures should be carefully controlled to prevent forcing the grout out from under the jacket sleeve; usually this exit is restricted by a grout retainer, but often the grout retainer will have been damaged during pile driving. Therefore a second entry grouting pipe is often provided, to permit the first grout to set and form a plug, and then the main grouting is carried out through the upper entry port.

References

API RP2A, 2007. Recommended Practice for Planning, Designing, and Constructing Fixed Offshore Platforms, 21 ST ed. American Petroleum Institute, Washington, DC.

Delton, N., 2009. Guidelines for Lifting Operations by Floating Crane Vessels. Report No:0027/NDI, Rev3, London.

Gerwick, B.C., 2007. Construction of Marine Offshore Structure. CRC Press, Boca Raton, FL.

Elreedy, M.A., 2013. Concrete and Steel Construction: Quality Control and Assurance. CRC Press.

Further reading

International Organization for Standardization (ISO), 2004. Petroleum and Natural Gas Industries – Offshore Structures – Part 2: Fixed Steel Structures. ISO/DIS 19902:2004.

Corrosion protection

6

6.1 Introduction

The basic concept of corrosion is not usually complex. Therefore the aim in this chapter is to describe corrosion in a simple form that emphasizes only those aspects that are important in understanding corrosion in offshore structures.

In general, one of the key factors in any corrosion situation is the environmental condition surrounding the structure. The definition and characteristics of this variable can be quite complex. In practice, it is important to realize that the environment is a variable that can change with time and conditions. It is also important to realize that the environment that actually affects a metal corresponds to the microenvironmental conditions of the local environment at the surface of the metal. It is the reactivity of this local environment that determines the real corrosion damage. Thus an experiment that investigates only the nominal environmental conditions without consideration of local effects such as flow, pH cells, deposits, and galvanic effects, is useless for lifetime prediction.

In general, corrosion is signaled by rust appearing on a steel surface. The chemical reactions are the main drivers in the corrosion process due to chloride attack. The corrosion of steel starts in the voids that contain water and the electrons will be released as per Eq. (6.1) and it presents an anodic reaction.

A steel offshore structure is exposed to saline water throughout its life time. The impact of water on the integrity of materials is thus an important aspect of system management. Since steels and other iron-based alloys are the metallic materials most commonly exposed to water, aqueous corrosion is discussed with a special focus on the reactions of iron (Fe) with water (H_2O). Metal ions go into solution in anodic areas in an amount chemically equivalent to the reaction at cathodic areas, as shown in Fig. 6.1. In the case of the corrosion of steel, the following reaction usually takes place at anodic areas:

The anodic reaction:

$$Fe \rightarrow Fe^{2+} + 2e^{-} \tag{6.1}$$

If the electrons accumulate on another part of the steel but cannot accumulate in huge amounts in the same part of the steel, another chemical reaction takes place as a combination of the electrodes with oxygen and water. This is called the cathodic reaction and is illustrated in Eq. (6.2):

Offshore Structures. DOI: https://doi.org/10.1016/B978-0-12-816191-3.00006-7

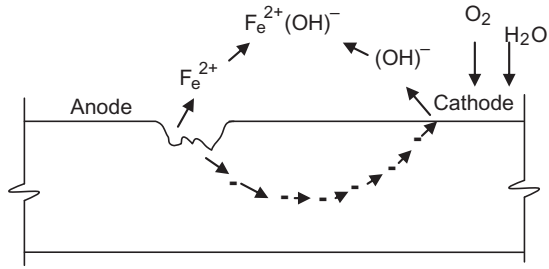

Figure 6.1 Corrosion process on the steel surface.

The cathodic reaction:

$$2e^- + H_2O + \frac{1}{2}O_2 \rightarrow 2OH^- \tag{6.2}$$

From Eq. (6.2) it is clear that the presence of (OH^-) occurs due to the cathodic reaction. The hydroxide ions cause alkalinity and reduce slightly the effect of chlorides. It is important to note from the above equation that water and oxygen are the main causes of the corrosion process.

As shown in the above equations and Fig. 6.1, the anodic and cathodic reactions are the first step in the process of corrosion. Hydroxide ions (OH^-) react with ferrous iron (Fe^{2+}) resulting in Eq. (6.1). This reaction produces ferrous hydroxide which reacts with oxygen and water again and produces ferric hydroxide. This chemical reaction is shown graphically in Fig. 6.1.

$$Fe^{2+} + 2OH^- \rightarrow Fe(OH)_2 \tag{6.3}$$

$$4Fe(OH_2) + O_2 + 2H_2O \rightarrow 4Fe(OH)_3 \tag{6.4}$$

$$2Fe(OH)_3 \rightarrow Fe_2O_3 \cdot H_2O + 2H_2O \tag{6.5}$$

From the above chemical reactions, the transformation of steel into ferrous hydroxides ($Fe(OH)_2$) starts with the reaction with oxygen and water to produce ferric hydroxides ($Fe(OH)_3$) and the final component is the hydration of ferric oxide (rust), with the chemical term $Fe_2O_3 \cdot H_2O$.

Saturated $Fe(OH)_3$ is almost neutral in pH. A magnetic hydrous ferrous ferrite, $Fe_3O_4 \cdot nH_2O$, often forms a black intermediate layer between hydrous Fe_2O_3 and FeO. Hence rust films normally consist of three layers of iron oxides in different states of oxidation.

6.1.1 Corrosion in seawater

Seawater systems are used by many industries, such as shipping, offshore oil and gas production, power plants, and coastal industrial plants.

The main use of seawater is for cooling purposes, but it is also used for firefighting, oilfield water injection, and desalination plants. The corrosion problems in these systems have been well studied over many years, but despite published information on materials behavior in seawater, failures still occur. Most of the elements that can be found on Earth are present in seawater, at least in trace amounts.

The concentration of dissolved materials in the sea varies greatly with location and time, because rivers dilute seawater, as do rain and melting ice, however seawater can be concentrated by evaporation. The most important properties of seawater are as follows:

- Remarkably constant ratios of the concentrations of the major constituents worldwide;
- High salt concentration, mainly sodium chloride;
- High electrical conductivity;
- Relatively high and constant pH;
- Buffering capacity;
- Solubility for gases, of which oxygen and carbon dioxide in particular are of importance in the context of corrosion;
- The presence of a myriad of organic compounds;
- The existence of biological life, to be further distinguished as microfouling (e.g., bacteria, slime) and macrofouling (e.g., seaweed, mussels, barnacles, and many kinds of animals or fish). Some of these factors are interrelated and depend on physical, chemical, and biological variables, such as depth, temperature, intensity of light, and the availability of nutrients. The main numerical specification of seawater is its salinity.

Salinity was defined, in 1902, as the total amount of solid material (in grams) contained in one kilogram of seawater when all halides have been replaced by the equivalent of chloride, when all the carbonate is converted to oxide, and when all organic matter is completely oxidized. The definition of 1902 was translated into Eq. (6.6), where the salinity (S) and chlorinity (Cl) are expressed in parts per thousand (‰).

$$S(‰) = 0.03 + 1.805Cl(‰) \tag{6.6}$$

The fact that the equation of 1902 gives a salinity of 0.03‰ for zero chlorinity was a cause for concern, and a program led by the United Nations Scientific, Education and Cultural Organization (UNESCO) helped to determine a more precise relation between chlorinity and salinity. The definition of 1969 produced by that study is given in Eq. (6.7):

$$S(‰) = 1.80655Cl(‰) \tag{6.7}$$

The definitions of 1902 and 1969 give identical results at a salinity of 35‰ and do not differ significantly for most applications. The definition of salinity was reviewed again when techniques to determine salinity from measurements of conductivity, temperature, and pressure were developed. Since 1978, the Practical Salinity Scale defines salinity in terms of a conductivity ratio:

The practical salinity, symbol S*, of a sample of sea water, is defined in terms of the ratio* K *of the electrical conductivity of a sea water sample of 15°C and the pressure of one standard atmosphere, to that of a potassium chloride (KCl) solution, in which the mass fraction of KCl is 0.0324356, at the same temperature and pressure. The* K *value exactly equal to one corresponds, by definition, to a practical salinity equal to 35.*

The corresponding formula is given in Eq. (6.8).

$$S = 0.0080 - 0.1692K^{0.5} + 25.3853K + 14.0941K^{1.5} - 7.0261K^{2} + 2.7081K^{2.5} \tag{6.8}$$

Note that in this definition ‰ is no longer used, but an old value of 35‰ corresponds to a new value of 35. Since the introduction of this practical definition, the salinity of seawater is usually determined by measuring its electrical conductivity and generally falls within the range 32−35.

It was shown earlier that when corrosion occurs, the anodic reaction rate is exactly equal to the cathodic reaction rate. It was not mentioned before, but it is true, that in environments of good conductivity as in seawater or seabed mud the corroding metal displays a single potential which lies between E_c and E_a. In Fig. 6.3A, this condition is met where the anodic and cathodic curves cross. The potential at the crossover point is referred to as the corrosion potential, E_{cor}. This is the single potential exerted by a corroding metal referred to above. The current, I_{cor}, is referred to as the corrosion current, and is an electrical representation of the corrosion rate. In practice, a corroding metal does not take up potential E_a or E_c, but spontaneously moves to E_{cor}.

While the shape of the individual $E-\log I$ curves may vary, depending on environmental conditions, the manner in which the diagrams, so-called polarization diagrams, are interpreted, in terms of E_{cor} and I_{cor} remains the same.

Fig. 6.2A presents an Evans diagram, which shows the polarization curves for separate cathodic and anodic reactions. When the cathodic and anodic current densities are equal, the two curves shall intersect at a point that defines the corrosion rate in terms of mean corrosion current density (I_{cor}). The electrode potential of the couple at this point is termed the corrosion potential (E_{cor}).

However, there is always some difference between the electrode potentials developed at anodic and cathodic sites on the metal surface. It may be that the amount is significant, with an ohmic drop (ir) under conditions where corrosion macrocells are formed when the anodic and cathodic areas are separated by a medium of high electrolytic resistance, so the Evans diagram will be modified as shown in Fig. 6.2D.

Therefore the mean corrosion rate, I_{cor}, is now reduced and the corrosion potential varies with the location between the limits of the anode E_{cor} and cathode E_{cor}, positions of local anodes being indicated by the region of low corrosion potential. In the absence of significant ohmic drops, the mean corrosion rate (I_{cor}) depends on the magnitude of the difference between the reversible potentials of the anodic and

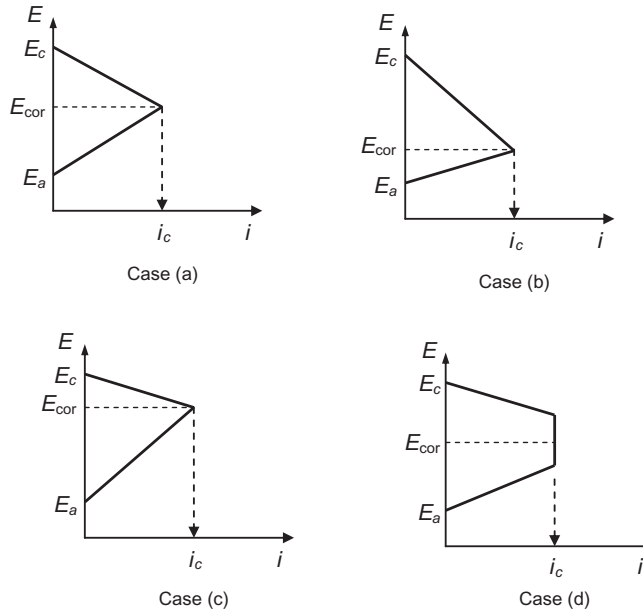

Figure 6.2 Evan's diagrams.

cathodic reactions and on the average slopes of the anodic and cathodic polarization curves. If the anodic reaction is steeply polarized, such as owing to the presence of a passive film, then I_{cor} is small and E_{cor} assumes a value which is close to the reversible potential of the cathodic reaction, as shown in Fig. 6.2C. On the other hand, if the cathodic reaction is steeply polarized, such as owing to limited oxygen availability, the situation is as shown in Fig. 6.2B. With I_{cor} again small, the corrosion potential is close to the reversible potential of the anodic reaction.

6.1.2 Steel corrosion in seawater

The corrosion of steel in seawater, and also seabed mud, is adequately represented by Eq. (6.1), although the process normally proceeds to the precipitation of Fe $(OH)_3$.

On clean steel in seawater, the anodic process occurs with greater facility than the cathodic. As a consequence, the corrosion reaction can go no faster than the rate of cathodic, oxygen reduction. The latter usually proves to be controlled by the rate of arrival of the oxygen at the metal surface, which, in turn, is controlled by the linear water flow rate and the dissolved oxygen concentration in the bulk seawater.

This may be represented on a polarization diagram as shown in Fig. 6.3. At first, the cathodic kinetics get faster as the potential becomes more negative from E_c. This has the effect of depleting the oxygen immediately adjacent to the metal

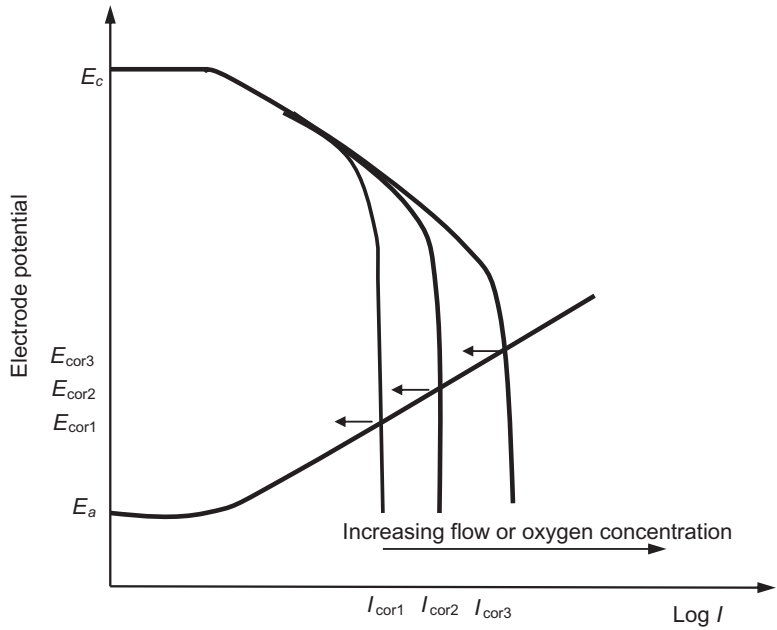

Figure 6.3 Polarization diagram with increasing oxygen concentration.

surface, thus rendering the reaction more difficult. Ultimately, a point is reached where the surface concentration of oxygen has fallen to zero and oxygen can then only be reduced as and when it reaches the surface. Further lowering of the potential cannot increase the cathodic reaction rate, because the kinetics are now governed by potential-independent diffusion processes. A plateau, or limiting, current is observed. Fig. 6.3 shows that the corrosion rate is then equal to this limiting current. The limiting current can be increased by increasing the oxygen flux either by raising the bulk oxygen concentration (the concentration gradient gets steeper) or increasing the flow rate (the oxygen-depleted layer gets thinner). Both serve to increase the corrosion rate as shown in Fig. 6.3.

To a first approximation, it may be stated that the corrosion rate of clean steel in aerated seawater under turbulent flow conditions is directly proportional to the bulk oxygen concentration and the linear velocity. Fick's first law of diffusion and the Chilton−Colbourn analogy can be used to calculate the precise effect of oxygen concentration and Reynolds number (flow rate) on corrosion. Using this technique, Ashworth (1994) estimated the maximum corrosion rates of clean steel in North Sea water at 7°C, as shown in Table 6.1.

In practice, corrosion products and marine fouling build up on steel as it corrodes in seawater. These generally produce lower corrosion rates.

As shown in Fig. 6.3, the polarization diagram represents control of the corrosion rate by sluggish cathodic, kinetics, and in this case controlled by the rate of oxygen arrival at the surface and the effect of increasing oxygen availability.

Table 6.1 Estimated maximum corrosion rates of clean steel in North Sea water at 7°C.

Linear flow rate (m/s)	O_2 concentration				
	6 ppm	7 ppm	8 ppm	9 ppm	10 ppm
0	0.080	0.094	0.107	0.120	0.134
0.3	0.091	0.107	0.123	0.138	0.154
0.4	0.096	0.111	0.128	0.144	0.160
0.6	0.104	0.121	0.138	0.156	0.174
1	0.120	0.140	0.160	0.179	0.199
2	0.160	0.187	0.213	0.240	0.266
4	0.240	0.280	0.320	0.360	0.400

The peak corrosion rate is often attributed to galvanic action between steel in contact with the oxygen-rich surface waters, which is the cathodic area, and the steel at somewhat greater depth exposed to waters of lesser oxygen content, which is the anodic area. It is difficult to conceive that the change in oxygen concentration with depth is sufficiently great to cause the effect, and it may be that other factors come into play. Nevertheless, while the explanations may remain in doubt, the general observation has been widely substantiated. However, if this is not possible, it is necessary to resort to alternative less conventional measures.

The following information is essential to gather before starting design of the cathodic protection (CP) system. This list of the required data can be considered as a checklist when collecting the information from the owner.

1. *Structure design data*
   - **a.** Design life for the CP system and the structure;
   - **b.** Construction drawings with full detailed and dimensions;
   - **c.** General arrangement drawings showing its relationship to the seabed, lowest astronomical tide level (LAT), mean water level, and maximum operational conditions;
   - **d.** Extent of use and application of protective coating;
   - **e.** Availability of electrical power;
   - **f.** Proposed construction schedule;
   - **g.** Structure fabrication methods and fabrication on site;
   - **h.** Use of metallic materials of construction more noble than carbon steel which would affect the CP system design;
   - **i.** Any weight limitations and constraints of the installed CP system;
   - **j.** Safety requirements;
   - **k.** Constraints and limitations on the installation and in-service maintenance and monitoring of the CP system;
   - **l.** Use of high-strength steels or other metals used in the structure which may be subject to a reduction in mechanical properties when under CP.
2. *Offshore site location data*
   - **a.** Water depth, oxygen content, velocity, turbulence, temperature, resistivity, tidal effect, and suspended soil;
   - **b.** Chemical compositions of water;
   - **c.** Presence in the water or seabed of pollutants, depolarizing bacteria, or marine borers;

d. Geological nature of sea bed and the probability for scour to occur;
e. Adjacent facilities including pipelines and details of their CP system;
f. Susceptibility to stratification of the water and the resultant effect or its resistivity temperature and oxygen content;
g. Performance history of previous or existing CP systems in the same environment;
h. Protective current density requirements to achieve the applicable protection criteria, obtained from site surveys or reliable documentary sources;
i. Susceptibility to adherent marine fouling, including type, rate of growth, and variation with water depth.

6.1.3 Choice of system type

There are three types of CP system, each of which, when correctly designed, installed and operated, can effectively protect a fixed offshore steel structure for its design life. These are:

- Sacrificial: comprising anodes made from reactive metals (normally zinc or aluminum alloys), which are more electro-negative than the structures requiring protection, and which require no external source of power.
- Impressed current: comprising anodes manufactured from materials which are essentially inert and powered by an external source of direct current.
- Hybrid: comprising a mixture of sacrificial anodes and externally powered impressed current anodes. The principal technical advantages and disadvantages of sacrificial, impressed current and hybrid systems are summarized in Table 6.2.

The use of the term "impressed current system" can be misleading because for most offshore applications an impressed current system is used in combination with a small number of sacrificial anodes, forming a hybrid system. Sacrificial anodes in hybrid systems are provided on structures to ensure that adequate polarization of the critical nodes is maintained at all times, even if the power supply to the impressed current anodes fails or is switched off temporarily to permit manual underwater inspection or cleaning of the structure by divers. Some early impressed current systems were provided with inadequate sacrificial anode back-up to perform this critical task and significant corrosion damage has been reported in times of unplanned and planned impressed current shutdowns (Table 6.3).

The same considerations apply equally to jacket structures with one important addition, namely that a power source to drive the impressed current system is generally not available until the topside power generation equipment is installed and commissioned. On large deep-water jackets in the North Sea, this may be a year or more after installation of the jacket, protection for the interim period being provided by high current, short-life sacrificial anodes.

It is strongly suggested that designers contemplating an impressed current system for North Sea applications should provide full sacrificial back-up. The sacrificial anodes should provide full protection for a minimum of 2 years, plus an allowance for periods of possible impressed current system shut-down during subsea surveys and maintenance throughout the design life.

Table 6.2 Comparison between different cathodic protection (CP) systems.

	Sacrificial anode	**Impressed current**	**Hybrid**
Advantages	• Simple, reliable and free from in-service operator surveillance • System installation is simple • System installation is simple • Permanent potential monitoring system not essential	• Flexible under widely varying operating conditions • Weight advantage for large-capacity, long-life systems	• Flexible under widely varying operating conditions • Weight advantage for large-capacity, long-life systems
Disadvantages	• Large weight penalty for large-capacity, long-life systems • Responses to varying operating conditions are limited • Hydrodynamic loadings can be high	• Relative complexity of system demands high level of detailed design expertise • System installation is complex, and a power source is required • Perceived driver risk from electric shock • In-service operator surveillance required • Permanent potential monitoring system essential • Vulnerable to loss of power • It is not recommended for the North Sea without full sacrificial back up (i.e., part of a hybrid system)	• Relative complexity of system demands high level of detailed design expertise • System installation is complex, and a power source is required • Perceived driver risk from electric shock • In-service operator surveillance required • Permanent potential monitoring system essential

The obvious technical attractions of sacrificial systems, as illustrated in Table 6.3, make this type most often chosen for offshore structures. Also, for many offshore structures, sacrificial systems are the most economical option to the owner when taking into account both capital expenditure and the running costs over the

Table 6.3 Comparison between the requirements for impressed current cathodic protection (ICCP) and sacrificial anode cathodic protection (SACP).

	ICCP	**SACP**
Power source and connections	External continuous power source required Can be inadvertently misconnected resulting in reversed DC polarity which will accelerate corrosion Isolation of anodes from the structure is essential Fewer connections required but more complex	Independent of any power source Straightforward, welded or bolted connections to structure Cannot be wrongly connected and connections are cathodically protected
Control	Simple controls—manual/automatic Automatic will maintain potentials within preset limits but requires additional fixed reference electrodes Monitoring required at regular intervals	A tendency for current to be self-adjustingDependent on initial design, if not adequate will require additional anodes
Anodes	Usually lighter and fewer numbers May effect other structures in close proximity to anodes and should be assessed for any interaction	Relatively heavy and large numbers Bulk of material may restrict water flow and induce turbulence and drag Less likely to cause interaction with neighboring structures as output is low Lifespan varies with conditions so replacement may be required at different times
Damage	Anodes lighter in construction and therefore less resistant to damage Loss of an anode can be more critical to the effectiveness of the system due to high current output for each anode	Anodes are robust and not susceptible to mechanical damage Where a system comprises a large number of anodes, the loss of a few anodes has little overall effect on the system
Maintenance	Equipment designed for long-life but regular checks on electrical equipment in service required	Generally maintenance-free Renewals usually required at regular intervals unless designed for life of structure

(*Continued*)

Table 6.3 (Continued)

	ICCP	SACP
Environment	May cause overprotection causing coating disbondment or hydrogen-induced cracking of high-tensile steels Less restricted by high-resistivity conditions	Not practical for use in high-resistivity conditions Limited current availability
Installation	Requires a high level of detailed design and installation expertise	Straightforward Often bulky and large numbers involved
Hazards	Diver risk from electrical shock, system needs to be switched off when diver is near anodes	Magnesium anodes can be used in potable tanks but never in areas containing hydrocarbons Aluminum and zinc anodes must never be used in potable water tanks
Cost	Generally initial cost high but service cost normally low	Initial cost dependent on design life but relatively low, periodic renewals necessary and cumulative costs high

design life of the structure. However, generalization of the economic advantages and disadvantages can be misleading, because they differ widely for each type and size of structure and according to the design constraints imposed by the environmental conditions prevailing at different offshore locations. For this reason, economics are not included in Table 6.2.

Faced with severe weight constraints, the designers of Murchison and Hutton platforms in the North Sea carried out detailed assessments of alternative sacrificial and impressed current designs. These showed that although sacrificial anodes could not be dispensed with entirely, substantial weight savings could be made by using impressed current systems as the primary means or protection, on both platforms.

This was despite their vastly different structural configurations, Murchison being a deep-water conventional jacket, and Hutton the world's first tension leg platform.

The adoption of hybrid systems for weight-saving reasons on Murchison and Hutton is significant, as this is perceived to be their primary advantage over sacrificial systems. In the case of Hutton, the installed weight of the primary impressed current system, plus supplementary sacrificial anodes located close to the main node joints, was approximately 60 tons. An equivalent totally sacrificial system would have weighed around 250 tons. In most cases, impressed current systems are more likely to be commercially competitive for buoyant structures such as tension leg platforms and submersibles than for conventional jacket structures.

The relatively simple geometry and large, flat surfaces of buoyant structures are ideally suited for protection to be provided by a small number of high-current, low-voltage, flush-mounted anodes. Cables to reference electrodes and anodes can be easily and economically routed through ballast tanks and the main access ways in the pontoons and columns of the hull.

Impressed current systems may also be cost competitive for conventional jacket structures of simple geometry, located in relatively benign offshore waters, and on which reference electrode and anode cables can be safely installed in substantial conduits routed along the outside of the structural tubular members.

However, the impressed current systems are less likely to be cost competitive on large jackets of complex geometry located in hostile environmental conditions. Complex node geometries are unlikely to allow large-capacity anodes to protect all surfaces adequately on account of shielding effects. Moreover, the hostile environment may demand the difficult and expensive routing of anode and reference electrode cables inside the structural tubular members in order to ensure their mechanical safety. This necessitates a large number of stress-raising penetrations in the tubular members below water adjacent to the anodes and reference electrodes.

As a general rule, increasing anode operating temperatures causes a decrease in both anode ampere-hour capacity and driving potential. At temperatures exceeding 50°C, zinc alloys experience intergranular corrosion and they should not be used at low anode current densities. On the other hand, the ampere-hour capacity of aluminum alloys tends to decrease significantly. In order to realize the performance claimed by anode manufacturers and thus to ensure the successful operation of the CP system, it is imperative that strict quality assurance and quality control of the anode manufacturing process be achieved and maintained throughout production. The quality assurance, quality control, and tests are discussed later in this chapter. It is worth mentioning that the requirements contained in Det Norske Veritas (DNV) RPB401 (2005) are considered to set the minimum standards for offshore work, with supplementary requirements for specific project applications to be determined and specified by the designer.

6.1.4 Geometric shape

Sacrificial anodes are generally cast in three basic geometric shapes: long slender stand-off type, flat plate flush-mounted type, and bracelet type. Typical examples of the first two basic geometries are shown in Figs. 6.4 and 6.5, respectively.

The most common anode shape used for offshore structures is the long slender type of trapezoidal or circular cross-section. The main advantages of this anode geometry is its high current output, good current distribution for a given mass, simple fabrication and casting requirements. Its wight is round 100 kg.

Flat plate anodes are generally best suited to complex fabrications where space limitations prevent the use of larger stand-off anodes and/or cathode current densities are low. Examples are heavily reinforced mud mats and large flat plate painted surfaces. The designer should determine if the chosen anode shapes can be more economically chosen from a manufacturer's standard units or whether, because of

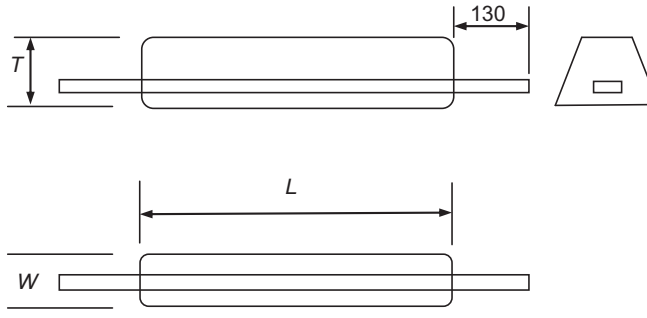

Figure 6.4 Flush-mounted anode.

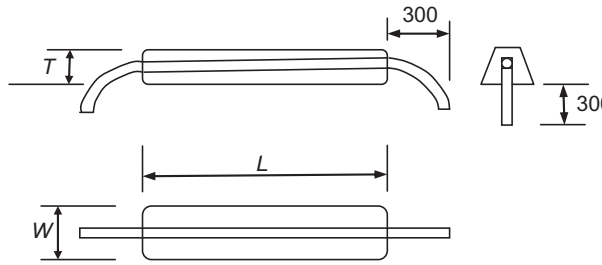

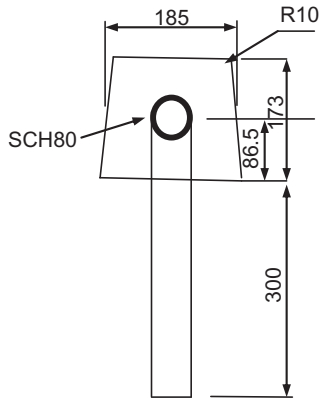

Figure 6.5 Stand-off anode type.

the large number required for a new structure, a preferred design could raise costs. Anode manufacturers offer a large variety of standard anodes and insert core types, the choice of steel insert usually being between a bar tube or rod, in either straight lengths or prefabricated, weld-jointed shapes.

There are three major types of anode for offshore structures:

- slender stand-off;
- elongated, flush mounted;
- bracelet.

Stand-off and flush-mounted anodes may further be divided into "short" and "long," based on the length to width ratio as presented in Figs. 6.4 and 6.5, respectively. The anode type is a main factor in anode resistance and utilization factor as illustrated later in this chapter.

The slender stand-off type is typically cast on a tubular insert and used for relatively large anodes, for example, on platform substructures and subsea templates. The current output, I_a (A), in relation to net anode mass, M_a (kg), is high, as is the utilization factor (u).

The modern type is created by putting the anode in a steel frame called a sled and connecting it with a special clamp to the steel structure. This system is very easy and less costly in case of retrofitting the existing structure.

Stand-off anodes can be manufactured and obtained up to a net anode mass of several hundred kilograms. In surface waters, drag forces exerted by sea currents are significant.

Bracelet anodes are used primarily for pipelines but they are now used also on platform legs in the upper zone, combining high current output to weight ratio with low drag. All flush-mounted anodes should have a suitable coating system applied on the surface facing the protection object. This is to avoid the build-up of anode corrosion products that could cause distortion and eventually fracture of anode fastening devices.

Type of anodes and any special requirements to anode fastening should be defined during the phase of conceptual CP design, taking into account forces exerted during installation, such as piling operation and the effect of wave forces during the structure life time. For stand-off type anodes, special precautions may be necessary during anode design and distribution of anodes to avoid impeding subsea operations.

The insert should be structurally suitable for the anode weight and for the forces it is likely to encounter during its lifetime, including impact, storm damage, wave action, and, possibly, ice. The insert should normally be made from materials that can be welded to the structural steel. The typical grades of steel usually used are BS4360 grades 40A, 43A or 50C, or API 5L grades B, X42, or X52.

If anode inserts are fabricated by welding, the latter has to be in accordance with a recognized, quality-controlled standard. Inserts should be prepared by abrasive cleaning to a minimum standard of SIS 05-59-00 1967 Sa 2.5. Zinc anode inserts are normally zinc coated to BS1729 or BS1706. National Association of Corrosion Engineers (NACE) recommended practice RP03-87 may be followed.

Aluminum anode steel insert specifications are similar to those for zinc, except that the surface must not be zinc coated nor galvanized after cleaning.

Bracelet anodes are the most commonly used type for protection of submarine pipelines and for which their wrap-around construction is ideally suited. They are rarely used on new offshore platform constructions, because of their low current output to mass ratio compared with long slender anodes. However, bracelet anodes do lend themselves to retrofitting on existing structures to supplement or replace original failed, deficient air end-of-life CP systems.

6.2 Coatings and corrosion protection of steel structures

The offshore platform steel is subject to different types of corrosion phenomena: atmospheric corrosion, splash zone corrosion, crevice corrosion, etc. Recently, many steel structures in service in seawater have been corroded by microorganisms spawned by the interaction of aerobic and anaerobic bacteria. Typical rates of corrosion of uncoated steel in seawater are 0.15 mm/year in the splash zone; 0.07 mm/year in the submerged zone, but more, up to 0.3 mm/year, in cold fast-running tides carrying silt or other abrasive sediments. Other studies for uncoated steel in seawater give rates of 0.127 mm/year.

Note that the corrosion rates in fresh water are about half of those in seawater. Painting and coating of steel members, where specified, should be carried out as far as practicable in the shop, under appropriate conditions of humidity and protection from extremes of weather. The joint surfaces should, of course, be masked to permit welding. Field coating of the joints and touchup of shop coats should be done only when the surfaces are dry and at the proper temperature. In some locations, portable tents or other protection will have to be provided. Heaters, dehumidifiers, or both may be required.

Coatings may delay initiation of corrosion by 10−20 years. It is extremely important that surface preparation be thorough and in accordance with the specified requirements. The offshore environment will quickly degrade any coatings placed on damp steel, or over mill scale, or rust. Morning dew can quickly degrade a well-prepared surface. DNV rules require that the provisions for coating include:

1. A description of general application conditions at the coating yard;
2. Method and equipment for surface preparation;
3. Ranges of temperature and relative humidity;
4. Application methods;
5. Time between surface preparation and first coat;
6. Minimum and maximum dry film thickness of a single coat;
7. Number of coats and minimum total dry film thickness;
8. Relevant drying characteristics;
9. Procedure for repair of damaged coating;
10. Methods of inspection, for example, adhesion testing and holiday detection.

Table 6.4 Guide on coating breakdown criteria for COP design.

Year	Coating breakdown (% of area)		
	Initial	Mean	Final
10	2	7	10
20	2	15	30
30	2	25	60
40	2	40	90

The relation between the coating breakdown as a percentage of area and the structure lifetime, which is considered in designing the CP system, is as shown in Table 6.4. Surface preparation and application of coating should be carried out when the surface temperature is more than the dew point or when the relative humidity of the air is below the limits recommended by the coating manufacturer. Coatings are usually applied to steel in the splash and atmospheric zones and to internal spaces that are exposed to seawater. In the case of sealed internal spaces permanently filled with seawater, corrosion inhibitors may be added to the water prior to sealing. The most effective coatings seem to be organic coatings over metallized zinc: vinyl mastic on urethane in temperate zones over zinc or zinc silicate and phenolic over the zinc primer in the Arctic and subarctic. The US Corps of Engineers is currently providing corrosion protection to lock gates in West Virginia by shot blasting a single coat of zinc primer 0.625−0.1 mm thick, followed by two coats of zinc-rich vinyl immersion coating to 0.175 mm. Underwater and in the splash zone they apply Copoxy Shop Primer, followed by a top coat epoxy to 1.0 mm.

Sacrificial anodes or impressed current CP are normally used to protect steel below water. Anodes must be carefully installed in accordance with the specifications to ensure that they cannot become dislodged during transport, launching, installation, pile driving, and service. An adequate electrical connection between sacrificial anodes and the steel structure is essential. Impressed current is believed to be more effective because it is less likely to be shielded, but requires continued monitoring and adjustment. If compressed current is turned off and on frequently, as happens on offshore platforms corrosion is actually accelerated. It is prohibited in closed spaces or where water flow is restricted because of the possibility of hydrogen generation. Sacrificial anodes discharge their ions on a line of sight through water. The anode demands on the exposed face and the back side of sheet piles are very different. Coatings may be applied to members that will be underwater in service in order to minimize the requirements for CP, provided the coating has adequate resistance to cathodic disbondment. Zinc-based and aluminum-based alloys have been applied by thermal spray. Titanium-clad steel tubular piles were used on the Trans-Tokyo Bay Bridge. In the splash zone, additional protection may be provided by means of Monel wrap, copper nickel, austenitic stainless steel, or carbon steel plate wrap. Fig. 6.6 illustrates a sketch of the relative metal loss from

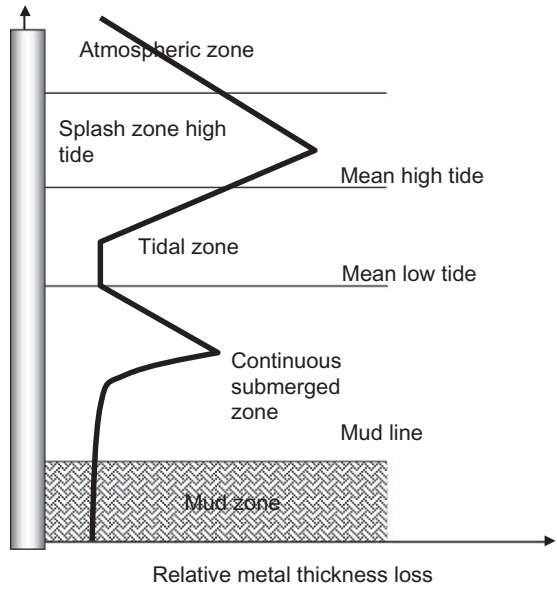

Figure 6.6 Corrosion profile of steel piling after 5 years exposure (Humble).

an offshore steel structure member. It is obvious that the maximum corrosion rate occurs at the splash zone.

The guide for the minimum design current densities for cathodic protection in different locations is presented in Table 6.5. For example, at least one offshore operator has so far successfully employed thermal sprayed aluminum coatings for critical high-strength steel components on a major North Sea structure, as an alternative to a conventional sacrificial anode system. The benefit in using this galvanic coating is that it provides an essentially uniform protected potential of −800 to −900 mV Ag/AgCl over the entire coated surface area (Table 6.6).

Corrosion of carbon steel in seawater is controlled by the availability of oxygen to the metal surface. Thus, under static conditions, carbon steel corrodes at between

Table 6.5 Guidance on the minimum design current densities for cathodic protection for bare steel.

Location	**Current densities (mA/m^2)**		
	Initial	**Mean**	**Final**
North Sea	180	90	120
Arabian Gulf	130	70	90
India	130	70	90
Gulf of Mexico (GoM)	110	60	80
Indonesia	110	60	80

Table 6.6 Potential limit for cathodic protection of steel.

	Positive limit	Negative limit
Aerated seawater	−800 mv Ag/Ag	−1050 mv
	+250 mv Zn	0.0 mv
Anaerobic condition	−900 mv Ag/AgCl	−1050 mv
	+150 mv Zn	0.0 mv

100 and 200 m/year, reflecting the oxygen level and temperature variations in different locations. As velocity causes a mass flow of oxygen to the surface, corrosion is very dependent on flow rate and can increase by a factor of 100 in moving from static or zero velocity to a velocity as high as 40 m/s. Galvanizing confers only limited benefit under flow conditions, as corrosion of zinc also increases with velocity. For the thickness normally used in seawater piping, it will extend the life of the pipe for about 6 months.

There is not available much information about the effect of temperature within the range normally encountered in seawater systems.

It has been noted, at the LaQue Centre, that corrosion of carbon steel increases by approximately 50% between the winter (average temperature 7°C) and summer (27°C−29°C) months. Although oxygen solubility tends to fall with a rise in temperature, the higher temperature tends to increase the reaction rate. Evidence from work on steel in potable waters suggests that the temperature effect is more important and that corrosion, for steel, will increase with temperature.

This part of ISO 12944 deals with the classification of the principal environments to which steel structures are exposed, and the corrosivity of these environments. It defines atmospheric corrosivity categories, based on mass loss (or thickness loss) by standard specimens, and describes typical natural atmospheric environments to which steel structures are exposed, giving advice on the estimation of the corrosivity; describes different categories of environment for structures immersed in water or buried in soil; gives information on some special corrosion stresses that may cause a significant increase in corrosion rate or place higher demands on the performance of the protective paint system. The corrosion stresses associated with a particular environment or corrosivity category represent one essential parameter governing the selection of protective paint systems. This part of ISO 12944 does not deal with the classification of those environments that consist of special atmospheres such as those in and around chemical and metallurgical plants.

6.3 Corrosion stresses due to the atmosphere, water, and soil

Atmospheric corrosion is a process that takes place in a film of moisture on the metal surface. The moisture film may be so thin that it is invisible to the naked eye.

The corrosion rate is increased by the following factors: an increase in relative humidity; the occurrence of condensation when the surface temperature is at or below the dew point; an increase in the amount of pollution in the atmosphere, the corrosive pollutants can react with the steel and may form deposits on the surface. Experience has shown that significant corrosion is likely to take place if the relative humidity is above 80% and the temperature above 0°C.

However, if pollutants or hygroscopic salts are present, corrosion occurs at much lower humidity levels. The atmospheric humidity and air temperature in a particular region of the world will depend on the climate prevailing in that part of the world.

The location of the constituent element of a structure also influences corrosion. Where structures are exposed to the open air, climatic parameters such as rain and sunshine and pollutants in the form of gases or aerosols affect corrosion. Under cover, the climatic influences are reduced. Indoors, the effect of atmospheric pollutants is reduced, although a locally high corrosion rate caused by poor ventilation, high humidity, or condensation is possible. For estimation of the corrosion stresses, an appreciation of the local environment and the microenvironment is essential. Examples of decisive microenvironments are the underside of a bridge (particularly over water), the roof of an indoor swimming pool, and the sunny and shady sides of a building.

Special care shall be taken when considering structures that are partly immersed in water or partly buried in soil. Corrosion under such conditions is often restricted to a small part of the structure where the corrosion rate can be high. Exposure tests for estimating the corrosivity of water or soil environments are not recommended. However, different immersion/burial conditions can be described. The type of water —fresh, brackish, or salt—has a significant influence on the corrosion of steel. Corrosivity is also influenced by the oxygen content of the water, the type and quantity of dissolved substances, and the water temperature. Animal or vegetable growth can accelerate corrosion. Three different zones for immersion in water can be defined: the underwater zone is the area which is permanently exposed to water; fluctuating water level in the intermediate zone, which is the area in which the water level changes due to natural or artificial effects, thus giving rise to increased corrosion due to the effects of both water and the atmosphere. The splash zone is critical and is defined as the area wetted by waves and where a water spray effect shall give rise to exceptionally high corrosion stresses.

Corrosion in soil is dependent on the mineral content of the soil and the nature of these minerals, and on the organic matter present, the water content, and the oxygen content. The corrosivity of soil is strongly influenced by the degree of aeration. The oxygen content will vary and corrosion cells may be formed. Different types of soil and differences in soil parameters are not considered as classification criteria in this part of ISO 12944.

For the selection of a protective paint system, special stresses to which a structure is subjected and special situations in which a structure is located shall also be taken into account. The design as well as the use of the structure may lead to corrosion stresses not being taken into consideration in the classification system.

6.3.1 Classification of environments

For the purposes of ISO 12944, atmospheric environments are classified into six atmospheric-corrosivity categories. To determine corrosivity categories, the exposure of standard specimens is strongly recommended. Table 6.9 presents the categories of corrosivity as a function of the mass or thickness loss of such standard specimens made of low-carbon steel and/or zinc after exposure for one year. For details of standard specimens and the treatment of the specimens prior to and after exposure refer to ISO 9226. Extrapolation of the mass or thickness losses from one year to shorter exposure times, or back-extrapolation from longer times, will not give reliable results and is therefore not permitted. The mass or thickness losses obtained for steel and zinc specimens may sometimes give different categories. In such cases, the higher corrosivity category shall be taken. If it is not possible to expose standard specimens in the actual environment of interest, the corrosivity category may be estimated by simply considering the examples of typical environments given in Table 6.9. The examples listed are informative and may occasionally be misleading. Only the actual measurement of mass or thickness loss will give the correct classification. Noting that, the corrosivity categories can also be estimated by considering the combined effect of the following environmental factors: yearly time of wetness, yearly mean concentration of sulfur dioxide, and yearly mean deposition of chloride as in ISO 9223.

Categories for water and soil

For structures immersed in water or buried in soil, corrosion is normally local in nature and corrosivity categories are difficult to define. However, for the purposes of this International Standard, various environments can be described. In Table 6.7, three different environments are given together with their designations. Note that, in many such situations, CP is involved, and this should be borne in mind.

Note from Table 6.8 that the loss values for the corrosivity categories are identical to those given in ISO 9223. In coastal areas in hot humid zones, the mass or thickness losses can exceed the limits of the category in the case of the marine structure category (C5-M) and special precautions must therefore be taken when selecting protective paint systems for structures in such areas.

In most cases the general conclusions arising that the corrosion behavior can be drawn from the type of climate. In a cold or dry climate, the corrosion rate will be lower than in a temperate climate; it will be greatest in a hot, humid climate and in a marine climate, although considerable local differences can occur. The main concern is the length of time a structure is exposed to high humidity, also described as time of wetness (Table 6.9).

6.3.2 Mechanical, temperature, and combined stresses

Erosion, which is an abrasive stress, may occur due to particles as in the case of sand being entrained by the wind. Surfaces which are subject to abrasion are

Table 6.7 Atmospheric corrosivity categories and examples of typical environments.

Corrosivity category	Mass loss per unit surface/thickness loss (after first year of exposure)				Example of typical environments in a temperate climate	
	Low-carbon steel		Zinc		Exterior	Interior
	Mass loss (g/m^2)	Thickness loss (μm)	Mass loss (g/m^2)	Thickness loss (μm)		
C1 very low	≤ 10	≤ 1.3	≤ 0.7	≤ 0.1		Heated buildings with clean atmospheres, for example, offices, shops, schools, hotels
C2 low	$>10-200$	$>1.3-25$	$>0.7-5$	$>0.1-0.7$	Atmospheres with a low level of pollution, mostly rural areas	Unheated buildings where condensation may occur, for example, depots, sports halls
C3 medium	$>200-400$	$>25-50$	$>5-15$	$>0.7-2.1$	Urban and industrial atmospheres, moderate sulfur dioxide pollution. Coastal areas with low salinity	Production room with high humidity with some air pollution, for example, food processing plants
C4 high	$>400-650$	$>50-80$	$>15-30$	$>2.1-4.2$	Industrial areas and coastal areas with low salinity	Chemical yards, swimming pools, coastal ship, and boatyards
C5.1 very high (industrial)	$>650-1500$	$>80-200$	$>30-60$	$>4.2-8.4$	Industrial areas with high humidity and an aggressive atmosphere	Buildings or areas with almost permanent condensation and high pollution
C5.M very high (marine)	$>650-1500$	$>80-200$	$>30-60$	$>4.2-8.4$	Coastal and offshore areas with high salinity	Buildings or areas with almost permanent condensation and high pollution

Table 6.8 Categories for water and soil.

Category	Environment	Examples of environment and structures
Im1	Fresh water	River installations, hydroelectric power plants
Im2	Sea or brackish water	Harbor areas with structures like sluice gates, locks, jetties, offshore structures
Im3	Soil	Buried tanks, steel piles, steel pipes

Table 6.9 Calculated time of wetness and selected characteristics of various types of climate (as in ISO9223:1992)

Type of climate	Mean value of the annual extreme values (°C)			Calculated time for wetness at RH > 80% and temperature >0°C h/year
	Low temperature	High temperature	Highest temperature with RH > 95%	
Extremely cold	−65	+32	+20	0−100
Cold	−50	+32	+20	150−2500
Cold temperature	−33	+34	+23	2500−4200
Warm temperature	−20	+35	+25	
Warm dry	−20	+40	+27	10−1600
Mild warm dry	−5	+40	+27	
Extremely warm dry	+3	+55	+28	
Warm damp	+5	+40	+31	4200−6000
Warm damp, equable	+13	+35	+33	

considered to be exposed to moderate or severe mechanical stresses. On the other hand, in water, mechanical stresses may be produced by boulder movement, the abrasive action of sand, wave action, etc.

Mechanical stresses can be divided into three classes—weak, moderate, and severe—and the criteria for each are as follows:

1. *Weak*: no, or very slight and intermittent, mechanical stresses, for example, due to light debris or small quantities of sand entrained in slow-moving water;
2. *Moderate*: moderate mechanical stresses due, for example, to solid debris, sand, gravel, shingle, or ice entrained in moderate quantities in moderately fast-flowing water, a strong current without entrained matter flowing past vertical surfaces, moderate growth such as animal or vegetable, moderate wave action;

3. *Severe*: high mechanical stresses due, for example, to solid debris, sand, gravel, shingle, or ice entrained in large quantities by fast-flowing water over horizontal or inclined surfaces, dense growth such as animal or vegetable, particularly if, for operational reasons, it must be removed mechanically from time to time.

Stresses will accumulate due to medium or high temperatures. In most standards special DNV define medium temperatures as those between +60°C and +150°C, and high temperatures as those between +150°C and +400°C. Temperatures of this magnitude only occur under special conditions during construction or operation. The case of higher temperature is seen usually in the case of fire, but medium temperatures are rarely found except in some areas in the Arabian gulf where the temperature can reach from 40°C to 60°C.

In the case of combined stresses affecting steel, corrosion will increase. In general, corrosion may develop more quickly on surfaces exposed simultaneously to mechanical and chemical stresses. This applies to steel structures near to salt water, in addition to mechanical stresses due to impacts, such as in the case of boats landing.

6.4 General cathodic protection design considerations

This section addresses aspects of CP which are primarily relevant to CP conceptual design, including the compatibility of CP with metallic materials and coatings.

The content of this section is informative in nature and intended as a guideline for owners and their contractors preparing for conceptual or detailed CP design. Nothing in this section shall be considered as mandatory if this RP has been referred to in a purchase document.

The corrosion allowance should be taken into consideration during design and cannot be ignored dependent on the CP system.

6.4.1 Environmental parameters affecting cathodic protection

The major seawater parameters affecting CP in situ are:

- dissolved oxygen content;
- sea currents;
- temperature;
- marine growth;
- salinity.

In addition, variations in seawater pH and carbonate content are considered factors which affect the formation of calcareous layers associated with CP and thus the current needed to achieve and maintain CP of bare metal surfaces. In seabed sediments, the major parameters are temperature, bacterial growth, salinity, and sediment coarseness.

The above parameters are interrelated and vary with geographical location, depth, and season. It is not feasible to give an exact relation between the seawater

environmental parameters indicated above and cathodic current demands to achieve and maintain CP. To rationalize CP design for marine applications, default design current densities, i_c (A/m^2), are defined in this document based on climatic regions, which are related to mean seawater surface temperature and water depth.

The ambient seawater temperature and salinity determine the specific seawater resistivity, ρ (ohm $\cdot$ m), which is used to calculate the anode resistance, R (ohm), a controlling factor for the current output from an anode.

6.4.2 Design criteria

The CP system for the substructure shall be designed in accordance with DNV RP B401-1993 and the requirements of this specification. The design criteria should also contain the condition and assumptions that were taken into consideration.

The retrofit CP design considerations may be limited only to the platform steel structure, pile guides, piles, and also any conductors, risers, or appurtenances.

When focusing on the platform, the design does not include pipelines or associated subsea structures that might be in close proximity and electrically connected to the platforms, other than making an allowance for some debris on the seabed.

The design life of the sacrificial anode cathodic protection (SACP) systems should be defined based on the owner requirement, which takes into consideration the lifetime of the platform, which in this case study is 25 years.

The retrofit CP design is based on using the conventional and modified CP criteria to be the target to maintain external structure potentials in the range from -800 to -1050 mV with respect to an Ag/AgCl reference electrode for seawater, throughout the remaining service life of the platforms.

A seawater resistivity of 20 Ω cm and an average seawater temperature of 22°C have been used in the design calculations.

In case of platforms that were originally fitted with aluminum flush-fit, long slender type anodes for more than 30 years ago, these anodes are now either totally consumed or almost at end-of-life. As these types of anode have a theoretical utilization factor of 85%, therefore the anode retrofit design will not consider allowance for any remaining anode alloy.

In the case of a retrofit, the designer should check that the original coating system applied to the splash zone is comparable with current standards equivalent to a DNV-Cat III standard coating. For the purposes of the CP retrofit design, an initial coating breakdown factor of 2% has been used and 1% each year thereafter. This is slightly less than DNV recommends but is comparable with other offshore operators, as being acceptable practice. Based on all platforms being originally installed for 30 years, the coating breakdown factors which will be used in the calculations for 25 years consider the initial coating breakdown failure (CBF) to be 35%, mean CBF 48%, and the final CBF equal to 60%.

Based on DNV RP B401 (2005), the CP design guideline provides the following current densities that can be used in design offshore structure CP systems; for wetted areas 150, 70, and 100 mA/m^2 for initial, mean, and final, respectively. In the case of a buried area, 20 mA/m^2 will be taken for initial, mean, and final CBF.

It is important to highlight that the above current densities are used for new uncoated steel structures in tropical waters ($>20^{\circ}$C) with a water depth to a maximum of 30 m. From a practical point of view the above criteria are conservative for retrofit designs in the case of platform steel structures that remain partially protected and as a result these figures would lead to have a large mass of anode alloy and a substantial number of anode sleds.

DNV and other international standard organizations have mentioned that the design parameters may vary depending on local conditions and operational experience.

As a case study has been carried out an assessment of the original CP design of SACP systems fitted to seven of the specified platforms. The assessment calculates the average current densities for the platforms based on potential levels over the last 25 years and compares these to total anode alloy weight loss over the same period. To obtain the most accurate current density figures the total surface areas for each platform have been added together, as have the number of anodes, to obtain the total mass of anode alloy consumed over 25 years.

The assessment concludes that based on potential data the average current density is 24 mA/m^2, whereas the anode weight loss over the same period gives an average current density of 23 mA/m^2. Based on the findings of the assessment, in some platforms it is recommended for the wetted area to be 35 mA/m^2 and for the buried area 10 mA/m^2, which are the same in the initial, mean, and final CBF. This is to reduce current density criteria for platform retrofit CP designs which are related to the design office experience.

6.4.3 Protective potentials

A potential of -0.80 V relative to the Ag/AgCl/seawater reference electrode is generally accepted as the design protective potential E_c° (V) for carbon and low-alloy steels. It has been argued that a design protective potential of -0.90 V should apply in anaerobic environments, including typical seawater sediments. However, in the design procedure advised in this RP, the protective potential is not a variable.

For a correctly designed galvanic anode CP system, the protection potential for the main part of the design life will be in the range -0.90 to -1.05 (V). Toward the end of the service life, the potential increases rapidly toward -0.80 (V), and eventually to even less negative values, referred to as underprotection.

The term "overprotection" is only applicable to protection potentials more negative than -1.15 (V). Such potentials will not apply for CP by galvanic anodes based on Al or Zn.

6.4.4 Detrimental effects of cathodic protection

CP will be accompanied by the formation of hydroxyl ions and hydrogen at the surface of the protected object. These products may cause disbonding of nonmetallic coatings by mechanisms including chemical dissolution and electrochemical reduction processes at the metal–coating interface, possibly including build-up of

hydrogen pressure at this interface. This process of coating deterioration is referred to as "cathodic disbonding." On components containing hot fluids, the process is accelerated by heat flow to the metal−coating interface.

Coatings applied to machined or as-delivered surfaces of corrosion-resistant alloys (CRAs) are particularly prone to cathodic disbonding. However, with surface preparation to achieve an optimum surface roughness, some coating systems (e.g., those based on epoxy or polyurethane) have shown good resistance to cathodic disbonding by galvanic anode CP, when applied to CRAs as well as to carbon and low-alloy steel. For coating systems whose compatibility with galvanic anode CP is not well documented, the owner should consider carrying out qualification testing, including laboratory testing of resistance to cathodic disbondment.

Testing of marine coatings' resistance to cathodic disbondment has been standardized in American Society of Testing material (ASTM) G8. CP will cause formation of atomic hydrogen at the metal surface. Within the potential range for CP by aluminum- or zinc-based anodes (i.e., −0.80 to −1.10 V Ag/AgCl/seawater), the production of hydrogen increases exponentially toward the negative potential limit. The hydrogen atoms can either combine forming hydrogen molecules or become absorbed in the metal matrix. In the latter case, they may interact with the microstructure of components subject to high stresses, causing initiation and growth of hydrogen-related cracks, here referred to as "hydrogen-induced stress cracking."

Copper- and aluminum-based alloys are generally considered immune to hydrogen-induced stress cracking, regardless of fabrication mode. For high-strength titanium alloys, documentation is limited and special considerations should apply.

Special techniques have been applied to control the CP protective potential to a less negative range (e.g., −0.80 to −0.90 V), including the use of diodes and special anode alloys, but practical experience is limited. A major disadvantage of this approach is that the individual component or system needs to be electrically insulated from adjacent "normal" CP systems.

CP in closed compartments without ventilation may cause the development of hydrogen gas to an extent that an explosive gas mixture (i.e., hydrogen/oxygen) may eventually develop. The risk is moderate with Al- and Zn-based galvanic anodes but at least one explosion during external welding on a water flooded platform leg containing such anodes has been related to this phenomenon.

A consequence of CP application is that a calcareous layer which primarily consists of calcium carbonate will form on bare metal surfaces. The thickness is typically of the order of a tenth of a millimeter, but thicker deposits may occur. The calcareous layer reduces the current demand for maintenance of CP and is therefore beneficial. A calcareous layer may, however, obstruct mating of subsea electrical and hydraulic couplers with small tolerances. This may be prevented by applying an insulating layer of a thin film coating such as baked epoxy resin. An alternative measure is to electrically insulate the connectors from the CP system and use seawater-resistant materials for all wetted parts. High-alloyed stainless steels, nickel-chromium-molybdenum alloys, titanium- and certain copper-based alloys such as nickel-aluminum bronze, have been used for this purpose.

Galvanic anodes may interfere with subsea operations and increase drag forces by flowing seawater. CP eliminates the antifouling properties of copper-based alloys in seawater.

6.4.5 Galvanic anode materials

Galvanic anodes for offshore applications are generally based on either aluminum or zinc. The generic type of anode material (i.e., aluminum or zinc-based) is typically selected and specified in the conceptual CP design report and/or in the design premises for detailed CP design.

Aluminum-based anodes are normally preferred due to their higher electrochemical capacity, ε (Ah/kg). However, zinc-based anodes have sometimes been considered more reliable (i.e., with respect to electrochemical performance) for applications in marine sediments or internal compartments with high bacterial activity, with both environments representing anaerobic conditions.

Based on practical experience, ferritic and ferritic-pearlitic structural steels with specified minimum yield strength up to at least 500 MPa have proven compatibility with marine CP systems. However, laboratory testing has demonstrated susceptibility to hydrogen-induced stress cracking during extreme conditions of yielding. It is recommended that all welding is carried out according to a qualified procedure with 350 HV as an absolute upper limit. With a qualified maximum hardness in the range 300−350 HV, design measures should be implemented to avoid local yielding and to apply a reliable coating system as a barrier to CP-induced hydrogen absorption.

The post weld heat treatment is very important to reduce the heat-affected zone hardness and the residual stresses due to welding processes as welding can change the steel formation.

Therefore there are recommendations for ferritic steels to be applied for hardness limits and design measures.

Design precautions should include measures to avoid local plastic yielding and use of coating systems qualified for, for example, resistance to disbondment by mechanical and physical or chemical effects.

Special techniques have been applied to control the CP protective potential to a less negative range (e.g., -0.80 to -0.90 V), including the use of diodes and special anode alloys, but practical experience is limited. A major disadvantage of this approach is that the individual component or system needs to be electrically insulated from adjacent “normal” CP systems.

A consequence of CP application is that a calcareous layer, which consists primarily of calcium carbonate, will form on bare metal surfaces. The thickness is typically of the order of a tenth of a millimeter, but thicker deposits may occur. The calcareous layer reduces the current demand for maintenance of CP and is therefore beneficial. A calcareous layer may, however, obstruct mating of subsea electrical and hydraulic couplers with small tolerances. This may be prevented by applying an insulating layer of a thin film coating (e.g., baked epoxy resin).

Table 6.10 Performance properties of the alloy

Environment	Nominal resistivity (ohm-cm)	Anode temperature (°C)	Min^{m} alloy capacity (Ah/kg)	Working potential (mV w.r.t.) Ag/AgCl/seawater
Saline mud	100	40	1500	−1050
Saline mud	200	25	1865	−1050
Seawater	25	25	2000	−1070

Galvanic anodes may interfere with subsea operations and increase drag forces by flowing seawater. CP eliminates the antifouling properties of copper-based alloys in seawater.

Anodes shall have a closed-circuit potential of minus 1.10 V (or more negative) to copper/copper sulfate electrode and shall have a minimum efficiency of 80% (maximum consumption rate of 3.68 kg per ampere-year) or such higher value as may be apparent. Each foundry pour shall be tested for chemical composition and closed-circuit potential. A suitable sample shall be retained from each pour to perform a rate of consumption test. A minimum of three tests shall be performed for rate of consumption during the production run. In the event that any test indicates a consumption rate of more than the above maximum, tests shall be performed on additional samples to confirm the adequacy of the anode composition.

The active anode material shall be a proven aluminum-zinc-indium-based alloy suitable for long-term continuous service in seawater, saline mud, or alternating seawater and saline mud environments.

Whoever delivers the anode shall propose an alloy offering the following minimum electrochemical performance characteristics, documented by long-term performance test reports (Table 6.10).

Prior to manufacture, the supplier shall demonstrate the ability of the proposed alloy to satisfy the above requirements, minimum anode capacities and working potentials shall be determined at operating anode current density in the range of 0.25−1.0 A/m^2 for saline mud and 0.25−4.0 A/m^2 for free seawater.

The supplier shall submit the full chemical analysis details and the specific gravity value of the proposed alloy to the client for approval and shall demonstrate that the specification requirements can be satisfied at the compositional limits.

6.4.6 Cathodic protection design parameters

This section describes the design parameters to be used for conceptual and detailed design of galvanic anode CP systems and gives guidance on the selection of such parameters. With the exception of the design life and possibly also coating breakdown factors, the actual design values to be applied for a specific project are normally selected by the contractor, based on environmental and other parameters identified in the project design. However, sometimes certain or all CP design parameters have already been defined by purchaser in a project document.

If reference is given to this RP in a purchase document, and unless otherwise agreed, the default design values referred to in this section shall apply.

The design values recommended in this section are consistently selected using a conservative approach. Adherence to these values is therefore likely to provide a service life that exceeds the design life of the CP system.

Owners of offshore structures may specify less, or in certain cases more conservative design data, based on their own experience or other special considerations. The contractor in addition to the owner may further propose the use of alternative design data, however, any such data shall then be accepted by the owner, preferably before the CP design work has started.

All electrochemical potentials associated with CP in this section refer to the Ag/AgCl/seawater reference electrode. The potential of this reference electrode is virtually equivalent to that of the standard calomel electrode.

By comparing the 1993 revision of this DNV RP with the major revisions of this 2004 revision it can be seen that the number of depth zones for design current densities have been extended from two to four, while the number of "coating categories" has been reduced from four to three.

Design life

The owner usually specifies the required life time for the CP system. The design life shall further take into account any period of time when the CP system will be active prior to operation of the protection object.

It is very important to take into consideration when defining the CP lifetime that the maintenance and repair of CP systems for fixed offshore structures are generally very costly and sometimes impractical.

It is therefore normal practice to apply at least the same anode design life as for the protection object. However, in certain circumstances planned retrofitting of sacrificial anodes may be an economically viable alternative to the installation of very large anodes initially. This alternative should then be planned such that necessary provisions for retrofitting are made during the initial design and fabrication.

Design current densities

The current density, i_c, refers to CP current per unit surface area (in A/m^2). The "initial" and "final" design current densities, i_{ci} (initial) and i_{cf} (final), respectively, give a measure of the anticipated cathodic current density demand to achieve CP of a bare metal surface within a reasonably short period of time. They are used to calculate the initial and final current demands which determine the number and sizing of anodes. The effect of any coating on current demand is taken into account by application of a "coating breakdown factor."

The initial design current density refers to the cathodic current density that is required to effect polarization of an initially bare metal surface, typically for structural steel surfaces with some rusting and/or mill scale.

The initial design cathodic current density is necessarily higher than the final design current density because the calcareous scale and possibly marine fouling

layer developed during this initial phase reduce the subsequent current demand as the "polarization resistance" is reduced. A sufficient initial design current density enables rapid formation of protective calcareous scale and hence efficient polarization.

The final design current density refers to metal surfaces with established calcareous scale and marine growth. It takes into account the current density required to repolarize a structure if such layers are partly damaged, or by periodic removal of marine growth.

An appropriate final design current density and hence CP polarizing capacity will further ensure that the protection object remains polarized to a potential of −0.95 to −1.05 V throughout the design life. In this potential range, the current density demand for maintenance of CP is lowest.

The initial and final current densities are used to calculate the required number of anodes of a specific type to achieve a sufficient polarizing capacity by use of Ohm's law and assuming the following:

- The anode potential is in accordance with the design closed circuit potential;
- The potential of the protection object (i.e., cathode) is at the design protective potential for C-steel and low-alloy steel, that is, −0.80 V.

It follows from the above relationship that the anode current and hence the cathodic current density decrease linearly when the cathode is polarized toward the closed circuit anode potential, reducing the driving voltage for the galvanic cell. The total CP current for a CP unit, It (A), becomes:

$$I_t = \frac{E_c - E_a}{R} \tag{6.9}$$

where R (ohm) is the total anode resistance, E_c (V) is the global protection potential and E_a (V) is the actual anode (closed circuit) potential.

The mean (or "maintenance") design current density, i_{cm} (A/m^2), is a measure of the anticipated cathodic current density once the CP system has attained its steady-state protection potential; this is typically 0.15−0.20 V more negative than the design protective potential.

The decrease in cathode potential (i.e., "cathodic polarization") reduces the anode current so that the average design current density becomes about 50% of the initial/final design current density. As the initial polarization period proceeding steady-state condition is normally short compared to the design life, the time-weighted cathodic current density becomes very close to the steady-state cathodic current density.

Cathodic current densities to achieve and maintain CP are dependent on factors that vary with geographical location and operational depth. Recommendations for initial/final and average design current densities are given in Tables 6.13 and 6.14, respectively, based on climatic regions and depth. These design current densities have been selected in a conservative manner to account for harsh weather conditions, including waves and sea currents, but not erosive effects on calcareous layers

Table 6.11 Recommended initial and final design current densities (A/m^2) for seawater-exposed bare metal surfaces, as a function of depth and climatic region based on surface water temperature.

Depth (m)	Tropical (>20°C)		Subtropical (12°C–20°C)		Temperate (7°C–11°C)		Arctic (<7°C)	
	Initial	Final	Initial	Final	Initial	Final	Initial	Final
0–30	0.150	0.100	0.170	0.110	0.200	0.130	0.250	0.170
30–100	0.120	0.080	0.140	0.090	0.170	0.110	0.200	0.130
100–300	0.140	0.090	0.160	0.110	0.190	0.140	0.220	0.170
>300	0.180	0.130	0.200	0.150	0.220	0.170	0.220	0.170

Table 6.12 Recommended mean design current densities (A/m^2) for seawater-exposed bare metal surfaces, as a function of depth and climatic region based on surface water temperature.

Depth (m)	Tropical (>20°C)	Subtropical (12°C–20°C)	Temperate (7°C–11°C)	Arctic (<7°C)
0–30	0.070	0.080	0.100	0.120
30–100	0.060	0.070	0.080	0.100
100–300	0.070	0.080	0.090	0.110
>300	0.090	0.100	0.110	0.110

by silt or ice. They further assume that the seawater at the surface is saturated with air (i.e., at 0.2 bar oxygen partial pressure).

The data in Tables 6.11 and 6.12 reflect the expected influence of seawater temperature and depth on the properties of a calcareous scale formed by CP and of the content of dissolved oxygen content. The properties of such layers are dependent on the seawater ambient temperature and, moreover, on certain depth-dependent parameters other than temperature. Oxygen is dissolved in the surface layer (by dissolution from air and photosynthesis) such that the oxygen content at a large depth in a tropical region is likely to be substantially lower than in temperate or Arctic surface waters of the same ambient seawater temperature. The higher design current densities in the uppermost zone are a result of wave forces and marine growth on degradation of calcareous scales and convective mass transfer of oxygen. In certain areas, decomposition of organic material may reduce and ultimately consume all oxygen in the seawater. No such reduction in oxygen content is accounted for in Tables 6.11 and 6.12.

In the case of bare steel surfaces buried in sediments, a design current density (initial/final and average) of 0.020 A/m^2 is recommended irrespective of geographical location and depth.

In the uppermost layer of seabed sediments, bacterial activity may be the primary factor determining the CP current demand.

Further down into sediments, the current will be related to hydrogen evolution.

The additional CP current density is to account for increased convective and diffusive mass transfer of oxygen induced by heat transfer.

The design current densities in Tables 6.11 and 6.12 shall also apply for surfaces of any stainless steel or nonferrous components of a CP system, which includes components in C-steel or low-alloy steel. For calculation of anode current output, a protective potential of -0.80 V shall then also apply for these materials.

Based on DNV, for aluminum components, or those coated with either aluminum or zinc, a design current density of 0.010 A/m^2 is recommended for initial/final as well as mean values. For internally heated components, the design current density shall be increased by 0.0002 A/m^2 for each °C that the metal/seawater is assumed to exceed 25°C.

The current density available to the structural steel surfaces shall be sufficient, at any time during the design life of the protected structure, to achieve the required potential range and maintain a calcareous deposit.

Locally determined maintenance current densities, if applied, shall be based upon well documented monitoring of cathode protection current densities. Locally determined values shall be provided by the principal and documented in detail.

Coating breakdown factors for cathodic protection design

The use of nonmetallic coatings is very important as it will reduce the CP current demand of the protection object and, hence, the required anode weight. For weight-sensitive structures with a long design life, the combination of a coating and CP is likely to give the most cost-effective corrosion control. For some systems with very long design lives, CP may be impractical unless combined with coatings.

The use of coatings should be considered for applications where the demand for CP of bare metal surfaces is known or expected to be high. This includes deep-water applications for which the formation of calcareous deposits may be slow. It should further be considered for surfaces that are partly shielded from CP by geometrical effects.

For large and complex structures like, for example, multiwell subsea production units, extensive use of coating is required to limit the overall current demand and to ensure adequate current distribution. To compensate for this, the design coating breakdown factors to be used for CP design are deliberately selected in a conservative manner to ensure that a sufficient total final current output capacity is installed. As a consequence, any calculations of the electrolytic voltage drop away from the anodes (e.g., by means of finite or boundary element analyses) and using these coating breakdown factors may result in excessively high CP in terms of the estimated protection potential.

This will primarily apply to relatively long design lives when the calculated coating breakdown, and hence current demands and electrolytic voltage drop, increase exponentially.

The application of coatings may not be suitable for parts of submerged structures requiring frequent inspection for fatigue cracks, for example, critical welded nodes of jacket structures.

Metallic coatings on zinc or aluminum bases are compatible with galvanic anode CP. However, compared to organic coatings, they have not been considered to afford any advantage in decreasing the current demand for CP. Zinc-rich primers have been considered unsuitable for application with CP due to susceptibility to low electrical resistivity, leading to high CP current demand.

The coating breakdown factor, f_c, describes the anticipated reduction in cathodic current density due to the application of an electrically insulating coating. When $f_c = 0$, the coating is 100% electrically insulating, thus decreasing the cathodic current density to zero. $f_c = 1$ means that the coating has no current-reducing properties.

The coating breakdown factor should not be confused with coating degradation as apparent by visual examination. A coating showing extensive blistering may still retain good electrically insulating properties. Conversely, an apparently perfectly coated surface may allow a significant passage of current.

The coating breakdown factor is a function of coating properties, operational parameters, and time. As a simple engineering approach, f_c can be expressed as:

$$f_c = a + b \cdot t \tag{6.10}$$

where t is the coating lifetime in, years, and a and b are constants which are dependent on coating properties and the environment.

The effect of marine growth is highest in the upper 30 m where wave forces may further contribute to coating degradation.

Another factor is periodic cleaning of marine growth in this zone.

Owner should preferably specify constants a and b for calculation of coating breakdown factors based on their own practical experience of specific coating systems in a particular environment. When the owner has not specified any such data, the default values in Table 6.13 shall be used.

Once a and b are defined, mean and final coating breakdown factors, f_{cm} and f_{cf}, respectively, to be used for CP design purposes, are to be calculated by introducing the CP design life, t_f (years):

Table 6.13 Recommended constants a and b for calculation of paint coating breakdown factors.

Depth (m)	**Recommended a and b values for coating categories I, II, III**		
	I ($a = 0.10$)	**II ($a = 0.05$)**	**III ($a = 0.02$)**
0–30 >30	$b = 0.10$ $b = 0.05$	$b = 0.025$ $b = 0.015$	$b = 0.012$ $b = 0.008$

$$f_{cm} = a + 0.5\, b\, t_f \tag{6.11}$$

$$f_{cf} = a + b \cdot t_f \tag{6.12}$$

For certain protection objects, with large uncoated surfaces, the initial coating breakdown factor, $f_{ci} = a$, may be applied to calculate the initial current demand to include coated surfaces.

If the calculated value exceeds 1, $f_c = 1$ shall be applied in the design. When the design life of the CP system exceeds the actual calculated life of the coating system, f_{cm} may be calculated as:

$$f_{cm} = 1 - \frac{(1-a)^2}{2 \cdot b \cdot t_f} \tag{6.13}$$

To account for the effect of a coating system on coating breakdown factors, three "coating categories" have been defined for inclusion in Table 6.13.

The criteria for the three categories as follows:

Category I: One layer of epoxy paint coating is not less than 20 μm nominal of dry film thickness;
Category II: One or more layers of marine paint coating by epoxy, polyurethane, or vinyl based with total nominal dry film thickness not less than 250 μm;
Category III: Two or more layers of marine paint coating by epoxy, polyurethane, or vinyl based, with total nominal dry film thickness not less than 350 μm.

Note that category (I) includes shop primer type of coatings. It is assumed for categories II and III that the supplier-specific coating materials to be applied have been qualified by documented performance in service, or by relevant testing. It is further assumed for all three categories that all coating work has been carried out according to manufacturer's recommendations and that surface preparation has included blast cleaning to minimum SA 2.5 in accordance with ISO 8501. The surface roughness shall be controlled according to the manufacturer's recommendation. For any coatings applied without blast cleaning surfaces, a coating breakdown factor of f_{cm} and f_{cf} will be taken equal to 1, while the initial current demand may be calculated as for category I.

Published data on the performance of coatings on cathodically protected structures are scarce, in particular for long service lives. The data in Table 6.13 should therefore be regarded as rather coarse but conservative engineering judgments. For any coating system not covered by the three coating categories above and with major potential effect on the overall current demand, the owner should specify or accept the applicable constants a and b.

The values of the factors a and b for a depth 30−100 m in Table 6.13 are applicable to calculations of current demands of flooded compartments and of closed compartments with free access to air.

It is worth mentioning that the constants in Table 6.13 do not account for significant damage to paint coatings during fabrication and installation. Therefore if such

damage is anticipated, the affected surface area is to be estimated and included in the design calculations as bare metal surface.

From the technical practice of Shell (1995), the paint coating category (I) is not applicable for structure nodes, the surface areas of welds and up to 0.25 m adjacent to the welds, shall be assumed to be bare and included for the calculation of current requirements.

The average and final coating coverage and breakdown factors shall be determined for the coated surface in each zone.

Galvanic anode material design parameters

Unless otherwise specified or accepted by the owner, the compositional limits for alloying and impurity elements for Al- and Zn-based anodes in Table 6.14 shall apply. The CP design parameters related to anode material performance are:

- design electrochemical capacity, ε (Ah/kg);
- design closed circuit anode potential, E_{oa} (V).

The design electrochemical capacity, ε (Ah/kg), and design closed circuit anode potential, E_{oa} (V). are used to calculate the design anode current output and the required net anode mass using Ohm's and Faraday's laws, respectively.

The design values for electrochemical capacity, ε (Ah/kg), in Table 6.14 shall be used for design unless otherwise specified or accepted by the owner. The data are applicable for ambient temperature seawater (i.e., up to 30°C as a yearly mean value).

Data on anode electrochemical efficiency from short-term laboratory examinations of galvanic anode materials will typically result in values close to the theoretical limit (e.g., $\geq$2500 Ah/kg for Al−Zn−In material). This is due to the relatively high anodic current densities that are utilized for testing. Such data shall not replace the recommended design values for electrochemical capacity at sea ambient temperatures. The use of electrochemical capacity greater than the default values based on DNV RPB401 (2005) in Table 6.15 should be justified by long-term testing.

Table 6.14 Recommended compositional limits for Al-based and Zn-based anode materials.

Alloying/impurity element	Zn-based	Al-based
Zn	na	2.5−5.75
Al	0.10−0.50	na
In	na	0.015−0.040
Cd	$\leq$0.07	$\leq$0.002
Si	na	$\leq$0.12
Fe	$\leq$0.005	$\leq$0.09
Cu	$\leq$0.005	$\leq$0.003
Pb	$\leq$0.006	na

na; not available

Table 6.15 Recommended design electrochemical capacity and design potential voltage for anode materials

Anode material type	Environment	Electrochemical capacity (Ah/kg)	Closed circuit potential (V)
Al-based	Seawater	2000	−1.05
	Sediments	1500	−0.95
Zn-based	Seawater	780	−1.00
	Sediments	700	−0.95

Even such testing will tend to result in slightly nonconservative values as the testing time is still relatively short and the anodic current density relatively high compared to the working conditions for real anodes. The design values for closed circuit anode potential, E_o a (V), in Table 6.15 shall be used for design. The data are applicable for all ambient seawater temperatures (i.e., maximum 30°C yearly average).

Anode resistance formulas

Unless otherwise agreed, the anode resistance, R (ohm), shall be calculated using the following formula that is applicable to the actual anode shape. Calculations shall be performed for the initial anode dimensions and for the estimated dimensions when the anode has been consumed to its utilization factor.

1. For long slender standoff $L \geq 4r$

$$R = \frac{\rho}{2\pi L}\left(\ln\frac{4L}{r} - 1\right) \tag{6.14}$$

where L is the anode length, ρ is the sea water resistivity, (ohm m), and r is the effective anode radius.

2. For short slender standoff $L < 4r$

$$R = \frac{\rho}{2\pi L}\left[\ln\left\{\frac{2L}{r}\left(1 + \sqrt{1 + \left(\frac{r}{2L}\right)^2}\right)\right\} + \frac{r}{2L} - \sqrt{1 + \left(\frac{r}{2L}\right)^2}\right] \tag{6.15}$$

The equation is valid for anodes with a minimum distance 0.30 m from the protection object. For an anode to object distance of less than 0.30 m but a minimum of 0.15 m the same equation may be applied with a correction factor of 1.3.

3. Long flush-mounted as L more than or equal to four times width and also thickness.

$$R = \frac{\rho}{2.S} \tag{6.16}$$

For noncylindrical anodes; $r = c/(2\pi)$ where c in m is the anode cross-sectional periphery. S is the arithmetic mean of anode length and width.

4. Short flush-mounted, bracelet, and other types.

$$R = \frac{0.315\rho}{\sqrt{A}} \tag{6.17}$$

where A is the anode surface area.

Seawater and sediment resistivity

The seawater resistivity, ρ (ohm m), is a function of the seawater salinity and temperature. In the open sea, the salinity does not vary significantly and temperature is the main factor.

In shore areas, particularly at river outlets and in enclosed bays, the salinity will vary significantly. It is recommended that the design of CP systems in such locations is based on resistivity measurements, reflecting the annual mean value and the variation of resistivity with depth.

Compared to seawater, the resistivity of marine sediments is higher by a factor ranging from about 2 for very soft clays to approximately 5 for sand. Unless sediment data for the location are available, the highest factor shall be assumed for calculation of the resistance of any buried anodes.

In temperate regions (annual average surface water temperature 7°C−12°C), resistivity of 0.30 and 1.3 ohm m are recommended as reasonably conservative estimates for the calculation of anode resistance in seawater and marine sediments, respectively, and independent of depth. Lower values are to be documented by actual measurements, taking into account any seasonal variations in temperature.

Seawater data used shall represent the structure's local annual average conditions versus depth. If the structure is exposed to seawater of which the temperature varies more than 5°C for a depth interval, that depth interval shall be split up into separate zones that cover no more than a 5°C interval each. The depth-averaged temperature shall be used for each zone created. Seawater resistivity (ρ) shall be determined from the above figure or from local seawater resistivity measurements corrected to the average annual seawater temperature conditions.

Anode utilization factor

Anode shape and core insert configuration have a major influence on the utilization factor of any particular anode design. This factor represents the maximum volume of cast anode alloy which can be consumed before the anode can no longer deliver the current required, and it has to take into account the reduced size of the anode alloy and disbandment of the anode alloy from the core at the end-of-life.

The anode utilization factor, u, is the fraction of the anode material of an anode with a specific design that may be utilized for calculation of the net anode mass required to sustain protection throughout the design life of a CP system.

When an anode is consumed to its utilization factor, the polarizing capacity (as determined by the anode current output) becomes unpredictable due to loss of support of anode material, or a rapid increase in the anode resistance due to other factors.

Table 6.16 Recommended anode utilization factors for cathodic protection (CP) design calculations.

Anode type	Anode utilization factor
Long slender stand-off $L \geq 4r$	0.90
Short slender stand-off $L < 4r$	0.85
Long flush-mounted $L \geq$ width and $L \geq$ thickness	0.85
Short flush-mounted, bracelet, and other types	0.80

The utilization factor is dependent on the anode design, particularly its dimensions and the location of anode cores. Unless otherwise agreed, the anode utilization factors in presented in Table 6.16 based on DNV RPB401 shall be used for design calculations and based on BS An anode utilization factor of 0.90 for the long slender stand-off type shall be used.

Current drain design parameters

All items which are expected to become electrically connected to a CP system shall be considered in current drain calculations.

Complex offshore structures often include temporary or permanent components which are not considered to require CP but will drain current from the CP system as the mooring systems for floating installations or secondary structural components such as piles and skirts which can readily tolerate some corrosive wear or casings installed in the sea bed and do not need corrosion protection for structural purposes due to high wall thickness relative to expected corrosion rates.

Calculations of current drain shall use the design current densities and coating breakdown factors for items requiring CP. Calculations of surface areas and current demands shall be carried out.

The design current densities and coating breakdown factors, respectively, are applicable for the calculation of current drains to components that are not considered to need CP, but will be or are expected to be electrically connected to the protection object by the CP system being designed.

For buried surfaces of mud mats, skirts, and piles, a current drain value of 0.020 A/m^2 shall be accounted for, based on the outer external surface area which is exposed to sediment. In some cases and based on the owner specification for parts of steel skirts and piles to be buried in sediments, a current density (initial/final and average) of 0.025 A/m^2 shall be used. The current drain to open pipes shall cover an internal surface area equivalent to 10 times π times their respective diameter.

For open pile ends, the top internal surface shall be included for a distance of five times the diameter and shall be regarded as seawater exposed. Internal surfaces of piles filled with sediments do not have to be included.

Unless otherwise specified or accepted by the owner, a current drain of 5 A/well casing shall be included in current drain calculations.

Casings for subsea wells are typically cemented, which reduces the current drain compared to platform wells which are normally not cemented. However, subsea wells may become exposed to significant current drain during installation and work-over equipment during subsea installations and interventions.

Current drain to anchor chains shall be accounted for by 30 m of chain for systems with mooring point topside only. For systems with a mooring point below the water level, the seawater-exposed section above this point shall also be included. A current drain of 30 m of chain shall also be included for CP of anchoring arrangements using chains.

6.4.7 Cathodic protection calculation and design procedures

For large protection objects such as platform substructures, the detailed design of a CP system is normally preceded by a conceptual design activity. During this conceptual design, the type of anodes and fastening devices should be selected, taking into account forces exerted on anodes during installation and operation. Moreover, any coating systems to be applied to specific areas or components would also normally be specified, allowing for a preliminary calculation of current demands for CP and the associated total net mass of anode material required.

If no CP conceptual report has been prepared, then the premises and basic concepts for detailed CP design shall be defined by the purchaser in some other reference document(s) to be included in an inquiry for CP detailed design.

The following information and any optional requirements (intended as a checklist) shall be provided by the purchaser:

- Conceptual CP design report;
- Design life of CP system to be installed;
- Relevant information from the project design basis; for example, salinity and temperature as a function of depth for calculation of anode resistance, location of seawater level and mud line for platform substructures, environmental and installation parameters affecting forces exerted on anodes;
- Structural drawings and information of coating systems as required for calculation of surface areas to be protected, including components which may exert temporary or permanent current drain;
- Identification of any interfaces to electrically connected components/systems with self-sufficient CP systems, for example, pipelines;
- Requirements to documentation and third party verification, including schedule for supply;
- Any specific requirement to CP design parameters to be applied, for example, coating breakdown factors and current drain to wells;
- Any specific requirements to anode material and anode design;
- Any further amendments and deviations to this RP applicable to CP design.

The purchaser shall ensure that valid revisions of drawings and specifications affecting calculation of current demand for CP and location of anodes are available

to the contractor during the design work. It shall be ensured that all necessary information is provided for the contractor to calculate the overall current demand, for example, conductors for production platform substructures and production control system for subsea valve trees.

In the design of CP systems for large and/or complex objects, it is always convenient to divide the protection object into units to be protected.

The division into units may be based on, for example, depth zones or physical interfaces of the protection object such as retrievable units within a subsea production system.

Current demand calculations

To calculate the current demand, I_c (A), to provide adequate polarizing capacity and to maintain CP during the design life, the individual surface areas, A_c (m^2), of each CP unit shall be calculated and multiplied by the relevant design current

$$I_c = A_c \cdot i_c \cdot f_c \tag{6.18}$$

Design current density, i_c (A/m^2), and the coating breakdown factor, f_c, and if applicable i_c and f_c are then to be selected, respectively.

It is practical to apply some simplification when calculating surface areas for objects with complex geometries.

However, it shall be ensured that the overall result of any such simplification is conservative.

For major surface areas, an accuracy of from -5% to $+10\%$ is adequate. For smaller components, the required accuracy may be lower depending on whether or not a coating will be applied to such items and to the major surfaces.

Surface area calculations for each unit shall be documented in the CP design report. Reference shall be made to drawings, including revision numbers.

The contractor shall make sure that all items affecting CP current demand are included in the surface area calculations. This may include various types of outfitting to be installed by different contractors.

For subsea production systems, production control equipment is typically manufactured from uncoated stainless steel (piping components, couplings, connectors, cable trays, etc.), which constitutes a significant current demand. remotely operating vehicle override components are also often manufactured from stainless steel without a coating.

Moreover, some components like valve blocks and hydraulic cylinders may have a coating applied directly to machined surfaces, increasing the coating breakdown factor to be used for design.

For items with major surfaces of uncoated metal, the CP current demands for both initial polarization and for polarization at the end of the design life, I_{ci} (A) and I_{cf} (A), respectively, shall be calculated, together with the mean current demand required to maintain CP throughout the design period, I_{cm} (A). For protection objects with current demand primarily associated with coated surfaces, the initial

current demand can be deleted in the design calculations. For future reference, all calculated data shall be documented in the design report.

Selection of anode type

The anode types, such as stand-off, flush-mounted, or bracelet anodes, may be specified by the owner, taking into account effects of, for example, sea current drag and interference with subsea interventions.

If the anode type has not been specified by the owner, then the contractor shall select the anode type taking into account, for example, net anode mass to be installed and available space for location of anodes. The anode type further affects the anode utilization factor and the anode current output in relation to weight.

Long stand-off type anodes are usually preferred for relatively large anodes (about 100 kg or more) to be installed on platform substructures and subsea templates. A flush-mounted anode with the same net anode mass will have a lower anode current output and lower utilization factor.

Anode mass calculations

The total net anode mass, M_a (kg), required to maintain CP throughout the design life, t_f (years), is calculated from I_{cm} (A) for each unit of the mean current demand including any current drain:

$$M_a = \frac{8760 I_{cm} \cdot t_f}{u \cdot \varepsilon} \tag{6.19}$$

Calculation of anode number

From the anode type selected, the number of anodes (N), anode dimensions, and anode net mass, ma (kg), shall be defined to meet the requirements for:

1. initial/final current output, I_{ci}/I_{cf} (A) and
2. anode current capacity C_a (Ah)

which relate to the CP current demand, I_c (A), of the protection object.

The preliminary sizing of anodes should be based on commercially available products, requiring liaison with potential anode vendors.

The individual anode current output, I_a (A), required to meet the current demand, I_c (A), is calculated from Ohm's law:

$$I_c = N \cdot I_a = \frac{N(E_{co} - E_{ao})}{R} = \frac{N \cdot \Delta E_o}{R} \tag{6.20}$$

where I_a (A) is the individual anode current output, E_{ao} (V) is the design closed circuit potential of the anode material, and R (ohm) is the anode resistance. The initial

and final current output, I_{ai} and I_{af}, are calculated using the initial and final anode resistances, R_{ai} and R_{af}, respectively.

For calculation of anode resistance, E_{co} (V) is the design protective potential which is −0.80 V. ΔE_o (V) is termed the design driving voltage.

As the design driving voltage in Eq. (6.20) is defined using the design protective potential for C-steel, the initial/final design current densities that define the anode current output capacity, and hence the driving voltage, refer to the required anode current output at this potential. Hence, the initial/final design current densities given in Table 6.11 are based on a protection potential of −0.80 V. This means that they shall always be used for calculations according to Eq. (6.20) in combination with this potential, also if a more negative protection potential (e.g., ≤ -0.90 V) is aimed.

The individual anode current capacity, C_a ($A \cdot h$), is given by:

$$C_a = m_a \cdot \varepsilon \cdot u \tag{6.21}$$

where m_a (kg) is the net mass per anode. The total current capacity for a CP unit with N anodes thus becomes $N \cdot C_a$ (A · h)

Calculations shall be carried out to demonstrate that the following requirements are met:

$$C_{at} = N \cdot C_a \geq 8760 \cdot I_{cm} \cdot t_f \tag{6.22}$$

$$I_{ati} = N \cdot I_{ai} \geq I_{ci} \tag{6.23}$$

$$I_{atf} = N \cdot I_{af} \geq I_{cf} \tag{6.24}$$

C_{at} in Eq. (6.22) is the total anode current capacity. $I_{cm}/I_{ci}/I_{cf}$ in Eqs. (6.22)–(6.24) are the current demands of a CP unit, including any current drain, and 8760 is the number of hours per year. I_{ai} and I_{af} in Eqs. (6.23) and (6.24) are the initial and final current outputs for the individual anodes.

If anodes with different sizes and hence, anode current capacities, C_a (Ah), and current outputs, I_a (A), are utilized for a CP unit, $N \cdot C_a$ and $N \cdot I_{ai}/N \cdot I_{af}$ will have to be calculated for each individual size and then added for calculation of the total anode current capacity (C_{at}) and total anode current output (I_{ati}/I_{atf}).

If the above criteria cannot be fulfilled for the anode dimensions and net mass initially selected, another anode size shall be selected and the calculations repeated until the criteria are fulfilled.

Optimizing the requirements in Eqs. (6.22)–(6.24) is an iterative process where a simple computer spreadsheet may be helpful. In general, if Eq. (6.22) is fulfilled, but not Eqs. (6.23) and/or (6.24), a higher number of smaller anodes, or the same number of more elongated anodes are to be used. On the other hand, if $N \cdot I_a$ in Eqs. (6.23) and (6.24) is much larger than I_{ci} and I_{cf}, fewer and/or more compact anodes may be applied.

Unless a high initial current capacity is deliberately aimed for, as in the case of protection objects consisting primarily of uncoated metal surfaces, the anodes to be

installed should have a similar anode current output (I_a) to the net anode mass (m_a) ratio. Small anodes with high anode current output to net mass ratio will be more rapidly consumed than large anodes with a higher ratio, which could result in an insufficient total anode current capacity toward the end of the design life.

For anodes with the same anode resistance and hence, same anode current output, but a major difference in net anode mass (i.e., due to different anode geometry), the anode with the lowest net anode mass will be consumed first. Similarly, for anodes with the same net anode mass but with a major difference in anode resistance and hence, anode current output, the anode with the lowest anode resistance will be consumed first.

From a practical point of view the following factors shall be used:

Design protective potential (E_{oc}) = −0.800 Volts Ag/AgCl/seawater;
Design closed circuit potential (E_{oa}) = −1.050 Volts Ag/AgCl/seawater.

The anode current output shall be calculated for the initial and final life of the CP system.

In the latter case anodes of 10% remaining mass shall be used.

The number of anodes shall be computed for the structure's initial and final currents, and the structure's current capacity, by zone, as follows:

Anodes for initial current needs (n)	=	I_c (initial)/I_a (initial)
Anodes for final current needs (n)	=	I_c (final)/I_a (final)
Anodes for current capacity (n)	=	M/m [m = mass of anode material per anode]

The number of anodes provided within each zone shall be greater than the required numbers as calculated by zone, and also greater than the minimum number of anodes required to assure adequate current capacity and proper current distribution.

The total number of anodes required shall be the sum of those needed for the three zones.

Calculation of anode resistance

The anode resistance, R (ohm), shall be based on the applicable Eqs. (6.14)−(6.17), using the actual anode dimensions and specific resistivity of the surrounding environment.

To calculate the initial anode resistance, R_i (ohm), the initial anode dimensions are inserted in the relevant anode resistance equations from Eqs. (6.14)−(6.17). The final anode resistance, R_f (ohm), is calculated based on the expected dimensions when the anode has been consumed to its utilization factor, u, as explained earlier.

When the anode has been consumed to its utilization factor, u, at the end of the design life, t_f (years), the remaining net anode mass, m_f (kg), is given by:

$$m_f = m_i \cdot (1 - u) \tag{6.25}$$

The final volume of the anode to be used for calculation of R can be calculated from the remaining net anode mass, m_f (kg), specific density of anode material, and the volume of insert materials. When details of anode inserts are not available, their volume should either be neglected or estimated to give a conservative approach.

For long and short slender stand-off anodes consumed to their utilization factor, a length reduction of 10% shall be assumed. Furthermore, assuming that the final anode shape is cylindrical, the final radius shall be calculated based on this length reduction, and the final anode mass/volume.

For long and flush-mounted anodes, the final shape shall be assumed to be a semicylinder and the final length and radius shall be calculated as above.

For short flush-mounted anodes, bracelet anodes and other shapes mounted flush with the protection object, the final exposed area shall be assumed to be equivalent to the initial area facing the surface to be protected.

Anode quantities have been calculated to ensure the correct total net mass of anode material is provided based on mean current density requirements and to be capable of providing sufficient current to maintain polarization throughout the 25-year design life of the platforms.

The total mass of sacrificial alloy required to protect the each platform and pipeline is calculated using the following formula

$$W = \frac{t_f \cdot E \cdot I_{cm}}{u} \tag{6.26}$$

where W is the total net anode weight alloy in kg, t_f is the design life per years, E is the consumption rate of anode alloy (kg/year), I_{cm} is the mean current to protect the structure, and u is the utilization factor.

Once the total weight of anode material has been calculated for each area to be protected the quantity of anodes is obtained by dividing the specified anode unit net weight into the total weight:

$$\text{Number of anodes} = \text{total weight}/\text{anode net weight}$$

The number of anodes for each area should also be capable of providing sufficient current throughout the remaining design life of the structure to maintain polarization.

This is verified by calculating the initial, mean, and final current output of each anode type used and comparing this with the platform or pipeline current demands based on surface areas and specified current densities.

The following formula is used to calculate long slender flush fit anode resistance:

$$\text{Number of anodes} = \text{Total weight}/\text{net weight of anode}$$

The above equation is valid for anodes with a minimum stand-off distance of 300 mm from the structure. A correction factor of 1.3 is applied for anodes between 150 and 300 mm from the structure.

For the initial anode resistance calculation, the anode resistance equation is a function of the initial anode dimensions. The final anode resistance is calculated based on the expected dimensions when the anode has been consumed to its utilization factor.

For long slender stand-off anodes consumed to their utilization factor, a length reduction of 10% shall be assumed.

Furthermore, assuming that the final anode shape is cylindrical, the final radius shall be calculated based on this length reduction, and the final anode mass/volume. For long flush anodes, the final shape shall be assumed to be semicylindrical.

Anode design precaution

The contractor shall specify in the CP design report tentative dimensions and/or net mass for anodes to be used.

For anodes that may become subject to significant forces during installation and operation, the design of anode fastening devices shall be addressed in the design report. Special considerations apply for large anodes to be installed on structural members subject to fatigue loads during pile-driving operations. Doubler and/or gusset plates may be required for large anodes.

For use of the anode resistance formula in Table 6.17 for stand-off type anodes, the minimum distance from anode to protection object shall be a minimum of 300 mm. However, for distances down to 150 mm, the formula can still be used by multiplying the anode resistance with a factor of 1.3.

The detailed anode design shall ensure that the utilization factor assumed during calculations of required anode net mass is met. Hence, it shall be ensured that the anode inserts are still likely to support the remaining anode material when the anode has been consumed to its design utilization factor. Unless otherwise agreed, anode cores of standoff type anodes shall protrude through the end faces.

With the exception of stand-off type anodes, a marine grade paint coating (min. 100 μm DFT) shall be specified for anode surfaces facing the protection object.

Distribution of anodes

The calculated number of anodes, N, for a CP unit shall be distributed to provide a uniform current distribution, taking into account the current demand of individual members due to different surface areas and any coatings used. On platform substructures, special areas to be considered when distributing anodes are, for example, nodes, pile guides, and conductor bundles. The location of all individual anodes shall be shown on drawings.

Whenever practical, anodes dedicated to the CP of surfaces buried in sediments shall be located freely exposed to the sea.

Table 6.17 Steps of cathodic protection (CP) design.

Item	Calculation and equations	Input/output data
Coating breakdown		
Jacket HAT to −3000 and risers all depths uncoated at installation		0.350
Jacket −3000 to mud line uncoated at construction		0.35
Jacket coating damaged prior to placement		1.00
Jacket f_c (initial) total factor at placement		0.00
Conductor coating damaged during construction		1.00
Coating breakdown factor per RP B401 paragraph 6.4.4		1.00
Average factor	$F_c\ (average) = a + b \cdot t_f/2$ $F_c\ (final) = a + b \cdot t_f$	
Average breakdown factors		
Jacket: HAT to −3.0	$F_c\ (average) = a + b \cdot t_f/2$	0.475
Jacket: −3.0 to −30.0	Bare	1.0
Jacket: −30.0 +		1.0
Conductors: HAT to −3.0		1.0
Conductors: −3.0 to −30.0		1.0
Conductors: −30.0 +		1.0
Risers: HAT to −3.0		0.472
Risers: −3.0 to 30.0		0.472
Risers: −30.0 +		0.472
Final breakdown factors		
Jacket: HAT to −3.0		0.6
Jacket: −3.0 to −30.0		1.0
Jacket: −30.0 +		1.0
Conductors: HAT to −3.0		1.0
Conductors: −3.0 to −30.0		1.0
Conductors: −30.0 +		0.6
Risers: HAT to −3.0		0.6
Risers: −3.0 to 30.0		0.6
Risers: −30.0 +		

(*Continued*)

Table 6.17 (Continued)

Current demand jacket				
I_c **(initial)**				
Zone	A_c **(m²)**	F_c **(initial)**	i_c **(initial) (A/m²)**	I_c **(A)**
Current demand jacket				
I_c **(initial)**				
Zone	A_c **(m²)**	F_c **(initial)**	i_c **(initial) (A/m²)**	I_c **(A)**
Jacket: HAT to −3.0 Jacket: −3.0 to −30.0 Jacket: −30.0 +	67.3563 692.6240 0.00	0.350 1.0 1.0	0.035 0.035 0.035	0.825 24.242 0.00
I_c (average)				
Jacket: HAT to −3.0 Jacket: −3.0 to −30.0 Jacket: −30.0 +	67.3563 692.6240 0.00	0.475 1.0 1.0	0.035 0.035 0.035	1.120 24.242 0.000
I_c (final)				
Jacket: HAT to −3.0 Jacket: −3.0 to −30.0 Jacket: −30.0 +	67.3563 692.6240 0.00	0.60 1.0 1.0	0.035 0.035 0.035	1.414 24.242 0.000
Current demand conductors				
$\mathbf{I_c}$ ***(initial)***				
Conductors: HAT to −3.0 Conductors: −3.0 to −30.0 Conductors: −30.0 +	30.099 151.736 0.00	1 1 1	0.035 0.035 0.035	1.053 5.311 0.000
$\mathbf{I_c}$ **(average)**				
Conductors: HAT to −3.0 Conductors: −3.0 to −30.0 Conductors: −30.0 +	30.099 151.736 0.00	1 1 1	0.035 0.035 0.035	1.053 5.311 0.000
$\mathbf{I_c}$ ***(final)***				
Conductors: HAT to −3.0 Conductors: −3.0 to −30.0 Conductors: −30.0 +	30.099 151.736 0.00	1 1 1	0.035 0.035 0.035	1.053 5.311 0.000

(*Continued*)

Table 6.17 (Continued)

Current demand jacket				
I_c (initial)				
Zone	**A_c (m^2)**	**F_c (initial)**	**i_c (initial) (A/m^2)**	**I_c (A)**
Riser demand conductor				
I_c ***(initial)***				
Risers: HAT to −3.0	11.124	0.35	0.035	0.136
Risers: −3.0 to 30.0	56.076	0.35	0.035	0.687
Risers: −30.0 +	0.00	0.35	0.035	0.00
I_c (average)				
Risers: HAT to −3.0	11.124	0.475	0.035	0.185
Risers: −3.0 to 30.0	56.076	0.475	0.035	0.932
Risers: −30.0 +	0.00	0.475	0.035	0.00
I_c (final)				
Risers: HAT to −3.0	11.124	0.60	0.035	0.234
Risers: −3.0 to 30.0	56.076	0.60	0.035	1.178
Risers: −30.0 +	0.00	0.60	0.035	0.00
Pile penetration I_c (initial/final and average)	634.219	1.00	0.01	6.342
Well casing	4 × (2.5) A/well			10
Total drain current required				16.342
Current demand for jacket buried				
I_c (initial)	49.551	1.00	0.01	0.496
I_c (Average)	49.551	1.00	0.01	0.496
I_c (final)	49.551	1.00	0.01	0.496
Total initial current I_c (initial)				49.092
Total average current I_c (average)				49.681
Total final current I_c (final)				50.269
	Mass (M) = I_c (average) × t_f × 8760/(u × e)			
Electrochemical anode efficiency				2.0
Utilization factor				0.90
Mass required				
I_c *(ave ttl)*	49.681			
I_c *(ave ttl)* × t_f × 8760/(u × e)	Total mass			6044 kg

(*Continued*)

Table 6.17 (Continued)

Current demand jacket				
***I_c* (initial)**				
Zone	**A_c (m^2)**	**F_c (initial)**	**i_c (initial) (A/m^2)**	**I_c (A)**
Anode resistance calculations				
Anode initial physical dimensions				
Anode length				2.420 m
Anode width				0.187 m
Anode depth				0.170
Anode radius				0.114 m
Alloy density				2700 kg/m^3
Net anode volume				0.06 m^3
Anode mass				189.76 kg
Anode final physical parameters	Anode final mass *m(final) = m (initial)* × *(1 − u)*			18.976 kg
	Anode final length *L*(final) = *L (initial) − 0.10* × *u* × *L(initial)*			2.202 m
Anode resistance, *R* (initial)				0.0453 Ω
Anode resistance, *R* (final)				0.0622 Ω
	Anode Output $(I_a) = (E_c - E_a)/R$			
Anode (Al) closed circuit potential				−0.95 V
Protected cathode potential				−0.80 V
Anode driving potential				0.15 V
Anode output I_a *(initial)*				3.310 A
Anode output I_a *(final)*				2.412 A
Anode number calculation				
Total initial current/I_a *(initial)*				14.829
Total initial current/I_a *(initial)*				15.0
Total final current/I_a *(final)*				20.845
Total final current/I_a*(final)*	Rounded up to integer			21.00
Anode number				32
Initial current available from anode number above				105.935 A
Total initial current required per calculation				49.092 A
Difference of initial current available and initial current required	Initial surplus			57 A
Final current available from anode number above				77.172 A
Total final current required per calculation				50.269 A

(*Continued*)

Table 6.17 (Continued)

Current demand jacket				
I_c (initial)				
Zone	**A_c (m^2)**	**F_c (initial)**	**i_c (initial) (A/m^2)**	**I_c (A)**
Difference of final current available and final current required	Final surplus			26.90 A
Mass check				
Mass of anodes per distribution				6072 kg
Mass required for life				6044 kg
Difference of mass available and mass required	Mass surplus			28 kg
Average current from mass for design life				55 A
Anode gross weight calculation				
Anode unit gross weight estimate				216
Anode gross weight estimated on numbers above				6912 kg
Total gross weight				6912 kg

HAT, Highest astronomical tide.

Anodes shall be located with sufficient spacing between each other to avoid interaction effects that reduce the useful current output. As far as practical, anodes shall be located so that those of its surfaces intended for current output are not in close proximity to structural members, reducing the current output.

With the exception of very large anodes, shielding and interference effects become insignificant at a distance of about 0.5 m or more. If anodes are suspected to interfere, a conservative approach may be to consider two adjacent anodes as one long anode, or as one wide anode, depending on their location in relation to each other.

No anodes shall be located for welding to pressure-containing components or areas with high fatigue loads. For the main structural components the minimum distance from anode fastening welds to structural welds shall be 150 mm. On jacket structures, no anodes shall be located closer than 600 mm to nodes.

The location of anodes shall take into account restrictions imposed by fabrication, installation, and operation.

Sequential priority for anode placement should be based upon the following:

1. Anode distribution should normally begin with placement upon larger members such as legs near nodes and continue to minor members.

2. Placement shall consider future added components, which in practice usually will be new conductors and risers as operations require.
3. Locations where attenuation effects will reduce good current distribution such as conductor clusters and complex pile guides which shall require a higher anode concentration.
4. Anodes shall be placed within 15 m of adjacent anodes.
5. Anodes shall be placed within 10 m of surfaces to be protected.

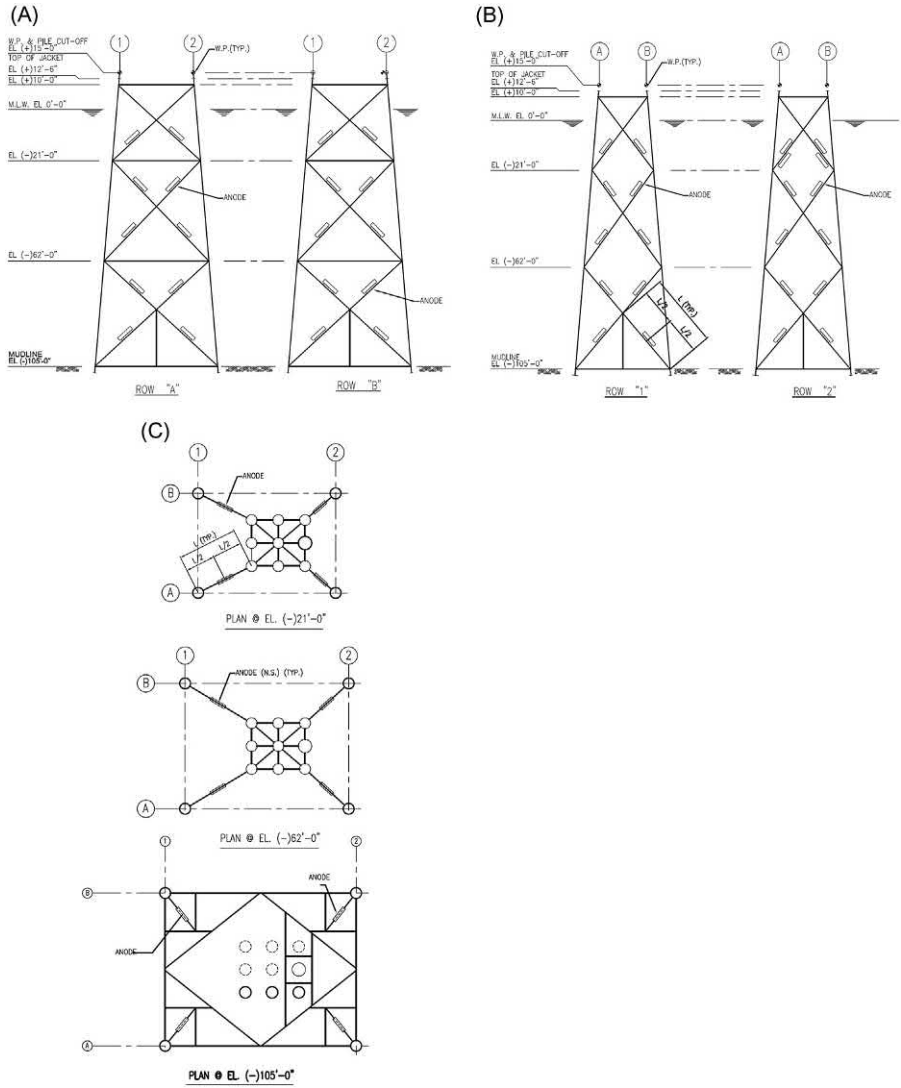

Figure 6.7 (A) The location of the anode to a four-leg platform. (B) The location of the anode to a four-leg platform for rows 1 and 2. (C) The location of the anode to a four-leg platform in a different horizontal plane.

Figure 6.8 Location of the anode in the jacket during construction.

Proper anode placement should be performed as an iterative process, in which initial design drafts are adjusted to an optimum configuration, using the above guidelines. The placement process may result in conservative adjustments to anode dimensions and in addition to the calculated total number to assure adequate current distribution.

Anodes designed to protect the buried surface area shall all be installed on the bottom elevation of the structure. Fig. 6.7A–C present the distribution of anodes (Fig. 6.8).

6.5 Design example

An example CP for an offshore structure platform is presented in Table 6.17. This table can be used as a logic step in a spread sheet to design a CP system.

6.6 General design considerations

Low-alloy steels with minimum yield stress ranging from 275 to 450 MPa are specified for substructures for fixed offshore platforms. Special attention should be given to the use of higher strength steels, particularly those with minimum yield stress above 400 MPa.

The sacrificial anodes shall be manufactured from an indium-activated aluminum alloy. The use of other aluminum activators shall be agreed by the principal. Tin-activated aluminum alloys shall not be used.

Mercury- or cadmium-activated aluminum alloys may only be considered under the circumstances that the indium-activated aluminum ones are proven to be ineffective in providing protection. However, statutory regulations limiting the use of these alloys may apply.

The core material shall be carbon steel and comply with the specification requirements for tubular structure secondary members and the core diameter and wall thickness shall be agreed with the principal. Anode core attachment by welding shall be as specified by drawings and in conformance with the welding specification for the associated structure.

Anodes shall be of the "slender stand-off" type, with a minimum stand-off (i.e., the closest distance between the aluminum alloy and the attached steel member) of 150 mm. Anodes shall have a cylindrical or trapezoidal shape. The anode core shall exit at the anode ends.

The sacrificial anode shall be an indium-activated aluminum alloy. The anode material shall have a capacity greater than 3.6 kg/A.year (efficiency = 2420 Ah/kg).

The anode material shall have a potential in the range of -1.05 to -1.15 V versus Ag/AgCl/seawater. The number of anodes, their capacity, and potential shall be sufficient to meet both the polarization and maintenance current requirements for the steel over the design temperature range.

The closed circuit anode potential (E_a°) used in design calculations for determination of indium-activated aluminum anode current output shall be -1.05 V Ag/AgCl/seawater.

The objective of the design calculations shall be to compute by iteration the number of anodes and anode dimensions to verify the following:

- Fulfill the initial current, final current, current capacity, and current distribution requirements of the structure, and
- Provide the lowest installed cost for the CP system, including cost of anode materials, molds, installation, and coating systems (if used).

To assure adequate and efficient use of the anode material, the submerged structure should be divided into "zones" to be protected. Three zones are normally classified as follow:

- *Zone 1*: The zone starts from mean sea level to just above the first horizontal member below it. The depth of this zone is either the trough depth of a 100-year extreme wave or 20 m, whichever is the larger. The calcareous coatings of this zone are subjected to damage by storm waves.
- *Zone 2*: The zone below Zone 1 and above the sea bottom.
- *Zone 3*: The zone below the sea bottom mud line.

In zone 3, instead of calculating the surface area for well casing strings extending beyond the end of the conductor, an allowance of 2.5−3 A per well shall be provided. This allowance shall be provided in addition to the surface area contributions from other components, such as conductors and piles.

The external surface area of the buried part of piles and conductors shall be included in the calculations only up to a depth of 30 m into the sea bed.

The current drain to open skirt piles, sumps, and caissons shall cover an internal surface area equivalent to 10 times π times their respective diameter.

The internal surfaces of all flooded structural members with unsealed flooding holes shall be included in the surface area calculations.

6.7 Anode manufacture

The anodes shall be manufactured in accordance with the requirements of the specification and the supplier shall submit detailed anode and steelwork manufacturing drawings, complete with tolerances, as well as manufacturing and testing procedures for the client's approval.

The stand-off supports shall be formed from single lengths of carbon steel seamless tube or bar, bent using purpose-built bending equipment of proven performance to provide the minimum clearance specified between the centerline of the anode and the nearest jacket member. The tubular supports shall have their ends square to the anode axis and to each other within a tolerance of ± 2 mm.

The bending method to be used for tubular inserts shall be proven to the purchaser's satisfaction to achieve consistent tolerances with a maximum flattering of 10% of the tube outer diameter. All production bends shall be checked for general dimensional tolerances and a minimum of 20% of bends shall be checked for flattering tolerance.

Inserts formed from flat steel bars shall be bent using reduced formers to produce bends of controlled radius. The supplier's proposed procedure shall be selected to ensure that the tolerances and acceptance criteria are fully complied with.

6.8 Installation of anodes

Installation of galvanic anodes on offshore structures will normally involve welding and sometimes also clamping of anode supports to structural steel components. In the latter case, electrical continuity is typically provided by a copper cable, attached to the anode support and the protection object by brazing, or by some special mechanical connection designed to ensure reliable electrical continuity. Electrical continuity cables may also be installed to provide electrical continuity to components of a CP unit without reliable electrical connection to anodes by welds, metallic seals, or threaded couplings. The design requirements for such connections shall apply.

Considerations of the mechanical integrity of anode fastening devices during installation and operation of the applicable structures and any special requirements shall be included in the CP detailed design report. For large anodes, the design may include use of doubler or gusset plates. No welding or brazing to pressure-containing components shall be performed.

Thermite welding is not recommended for CRAs. Alternative methods like pin brazing or soft or both soldering may be considered.

The following information and any optional requirements (intended as a checklist) shall be enclosed by the purchaser:

- anode drawings from detailed CP design, or by manufacturer if completed;
- drawings from detailed CP design showing location of individual anodes;
- any requirement for preparation;
- any special requirements for documentation.
- any further amendments to and deviations from this order

Contractor may specify that all work related to anode installation shall be described in an installation procedure specification. If applicable, this document shall include, as a minimum:

- specification of materials and equipment to be used, including certificates and material data sheets;
- receipt, handling and storage of anodes and materials for anode installation;
- reference to welding and/or brazing procedure specifications and qualification of personnel carrying out welding/ brazing;
- inspection and testing of anode fastening;
- documentation of materials and inspection records.

All welding associated with anode installation shall be qualified according to a recognized standard. Only qualified welders and/or operators of brazing equipment shall be used.

Installation of anodes shall be carried out according to drawings approved for construction, showing locations of individual anodes and any other relevant specifications for fabrication of the protection object. All welding associated with anode installation shall be carried out according to the qualified WPS and by qualified welders.

Any significant changes of anode installation from approved drawings shall be approved by the purchaser. However, for ease of installation, stand-off anodes to be mounted on structural components may be displaced laterally not more than one anode length and circumferentially a maximum of 30 degrees.

For welding of anodes to components subject to high external loads, welded connections shall be placed at least 150 mm from other welds, and a minimum 600 mm from structural nodes of jacket structures.

Installed anodes shall be adequately protected during any subsequent coating work. Any spillage of coating on anodes shall be removed. For coated objects, exposed anode cores shall be coated to the same standard.

Inspection of anode installation shall, as a minimum, include visual examination of welds and any brazed connections.

For welding to structural components, further nondestructive testing (NDT) may apply in accordance with the applicable fabrication specification.

Subsequent to completed anode installation, compliance with drawings for anode installation shall be confirmed.

For brazed and mechanical connections for electrical continuity, measurements shall be carried out according to a documented procedure and with an instrument capable of verifying an electrical resistance of 0.1 ohm maximum (Fig. 6.9).

Figure 6.9 Cow horn anode of 189 kg.

6.9 Anode dimension tolerance

In most cases, the anode tubular core shall be 80 mm NB, schedule 80 pipe, extended for the full length of the anode casting, have a minimum standoff height of 300 mm and be fabricated from ASTM 106 Grade B or similar material. Welding shall be in accordance with AWS D1.1, Structural Welding Code. Steel anode cores manufactured from channel sections are not acceptable.

The anodes shall be located on the supporting structural members to minimize the impact of wave loads on the structure.

The weight of each anode shall be within −0% to +5% surface defect tolerance.

Dimensional tolerances for the long slender stand-off anodes and flush-mounted anodes shall conform to the following:

- The smaller of 2.5% on the anode length or ± 20 mm, for anodes with tubular stand-off supports;
- The smaller of 2.5% on the anode length or ± 10 mm, for flush-mounted anodes;
- The smaller of 2.5% on the thickness, width, or diameter or ± 5 mm, for all anodes.

The straightness of each anode shall not deviate by more than 2% from the longitudinal axis over the nominal anode length.

Bends on anode tubular supports shall be checked to ensure that flattering (ovality) of the pipe due to bending is within specified limits. Wrinkling of the inside of the bend shall not be acceptable.

The core shall be centrally located within the casting length. A tolerance of ± 5% on the nominal position of the core in the anode is permitted provided the stand-off distance meets the specified minimum anode/member clearance.

The stand-off support fixing centers (to the structure) shall be within 20 mm of the nominal dimensions.

Each structural anodes shall be weighed and shall conform to the following weight tolerances:

1. Net weight of individual anodes shall be greater than 97% of the design net weight.
2. Total anode net weight supplied shall not be below the contract net weight.

6.9.1 Internal and external inspection

Verification of anode weight and dimensions shall be carried out with the frequency and acceptance criteria specified in NACE RP0387. The anode shall comply with tolerances in the manufacturer's drawings and shall be checked for a minimum of 10% of the anodes of a specific design and based on the tolerance dimensions as it is discussed before.

In any case, the anode surface should be generally free from defects affecting anode efficiency. Inspection for cracks and other surface irregularities shall be carried out on all anodes with the acceptance criteria as specified in NACE RP0387. Anodes exhibiting the following defects will be rejected:

- For zinc-based anodes, no cracks visible to the naked eye are acceptable;
- Cracks that are seen to penetrate to anode inserts are not accepted;
- Shrinkage pits or cavities exceeding 10% of depth of anode thickness;
- Cracks exceeding 2 mm in width or greater than 150 mm in length intersecting each other;
- Cracks exceeding 4 mm in width or 300 mm in length;
- Cracks penetrating to the core;
- Apparent slag or dirt inclusions;
- All anodes shall be free from slag, dross, and any other inclusions having a particle size of 2 mm or greater;
- Surface irregularity on the top anode surface due to "topping-up" during solidification of the anode shall not exceed ± 5 mm of the nominal level. Such "topping-up" shall not exceed 0.5% of the total anode alloy volume and shall be mechanically well-bonded to the main body of the anode;
- Cold shuts or surface laps shall not be permitted.

Unless otherwise agreed, a minimum of two anodes of each size shall be subject to destructive testing to verify the absence of internal defects and adequate location of anode inserts. The cutting procedure and acceptance criteria in NACE RP0387 shall apply.

As a minimum, electrochemical testing shall be performed in the first day production test for purchase orders exceeding 15,000 kg of net anode material and for each further 15,000 kg of production.

The anodes shall be transversely sectioned by single cuts at 25% and 50% of the nominal length.

The cut faces, when examined visually without magnification, shall not contain more than:

- 0.25% of surface areas as gas holes or porosity with individual pore size limited to 10 mm^2;
- 20% of the insert perimeter with voids porosity adjacent to the insert or any one face and no greater than an aggregate of 10% on all faces.

The cut faces shall be dimensionally checked to ensure compliance with the requirements of the core location. All anodes represented by a failed test shall be rejected.

Reference

Ashworth, V., 1994. Corrosion. In: 3rd edition Shreir, L.L., Jarman, R.A., Burstein, G.T. (Eds.), Corrosion Control, vol.2. Butterworth-Heinemann, Oxford, p. 10.15.

Further Reading

Aluminium and aluminium alloys. Castings. Chemical composition and mechanical properties, BS1706.

Baboian, R., 1983. Performance of platinum clad columbium impressed current anodes in fresh water. Mater. Perform. 22, 15–18.

Butler, G., Mercer, A.D., 1975. Corrosion of steel in potable waters. Nature 256, 719–720.

Design and operating guidance on cathodic protection of offshore structure subsea installation and pipeline, the marine technology director limited. 1990.

Det Norske Veritas (DNV), 1993. Recommended Practice, Cathodic Protection Design, DNV RP B401-1993.

Efird, K.D., 1982. Current waveform initiated corrosion failure of platinum niobium anodes in seawater cathodic protection systems. Mater. Perform. 21, 51–55.

Hayfield, P.C.S., 1981. Electrochemical properties of niobium in impressed current cathodic protection. Mater. Perform.

Linder, B., 1979. Magnetite anodes for impressed current cathodic protection. Mater. Perform. NACE International. Dallas, Texas. 18 (8), 17.

National Association of Corrosion Engineers (NACE), RP 0176-94 Corrosion control of steel fixed offshore platform associated with petroleum production, NACE, Houston, TX, 1994.

National Association of Corrosion Engineers (NACE), RP 0387-99 Metallurgical and inspection requirements for cast sacrificial anodes for offshore applications, NACE, Houston, TX, 1999.

Pourbaix, M., 1974. Atlas of Electrochemical Equilibria in Aqueous Solutions, NACE International, Houston, TX.

Rowlands, J.C., 1994. “Sea Water” Corrosion: Metal/Environment, third ed. Butterworth-heinennan, Oxford, pp. 2:60−2:71.

Smith, M.L., Weldon, C.P., 1997. Impressed current tensioned anode strings for offshore structures. NACE − CORROSION 97, Paper 97476, NACE International, Houston, TX.

Warne, M.A., 1979. Precious metal anodes—Options for cathodic protection. Mater. Perform. NACE International, Houston, TX. 18, 8.

Warne, M.A., Hayfield, P.C.S., 1976. Platinized titanium anodes for use in cathodic protection. Mater. Perform. Houston, TX. 15, 3.

Assessment of existing structures and repairs

7

7.1 Introduction

Worldwide, oil and gas offshore projects are experiencing the same problems as the platforms are aging due the peak of exploration and development in oil projects which started in the mid-1970s until the mid-1980s, particularly in the Middle East. These platforms are now over 40 years old. Offshore platforms are unique structures from the nature of their design, construction, and also the applied load. Offshore platforms and the normal steel structure projects or onshore concrete structures are very different. For onshore structures, there are millions of steel structures worldwide and many researches in universities for steel structure design, and there are American Institute of Steel Construction (AISC), BS, EC, and Egyptian and Indian codes, and many others because there is a huge amount of these types of structures worldwide. In addition, due to the huge amount of onshore steel structures there are many structures that have failed for different reasons which have been studied and the results included in the codes and standards, so the assessment and evaluation of old structures is easy and there are technical resources competent for this assessment. On the other hand, offshore structure platform design is usually based on American Petroleum Institute (API) RP2A. The Gulf of Mexico (GoM) was the first area in which these types of structures were constructed. Around 1960 the platforms were design based on the experience of engineering offices and the standards were based on their experience. Since developing API RP2A, there have been many developments. There are now a few thousand platforms, and of that number, very few have failed, and most of these were due to fire, which is outwith the structure capacity. Therefore there are few case studies to use in evaluating offshore structures, in addition, there are very few engineering companies that have experience in the realistic assessment of platforms compared with similar companies working with onshore structures. In the process of the assessment, structure analysis of the old platform is done manually, in addition, offshore structures have special characteristics, as the main force effect is due to wave and wind, which change with time due to the climatic change, and this point is very critical and should be taken into consideration.

Offshore Structures. DOI: https://doi.org/10.1016/B978-0-12-816191-3.00007-9

7.2 American Petroleum Institute RP2A historical background

Knowing the history of API for offshore structure is very important as it evaluates and assesses existing structure in 1966.

API was formed in 1919, starting in the offshore structures field with the formation of the "Committee on Standardization of Offshore Structures." The target of the committee was to provide guidance to avoid problems and to serve as the basis for future regulations for offshore structures.

RP2A was the first publication of the Committee and when issued in 1969 it was only 16 pages long. API RP2A is now on its 20th edition, and also has an alternative version—RP2A-load resistance factor design (LRFD)—which contains 224 pages. RP2A has always been recognized as an evolving document, and every edition has stated in the foreword that as offshore knowledge continues to grow, this recommended practice will be revised as there is continuing research in this area.

From its start RP2A was not intended to be a complete specification, but rather a supplement to other engineering codes and specifications. Furthermore, as a note in the more recent editions states, API RP2A is intended to supplement rather than replace individual engineering judgment.

The development of the API RP2A guidance is reviewed in the following for each of the main topics.

For systems considerations, until recently RP2A has been primarily concerned with the design of each member separately. In the latest edition a separate subsection is devoted to structural redundancy and system considerations, with guidance on framing patterns as consideration should be given to providing redundancy in the structure and the framing system that provide substitute load paths are preferred in the design.

In the 19th edition (1991) a section on the reuse of platforms was added, and in the 20th edition (1993) a separate section on minimum structures was included. Minimum structures are defined as offshore structures which provide less redundancy than typical four-leg template-type platforms, or free-standing caisson platforms. On the other hand, RP2A recognizes that the consequences of failure for minimum structures are usually less than those for conventional structures. Therefore it is suggested by API that the minimum structure should be checked by evaluating its reserve strength and redundancy.

7.2.1 Environmental loading provisions

Based on OTO (1999), one of the most important topics in RP2A is the load effect due to environmental conditions, however in the early editions this guidance was brief.

Morison's equation has always been recommended for evaluating the horizontal wave force, and it has always been recognized that the appropriate drag and inertia coefficients depend in part on the wave theory being used. However, the

recommended values for the drag and inertia coefficients have been revised over the years, with the most substantial change in the latest edition. The recommended value of drag coefficient has changed from 0.5 in the early editions, to 0.6, and is now 1.05 for rough members.

In the 1st edition no guidance was given for the most appropriate wave theory to use. Stokes fifth and modified solitary wave theory were suggested by the 3rd edition; and as new wave theories became accepted they were recognized in RP2A. The 20th edition contains detailed guidance on zones of applicability for wave theories, including stream functions, Stokes fifth, and Airy wave theory.

API RP2A has always recommended that the selection of design environmental conditions data to which platforms will be designed should be delivered to the owner. Until 1986 in the 16th edition factors suggested to be considered in the selection of the design conditions included whether the platform was manned, the planned life of the platform, and the cost of the platform, including estimated losses if the design criteria were to be exceeded. In the more modern editions, the intent is the same although recognition of risk analysis has been added to justify the choice of the design event return period.

Prior to 1986, and the introduction of the 16th edition, RP2A did not state an explicit recurrence interval for the design conditions. Instead it was suggested as a guide that the recurrence interval of the design event should be several times the planned life of the platform.

In practice, in the GoM, apart from some of the earliest structures constructed before 1970 and some unmanned satellite/wellhead structures which were designed using 25-year criteria, a recurrence period of 100 years has generally been used for platform design. The regional guideline hydrodynamic parameters introduced from 1976 are believed to have been based on a 100-year recurrence period, and a 100-year recurrence interval was also accepted and used for the reliability-based calibration of the LRFD version of RP2A which began development in the late 1970s. However, it was not until the 16th edition (1986) that it was explicitly recommended in RP2A that not less than 100-year environmental design criteria should be considered where the design event may occur while the platform is manned.

Morison's equation

Morison's equation, as described in Chapter 3, Offshore structure platform design, is suggested for evaluating the hydrodynamic loading on individual tubular members. Prior to the 13th edition, in 1982, the equation had only been written in terms of horizontal wave force; after this date it was rewritten in terms of force normal to the axis of the member.

It was always recognized, by API RP2A, that the appropriate drag and inertia coefficients (C_d and C_m) depend in part on the wave theory being used. In the 1st edition, in 1969, the recommended range of typical values for C_d ranged from 0.5 to 1.0, and C_m from 1.3 to 1.7. By the 3rd edition (1972) the recommended range for C_m was increased to 1.5−2.0.

In 1975, the 6th edition presented a revision to the recommended range of typical values for C_d; the lower value was increased so that the range became 0.6−1.0. These values remained unchanged until the 16th edition, which saw a further revision to the coefficients, and the range was became 0.6−1.2 for C_d, and 1.3−2.0 for C_m.

However, when regional specific guidance was introduced in the 7th edition (1976), the recommended values for use in the GoM were 0.6 and 1.5 for C_d and C_m, respectively. In 1980, the 11th edition was modified slightly, and remained unchanged until the 20th edition, to a constant drag coefficient of 0.6 and an inertia coefficient of 1.5 for members 1.8 m (6 ft.) or less in diameter, increasing linearly to 2.0 for members 3 m (10 ft.) in diameter and greater.

The 20th edition (1993) provided a major revision to the environmental loading provisions with significant changes in the recommended values of drag and inertia coefficients for use in conjunction with other factors which are discussed below. For typical design situations the following values are now recommended for unshielded tubular members in the case of smooth members, C_d equal to 0.65, C_m equal to 1.6; on the other hand, for the rough members, C_d was equal to 1.05, and C_m equal to1.2.

Wave theories

In the 1st edition no guidance was given for the most appropriate wave theory to use. Stokes fifth and modified solitary wave theory were suggested by the 3rd edition, and as new wave theories became accepted they were suggested in RP2A. The 5th edition illustrated Chappelear wave theory, however Dean's stream function and extended velocity potential wave theory were added from the 7th edition (1976).

The 20th edition contains detailed guidance on zones of applicability for wave theories including stream functions of various order, Stokes fifth, and Airy wave theory (Table 7.1).

Selection of design condition

API RP2A has always stated that the selection of design environmental conditions to which platforms are designed should be the provided by the owner.

In the early editions a classification system was suggested for platforms based on the class number which was added to reflect the probability of the design condition being equaled or exceeded. Thus, a Class 100 platform would be designed to resist environmental loads which correspond to a one percent annual probability. Noting that, the class is defined in terms of platform environmental loading. Factors to be considered in selecting the class of the structure, and hence the design condition, were suggested to include:

1. probability of personnel being on the platform;
2. prevention of possible pollution;
3. intended use of the platform;

Table 7.1 Development of American Petroleum Institute (API) RP2A guidance for member wave loading.

RP2A edition (year)	Typical values of C_d	Typical values of C_m	Suggested wave theories
1st, 2nd (1969–71)	0.5–1.0	1.3–1.7	No guidance
3rd–5th (1972–74)	0.5–1.0	1.5–2.0	Stokes fifth and modified solitary; Chappelear added from 5th edition
6th–15th (1975–85)	0.6–1.0	1.5–2.0	Stream function and extended velocity potential added from 7th edition
16th–19th (1986–92)	0.6–1.2	1.3–2.0	As above
20th– (1993–2007)	Smooth/ rough 0.65/1.05	Smooth/ rough 1.6/1.2	Detailed guidance on zones of applicability

4. planned life of the platform;
5. cost of the platform, giving consideration to both initial cost and estimated losses if the design criteria are exceeded.

In 1969 in the 1st edition it was stated that economic risk evaluations for offshore platforms have indicated that the optimum class number is several times the planned life in years.

This design guide remained almost unchanged until the 16th edition in 1986, the only change being to remove the terminology class *number* in the 5th edition. In the next editions the intention has remained the same, although explicit recognition of risk analysis has been added.

Prior to the 16th edition RP2A did not state an explicit recurrence interval for the design conditions. On the other hand, it was suggested that the recurrence interval of the design event should be several times the planned life of the platform. It is important to highlight that some of the earliest structures in the GoM and other locations around the world, that is those designed before 1970 and RP2A, and some unmanned satellite wellhead structures, were designed using 25-year criteria, in practice a recurrence period of 100 years has generally been used for platform design in the GoM and US waters. The regional guideline hydrodynamic parameters introduced from 1976 are believed to have been based on a 100-year recurrence period, and a 100-year recurrence interval for storm conditions was also accepted and used for the reliability-based calibration of the LRFD version of RP2A which began development in the late 1970s.

However, it was not until the 16th edition (1986) that an explicit recurrence interval was given in RP2A for the design event; it was recommended that not less than 100-year environmental design criteria should be considered where the design event may occur while the platform is manned.

The definition of environmental loading for the extreme design condition in API RP2A (for use in US waters) has always been based on a wave height of the given return period (usually 100 years) acting together with "associated" wind and "associated" current. However, in practice, no current was included in the design criteria for many of the platforms in the GoM. The regional guideline values have only recently been introduced in RP2A (20th edition). The term "associated" has not always been clear. In the 16th edition (and subsequent editions) the following sentence was added without amplification: *Where there is sufficient knowledge of wave current joint probability, it may be used to advantage*. In the draft edition RP2A-LRFD, which was published in 1989, the definition of combined extreme wind, wave, and current is discussed. The following three definitions are discussed:

1. 100-year wave + associated current and wind;
2. 100-year platform load;
3. 100-year wave + 100-year current + 100-year wind.

Offshore structures are affected by wave loading, and the definition preferred by API is to use the 100-year return period wave height with the *statistically expected* value of current and wind. It is noted that for structures whose extreme fluid loading is not dominated by waves any "reasonable" combination of parameters leading to the 100-year return period load, as base shear or overturning moment, may be used.

Using the 100-year return period wave height combined with the 100-year return period current speed and the 100-year return period wind speed is recognized as conservative, and for some structures, for example, in areas of the GoM, too conservative.

Deck clearance or air gap

The air gap is a very simple and very important factor that affects the structure safety. In the case of waves striking a platform's deck there will be a large force affect the deck, however it is only in the latest edition that general (nonregional) guidance is offered in RP2A.

The air gap was first discussed in RP2A in the 7th edition (1976) when regional guidance was introduced for the GoM. Then it was recommended that use of the reference level wave heights for water depths greater than (200 ft.) 61 m in the GoM *should result in a deck clearance elevation of at least 48 ft*. (14.6 m) *above mean low water* (MLLW). This allowed for storm and astronomic tides, but did not include an explicit safety margin.

When guidance for other regions in US waters was introduced from the 11th edition (1980), tabulated values of corresponding reference deck elevations were also included. The values included *an appropriate safety margin* and were unchanged until 1986 when the 16th edition was introduced. Then, instead of providing values of minimum deck elevation, detailed guidance was provided for its evaluation; this included an explicit safety margin or air gap of at least 5 ft. (l.5 m).

These recommendations still apply in the 20th edition and the LRFD version, however they are now considered part of the general provisions and not region-specific. In the latest editions it is also recommended that an additional air gap should be provided for any known or predicted long-term seafloor subsidence. For the GoM, explicit values for guideline deck height have been reintroduced; for deep water [> 500 ft. (152.4 m)] the recommended deck elevation remains at 48 ft. (14.6 m) above MLLW, however for shallower waters this has been increased up to 53.5 ft. (16.3 m) for water depths of 100 ft. (30.5 m).

The latest editions of RP2A working stress design and load resistance factor design

In general, the change to the loading guidance between subsequent editions of RP2A has, in general, been small. However, in 1993 with the publication of the 20th edition of RP2A and the simultaneous introduction of the 1st edition of RP2A-LRFD, the environmental loading guidance was extensively revised and updated. A number of factors have been introduced or modified which are intended to produce more realistic estimates of platform hydrodynamic loading.

These changes include the following:

- Doppler effect of current on wave period as a current in the wave direction tends to stretch the wavelength, thus making the wave less steep. Guidance is provided on the evaluation of an apparent wave period.
- Wave kinematics reduction factor as the "real" waves are not two-dimensional. The kinematics reduction factor is applied to the horizontal particle velocities and accelerations from two-dimensional wave theory in order to approximate the effects of directional spreading. For tropical storms the factor is given in RP2A as being in the range 0.85−.95 and for extratropical storms it is in the range 0.95−1.00. The Commentary provides some further guidance on assessing the reduction factor, and also discusses an irregularity factor to account for the nonsymmetric shape of real waves.
- Current blockage factor due to the current speed in the vicinity of the platform is reduced from the free stream value by "blockage," as the structure causes the incipient flow to diverge. The factor is in the range 0.7−1.0 depending on the "drag area" of the platform. The multiplying factor on current velocity is evaluated from the following equation:

$$1/\left(1 + \left(\text{hydrodynamic drag area}/4 \times \text{frontal area}\right)\right)$$

- Conductor shielding factor effect depending on the configuration and spacing of the well conductors, the wave force may be reduced due to hydrodynamic shielding. Guidance on the reduction factor to apply to the drag and inertia coefficients for the conductor array is given; the factor ranges from approximately 0.5 for very closely spaced conductors, to 1.0 for spacing-to-diameter ratios greater than four.
- Current profile stretching, as the design current profile is specified only to the mean water level, the profile must be stretched to the local wave surface. "Nonlinear stretching" is the method preferred in RP2A, although linear stretching is considered to be a good approximation in some circumstances.

Together these loading provisions provide a package which is intended to model platform hydrodynamic loading more realistically.

7.2.2 Regional environmental design parameters

The selection of design parameters is the responsibility of the platform owner as stated by API RP2A and also is usually requested by the engineering companies.

RP2A did not contain any recommendations for regional design parameters until the 7th edition in 1976 when guideline wave heights for the GoM were introduced. These values were referred to as the *reference level* and together with guideline values of Morison coefficients, wave steepness (1/12), and other specific guidance noting that current was not mentioned were intended to lead to the *reference level* base shear and overturning moment for design. By the 11th edition (1980) guideline wave parameters were provided for 10 areas in United States waters covering offshore Alaska, California, and the Atlantic coast. This has gradually been increased, and in the 20th edition a total of 20 areas are covered.

The guideline environmental data have been developed from mathematical hindcasting based largely on wind measurements, and supplemented with hurricane data taken from aircraft and free-floating buoys. It is understood that the peaks-over-threshold method is used to estimate significant wave height from 3-hourly sea state data. Based on Forristall (1978), the short-term distribution of wave height within a sea state is assumed to be based on a two-parameter Weibull distribution.

As illustrated in Table 7.2 for omnidirectional wave heights for the GoM, the guidelines were very uncertain to begin with, and with time the range of values has been narrowed.

API recognized that based on specialist oceanographic and hydrodynamic advice alternative metocean design parameters can be used; however, RP2A does not detail the specific methodology to be followed.

7.2.3 Member resistance calculation

There have only been three occurrences of major changes to the member resistance equations in RP2A.

The first was the introduction of member resistance formulations into RP2A in the 6th edition in 1975. Prior to this date RP2A recommended that the AISC provisions be used. Guidance for local buckling was introduced, along with provisions

Table 7.2 Guideline wave heights for the Gulf of Mexico (GoM) by water depth.

RP2A edition (year)	Reference level wave height (m)	Range of values (m)
1st to 6th (1969–75)	No guidance	–
7th–15th (1976–84)	21.2	17.4–25.3
16th–19th (1984–91)	21.64	19.5–23.8
20th (1993–2000)	20.73	Directional factors

for hydrostatic pressure, and interaction equation for axial compression and bending stress, and axial tension and hoop stress.

In 1980, the second change was with the publication of the 11th edition. Equations were introduced for the assessment of allowable hoop stress, rather than using a design chart, and a formulation for the combined effects of axial compression, bending, and hydrostatic pressure was introduced.

The third change occurred in 1987 with the introduction of the 17th edition. This edition saw a major change in the allowable bending stress, which was increased from $0.66F_y$ to $0.75F_y$ for members not susceptible to local buckling.

Finally, in 1993, the LRFD version (1st edition) introduced some equations which have been modified. These modifications have not yet been introduced into the WSD version, and the member resistance formulations in the 20th edition (introduced at the same time as LRFD) are identical to those in the 19th edition.

7.2.4 Joint strength calculation

Ever since the 1st edition it has always been recommended that connections should be designed to develop at least 50% of the effective strength of the members. However, in the first two editions of RP2A no provisions for tubular joint strength were given except for stating that *design and detailing of joints shall be in accordance with good current practice*. It was not until 1972 and the issue of the 3rd edition that some specific guidance was given for joint strength design. This was based on the punching shear concept and was very simplistic. Later the 4th edition in 1972 was issued which introduced factors into the allowable stress formula to allow for the presence of load in the chord and the brace-to-chord diameter ratio.

However, it was not until late 1977 and the 9th edition that allowance was made in the allowable stress formulation for the joint configuration, as T, X, K. A plastic reserve factor was also introduced to account for the interaction between brace axial and bending stress, however this term was later dropped in the 14th edition.

In 1984 in the 14th edition a major change was added to the joint design recommendations in API since new test data had proved that the previous API joint strength equations and guides were unconservative. The allowable stress formula was modified considerably, and included a new and more realistic expression to account for the interaction effect of chord loads. The applied stress formula was also modified and based on the *nominal* stress in the brace. The previous API formula is believed to have underestimated the calculated punching shear stress. In addition, an interaction equation was introduced to account for the combined effect of axial and bending stresses in the brace.

The 14th edition stated the introduction of the *nominal load approach*. The punching shear and the nominal load approaches are intended by API to give *equivalent results*. The nominal load approach was introduced because the punching shear approach does not always reflect the actual mode of failure.

Noting that, based on OTO (1999), the 14th edition contained a number of printing errors, largely in the joint strength provisions, and was withdrawn shortly after issue. In 1984, the 15th edition, which contained the corrections, was submitted.

The guidance has remained unchanged, however in the 20th edition (1993) further recommendations have been added on load transfer through the chord. Note that there is a major change to the joint strength calculation in API RP2A-WSD (2007).

7.2.5 Fatigue

In the early editions of RP2A the guidance on fatigue was rudimentary, and simply stated that in the design of tubular joints due consideration shall be given to the problems of high stress, low cycle fatigue, and brittle fracture, and also to the effects of saltwater corrosion. Allowable design stresses for fatigue loading were suggested in AISC (1969), and by the 5th edition the fatigue provisions of AWS D1.1 (1972) were referenced. From the 3rd edition it was recommended that based on a typical GoM storm history, and in lieu of a more rigorous analysis:

- Nominal brace stress due to design loading of a cyclic nature should not exceed 138 MPa at the joint;
- Simple joints are preferred for jacket leg joints;
- Complex joints used should be detailed with smooth flowing lines.

In later editions the above recommendations were modified slightly to form the basis for fatigue design. However, it was not until 1980, and the 11th edition, that specific guidance on fatigue analysis and cumulative fatigue damage assessment was provided along with design curves of stress range versus predicted number of cycles (S−N curves). In 1986, in the 17th edition, API adjusted the fatigue guidance in the light of new research on the effects of the weld profile and produced a lower fatigue design S−N curve. In addition, a simplified fatigue design approach was introduced to assess the allowable peak hot spot stress as a function of water depth; the curves were calibrated for a typical GoM wave climate.

In 1993, the 20th edition presented a modification to the peak hot spot stress curves to account for the new wave force recipe. The 20th edition has also seen the introduction of a correction to the S−N curves to account for the scale effect due to plate thickness.

7.2.6 Foundation design

Foundation design guidance in API RP2A for tubular piles was initially limited. It is worth mentioning that, from the 1st edition in 1969, safety factors were 1.5 and 2.0 for the extreme and operating conditions, respectively, and these remained unchanged until the last edition.

The design guidance for the axial capacity of tubular piles in clay was initially based on engineering practice that had previously been followed for about 30 years for the GoM. This guidance was unchanged until the 6th edition in 1975 when it was replaced by the so-called API method 2. This was a substantial change which led to a significant increase in design pile penetration. As stated by OTO report that, due to the concerns raised by the industry, the previous method was reinstated

a year later in the 7th edition for highly plastic clays such as those found in the GoM; the API method 2 was categorized for use with other types of clay. The design guidance for clays remained almost unchanged until, in 1987, in the 17th edition it was completely changed and a new method introduced, however methods 1 and 2 have been retained in the commentary clause.

Guidelines for bearing capacity factors and soil friction angles for sands and silts were recommended for a limited range of soil types, along with limiting values in the first two editions of RP2A. In the 3rd edition the limiting values were removed, and this guidance remained almost unchanged until the 15th edition was introduced in 1984. Following an extensive review of all the available test data the guidance was changed extensively.

One of the most significant changes was for piles under tension where the earth pressure coefficient was increased from 0.5 to 1.0 for *full displacement* piles that were plugged or closed-ended. Other changes were to expand the range of soil types covered by guideline parameters, and to reintroduce limiting values on end bearing and skin friction pile.

7.3 Historical review of Department of Energy/Health and Safety Executive guidance notes

In 1974, the guidance notes were originally produced by the UK Department of Energy, and have since been re-issued by the UK Health and Safety Executive. The main purpose of the notes is to explain the Department's view on the procedures and requirements of the offshore construction, installation, and survey. For areas where no detailed guidance is given in the notes other codes and design standards are referenced, including API and Det Norske Veritas.

New editions of the guidance notes have been published every 5 years or so, and the latest edition, the 4th, was published in 1990. However, amendments to the notes are issued as and when new information or guidance is available; seven amendments were issued to the 2nd edition, and six were issued to the 3rd edition. In addition, background documents are published on a frequent basis to supplement the guidance.

As a result of the Cullen Report and the Offshore Installations (Safety Cases) Regulations (1992) some aspects of the guidance notes have been superseded.

The guidance notes contain guidance on a wide range of design considerations for offshore installations, some like environmental loading are covered in detail, whilst other areas are only briefly mentioned.

The extreme environmental condition in Health and Safety Executive (HSE) guidance underpins UK regulatory requirements. However, the guidance on environmental loading in the notes has evolved progressively to reflect new information and trends in design practice. The guidance on environmental considerations is both descriptive and detailed, and in later editions indicative values of most of the important environmental design parameters are presented.

Initially the guidance on environmental design loading in the Department of Energy (Den)/HSE notes was not very detailed. More guidance and indicative values of wave height were introduced into the 2nd edition in 1977, and this was largely unchanged when the 3rd edition was published in 1984. When the 4th edition was introduced in 1990 the environmental loading provisions were overhauled and much more detailed guidance was added.

The latest guidance on environmental loading is based on widely used present practice, and for overall structural load involves a "package" of interdependent assumptions which are considered to provide estimates of *sufficient accuracy for design purposes*.

7.3.1 Environmental loading provisions

The environmental loading sections in the guidance notes have evolved progressively to reflect new information and trends in design practice. In the latest edition, guidance is given on all types of environmental effects influencing platform loading, including wind, waves, tides and currents, water depth, marine growth, air and sea temperatures, and snow and ice accretion.

In the 1st edition much of the hydrodynamic guidance was discursive, but by the 2nd edition detailed guidance was given together with indicative values of the main parameters. The guidance on environmental loading was virtually unchanged in the 3rd edition, but was completely changed and updated in the 4th edition.

Noting that, the indicative values in the notes are only intended for use when site-specific measurements or other authoritative studies are not available. The data are generally presented as contours on maps covering the North Sea (NS) and North East Atlantic. The contours are based on long-term measurements supplemented by mathematical modeling, and do not take into account small-scale local effects.

7.3.2 Joint strength equations

In 1984, simple guidance on joint detailing was provided in the 3rd edition. When the 4th edition was published in 1990 detailed formulations for joint strength were introduced. These equations, produced following an extensive testing program and an assessment of worldwide test results, are based on the load approach, as opposed to punching shear approach. As for the contemporary API guidance, the equations are presented according to joint type and loading type, along with an interaction equation for combined load effects. However, as opposed to the API recommendations, the DEn/HSE formulations are based on characteristic strength, which is the value at which not more than 5% of results in an infinite number of tests would fail. Also contrary to API practice, explicit safety factors are defined in the guidance notes; 1.28 for extreme conditions, and 1.70 for operating conditions. The joint type classification system is similar to API's.

7.3.3 Fatigue

Extensive guidance on fatigue analysis and assessment was presented in the 2nd edition (1977). This included detailed weld type classification, a range of S−N curves (which differed significantly from the corresponding A WS curves), and guidance on a number of factors which modify the standard S−N curves. These modification factors account for unprotected joints in seawater, and measures taken to improve the profile of welds. In 1984, in the 3rd edition, further guidance on weld profiling was included, and measures to account for the scale effect between the actual plate thickness and standard thickness for the S−N curves were introduced. This later correction term has only recently been introduced into the API recommendations. In the 4th edition guidance on avoiding brittle fracture was introduced. The guidance notes are also supplemented by a number of background documents with additional information, and covering corrosion fatigue and brittle fracture in more detail.

7.3.4 Foundations

Some general guidance on factors to be considered when designing piled foundations is included in the notes, and additional guidance on foundations and site investigations is contained in another document which was published in 1986. The minimum safety factor for use with the extreme condition is recommended as 1.5. From the 3rd edition (1984) it is suggested that the safety factor to be used should be chosen depending on the reliability of the soils data, load estimates, analytical methods, and installation technique.

7.3.5 Definition of design condition

Prior to the publication of the 4th edition the extreme design condition in HSE guidance was based on the combination of the following minimum values:

- maximum wave height with average recurrence period of 50 years;
- the maximum current;
- the one-minute mean wind speed within a 50-year period and average recurrence.

In practice these factors were assumed to be acting in the same direction. The DEn/HSE note also stated that any other combination of environmental factors which may cause greater stress either in the structure as a whole or in any element of the primary structure, should be taken into account.

By 1990 and the introduction of the 4th edition, information on currents had improved somewhat and the definition of the minimum current for design was changed to current with an average 50-year return period.

In the 4th edition the use of joint probability is recognized for assessing combinations of extreme parameters, but it is not believed to have been used in practice for NS platform design.

7.3.6 Currents

For the design condition in the 2nd and 3rd editions the term maximum current was not specified other than that it should take into account the tidal current, which is associated with surges, wind-generated currents, and any currents due to other causes. Even in 1984 it was recognized that there was a lack of adequate measured data and theoretical understanding of near-surface currents and its variation with depth, and a map giving information on extreme currents in the NS had not been published. However, a contour map of maximum tidal surface currents based on mean spring tides was presented; these data may have inadvertently been used for design in some cases.

In 1990, for the 4th edition, the guidance on currents was improved considerably, and the design event is now defined using the current with a minimum average return period of 50 years; this is evaluated using the mean spring tidal current and the 50-year return surge current. Contour maps are now presented for depth-averaged speed and direction of an average spring tide, and 50-year return period depth-averaged hourly mean storm surge currents. Guidance on depth profiles is given, along with a discussion of other effects.

7.3.7 Wind

The 1st edition presented the values of maximum 3-second gust speed and hourly mean wind speed in the form of contour maps. Recommended ratios were presented for other averaging periods, and a table of factors was provided to account for the effect of height above sea level.

The guidance on wind loading remained until the 4th edition when it was extensively revised, and a new contour map of hourly mean wind speed was introduced.

7.3.8 Waves

In the 2nd and 3rd editions contour maps of indicative 50-year wave heights and associated zero-crossing period were presented. In this document, the wave heights were defined as the most probable value of the height of the highest wave in a fully developed sea state lasting 12 hours. The maps were developed in 1977 by the Institute of Oceanographic Sciences, and the data were derived from instrumental field measurements and wind data.

In 1990 the 4th edition was published, and the definition of the design wave was fundamentally changed—instead of a 12-hour storm the wave height was based on a 3-hour sea state. However, as a result of the simplified method used to derive the 1984 values, the overall effect on the values of the design wave was largely canceled out.

In the 4th edition, the indicative values of design wave height have been consistently evaluated and are estimated by generating from long-term data sets and mathematical models. However, it is recognized that the values are not definitive, and that other values may be used where they can be justified.

In addition, in the 1990 edition a table of factors is provided relating the 50-year significant wave height with individual wave height for a range of return periods from 50 years to 10,000 years. These factors are based on a sophisticated procedure which accounts for the fact that waters in the NS are not narrow-banded, and allows for the possibility that the highest wave may not occur in the worst storm.

$$H_{\max,n}/H_s = kFq \tag{7.1}$$

where, k is a factor defining the relationship between individual wave height and associated crest elevation, c, $h = 2kc$. For HSE guidance purposes it is recommended that $k = 0.9$. Noting that, q, will be obtained by evaluating using Eq. (7.2):

$$q = (1/2\log_e(n))^{1/2} + 1/16(1/2\log_e(n))^{-3/2} \tag{7.2}$$

It is worth mentioning that the product of, k and F is very close to one. Thus the factors are very close to a commonly used approximation to the ratio between the most probable maximum height in a sea state and corresponding significant wave height, as F allows for the possibility of extreme waves occurring in less than extreme sea states. It can be derived numerically from a modeling of the total population of individual waves in a return period. In the NS, for a 50-year return period, F can be shown to be around 1.12.

$$H_{\max,n}/H_s = \left(1/2\,\log_e(n)\right)^{0.5} \tag{7.3}$$

There was another change in the 4th edition which introduced conversion factors to define a range for associated wave period rather than a contour map of values. The design is intended to be based on the wave period within the recommended range producing the worst effect.

7.3.9 Deck air gap

In the early editions of the code there was no detailed guidance given on the air gap, other than in the 2nd and 3rd editions to state that the maximum crest elevation from the 50-year wave was required for calculating the clearance height of the superstructure.

However, in the 4th edition a subsection was devoted to the topic. The notes state that the air gap should be based on an assessment of the probability of encountering extreme wave crests of return period greater than 50 years, but the air gap relative to the design extreme wave crest elevation should never be less than 15 m. Further guidance is given for structures with large-diameter members which diffract waves ($D/L > 1/5$) and which may increase the maximum crest elevation

7.3.10 Historical review of major North Sea incidents

It is worth having knowledge of the major offshore incidents in order to ensure the design can avoid a repetition. The Piper Alpha disaster had a major impact on the

Table 7.3 Major North Sea incidents.

Date	Platform	Type of incident
1965	Sea Gem	Jack-up collapse due to brittle fracture. fatalities
1974	Auk A	Collision damage to platform
1976	Heather A	Jacket damaged by pile driving
1978	Transworld 58	Semisub fatigue damage to critical member.
1980	Alexander Kielland	Semisub capsize because of loss of column resulting from fatigue damage, causing Fatalities
1984	Ninian	Damage due to fabrication defect in primary structure
1984	Claymore	Damage due to fabrication defect in subsea brace
1988	Piper A	Platform collapse due to fire and explosion. 167 fatalities

development of offshore design, particularly in the NS. The repercussions following any major incident inevitably lead to changes in design guidance and practice. Where fatalities occurred, as at Sea Gem, Alexander Kielland, and Piper Alpha, the changes in practice have been far reaching. Table 7.3 summarizes the major North Sea incidents,

7.4 Historical assessment of UK environmental loading design practice

Historically, and also in present practice, environmental design loading is defined largely on the basis of owner company preference. Some companies take a conservative approach when choosing environmental design parameters using 100-year events as the basis for the design condition, whilst others take a less onerous approach.

Even today, there is no standard practice for establishing environmental design parameters and methods of design that analyze procedures, and design wave heights as they vary widely between various, even adjacent, fields. Different approaches are also taken in the choice of design current velocity and profile, drag coefficient, and other factors.

7.4.1 Design environmental parameters

In practice the extreme wave height and current used in the design of individual NS platforms have usually been derived using historical data from nearby sites.

While there is no standard procedure that is followed by all companies for establishing design wave heights in the NS, the common method is to fit a cumulative probability distribution for H_s to long-term field measurements, and the short-term distribution of wave heights in a sea state is then often assumed to follow Rayleigh distribution.

In some cases the resulting wave heights have then been arbitrarily adjusted upward for design purposes.

Although the wave climate has not changed, the estimates of design environmental criteria have changed over the years. There are several reasons for this, and one of the main reasons is that additional years of data measurement are available. Recording of wave measurements in the NS did not really begin until the early 1970s. Thus the early platforms had to rely on design parameters extrapolated from a very limited number of years of data. Clearly as time has gone on more years of data have been accumulated, and the statistical uncertainty in deriving design parameters has been reduced.

In addition, data have been recorded at more sites, and thus much of the uncertainty associated with interpolating values for new sites has been reduced.

For wave heights the method of measurement and data recording and analysis has improved over the years, and the definition of significant wave height has been refined. Up until the mid 1970s waves were usually measured using "waverider" buoys or wave staffs, and data were recorded for 20 minutes every 3 hours on paper chart recorders.

As discussed in Chapter 3, Offshore structure platform design, significant wave height was defined as the mean of the third highest waves. From the mid to late 1970s, analogue magnetic tapes were used more widely, and the data processed to derive significant wave heights defined using the root mean square (rms) of the sea state wave heights ($H = 4H_{\text{nns}}$). From the early 1980s the definition of significant wave height was based on the spectral moment ($H = 4\ (\text{mo})^{05}$).

Methods of data reduction and statistical analysis have improved considerably from the manual methods of the early 1970s to the sophisticated computations undertaken nowadays. In the early years it was not unusual for only one or two distribution types to be considered and a best-fit line fitted by eye; now a wide range of distribution types are considered, a variety of data reduction methods are used, a number of sophisticated fitting methods employed, and significance or goodness-of-fit tests undertaken.

North East Storm Study (NESS) is a hindcast study of environmental parameters based on 25 years of winter storms covering the period 1964–89—data are available on a 1-km grid covering the NS and the NE Atlantic Ocean. Since 1989, the results of the NESS have been available to contributory participants.

7.4.2 Fluid loading analysis

In the early years of NS development, only Airy and Stokes third and fifth wave theories were available to designers for practical use. All theory was used for its simplicity, particularly for appurtenance design, but as design became more sophisticated Stokes theories were used more widely, and even today Stokes fifth wave theory is still the most widely used theory for design.

Dean, in 1970, was following work primarily by Airy and Stokes wave theories that were shown to inaccurately predict wave particle kinematics for some combinations of water depth and wave period. The selection of the most suitable wave

theory was improved further following work by Le Mehaute in 1976, and Barltrop et al. in 1990. With advances in computing power, stream theory has become more popular, particularly in shallower water and for waves close to breaking. Stream function theory up to 11th order, as developed by Dean in 1965, or Chappelear velocity potential are now used.

All of the above are regular wave theories. Tromans et al. (1991) proved a theory based on random waves by new wave theory that has recently been developed by and is now being used by Shell company. It is said to model the irregular nature of real seas better.

Along with advances in wave theories there were more researches and development in the computer analysis software used to assess structural loading which has become increasing fast.

It is very important to highlight that marine growth was not usually considered in design before the late 1970s. Whilst the effects of marine growth on platform loading have usually been considered in the design of NS structures from at least the late 1970s, guidance on marine growth was only included in RP2A in 1993 with the introduction of the new loading provisions in the 20th edition. Detailed guidance on marine growth is now given in the 4th edition DEn/HSE notes, but only descriptive guidance was given in the 2nd edition (1977).

Due to the increase in knowledge and experience, the effects of breaking waves, wave slam, and slap can now be assessed.

Techniques have improved for allowing for wave−current interaction and for stretching the current profile to the instantaneous wave surface. The so-called mass continuity method was widely used until the 1980s, but this assumption can be shown to be unconservative. Until the mid 1980s highly sheared current profiles were assumed for design; nowadays a more uniform slab profile is generally preferred for extreme design conditions. In the 20th edition RP2A, the Doppler effect of the current on wave period is included.

One of the other main areas of change has been in the hydrodynamic coefficients used in Morison's equation. Considerable research has been done over the years to try to quantify the coefficients. A variety of tests in wave flumes, if-tubes, involving multiple and inclined members, and full-scale test structures have been undertaken. The use of these data by operators in practice cannot be easily quantified.

The following Morison's coefficients are based on information from one major NS operator, and may be considered indicative of general practice:

Up to 1971	$C_d = 0.5$	$C_m = 1.5$
1972−80	$C_d = 0.6$	$C_m = 1.8$
From 1981	$C_d = 0.7$	$C_m = 2.0$

7.5 Development of American Petroleum Institute RP2A member resistance equations

According to OTO (1999), the research mentioned that, every edition of API RP2A (WSD) has included clause referring to AISC for member design in cases which is not covered by RP2A with minor modifications to the wording.

The platform structure design shall comply with AISC-allowable stress design and specification.

The structural steel fabrication and erection shall follow the latest edition AISC. If there are types of loading not mentioned in API or not included in AISC, in this case the expert judgment with technical practice should be used to define the allowable stresses based on a reasonable factor of safety which matches with the AISC factor of safety.

The earliest editions of RP2A did not contain any recommendations for allowable stresses and relied totally on the AISC or *rational analysis*. This reliance has been eroded over time, with more and more guidance being given in RP2A. The later editions of RP2A (WSD) warn that the AISC load and resistance factor design code is not recommended for the design of offshore platforms.

The RP2A-LRFD does not mention AISC in the main body of the code, but gives guidance on the use of AISC-LRFD in the Commentary for nontubular members.

In every edition of API RP2A-WSD the wording has been unchanged for increasing the allowable stresses for the extreme environmental condition:

> *Where stresses are calculated by the effect of the lateral and vertical forces imposed by the design environmental conditions, the basic AISC allowable stresses may be increased by one-third. The required section properties computed on this basis should not be less than required for design dead and live loads computed without the one-third increase.*

7.6 Allowable stresses for cylindrical members

7.6.1 Axial tension

API RP2A did not contain a recommended expression for an axial tensile check until one was introduced in 1987 in the 17th edition. Until then reliance was on the AISC. In 1969, as now, AISC recommended that the allowable tensile stress was given by the following equation as presented in Chapter 3, Offshore structure platform design:

$$F_t = 0.6\, F_y \tag{7.4}$$

From the 17th edition, RP2A (WSD) adopted this recommendation explicitly.

7.6.2 Axial compression

Unstiffened tubular under axial compression is subject to the following three failure modes:

- material yield;
- Euler column (overall) buckling;
- local buckling.

In general, members with low *D/t* ratio are not subject to local buckling under axial compression. All editions of RP2A recommend that unstiffened tubular members be investigated for local buckling once the member *D/t* ratio exceeds a limiting value.

For editions 1−3, that is until 1972, local buckling should be investigated for $D/t > E/12F_y$. For example, for $F_y = 345$ MPa, the limiting value is about 50.

For editions 4−10, that is until 1979, local buckling should be investigated for $D/t > 22{,}750/F_y$ (F_y in MPa). For example for, $F_y = 345$ MPa, the limiting value is about 66. For later editions, the limiting value is 60.

No further guidance on local buckling stress or allowable compressive stress was given in the first five editions of RP2A. AISC also did not contain any guidance on local buckling for tubular members until 1978, when the 8th edition AISC was introduced, but AISC did contain formulae for overall buckling, as presented in Chapter 3, Offshore structure platform design, Eqs. (3.81) and (3.82).

From 1975, that is the 6th edition, API recommended that where the limiting *D/t* ratio was exceeded the allowable axial compression and bending stress for an unstiffened member should be determined by substituting a reduced yield stress F_{yr} for F_y in the appropriate AISC design formulae, where:

$$F_{yr} = \left[1 - \left(1 - \frac{22750/F_y}{D/t}\right)^2\right] F_y \tag{7.5}$$

From the 11th edition, in 1980, where the *D/t* exceeded 60, expressions were provided for elastic and inelastic local buckling. These were valid for *D/t* ratios up to 300, and for $t = 6$ mm. The elastic local buckling stress was calculated by the following equation:

$$F_{xe} = 0.6\, E\, t/D \tag{7.6}$$

In the 12th edition the constant 0.6 was replaced by a term (2*C*), where *C* was recommended as 0.3, thus giving the same result as the 11th edition.

$$F_{xc} = [1.64 - 0.23(D/t)1/4]F_y \tag{7.7}$$

It was then recommended that the minimum of $\{F_y, F_{xe}, F_{xC}\}$ should be substituted for F_y in the expressions for evaluating the allowable compressive stress.

Until 1987, and the 17th edition, API RP2A did not contain an expression for an allowable compressive stress; instead the AISC was suggested.

In the 17th edition RP2A introduced the following equation from AISC for the allowable compressive stress as stated in Chapter 3 as Eqs. (3.81) and (3.82).

7.6.3 Bending

In the case of pure bending the failure of a tubular member is usually precipitated by localized axisymmetric bulges on the compression side of the cylinder. As with

the local buckling for axial compression, the buckling behavior depends on the *D/t* ratio; at larger *D/t* ratios both the moment and rotational capacities of the tube decrease.

In the first five editions RP2A did not contain any expressions for an allowable bending stress, until 1987 the allowable stress for bending was treated very simply. AISC also did not contain any explicit guidance for tubular members until 1978, however for noncompact members, the allowable bending stress was given as $F_b = 0.6F_y$.

In 1975, in the 6th edition RP2A, the allowable bending stress was given as (for F_y in MPa):

$$F_b = 0.66\,F_y \quad \text{for } D/t \le 22750/F_y \tag{7.8a}$$

$$F_b = 0.66\,F_{yr} \quad \text{for } D/t > 22750/Fy \tag{7.8b}$$

where F_{yr} is the reduced yield stress as given in Eq. (7.5).

In the 11th edition, in 1980, F_{yr} was replaced by F_{xc}, and the limiting value was changed to 60, that is:

high rotational capacity; ductile failure mode exhibiting very gradual load decay; intermediate rotational capacity; semiductile failure mode;

$$F_b = 0.66\,F_y \quad \text{for } D/t \le 60 \tag{7.9a}$$

$$F_b = 0.66\,F_{xc} \quad \text{for } D/t > 60 \tag{7.9b}$$

In the 17th edition, in 1987, there was a substantial change in the allowable bending stress from a maximum value of $0.66F_y$ to $0.75F_y$, and allowance for local buckling was formulated explicitly in the expressions. Formulations for three regions are now provided in RP2A which can be classified according to rotational capacity:

- high rotational capacity; ductile failure mode exhibiting very gradual load decay;
- intermediate rotational capacity; semiductile failure mode;
- low rotational capacity; little postyield ductility, susceptible to local buckling and rapid load decay.

As shown in Eqs. (3.84) and (3.85) in Chapter 3, Offshore structure platform design, based on API RP2A (2007), however an unstiffened tubular with such a high *D/t* is unlikely to be practical in offshore structures, and in the 18th edition the upper limit for *D/t* was changed to 300.

7.6.4 Shear

In the 6th edition of RP2A it was recommended for the first time that for tubular members the applied beam shear stress should be evaluated using one half of the gross cross-sectional area. However, it was not until 1987 and the 17th edition that

the allowable shear stress recommended by AISC was introduced, as presented in Chapter 3, Offshore structure platform design, and the 17th edition also saw the introduction of an expression for the applied torsional shear stress, for torsional shear calculation.

In 1980, the 11th edition, the equation for acting hoop stress from hydrostatic pressure was modified slightly by replacing the constant by ρ, where ρ is the density of seawater.

7.6.5 Hydrostatic pressure

Unstiffened tubular members under hydrostatic pressure are subject to local buckling of the shell wall anywhere between restraints. The effect on the tube of pressure is magnified by any initial geometric imperfection or out-of-roundness. For closed-end tubulars, as braces, hydrostatic pressure also imposes an axial compressive stress of 0.5 f_h, some of which is taken by the structure and some of which passes into the member; the treatment of this force has always been a little unclear in RP2A, although the more recent editions are more definitive.

No provisions were included for hydrostatic pressure until the 6th edition in 1975. Then the acting hoop stress from hydrostatic pressure was given as in Eq. (3.55) in Chapter 3, Offshore structure platform design.

The allowable hoop stress was evaluated using a design chart. The *L*/*D* ratio and *D*/*t* ratio were used to derive the critical hoop strain, and the ultimate hoop stress was read from the chart using F_{ys}, which in the absence of interaction with axial stress was taken as F_y. For combined axial and hydrostatic stresses, F_{ys} was derived from the chart for later use. The allowable hoop stress was obtained from the ultimate value by dividing by an appropriate safety factor; suggested safety factors were given as:

1.25−1.5 Where the one-third increase in allowable stresses is appropriate, as when considering interaction with storm loads;
1.67−2.0 Where the basic allowable stress would be used, as pressures which will definitely be encountered during the installation or life of the structure.

In 1980, in the 11th edition, the equation for acting hoop stress from hydrostatic pressure was modified slightly by replacing the constant by $\gamma/2$, where γ is the density of seawater. Also at this time, API introduced a new method for evaluating the allowable hoop stress. This is based on a critical hoop buckling stress derived according to whether the collapse mode is elastic or inelastic. The allowable hoop stress is the critical hoop stress divided by the safety factor which was hardened in the 11th edition to become 1.5 for extreme conditions and 2.0 for other conditions. Hope buckling stress is calculated in Eq. (3.91).

In the 11lth edition, in 1980, the critical hoop buckling stress was defined as follows:

$$F_{hc} = F_{he} \quad \text{for } F_{he} \leq 0.667F_y \tag{7.10}$$

$$F_{hc} = 2.53\ F_y/\left(2.29 + \left(F_y/F_{he}\right)\right) \quad \text{for } 0.667\ F_y < F_{he} < 4.2F_y \tag{7.11}$$

$$F_{hc} = F_y \quad \text{for } F_{he} \geq 4.2F_y \tag{7.12}$$

Elastic buckling as in Section 3.6.2.8 part (b) is about critical hoop buckling stress. For formulations to evaluate F_{hc} for inelastic buckling, the following equations were modified in the LRFD version issued in 1993.

$$F_{hc} = 0.45F_y + 0.18F_{he} \quad \text{for } 0.55F_y < F_{he}$$

$$F_{hc} = 1.31\ F_y/\left(1.15 + F_y/F_{he}\right) \quad \text{for } 1.6F_y < F_{he} \leq 6.2\ F_y$$

$$F_{hc} = F_y \quad \text{for } F_{he} > 6.2\ F_y$$

7.6.6 Combined axial tension and bending

Prior to 1987 RP2A did not contain any provisions for this combination of stresses, however AISC contained the following equation:

$$\frac{f_a}{0.6F_y} + \frac{f_{bx}}{F_{bx}} + \frac{f_{by}}{F_{by}} \leq 1.0 \tag{7.13}$$

In 1987, in the 17th edition, an interaction equation for combined axial tension and bending was introduced for the first time. This was simply a modification of the AISC equation to allow for the circular cross-sectional shape:

$$\frac{f_a}{0.6F_y} + \frac{\sqrt{f_{bx}^2 + f_{by}^2}}{F_b} \leq 1.0 \tag{7.14}$$

The form of the interaction in Eq. (7.14) has been modified in the LRFD version.

7.6.7 Combined axial compression and bending

RP2A did not contain any provisions for combined axial compression and bending load effects until the 6th edition was introduced in 1975. In the 8th edition AISC contained the following two interaction equations; one to verify member stability and the other for plasticity. Where the axial component was small ($\leq$0.15) an alternative equation was suggested.

$$\frac{f_a}{F_a} + \frac{C_{mx}f_{bx}}{(1 - f_a/F'_{ex})F_{bx}} + \frac{C_{my}f_{by}}{(1 - f_a/F'_{ey})F_{by}} \leq 1.0 \tag{7.15}$$

and

$$\frac{f_a}{0.6F_y} + \frac{f_{bx}}{F_{bx}} + \frac{f_{by}}{F_{by}} \leq 1.0 \tag{7.16}$$

where

$$F_e = \frac{12\pi^2 E}{23(Kl/r)^2}$$

The reduction factors C_{mx} and C_{my} depend on the support conditions of the member, end moments, and whether transverse loading is applied: the factors take a value between 0.4 and 1.0.

In 1975, in the 6th edition, RnA adapted these interaction equations for circular cross-sections as in Eqs. (3.94) and (3.95).

When $f_a/F_a \leq 0.15$, there are two equations used as discussed in Chapter 3, Offshore structure platform design, as in Eq. (3.96).

Guidance was given on the evaluation of the reduction factor C_m for different types of jacket and deck components and has remained unchanged. However, in the 11th edition (1980) allowance was made for having different e_m and F_e values about the x and y axes, as in Eq. (3.97).

The interactions in Eqs. (3.96) and (3.97) have been modified in the LRFD version issued in 1993.

7.6.8 Combined axial tension and hydrostatic pressure

This load combination was originally called the *tension and collapse interaction* when it was introduced in the 6th edition. The title of the classification is now slightly misleading since the formulation also caters for bending. In the 6th edition the following interaction equation was introduced

$$(F_{ys}/F_y)^2 + (F_{ys}/F_y)A + A^2 \leq 1.0 \tag{7.17}$$

where

$$A = \frac{f_a + f_b - 0.5f_h}{0.6F_y} \tag{7.18}$$

F_{ys} was read from the design chart. It was stated that under cyclic loads, tension and collapse interaction need not be investigated where both of the following apply:

SF ≥ 2 for collapse alone

$F_a + f_b \leq 138$ MPa

Table 7.4 American Petroleum Institute (API) RP2A safety factors for use with hydrostatic interaction.

Design condition	Loading			
	Axial tension	**Bending**	**Axial compression**	**Hoop compression**
1. Where the basic allowable stress would be used, for example, pressures which will definitely be encountered during the installation or life of the structure	**1.67**	F_y/F_b	**1.67−2.0****	**2.0**
2. Where the one-third increase in allowable stresses is appropriate, for example, when considering interaction with storm loads	1.25	$F_y/1.3^3F_b$	1.25−1.5**	1.5

Notes: The asterisks were added in March 1983, in a supplement to the 13th edition: The value used should not be less than the AISC safety factor for column buckling under axial compression.
Source: From 17th Edition (1987).

In 1980, the 11th edition, this was replaced by an interaction equation based on the maximum strain energy theory for biaxial loading by Beltrami and Haigh as in Eqs. (3.98)−(3.100). The interaction equation was modified in the LRFD version introduced in 1993.

In RP2A the safety factor, SF, was tabulated as in Table 7.4, however it was not until the 17th edition that a separate safety factor for bending was introduced.

7.6.9 Combined axial compression and hydrostatic pressure

This combination was originally called the compression and collapse interaction when it was introduced in 1980 in the 11th edition; again the title is slightly misleading since bending is included in the equations. In 1980 three criteria had to be satisfied:

$$\frac{f_x - 0.5F_{ha}}{F_{aa} - 0.5F_{ha}} + \left(\frac{f_h}{F_{ha}}\right)^2 \leq 1.0 \tag{7.19}$$

$$\frac{f_x}{F_{xc}} SF_x \leq 1.0 \tag{7.20}$$

$$\frac{f_h}{F_{hc}} SF_h \leq 1.0 \tag{7.21}$$

Table 7.5 Historical American institute of steel construction (AISC) allowable stresses (N/mm^2) for weld in ASD.

Year	Steels and welding materials	Fillet weld shear	Tension	Compression
1934	A7/A9 steel	78	89.6	103.4
1939	A7/A9 steel	78	89.6	124.1
1946	A7/A9 steel: 60XX electrodes	93.8	137.9	137.9
1961, 1963	All steels: 60XX electrodes or subarc grade SAW-1	93.8	Same as member for all cases	Same as member for all cases
	A7 and A373 steels: 70XX or subarc grade SAW-2	93.8		
	A36, A42, A441 steels: 70XX or subarc grade SAW-2	108.9		
1969	All steels and weld processes[a]	0.3 F_{uw}	Same as member for all cases	Same as member for all cases
1989	No significant changes	0.3 F_{uw}	Same as member for all cases	Same as member for all cases

Noting that, for shear in but weld the strength 93 N/mm^2.
[a]Allowable shear stress = 0.30 F_{uw} in supplement 3, 1974, permitted weld metal with a strength equal to or less than base metal strength, except for tension members.

where

$$f_x = f_a + f_b + (0.5\, f_h) > 0.5F_{ha} \tag{7.22}$$

In the 17th edition the change in the safety factor for bending was allowed for, and the second criterion was replaced by:

$$\frac{f_x + (0.5f_h)}{F_{xc}} SF_x + \frac{f_b}{F_y} SF_b \leq 1.0 \tag{7.23}$$

In addition, in the 17th edition it was recognized that if $f_b > f_a + 0.5\, f_h$, the combined axial tension, bending, and hydrostatic pressure criteria should also be satisfied.

7.6.10 American institute of steel construction historical background

Based on Brockenbrough (2003), the welding specification based on the AISC was changed as shown in Table 7.5.

7.6.11 Pile design historical background

The pile design depends on the configuration of the platform, the water depth, and the construction practical method onsite at the time of execution. There has been a growth in the number of platforms with time and also the number of platforms that have been installed at greater water depths.

As the water depth is the most effective value on platform design, Fig. 7.1 presents the platform number in the North Sea until 1994. It is shown that the number of platforms with a water depth of over 100 m (300 ft.) increased rapidly after 1974.

From Tables 7.2 and 7.3 the effect of the limiting friction and end bearing values can be seen at around 35 m (for this example) for both the 1st and 15th editions. For compressive capacity there is very little difference between the ultimate capacities predicted by the 1st edition and the 15th edition; the only real change for dense sand is in the value of lateral earth pressure coefficient, K, which has changed from 0.7 to 0.8. For the 3rd to 10th editions (1972−84), there is a reduction in ultimate compressive capacity of up to 30% for a given pile length if K is taken as 0.5. In terms of pile length for a given pile load the 3rd to 10th editions would lead to a pile length of up to 7 m longer than the 15th edition for this example.

The ultimate tensile capacity predicted by the recommendations in the 1st edition is almost identical to that in the 3rd edition. However, the ultimate tensile capacity has been increased by up to 50% for the same pile length according to the 15th edition. In terms of pile length for a given pile load, the 15th edition leads to a reduction of around 7 m for this example.

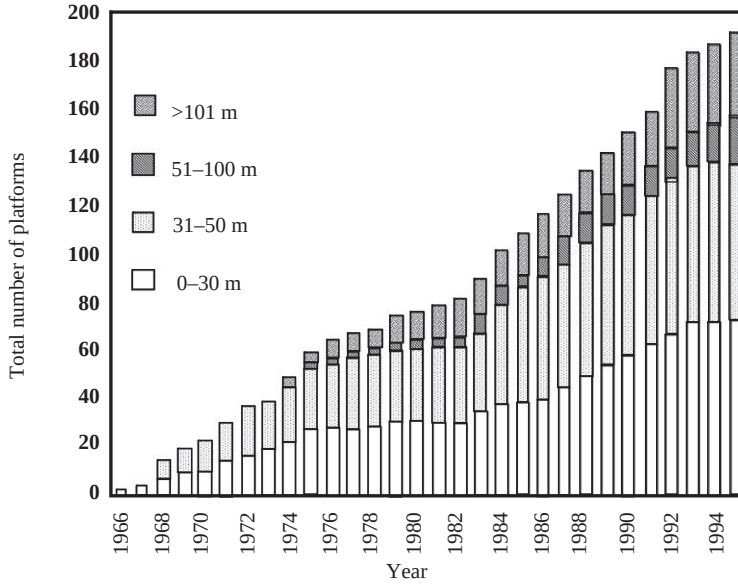

Figure 7.1 Bar chart of development with water depth.

Table 7.6 Change in ultimate capacity for a 30 m penetration.

RP2A edition (year)	Ultimate compressive capacity (MN)	Ultimate tensile capacity (MN)
1st and 2nd (1969– 1971)	11.5	3.8
3rd to 14lh (1972– 1984)	9.0	3.8
15th to 20th (1984–2000)	12.4	5.7

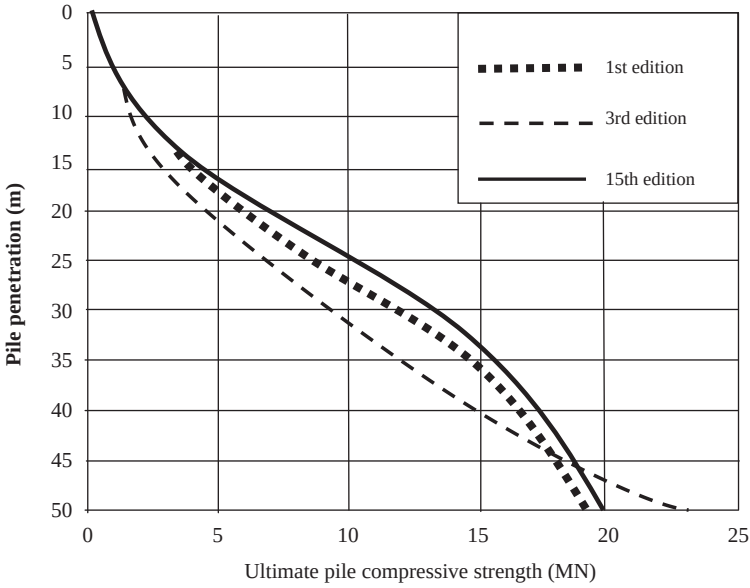

Figure 7.2 Changes in American petroleum institute (API) edition in pile ultimate compressive capacity calculation for a dense sand.

Table 7.6 presents the ultimate capacities for the pile with a diameter 1 m and depth 30 m in homogeneous dense sand (Figs. 7.2 and 7.3).

Fig. 7.4 illustrates the significant reduction in ultimate pile capacity for guidance in the 6th edition, particularly at deeper penetrations. The 17th edition guidance has led to a reduction in capacity of around 25% from the guidance introduced in the 7th edition for a given pile length. In terms of pile length for a given capacity the 17th edition leads to an increase of around 9 m for this example.

Table 7.7 presents the change in the ultimate capacity for 30 m penetration in homogeneous normally consolidated clay.

Noting that there are no more differences between the pile ultimate tensile and compressive capacity for different editions in normally consolidated clay.

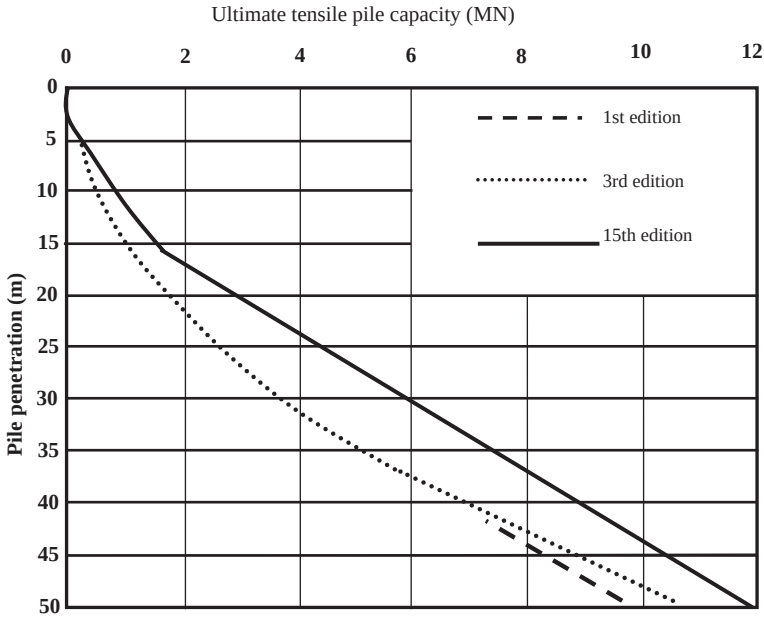

Figure 7.3 Changes in American petroleum institute (API) edition in pile ultimate tensile capacity calculation for a dense sand.

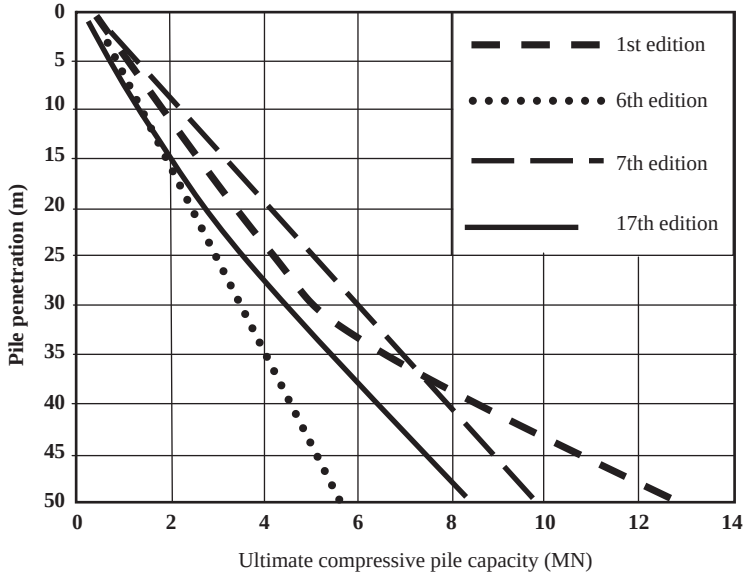

Figure 7.4 Changes in American petroleum institute (API) edition in pile ultimate compressive capacity calculation for a normally consolidated clay.

Table 7.7 Change in ultimate capacity for a 30 m penetration.

RP2A *e*dition (year)	Ultimate compressive capacity (MN)	Ultimate tensile capacity (MN)
1st to 5th (1969–74)	5.06	4.64
6th (1975)	3.53	3.10
7th to 16th (1976– 87)	6.08	5.65
17th to 20th (1988–)	4.58	4.16

Table 7.8 Effect of change in resistance formulations only on the average reliability index based on HSE.

Date of code	Average reliability index
1969–75	2.15
1975–78	2.3
1978–94	2.25

Table 7.9 Effect of change in resistance formulations and hydrostatic component database on the average reliability index.

Date of code	Average reliability index
1969–81	2.25
1981–87	2.32
1987–91	2.25

7.6.12 Effects of changes in tubular member design

As in Chapter 6, Corrosion protection, the loading was kept with minor changes, and all that was changed were the resistance formulae.

Table 7.8 illustrates the average reliability index evaluated for the resistance formulations in each RP2A edition.

The table illustrates clearly that there has been very little change in average reliability index over the years as a result of changes in the equation of resistance. The average reliability index for the 20th edition, which is applicable from the 17th edition, is 2.25, and the averages for the various stress combinations vary from 2.12 for tension and bending to 2.85 for compression, bending, and hydrostatic pressure.

The reliabilities evaluated for the early editions have been influenced by components designed with hydrostatic pressure which was not included in the early editions. NS structures generally were not installed in waters over 50 m deep until the mid 1970s, and thus hydrostatic pressure was not a critical design factor until then.

Table 7.9 illustrates the average reliability index with the hydrostatic pressure components for the early editions. The average reliability index due to changes in

Table 7.10 Effect of change in Morison coefficients on the average reliability index based on HSE.

Date of code	Average reliability index
1970–72	1.45
1972–81	1.8
1981–94	2.25

the resistance equations has remained virtually constant since RP2A was first introduced. It can be shown that the maximum change in the average reliability is from a reliability index of 2.25 for the 20th edition to a value of 2.32 for the 11th edition.

To illustrate the importance of the environmental loading, Table 7.10 shows the effect on average reliability index of changes in the Morison coefficients. For the purposes of the table the designs have been based on the latest resistance formulations in the 20th edition, and all that has been changed are the drag and inertia coefficients.

In general, the main reason for the consistency in the results is that component reliability is most sensitive to the environmental loading, and in particular extreme wave height.

7.7 Failure due to fire

The decks of offshore structure platforms in the oil and gas industry may be exposed to fire in the case of an incident. Therefore in most cases, after a fire it is requested to assess the deck to see whether it should be used or needs strengthen. There are many studies and researches about the reduction on steel structure exposed to fire, such as the analysis of catenary action in steel beams under fire conditions, based on the study by Yingzhi Yin at Manchester University.

The large deflection behavior of steel beams at elevated temperatures has been investigated.

A simple hand calculation method for predicting the deflections and catenary forces in steel beams at elevated temperatures has been developed at Manchester University.

The study was performed for uniform and nonuniform temperature effects in the case of lateral and axial restrain, with axial restrain only, or without any restrain axially or laterally. According to European code EC3, steel strength will soften progressively from 100°C to 200°C. Note that only 23% of ambient-temperature strength remains at 700°C. At 800°C strength is reduced to 11% and at 900°C to 6%, and steel melts at about 1500°C.

The EC1 (ISO834) standard fire curve is shown in Fig. 7.5. Fig. 7.5 which presents a different EC1 time temperature curve.

Fire resistance times are based on standard e tests—NOT on survival in real fires. European code EC1 Parametric Fire temperature–time curves are based on

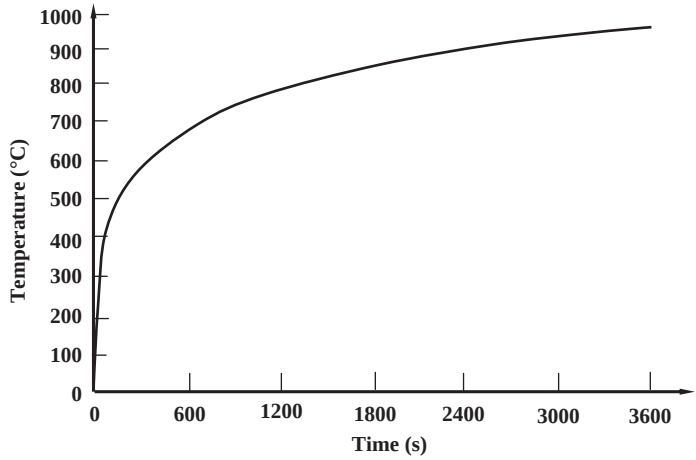

Figure 7.5 Standard fire test based on ISO834.

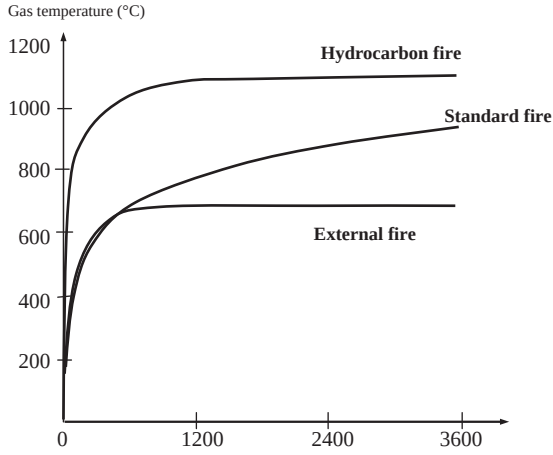

Figure 7.6 Type of fire and maximum temperature.

fire load and compartment properties ($<100\ m^2$), and are only allowed with calculation models.

As shown in Fig. 7.6, there are differences between hydrocarbon fire, external fire and a standard fire.

They are used to rate fire severity or element performance relative to the fire test. The fire testing usually is performed by load kept constant, with the fire temperature increased using a standard fire curve and then measuring the maximum deflection criterion for fire resistance of beams. Then the load capacity criterion for fire resistance of columns is defined.

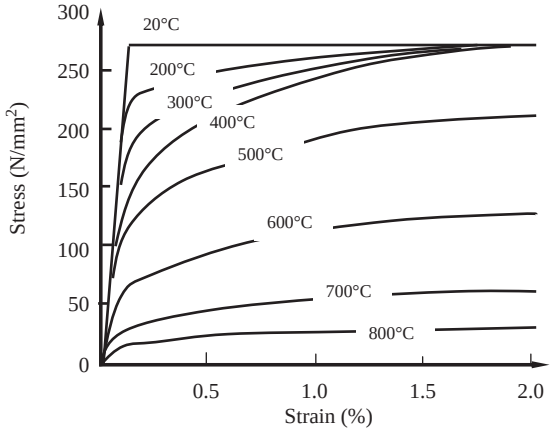

Figure 7.7 Relationship between stress and strain at different temperatures.

The effect of fires on steel structure depends on the limited range of spans, and the structure system if it is simply supported beams only, or restraint to thermal expansion by surrounding structures.

In some oil and gas projects, a passive protection technique should be used, of which there are different types as follows:

1. *Insulating board*
   - **a.** Consists of gypsum, mineral fiber, vermiculite;
   - **b.** Easy to apply, architecturally accepted;
   - **c.** Difficulties with complex details.
2. *Spray by cementitious materials*
   - **a.** Mineral fiber or vermiculite in cement binder;
   - **b.** Cheap to apply, but may need expensive cleaning after application;
   - **c.** Poor esthetics; normally used behind suspended ceilings.
3. *Painting by intumescence (commonly used in offshore structures)*
   - **a.** This painting expands by heating to produce an insulating layer;
   - **b.** It can provide a decorative finishing under normal conditions;
   - **c.** Nowadays it can be applied off-site.

Steel stress−strain curves at high temperatures are presented in Fig. 7.7. Strength and stiffness reduction factors for elastic modulus and yield strength are at 2% strain. Noting that, the elastic modulus at 600°C is reduced by about 70% and the yield strength at 600°C is reduced by over 50%.

From Fig. 7.8, it can be seen that steel softens progressively from 100°C to 200°C up. Only 23% of ambient-temperature strength remains at 700°C. At 800°C strength is reduced to 11% and at 900°C to 6%. In general, steel melts at about 1500°C. Stress−strain curves at different temperatures are shown in Fig. 7.7.

Degradation of steel strength and stiffness is presented in the curve in Fig. 7.8. Strength and stiffness reductions are very similar for S235, S275, S355 structural steels and hot-rolled reinforcing bars.

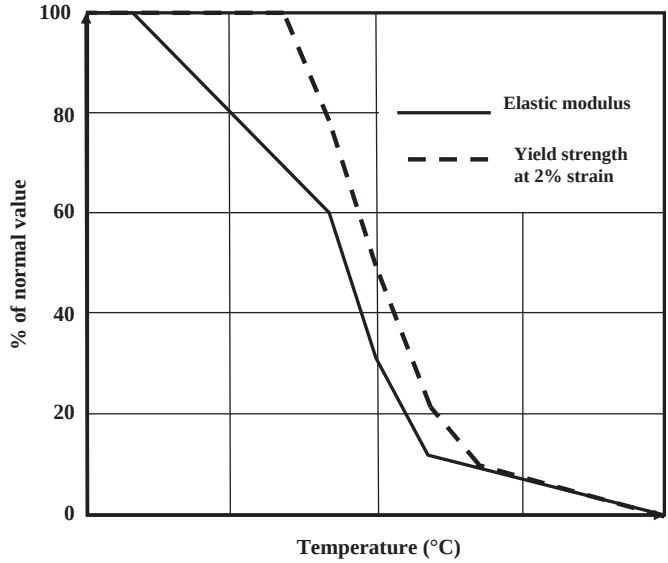

Figure 7.8 Percentage reduction in yield strength and elastic modules by increasing temperature.

7.7.1 Degree of utilization

Based on the EC3 European code for steel, the utilization degree will be presented by the following equation:

$$\mu_o = \frac{E_{fi.d}}{R_{fi.d.0}} \tag{7.24}$$

where $E_{fi.d}$ is the design loading of a member in fire, and $R_{fi.d.0}$ is resistance proportion at normal and ambient temperature, but including material safety factor for fire limit state.

A simple version of degree of utilization shall be used if there is no possible occurrence of overall or lateral-torsional buckling, which is conservative if η_{fi} is calculated as a proportion of the design loading at ambient temperature

$$\mu_0 = \eta_{fi}\left(\frac{\gamma_{M.fi}}{\gamma_{M1}}\right) \tag{7.25}$$

where η_{fi} is the reduction factor for the design load level for the fire situation.

For steel, material partial safety factors $\gamma_{M1} = 1.1$, $\gamma_{M.fi} = 1.0$

$$\eta_{fi} = \frac{E_{fi} \cdot d \cdot t}{E_d}$$

The is relative to the ambient temperature design load.

$$\eta_{fi} = \frac{\gamma_{GA} G + \psi_{1.1} Q_{k.1}}{\gamma_G G_k + \gamma_{Q.1} Q_{k.1}} \tag{7.26}$$

where $Q_{k.1}$, G_k is the characteristic value of the variable and permanent load, respectively.

The partial safety factor for permanent load γ_G is equal to 1.35, and the partial safety factor variable load $\gamma_{Q.1}$ is equal to 1.5 in a fire limit state where

$\gamma_{GA} = 1$ permanent loads; accidental design situation
$\psi_{1.1} = 0.5$ combination factor; variable loads, offices

Q_{k1}/G_k	1	2	3	4
η_{fi}	0.53	0.46	0.43	0.41

7.7.2 Tension member design by EC3

Design loading: $N_{Sd} = 247.95$ kN

Try IPE 100: $(100 \times 55 \times 8$ kg/m)

Design resistance: $N_{pl.Rd} = A_{net} f_y / \gamma_{M0}$
$= 1030 \times 0.275/[1.1] = 257.5$ kN > 247.95 OK

Design loading in fire: $N_{fi.d} = \eta_{fi} N_{Sd}$

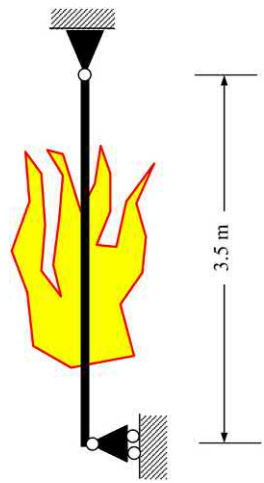

Combination factor, $y_{1.1} = 0.5$
$G_{k.1}/Q_k = 2.0$
Load reduction factor, $h_{fi} = 0.46$
$N_{fi.d} = 0.46 \times 247.95 = 114$ kN

Table 7.11 Reduction factors for the stress−strain relationship of carbon steel at elevated temperatures.

Steel temperature (Θ)	**Reduction factors at temperature Θ_a relative to the value of f_y or E_a at 20°C**		
	Reduction factor (relative to f_y) for effective yield strength $k_{y,} = f_{y,}/f_y$	**Reduction factor (relative to f_y) for proportional limit $k_{p,} = f_{p,}/f_y$**	**Reduction factor (relative to E_a) for the slope of the linear elastic range $k_{E,} = E_{a,}/E_a$**
20°C	1.0	1.0	1.0
100°C	1.0	1.0	1.0
200°C	1.0	0.807	0.900
300°C	1.0	0.613	0.80
400°C	1.0	0.42	0.700
500°C	0.780	0.360	0.600
600°C	0.470	0.180	0.310
700°C	0.230	0.075	0.130
800°C	0.110	0.050	0.090
900°C	0.06	0.0375	0.0675
1000°C	0.040	0.025	0.045
1100°C	0.02	0.0125	0.0225
1200°C	0.00	0.0	0.0

Design resistance at 20°C, using fire safety factors:

$N_{fi.20.Rd} = k_{y.20} N_{Rd} (\gamma_{M.1}/\gamma_{M.fi})$
Strength reduction factor $k_{y.20} = 1.0$ as in Table 7.11.
$N_{fi.20.Rd} = 1.0 \times 257.5 \times ([1.1]/[1.0]) = 283.25$ kN

Critical temperature: Degree of utilization $\mu_0 = N_{fi.d}/N_{fi.20.Rd}$

$= 114/283.25 = 0.40$

Critical temperature $\theta_c = 619$°C as in Table 7.12.

Note that in Table 7.11 for the intermediate value the linear interpolation can be used.

The relative thermal elongation of steel $\Delta l/l$ should be determined from the following:

- for $20°C \leq \theta_a < 750°C$

$$\Delta l/l = 1.2 \times 10^{-5}\theta_a + 0.4 \times 10^{-8}\theta_a^2 - 2.416 \times 10^{-4}$$

- for $750°C \leq \theta_a \leq 860°C$

$$\Delta l/l = 1.1 \times 10^{-2}$$

Table 7.12 Critical temperature $\theta_{a,cr}$ for values of the utilization factor μ_o

μ_o	$\theta_{a,cr}$	μ_o	$\theta_{a,cr}$	μ_o	$\theta_{a,cr}$
0.22	711	0.42	612	0.62	549
0.24	698	0.44	605	0.64	543
0.26	685	0.46	598	0.66	537
0.28	674	0.48	591	0.68	531
0.30	664	0.50	585	0.70	526
0.32	654	0.52	578	0.72	520
0.34	645	0.54	572	0.74	514
0.36	636	0.56	566	0.76	508
0.38	628	0.58	560	0.78	502
0.40	620	0.60	554	0.80	496

- for $860^\circ C < \Theta_a \leq 1200^\circ C$:

$$\Delta l/l = 2 \times 10^{-5}\Theta_a - 6.2 \times 10^{-3}$$

where l is the length at temperature 20°C; Δl is the temperature-induced elongation; and Θ_a is the steel temperature in °C.

7.7.3 Unrestrained beams

In the load resistance domain lateral-torsional buckling capacity at compression flange maximum temperature $\theta_{a.com}$ is presented by the following equation:

$$M_{b.fi.t.Rd} = W_{pl.y}K_{y.\theta.com}f_y\left(\frac{\chi_{LT.fi}}{1,2}\right)\frac{1}{\gamma_{M.fi}}$$

- Reduced yield strength of compression flange = $k_{y.q.com}\,f_y$ at $\theta_{a.com}$
- Reduction factor $\chi_{LT.fi}$ for flexural buckling based on normalized slenderness:

$$\overline{\lambda}_{LT.\theta.com} = \overline{\lambda}_{LT}\sqrt{k_{y.\theta.com}/k_{E.\theta.com}}$$

Noting that, there is no need to consider lateral-torsional buckling unless $\overline{\lambda}_{LT.\theta com} > 0.4$ and a correction factor of 1.2 simply allows for uncertainties.

Compression members of Class 1, 2, or 3

- In the load resistance domain buckling capacity at maximum temperature $\theta_{a.\max}$ is

$$N_{b.fi.t.Rd} = Ak_{y.\theta.\max}f_y\left(\frac{\chi_{fi}}{1.2}\right)\frac{1}{\gamma_{M.fi}}$$

- In the load resistance domain buckling capacity at maximum temperature $\theta_{a.\max}$ is
- Reduced yield strength = $k_{y.q.\max}\,f_y$ at $\theta_{a.\max}$

- Reduction factor χ_{fi} for flexural buckling based on:
  - Buckling curve (c)
  - Effective lengths in fire as shown.
  - Correction factor of 1, 2 simply allows for uncertainties.
  - Normalized slenderness is

$$\overline{\lambda}_{\theta.\max} = \overline{\lambda}\sqrt{k_{y.\theta.\max}/k_{E.\theta.\max}}$$

7.7.4 Example: strength design for steel beam

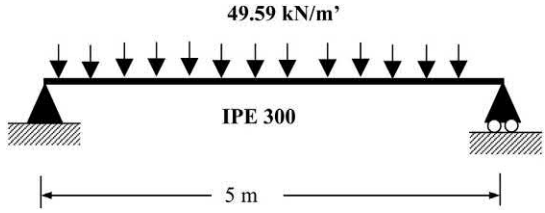

$$M_{Sd} = 49.59 \times (5)^2/8 = 154.97 \text{ kNm}$$

Try IPE 300: ($300 \times 150 \times 42$ kg/m)
Section classification:

$\varepsilon = \left(235/f_y\right)^{0,5} = 0.92$
$d/t_w = 248.6/7.1 = 37.5 < 72 \times 0.92$
$c/t_f = 7.0 < 10 \times 0.92\ldots$ The section is class 1 (compact section).

Moment resistance:

There is a full restraint to top flange; so there is no effect of lateral-torsional buckling.
Resistance moment $M_{pl.Rd} = W_{pl.x}\ f_y/\gamma_{M.0} = 157$ kNm > 154.97.

Shear resistance:

Applied shear $V_{Sd} = 123.97$ kN
Shear area $A_v = 2567$ mm^2
Resistance $V_{\text{pl.Rd}} = 2567 \times 0.275/(1.732 \times [1.1]) = 370$ kN > 123.97.

Steel beam: design resistance at 20°C
Design loading in fire:

$M_{fi.d} = \eta_{fi} M_{Sd}$
Combination factor $y_{1.1} = 0.5$
$G_{k,1}/Q_k = 2.0$

Fig. 2.1 Reduction factor $\eta_{fi} = 0.46$

$M_{fi.d} = 0.46 \times 154.97 = 71.25$ kNm

Design resistance at 20°C, using fire safety factors:
For a class 1 beam with uniform temperature distribution,
Resistance moment at temperature θ is $M_{fi.\theta.Rd} = k_{y.\theta}\ (\gamma_{M.1}/\gamma_{M.fi})\ M_{Rd}$
Strength reduction factor for 20°C: $k_{y.20} = 1.0$
$\gamma_{M.1} = [1.1]$ and $\gamma_{M.fi} = [1.0]$
Resistance moment for strength at 20°C is $M_{Rd} = 157$ kNm
$M_{fi.20.Rd} = 1.0 \times ([1.1]/[1.0]) \times 157 = 172.7$ kNm

$$M_{fi.t.Rd} = M_{fi.q.Rd}/k_1 k_2$$

$k_1 = [1.0]$ for beam exposed to fire from all sides;
$k_2 = 1.0$ noting that k_2 is equal to 0.85 at the support for statically indeterminate beam;
$M_{fi.t.Rd=}172.7/([1.0] \times 1.0) = 172.7$ kNm.

Critical temperature of the beam:

Degree of utilization $\mu_0 = 71.25/172.7 = 0.41$
Critical temperature of beam $\theta_{cr} = 616$°C

7.7.5 Steel column: strength design

Design loading: $N_{Sd} = 991.8$ kN

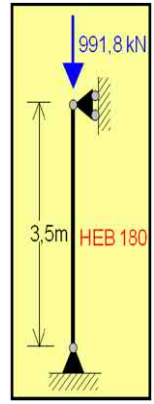

Try HEB 180:$(180 \times 180 \times 51$ kg/m)
Section classification: $\varepsilon = (235/f_y)^{0.5} = 0.92$

$d/t_w = 122/8.5 = 14.4 < 33 \times 0.92$
$c/t_f = 90/14 = 6.4 < 10 \times 0.92$ . . . class 1

Compression resistance:

Slenderness $\lambda = 3.5/0.046 = 76.6$
$\lambda_1 = 86.8$
Normalized slenderness $= \lambda/\lambda_1 = 0.88$

Reduction factor $\chi = 0.61$
$\beta_A = 1$ for class 1 sections
Buckling resistance $N_{b.Rd} = \chi \beta_A A f_y / \gamma_{M.1}$
$= 0.61 \times 1 \times 6530 \times 0.275/1.1 = 997$ kN > 991.8

Steel column: design resistance at 20°C

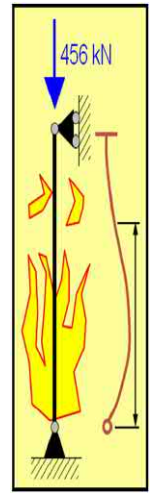

Design loading in fire: $N_{fi.d} = \eta_{fi} N_{Sd}$

Combination factor $y_{1.1} = 0.5$

$G_{k.1}/Q_k = 2.0$

Reduction factor $\eta_{fi} = 0.46$

$N_{fi.d} = 0.46 \times 991.8 = 456$ kN

Design resistance at 20°C, using fire safety factors:

$N_{b.fi.t.Rd} = (\chi_{fi}/1.2)\, A k_{y.q.\max}\, (f_y/\gamma_{M.fi})$

Effective length factor = 0.7 (pinned base)
Slenderness $\lambda = 53.6$
$\lambda_1 = 86.8$
Normalized slenderness $\lambda = \lambda/\lambda_1 = 0.62$

$\lambda_{20} = 0.62\ (k_{y.20.\max}/k_{E.20.\max})$
for $\theta = 20$°C, $k_{y.20.\max} = k_{E.20.\max} = 1.0$

Reduction factor in fire, $\chi_{fi} = 0.77$

$N_{b.fi.t.Rd} = (0.77/1.2) \times 6530 \times 1 \times 0.275/1 = 1159.6$ kN

Critical temperature of column:

Degree of utilization $\mu_0 = 456/1160 = 0.39$
Critical temperature $\theta_{cr} = 622.4$°C.

7.7.6 Case study for a deck under fire

This platform is used for drilling. The fire occurred in 2003 due to a sudden rupture of the gas riser. As a result of this rupture, the riser which contained a gas under pressure, caused a hydrocarbon fire jet which was directly exposed to the bottom of the main deck. The process of the assessment will be as follow:

- The onsite inspection survey revealed different levels of damage in various structural and piping components on the platform.
- Categorize the damage level of different structural elements of the platform in accordance with API579, Section 11.
- Measure the actual dimensions of structural elements of the platform.
- Assess the material properties of different structural elements of the platform.
- Provide necessary information to allow structure modeling of the platform to be performed (Figs. 7.9–7.13).

Figs. 7.14 and 7.15 present the location of damage on the platform due to exposure to fire.

The plot plan in Fig. 7.14 presents the deck beam which is directly affected by the fire, with observations of damage status in the structural elements of the platform due to fire. Site measurements for a sample of the structural elements of the platform for nonaffected and affected elements include:

- Structural dimensions;
- Hardness readings.

Estimating the material properties is based on the hardness readings. All materials weaken with increasing temperature, and steel is no exception. Strength loss for steel is generally accepted to begin at about 300°C and increases rapidly after

Figure 7.9 The fire on the main deck.

Figure 7.10 The effect to the main truss.

Figure 7.11 Deformation of the main and secondary beam for the deck.

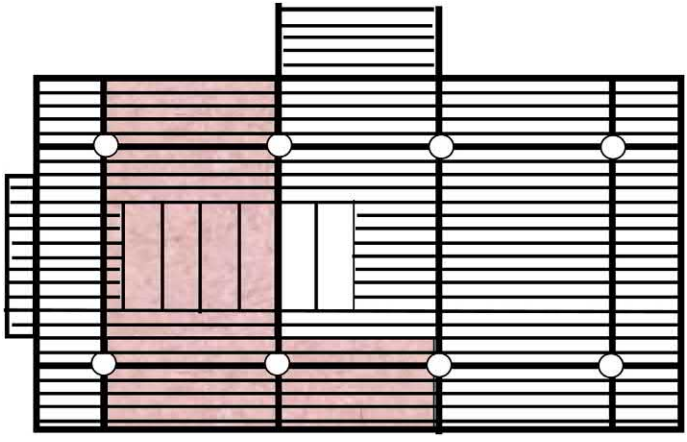

Figure 7.12 Deck layout showing the fire-affected zone.

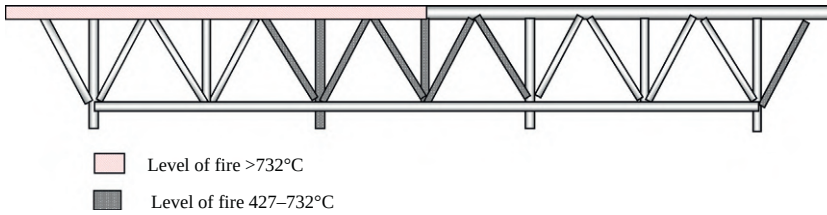

Figure 7.13 Fire classification effect on the main truss.

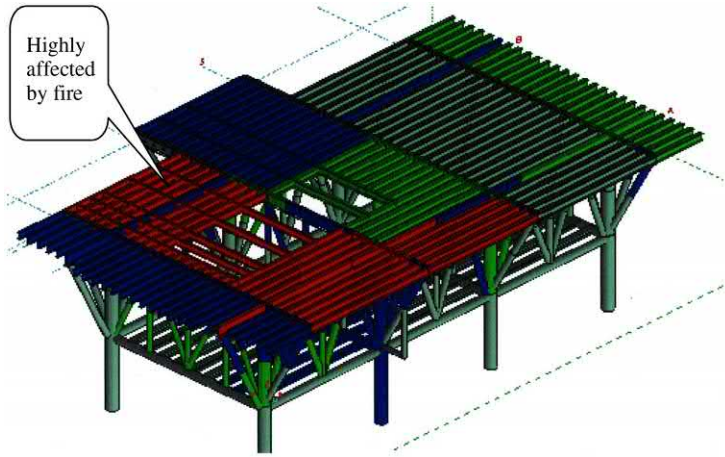

Figure 7.14 Deck categories based on the fire effect.

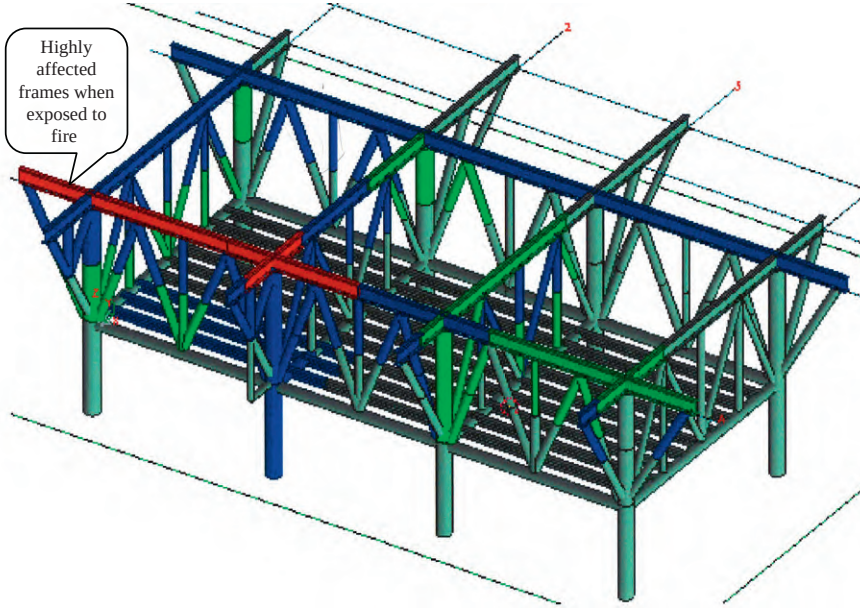

Figure 7.15 The main frame categories exposed to fire.

400°C, by 550°C steel retains only about 60% of its room temperature yield strength.

As a rule of thumb, in the case of fire-affected hot-rolled structural steels, after visual inspection it was found that if the steel member is straight without obvious deformation then it can be used again. If the temperature reached to 600°C then the steel yield strength is equal to about 40% of its nominal yield strength value at room temperature. Based on this, if during a visual inspection a steel member is straight with distortions this means that the steel member was carrying an appreciable load and was probably not heated beyond 600°C, so there will be no metallurgical changes that have occurred and so it is fit for reuse.

When calculating the yield strength by testing the steel the following precautions, as specified by Brockenbrough (2003), should be considered. During steel testing in laboratories and mill reports as per American Society of Testing materials (ASTM) methods, the value of yield strength is higher than the static yield strength as a result of the dynamic effect during testing. In addition, the test specimen location has an influence on the yield strength value. All these influences and variabilities are considered in defining the value of the nominal yield strength in the specification. However, if the load test is applied to perform an evaluation, these effects should be taken into consideration in the test plan as yielding will occur earlier than expected.

The static yield stress, F_{ys}, can be estimated from that determined by routine application of ASTM methods, F_y, by the following equation (Galambos, 1978, 1998).

$$F_{ys} = R\left(F_y - 4\right)$$

where F_{ys} is the static yield strength, ksi (MPa); F_y is the test reported yield strength, ksi (MPa); $R = 1.00$ for tests taken from flange specimens; and $R = 0.95$ for tests taken from web specimens.

The R factor covers the specimen coupon location effect on the reported yield stress from the laboratory test. As per ASTM A6/A6M prior to 1997, the reports from certified mill tests for structural shapes were based on specimens taken from the web, after that the coupon specimens location was changed to be from the flange. During 1997−98, new provisions of ASTM A6/A6M were adopted, so there was a transition from web specimens to flange specimens.

On the other hand, the material properties of the damage part are estimated using a hardness tester in a fire-unaffected zone in order to obtain the original material ultimate strength and consequently the material grade. Table 7.13 provides the relation between the hardness reading using the Birnell method to the steel ultimate strength.

A beam with deformation should be replaced by a new one. The main problem is on the main frame structure, which is very expensive to strengthen, so the hardness test is obtained and due to fire the properties of steel change as the percentage of carbon increases, which affects the ductility of the materials of the structure. An offshore structure platform is always affected by the wind and waves, so the structure should be ductile enough to enable drift without failure.

Table 7.13 Relation between the Birnell number and ultimate strength.

Birnell reading	Ultimate strength (MPa)	Birnell reading	Ultimate strength (MPa)	Birnell reading	Ultimate strength (MPa)
240	795	180	596	135	447
234	775	176	583	130	431
228	755	172	570	125	414
222	735	169	560	120	397
216	715	162	537	115	381
210	696	159	527	110	364
205	679	156	517	105	348
200	662	153	507	100	331
195	646	150	497	95	315
190	629	145	480	90	298
185	613	140	464	85	281

Due to the hardness reading, the zone of the high effect of fire is found in the main bracing system. The yield strength is considered about 0.85 from the actual yield strength. After performing the structure analysis on the main deck, the steel structure will be revealed as unsafe so the first option is to reconstruct the deck, but in making this decision we should look at the business as a whole as the target is the delivery of oil by this platform. Therefore due to the age of the field, the best economic decision is to reduce the load from the deck and prevent any work on the above deck, however this solution may not be the best in another platform.

7.8 Platform failure case study

Most platforms in the Gulf of Suez have an age of more than 30 years. The integrity management system (IMS)is developed and implemented based on the industrial practice. One role of the integrity management is to perform assessment of the existing structure based on API RP2A.

The API RP2A in general is tailored for platforms in GoM. Therefore when we deal with fixed offshore structures in different location the code needs to be modified and adapted to the platform location. The risk of the structure is based on the platform probability of failure and consequence, after analysis of this failure of the platform, it is clear that this method of approach needs to be changed when delivering the offshore structure platform maintenance plan.

Fatigue is the main factor defining the structure lifetime. In the case of an existing structure with a flooded member more comprehensive study is needed. The remote operating vehicle (ROV) survey is usually used as a part of API RP2A, but it needs to be changed based on each location and the environmental conditions.

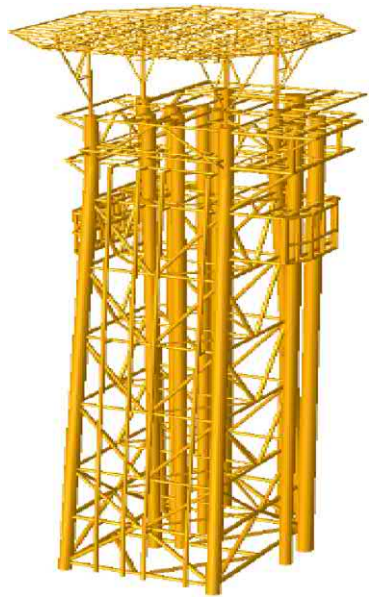

Figure 7.16 Platform configuration.

This case study of platform failure and the reason for it clarify the pitfalls in IMS philosophy and also in API RP2A for assessment of existing structures.

This platform shown in Fig. 7.16 is a well protector platform with four legs in a water depth of 39 m (130 ft.). It was constructed in 1973 with an inverse K-bracing system. There was a subsea survey performed by a ROV 7 years before the failure. From this inspection it was observed that there were five flooded members in this platform. The topside facilities weight is 27 tons with six risers and four conductors. The deck weight is 46 tons and the jacket weight is 73 tons. The platform was designed prior to the 1st edition of API RP 2A "Recommended Practice for Planning, Designing and Constructing Fixed Offshore Platforms, Working Stress Design" in 1969, which is a 16-page document, and the design would have been done by the engineering company specifications, possibly supplemented by owner recommendations.

There is no evidence that accidental loads such as vessel impact, fatigue load, seismic load, or the effect of corrosion or marine growth were accounted for in the design as these were not design practice at the time.

In addition, the pushover study using an Structural Analysis Computer System (SACS) model was performed on the platform 4 years before failure and the reserve strength ratio is suitable.

Failure is usually caused by the lowering of strength and raising of the affected load at the same time as presented in the cause of failure.

7.9 Failure mechanism

It is observed that the topsides are inclined 5−10 degrees toward the south, indicating a significant horizontal force was most likely applied well above the base of the jacket structure.

The leg members above the pile stabbing points are cracked in a manner consistent with a horizontal shear-type action as presented in previous figures.

The subsea survey indicated multiple joint failures on the east and west faces, with bright steel on most visible failure surfaces and lack of corrosion and marine growth on most exposed pile surfaces where the joint failure led to pull out of the leg. Thus these surfaces had only recently been exposed to seawater.

Fig. 7.17 presents bracing failure in the tubular joint and Figs. 7.18 and 7.19 present the shear failure on the leg.

Figure 7.17 Failure on the bracing member.

Figure 7.18 Failure on the leg.

Figure 7.19 Shear cracks on the leg with rotation.

Figure 7.20 Clean detachment of the brace member from the leg.

The leg has loads applied that cause shear stress with a torsion effect that revealed a shear crack on the leg with rotation, as shown in Fig. 7.19.

For the subsea inspection after failure there are a punching shear and detachment of a brace member from the leg as shown in Fig. 7.20.

7.9.1 Strength reduction

Four braces near the base of the jacket were reported to be flooded from a previous subsea survey, potentially indicating that some cyclic fatigue action had led to through-thickness cracking of these members. It is considered unlikely that these flooded members led directly to the subsequent structural failure since the ROV survey.

Some joints in the postcollapse subsea survey appeared to have a discolored surface and marine growth over cracks, suggesting failure some time before the date of failure.

The tubular steel used offshore at the time would have had a high carbon equivalent value and consequently be more brittle and less ductile than other offshore steel rolled sections.

Welding visually appears satisfactory with no gross defects detected. No obvious weld fabrication problems have been identified on this platform in particular, or any platforms in the fleet in general.

In general, the K-braced type system of jacket with no joint cans has little scope to redistribute load following an initial joint failure.

Joint plasticity would normally be associated with structural overload but there was little evidence of this from subsea ROV inspections postcollapse. This may be due to the more brittle steel employed in the late 1960s/early 1970s when this platform was fabricated, and/or the relatively thin steel sections as the member thicknesses are around 7−10 mm, and/or other factors discussed below.

In most cases the failure cause will be a combination of many factors at the same time.

7.9.2 Environmental load effect

The catastrophic structural failure of this platform, which is an unmanned satellite platform, was observed and most likely occurred at the peak of the preceding storm before failure after 2 days when onshore maximum gust wind speeds higher than 50 knots (25.7 m/s) were recorded at the nearest onshore location.

The mode of failure was structural overload primarily caused by severe wave loading from the north and northwest (N−NW) direction impacting the platform over a prolonged period.

The failure characteristics were similar to the pushover collapse analyses performed before failure of 5 years and another study for a similar platform before failure by 1 year.

There was no evidence of vessel impact, a seismic event, or other possible source of loading identified as a hazard to this platform, with the exception of the operated support vessel tying up to the boat landing to ride out a storm.

While the vessel tie-up option cannot be completely discounted, it would be very unlikely as this platform is near a natural sheltered location and the bollards show no signs of damage.

The storm conditions recorded for 2 days before structure failure were typical of storms recorded around 3−4 times per year from 7 years from failure. Based on the onshore gusts measured, the estimated maximum wave height and maximum 1-hour average wind speed during this storm are considered to be roughly wave height ($H_{\max}$) from 6.5 to 7.5 m and wind speed (W_s) equal to 19.5 m/s, respectively.

A previous storm 2 months prior to the failure was more severe and more typical of storms recorded around once every 2 years. Estimated maximum wave height and maximum 1-hour average wind speed during this storm are considered to be around $H_{\max} = 6.7-8.7$ m and W_s equal to 21 m/s, respectively.

There have been other severe storms 3, 4, and 7 years prior to the failure of similar peak gust and duration. Without offshore metocean data, the relative severity of these storms cannot be further quantified.

7.9.3 Structure assessment

The platform subsea jacket is considered to have been in a degraded condition prior to the catastrophic collapse.

The collapse analysis of this platform is performed by an SACS model with no joint failure modeled and the estimated minimum reserve strength ratio (RSR) equal to the load at collapse divided by load under 100-year environmental conditions was found to be 1.25 at collapse. RSR equal to 1.13 at first failure was due to pile yield, that is, an environmental load 25% greater than H_{max} equal to 7.72 m combined with Ws equal to 31.4 m/s—the wave contribution being the most significant factor.

The collapse analysis for a similar platform was performed by USFOS pushover analysis as per Soreide et al. (1986), and the estimated minimum RSR was equal to 2.19 at collapse and 1.76 at first failure in the leg joints at −8.5 m elevation, that is, an environmental load from the NW direction was 119% greater than H_{max} equal to 6.3 m combined with Ws equal to 15.6 m/s. The effect of 15% and 30% wall thickness loss reduced the RSR values to 2.02 and 1.55, respectively, however there is no report that corrosion loss had been an issue on this platform.

Four braces near the base of the jacket were reported to be flooded in the subsea survey, potentially indicating that some cyclic fatigue action had led to through-thickness cracking of these members. It is considered unlikely that these flooded members led directly to the subsequent structural failure since ROV footage implies that two were intact after failure.

Some joints in the postcollapse subsea survey appeared to have discolored surfaces and marine growth over cracks, suggesting failure some time before failure.

The collapse analysis is performed regardless of the flooded member data as the crack in the joint increased with time, causing a sudden failure in a high storm.

From the in-place analysis by the SACS model it was found that 90% of the joint had a unity check (UC) higher than 1.2. Also, some joint at elevation −11, −28, and −46 had UC higher than 2.0.

In addition, the minimum pile capacity factor of safety in compression for storm condition is equal to 1.08 and the minimum factor of safety for tension is 1.00, which is outwith the API RP2A.

The collapse analysis was performed by taking pile soil interaction, and in this case the RSR was equal to 1.25. The other collapse analysis was performed using a dummy pile stub to define the RSR for the jacket and in this case the RSR was equal to 1.65. Therefore the joint flexibility option is included in the analysis.

From a dynamic analysis point of view, the natural frequency is calculated through the eigen value problem which takes the form:

$$K\phi = \lambda M\phi \tag{7.27}$$

where K and M are the stiffness and mass matrices, respectively, and ϕ is the model shape factor of the structure and the software program calculates the lowest eigen value λ and the corresponding eigen vector. From the above it can be seen that the structure stiffness is the main factor in calculating its dynamic analysis. The reason for the flooded member is very important to consider as if there is a crack on the joint it will affect the global stiffness and so the natural frequency will increase, which will increase the dynamic amplification factor (DAF), which should be considered in the collapse analysis.

The DAF is calculated from the following equation.

$$DAF = \frac{1}{\sqrt{\left\{\left[1-\left(\frac{T_n}{T}\right)^2\right]^2 + \left(2D\frac{T_n}{T}\right)^2\right\}}} \tag{7.28}$$

where T is the wave period in consideration; T_n is the natural period of the structure; and D is the damping ratio.

On the other hand, the reduction in stiffness under wave load will increase the vibration, which will affect the fatigue and accelerate opening of the cracks and so also shorten the structure life time.

The natural period of the structure was calculated and found to be 2.78 seconds, which is less than 3 seconds, and so there is no need to add the dynamic amplification factor to the in-place analysis. There was another pushover analysis performed by USFOS software and in this study the natural period was 2.36 and was added to the DAF in this collapse analysis.

The effect of reducing the stiffness is presented by the following curve as when the structure is loosening the stiffness in the natural period will increase and then the DAF will increase also gradually, as shown in Fig. 7.21.

For the last study the RSR at first load failure was 1.76, 1.24, and 0.874 in the case of 0%, 15%, and 30% corrosion loss, respectively.

RSR is equal to 0.874 in the case of 30% corrosion and at the first plasticity point formulation.

In these two studies the five flooded members are not taken into account.

Fig. 7.22 presents the point of first collapse joint in the structure. Fig. 7.23 illustrates the global platform displacement versus the global load effect on the structure until complete collapse.

From the previous collapse analysis with the maximum RSR 1.76 and from the DAF curve, it can be seen that the wave load can increase 76% if the structure natural period is less than 4 seconds; its mean there is no change on the platform stiffness.

Therefore the minimum RSR for the old structure for a cutting or flooded member should be studied against the DAF that added value statically to the wave load on the structure.

The field platform is located under an IMS. In general an IMS for an offshore structure is based on risk-based inspection as clarified by APRPISM and API RP2A

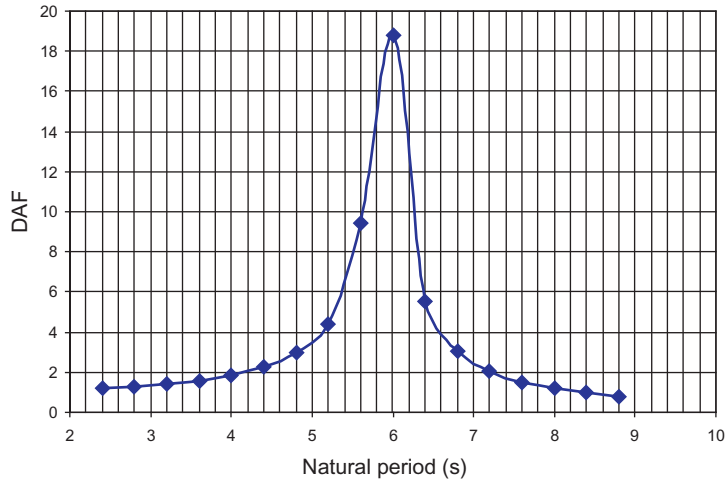

Figure 7.21 Relation between the natural period and the dynamic amplification factor (DAF).

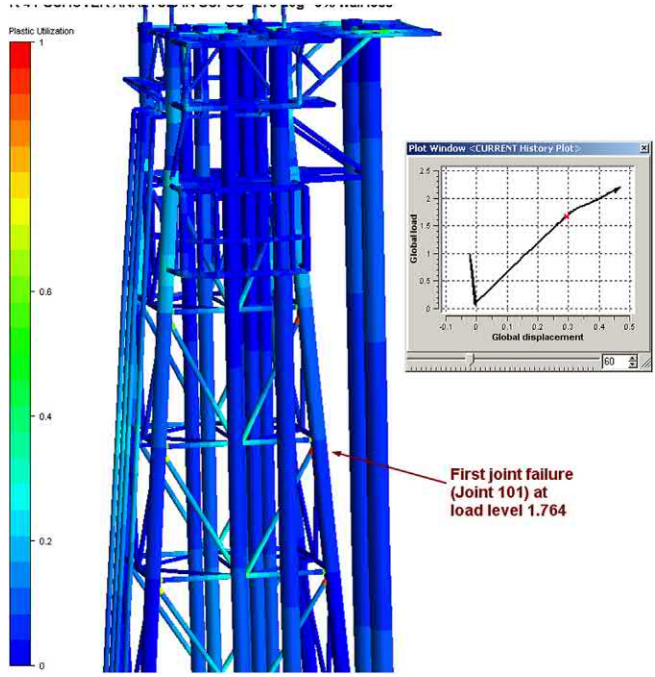

Figure 7.22 The location of the first joint failure.

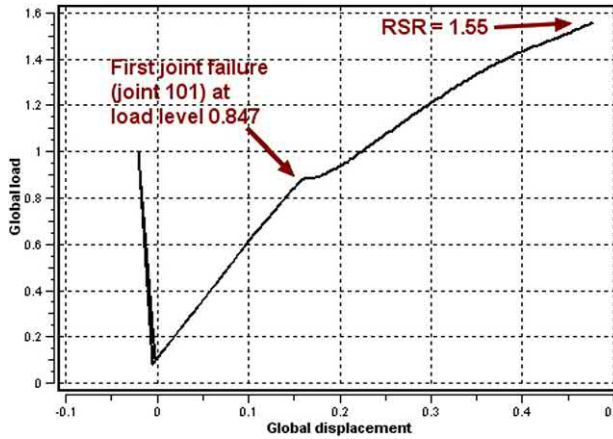

Figure 7.23 Load−displacement curve to complete collapse.

clause 17 about the assessment of existing structures. The term risk is a function of multiplying the probability of failure to consequence. Therefore if the probability of failure increases the risk may still be low as the consequence may be very low; in this platform the risk ranking is 26 for 120 offshore structures. The risk is not high so it is indicated that the risk assessment of the platform is a matter of managing the business and goals of the owner organization but not reflecting the actual condition of the structure itself. If the risk is low this means also that a failure can occur at any time. Therefore to maintain the offshore structures from a structural point of view, the likelihood of failure should be focused on.

For assessment of the platform, the in-place analysis is very important to define the condition of the structure. In most cases the piles are outwith the code and also the joint as presented in this platform. However, it is important to concentrate the survey for the connection in a short period with a closed visual inspection.

From an engineering point of view, if the probability of failure is high, this means that the structure may fail at any time regardless of its risk ranking, which is the main focus of the business goal.

The in-place analysis is enough to define the preliminary main points, that have a lack of structure reliability. Therefore the maintenance scope can be defined based on that.

The pushover analysis should present the exact condition of the platform if there are any deviations that the RSR does not identify exactly in the condition of the platform. If there are any flooded members, the fatigue assessment is critical with the dynamic analysis, as vibration of the structure is affected by that. From many learned lessons revealed that, the survey results and the collapse analysis should be very accurate and cover everything in as is condition of the structure at the time of the analysis or do not do it to avoid waste of time and money, as there is no optimization in assessment of the existing structures. Check list that is using to gurantee the outpout of the pushover analysis is presented in Table 7.14.

Table 7.14 Checklist for pushover analysis.

	Yes/No
General checks	
Is the scope of analysis clearly defined? Are the content and standard of presentation reasonable? Are all units defined and consistent? Are all specifications, standards, and codes listed? Does work satisfy the requirements of the design brief, design spec., and/or other relevant documents? Have the correct conditions been included in the analysis (in-place, future, ship impact, fire, others)? Has the analysis been set up in a clear and logical file structure? Have the recommendations of the latest codes been adhered to? Do you have a project working folder with all relevant information reported on it?	
Checks for new or converted models	
Is the model orientated in the correct coordinate system? Have coordinates of key geometry points been checked? Have variables been defined in consistent units of weight, length, and time? Do you check the beam element properties and orientation? Did you modify the general section properties? Have section, material, and other names (ID) been updated? Have basic and combined load cases been checked and/or updated? Do you check the member releases? Have the appropriate appurtenances been included? Do you define the joint cans and stubs? Have you defined or checked the brace offsets and gaps at joints? Have model sets been defined and checked? Does the model have duplicated nodes? Have you checked that all section property shear factors are 1? Have correct C_d and C_m coefficients been used? Is water depth in accordance with the latest air gap measurements? Are wave heights in accordance with metocean? Have the mudline and waterline been defined correctly? Have flooded members been defined correctly? Have member-specific Morison coefficients been defined correctly? Have marine growth thickness and mass been included? Has the associated current been defined correctly? Have anodes CD and CM been included? If not increase by 1.07 the wave force in the analysis Are wave directions and headings consistent? Have the correct wave frequencies been defined? Have sea state directions been checked? Have the correct wave amplitudes been defined?	

(*Continued*)

Table 7.14 (Continued)

	Yes/No
Has the wave steepness been checked? Have groups/sets been checked? Have base shear and OTM been checked/compared? Have you checked that buoyancy was not apply twice (storm case must not have buoyancy)? Did you check the output file for possible warnings/errors? Have you reported all relevant information in the working folder?	
Checks in case of a modified existing model	
Have new or updated flooded members been defined correctly? Have the specific Morison, C_d, and C_m coefficients and marine growth thickness and mass been defined correctly for new/updated members? Have anodes CD and CM been included? If not increase by 1.07 the wave force in the analysis. Have groups/sets been checked/updated/included? Did you check or compare the base shear and the overturning moment? Have you checked that buoyancy was not applied twice (storm case must not have buoyancy)? Have you checked the .out file for possible warnings/errors? Have you reported all relevant information in the working folder? *Model conversion* *Foundation* Have soil spring definitions been checked? Do you have the latest information about pile capacities? Have individual piles been limited in tension and compression according to the latest information about pile capacities? Have groups of piles been limited in tension and compression according to the latest capacities? Have you reported all relevant information in the working folder? *Geometry* Have you selected correctly the node/element number? Have you defined the correct pile head node? Have the boundary conditions of piles, sleeves, etc. been defined correctly? Have the software basic load cases been checked? Have you checked that the genie sets are correct in the software? *USFOS analysis checks* *Before analysis* Have you got the soil data for still and storm conditions? Have initial imperfections of 0.2% L for still and storm conditions been defined? Has MSL joint formulation been defined? Has hydrostatic pressure been included for member strength? Has the fracture module been included in the analysis? Have appropriate load and material factors been applied?	

(*Continued*)

Table 7.14 (Continued)

	Yes/No
Have local buckling and lateral-torsional buckling been considered (i.e., will local buckling occur before the full plastic capacity is achieved?)?	
Has the software model been validated against the results of a known loading case?	
Have you checked the topside load combination CoG via reaction loads?	
Has the wave OTM been checked via fixing the jacket at a known elevation?	
Have pile reactions from the output file been added up and make sense against what is expected?	
Has the pile model been checked by plotting the pile head axial force (with a linear jacket to ensure soil failure)?	
Have you considered a D/t yield strength reduction in the header file (elastic and plastic local buckling)?	
During analysis	
Has gravity (still water) pushover been completed for various and worst drilling rig location with appropriate load factors (American Petroleum Institute, API and International Standards Organization, ISO)?	
Have soil data (factor = 0.80) for API still condition been used?	
Has 100-year storm [100-year wave + associated (1-year) current] pushover for various/worst drilling rig location been completed with appropriate load factors (API and ISO)?	
Have soil data (factor = 0.94) for API storm condition been used?	
Have you checked the serviceability limit (strain levels 5% and 15% + tension, −tension)	
Has 10,000-year storm (10,000-year wave + associated current) pushover for various/worst drilling rig location been completed with appropriate load factors (API and ISO)?	
Have soil data (factor = 1.0) for API and $1.15F_y$ for ISO in the 10,000-year assessment been used?	
Have you checked the API spreadsheet maximum member capacity predictions versus the software results?	
Have the output files been checked for additional failure information as buckling, join failure, fracture, and other, in order to understand the analysis behavior?	
Has a 100-increment only solution been performed (no iterations) and checked with a 1000-increment solution (worst cases)?	

A dynamic analysis with a fatigue study is more critical in defining the structure life time than the collapse analysis.

For an old platform with cracked or cutting members the RSR should be compared with the maximum amplification factor. As the minimum RSR is equal to 1.6, this depends on the maximum wave height within a period in the year with the probability of failure and it is reasonable in a new platform or a platform without joint cracks.

7.10 Assessment of platform

The criteria for assessment of the platform were under development at the time of preparing this book, and only the draft of API SIM was available, which will be focus of the assessment of existing structures.

The acceptance criteria will determine whether a structural assessment has confirmed the platform fit for continued operation in its present condition or not.

The ultimate structural capacity of an offshore platform may be characterized either in terms of the platform RSR or in terms of the probability of increasing the environmental load due to wind, wave, or current and causing the platform to collapse. The RSR is defined as the ratio of the environmental load set causing collapse to the environmental load set with a 100-year probability of exceedance. Therefore a platform with an RSR of 1.0 will have a deterministic probability of failure in the region of 1 in 100 (10^{-2}).

Noting that the design of an offshore platform under 100-year actions from wave and wind, based on API RP2A, will have an ultimate capacity, or design capacity, about 1.8−2.5 times the design load. This design capacity represents the explicit factors of safety in the design code as well as the implicit margins due to different factors such as mean steel strength, conservatism in foundation capacity assumptions, and the presence of additional steel as a result of temporary load conditions in the case of construction, transportation, and installation, and the increased capacity associated with structure analysis in a three-dimensional space frame structure.

Fig. 7.24 shows a comparison of two geographical regions; region (1) and region (2). The plot origin represents the design point for both regions (1) and (2). In both cases the design capacity of the structures is assumed to be in the range of

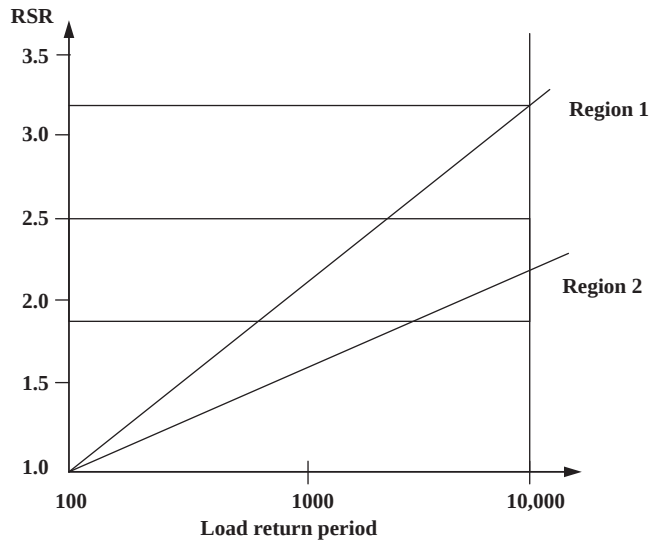

Figure 7.24 Comparison of regional hazard curves.

1.8−2.5 times the 100-year (storm condition) loads indicated by the shaded region of the graph. This reserve described above for 100-year design is referred to as the RSR.

The two curves shown in the figure represent the relationship between the load associated with the 100-year environmental event and the load from *n*-year events.

These curves are referred to in APISIM as region hazard curves. This figure present a typical platform structure in region (1) with a shallower hazard curve that would be expected to have sufficient reserve strength to survive the 10,000-year regional environmental event with an RSR of approximately 2.3 being required. On the other hand, a typical platform structure in region (2) with a steeper hazard curve would not be expected to survive the 10,000-year environmental event since it would require an RSR of approximately 3.4 to do so, which is greater than that explicit in API RP2A.

This example presents a case of regions with different hazard curves, the same RSR being associated with significantly different structural reliability or probabilities of failure. Based on that it is clear that every region in the world has its own environmental hazard curve, so the acceptance criteria are different from one region to another to obtain the optimum reliability against the environmental load.

The probability of structural failure of a range of offshore platforms that exist in the region in question should be well understood. This can be done by performing a structural reliability analysis of the selected platforms as the fleet representatives. The sensitivity studies may be required to establish whether certain characteristics are significant or not.

To account for uncertainties in the derivation of both the loading and response, the probability of failure should be estimated using reliability analysis.

7.10.1 Nonlinear structure analysis in ultimate strength design

A normal structural analysis procedure is based on an idealized linear-elastic model to define the internal forces at each structure member. After that the member section size is selected based on the design codes that achieve the required safety factor from the design code.

In the case of an ultimate strength analysis approach, nonlinearities associated with the plasticity and large deformations of components under extreme loads shall be considered in the element modeling. Nonlinear analysis software tracks the interaction between components as member end restraints are modified and forces are redistributed as a result of local stiffness changes due the member reaching plasticity. The sequence of nonlinear events to many elements will lead in the end to a global collapse mechanism and then the associated system capacity is defined.

Thus, while the typical linear design process checks for the adequacy of each individual component, the nonlinear ultimate strength analysis models the performance of the system as a whole.

A comparison between the elastic structure analysis and nonlinear structure analysis is shown in Figs. 7.25 and 7.26.

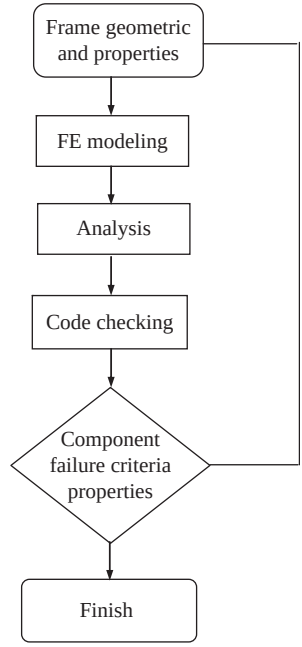

Figure 7.25 Procedure for conventional analysis design.

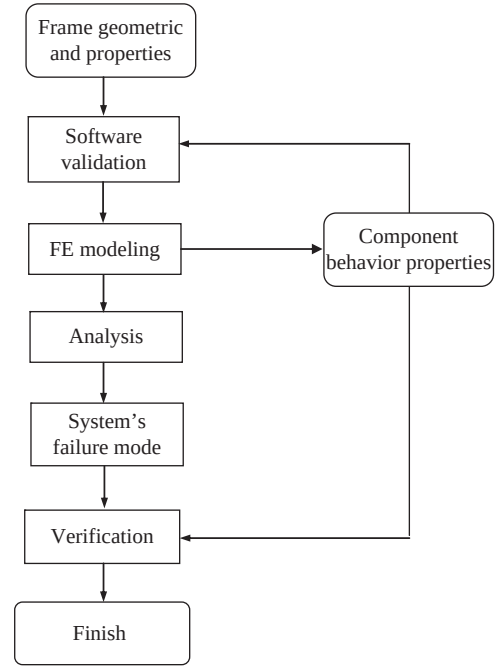

Figure 7.26 Nonlinear ultimate strength analysis.

In general, nonlinear analysis techniques have four basic types, as follows:

- General purpose nonlinear beam column models;
- Plastic hinge beam column models;
- Phenomenological models;
- Shell finite element models.

General purpose nonlinear beam column models

Beam elements do not generally incorporate geometric nonlinearity at the element level and multiple beam elements along a member are required to accurately model buckling responses.

The equation of equilibrium is usually evaluated in the deformed condition, which is the largest displacement.

The stiffness is integrated numerically from the stress distribution at points across the section due to the combined action of axial forces and moments.

When proceeding with the detailed stress−strain material modeling formulations including strain hardening may be available, these may require definition in true rather than engineering format, and components may also be modeled by shell elements or with a combination of shell element as for joint damage representation of members and beam element with a greater modeling and analysis demand.

Plastic hinge beam column models

Some technique have been developed specifically for the ultimate strength analysis of frame structures.

The elements have been derived to model beam column behavior and each member requires only a single element to model the buckling response.

The plasticity may be presented by modeling the propagation of yield through the section and along the element sections or by the formation of annualized hinges.

The plastic hinges are defined using the basic relationships of plasticity and yield surface.

Depending on the element formulation, hinges may form at the calculated locations of first fiber yield for a representative end and mid point location.

Elastic plastic behavior analysis or gradual strain hardening may be accommodated relative to the energy dissipated in the element specification, which can be adjusted to account for the imperfection or to calculate responses to characteristics rather than mean component strength given by test data.

Phenomenological models

In a phenomenological model, component responses are prescribed with force and deformation relationships which can be empirically related to element geometry or determined through analysis. A single element represents the member behavior.

In some software, the type of failure must be anticipated for each component and loading mode prior to analysis and the element type and its nonlinear characteristics defined accordingly, for example:

- elastic members;
- buckling members;
- beam members;
- frame members;
- joints.

Material nonlinearity and initial imperfections are embodied in the phenomenological representation of the test data section yielding and may be determined from the full-section forces and a specified interaction surface.

Shell FE models

Any member or joint can have components that may also be modeled by shell elements or with a combination of shell element as for joints, damage representation of members and beam elements, even in the case of a greater modeling and analysis demand.

Steel usually yields before it fractures, because the uniaxial yield stress is significantly less than the stress required for a cleavage fracture. However, in three-dimensional stress fields the individual stress components can be much greater than the uniaxial yield stress. Without yield occurring in the vicinity of a crack tip, a simple elastic calculation of the stress distribution combined with the von Mises equation predicts that the stresses may reach 2.5 times the uniaxial yield stress before yielding occurs.

Fracture is much more dependent on the largest stress and is less affected by the triaxial stress pattern. Therefore in the triaxial stress field, the yield stress may exceed the fracture stress so that fracture becomes the failure mechanism. This effect is particularly important in the center of thick plates, owing to the through-thickness stresses generated in the plane strain conditions by the Poisson's ratio effect.

Brittle fracture is more likely to occur in cold conditions and at high rates of loading, for example, under impact. The toughness grade of material specified for any application should be carefully selected to account for these factors as well as the likely stress levels, crack growth through fatigue, inspection procedures, and consequences of failure.

Modeling the element

The sliding action of piles within legs should be modeled with the approximate constraint conditions, which allow unrestrained differential axial displacement and rotations, but couple the lateral displacements of piles and legs.

Grouted piles can be modeled as composite leg-pile members. On the other hand, leg and pile members can be modeled as separate elements with full coupling between end degrees of freedom.

For ungrouted piles, the lateral displacements for pile and leg are usually coupled at each horizontal elevation, but some differential movement can occur between elevations.

Conductors provide a limited contribution to the strength of the steel frame system. In most cases, they can be modeled as pure load-attracting members; as long as their load contributions are correctly captured, the conductors can be omitted from the strength calculations.

However, for structures with limited foundation resistance, conductors can contribute significantly to the foundation stiffness and collapse strength of the structure.

In that case, the conductor should also be modeled and analyzed as a structural element and included in the integrated structure soil model. The conductor guide framing at the mudline may then be highly loaded and may need more detailed inclusion in the structural model as primary framework.

Conductor connectivity

Conductor guides should be modeled in sufficient detail to transfer the required loads into the primary framework. Local overstresses in conductor guides should not cause concern if they occur in areas where the model has been purposely simplified and the surrounding primary members have sufficient capacity.

If conductors are included as structural members, the sliding action of conductors is within the guide frames. Differential rotations should also be unrestrained.

The contract action between curved conductors and their guide frames due to the imposed conductor curvature and friction may require specific consideration

7.10.2 Structural modeling

The structures must be modeled in sufficient detail to ensure that the nonlinear analysis program adequately captures the relevant global and local failure modes and load redistribution.

The models for component strength, such as member compressive strength and joint strength, are semiempirical. They have a theoretical basis, but are formulated to conform to experimental data. In general, all theoretical formulations need some calibration in order to represent the behavior of "real" structural components with sufficient accuracy.

Moreover, it should be possible for an engineer to select specific failure criteria and have the analysis tools calculate the structure's strength based on those criteria. In such a case, the requirement for the analysis tool is not to present theoretically correct solutions for the structure, but rather to present a consistent strength estimate based on the engineer's specifications.

This implies that the analysis tools should be able to represent different failure criteria, from the theoretical "idea" solution to characteristic lower-bound solutions, as specified by different codes of practice.

Some nonlinear analysis programs have built-in features to calibrate component failure modes to specific criteria. For other programs, the engineer must give special consideration during the modeling of the structure in order to make the program represent the required failure modes or limiting criteria. Which consideration to take depends on the component as member, joint, or foundation and on the mathematical formulation.

If there is any doubt about the FE formulation, a simple model should be subjected to a well-defined load and deformation path. This will allow the results to be judged and calibrated against engineering practice.

Instead of modeling the structure out of purely geometric considerations, the modeling must consider the analysis tool that will be used for the nonlinear analysis, and the mathematical formulation that is embedded within the program.

This discussion gives a set of modeling recommendations to help make the nonlinear analysis tool produce reliable results that conform to recognized failure criteria and design formulations.

Load modeling is treated in Chapter 6, Corrosion protection, while this chapter discusses the actual analysis execution.

Frame modeling of the space frame model should describe the three-dimensional geometry of the platform.

The model for ultimate strength assessment can usually be significantly simpler than models required for design and fatigue analysis. The primary framework essential in maintaining overall integrity of the structure for the in-place condition must be included in the structure model. Secondary structures and members generating dead loads and/or environmental loading need only be represented in sufficient detail to introduce the relevant loads on the primary structure.

The analytical models should consist primarily of beam elements. the structural members of the framework may be modeled using one or more beam elements for each span between the nodes of the model of the primary framework.

The primary framework of the structure comprises those members that provide the stiffness and strength to the structures. These are usually the legs, the piles, the vertical diagonal members, and the main plan frame bracing members.

Secondary framework

The secondary framework consists of members that do not contribute to the global stiffness and strength of the framework in general. Their structural contribution may be neglected and they do not need to be included in the model as structural members. Boat-landing/fenders, spiderdeck, walkways, and others are examples of secondary members. Secondary frameworks should be modeled in sufficient detail to transfer the required loads into the primary framework.

Some local overstresses in secondary frameworks should be accepted if they occur in areas where the model has been purposely simplified and where the adjacent primary members show sufficient capacity. This should, however, be subject to separate justification in each case.

The following secondary framework should be included in the model:

1. Members or joints which are essential for transfer of reaction loads from conductors and appurtenances, etc. to the main structural elements.

2. Members or joints which are highly loaded by local wave action, a separate assessment may be done on the local behavior. The global assessment may be performed with a simplified model if it is demonstrated that the load can be carried and transferred by the secondary framework.

Secondary members associated with launch framing, mudmats, conductor support during transportation, and others should be included in the model if they share in the system capacity with the primary members.

When neglecting the structural contribution of secondary members, their load-attracting properties, that is loading due to self-weight or hydrodynamic loading, should still be accounted for and included in the appropriate loading condition.

Conductors and other appurtenances such as launch cradles, mudmats, J-tubes, risers, skirt pile guides, etc. should be included in the model if they contribute significantly to the overall strength of the structure or foundation. Otherwise, they may be disregarded as structural elements.

Dented beam and cracked joint

In the case of a dented member which traditionally happened due to a dropped object on the bracing, the strength of the member will be reduced by the following formulas in the case of normal strength and bending strength:

$$\left(\frac{N_U}{N_P}\right) = \exp(-0.08\frac{D_d}{t})$$

$$\left(\frac{M_U}{M_P}\right) = \exp\left(-0.06\frac{D_d}{t}\right)$$

where D_d is the denting depth and t is the wall thickness.

The damaged member should be modeled in sufficient detail to assess the impact of the damage on the global behavior of the structure. A lower bound on the remaining structure's strength can usually be obtained by removing the affected member(s) from the model. A less conservative strength estimate is obtained by modeling the damage in the nonlinear analysis. Some nonlinear analysis tools include special formulation to model dented or distorted members. Alternately, the damage can be modeled explicitly by shell elements, or a reduced cross-sectional area can be specified in the damage zone.

The same philosophy can be applied in the case of cracked joints as they eliminate the member from the model. The less conservative approach can be done by reducing the strength of the affected joint by some fraction. Noting that, the presence of a crack will also limit the ductility and the cyclic capacity of the cracked joint. These properties should be evaluated by refined analysis indicating that a cracked joint is loaded up to its static capacity.

Due to the crack there will be a reduction factor, F_{JR}

$$F_{JR} = \left(1 - \frac{A_C}{A}\right)\left(\frac{1}{Q_\beta}\right)^{m_q}$$

where A_C is the cracked area and A is the weld length multiplied by the thickness, T. Q_β allows for the increased strength observed at β values of 0.6, where β = brace diameter/chord diameter. Q_β is known as the geometrical modifier, usually used in design codes to account for the increasing capacity of uncracked tubular joints at high β:

$$Q_b = 1 \quad \text{for } \beta \leq 0.6$$

$$Q_b = 0.3/\beta(1 - 0.833\beta) \quad \text{for } \beta > 0.6$$

M_q is the power allocated to Q_β and depends on the approach used to estimate the capacity of the uncracked joint.

For tubular joints containing part-thickness flaws, $m_q = 0$.

For tubular joints containing through-thickness flaws, validated correction factors giving lower-bound estimates of the collapse load are at present limited to joints with β ratios less than 0.8 and the following configurations:

- K-joints with a through-thickness crack at the crown subjected to balanced axial loading;
- Axially loaded *T* and *DT* joints with a through-thickness crack at the saddle.

7.10.3 Determine the probability of structural failure

It is necessary to understand the probability of the structural failure of the range of offshore platforms that exist in the region in question. This can be done by selecting a number of platforms that represent the fleet and then applying the structural reliability analysis on these platforms. As discussed above, sensitivity analysis may be required to identify if certain parameters are significant or not, and its weight.

The platform probability of failure shall be calculated by using reliability analysis to consider the uncertainties and variabilities for the load and strength. The analysis procedure is outlined in the flow chart in Fig. 7.27.

7.10.4 Establish acceptance criteria

In order to establish the assessment acceptance criteria it is necessary to establish the relationship between the probability of failure of the representative structures and their reserve strength, defined in terms of RSR.

In the reliability analysis procedure described above the structural capacity of the platform, R, is assumed to be a random variable with a lognormal distribution. The mean value of R is estimated from an ultimate strength (or pushover) analysis as described in Section 7.5. By arbitrarily moving the mean structural capacity to represent a range around the calculated capacity it is possible to estimate the probability of failure of a range of designs of the same structural type. This allows the

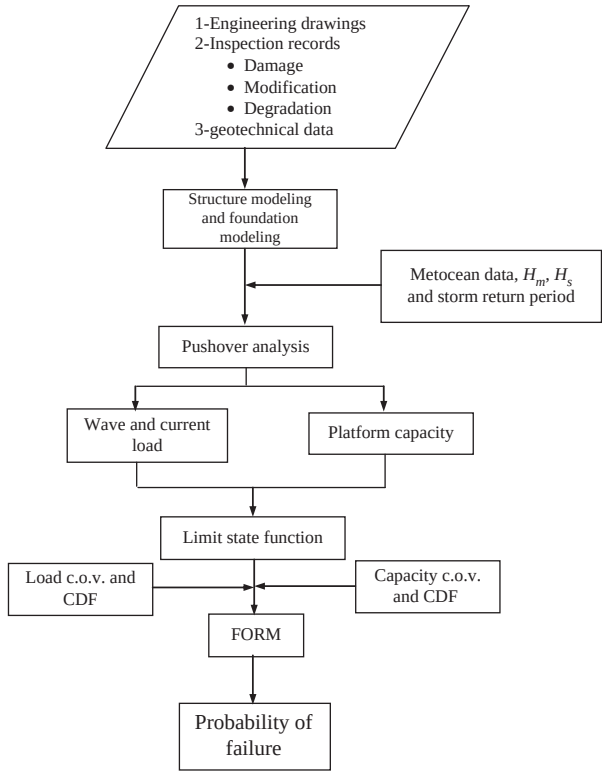

Figure 7.27 Probability of the failure calculation procedure.

relationship between RSR and probability of failure (POF) to be approximated and plotted. It should be noted that the approach is an approximation and assumes the load on the structure remains constant. In fact, it may be argued that increasing RSR would perhaps also increase load; assuming larger members and therefore increased fluid drag loading—and conversely reducing the RSR may reduce the load. If this effect was felt to be significant for the structures in question the effect on the load could also be estimated and included by adjustment of the estimated mean load.

Fig. 7.28 illustrates, for example, a minimum RSR corresponding to a probability of failure is 1×10^{-3}; representative of potential assessment criteria for this (fictitious) region for medium failure consequence.

7.10.5 Reliability analysis

The probability of failure may be calculated for the dominant direction, in the case of platforms that experience storm waves from a dominant approach direction. However, it may be necessary to calculate the failure probability for the eight wave

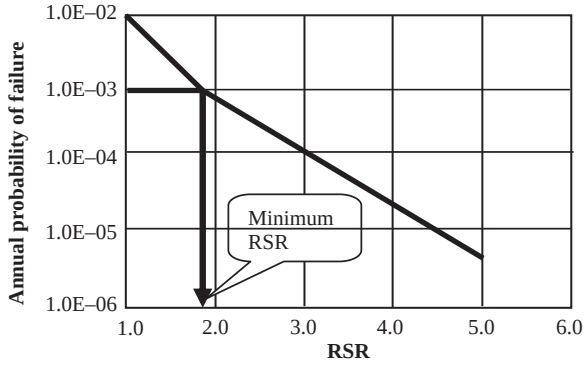

Figure 7.28 Relation between reserve strength ratio (RSR) and the probability of failure.

approach directions to be four orthogonal directions and also four diagonal directions, for platforms that do not have a dominant wave-approaching direction. In this case, failure in each direction is treated as a failure element, and the multiple direction failure forms a series system for reliability calculations.

For each wave direction, the annual platform probability of failure shall be obtained by a system reliability approach. In the platform system reliability analysis, a platform consists mainly of two basic subsystems which are:

- The jacket structure including piles foundation;
- The topsides structure.

The platform fails if either the jacket subsystem or the deck subsystem fails. The platform system reliability analysis models consist of the two correlated subsystems as a system in series. In most cases the topsides subsystem failure does not occur in advance of the jacket/foundation subsystem, even with large wave inundation of the topsides under extreme storm conditions. The failure of the topsides subsystem is not considered acceptance criteria against environmental overload.

Limit state function

The limit state function for estimating the failure probability may be defined as

$$g(X) = R - L, \tag{7.29}$$

where R is the platform capacity in terms of maximum lateral load that the platform can withstand before system failure or collapse. S is the total environmental load, which consists of wave and current load W_v and wind load W_l, that is,

$$g(X) = R - W_v - W_l. \tag{7.30}$$

The limit state function $g(X)$ provides a failure criterion that is a function of all random variables X. A principal failure occurs when the load L is more than the capacity R or when $g(X) < 0$.

First-order reliability method

With the establishment of a limit state function, the conventional formula for computing the probability of failure is:

$$P_f = \int_0^{\infty} (1 - F_s(x)) \cdot f_R(x) \cdot dx \tag{7.31}$$

where F_s is the cumulative distribution function (CDF) for the total environmental load variable S, and f_R is the probability density function (PDF) for the capacity variable R.

The probability of failure can be calculated using the Rackwitz–Fiessler FORM method. The probability of failure is calculated by this method using first-order approximation to the limit state at the design point. The Rackwitz–Fiessler FORM method consists of the following steps:

1. Transform nonnormal distribution random variables that are used to define the limit state function to equivalent normal distribution variables. Therefore the PDFs of the actual variables and the equivalent normal variables are equal on the failure surface at a certain iteration point.
2. The failure most probable point in the limit state surface based on Newton-type recursive equation shall be obtained by iteration.
3. Then, calculate the reliability index, β.
4. After that, the probability of failure is obtained by using the following equation:

$$= \Phi(-\beta) f\ P, (2.3 - 2)$$

where $\Phi(\cdot)$ is the CDF of a standard normal variable.

7.10.6 Software requirement

The fundamental requirement of the software is that it should adequately represent the relevant failure modes for the basic components in framed offshore structures:

- members;
- joints;
- foundation;
- loading.

The software should have clear documentation as to which facilities are available and how they should be applied.

The software should include specification of any limits of validity for special features, for example, D/t limits for a particular local buckling formulation β-range for a joint capacity formulation, etc.

From the quality assurance point of view. It is essential that the software can document compliance with theoretical solutions and test results for single components, substructures, and structural systems.

If there is any doubt about the formulation, a simple model should be subjected to a well-defined load and deformation path. This will allow the results to be judged and calibrated against engineering practice.

Simple program input reduces the possibilities of modeling errors and errors in result interpretation.

The input should be given in familiar engineering terms. Unfamiliar or specialized input parameters increase the possibilities for input errors.

The software should include preprocessing tools and default parameters to reduce the need for detail information from the user.

This is especially relevant for specialized information outside the main engineering focus, for example, parameters concerning numerical integration, mathematical stability, or detail parameters for special program features.

Program default parameters should be listed with a description of what they imply and what any variation may represent.

The primary and essential validation of nonlinear analysis results comes from understanding the development of the global collapse mechanism.

The software should present the analysis results in an efficient manner such that the structural behavior is easily understood by the engineer and is readily conveyed to others. Extensive use of computer graphic capabilities is recommended.

Identification of critical members should be made along with documentation of their strength as a buckling load.

The software should contain a self-checking mechanism such that clear indications are given if the analysis results at any stage in the analysis violate basic assumptions of the theory.

The treatment of different failure modes will vary from formulation to formulation. Different failure modes may typically be treated at one of the following levels:

1. As specialized features implemented in the program. For example, local buckling criteria implemented in the program, including dent growth and modification of postbuckling load shedding.
2. As modeling guidelines, for example, describing how the program's input parameters should be modified to capture the appropriate reduction in axial capacity and the accelerated load shedding in the postcollapse range.
3. As a provision for separate, manual checking after the analysis is completed.

Program modules separate from the structural analysis module are often used to calculate soil parameters and environmental loading.

The interface between the modules should then be well defined and clearly documented, to prevent user errors or misunderstandings during transfer of data.

The following is a list of general modeling requirements for nonlinear analysis of framed offshore structures.

Material properties

- yielding/yield hinges;
- strain hardening;
- strain rate effects.

Section properties

- first fiber yield;
- gradual plastification of cross-section;
- fully plastic capacity;
- interaction between axial force and bending capacity;
- strain hardening.

Member properties

General

- elastic;
- compression (crushing) failure;
- yield (tension) failure;
- stability failure;
- postcollapse behavior.

Behavior modes

- beam bending;
- column buckling;
- residual stresses/initial imperfections;
- member ductility;
- local buckling;
- hydrostatic pressure.

Special formulations

- dented members;
- cracked members;
- grouted members;
- cyclic degradation.

Tubular joint properties

Formulae

- API;
- HSE;
- user defined;
- mean;
- characteristic.

Behavior modes

- elastic flexibility;
- ultimate capacity;
- nonlinear deformation.

Special formulations

- grouted joints;
- ring-stiffened joints;
- cracked joints;
- ground joints;
- cyclic degradation.

Foundation properties

- behavior modes;
- lateral soil failure;
- axial failure;
- monotonic behavior;
- fully degraded behavior.

General FE modeling
General

- joint eccentricities;
- linear dependencies;
- shim elements;
- locked-in forces;
- linear springs;
- nonlinear springs;
- pinned supports;
- fixed supports;
- spring supports;
- prescribed displacement;
- prescribed acceleration;
- load modeling.
- load combinations;
- concentrated nodal loads;
- linearly distributed member loads;
- thermal loading;
- environmental loading;
- self-weight calculated from density and section properties.

Wave kinematics

- stokes fifth;
- airy;
- wheeler;
- stream function;
- current loading;
- buoyancy loads;
- marine growth.

Loading algorithms

- initial loads (self-weight and buoyancy);
- proportional loads;

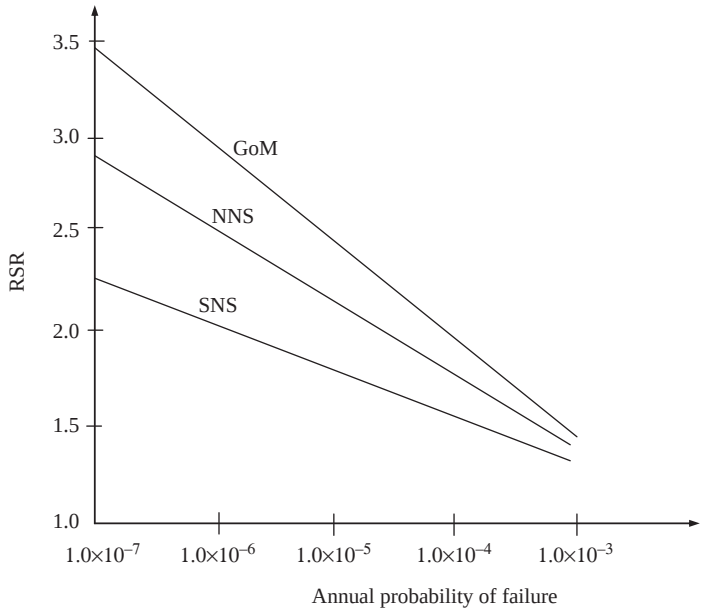

Figure 7.29 Relationship between RSR and annual probability of failure in different locations.

- nonproportional loading;
- wave height incrementation;
- wave-in-deck forces;
- cyclic storm loading.

As presented by Van de Graaf et al. (1994), the relation between the probability of failure and the reserve strength ratio for the offshore structure in GoM the South north sea and north north sea is presented in Fig. 7.29.

Based on El-Reedy and Ahmed (2002), the probability analysis of the tubular joint of offshore structures under axial tension, compression, in plan bending, and out of plan bending at yield is discussed considering the capacity of the tubular joint.

The probabilistic analysis is performed using a Monte-Carlo simulation technique based on the API LRFD model. The ratio between the tubular joint capacity mean value and its nominal value is presented and it is seen that in any case the tubular joint capacity follows a gamma distribution. The parametric study is performed taking into consideration a different chord to branch ratio and different values of steel yield strength.

This study is compared with an experimental test done to a tubular joint for offshore structure and from the study the variation of the model calculation is presented.

Evaluating the strength variability of a tubular joint is an essential requirement in developing probability-based design criteria in assessing the safety of an existing design.

Probabilistic analysis of the tubular joint capacity has been performed using a Monte-Carlo simulation technique and including the variability of the steel yield strength and dimension of the brace and chord.

The capacity of the tubular joint in all cases of loading and different values of β is well presented by a gamma distribution with average bias factor 1.15 and coefficient of variation is equal to 0.28.

The value of the chord thickness has a major effect on the variation of the capacity of the tubular joint. Therefore the thickness of the tubular must be under highly quality control. The bias factor has a slight effect on the β values.

7.11 Offshore platform decommissioning

As discussed in Chapter 1, Introduction to offshore structure, oil production started more than 50 years ago, during which time many fields have matured and there has been a reduction in production below the economic limit. Therefore there are many projects worldwide heading toward decommissioning.

In 1947, the offshore oil industry started in the GoM. Since then, the oil and gas industry has designed, built, and installed more than 6500 structures. The numbers of offshore installations around the world are around 4000 in the GoM, 1000 in Asia, around 700 in the Middle East, around 500 in Africa, around 350 in South America, and around 500 in Europe.

The basic types of offshore installation, with their approximate numbers in 1998, are as follows:

- Around 6000 steel-jacketed platforms (shallow water $<$ 75 m);
- Around 60 concrete gravity platforms;
- Around 100 FPSOs;
- Around 600 steel-jacketed platforms (deep water $>$ 75 m);
- Around 12 tension leg platforms (TLPs).

The physical process of taking offshore platforms out of service safely and securely is a sensitive, complex, and technically formidable undertaking.

In general, as these structures come to the end of their economic lives, they must be decommissioned. Platform abandonment has five steps:

- Obtaining necessary permits and approvals;
- Plugging the well;
- Decommissioning (removing hydrocarbons from equipment);
- Removing the platform;
- Clearing the site.

There are many challenges to the decommissioning process, some of these include finding the right balance in decommissioning between:

- Technical feasibility;
- Environmental protection;
- Health and safety;

- Cost;
- Public opinion.

7.11.1 Decommissioning methods

In general, there are three methods for decommissioning dependent on the condition of the platform and the existing production facilities, and the available crane depending on the location and the possibility of hiring a heavy barge crane. The other main factors in the strategy for decommissioning parts are whether to use part of it or the whole deck, or to sell it as scrap. Therefore the decommissioning decision depends on all of these factors. The three methods and their advantages and disadvantages are discussed below.

Small pieces

This approach means removal of the platform in small sections, typically not more than 20 tons. The advantage of this method is that it limits the size of assemblies that can be removed for reuse or resale. In addition, this approach allows for the opportunity for early removal from the equipment of individual items, which may increase the opportunities for reuse of some of the equipment parts and it will also limit the level of deterioration.

Advantages

- There is no need for a heavy-lift vessel, providing greater flexibility around availability and timescales.
- It can start during late life, and so can add value by providing free space on the deck, reducing periodic maintenance cost and reducing topside weight.
- All plant, equipment, and structural sections can be removed and materials segregated into the various recycle streams and loaded onto a supply boat or barge.
- At an early stage resale or reuse items can be removed and sent to the end user rapidly.
- The advantage of reuse equipment or parts is it reduces the procurement cycle and delivery time. This will allow for identified critical equipment to become available for other operating platforms at an earlier stage.

Disadvantages

- Remove the contamination (decontamination)from the plant and equipment by using high-level technique prior to topside “dismantling” to prevent potential loss of containment. The heavily contaminated material may need some special precautions to be sealed up and lifted whole and transported to shore for further decommissioning.
- More offshore manhours are required for this type of decommissioning.
- There is a high working manhour number, which is a safety concern in addition to multiple vessel trips to shore.
- There is a limited number of experienced workers for demolition offshore.
- The demolishing rate may be influenced by the initial availability of the deck area for material handling.
- Small piece removal of the jacket will require significant additional subsea working than other removal options by using divers or ROV.

- As a safety issue the work will stop whilst supply vessels transport dismantled items to shore.
- There will be an increase in the probability of dropping items to the seabed.
- HSE procedures will need to be reviewed and modified. A professional risk assessment needs to be carried out with those involved with process, instrument, and piping engineers to identify the decommissioning procedure and guarantee safe operations.

Large pieces

Large piece removal is the removal of the platform in sections or modules of up to 5000 ton. This can allow reuse of assemblies up to the size of complete modules. Reuse will be dependent upon ensuring that adequate preservation routines are in place prior to removal.

Advantages

- A wider range of heavy-lift vessels are now available, this will allow for greater flexibility when planning removal activities.
- In this method less offshore manhours are required, which lowers cost and safety concerns.
- Every separate module is prepared for lifting, reducing the preparation time and the risk of loss of containment.
- One crane in a single campaign can lifted modules and lay them on transportation barges for transport to onshore.
- It is preferred for the removal to be done within 24 hours, to reduce the risk of delays from adverse weather conditions.
- In most cases there is an available onshore yard to receive and process the modules.
- Plant or equipment that shall be for resale or reuse will remain in situ and be removed once delivered to onshore.
- As a rule of thumb "less lifts equals less opportunity for damage."

Disadvantages

- If there are lifting points on the modules it must be tested before lifting or installing new lifting points if they do not exist.
- Platform in most cases have been significantly modified since original construction. In most cases it is required to remove some equipment to have a reasonable center of gravity as per the engineering study.
- Some manhours will be spent with the work required to separate the modules for a single lift, but will be less than that required for the small piece method.
- The likelihood of delays due to bad weather, as some lifts are by a lift vessel.
- In some cases multiple repositioning is required, due to the difficulty associated with handling items out of the reach of the cranes. This depends on the type and size of the available crane.
- Greater cost certainty, with the potential for costs to run away reduced.
- In some cases as an outcomes of the engineering study, the jacket may require additional structural stiffening to allow for lifting to prevent the jacket collapsing while tailing and lowering onto the transport barge.

Single lift

This method removes the whole platform topsides in a single lift. The jacket structure can also be removed in a similar manner. This option is mandatory in case of reusing the full platform topsides in another location. If the weight and conditions surrounding the platform prevent the application of this method it can be used for assemblies up to module size following onshore dismantling.

It is also possible to reuse smaller pieces of equipment as spare parts to another similar facilities, therefore care is required to avoid damage during the removal process considering that it is mature facilities.

Advantages

- The same lift vessel can be used for both the topside and jacket to save time and money.
- There are fewer lifts, therefore less time is required for module separation and time at sea.
- Less cleaning is required of the platform offshore, reducing the risk of loss of containment.
- It has the lowest offshore manhours, resulting in lower cost and greater safety.
- Greater cost estimate certainty due to weather delay for the first two methods.
- Resale/reuse plant and equipment will remain in situ and be removed once delivered to shore, where it will be potentially easier to remove.
- There will be less opportunity for damage as it is only a single lift.

Disadvantages

- There are a limited number of heavy-lift vessels and also disposal yards that can cope with the potential high demand, all these factors have an impact on the cost.
- Some maintenance costs may be required as the platform is unloaded with topside for a significant period of time prior to removal as per the decommissioning study.
- In most cases a modification to the platform is required, with additional structural steelwork fitted to provide suitable lifting points.
- The flare, for example, may have to be cut and removed in sections or other modules to ensure a more secure center of gravity for lifting.
- There is a limited number of yard facilities to receive heavy integrated decks. This could become the bottleneck, resulting in removed topsides/jackets being transported greater distances to find suitable disposal yards.
- The jacket may require additional structural stiffening to allow for lifting to prevent the jacket collapsing while lowering onto a transport barge, and this depends on the engineering study.
- There may be a delay in removing the resale/reuse plant and equipment, so preservation measures will be required.

Many of the structures were constructed and installed in the 1970s and hailed as technological feats. However, when they were designed and installed, little or no consideration was given to decommissioning and removal at the end of the field life. Decommissioning of the platform become a challenging subject, as in the offshore oil and gas industry in the UK which has seen a large increase in the anticipated cost of decommissioning over the past 7 years from an estimated £14bn in 2008 to over £40bn currently.

After decommissioning there are only three outcomes: reuse, recycle, or resale. This is the sole decision of the owner as this decision has many constraints dependent on the owner capability in the market, the condition of the facilities, and the market economics.

Decommissioning requires a very restricted plan with competent engineering and contractor. and it is preferred in this type of project to be engineering, procurement and construction (EPC) with a lump sum approach but the engineering in the decommissioning will be as follows:

- The first stage is to collect the available data and the last survey results;
- Provide a study about removal, disposal, remediation, and environmental impacts;
- Modeling and sampling; waste mapping and handling;
- It is important to define the main stakeholder to permit the decommissioning plan and ensure it matches with the regulatory requirements;
- As-lift assessment, impact assessment study, and a decommissioning plan;
- HAZID and safety screening; removal of equipment with NORM if applicable;
- Site inspection and weight estimation, which requires a competent engineering firm that has the capability to estimate the weight of a mature structure with little engineering activities, as drawings and equipment data sheets may not be available;
- The engineering firm shall perform the stress analysis, lifting eye check, and lifting and rigging procedures;
- The transportation and sea fastening of the equipment with the coordination of the installation company is very important.

7.11.2 Cutting tools

One of the main challenges affecting the decommissioning is selection of the cutting tools, as will be presented in the following case study using a rotating machine by a diver, and the other method is by a water jet.

The cutting abrasion materials shall be injected into a water jet and abrasively wear away steel. The abrasion materials include sand cutters, abrasive jet cutters, or abrasive slurry cutters.

There are two types of cutters presently in use:

1. Sand or slag mixed with water with a high volume from 80 to 100 gallons/minute at low pressure from 4000 to 10,000 psi.
2. Garnet or other abrasive materials injected at the nozzle with lower water volume at high water pressure ranging from 50,000 to 70,000 psi. This is used in cutting pile, well-protector jackets with single thickness, small vertical caissons, and wells with uncemented casing strings in shallow water.

The other methods using hydraulic shear cutting are shown in Figs. 7.30 and 7.31.

The other method of cutting by a subsea water jet uses ultra-deep and ultra-high pressure. This method can be carried out using a water jet with high pressure or ultra high pressure. It can be used for cutting 50 mm steel thickness and can be used by an ROV.

In the case of a large cylinder member, it can be cut by using oxy-arc cutting, but extensive precautions are required.

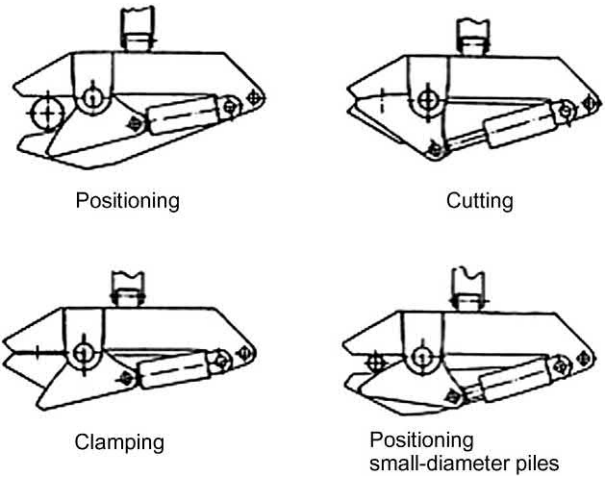

Figure 7.30 Hydraulic shear cutting.

Figure 7.31 Shear cutting on a barge.

7.11.3 Case study for platform decommissioning

This platform required demolition due to its failure.

It was identified after visual survey that the condition of the platform would not allow for safe operations for long-term topsides intervention, due to instability of the platform. It was recommended to prepare the structure for a controlled toppling.

Additionally, it was identified that diver operations would not be possible due to significant overhead and dropped object hazards.

Once the platform is resting on the bottom, the wells can be secured in a similar fashion to the numerous platform and well projects that have been demolished before. The main principle of the toppling process is to disconnect risers near the sea floor, and create hinges in the conductors and north legs, thus creating the potential for the platform to fall in a general southerly direction. All subsea operations are conducted with ROVs. Tug boats are then be utilized to pull the platform over for the final toppling.

The following will outline the steps required to achieve toppling with full control. Due to the dynamic nature of this type of work, the work plan may change due to weather, safety, or operational restrictions to ensure continued work flow efficiencies.

It is worth predicting whether the platform would fail with continued regular weather forces that affect it. It is possible that collapse could also occur after any structural cutting. Therefore it is important to prepare for this potential situation by proposed tooling packages that can be used for toppling, post-toppling debris removal, and any intermediate situation.

A toppling analysis is developed through basic overturning and beam-bending calculations. It has been shown that the platform would require around 85−120 tons of force to topple the platform after proposed cuts to the riser and reducing the conductor and leg capacity by making a notch to convert its behavior as hinges from a structural point of view.

The platform will be rigged at two points to ensure that the deck structure and jacket collapse together. The barge will be used to transfer personnel and rigging to the platform and will be utilized also to handle the long rigging and make the connections to the buoy.

In this type of project a crane vessel must be on-site, as per the site safety procedure and safe boarding.

A plan to help shelter the platform from weather and to be utilized to remove personnel from the platform in case of any issues with the barge crane should be made.

All platform boarding and prerigging will be completed after an ROV survey of the jacket below the waterline, and in a period of limited wind or waves.

All slings and shackles used in the toppling operation will be used at a safety factor of 2. This allows the slings to be smaller and greatly improve the ease of handling, which will be essential for maintaining safe working conditions on the platform.

In most cases, to obtain better overhead access to the wellhead deck below, it will be required to cut and remove the member, in our case in the southern fence on the helideck.

Prior to beginning subsea cutting operations a structural survey should be performed to identify the integrity of the jacket and conductors before starting any cutting operations. This survey will include a review of previous structural data regarding existing failures and be used to track any additional failures that occur during the cutting portion of the toppling.

Figure 7.32 A platform 3D model.

All survey information will be used to develop the 3D model that will be continuously updated (in the field) throughout the project, as shown in Fig. 7.32. This will include a final model showing the platform lying on the seafloor after toppling, as shown in Fig. 7.37.

Noting that, if during the cutting process a significant structural movement is noticed, a brief survey will be conducted to review any additional changes to the global structure. In this case, to give the ROVs proper access to the conductor bay for notching or cutting operations.

For this platform, the first important step is to inspect members before cutting to ensure they are still intact, cut and drop the brace and the horizontal member as shown in Fig. 7.33, and identify any other structural obstructions to conductors from the east face.

In this platform in the south side, there are two rises that will be notched on the south face.

Great care will be taken with these risers as they may be providing some restraining force to the platform. All cuts will take place to confirm the correct location.

On the other hand, there are four rises that will be cut on the north face of the platform. All cuts will take place to confirm the correct location.

In addition, when rigged up to the north face the vertical bracing should be cut prior to final cutting of the north legs, as shown in Fig. 7.37.

After cutting the risers the next step is to cut the leg. The expected final cuts will be the complete severing of the north legs. This operation will require running

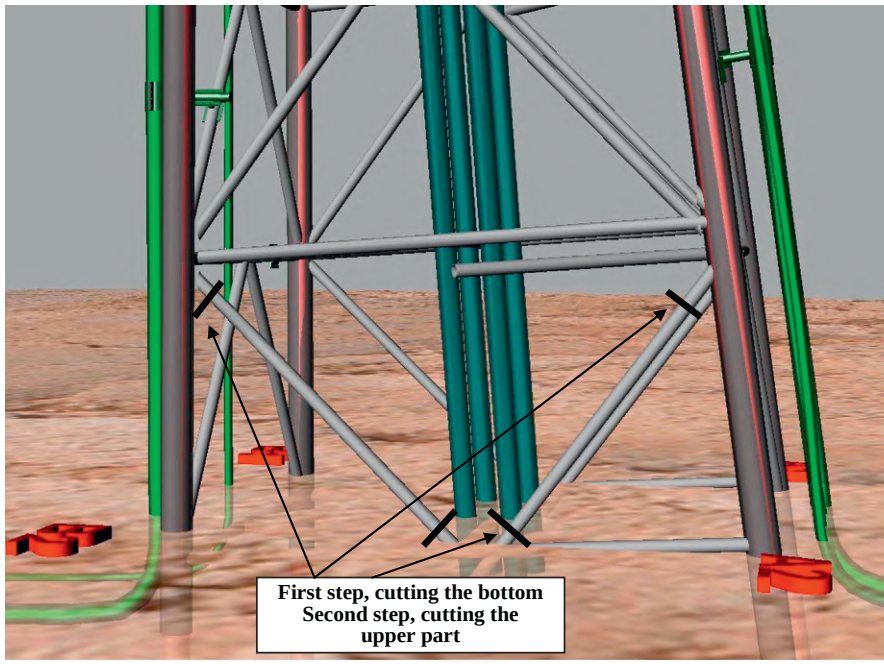

Figure 7.33 Location for the cutting bracing.

Figure 7.34 Notch the conductor machine.

two 36″ diamond wire saws simultaneously. The notching and cutting machines are shown in Figs. 7.34 and 7.35, respectively (see also Fig. 7.36).

The operations will proceed by connecting the tugboats to the toppling rigging on the buoys and standby for direction. A diamond wire saw will be set up on deck, hydraulics attached and tested, and the diamond wire saw lowered to the seafloor by crane and unhooked by the ROV. The ROV will maneuver saws into place (just above the mudline) and clamp onto the leg utilizing surface hydraulics. Take into consideration that the ROV will monitor the cut from a safe distance.

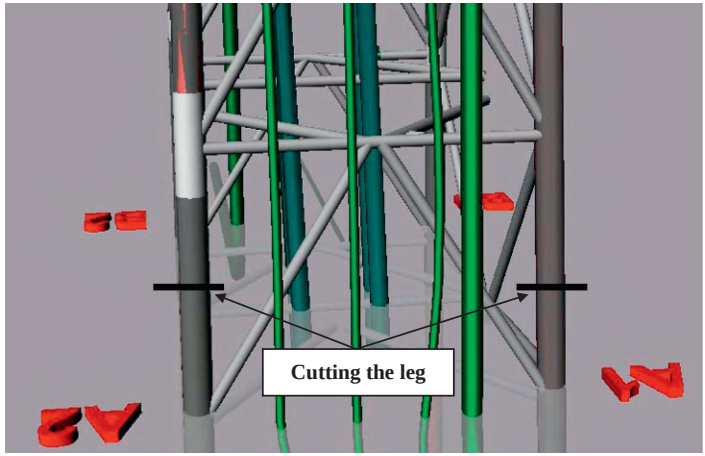

Figure 7.35 Location of cutting leg.

Figure 7.36 Cutting machine.

The north side jacket leg cuts, and the tugs will tie onto the platform prior to beginning the cutting operations.

Tug #1 will pull directly to the south, while tug #2 will pull to the southeast.

During this time it will direct tugs based on two criteria.

The reaction of the global structure is to ensure that once the platform gains momentum it is guided to continue falling.

There is the potential for pollution during the toppling work from any required decommissioning platform parts, such as pipeline/risers (if they have not been recently pigged), trapped annular and other wellbore fluids, and deck storage tanks.

This includes necessary response vessels, containment boom, sorbent boom, and skimmer/separator equipment. All equipment should be ready to be deployed.

Figure 7.37 Model of the platform lying on the seabed.

After the platform is toppled it will be necessary to survey and depict the new orientation and altitude of the platform on the bottom. Utilizing ROV visual survey and single-side band sonar, data will be collected to create a revised 3D model of the platform resting on the seabed, as shown in Fig. 7.37.

Once the platform has been surveyed in its new orientation, it is recommended that additional structural debris removal is required to clear the direct wellbay area ahead of another step by diving operations.

Then, it is anticipated that we will keep the bell at approximately −100'FSW. The structure will also need to be surveyed for any high points that are above this depth and these items will need to be removed as well, utilizing the phase 1 assets.

Based on the toppling analysis, approximately 85−120T of bollard pull will be required to topple the platform after the cutting and notching have taken place. Therefore it has been recommended that a combination of two 60-T (minimum) bollard pull tugs be utilized for this operation. Each tug will pull against the single rigging point defined. An analysis of the tow line distances, compared with fall path was completed.

Drive pipe cutting operations include:

- Based on the conductor survey results, measure down the drive pipe and mark the cut location.
- Survey for any obstructions that could prevent setting the cutting tools.
- Drill rigging holes at the top of the drive pipe for installing shackles for drive pipe removal.
- Clean out any grout in the drive pipe annulus for shackle installation.
- Install the set clamp on the drive pipe.
- Install a roto-mill on the set clamp and secure in place. Note: all hydraulic tools are to be function tested on the surface prior to being sent subsea.
- Connect hydraulics to the roto-mill subsea and test the run tool under direction of a tooling technician.
- Plunge cut drive pipe to required depth.
- Start travel of the roto-mill with the diver monitoring cut. When entering a tight area between two casing strings, the tool will need to be stopped and checked frequently to ensure the internal casing is not being damaged.

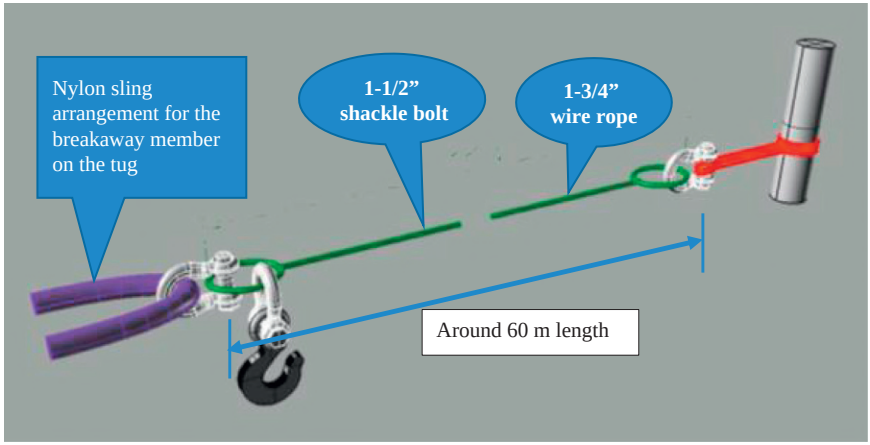

Figure 7.38 Rigging arrangement.

- When the cut is complete, diver to disconnect hydraulics, roto-mill, and set clamp and recover to surface.
- Install rail-mill cutter on the drive pipe to split casing. (Only necessary if casing is cemented.)
- Complete the splitting of the drive pipe. This may also require the use of hydraulic hand cutting tools for making final cuts.
- Rig and strip off casing and deposit on bottom.
- Remove grout using hydraulic chipping hammer to expose next casing string.

The rigging arrangement described in Fig. 7.38 is used for each tug boat.

7.12 Scour problem

There are several methods for scour prevention and repair. Angus and Moore (1982) detail the methods used in the southern North Sea. Gravel grout bags and sandbags have been used effectively to fill in the scoured area and raised the seabed profile up to the original level, based on car tires that have also been used successively.

They are tied together to suit the geometry of the local scour holes, dropped to the seabed, and then moved into position by the divers.

Plastic seaweed is another useful method. The seaweed reduces the water velocity and thus encourages deposition of sediments. This system is mainly based on continuous lines of overlapping buoyant polypropylene fronds that in water generate a viscous drag barrier that reduces current velocity significantly around the piles. The frond lines are fixed to a polyester webbing mesh base that is itself fixed to the seabed by anchors preattached to the mesh base by polyester webbing lines.

Due to reduced current velocity around the pile, it directly prevents seabed sediment in the immediate area of the fronds from being transported out, which is

called "scoured out," and as a reverse action it causes the sediment that is transported across the fronded area to fall into it and be collected in its area.

At the design stage, jacket structures can be made less sensitive to scour by providing stronger piles and jacket legs and this is done be using scour about 1.5 times the pile diameter based on API and up to two times in the case of special situations according to the soil type and previous experience.

7.13 Offshore platform repair

7.13.1 Deck repair

The topsides structure system is robust as it is designed to resist the effects of all loads, hazards, and their probabilities of occurrence, to ensure that damage consequences are very low. Therefore if there is damage from an event with a reasonable likelihood of occurrence it should not cause a complete loss of structure integrity. In such cases the structural integrity with its damage portion shall be enough to allow safe evacuation for personnel.

According to the maintenance plan, which should be performed also by the risk-based inspection technique that will be presented in Chapter 8, Risk-based inspection technique, the first tool of the inspection is the visual inspection that should be performed periodically to follow-up the degradation of the structure. Figs. 7.39 and 7.40 present a sample that may be faced during inspection as the corrosion of the main steel for the stairs and the main supports on the helideck truss support, respectively. The repair of the deck structure is usually easy to perform as for the stair shown in Fig. 7.39 which can be replaced by a new one and also the helideck is

Figure 7.39 Severe corrosion damage to the stair.

Figure 7.40 Severe corrosion to the helideck main truss.

usually replaced and then the existing one repaired to be transferred to another platform if the company has a large fleet, or if not it is repaired it

7.13.2 Reduce the loads

Removing marine growth can be performed by different techniques.

Marine growth removal

Marine growth accumulates on the legs and the bracing with time. As a result the diameter of the members affected by waves is increased. Therefore the lateral load due to wave will increase also with time and be critical if the marine growth thickness increases more than predicted in design based on API or technical practice. Therefore removing the marine growth can enhance the structural capacity. There is a new technique using marine growth removal that is fixed on the leg and bracing as shown in Figs. 7.41 and 7.42.

This technique generates substantial savings in cleaning and prevention costs (up to an 80% reduction) for existing structures, reduces fabrication and installation costs for new structures, and offers both removal and prevention capabilities.

It can be easily installed by riggers or abseilers from above water and divers or ROV from underwater and enables instant visual inspection of substructure without prior cleaning and also is harmless to the environment. This technique is effective in reducing the weight of marine growth for decommissioning of structures and eliminates safety hazards encountered by divers when using high-pressure water jetting which is the traditional method, especially in the splash zone environment

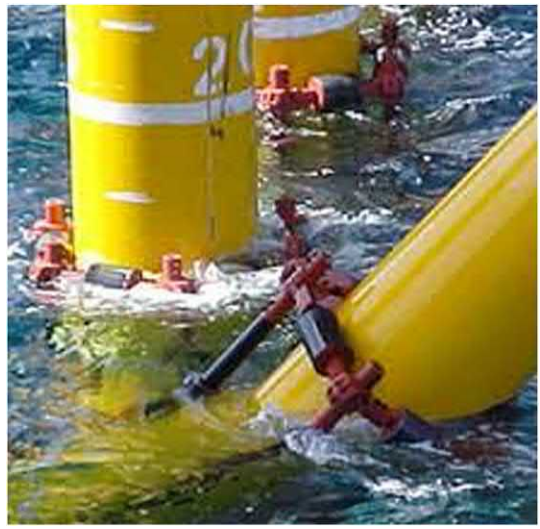

Figure 7.41 Marine growth remover fixation.

Figure 7.42 Working mechanism for marine growth removal.

The fouling system is a painting technique that prevents the accumulation of marine growth on the members but marine growth preventers subsequently maintain existing structures free of regrowth after the removal of existing growth.

Vibration monitoring

Structural vibration monitoring offers a low-cost method of assessing structural integrity. The cost is low because monitoring is done exclusively above water at the deck level by a small crew using lightweight portable equipment.

Platform natural frequencies and mode shapes are typically measured using sensitive accelerometers. These are mounted horizontally and detect the small sway movements of the platform. These movements occur primarily at the wave period but the platform natural frequencies are usually clearly identifiable. By measuring the platform movements at different locations on the deck it is possible to define the sway and torsional natural frequencies.

Theoretically, using the same principle, by measuring movements at different elevations on the jacket it is possible to distinguish between the first sway natural frequency and higher order sway natural frequencies, although in practice higher order natural frequencies will not be strongly excited.

The effect of single member damage on the overall natural frequencies will depend on the jacket structure system redundancy and the member location on the structures, and also on the contribution of that member in the dynamic stiffness of the platform at that particular natural frequency.

The offshore platform natural frequencies depend, of course, on deck mass as well as jacket stiffness. Other factors may have a secondary effect, including variations in the effective mass of entrained water and nonlinearity of foundation stiffness. Further, the mathematical calculation of natural frequencies is a statistical process and each estimate of natural frequency has an associated error. Natural frequency data from continuously monitored platforms are available and can be used to show day-to-day variations.

The above discussion indicates that natural frequencies are adequately stable and sensitive to damage that they can be used in the detection of changes in stiffness of the order of $\pm 3\%$ ($\pm 1\%$ change in natural frequency). Damage to one of the bracings can be detected on platforms with low-redundant member configurations, whereas several or many member failures may occur on higher redundant structures before a change is detected. For example, a loss of a diagonal on a K-braced structure results in a frequency change of $9.5\%-11.5\%$, whereas a similar loss on an X-braced structure results in a change of only $1\%-2\%$. The former is detectable and indicative of a significant loss of overall stiffness.

Topside accelerometers, as shown in Fig. 7.43, are cabled back to a central data collection station using conventional methods. A significant change in recent years has been the development of cableless underwater sensor packages. These systems are battery powered, and data are transmitted by hydroacoustic telemetry.

Nowadays vibration monitoring is widely used as it is cheap compared with follow-up and monitoring of the performance of the structure and provides us the capabilities to use the required action in a reasonable time.

7.13.3 Jacket repair

There are many methods of strengthening and repairing offshore structure platforms. The main element of repair is the clamp, as shown in Fig. 7.45 which presents the shape of the traditional clamp connected to the leg of the platform.

Fig. 7.44 presents the traditional procedure for repairing the leg due to severe corrosion. When reconnecting the leg in step 2 the bracing will be removed and also half the leg is fixed by installing a clamp which is connected to the bracing.

Figure 7.43 Vibration monitoring attached to the deck beam.

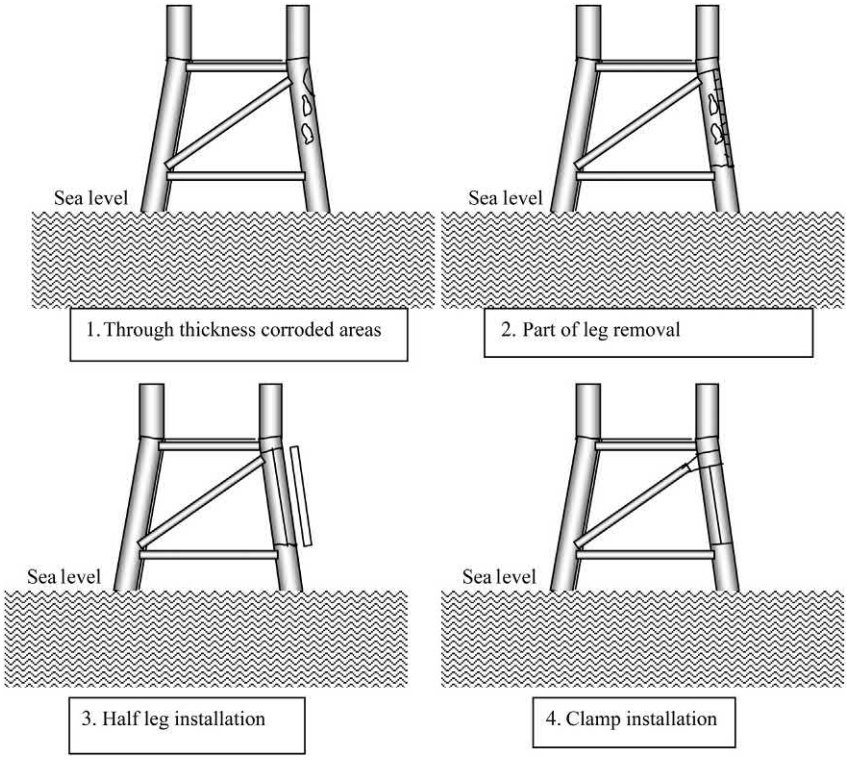

Figure 7.44 Repair procedure.

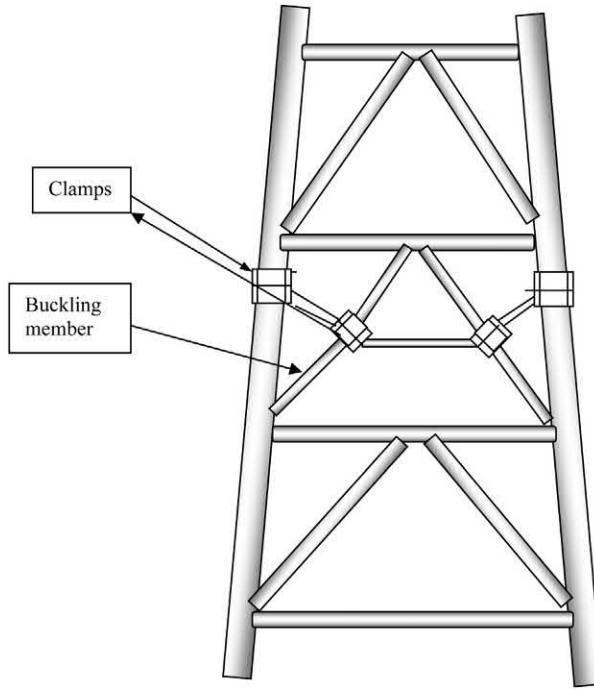

Figure 7.45 Bracing repair.

The other method of repair to strengthen a buckling bracing member is shown in Fig. 7.45. As presented in this figure connection is carried out on the buckling member from the mid point to the leg by two clamps on the leg and on the bracing.

A case of corrosion of the horizontal member is shown in Fig. 7.46. The main principle of strengthening this member is adding a new horizontal member which is connected to the corroded member by clamps.

Clamps can also be used to strengthen the jacket face, as shown in Fig. 7.47.

7.13.4 Dry welding

Welding is often regarded as the best strengthening, modification, and repair (SMR) technique, and no doubt it would be used more often if there were not operational difficulties in its execution. There are several welding techniques and a number of welding processes that can be considered, as follows:

- Dry welding topsides;
- Dry welding at or below the sea surface at one atmosphere using cofferdam or pressure-resisting chambers. All normal welding processes can be used but gas tungsten arc welding (GTAW), shielded metal arc welding (SMAW) and, to a lesser extent, flux cored arc welding (FCAW) are the main methods used in practice;

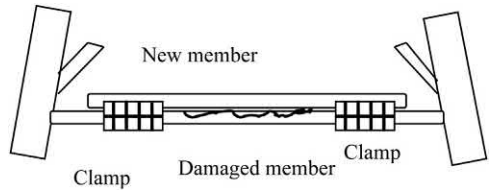

Figure 7.46 Corroded member repair.

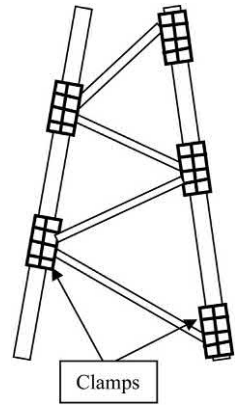

Figure 7.47 Repair by clamps.

- Hyperbaric welding using habitats. The main processes used are GTAW and SMAW, although FCAW and gas metal arc welding (GMAW) are sometimes employed.

Repairs by both cofferdam and hyperbaric habitat welding techniques have proven track records. Since 1970, particularly in the NS, hyperbaric welding has been used as an underwater SMR technique.

Most of the time required for an underwater welding repair is not taken in the preparatory work but rather in the welding process, and this must be planned with considerable care. Around the more complex node geometries, assembling and sealing the welding chamber can take time comparable to the welding operation. There needs to be optimization between separating the chamber into a few pieces to minimize subsea assembly work, but in the case of large chamber components diver risk is increased, especially if the work is in tidal or splash zone conditions.

In most cases the condition of the structure geometry is not exactly the same as in the design, so it is essential to carry out a survey of the location before building the welding chamber.

One of the first and most important tasks is to clean portions of the structure to guarantee that an effective seal can be achieved, allowing the chamber to be dewatered. The welding chamber must be made sufficiently large to enable the welders to have effective access to the weld site.

Dry welding in topsides

Dry welding is a routine and traditional method for the repair of topsides structures above the water level.

The area where dry welding is undertaken is normally designated as a temporary hazardous area and all routine safety precautions must be followed. Hot works are a consideration when welding topsides. Platform shut-in may be required, depending on the location of the welding relative to the well bay and equipment/piping.

It is the most widely used form of SMR, and the only limitation is the requirement for hot works.

Dry welding at or below the sea surface

Since a large body of welding technology exists relating to normal atmospheric pressure, a logical approach to underwater welding repair is to duplicate surface welding conditions by providing a one-atmosphere environment at the repair site. This method is limited to shallow water depths. Two methods are available which can achieve this:

- Cofferdam: This essentially is a watertight structure which surrounds the repair location and is open to the atmosphere. The structure can be open topped, or have a closed top with an access shaft to the surface.
- Pressure-resistant chamber: The worksite is surrounded by a chamber constructed as a pressure vessel, capable of withstanding the water pressure at the depth of the repair location. Once the chamber is in place and sealed to the structure, it is dewatered and the pressure can then be reduced to one atmosphere. The repair crew can transfer to the welding chamber in a one-atmosphere environment, within a diving bell, to perform the repair.

Dry welding is also possible at pressure below the sea surface using a hyperbaric habitat or chamber. The chamber is filled with gas equal to the hydrostatic head at the weld depth. The following factors govern the selection of the habitat:

- The extent of welding required;
- The repair site geometry complexity;
- Depth of repair;
- Welding process and ancillary equipment;
- Environmental conditions.

Given that conditions within the cofferdam or welding chamber duplicate those on the surface, any normal welding process could be used. In practice, GTAW and SMAW predominate, with only minor usage of FCAW.

The primary limitation for atmospheric welding below sea surface is the depth. Differential pressure at depth precludes the use of cofferdams or pressure-resistant chambers due to size and related cost.

Good-quality welding is guaranteed, but there are water depth limitations and it is potentially costly.

Hyperbaric welding

Hyperbaric welding is the most widely used dry weld repair technique for primary structures and pipelines. The repair site is again enclosed within a working habitat, which is dewatered by filling the habitat with gas. Since the gas and water will be at equal pressure at a point close to the bottom of the chamber, the maximum differential pressure will be at the top of the chamber, and obviously depends on the height of the chamber. This differential pressure [normally a few tenths of a bar (10s of kPa)] is easily resisted by lightweight habitats and simple flexible seals, making deployment and sealing of the work chamber operationally feasible. Hyperbaric welding is only limited in depth by access.

A typical hyperbaric welding operation will require the following items of equipment:

- Purpose-built cofferdam or pressure-resistant chamber;
- Diving support;
- Environmental control equipment;
- Pre- and postweld heating equipment;
- Welding equipment (often GTAW and one other);
- Weld inspection equipment;
- Equipment to remove marine growth and grit blast;
- Temporary holding clamps to take the weight of additional members and maintain root gaps, as needed;
- Crane capacity.

The problem with hyperbaric techniques is that the environmental pressure at which the weld is carried out is essentially that of the worksite. These elevated pressures affect the gas/slag/metal reactions for all welding processes, and the high-density gas enhances the rate of heat loss from the weld. Hyperbaric welding research is mainly concerned with ensuring that for any specific environmental pressure and composition, welding parameters can be specified which will ensure the production of welded joints with properties acceptable to the certification authorities responsible for the structure on which the weld is being made. Given that the welding process has to be especially optimized for hyperbaric conditions, the number of techniques used has been limited. The great majority of the welding is carried out using GTAW and SMAW techniques, with small amounts of FCAW and GMAW.

A variety of habitats have been used, dependent on such factors as the extent of welding required, the complexity of the repair site geometry, depth of repair, welding process and ancillary equipment, and environmental conditions. Generally, designs of dry hyperbaric habitat fall into one of the following four groups:

- *Lightweight steel habitats*: These are of stiffened plate construction and are fabricated in two or more sections to allow their placement around jacket members. They may have an open grate floor with an access hole, or be fitted with a closed floor and access shaft. The latter is used in shallow depths where the shaft acts as a surge tube, thereby reducing the volume and pressure changes in the habitat which otherwise could affect diver physiology.

- *Inflatable flexible habitats*: Where the differential pressures are expected to be low, flexible habitats of sufficient strength are practicable. Since differential pressures are low, flexible habitats of sufficient strength are practicable and have been used. The skin of the habitat takes up a shape dictated by the skin membrane stresses and the depth-dependent differential pressure, and is the same shape that would be obtained onshore by turning the habitat upside down and filling it with water.
- *Mini habitats*: These habitats are of small construction with just enough room for the arms and sometimes the head of the welder/diver. These, in essence, only protect the welding head and a small area around the weld. The clear plastic box, fitted with sponge or flexible rubber seals, moves with the head. These devices have not undergone as much development as either large habitat welding or wet welding.
- *Portable dry spot habitats*: These, in essence, only protect the welding head and a small area around the weld. The clear plastic box, fitted with sponge or flexible rubber seals, moves with the head. These devices have not undergone as much development as either large habitat welding or wet welding.

The hyperbaric conditions require that the welding is specially optimized for the elevated pressure, which affects the gas, slag, and metal reactions for all welding processes, and the high-density gas enhances the rate of heat loss from the weld.

The following equipment and tools are required due to this special repair process for the hyperbaric welding operation:

- Purpose-built habitat;
- Saturation diving support;
- Environmental control equipment;
- Pre- and postweld heating equipment;
- Welding equipment;
- Weld inspection equipment;
- Equipment to remove marine growth and grit blast;
- Temporary holding clamps to take weight of additional members and maintain root gaps, as needed;
- Crane capacity.

Platform underwater repair

The platform is a four-leg jacket platform operating in 21 m of water depth. The jacket structure is horizontally braced at four levels with K diagonal braces.

The platform was inspected immediately after Hurricane Andrew. The inspection discovered that two midpoint joints, which are located at EL (−)12 m level between the four legs were damaged, as shown in Fig. 7.48.

The divers performed the wet welding repair work of replacing the two damaged joints.

The repair procedure was as follows:

- The new joint was designed as shown in Fig. 7.49.
- Determined proper welding technique by collection specimens from jacket structure and measuring the carbon equivalent.
- Wet welding specimens were tested.
- Removal of the two damaged joints.
- Grit blasting the remaining structural members in preparation for welding.

Figure 7.48 Corroded part removal.

Figure 7.49 New replacement part.

- Final dimensions were measured to insure the new joints fit.
- Install new joints.
- Inspect all welds using magnetic particles.

There are different repair options. Mechanical clamps, dry hyperbaric welding, and wet welding repairs were considered as repair options. It was estimated that wet welding would save 40% and 60% when compared to dry hyperbaric welding and mechanical clamps, respectively.

7.13.5 Platform "shear pups" repair

The platform consists of two eight-leg jackets in 8ft. of water that are connected above water by a common deck structure and horizontal braces.

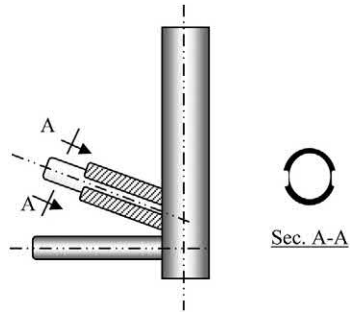

Figure 7.50 Shear pup.

Figure 7.51 Shear pups installed on the platform.

The platform sustained several buckled members as well as small cracks at several above- and below-water joints following a large storm in 1997.

It was found from a subsea survey that there were small cracks in the bracing member which were identified by magnetic particle inspection (MPI). The damaged members were repaired using traditional slip-sleeve replacement members. The cracked joints were repaired using "shear pups" as shown in Figs. 7.50 and 7.51 to strengthen the joints. The shear pups consisted of one-third circumference pipe pieces about 24″ long that "piggyback" on the brace at the joint in order to provide an additional path for loads from the brace into the joint. The shear pups are wet welded into place. The shear pups were considered a better repair than mechanical clamps due to the complexity of the joint configuration, making it difficult for a clamp. In addition, the cracks were small at these locations, identifiable only by MPI, or were an order of only a few inches or less.

The repair procedures was as follows:

- As with any wet weld, take a material sample of the jacket to be sure that wet welding can be performed;

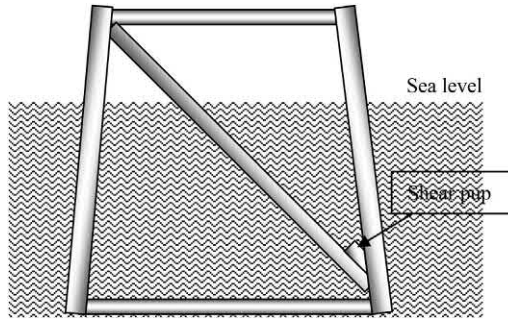

Figure 7.52 Sketch of proposed wet weld repairs.

- Clean joint for fitting the shear pup and wet welding;
- Multiple "generic" 24″ shear pups are cut and prepared on-deck, including approximate copping of ends at the joint connection;
- The ends of the shear pup opposite the joint are also copped via transition to a narrow section in order to eliminate the potential for fatigue cracking;
- The diver fits a generic shear-pup into place and notes additional copping needed, if any, as shown in Fig. 7.51;
- Final copping on shear pup above water;
- The diver wet welds the shear pup into place and inspect the welds.

7.13.6 Underwater repair for a platform structure

The platform is a four-leg, fixed steel jacket platform operating in 43 m of water. The jacket is a vertical diagonal braced structure.

The underwater inspection revealed a buckled vertical diagonal. The buckled area is located approximately in the center of the member. Replacement of the member and wet welding work for the buckled vertical diagonal member were performed.

Repair procedure

- Remove vertical brace leaving a 2-foot stub at top and a 6″ stub at bottom.
- Install single telescoping vertical diagonal member over stubs.
- Wet weld the sliding sleeve as shown in Fig. 7.52 (see also Fig. 7.53).

7.13.7 Case study 2: platform underwater repair

The platform is a fixed-steel jacket platform operating in 7.8 m of water depth. The jacket structure is braced with vertical diagonal bracing members.

An inspection revealed a 10¾″ diameter vertical member, with a 30″ crack located at the midpoint around the circumference, as shown in Fig. 7.54. An additional 6″ diameter hole was located on the horizontal bracing member.

Contractors performed the wet welding replacement work of the vertical diagonal member and the dry welding work of the corrosion hole patch.

Figure 7.53 Underwater repair.

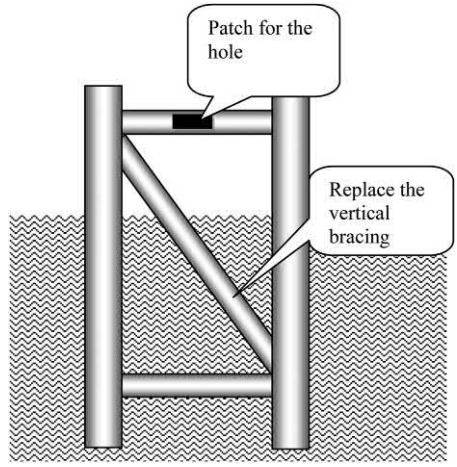

Figure 7.54 Repairs to the members.

7.13.8 Clamps

Repair clamps are normally constructed from low-carbon steel and consist of a reinforcing sleeve which may include brace attachments. For ease of installation, the clamps can be split or hinged. Whether used for repair of a member or node, a clamp will typically take on the same general appearance as the part of the structure it is to reinforce. In general typical joint clamps weigh between 0.5 and 10 tons, although clamps weighing some 50 tons have been used, and they may require grouting, bolting, or some other structural bonding technique.

Clamps may be used to repair a member, by installing an additional brace, and it is normally used for a connection to a riser or caisson if there has been loss of support to such an appurtenance.

However, the principal use of steel repair clamps is in repairing primary structural joints. There are four clamp types traditionally use in offshore platform repair. Their classification is based on the installation and fixing method rather than the terms of usage.

- The stressed mechanical (friction) clamp uses long stud bolts to produce a friction grip on the repaired structural elements.
- The unstressed grouted repair clamp relies on grout shear strength to affect load transference, working in a similar way to a grouted pile sleeve connection.
- The stressed grouted clamp is a hybrid of the above two clamp types with load being transferred partly by grout bond but mainly by friction. It is popular for its ability to tolerate dimensional variation while achieving load transfer in a reasonable sleeve length.
- The stressed elastomer-lined clamp is similar to a mechanical clamp but for an elastomer there is usually a neoprene liner that lies between the member and the clamp. Such clamps are often selected for repairs to caissons and other secondary structural elements.

The basis of any clamp design must be the establishment of the forces in the structural elements under operating and storm loading conditions. It is normal to evaluate such forces for the undamaged condition and then design the clamp so that load transfer is accomplished within the body of the repair clamp.

The technology surrounding clamp installation is highly developed and a number of specialist companies are now able to provide the necessary equipment and materials on a contract basis.

Stressed mechanical (friction) clamps

A stressed mechanical clamp is a steel-to-steel friction clam that is connected by long tension stud bolts, it comprises two or more segments of closely fitting stiffened saddle plates, stressed directly onto a tubular section by means of long stud bolts. The strength of a mechanical connection is obtained from steel-to-steel friction generated by compressive forces normal to the tubular/clamp saddle interface, applied by the external bolt loads.

These clamps are generally used for the strengthening and repair of damaged members or connecting new members. A high degree of tolerance is required for close contact between the clamp and the tubular member, therefore these clamps are unsuitable for repair of tubular joints.

The major advantage of a mechanical clamp is that large forces can be transferred through friction over a short clamp length, limited only by the hoop resistance of the member.

The time of installation for stressed mechanical clamps varies depending on the complexity of the clamp (for instance, number of clamp segments), space limitations, and water depth of the repair site. Typically, installation times vary between 2 and 6 days, depending on size and complexity.

Over the past 20 years there have been numerous applications of stressed mechanical clamps worldwide. Their use has principally been to repair or strengthen jacket components damaged due to boat impact, fabrication flaws, fatigue cracking, and corrosion.

In this type of clamp full contact between the clamp and member surface interface is required, and the clamp offers minimal translation or angular tolerances. Thus, extremely accurate offshore surveys are needed for its proper construction.

Therefore the clamps require very tight tolerances in fabrication. The connection between clamp and tubular is susceptible to crevice corrosion. Therefore it needs periodical inspections to confirm bolt tension.

These are one of the quickest clamps to deploy and have good transfer capacity. They require detailed survey and good fabrication tolerances, and are ideal for clamping on intact tubular members to strengthen, replace, or add members.

For diver installation of a stressed mechanical clamp, the following items of equipment/support are required:

Diving spread and divers;
Crane for lifting and placing in position;
Rigging for installation;
Underwater cutting and grinding equipment, if obstructions have to be removed;
Stud bolt tensioning equipment;
Monitoring equipment, such as a video camera;
Equipment to remove marine growth and grit blast.

Unstressed grouted clamp connections

The grouted sleeve type clamp uses short bolts. An unstressed grouted clamp or sleeve connection comprises sleeves placed around a tubular member or joint with the annular space filled with grout. The sleeves may be split, as in the case of a clamp, or continuous as in a sleeve connection. For split sleeves, short bolts are provided and these are tightened prior to injection of grout into the annulus.

The bond at the grout−steel interface provides the only means of transfer of load between the tubular member and the clamp. To increase the capacity of the clamp, often the length of the clamp needs to be increased. The provision of shear keys, usually in the form of weld beads, can increase the clamp capacity, but it should be borne in mind that the underwater welding option is very expensive.

Unstressed grouted clamps and connections offer a versatile means for strengthening or repair of tubular joints and members since they require less accurate offshore survey. Both angular and translation tolerances can be readily accommodated by the annulus. However, the loading regime and the availability of space are dominant in deciding the suitability of an unstressed grouted connection or clamp.

The time of installation for this type of clamp varies depending on the complexity of the clamp and the number of pieces in which the clamp is installed. The number of bolts that have to be tensioned and the amount of grout will influence the timescales. As an example, two X joints strengthened using unstressed grouted split sleeve connections have been reported with a total dive time of 50 hours. The dive

time comprised 10 hours each for survey and cleaning, 20 hours for clamp installation and bolting, 5 hours for grouting, and 5 hours for inspection.

It is important to note that curing time should be allowed in the program to ensure that the unstressed grouted clamp/sleeve connection is not subjected to the loading before the grout has gained sufficient strength. In some instances, temporary clamps may be necessary.

Several applications of unstressed grouted clamps and sleeve connections are evident. Pile or sleeve connections for numerous jackets make use of this technique. For repair/strengthening, unstressed grouted clamps/sleeve connections have often been used to overcome fatigue cracks and damaged members due to boat impact.

The advantage of this technique is that it has reasonable transfer capacity, good tolerance for fit-up and is ideal for clamping on joints and members. It is also particularly good for strengthening dented members.

Without the use of shear keys, the required connection length may be unacceptably long. Grout seal, if improperly fitted, often results in leakage of grout resulting in loss of friction.

The following equipment is required for diver installation of an unstressed grouted connection or clamp:

- Diving spread and divers;
- Crane for lifting and placing in position;
- Rigging for installation;
- Underwater cutting and grinding equipment, if obstructions have to be removed;
- Bolt torque/tension equipment for spilt-sleeve clamp;
- Grouting spread;
- Monitoring equipment (e.g., a video camera);
- Equipment to remove marine growth and grit blast.

Stressed grouted clamps

A stressed grouted clamp is formed when two or more segments of strengthened saddle plates are stressed by means of long stud bolts onto a tubular member after grout has been injected and allowed to cure in the annular space between the clamp and the tubular member.

This type of clamp is a hybrid between a stressed mechanical clamp and an unstressed grouted clamp. The strength of the clamp is obtained from a combination of "plane pipe" bond and grout/steel friction developed because of the compressive force applied normal to the grout/tubular surface interface by the stud bolt tension.

Stressed grouted clamps offer the benefits of stressed mechanical clamps of high strength-to-length ratio, and the benefits of unstressed grouted clamps of the ability to absorb significant tolerances.

As an example, eight stressed grouted clamps were fully installed on a platform in the GoM in a total of 18 days. About one-third of this time was used in removal of obstructions, while cleaning, clamp installation, grouting, and stud bolt tensioning took an equal amount of time. It is important to recognize, however, that installation time is very dependent on the complexity of the clamp, access at the repair

site, water depth at the repair site, and environmental conditions that may severely limit dive time and greatly influence weather downtime.

Stressed grouted clamps can be viewed as representing the strength advantages of stressed mechanical clamps with the tolerance advantages of unstressed grouted clamps; it is therefore not surprising to note that stressed grouted clamps are the most popular form of clamp concept and are used widely these days.

Grout seals, if improperly fitted, often result in leakage of grout resulting in loss of friction. They have good transfer capacity, good tolerance for fit-up, and are ideal for clamping on joints and members, they are particularly good for repair of joints.

The required equipment and tools are the same as for the unstressed grouted clamp.

Stressed elastomer-lined clamp

The elastomer-lined clamp is used in secondary members as the stiffness is not critical to its performance because this liner is flexible, which reduces the repair system efficiency and so it is not used in main members. This type of clamp is used for stub connections, appurtenances and seal holed caissons.

The time duration for installation varies depending on the complexity of the clamp (for instance, number of clamp segments, space limitations, and water depth of the repair site). In general the installation time is similar to that for stressed mechanical clamps.

It is worth mentioning that stressed elastomer-lined clamps are similar to stressed mechanical clamps, the only difference being that an elastomer lining is bonded to the inside faces of the clamp saddle plates. The lining is made up of solid polychloroprene, which is commercial neoprene sheets.

The strength of the clamp is derived from external bolt loads, which impart compressive force normal to the interface of the liner and the tubular member. This type of clamp is not recommended for the transfer of forces between structural components. It is recommended for the attachment of components such as guides for appurtenances.

The elastomer lining offers a degree of angular and translation tolerance, eliminating the need for very accurate offshore surveys as required for stressed mechanical clamps.

The relatively low stiffness of the liner gives rise to significant stud bolt load fluctuations due to elastomer relaxation. Fatigue of stud bolts therefore requires careful consideration. Large-scale tests have demonstrated that this type of clamp does not transfer structural forces. Furthermore, the typical coefficient of friction between liner and steel is considerable lower than previously assumed values. These clamps require periodic inspection to confirm bolt tension.

It is one of the quickest clamps to deploy, requires reasonably detailed survey, has poor axial and bending load transfer capacity, and is ideal for clamping on intact tubular members or adding to members and appurtenance supports.

The required equipment for installation is the same as the equipment for the stressed grouted clamp.

Drilling platform stabilization post Hurricane Lili

A drilling platform that was severely damaged when Hurricane Lili passed through the GoM is located in 71 m water depth.

In order to stabilize the platform during well plug and a bonded process, additional templates and piles were installed to strengthen the damaged platform.

The leeward pile was severed at 6.3 m below the base of the jacket leg. The pile severance was located at the mudline due to leaning of the platform. In addition, the remaining three piles were assumed to be damaged at or below the mudline due to the platform rotation.

The diving activity performed member cleaning, clamp installation, and grouting operations. Once the grout had been sufficiently cured within the clamp annulus, the stud-bolts were tensioned to the required tensile loads. Heavy lifting and pile installation was carried out. The prestressed grouted clamp is as shown in Fig. 7.55.

Note that several repair methods were considered, such as guy wires to piles, props, and attached to the undamaged production platform. It is also worth mentioning that analyses indicated that templates were required in addition to severed pile reinstatement to provide sufficient torsional resistance against potential hurricane wave loads. The strengthening scheme consisted of two templates, a stressed grouted clamp, and five piles.

The repair procedure was as follows for this platform:

- Clean the exposed pile;
- Cut holes in the base of the severed pile and place the support clamp;
- Install the sleeve clamp around the exposed pile using the support clamp;

Figure 7.55 A prestressed clamp.

- Close the clamp and hand-tighten several bolts;
- Check seals for leakage and place grout;
- Once grout has reached the required cube strength, stress the 32 2″ stud-bolts to required tensile load;
- Lower piles through sleeves to the self-penetration depth;
- Hammer piles to the required 200′ penetration;
- Grout pile sleeves.

7.13.9 Grouting

Using grouting by filling of structural members is a cheap and effective solution to several repair and strengthening problems. It is most beneficial in the following conditions:

- Compressively loaded dent-damaged elements where the grout prevents any further deformation of the tubular section. In such cases the grout filling need only be extended to the immediate region of the damage;
- Improve the strength and fatigue performance of a tubular joint by grouting the chord in the location of the entire tubular joint.

There is no benefit accrued under the following situations:

- Tensile loads in the element (unless there is a problem with hydrostatic/tension interaction collapse);
- Unchanging compressive or bending loads in element (because a repair can only carry a load which is applied after the grout has set);
- Partially filled compressive elements—because there is no guaranteed load transfer mechanism between the grout and the steel.

The work with grout should be through a competent company as this should deliver a grouting design mix to reduce the heat of hydration effects, grout shrinkage, grout port locations, and ensuring complete element filling if deemed essential.

In general, grout-filled elements and joints will be stiffer than their pure steel counterparts, and as such they may attract more load in a statically indeterminate frame. In seismic zones, the additional mass associated with grout filling may need to be considered in the structural analysis. On any structure the additional weight imposed by grout may constitute a significant load, particularly if the grouted joint or element lies in a horizontal plane, as is the case with conductor bracing.

Based on typical offshore timescales, a grouting operation should be achievable with 2−3 days offshore work.

Joint grouting

In general joint grouting is perform by filling of a chord with grout in the region of a tubular joint. Grouted joints have the chord member fully filled with a cementitious grout material. Double-skin joints are those in which the chord member contains a pile and a grouted annulus.

For a member rather than the jacket leg, it is easy to fill a chord member over its full length, as this method avoids cutting windows in the member to insert seals to localize the grout plug. The grout can be placed through small-diameter inlets and outlets, which can be drilled and tapped into the tubular wall. Jacket legs need only be filled up to the level which is required in view of the quantity of grout needed.

Filling tubular chord members with a cementitious material will increase their strength and improve ductility, and the radial stiffness of the chord member will increase due to grout. The grout restricts local chord wall deformations leading to a reduction of deformation-induced bending stresses and associated SCFs. Therefore it will improve the fatigue life.

Therefore grout filling of tubular chord elements is used to improve the static strength of the joint and to extend the fatigue life of the connections made at the joint. The repair method has the advantage of introducing no additional wave and current loads on the platform but the local dead loads can be increased.

Only grout-filled joints have been considered. It is therefore assumed that the material is cementitious and not reinforced. If the joint is simply pumped full of grout then a simple grout-filled joint is created. In some instances there will be a concentric pile within the joint as is the case with many leg sections, and the resulting construction is then termed double-skinned. The grout is assumed to completely fill the available annulus in the joint.

Ring stiffening is sometimes used at the joint to increase the resistance of the chord wall to applied member forces. Both of these details as increase can diameter and stiffening it, may cause problems in ensuring complete grout filling in the joint.

In most cases of grouting the joint takes about 3−4 days as the time should be enough for installing grout bag seals, allowing seals to set and cure, and then grouting the plug.

Void formation is a potential problem at ring-stiffened joints and at joints with an expanded can diameter. There is increased strength and fatigue performance of a tubular joint, and no increase in hydrodynamic load but mass is added to the structure.

If a large volume of grout is used, excessive heat while setting will need addressing. Consideration of the mix design and heat loss will be required.

The following equipment is required for a typical grout-filling operation:

- Diving spread;
- Drilling and tapping tools for grout ports;
- Underwater cutting and grinding equipment if temporary seals are to be placed;
- Grouting spread;
- Monitoring equipment, such as a video camera;
- Marine growth-removing equipment.

Grout filling of members

Grout filling of a member increases both its cross-sectional strength and its overall stability. This process provides a relatively easy method for strengthening tubular members, particularly compression members with or without bending. Grout filling

of the compression member increases the axial load capacity and prevents local buckling.

As a direct effect of grout filling, the additional mass of the member, the additional earthquake load due to increased inertia, and the extra stiffness of the member and tubular joints along its length need to be considered in the design.

This technique is most beneficial for tubes with low L/D ratios and high D/t ratios.

It is important that the grout completely fills the tubular, as small voids close to the tubular inner wall may reduce the load-carrying capacity of the strengthened member significantly. Void formation is also a potential problem for all ring-stiffened tubulars.

If there is no damage to the member but an increase in axial load-carrying capacity is sought, then a few preliminary calculations will indicate if there is likely to be a sufficient increase in the member capacity. If the member is short and has a low kl/r ratio then the axial load capacity in compression will be increased if the element is completely filled and load transference can be made from the node capping plate to the grout body. If the element has a high D/T ratio then there may be an improvement in load-carrying capacity due to the prevention of local instability.

The design mix should be done professionally to prevent the generation of excess heat during setting as a large volume of grout will be used.

On the other hand, grout filling has little benefit for tension members. In addition, full grout filling must be achieved and an increase in mass due to the filling of a member with grout may result in overstress of the member under seismic and/or in-place conditions.

It will result in an increase in the strength of a member but not an increase in hydrodynamic load and it adds mass to the structure.

For grouting the members operation requires the same equipment as specified above for grouting joints. In the case of filling the annulus between the pile and leg by grouting, the load is transferred to the pile from the structure across the grout. As per the experimental work that was done for the grouting annulus pile present, the load transferred is a combination of bond and confinement friction between the grout and the steel surfaces and if shear keys are used they bear part of the transfer load.

To have a uniform annulus or space between the pile and the surrounding structure, centralizers should be considered. As per API RP2A the minimum annulus width of 38 mm (1½ in) should be provided, if the grout is the only means of load transfer. The dimensions of shear keys should be considered to have adequate clearance between the pile and sleeve.

Packers should be used as necessary to confine the grout. Grouting good-quality control and installation are needed to avoid any possibility of dilution of the grout and to minimize the formation of voids in the grout.

Allowable axial force calculation

If there are no reliable detailed data that assist in the use of other values of connection strength, then the allowable axial load transfer shall be considered the smaller

value from the pile or leg of the force calculated by multiplying it for the contact area between the grout and steel surfaces. The allowable axial load stress is f_{ba}, where f_{ba} is calculated by a reasonable value that must be greater than or equal to the calculated applied axial force.

The value of the allowable axial load transfer stress, f_{ba}, should be taken as 0.138 MPa for loading conditions 1 and 2, and 26.7 psi (0.184 MPa) for loading conditions 3 and 4, where the loading conditions based on API are as follows:

1. $E_o + D_L + L_{max}$
2. $E_o + D_L + L_{min}$
3. $E_D + D_L + L_{max}$
4. $E_D + D_L + L_{min}$

where E_o is the operating environmental condition, D_L is the dead load, L_{max} and L_{min} are the maximum and minimum live loads, respectively, and in both cases the live load is appropriate to the normal operating condition of the platform. E_D is the design environmental condition in extreme environmental conditions.

Where shear keys are used at the interface between steel and grout, the value of the nominal allowable axial load transfer stress, f_{ba}, should be taken as:

$$f_{ba} = 0.138 + 0.5 f_{cu}.\frac{h}{s}; \text{MPa} \tag{7.32}$$

for loading conditions 1 and 2, and should be taken as:

$$f_{ba} = 0.184 + 0.67 f_{cu}.\frac{h}{s}; \text{MPa} \tag{7.33}$$

for loading conditions 3 and 4, where f_{cu} is the unconfined grout compressive strength; MPa;h is the shear key outstand dimension, mm; and $s$is the shear key spacing, mm.

Shear keys designed according to Eqs. (7.32) and (7.33) should be detailed in accordance with the following requirements:

1. Shear keys may be circular hoops at spacing "s" or a continuous helix with a pitch of "S_s." Shear keys should be one of the types indicated in Figs. 7.56 and 7.57.
2. For driven piles, shear keys on the pile should have sufficient length to guarantee that, after driving, the pile length in contact with the grout has the required number of shear keys as designed.
3. The cross-section for each shear key and weld shall be designed to transfer that part of the connection capacity which is attributable to the shear key for different loading conditions.

The shear key and its welding should be designed as per the allowable steel and welding stresses to be capable of transferring an average force equal to the shear key bearing area multiplied by 1.7 f_{cu}, except for a distance of two pile diameters from the top and the bottom end of the connections as to be 2.5 f_{cu} should be used.

The following limitations should be observed when designing a connection.

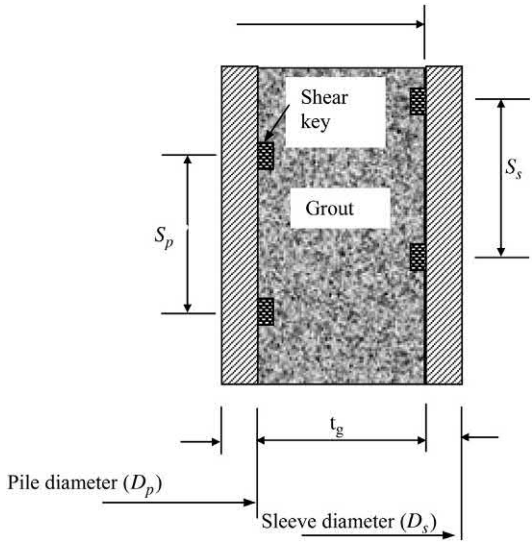

Figure 7.56 Grouting the annulus between piles and legs.

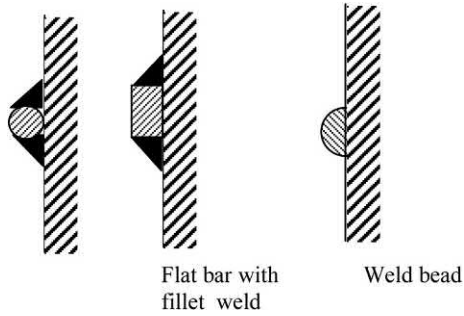

Figure 7.57 Recommended American petroleum institute (API) shear key detail.

- 17.25 MPa $\leq f_{cu} \leq$ 110 MPa;
- Sleeve geometry $D_s/t_s \leq 80$;
- Pile geometry $D_p/t_p \leq 40$;
- Grout annulus geometry $7 \leq D_g/t_g \leq 45$;
- Shear key spacing ratio $2.5 \leq D_p/s \leq 8$;
- Shear key ratio $h/s \leq 0.10$;
- Shear key shape factor $1.5 \leq w/h \leq 3$;
- f_{cu} $(h/s) \leq 5.5$ MPa.

Composite technology

The definition of composite technologies is to use a combination of two or more materials. Composite materials have been extensively used onshore, however, the

use of composites for offshore structural applications has been somewhat limited. Composites have been used widely for pipeline and piping on topsides, and they are seeing greater use for tertiary steel structures such as handrails and gratings.

There are two main groups of composites that have been used in offshore applications, namely:

- Reinforced epoxy grout—A rebar reinforced epoxy grout typically used for the repair of conductors.
- Fiber reinforced polymer (FRP) is a structure, which contains an arrangement of unidirectional fibers or woven fiber fabrics embedded within a thin layer of light polymer matrix material. The fibers, composed of carbon or glass, provide the higher strength. The matrix in most cases is from polyester, epoxy, or nylon, which binds and protects the fibers from damage, and mainly transits the stresses between fibers. The matrix also provides a bond and thus an interface for the transfer of forces between the parent structure and the composite component. FRP can be molded or pultruded to form many shapes for topsides applications.

Composite applications can consist of either of the above or a combination of both. One variation of the above grouted clamps/sleeves is covered in the clamps section in this chapter.

The use of composites to date, particularly for offshore applications, has been limited largely by lack of design guidance, unfamiliarity by designers, combustibility concerns, lack of performance data, and fabrication scale. These have in the main been addressed, with specialist contractors offering off-the-shelf solutions and data providing proof of performance. A range of resins are available for different applications including low generation of smoke and toxicity in fires.

The application of composite is different in repairing topsides rather than for subsea applications. Composite technology to date has shown little success in the use of composites subsea when the laminates are formed in situ. Preformed components can be used, however, and are typically limited to nonstructural applications. The use of composites in the topsides are as follows:

- repair wraps to tubular members;
- wraps to deck legs for corrosion prevention;
- grating;
- stair treads and ladders;
- handrails;
- mudmats;
- fire and blast walls;
- access platforms.

Many of the topsides composite applications can be utilized as part of strength and repair or for new builds. A number of notable new-build offshore facilities have made extensive use of composites for a range of applications. As much as 10% of the topsides weight has been represented by composite components.

Reinforced epoxy grout

A rebar reinforced epoxy grout is typically used for the repair of conductors. Reinforced epoxy grout provides a method of repair which requires little

preparation onshore prior to implementation of the repair offshore. The repair technique can readily conform to the structure geometry without the requirement for a detailed survey. The main advantages of using epoxy grout are as follows:

- Transportation to site and installation is very easy;
- Can be implemented without the requirement for hot works;
- Minimal lift equipment is required, particularly if rebar cage is assembled in situ;
- Significantly improved corrosion resistance compared to steel;
- Prevents further deterioration, particularly corrosion in the case of conductors;
- Limited requirement for design with minimal fabrication.

Reinforced epoxy grout has been mainly limited to axially loaded members such as conductors under compression loading and mainly used for above-water applications. In addition it is easily transported and utilized for repairs to conductors.

In general, the following equipment and support may be needed:

- grouting spread;
- composite materials;
- other components depending on the repair type, such as a temporary outer jacket to provide formwork;
- Installation aids.

Fiber reinforced polymer composites

A linear elastic response of FRP to axial stress is one of the main attractions of its use in structural engineering. The response of FRP to axial compression is subject to the volume of fibers and the fiber properties and resin, and the interface bond strength. If there is fiber buckling due to rapid side sway or deflection, FRP composite compression failure occurs.

The base fiber matrix is available in many forms from random mixed fibers to woven fiber blankets consisting of either glass fibers or carbon fibers. The woven matrix provides the necessary bidirectional fiber strength depending on the strength requirements and application.

FRP's response to transverse tensile stress is very much dependent on the properties of the fiber and matrix, the interaction between the fiber and matrix, and the strength of the fiber−matrix interface. Generally, however, tensile strength in this direction perpendicular to the fiber direction is very poor so the greatest tensile strength is in the direction of the fibers. The shear strength of FRP is difficult to quantify. To avoid this weakness, the direction of fibers is in two directions and the other in the other two diagonal directions. Therefore it can carry the load in four directions. This type of repair is used for a repair on site, but prefabricated FRP as grating is usually in one direction.

FRP has higher strength, and its main advantages are its durability and corrosion resistance. In addition, its high strength-to-weight ratio is of significant benefit; a member composed of FRP can support larger live loads since its dead weight does not contribute significantly to the loads that it must bear. Other features include ease of installation, versatility, electromagnetic neutrality, excellent fatigue behavior, fire resistance, and possible maintenance-free use. FRP has increased reliability

due to good corrosion resistance and structural superiority through weight savings, higher stiffness, and ability to better tailor the structure to the load.

The composite repair method takes a shorter time offshore and involves light material handling. This method often proves to be more cost effective than other repair solutions.

FRP has the following limitations, which can be easily overcome through design and application and by searching for advanced products on the market:

- brittle behavior;
- susceptibility to deformation under long-term loads;
- UV degradation and photo-degradation (from exposure to light);
- temperature and moisture effects.

Limitations also lie in the level of previous experience of the contractor. However, the number and experience of contractors are growing and enhancing the properties of FRP.

7.13.10 Example of using fiber reinforced polymer

Davy and Bessemer are two shallow-water monopod platform structures located in the southern North Sea that commenced production in 1995. These two platforms used FRP. The fiberglass components consisted of 10% by weight of composites, including the following:

- office and equipment modules;
- diesel and water storage tanks;
- pultruded glass/phenolic gratings for floors;
- ladders;
- walkways;
- handrails;
- enclosures and heat protection walls;
- glass-reinforced epoxy was also widely used for the pipework and tubular.

Fig. 7.58 presents the topside structure prior to transportation. Davy and Bessemer were installed as single-lift structures.

The main benefit was the reduction in weight, which was important for these lightweight structures as it reduced the cost as the topside weight is lowered and the cost of regular maintenance in the future is much lower.

7.13.11 Case study for conductor composite repair

An eight-leg jacket drilling platform was operating in 75 m water depth in GoM. The platform was installed in 1964.

The original conductors were heavily corroded. A 5-year conductor maintenance plan identified the required conductor restoration work.

The cost analysis revealed a composite repair system to be the most cost-effective repair method, with the following preparartion and process:

- Underwater and above-water repair site inspection.
- Plan staging area for equipment and material.

Figure 7.58 Topsides from fiber reinforced polymer (FRP).

Figure 7.59 Severely corroded conductor.

- Surface preparation including removal of excess scale; removal of grout if it is not structurally sound; and grit blasting to near white metal.
- Install shear lug, rebar cage, and translucent FRP jacket outside rebar cage.
- Pump epoxy grout into FRP jacket from bottom up.
- Install wear pads and conductor centralizers at the guide bell (Fig. 7.59).

7.13.12 Fiberglass access decks

For 10 years fiberglass use for grating and handrail has grown in offshore structures, and it is now used for new platforms or for replacing existing ones.

Fiberglass access decks and stair towers are lighter than their steel equivalent and easier to install.

Figure 7.60 An fiber reinforced polymer (FRP) deck.

Fiberglass structural decks can be designed to meet any load requirements. The decks can be custom built and installed offshore with no welding and/or heavy lift equipment required.

Fiberglass access decks consist of pultruded structural sections which are bolted together. Fiberglass gratings and handrails complete the full deck.

The benefits of fiberglass access decks include that they can be installed without hot work and there is no long-term maintenance or painting. They can be readily transported to site and handled using lighter lifting equipment compared to steel decks. The main advantages of the fiberglass access decks are that they do not corrode—eliminating maintenance and costly repairs or replacement of steel decks.

In some cases the small deck will be from fiberglass, as shown in Fig. 7.60.

Fiberglass access decks, primarily well access decks, have been used throughout the world on projects ranging from minimal structures to deep-water TLPs and spars.

Fiberglass grating products and resins are available to cover a range of requirements including:

- strength;
- chemical resistance;
- impact resistance;
- fire resistance.

A number of attachment options are available including bolting, welding, clips, and friction welding. The choice of attachment depends on the location (wave zone or nonwave zone) and whether or not hot works are possible.

Fiberglass grating systems have been proven to perform even after being subjected to hurricane wave forces. Grating is typically designed to last for the lifetime of the structure, without replacement.

Figure 7.61 Fiber reinforced polymer (FRP) grating.

Figure 7.62 Nonwave zone fiberglass stairs.

Fiberglass grating does not corrode, which is the primary cause for the replacement of steel grating and plating (Fig. 7.61).

Fiberglass access stairs and treads are lighter than the steel equivalent and easier to install.

Fiberglass stairs can be designed to meet any access requirements.

Fiberglass stairs consist of pultruded structural sections with fiberglass stair treads. Fiberglass handrails complete the full stair. Fiberglass stairs can be replacement items for steel stairs. They can also be used for new design or new access requirements. Fiberglass stairs are installed using lighter lifting equipment compared to their steel equivalent.

Fiberglass treads have been proven to perform even after being subjected to hurricane wave forces. Stairs and treads are typically designed to last for the life of the structure and not require replacement.

Fiberglass stairs and treads do not corrode, which is the primary cause for the replacement of steel stairs, as shown in Figs. 7.62 and 7.63.

Fiberglass stairs and treads have been used throughout the world on offshore platforms.

Figure 7.63 Stair tread covers.

Figure 7.64 Glass fiber reinforced polymer (GFRP) handrails.

Fiberglass handrails can be used for jacket walkways, boat landings, and deck perimeters.

Handrail sockets are typically fabricated from stainless steel and are welded to the structure. If hot work is not permitted, then bolted attachments are available. The attachment of the handrails can be modified for installation where hot work is not permitted.

Fiberglass handrail systems have been proven to perform even after being subjected to hurricane wave forces. Handrails are typically designed to last for the life of the structure, without replacement.

Fiberglass handrails do not corrode, which is the primary cause for the replacement of steel handrails (Fig. 7.64).

Figure 7.65 Fiber reinforced polymer (FRP) mudmat system.

7.13.13 Fiberglass mudmats

Fiberglass mudmats are more economical than traditional steel systems. Due to the high potential flexural strength, as high as 427 N/mm^2, coupled with the high flexural stiffness (*EI*), as high as 64,121 N/mm^2, mudmats can span 2−3 times further than unstiffened steel plate mudmat skins. As many as one-half to two-thirds of the beams required to support a steel mudmat skin can be eliminated when using fiberglass mudmats.

In addition, fiberglass mudmats, shown in Fig. 7.65, reduce steel fabrication tonnage and eliminate the need for mudmat cathodic protection that steel mudmats require. The service life of any mudmat system is very short, and after the piles have been driven and welded to the jacket structure, mudmats provide no further service, however, a steel mudmat system continues to draw from the platform's cathodic protection system.

A fiberglass mudmat system is significantly lighter than steel, ranging from 44 to 58 kg/m^2 in air and 49 to 58 kg/m^2 submerged.

A mudmat constructed using fiberglass has the following advantages:

- high flexural strength;
- high flexural stiffness;
- reduced number of support beams;
- reduction in fabrication costs;
- reduction in anodes;
- saves weight;
- easily installed—no bolting.

Fiberglass mudmats have been utilized on approximately 20 jackets in the GoM since the late 1990s by a number of companies

7.13.14 Case study 1: flare repair

This is a conventional repair method that is usually used to repair offshore structure platforms.

Figure 7.66 Hole on the leg.

Figure 7.67 Corrosion in horizontal bracing.

The horizontal bracing shown in Fig. 7.66–7.67 has severe corrosion highlighted as the result of an inspection survey, but after reviewing the old document (which is essential in evaluating the existing structure) it was found that there was an alternative bracing system used previously. This alternative system is presented by the inspection survey. Therefore in this situation there is no need to carry out any repair or to strengthen these horizontal bracings. The final repair is presented in Fig. 7.68.

Figure 7.68 After strengthen the leg.

Figure 7.69 Loosening the clamp and corroded member.

7.13.15 Case study 2: repair of the flare jacket

This flare was constructed in 1970. After performing the survey cracks on the bracing due to corrosion were found, as shown in Figs. 7.69 and 7.70. The flare jacket leg brace clamps were designed in 1984 but not fitted until 1994. They are ungrouted, loose, and heavily corroded. The vertical diagonal braces in all three elevations in the vertical interval between the upper bay are totally corroded with extensive holes through most of the perimeter. The horizontal braces in all three

Figure 7.70 Corroded bracing.

elevations are totally corroded with extensive holes through most of the perimeter. After visual inspection it was shown that the roller bearings at deck level supporting the flare bridge were highly corroded and frozen, as shown in Fig. 7.71. In addition, the dead load deflection of the last span of the flare bridge caused a rotation of the roller shoe beam with the result that the flare bridge load was carried only on the inner one or two rollers and the thermal expansion/contraction was causing excessive loading of the jacket structure.

Prior to the start of diving operations, the current condition of the submerged structure is assessed by an ROV. While the underwater inspection should make a general inspection of the structure for potential hazards to divers, there should be a particular focus on the first bay up and vertical diagonal braces and horizontal plan bracing members.

Face brace members on elevations as shown in Fig. 7.71 should also be generally inspected. If cyclic lateral movements of any braces or leg clamps are detected in a running sea, remedial measures should be taken up to and including, removal of members which could present a hazard and which would not further reduce the strength and stability of the structure.

Manual access will be required to the underside roller bearing deck to attach beam clamps to support the weight of the new brace members during installation. Scaffolding to enable safe access to these locations from the flare bridge and to provide a working platform shall be constructed prior to the start of repair operations.

Repairs shall be carried out in the following sequence:

1. Pile wall thickness survey;
2. Refurbishment of roller bearings;
3. Grouting of leg/pile annuli;
4. Cutting of legs or crown weld shims;
5. New horizontal braces for the two levels.

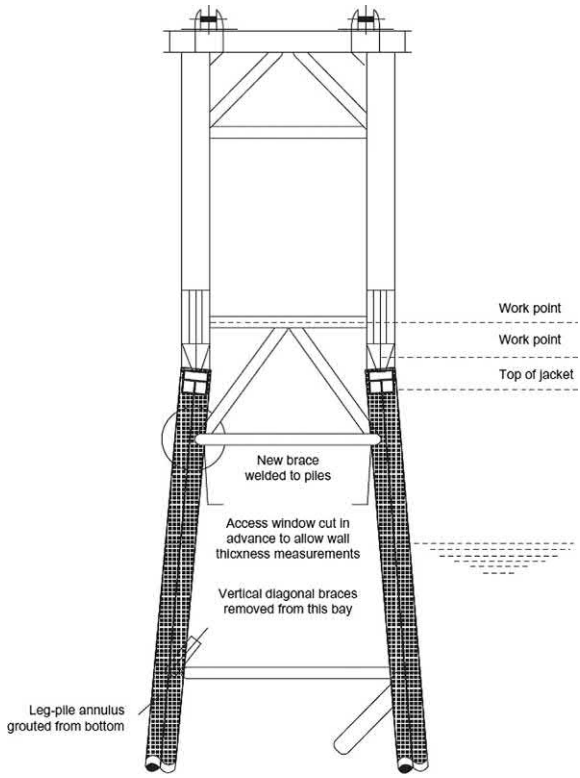

Figure 7.71 Flare jacket configuration and location of grouting.

7.13.16 Case study 3: repair of the bearing support

The bearing support of the bridge, as shown in Fig. 7.72A, was seen to have severe corrosion, as shown in Fig. 7.72B.

The severe corrosion of the bearing as shown in Figs. 7.72A and B. The procedure for refurbishing the roller bearings is very critical as it is based on removal of the old corroded rollers and cleaning up the existing steel work and bronze bearing bushings.

1. Machine sleeves to final outside diameter to fit, on the basis of the surveyed gaps, above the existing rollers.

2. Install temporary lateral bracing to support the flare bridge lower chord during refurbishment of rollers.

3. Install hydraulic jacks to lift and support the flare bridge (4×50 tons) are foreseen as required and jack-up the flare-bridge by 30 mm to unload rollers, as shown in Fig. 7.73.

4. Place heat-shield under flare-bridge lower beam underside.

5. One at a time, flame cut the rollers 50 mm from the inside face on each side.

Figure 7.72 (A) Corrosion of bearing. (B) Corrosion of the bearing stud.

Figure 7.73 Flare bridge support.

6. Cut or burn off keeper plates from outside ends.

7. Remove all corrosion on outer parts by needle-gun and grit-blast to reduce the diameters of the protruding parts so that they can pass through the bushings without causing damage.

8. Hammer drift the remaining roller portions through the bronze bushings from outside and remove remaining roller portions.

9. Clean-up and remove corrosion products and rust scale from surfaces and apply paint system to bearing support steelwork.

10. Inspect, clean, and grease the bronze bushings. The bearings are believed to be intact. If there is wear or corrosion then they should be cleaned up as far as possible and the surfaces of the bushings polished without increasing the diameter by more than 2 mm.

11. Insert new rollers from outside; by pushing the jacks and using the hammer across through opposite bushings and fit new stainless steel sleeves (in three sections each) onto new rollers as they are inserted.

12. Achieve symmetrical projecting ends.

13. Install new keeper plates, weld keeper plates to ends of rollers.

14. Finally, grease rollers and apply paint system to roller ends.

References

AISC, 1969. Specification for the Design, Fabrication and Erection of Structural Steel for Buildings, seventh ed. American Institute of Steel Construction, New York, 12 February 1969.

American Welding Society, 1972. AWS D1.1, Structural Welding Code, First ed American Welding Society, USA.

Angus, N.M., Moore, R.L., 1982. Scour repair methods in the southern North Sea. In: Proceedings of the Fourteenth Annual Offshore Technology Conference, Houston, TX. OTC paper 4410.

API RP2A, 1976. Recommended Practice for Planning, Designing and Constructing Fixed Offshore Platforms, seventh ed. American Petroleum Institute, Washington, DC, January 1976.

API RP2A, 1980. Recommended Practice for Planning, Designing and Constructing Fixed Offshore Platforms, eleventh ed. American Petroleum Institute, Washington, DC, January 1980.

API RP2A, 1982. Recommended Practice for Planning, Designing and Constructing Fixed, Offshore Platforms, thirteenth ed. American Petroleum Institute, Washington, DC, January 1982.

API RP2A, 1986. Recommended Practice for Planning, Designing and Constructing Fixed Offshore Platforms, sixteenth ed. American Petroleum Institute, Washington, DC, April 1986.

API RP2A, 1987. Recommended Practice for Planning, Designing and Constructing Fixed Offshore Platforms, seventeenth ed. American Petroleum Institute, Washington, DC, April 1987.

API RP2A, 1991. Recommended Practice for Planning, Designing and Constructing Fixed Offshore Platforms, nineteenth ed. American Petroleum Institute, Washington, DC, August 1991.

API RP2A, 1993. Recommended Practice for Planning, Designing and Constructing Fixed Offshore Platforms, twentieth ed. American Petroleum Institute, Washington, DC, August, 1993.

API RP2A-WSD, 2007. Recommended Practice for Planning, Designing, and Constructing Fixed Offshore Platforms, American Petroleum Institute, Washington DC. Twentieth ed, Supplement 3, October, 2007.

Brockenbrough, R.L., 2003. AISC Rehabilitation and Retrofit Guide: A Reference for Historic Shapes and Specifications. American Institute of Steel Construction, Inc., Chicago, IL.

El-Reedy, M.A., Ahmed, M.A., 2002. Reliability-based tubular joints. In: Proceedings of 8th International Conference of Structural Safety and Reliability, ICOSSAR 01, USA.

Forristall, G.Z., 1978. On the statistical distribution of wave heights in a storm. J. Geophys. Res 83, 2353−2358.

Galambos, T.V., 1998. Guide to Stability Design Criteria for Metal Structures. John Wiley, USA.

OTO report index, 1999. http://www.hse.gov.uk/research/otohtm/1999/index.htm

Soreide, T.H., Amdahl, J., Granli, T., Astrup, O.C., 1986. Collapse Analysis of Framed Offshore Structures, OTC 5302, Houston, TX.

Van de Graaf, J.W., Tromans, P.S., Shell Research, B.V., Efthymiou, M., 1994. The reliability of offshore structures and its dependence on design code and environment. In: Offshore Technology Conference, OTC 7382, Houston, TX.

Further Reading

AISC, 1978. Specification for the Design, Fabrication and Erection of Structural Steel for Buildings, eighth ed. American Institute of Steel Construction, Chicago, IL, 1 November 1978.

AISC-ASD, 1989. Specification for Structural Steel Buildings—Allowable Stress Design and Plastic Design, nineth ed. American Institute of Steel Construction, Chicago, IL, 1 June 1989.

API, 1969. Recommended Practice for Planning, Designing, and Constructing Fixed Offshore Platforms, first ed. API RP 2A-WSD.

API, 2000. Recommended Practice for Planning, Designing, and Constructing Fixed Offshore Platforms, twelfth ed. API RP 2A-WSD, Supplement 1, December 2000.

API RP2A, 1969. Recommended Practice for Planning, Designing and Constructing Fixed Offshore Platforms, first ed. American Petroleum Institute, Washington, DC, October 1969.

API RP2A, 1971. Recommended Practice for Planning, Designing and Constructing Fixed Offshore Platforms, second ed. American Petroleum Institute, Washington, DC, January 1971.

API RP2A, 1972a. Recommended Practice for Planning, Designing and Constructing Fixed Offshore Platforms, third ed. American Petroleum Institute, Washington, DC, January 1972a.

API RP2A, 1972b. Recommended Practice for Planning, Designing and Constructing Fixed Offshore Platforms, fourth ed. American Petroleum Institute, Washington, DC, October 1972b.

API RP2A, 1974. Recommended Practice for Planning, Designing and Constructing Fixed Offshore Platforms, fifth ed. American Petroleum Institute, Washington, DC, January 1974.

API RP2A, 1975. Recommended Practice for Planning, Designing and Constructing Fixed Offshore Platforms, sixth ed. American Petroleum Institute, Washington, DC, January 1975.

API RP2A, 1977a. Recommended Practice for Planning, Designing and Constructing Fixed Offshore Platforms, eighth ed. American Petroleum Institute, Washington, DC, April 1977.

API RP2A, 1977b. Recommended Practice for Planning, Designing and Constructing Fixed Offshore Platforms, nineth ed. American Petroleum Institute, Washington, DC, November 1977.

API RP2A, 1979. Recommended Practice for Planning, Designing and Constructing Fixed Offshore Platforms, tenth ed. American Petroleum Institute, Washington, DC, March 1979.

API RP2A, 1981. Recommended Practice for Planning, Designing and Constructing Fixed Offshore Platforms, twelfth ed. American Petroleum Institute, Washington, DC, January 1981.

API RP2A, 1984a. Recommended Practice for Planning, Designing and Constructing Fixed Offshore Platforms, fourteenth ed. American Petroleum Institute, Washington, DC, July 1984.

API RP2A, 1984b. Recommended Practice for Planning, Designing and Constructing Fixed Offshore Platforms, fifteenth ed. American Petroleum Institute, Washington, DC, October 1984.

API RP2A, 1989. Recommended Practice for Planning, Designing and Constructing Fixed Offshore Platforms, eighteenth ed. American Petroleum Institute, Washington, DC, September 1989.

API RPZA-LRFD, 1989. Recommended Practice for Planning, Designing and Constructing Fixed Offshore Platforms—Load and Resistance Factor Design, Draft ed. American Petroleum Institute, Washington, DC, 15 December 1989.

API RP2A-LRFD, 1993. Recommended Practice for Planning, Designing and Constructing Fixed Offshore Platforms—Load and Resistance Factor Design, first ed. American Petroleum Institute, Washington, DC, 1 August 1993.

Barltrop, N.D.P., Adams, J.A., 1991. Dynamics of Fixed Marine Structure. Butterworth and Heinemann.

Barltrop, N.D.P., Mitchell, G.M., Atkins, J.B., 1990. Fluid Loading on Fixed Offshore Structures. OTH 90 322, HMSO.

Health and Safety Executive, 1990. Offshore Installations: Guidance on Design, Construction and Certification, fourth ed. HMSO, London.

HSE, 1997. Offshore Technology Report, OTO 97 040.

Le Mehaute, B., 1976. An Introduction to Hydrodynamics and Water Waves. Springer-Verlag, Dusseldorf.

Trornans, P.S., Anaturk, A.R., Hagemeijer, P., 1991. A new model for the kinematics of large ocean waves—application as a design wave. In: Proc 1st ISOPE Conf, Edinburgh, vol. 3, p. M-71, August 1991.

Ultiguide, 1999. Best Practice Guidelines for Use of Non-linear Analysis Methods in Documentation of Ultimate Limit States for Jacket Type of Offshore Structures. Det Norske Veritas, Norway.

Risk-based inspection technique

8

8.1 Introduction

This chapter presents a risk assessment methodology based on current industrial practice. In addition, methods of subsea inspection and methods for implementing inspection programs are illustrated at every inspection level.

The implementation of a structure integrity management (SIM) system is presented in Fig. 8.1. The first step is to collect and evaluate all available data about all the offshore structures in the fleet. Structures should include supports, such as flares, and bridges connecting platforms if they exist. In general, all available data should be on hand, and, if there are missing data that are critical, a special survey or study can be performed to obtain this data.

The data should include:

- year of design;
- year of construction;
- water depth;
- calculation report;
- construction drawings;
- as-built drawings;
- management of change records, additional risers, conductors, equipment or deck extensions, or other additional load or change of configuration;
- number of risers and conductors;
- pile depth and driving records;
- existing metocean data;
- last inspection findings;
- soil report;
- any previous structure study performed;
- records of any accidents or fire or other events affecting the structure.

The next step is to evaluate the structure's integrity and to obtain its fitness for service. Also in this phase, the data can be used to define the structure's risk assessment ranking. Based on the risk rankings for all offshore structures in the fleet, the overall inspection philosophy, strategy, and plan for all the structures can be defined.

After the plan has been determined, the scope of the inspection will be implemented and the inspection program will be executed. Finally, when the data are updated, the cycle begins again, as shown in Fig. 8.1.

Offshore Structures. DOI: https://doi.org/10.1016/B978-0-12-816191-3.00008-0

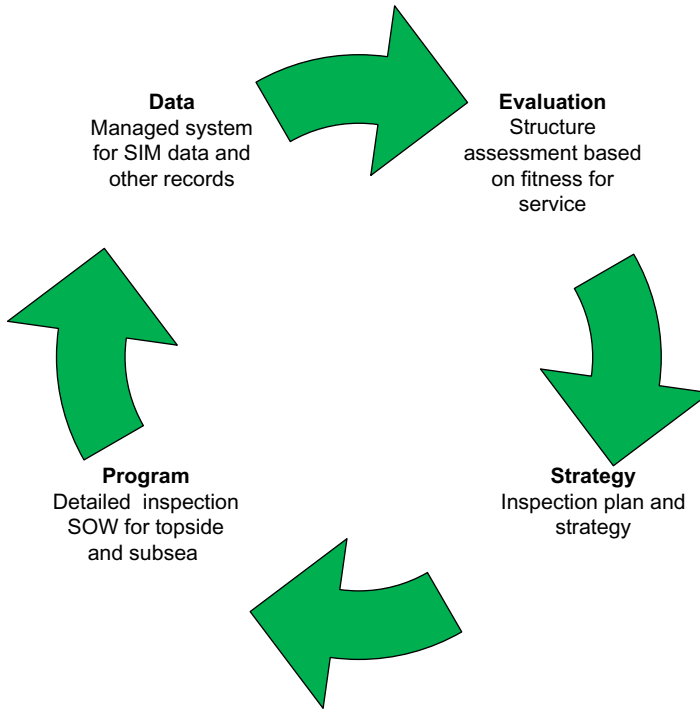

Figure 8.1 Structure integrity management (SIM) main steps.

8.2 Structure integrity management methodology

The structure integrity management (SIM) system needs to be a strong system for maintaining a reliable structure during its lifespan. The SIM system requires procedures, resources, budget, and a timeline.

The steps of SIM (summarized in Fig. 8.1) start with collection of data about all offshore fixed platforms in the fleet of the owner company and input of the data into the computer. The second step is to evaluate the data and to identify each structure's reliability and its fitness for service. The next step is to develop an inspection and repair plan designed for needed minor or major repairs. Then a comprehensive inspection plan and detailed scope of work are developed for the remotely operated vehicle (ROV) crew. After the ROV inspection has been performed, data are again input into the system, the structure is re-evaluated and so on until all the structures in the fleet are under control and their condition is clear. In future decision-making, management can define the required annual budget for maintaining the SIM cycle without stopping.

The core of the structure evaluation and ranking is to perform qualitative risk assessment by identifying the likelihood of failure and the impact of that failure.

For example, the likelihood of failure can be the result of the strength and the affected loads as per the following factors:

- the date of construction;
- the structure's configuration;
- the number of legs;
- marine growth;
- date of the last inspection.

The possibility of failure is affected by:

- manned or unmanned platform;
- distance (near or far away) from the shoreline.

The core of the SIM system for defining the action plan for inspection and repair is by using a risk-based inspection technique. Risk is determined through qualitative risk assessment, which is easy to do for a fleet of structures rather than quantitative risk assessment which needs a sophisticated structure analysis combined with a probabilistic study that requires a budget and takes time.

Factors that indicate platform-strength deterioration are:

- splash zone corrosion;
- cathodic protection (CP) survey;
- damaged or missing members;
- inspection history;
- cutting member;
- others.

Factors that indicate extreme platform loads are:

- boat landings;
- marine growth;
- scour;
- additional conductors or risers;
- design loading;
- others.

8.3 Quantitative risk assessment for fleet structures

The philosophy adopted for developing the offshore structure jacket ranking methodology is risk-based. Risk in this context is the combination of the likelihood of failure and the consequence of failure for the platform (risk = probability of failure × consequence). The likelihood of failure is the practical definition for the probability of failure.

The consequence of failure is the combination of losses that could be incurred as a result of a failure.

Classification factors that do not require any analytical assessment are presented that enable the likelihoods and consequences of failure to be quantitatively evaluated or qualitatively categorized.

The likelihood of structural collapse is a function of two main factors, which are the platform strength or capacity, and the maximum loads that affect the offshore structure. The likelihood identification system defines the platform factors that decrease or increase the platform strength and loads. For example, factors that decrease the strength of the platform and its capacity to carry the applied load will increase the likelihood of platform failure. Factors that contribute to increasing the applied load on the platform or the offshore structure in general will also increase the probability of failure.

The overall consequence of failure is the sum of three main components: environmental losses, business losses, and injury/safety-related losses. The effect of each of the three consequences is converted to a dollar value (in USD) and the effects are summed to result in the overall consequence. While the resulting dollar value does not represent the total amount of money that could be lost due to a failure, the monetary concept allows the three components to be combined.

After each platform is categorized in terms of likelihood and consequence of failure, the categories are entered into the risk matrix to establish the overall relative risk ranking. Note that the risk matrix has a variety of shapes, such as a 4×4 matrix or a 5×5 matrix. The relative risk rankings are high (red), moderate (yellow), low (green), and insignificant (white).

In parallel with the risk assessment, the platforms have also been grouped into "families" that represent platforms with similar configurations and similar duties. Hence, in addition to identifying and ranking the high-risk platforms across the overall fleet of offshore structures, the high-risk platforms can also be identified within each family. The two rankings make possible rational decisions about where to focus and how to distribute the resources of the rehabilitation project.

8.3.1 Likelihood (probability) factors

This section presents the factors that influence the likelihood of jacket structural failure (the likelihood is equal to the probability of failure in quantitative risk assessment). The factors consist of two groups, those that relate to the strength of the platform, listed in Table 8.1, and those that relate to the loadings applied to the structure platform, listed in Table 8.2.

The factors should be defined separately for different locations, based on the expertise of the owner companies and regional data about the factors that can affect the structures. In addition, as more detailed inspections are undertaken, the number of factors can be increased. Therefore it is very important to mention that the values in Table 8.2 and subsequent tables are purely guidelines to illustrate this approach and should be examines for individual fleets based on the condition of operation, environment, and the back history, and the data that have been collected. For example, if, for a certain structure, no member thicknesses have been measured to check for corrosion, member thickness is not included. However, once thickness measurements become available in the future, this factor should be introduced. Examples of factors include the following.

Table 8.1 All strength factors related to platform likelihood of failure.

Item	Factor	Influence of the factor	Weight	Score
1	Design practice	To consider the modification in the new revision of codes and specification considering improving design calculation and fabrication practice	6	0–60
2	Number of legs and bracing type	To consider the effect of the number of legs and the bracing system on the structure probability of failure	10	10–100
3	Pile system	To consider the effect that the pile system has on the likelihood of failure and account for the uncertainty results in case of potential damage in the pile or where there are no record data to the pile driving	10	0–120
4	Risers and conductors	To account for the number of conductors and risers that affect the hydrodynamic loading and its service of carrying hazardous materials that affect the probability of structure failure	7	0–70
5	Boat landings	To account for nondesigned hydrodynamic loads from boats	5	0–50
6	Grouted piles	To recognize the reduced likelihood of failure if piles are grouted	3	0–30
7	Damaged, missing, and cut members	To account for the effect of damaged, removed, or cut members on the platform likelihood of failure	21	0–210
8	Splash zone	To consider the platform probability of failure due to a corroded member in the splash zone	8	0–80
9	Flooded members	To account for the effect that flooded members have on the likelihood of failure	8	0–80
10	CP surveys and anode depletion	To consider the condition of the CP system as lack of a CP system increases the likelihood of platform failure	6	0–60
11	Inspection history	To account for the inspection history on the platform likelihood of failure	6	0–60
12	Remaining thickness	Remaining wall as a percentage of nominal wall thickness. Number of members marked as corroded. Penalizes platforms where inspections have detected actual member wall corrosion	$8 \times BL$	0–80
Strength only—subtotal				10–1000

Table 8.2 All load factors related to platform likelihood of failure.

Item	Factor	Effect factor	Weight	Score
13	Design loading	To account for the effect that design loading has on the likelihood of failure. This differs from the design practice factor, which accounts for design details of the structure, such as joints and framing schemes	8	0–60
14	Marine growth	To consider the increase of platform likelihood of failure by increasing the marine growth	5	0–50
15	Scour	To account for the effect that scour has on the likelihood of failure	6	0–60
16	Topside weight change	To account for the likelihood of failure of the platform due to changes in deck weight due to deck extensions, additional equipment, or change of use	10	0–100
17	Additional risers, caissons, and conductors	To account for the effect that additional risers, caissons, and conductors, over and above those that the structure was originally designed for, have on the likelihood of failure of the platform	10	0–100
18	Wave-in deck	To consider an increase in the platform probability of failure as a result to storm-wave crests hitting the lower platform deck	25	0–250
19	Earthquake	To account for whether design considered earthquake loads. Penalizes platforms that have not been designed for earthquakes in areas where earthquakes are likely	8	0–80
Load only—subtotal Total score				0–700 10–1700

Strength factors:

- design practice;
- number of legs and bracing type;
- foundation;
- risers and conductors;
- boat landings;

- grouted pile;
- damaged, missing, and cutting members;
- splash zone;
- flooded members;
- CP survey and anode depletion;
- inspection history;
- remaining wall thickness.

Load factors:

- design loading;
- marine growth;
- scour;
- topside weight change;
- additional risers, conductors, and caissons;
- wave-in deck;
- earthquake load.

Interactions

Most of the above factors are not truly independent, some have strong interactions. For example, the bracing type and the number of legs affect how much a damaged member decreases the strength of the platform and how much it increases the likelihood of failure.

According to De Franco et al. (1999), the complex interactions between different platform characteristics may make it impossible to develop a risk-based inspection system that does not depend on a great deal of structural details. The team evaluated the interaction of each pair of factors, and the resulting relations between the likelihood factors and their interactions are presented in the matrix in Table 8.3, where H, M, and L are high, moderate, and low interactions, respectively.

The investigators arrived at the matrix by identifying the following:

- Whether the parameters are related to each other or not. That is, whether the first factor is correlated to the second parameter or not. For example, the design year of the platform implies that certain safety factors and detailing practices were followed in the platform's design, therefore in this case, the year of the platform design will be in conjunction with the design practice in that year as it will be correlated with the design load as described in Chapter 7, Assessment of existing structures and repairs.
- The weight of the correlation between these two factors. For example, the number of legs and the bracing system together strongly affect the redundancy and possibility of damage to the platform. In contrast, the effect of marine growth on the loads was considered small.

For various reasons, not all of the strong interactions were covered. In some cases when the interaction was reconsidered during construction, it was decided that it was either too complex to describe adequately or that the interaction may not have been as strong as originally believed. In other cases, such as in the case of corrosion, the effect of locality, which is captured in the calculation, was determined to be more important than the interaction with the type of structural system, and as

Table 8.3 Matrix for correlation between failure likelihood factors.

	Year of design	**Bracing system**	**Location**	**Number of legs**	**Grouted piles**	**Sensitivity to corrosion**	**Splash zone**	**Damaged and flooded members**	**Deck elevation**	**Scour**	**Inspection history**	**Remaining wall thickness**	**Topside weight change**
Year of design		L	**H**	M	**H**	M	L	H	H	M	L	L	M
Bracing system			H	H	M	**H**	**L**	**H**	H	H	M	H	L
Location				**H**	**L**	H	**L**	**H**	L	H	H	M	L
Number of legs					M	**H**	L	H	L	M	L	L	H
Grouted piles						L	L	M	L	L	L	L	L
Sensitivity to corrosion							H	H	L	L	H	H	M
Splash zone								M	L	L	H	H	M
Damaged and flooded members									L	L	H	M	L
Deck elevation										L	L	L	L
Scour											H	L	L
Inspection history												H	L
Remaining wall thickness													L
Topside weight change													

a result it was omitted. Furthermore, two other parameters were already bound to the bracing systems and leg factors, and tying in a third would make this factor overpower most of the other factors that affect likelihood.

In the case of the interaction between location and grouted piles, where the initial assessment ranked it as low, a factor was developed for a reason other than the physical interaction of piles with the local load environment. Instead, the factor for grouted piles included the location to reflect design, detailing, and construction practices that would lessen the impact of retrofitting a platform by grouting its piles.

Likelihood calculation for strength

The definition of the parameters mainly depends on the characteristics of the fleet of fixed platforms to be maintained, as some factors exist in some locations but do not exist in other locations. The discussion of the factors here is just an example of the effect of each factor, which should be tailored to each location and region worldwide. This is done by collecting the data for the whole structure and then a comprehensive study is required to evaluate the role of each factor. For example, one owner may have an old platform constructed in 1995, while another owner may have a platform from 1960, and so the weights and scores will be different. On the other hand, some areas of the world are affected by seismic load, while other regions have no snow load at all, as in the Middle East. Therefore the numbers in Tables 8.1 and 8.2 are only guidelines and cannot be used in a standard. The normal procedure for qualitative risk assessment is that a team, consisting of the owner, the operator, and the engineering group with expertise, hold a meeting and use brainstorming or other techniques to define the interactions between the factors and their weight.

Design practice

Design practice accounts for platform design attributes, such as member sizing, joints, pile design, etc. The intent is to quantify the inherent strength in a platform depending on the point in time at which it was designed. The year it was designed was selected as this is most reflective of the strength of the platform. The year of design should be different from the date of installation; in some cases, the platform may have been designed several years prior to being installed.

The indicated dates generally match up with the continued development of the API RP2A recommended practice for design of offshore platforms in US waters. The first version of API RP2A, issued in 1969, was the first good guideline for platform design. The year 1970 is used here (conservatively) to reflect the fact that, although the first edition was issued in 1969, the document did not become common practice for about a year. The next major update to RP2A was the inclusion of joint design practices, in approximately 1975. In 1979, API RP2A was updated to the point that the API Section 17 Committee on assessment of existing platforms deemed that the guideline had reached maturity and that platforms designed to the guideline since that time are of good quality.

Table 8.4 Design practice factor.

Year of design		Score
≥	≤	
	1970	10
1971	1974	7
1975	1979	4
1979		0
Unknown		9

Table 8.4 presents an example for a score between 0 and 10 for the year of design of the platform, a factor that estimates the level of confidence that can be placed on it due to the state of design practices prevalent at that time. A platform designed later than 1979 scores 0, to indicate that the platform is reliable due to the good and improved design practices. Platforms designed before 1970 score 10 because they tend to have the highest probabilities of failure. Note that the overall weight of the total score is 5.

Sometimes the year of design is not known for old platforms, but the drawings for them indicate the construction or installation year, so the design year is taken to be 2 years prior to the year of installation.

If a platform design has been repeated as a standard, the year of design should be taken as the first time of design or the installation year for the first platform the design was applied to.

The "year designed" input parameter is in the general category of the platform data. As already mentioned, this parameter is used for estimating the reliability of the platform based on design practices. This factor is independent of other factors as it does not have a relation to any of the others. However, the "year designed" input parameter is also used in the "year designed and location" factor and the "grouted piles" factor because the input has a high interaction with the loading and resistance aspects in these factors.

Number of legs and bracing configuration

It is well known that the number of legs and framing scheme contribute to the strength of a platform and, more importantly, its ability to sustain damage and still "survive" extreme loading events. (The relation between the structure configuration and its strength is discussed in Chapter 7, Assessment of existing structures and repairs.) For example, a three-legged platform with several damaged *K* braces has a significant decrease in capacity compared to the same number of damaged members on an eight-legged platform that is *X*-braced. The number of legs provides for an increased number of major load paths, while the *X*-brace scheme provides redundant framing at each major joint. Note that the "preferred" platform framing scheme per American Petroleum Institute (API) for earthquake regions (where redundancy and ductility are important) is an eight-legged (or more) structure that is *X*-braced.

In terms of score, an *X*-braced eight-legged (or more) structure was assigned the highest value and the *K*-braced three-legged (or less) structure was assigned the lowest value. Values in between were based upon subjective ranking, based upon experience, where available. For example, based on Puskar et al. (1994), Hurricane Andrew in 1992 caused failure in some eight-legged *K*-braced platforms, but numerous four-legged *X*-braced platforms survived without any failures. Hence the score for eight-legged *K*-braced structures is slightly higher than the score for four-legged *X*-braced structures.

This criterion is required to account for the effect that the number of legs and conjunction with the bracing system have on the likelihood of failure. Therefore the leg number and the bracing structure system are mandatory to be known. Table 8.5 presents the criteria and score based on the number of legs and the structure system.

If the platform has different types of bracing schemes in different directions (e.g., *K* in the transverse direction and diagonal in the longitudinal direction), then the framing scheme that results in the highest score is used (*K* in this example).

Note that an increase in the number of legs increases the redundancy of the platform. Of the bracing systems, *X* bracing is the most efficient, while *K* bracing is the least efficient. The overall weight in the total score is 10.

The inputs for this factor are available in the "arrangement" data sheet. There is a high interaction between the number of legs and the bracing system because both these inputs give a strong indication of the damage tolerance of the platform. The number of legs relates directly to the redundancy of the platform. Because failure in a platform initiates at the brace, the bracing pattern dictates the damage sensitivity of the platform.

As mentioned elsewhere, this factor interacts significantly with damaged members and flooded members. The significance of any damage affecting the likelihood of failure is dependent on the damage tolerance of the platform.

Piles system

This factor accounts for the pile system effect on the likelihood of failure. Uncertainty shall exist due to unavailable records relating to the design and installation of the piles and to potential damage to the piles from soil disturbance caused by the feet of jack-up rigs. In this factor your should answer the following three inquiries:

Table 8.5 Bracing configuration and number of legs factor.

Bracing system	**Number of legs**			
	3	**4**	**6**	**8**
K and diamond	10	8	6	5
Diagonal	7	6	4	3
X	5	4	2	1
Unknown	10	7	5	4

1. Does pile design exist (Y/N)?
2. Are there actual pile penetration records (Y/N)?
3. If answers to the above are Y, does actual penetration meet the target requirement (Y/N)?

From the above answers, select the appropriate score in Table 8.6. The overall weight of the total score is 10.

Note that the accuracy factor of the foundation design itself has not been included in the above table.

Risers and conductors

Previous factors have been associated directly with the strength and redundancy of the platform and how the particular issue affects the platform's ability to withstand extreme events, such as waves and earthquakes. However, appurtenances like risers and conductors also contribute to the platform's likelihood of failure and need to be included in the quantitative risk calculation since inspection of these items is also typically included in an underwater inspection.

Caissons for fire-control water and other important activities are considered a riser. Note that appurtenances like boat landings, walkways, and barge bumpers have been excluded since they generally play a much smaller role in platform risk than risers and conductors do.

Risers and conductors that contain hydrocarbon gas or oil can result in an explosion or fire that can damage or fail the platform. The score increases with the number of risers or conductors, since there is an increased likelihood of damage as their number increases.

Table 8.6 Pile strength factor.

Criteria	**Answers to input questions**	**Score <1975**	**Score ≥1975**
Existing pile penetration achieves target	Y, Y, Y	2	0
Existing pile penetration known but not target	N, Y, (N/A)	3	2
Target pile penetration known but not existing	Y, N, (N/A)	7	3
Existing pile penetration does not meet target	Y, Y, N	8	7
Target and existing pile penetration unknown	N, N, (N/A)	10	10
Disturbance from jack-up feet			**Factor**
No sea-bed disturbance			1
Depression > 0.3 m < 5 m from pile			1.4
No data			1.4

Score = Score from table × factor (max score equals 14).

In terms of weight, the risers were assigned a higher value than conductors: one riser was assumed to equal five conductors. This bias toward risers is because conductors are less likely to fail than risers, for the following reasons:

- They are often located on the interior of the platform and therefore are less vulnerable to boat impact or other external damage.
- They have multiple layers of pipe and drill string, which decrease the probability of a complete breach.
- They typically have subsurface safety valves that shut off quickly in the event of a breach.

The 20% value was based upon testing of the weighted score for several platforms in the Amoco database and determining how much of an effect there was on the rank of the platform if the number of risers and/or conductors was increased or decreased.

This criterion accounts for the effect that risers and conductors have on the likelihood of failure. Risers and conductors attract hydrodynamic loading, which increases the global loading on the structure, increasing its likelihood of failure. Also, damage to risers may cause loss of containment, which could result in a major incident, significantly increasing the likelihood of failure.

The input data should be the number of risers and conductors, and also define whether the riser and conductor are carrying oil or gas, and in the case of gas should define whether it is high- or low-pressure gas. Key caissons, such as firewater caissons, should be counted as "oil" risers.

Table 8.7 illustrates an example of a score between 0 and 10 for both risers and conductors, depending upon their contents. These scores are then multiplied by a weighted factor (1 for risers and 0.2 for conductors) and the sum of the two scores gives the total score. The total score can vary from 0 to a maximum of 13.6. The overall weight of the total score is 5.

Risers and conductors do not have any interdependence with others, as the appurtenances do not directly contribute to the redundancy or strength of a

Table 8.7 Risers and conductors.

Number	Type		
	Risers and caissons		Conductors
	Oil and water	Gas	
0	0	0	0
<3	0	1	0
4–7	1	3	1
8–14	2	6	2
14–20	3	8	3
>20	4	10	3

Score = Riser score × 1.0 + Conductor score × 0.2.

platform. On the other hand, riser failure increases the overall risk in a platform (Table 8.8).

Damage to appurtenances is mainly detected through different levels of inspection. The causes of damage are mainly internal or external corrosion, external impact, vibration, or natural hazards.

Boat landings

Both excessive marine growth and additional boat landings, for which the jacket has not been designed, increase the global loading on the structure, increasing the likelihood of failure. Corrosion and uncontrolled modifications may result in boat-landing failure, creating a dropped-object hazard to the jacket.

The number of boat landings should be identified, because the score for this factor depends on this number and ranges from 0 to 10. The overall weight of the total score is 5.

Grouted piles

Grouting is usually to fill the annulus between the leg and pile, and increases the effective wall thickness of the leg since it would then be a combined section of leg, grout, and pile together, which increases the capacity of the joints of braces that frame into the leg. In many areas, particularly older Gulf of Mexico platforms, the weak links in the platform design are these joints. Therefore grouting of the annulus between the leg and pile of some platforms is a reasonable measure for reducing the likelihood of failure.

The 1975 threshold date is meant to capture the impact of API RP2A factors at that time that resulted in better joint design, hence a lower score, since the joint may be already well designed and the grouting will not provide much improvement. Similarly, the North Sea factor was included since platforms in this region tend to have better joint design and therefore grouting will have less of an impact.

It is worth mentioning that in the case of grouting the piles, this will increase the structure strength as discussed in Chapter 7, Assessment of existing structures and repairs, and so this will reduce the likelihood of failure.

If the pile is grouted this factor is ignored for increasing the likelihood of failure.

This factor is presented by Table 8.9, where the score of the nongrouted pile is dependent on the year of design of the platform. From a practical point of view this score can be reduced by around 60% if the platform location is in the North Sea as

Table 8.8 Additional boat landings.

Number of boat landings	Score
0	0
1	5
2	8
≥ 3	10
No data	10

Table 8.9 Grouted piles.

No. grouted piles	Year designed	
	<1975	≥1975
	10	4

Score = tabulated score × weight.

joint designs there tend to be much better than in other areas of the world, hence grouting would have a much lower effect, as discussed in Chapter 7, Assessment of existing structures and repairs.

As evident from the table for this factor, grouted piles will interact with the year designed and location. A weight factor has been added to reduce the effect considerably in the North Sea, where platform joints have historically been better designed.

Damaged, missing, and cut members

In the initial risk-based underwater inspection (RBUI) calibration work done in 1997, the change in the failure probability was estimated primarily using results from the Joint Industry Projects and Puskar et al. (1994) relating the reserve strength ratio (RSR) to the failure probability for a number of locations worldwide. The calculation of the likelihood requires collecting numerous criteria about the platform's configuration and its current condition to assign risk. One of the key components is the number of damaged members, as they can have a significant impact on the strength of the platform.

The AIM Phase III project, which was performed in 1988, evaluated a platform with numerous postulated damaged conditions, including several scenarios of damaged members ranging from one to three or more. The damaged members were located at different regions of the jacket, including the waterline, mid-depth, and near the sea bed. The results indicated that the overall platform capacity reduced little with one damaged member and that numerous damaged members, for example, over five members, will cause a noticeable reduction in platform capacity. This led to the ranges shown in the scoring table above.

As discussed by Puskar et al. (1994) and Gebara et al. (1998), *K*-braced platforms are more sensitive to damage than *X*-braced platforms. Based upon this background, it was decided that the *K*-braced platforms would be 10 times more sensitive to damaged members than *X*-braced platforms.

The probability of failure is affected by the existing number of damaged, missing, or cut members. Damaged members are defined as members that remain in place but have dents, holes, cracks, out-of-straightness, or other defects that reduce their strength.

The number of missing, cut, or damaged members should be known from the underwater survey or can be estimated from previous experience in limited cases. If there is no available underwater survey information, the score depends on the

platform type, as well-head protectors are particularly vulnerable to having members cut out.

Note that if the expected platforms have been only partly surveyed, the numbers of damaged, missing, or cut members should be extrapolated from the available survey data.

Tables 8.10 and 8.11 illustrate the scores for damaged and missing members. The platform's damage tolerance is calculated by multiplying the tabulated scores by the "legs−bracing" score and dividing by 10. The resulting score is limited to a maximum of 10. The overall weight of the total score is 20.

The number of damaged members is an inspection result. Consequently, this factor is taken as one of the strongest indicators of the current condition of the platform. Inspection-related inputs are given a stronger overall weighting in the scoring, because the goal of the system is to examine the effect of different inspection policies on risk.

The number of damaged members also interacts with the type of framing system in any given platform. Three-legged, *K*-braced platforms have few redundant load paths and are, therefore not very damage tolerant, while eight-legged, *X*-braced platforms are not as affected by missing or damaged members.

The total weight given to damaged members is 10.5. This was obtained by testing the database, which showed that this level of weight was required to increase the risk of platforms with significant damage, for example, if the platform has four damaged members the platform rank should be changed to a ranking number that enables this platform to have more frequent underwater inspections. Therefore the

Table 8.10 Damaged members.

Number of damaged members	Score
0	0
1−4	2
5−9	3
More than or equal to 10	5
No data for well-head, tender, or drilling platforms	5

Table 8.11 Missing or cut members.

Number of missing members	Score
0	0
1−3	6
4−9	8
More than or equal to 10	10
No data for well-head, tender, or drilling platforms	10

Total score (limited to 10) = (tabulated score for damaged members + tabulated score for missing members) × leg-bracing score/10.

Table 8.12 Splash zone corrosion and damage.

Extent of corrosion	Score
None and light corrosion	0
Moderate corrosion (approximately 50% coverage)	3
Heavy corrosion	10
No corrosion data	10 or go to Table 8.13

Table 8.13 Corrosion condition against topside loads where no data exist on extent of corrosion.

	Original topside weight	
	Known	Estimated
No weight growth or known/believed weight growth $\leq 10\%$	3	7
Known/believed weight growth $>10\%$ or no data	8	10

score is only a guide and should be done by trial and error for the fleet of platforms in the same location to define reasonable weights and scores.

Splash zone corrosion and damage

In the some regions of the world, such as in the Red Sea, splash zone corrosion is a major hazard. The survey data of the splash zone members should be collected.

Where no survey information is available, the score depends on the topside weight growth. Tables 8.12 and 8.13 are guides for scoring this factor. The overall weight of the total score is equal to 10.

This factor is essential when the pile-leg annulus is not grouted and the jacket therefore hangs from the crown weld, so that the highest utilized leg members are in the splash zone.

Flooded members

Flooded member detection (FMD) is a common approach to inspection of offshore platforms. A flooded member provides an indication of the current condition of the member and possible existence of damage or defects, since most platform members are designed to be buoyant. Basically, damage such as a crack or hole allows water to enter the flooded member. In some cases, the cause of the flooding cannot be found, and this is the condition considered here. The basic assumption is that, although the specific damage is unknown, it is still significant enough that it will affect member strength, and if enough members are flooded, it will affect platform strength.

In terms of the scores assigned for the number of flooded members, the logic previously described for damaged members when applied to the flooded members will be different as it has little impact on the platform strength due to redundancy

in the platform structure system. A larger number of flooded members has a greater impact. As with damaged members, the number of legs and the type of framing scheme also have an impact on the score.

The number of flooded members does not include members known to be "damaged." For damaged members, the damaged member factor overrides the flooded member likelihood of failure score. Only flooded members that have an unknown cause of flooding are counted.

Table 8.14 is very similar to the damaged members table. It illustrates a score between 0 and 10, where a score of 0 corresponds to no flooded members and hence no increase in the likelihood of failure, and a score of 10 corresponds to 10 or more flooded members and a significantly increased likelihood of failure. The platform's damage tolerance is calculated by multiplying the tabulated scores by the "legs−bracing" score and dividing by 10. The resulting scores range from 0 to 10. The overall weight of the total score is 6.

If underwater survey data relate to a percentage of the members, the number of flooded members is factored up to reflect the total number of members. For example, if a survey of 25% of the members detected one flooded member, then a total of four flooded members should be assumed for the structure.

The number of flooded members is an inspection result and gives a strong indication of the current condition of the platform. As the objective of the system is to examine the effect of different inspection policies on risk, inspection-related inputs are given a stronger overall weight in the scoring.

The number of flooded members also interacts with the type of framing system in any given platform. Three-legged, *K*-braced platforms have few redundant load paths and are, therefore not very damage tolerant, while eight-legged, *X*-braced platforms are not as affected by missing or flooded members.

CP surveys and anode depletion

An ineffective CP system will result in corrosion, which will increase the likelihood of failure.

Anode survey data by "Grade" should be defined. Note that, if an overall "Grade" for the platform has not been established, then the platform "Grade" shall

Table 8.14 Flooded member effect.

Number of flooded members		**Score**
≥	≤	
	0	0
1	3	3
4	9	8
10		10
No data available		10 (or estimated)

Total score = tabulated score × leg-bracing score/10.

Table 8.15 Cathodic protection (CP).

Criteria	Score
Grade 1: <10% consumed	0
Grade 2: <50% consumed	3
Grade 3: >50% consumed	7
Grade 4: 100% consumed	10
No data (assume worst)	10

be calculated by averaging the anode survey results of the worst 30% of the structure's anodes. Table 8.15 illustrates a score between 0 and 10, where a higher score signifies greater risk. The overall weight of the total score is 6.

Inspection history

This factor consists of two approaches, the time period and the level of the survey, as if the time period between inspections is long the probability of failure of the platform increases as there is a high probability of increased unpredicted local failure during the gaps between inspections. On the other hand, underwater surveys, as more detailed inspections, are less likely to result in undetected local failures or deficiencies in strength or increased load. A well-inspected platform is defined as a platform which has been checked for flooded members and for which several joints have been cleaned/inspected and which should be able to have a longer period without an inspection update than a platform that was inspected with only a swim-by.

When a platform is inspected, the risks based on the data obtained are recomputed and the platform is re-ranked. In this way, if two platforms have the same likelihood prior to the inspection of one, the inspected platform's likelihood drops, as does its overall risk. The platform with the lowered risk is then a lower inspection priority, while the uninspected platform becomes a higher inspection priority.

The quality of the inspection also affects the ranking. Two platforms with the same risk just prior to being inspected—one with a level II inspection and the other with a level III—will have the same risk immediately after the inspection. While not strictly true, it is assumed that both levels of inspection will be able to determine the current condition of the platform with the same level of confidence. However, the level III or close visual inspection (CVI) is assumed to be able to detect impending problems with more confidence than the level II. Four years after the inspection, the score of the platform with the level II inspection increases to 8, while the score for the level III platform increases to 5, indicating the system considers that the predictive capabilities of the level III inspection are significantly better than those of the level II inspection.

In the case of level I inspections, the definition in API RP2A is above-water walk-around inspections—these have been excluded because they should be performed every year for all platforms.

Table 8.16 Inspection history.

Years since inspection	Level of last inspection		
	Level II	**Level III**	**Level IV**
1	0	0	0
2	2	0	0
3	4	2	1
4	8	5	3
5	9	7	5
6	9	8	6
7	10	9	8
8	10	10	9
9	10	10	10

For each inspection level, calculate tabulated scores, *SII* for level II, *SIII* for level III, and *SIV* for level IV.
Score = min (*SII*, *SIII*, *SIV*).

As shown in Table 8.16, the input data will be the year of the last level II, III, and IV inspections. The overall weight for the inspection history factor in the total score is 5.

For each inspection level II through III the following formula applies:

$$\text{The years since inspection} = \min(9,\ \text{this year} - \text{inspection year})$$

The last inspection factor does not interact with any other factors, as it is totally independent of the design or the condition of the platform; it is a matter of operation and the maintenance plan, which depend mainly on the budget and the existing robust plan. This factor highlights the necessity for different levels of inspection in order to eliminate or lower the perceived risk factors of a platform.

Remaining wall

Similar to damaged and flooded members, the number of corroded members has a major effect. However, in this factor, the *amount* of corrosion is also important (for damaged or flooded members, the amount of damage is not considered).

In terms of remaining wall thickness, it was felt that at least a 20% decrease is required to affect the strength. Corrosion is typically localized on the member and this has been accounted for in the approximation, noting that the score would be higher if the entire member were corroded. Corrosion above 50% was considered extreme and was assigned the highest score.

The extent of corrosion refers to the number of members affected. The quantitative calculation for this factor follows the same logic as for damaged and flooded members. Note that, in this case, the score is inverted compared to damaged and flooded members since the remaining wall is the key factor. The remaining wall is expressed as a percentage of the nominal thickness.

Table 8.17 Remaining wall thickness.

Remaining wall (%)		**Score**
>	≤	
50 80 100	50 80 99	10 8 3 0
Number of members		**Weight**
≥	≤	
5 10	4 9	0.2 0.4 1

Total score = tabulated score × weight.

Table 8.17 presents a score between 0 and 10, where a score of 0 corresponds to a wall retaining 100% thickness and a score of 10 corresponds to a wall that has thinned to less than or equal to 50%. This score is then multiplied by another factor that is determined by the number of members thinned. The resulting scores range from 0 (no risk of failure) to 10 (increased risk of failure). The overall weight of this factor in the total score is 7.5.

The remaining wall and the extent are both inspection results. Consequently, the corrosion factor is taken as a strong indicator of the current condition of the platform.

However, for this factor, the effect on likelihood of failure has been kept independent of the bracing pattern and number of legs, because a member with a corroded wall would still be considered to be contributing to the structural stiffness and thus would carry load with a reduced capacity. When the remaining wall turns into a through-thickness hole, a crack, or a dent, it would be recategorized as a damaged member, for which separate qualitative calculations exist, as described above.

Likelihood calculation for load

Design loading

Previous studies concluded that the first generation of platforms in the Gulf of Mexico were designed for a hydrodynamic loading that is 55% of today's design load. The metocean data were subsequently revised and the design loading became more severe as the years progressed.

As per the discussion in Chapter 7, Assessment of existing structures and repairs, in the North Sea the earlier platforms of the late 1960s and early 1970s were designed for loading that is 70% of today's design load. However, in the years

between 1980 and 1986, the metocean data produced design loads that were 45% more severe than the present loads. This explains the separate tables for the North Sea. At other locations, the Gulf of Mexico trend is used.

The design loading factor differs from the design practice factor, which accounts for the level of confidence in the design of structural components such as joints and members.

Note that the "year designed" can generally be taken as 2 years prior to the year of installation.

The scores for this factor vary from 0 to 10 for different ranges of year designed. Low scores correspond to higher values of design loads and thus low likelihood of failure, while high scores indicate lower values of design loads and increased likelihood of failure. This factor has two tables, one for the North Sea and another for elsewhere (combined into one table in Table 8.18). However, the scoring principle is the same for both. The scores vary from 1 to 10 for different ranges of year designed. The overall weight in the total score is 5.

Where the design is a repeat of a standard design, the year designed should be taken as the year designed for the first of the standard platforms. Where the year designed for the first of the standard platforms is not known, a date 2 years prior to the year of installation may be taken, although this may not be conservative.

It is evident from Table 8.18 that the year designed parameter interacts with location to distinguish the North Sea from the remainder. The scores are based on the design hydrodynamic loading adopted from the metocean data as per practice in the year of design.

Marine growth

Marine growth is a very simple factor but can cause many problems, as discussed in Chapter 3, Offshore structure platform design. The wave force that affects the

Table 8.18 Year of design.

North Sea	**Year designed**		**Score**
	≥	≤	
	1973	1972	10
	1981	1980	6
	1987	1986	1
			5
Another location	**Year designed**		**Score**
	≥	≤	
	1971	1970	10
	1975	1974	7
	1979	1978	4
			1

Table 8.19 Marine growth factor.

Measured/allowable marine growth in design		**Score**
>	≤	
	90%	0
90%	135%	3
135%	150%	8
150%		10
No data	10	

load on the structure is a function of the member diameter, so marine growth will increase the member diameter and increase the wave force correspondingly. This factor uses actual measured marine growth (mm)/design marine growth (mm).

Table 8.19 illustrates scores for this factor between 0 and 10, where a higher score signifies greater risk. If the measured marine growth exceeds the design value, it increases the environmental loading on the platform and therefore increases the likelihood of failure for the platform. The table allots a score of 10 to platforms whose measured marine growth exceeds the design value by 50% or more.

If there are no data available, the score may be reduced to 5 if underwater surveys undertaken indicate that the levels of marine growth are low, that is <50 mm thick.

This parameter does not have any interdependence with other factors or parameters in the likelihood category. The measured marine growth is an inspection item. It is divided by the design marine growth (design data sheet) to obtain the ratio in terms of percentage.

Although this is an inspection-related input, the parameter to cause failure is the environmental loading. Excessive marine growth, especially when it far exceeds the design growth, results in higher loading on the platform than it was originally designed for.

Note that there is not a 1:1 correspondence in the percent increase in marine growth and the increase in global base shear on the structure. This is because the computed ratio is the percent increase in marine growth only, with the marine growth typically only being a small portion of the total diameter of a tubular member (the member diameter is by far the largest contributor). This is why the marine growth ratio has to exceed a large value (150%) before there is a significant effect.

Scour

Although scour is an inspection-related input, the parameter to cause failure is the resultant stress. Excessive scour, especially when it far exceeds the design depth, may result in an increased stress level on the piles and the lower portion of the jacket, which may increase the likelihood of failure.

This factor uses measured scour depth (ft. or m) divided by the design scour depth (ft. or m). Table 8.20 presents a score between 0 and 10, where a higher score signifies greater risk. If the measured scour exceeds the design value, it increases

Table 8.20 Scour factor.

Scour measured/design		Score
≥	≤	
	90%	0
90%	125%	3
125%	150%	7
150%		10

the stresses on the pile and lower portion of the jacket and therefore increases the likelihood of failure for the platform. This table allots a point of 10 to platforms whose measured scour exceeds the design value by 50% or more.

Although scour is a concern, it does not typically result in a significant increase in stresses in the piles and lower portion of the jacket (although the stresses are higher than if there were no scour). Therefore it has been assigned a low overall weight of 2.

The "No data available" score may be reduced to 3 if underwater surveys undertaken across the assets indicate that typical scour levels are low, that is, <1 m.

This factor does not have any interdependence with other factors or parameters in the likelihood category. The measured scour is divided by the design scour depth (design data sheet) to obtain the ratio in terms of percentage.

Topside weight change

This factor accounts for the likelihood of failure of the platform due to changes in deck weight due to deck extensions, additional static or rotating equipment, or change of use. To access these data is not easy as in the past, there were no computers to maintain an archive system for drawings and calculation reports, and the data may go back over 40 years. Therefore the main source is the original drawings, if they exist, and the actual condition, and the other main source is information collected from the people who have worked on the platform previously.

Therefore there are four scenarios: the first one you have no data at all, the second you have minor data but do not know if the weight is increasing or decreasing from the original. You already have data and expect the growth on weight is less than 10% or you expect the weight growth to be higher than 10%, the score of this factor is shown in Table 8.21. Note that the weight growth means the percentage of the actual weight to the original weight after commissioning and start up of the platform and is the sum of the dead, operating, and live loads, including live loads on all open and laydown areas.

Additional risers, caissons, and conductors

This factor is intended to consider the additional risers, caissons, and conductors (over and above those that the structure was originally designed for) that have an impact on platform failure.

Table 8.21 Topside weight change.

Criteria	Score
Not known if weight growth or weight reduction	2
Estimated believed weight growth $\leq 10\%$	5
Estimated weight growth $>10\%$	8
No data	10

Table 8.22 Additional risers or conductors.

(A) Number of additional risers, caissons, and conductors	Number of risers, caissons, and conductors designed for		
	1–10	11–20	>20
0	0	0	0
2	2	1	0
4	4	3	1
6	6	4	2
8	8	5	2
>8	10	7	3
Not known	5	3	2
(B) Sum of diameters for existing riser/ sum of diameter of original design	**Score**		
0	0		
1%–20%	2		
20%–50%	5		
50%–80%	8		
80%–100%	10		
Higher than 100%	10		
Not known	10		

The score depends on both the number of risers, caissons, and conductors that the structure was designed for, and the additional number subsequently installed (Table 8.22a). Note that the overall weight in the total score is 5.

If there is uncertainty concerning the basis of the original design, a conservative estimate of the number of additional risers, caissons, and conductors is used.

This factor can be calculated by another approach if the diameter of the original riser and conductor design and the actual existing riser and conductors are available. By obtaining the ratio of the sum of the diameters of the existing risers and conductors, the sum of the diameters for the original design of conductors and risers can be obtained. Table 8.22b provides the score for every case.

Wave-in-deck

The wave-in-deck factor is intended to consider the likelihood of platform failure due to storm wave crests that strike the platform's lowest deck. This might occur if the platform has improper design or there has been a change in metocean data so that the lowest deck elevation fails to satisfy the minimum air gap requirement. This would mean that, in the case of an extreme event, the maximum wave could potentially hit the deck levels and cause damage. This affects the reliability of the structure in terms of both structural integrity and human safety. Therefore it is essential that this situation be reported to the operating and engineering group.

Since this problem seldom occurs, if the review study reveals that there is a problem it should be raised at once and action taken.

So, this phenomena may be happened before, or not happened, so if it was not happened before, in this case this factor will be neglected but if it is happened it will take the higher score which is 10. So the overall weight in the total score is <20.

Earthquake load

Amoco's platforms in Trinidad lie in an earthquake zone. Although recent platforms installed in the area have been designed for earthquakes, a majority (if not all) of the older platforms did not account for earthquakes in their original design. This inadequacy in design increases the likelihood of failure for those platforms when compared with platforms that have been designed for earthquakes or those that are located in nonearthquake zones.

ISO Zone 2 correlates to an effective ground acceleration of 0.2 g (ISO zones have ground accelerations that are 10% of the zone value: that is, Zone 1 = 0.1 g, Zone 2 = 0.2 g, etc.). Typical offshore platforms that are designed for waves only can normally withstand ground accelerations of 0.15−0.2, provided that they were initially designed for a reasonable wave height and have good joint detailing. Ground accelerations higher than this can cause problems, with an ISO Zone 4 or larger requiring specific earthquake design features for ductility (special kl/r values, extra-heavy cans, redundant framing schemes, etc.).

Obviously, it is important to define the earthquake zone. Table 8.23 presents a score of between 0 and 10. Higher scores are used for platforms in higher earthquake zones to penalize them for design inadequacy. In an earthquake zone, this is a major design consideration, therefore the overall weight in the total score is 8.

Table 8.23 Seismic load.

ISO seismic zone		**Score**
≥	≤	
0	2	0
3	3	4
4	4	7
5	5	10

This factor does not have any interdependence with other factors or parameters in the likelihood category. It is formulated with the earthquake zone and earthquake design (yes or no) parameters from the design category of the datasheets.

Likelihood categories

Most factors provide a score of between 0 and 10. Factors like bracing-legs and year-load location have values ranging from 1 to 10 and scores for appurtenances range from 0 to 12. The factors value has a negative or positive effect on the likelihood of failure. A value of 0 indicates that the factor has the least effect on increasing the probability of failure. A value of 10 indicates that the factor has a maximum detrimental effect on the likelihood of failure.

The weights indicate how strongly the effect assessed by each factor affects the overall likelihood of failure of the platform. The total score is calculated by the formula: $\sum_i w_i s_i$, where w_i is the weight of the ith factor and s_i is the score. This score can mathematically range from 15 to 2255, but for practical purposes scores range from about 40 to 350.

The total weighted scores are converted to a likelihood category according to the ranges in Table 8.24. These ranges have been developed from the ranges presented in the DNV paper.

After scores for all the platforms in the fleet have been obtained, the cumulative percentage can be calculated and, using statistical data, the cumulative distribution function can be obtained, as shown in Fig. 8.2. Because the category limits identify the best and worst 5% of the platforms, it is assumed that 5% of the platforms have a high likelihood of failure and 5% of the platforms have an insignificant likelihood of failure. The intermediate category limits are intended to represent the 50th and 70th percentiles. This distribution of the category limits assigns two category ranges for platforms that have better than average likelihood scores and three ranges for platforms that have worse than average scores. Consequently, it will be necessary to review and modify the ranges once data from the jacket evaluation and scoring become available, to ensure that the intent is being realized. The values of the categories S1, S2, S3, and S4 are obtained from the cumulative density function (CDF).

Table 8.24 Likelihood category.

Category	Range
1	$\leq$ S1
2	S1−S2
3	S2−S3
4	S3−S4
5	$>$ S4

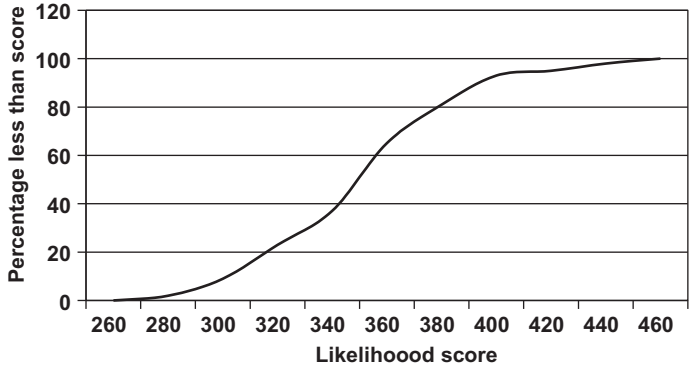

Figure 8.2 Cumulative density function (CDF) for likelihood score strength.

Consequence factors

In general, the consequences of platform failure are the sum of three main factors, where the components account for:

- environmental losses (C_E);
- business losses (C_B);
- injuries and safety-related losses (C_S).

Each of the above consequences is converted into a monetary value in USD, and the three factors are then summed to give the overall consequence.

While the summation of the monetary values obtained does not represent the total amount of money that could be lost due to a failure, the concept of a monetary value for consequences has been adopted to measure and sum the effect of safety, environmental, and business losses.

Each type of consequence is measured in the common unit of USD or Euros, with different factors determining the value of each type of loss. When possible, the consequence calculations are quantitative and related to actual economic values during the time of calculation. One of the main factors is the price of oil and gas and the cost of offshore reinstatement. The factors affecting each type of consequence and the factors for calculating their monetary value are described next.

The total cost is calculated as follows:

$$C_T = C_E + C_B + C_S \tag{8.1}$$

Each category is calculated separately in the following sections.

Environmental losses

Environmental losses are calculated based on the amount of liquid that was spilled, which is calculated by the daily production or the amount of liquid released if it can be computed. There is a fixed cost which includes the mobilization of personnel

and equipment to perform the clean up, in addition to the regulatory cost. The cost will vary depending on the volume of oil spill. It is worth mentioning that the fixed and variable costs vary with the global location, reflecting the regional differences in clean-up and regulatory costs. For example, strong wave action in some regions will quickly break up, dissipate, and volatize spilled oil, reducing the overall environmental impact of an oil release (Table 8.25).

- The cost is adjusted by multiplying the calculated cost by a factor to account for the distance offshore. The distance from shore is important because both the clean-up cost and the damaging effect of an oil spill increase if oil is washed up on shore. On the other hand, the spill can affect rare coral reefs or destroy the tourist areas, such as in Egypt where the oil field is close to tourist areas.

  Estimated environmental loss calculations are presented in Eq. (8.2).

$$C_E = f(d) \times \left\{ F_C + V_C \times \min(D_P, R) \right\} \tag{8.2}$$

where

$$f(d) = 1 \quad d > d_m \tag{8.3}$$

$$f(d) = 1 + \left(\frac{d_s - d}{d_s} \right)^2 \quad d \leq d_m \tag{8.4}$$

and where C_E is the environmental loss, in USD; V_C is the variable cost, in USD/bbl; F_C is fixed environmental cost, in USD; R is minimum released oil volume, in bbl; D_P is daily production, in barrels of liquid, bpl; d is distance offshore, in km; and d_s is the maximum significant distance offshore, which is the distance from the shore line in km.

These calculations are followed only when the environmental loss, C_E, has not been determined for a given platform. The estimate is based on the assumption that the environmental losses are proportional to the daily production. The fixed cost, F_C, and the marginal cost, V_C, depend on the location accounting for worldwide variations in the costs associated with clean-up, regulations, and other factors.

Eq. (8.1) also accounts for the increased environmental effects of near-shore spills where a spill is more likely to threaten beaches and other ecosystems. In these locations, clean-up and regulatory costs are likely to be higher than in the open sea, where wave action and weather can dissipate and volatize a large portion of a spill.

The value of the significant distance should be defined in each region separately based on the geographic location.

Note that, for input variables that are unknown, the variables can revert to default values.

It is worth mentioning that environmental factors alone made the oil spill that occurred in the Gulf of Mexico in 2010 a disaster for BP: the cost may reach to 60 billion USD according to new analysis from Moody's, the rating agency. In

Table 8.25 Worldwide variation in default values for consequence costs.

Variable	Location						Description
	G	N	C	M	E	Units	
i	10%	10%	10%	10%	10%	%	Discount rate
P_{oil}	$120.00	$130.00	$110.00	$130.00	$110.00	$/bbl	Oil revenue per bbl
P_{gas}	$1.50	$3.00	$1.50	$1.50	$1.50	$/mscf	Gas
C_{ex}	$1 MM	$1 MM	$1 MM	$1 MM	$1 MM	$	Personnel marginal exposure cost
n	200	545	180	180	400	Days	Default deferred production period
FC	$500 M	$750 M	$400 M	$350 M	$500 M	USD	Fixed environmental cost in open sea
VC	$500	$500	$500	$500	$500	$/bbl	Variable environmental cost in open sea
d	50	65	25	25	50	Miles	Default distance offshore
d_m	100	100	100	100	100	Miles	Distance offshore to open sea
—	$5 M	$5 M	$5 M	$5 M	$5 M	$/ton	Default replacement value
M	$150 M	$150 M	$150 M	$150 M	$150 M	$	Default daily production value
RV	250	250	250	250	250	Bbl	Default spill volume
N_{crew}	20	20	20	20	20	Persons	Default crew size: service unknown
N_{crew}	30	30	30	30	30	Persons	Default crew size: production platform
N_{crew}	20	20	20	20	20	Persons	Default crew size: drilling platform
N_{crew}	50	180	50	50	50	Persons	Default crew size: quarters platform
N_{crew}	10%	10%	10%	10%	10%	%	Percent of crew exposed if evacuated
N_{crew}	2	2	2	2	2	Persons	Default crew size: unmanned platform
—	20%	20%	20%	20%	20%	%	The percent increase in the expected safety losses in gas production platforms.

G, Gulf of Mexico; *N*, North Sea; *C*, Canada; *M*, Malaysia; *E*, elsewhere.

addition, there is also an effect on the reputation of the company. The reputation factor should be considered as another consequence of platform failure.

Business losses

To assess the business consequences of a platform failure, two terms are considered. First, there is the replacement cost of constructing a new platform. Second, there is the impact of deferred production, which reflects the cost of not being able to produce for the time that it takes to replace the platform.

For water and gas injection platforms and jackets supporting vent lines and flares, this value should reflect the loss of production should the structure fail.

Eq. (8.1) estimates the total business loss component of the failure consequences. There are two main factors that influence the business loss cost, as follows:

- Replacement as, in the case of a failure, there will be a cost of constructing a new platform;
- Deferred production due to the platform structure failure completely or partially, as this is the cost due to stopping production and shutting off the well until replacement of the platform or a major repair has been performed. In this calculation the oil and gas reserve is modeled as an investment present value (PV). The value of the deferred production is equal to the difference between the present value and the value of the reserve discounted for the time it takes to return it to production after a failure at a given interest rate.

The owner company should define the estimated cost of the platform (e.g., it can estimate the cost as $5500 per ton of platform) if there is no given replacement value for the platform.

The deferred production losses are a function of the platform's production rate. The production rate can be expressed as either the value of a month's production or the volume of oil and gas produced in a month. When the volume is given, the value of the production is estimated using default oil and gas prices that vary with location to reflect the actual value of the oil and gas in any given region of the world.

The value of all the oil in the reserve is simplistically modeled as the net present value of an annuity that makes monthly payments equal to the monthly production. If the reserve lifetime is unknown, it is assumed to be infinite and the value of the reserve is the "capitalized cost" of the reserve. This is equal to monthly production in dollars divided by the monthly interest rate (M/I). This is the value of the reserve if production is never interrupted. But if the platform fails and production must be deferred, the value of the reserve decreases because monthly payments on the annuity are suspended for the period it takes to replace the platform.

The deferred production loss is the difference between the value of the uninterrupted production and the present value of the interrupted production. The day production resumes, the value of the reserve is equal to the value of the reserve based on the uninterrupted assumption. This is converted to a net present value by discounting the value of the reserve for the interruption period. By default, this is calculated at an interest rate of 1% per month.

In determining the business loss for collapse of the structure, if C_{DP} is not given, then its default value is determined.

Calculate the net monthly production from Eq. (8.5):

$$P_M = (D_{Poil} \times P_{oil} \times D_{Pgas} \times P_{gas}) \times (30 \text{ days}) \tag{8.5}$$

where D_P is the daily production in bpd or MSCFD, in USD; P_{oil} is oil price/bbl, in USD/bbl; P_{gas} is gas price/mscf, in USD/MSCF; and P_M is the net monthly production.

The present value will be as shown in Eq. (8.6), as r_m is the monthly return investment as equal approximately to $r/12$, which will be obtained by defining, r, which is the annual rate of return on investment.

$$PV = P_M / r_m \tag{8.6}$$

$$C_{DP} = P_m \sum_{k=1}^{n} \left(\frac{1}{1+r} \right)^k \tag{8.7}$$

where n is calculated from $N/30$, where N is the total amount of downtime per day.

Noting that Eq. (8.7) assumes the volume of oil is fixed for the period of shutdown, it is however not true as in most cases there is a decline in production which depends on the reservoir characteristics.

$$C_B = C_{DP} + C_R \tag{8.8}$$

where C_R is replacement cost, in USD; C_{DP} is deferred production loss, in USD; C_B is business loss, in USD. The value of deferred production is based on the total present value of production. If this is not given, PV is estimated from the monthly production in dollars by assuming an infinite reserve life.

The values for deferred production, replacement, and total business loss can be input into the system from a variety of sources. The values here are default values for these losses when no additional information is available. The defaults for net oil price, expected return on investment, etc., can be assigned from region to region to reflect the differences in each home market.

The loss from failure of the structure is the sum of the replacement cost and deferred production. If the replacement cost is unknown, it can be estimated using the approximate weight of the structure.

Safety consequences

To assess the safety consequences of a platform failure, two terms are used. The calculation is simply equal to the product of the crew size and a marginal safety cost per crew member. Because there is an increased hazard potential when the platform handles gas, the product is increased by 20% for gas-producing and gas compression platforms. The consequence value is recommended to increase by

around 50% when the platform handles H_2S. If the platform is bridge-linked to another platform, the consequence value is halved.

The default safety loss is proportional to the average number of people on a platform. The estimated safety loss is the product of a mean per capita safety loss and the average platform crew. As in other consequences, default crew sizes can vary from location to location, so the resulting consequences reflect the relative differences in hazard exposure costs worldwide.

This calculated loss is adjusted downward when the platform is evacuated during severe storms. The expected consequence is increased if the platform handles gas production, because gas production implies that fire could result from an underwater structural failure. In the case of unmanned platforms, a minimum safety loss is assumed.

Regional factors, such as workplace safety regulations, fines, or other legal costs, are accounted for using regionally specific default mean per capita safety losses.

The safety-related losses, C_S, are proportional to the number of people exposed, the location and the marginal safety loss per person as a result of failure

$$C_S = C_{ex} \times N \times G \tag{8.9}$$

where N is the number of crew on a platform.

The penalty that increases expected losses by 20% for gas platforms is

$$G = 1 \quad \text{if } DP_{gas} = 0$$
$$G = 1.2 \quad \text{if } DP_{gas} \neq 0$$

Input data depend on the location, platform service, and type of production. Default values for each of the inputs can be specified for different worldwide locations to reflect local conditions and expectations.

Consequence categories

The estimated loss in dollars is converted to consequence categories. This is in order to determine the ranges for the consequence categorization, if you have a fleet of platforms structures. It need to calculate the total losses in all platforms, the present cumulative distribution of the estimated total losses is plotted on probability using the appropriate software and the results are used to estimate the consequence against 5%, 50%, 75%, and 95% probability. These four values C1, C2, C3, and C4 are obtained and used as the bounds to define the consequence categories as shown in Table 8.26.

In order to reflect local differences in the factors that affect the consequences, Table 8.26 shows which values can be changed for the various locations worldwide. The factors C1−C4 should be defined in each category as their values will differ from one region and company to another.

Table 8.26 Relationship between estimated consequence and consequence category.

Category	Percentage of the platform fleet	Consequence (US $M)
A	< 5%	< C1
B	5%–50%	C1 to C2
C	50%–75%	C2 to C3
D	75%–95%	C3 to C4
E	> 95%	> C4

Consequence

Likelihood	A	B	C	D	E
1	Yellow	Yellow	Yellow	Red	Red
2	Green	Green	Yellow	Yellow	Red
3	White	White	Green	Yellow	Red
4	White	White	Green	Green	Yellow
5	White	White	Green	Green	Yellow

Figure 8.3 Risk matrix proposed by American Petroleum Institute (API) for the categorization of qualitative risk.

The environmental, business, and safety losses are summed to calculate the overall loss in terms of dollars or other currency depending on the country. This overall loss is converted to a consequence category according to the ranges presented in Table 8.26.

As with the likelihood of failure, the consequence category limits are intended to identify the best and worst 5% of the platforms. The intermediate category limits are intended to represent the 50th and 70th percentiles. This distribution of the category limits assigns two category ranges for platforms that have better-than-average likelihood scores and three ranges for platforms that have worse-than-average scores.

8.3.2 Overall risk ranking

After each platform has been categorized in terms of likelihood (1–5) and consequence (A–E), the categories are presented through the risk matrix presented in Fig. 8.3 to establish the overall relative risk ranking. The overall rankings are high (red), moderate (yellow), low (green), and insignificant (white).

The highest risk items fall into category E5 and the lowest risk items fall into category A1. The different colors show that the relative risks are grouped into high, moderate, low, and insignificant risk levels.

Where guidance in terms of ranking within each of the four risk categories may be useful, a preliminary assessment can be made by multiplying the total likelihood

score by the total loss in abstract dollars. This approach is far from rigorous, so the resulting listing should be treated as indicative only.

Fig. 8.3 shows the qualitative risk matrix proposed by the API Committee for Refinery Equipment and based on Bea et al. (1988) for the assessment of refinery and petrochemical plants. The same 5×5 matrix has been adopted for the RBUI system.

Puskar et al. (1994) delivered other risk matrices that have been used for offshore risk assessment. Many of these systems are based on every company's practical experience. The 5×5 matrix elements, as shown in Fig. 8.3, are preferable as they present enough range in likelihood and consequence for it to be easy to differentiate between the platform fleet. The categorization scheme summarized by the API risk matrix in Fig. 8.3 appears to be biased toward high-consequence events. High-consequence and moderate-likelihood equipment (E3) is classified as high risk, while high-likelihood, moderate-consequence equipment (C5) is classified as moderate risk. Because the API group that developed this matrix felt that avoiding very high-consequence failures was a priority, the bias was intentional. It was included as a precaution against uncertainties in categorizing the likelihood of high-consequence equipment, but since neither the likelihood nor consequence categories correspond exactly to a precise quantitative value, this bias may not be as significant as it appears in the diagram.

Note that API RP2-SIM recommends the matrix in Table 8.27 to present the risk level of the platform.

High consequence is in the cases of E5, D5, E4, and E3 and medium consequence will be A5, B5, C5, C4, D4, D3, E2, E1, where the low risk ranking applies to the remaining cells. Some references, such as API RP2-SIM, have three categories only.

The structure should be classified into one of three categories:

- red = high risk;
- yellow = medium risk;
- green = low risk.

The other way to manage the platform is by put all the ranking values of the platform as in Table 8.27 and then divide all the platforms into three categories with an equal number of platforms from red, yellow, and green, for example, if you

Table 8.27 Risk matrix based on American Petroleum Institute structure integrity management (API SIM).

		Likelihood of failure		
		Low	**Medium**	**High**
Consequence of failure	High	Risk level 2	Risk level 1	Risk level 1
	Medium	Risk level 3	Risk level 2	Risk level 1
	Low	Risk level 3	Risk level 3	Risk level 2

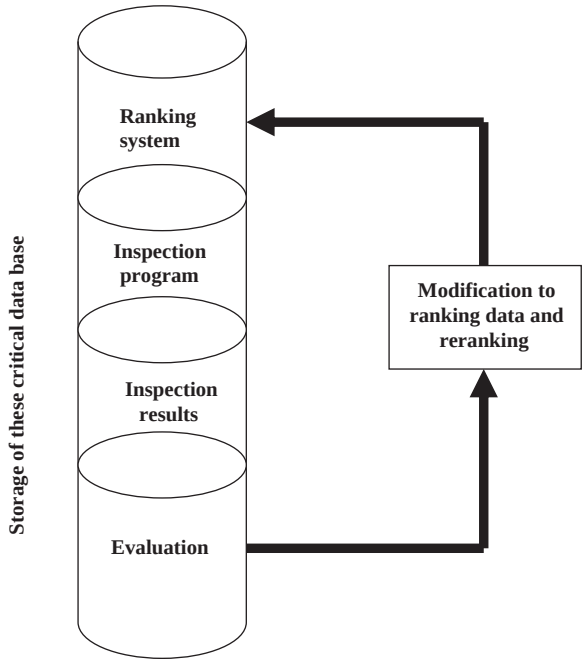

Figure 8.4 Risk ranking procedure.

have 150 platforms each category will have 50 platforms, and the priority for inspection will follow platforms based on their individual numbers. The qualitative risk assessment method makes it very easy to manage a large number of offshore structure platforms.

It is very important to highlight that, as engineers, we focus on the likelihood of failure, however company management usually focuses on the business, so the consequence should be in the risk equation. Therefore if you implement the risk categories based on the consequence and the likelihood of failure, the maintenance plan will be business oriented, as in this case you may spend no money on a platform with high probability of failure, and with a very low consequence cost you should predict that the platform will fail, which is considered tacitly in this approach. However, if you need to insert a maintenance and inspection plan to prevent any failures, you should rank the platforms by probability of failure only. Fig. 8.4 presents a summary for the main steps for the structure integrity management system.

8.4 Underwater inspection plan

After defining the risk ranking for all fixed offshore platforms in the fleet, the next step is to define the future inspection plan for the topsides and for the subsea

structure. The inspection program focuses on underwater inspection because it is more costly: it requires a vessel and divers or an ROV.

8.4.1 Underwater inspection (according to API SIM 2005)

Periodic underwater inspection should be carried out at intervals consistent with the SIM strategy adopted by the owner or the operator. Inspection intervals are provided based on the platform consequence of failure; there are default intervals in lieu of intervals developed based on risk of failure. Periodic underwater inspection intervals may also be influenced by operational considerations, such as riser importance and condition, sea-bed movement, CP system condition, etc.

The purpose of routine underwater inspection is to provide the information necessary to evaluate the condition of the platform and appurtenances.

In the absence of a risk-based SIM strategy, default inspection intervals, shown in Table 8.28, based on the consequence of platform failure, should be used. These default intervals are based on historic industry practice that has resulted in satisfactory in-service performance of the platform, CP system, and appurtenances.

Note that the timing of the first underwater periodic inspection is determined from the date that the baseline inspection was completed.

If the owner or operator responsible for SIM has adopted a risk-based SIM strategy, the inspection intervals shown in Table 8.29 based on the risk of platform failure should be used. The risk-based inspection intervals should be adjusted as described in Table 8.29 to recognize the existence of high-consequence appurtenances, in particular risers, and also to ensure the uninterrupted operation of the underwater CP system. This should be based on data from prior inspections.

The risk-based inspection interval should not exceed 5 years for high-consequence platforms where the consequence category is driven by the presence of pipeline risers at the platform.

API SIM defines the requirement for survey level as shown in Table 8.30. The general visual survey in level II, as described in Table 8.31, is the basis for initiation of a level III survey. The scour survey in a level II survey will be done if the seafloor is composed of loose sand or from previous experience or if it is suspected that the seafloor is instable. As presented in Table 8.31 for the under water survey categories, the visual corrosion in a level III survey in a medium consequence category is not required, and also for a low consequence category if it was indicated previously that there is a cell record of continuous annual drop.

Based on the number of platforms that need inspection we can obtain the required budget cost estimate to enable management to define the required annual budget for the inspection.

8.4.2 Baseline underwater inspection

A baseline for underwater platform inspection is required to define the as-installed condition of the platform. The minimum scope of work should consist of the following, unless data are available from the installation survey:

Table 8.28 Data for platforms constructed in 1980−1990.

Platform	Design year	Total score
P49	1985	410
P50	1985	470
P51	1984	465
P52	1986	473
P53	1985	399
P54	1985	394
P55	1985	394
P56	1985	323
P57	1985	405
P58	1985	416
P59	1985	391
P60	1984	418
P61	1987	423
P62	1981	483
P63	1984	348
P64	1986	463
P65	1983	439
P66	1984	458
P67	1984	463
P68	1987	420
P69	1985	503
P70	1985	333
P71	1982	463
P72	1983	473
P73	1989	407
P74	1989	449
P75	1989	444
P76	1984	458
P77	1989	421
P78	1982	503
P79	1985	463
P80	1985	645
P81	1981	458
P82	1981	662

Table 8.29 Default inspection intervals.

Consequence category	Maximum inspection interval (years)
High	3
Medium	5
Low	5

Table 8.30 Risk-based inspection interval ranges.

Risk category	Inspection interval ranges (years)
High	3–5
Medium	6–10
Low	11 or more

Table 8.31 American Petroleum Institute structure integrity management (API SIM) definitions of requirements for survey, by level.

Subsea survey level	Consequence categorization		
	Low	Medium	Higher
Level II			
General visual survey	●	●	●
Damage survey	●	●	●
Debris survey	●	●	●
Marine growth survey	●	●	●
Scour survey*	●	●	●
Anode survey	●	●	●
Cathodic potential	●	●	●
Riser/J tubes/ caissons	●	●	●
Level III			
Visual corrosion		●	●
Flooded member detection (FMD)		●	●
Weld/joint close Visual		●	●
Level IV			
Weld/joint nondestructive test (NDT)		●	●
Wall thickness			●

- A general visual survey of the platform from the mud line to the top of the jacket, including all members and joints and also including coating integrity through the splash zone;
- Below-water boat-landing and barge-bumper integrity;
- Anode count and verification of their presence and integrity, in addition to measurement of the CP reading;
- Appurtenance survey;
- Measurement of the mean water surface elevation, as installed, with appropriate correction for tide and sea-state conditions;
- Tilt and platform orientation;
- Riser and tube soil contact;
- Scour survey (sea-bed profile).

8.4.3 Routine underwater inspection scope of work

Routine underwater platform inspections are required to detect and properly measure and record any platform defects, deterioration, or anomalies that affect its structural integrity and performance. Platform deterioration may include excessive corrosion of welds and members, weld/joint damage due to overload or fatigue damage, and mechanical damage such as dents, holes, bows, and gouges. Platform anomalies may include a nonoperating or ineffective corrosion protection system, scour, seafloor instability, hazardous or detrimental debris, and excessive marine growth.

The whole structural integrity management system relies on the accuracy and completeness of the inspection, both topside and underwater.

The underwater inspection program may include one or more of the following surveys:

- General visual survey;
- Damage survey;
- Debris survey;
- Marine growth survey;
- Scour survey;
- Anode survey;
- CP surveys;
- Visual corrosion survey;
- Appurtenance inspection;
- FMD survey;
- Weld/joint CVI;
- Weld/joint nondestructive testing (NDT) by using magnetic particle test (MPI);
- Wall thickness.

8.4.4 Inspection plan based on ISO 9000

The inspection plan is defined after determination of the exposure level, as shown in Table 8.32.

It is important to highlight that the timing of the first periodic level (I) inspection should be determined by knowing the platform installation completion date.

Table 8.32 Determination of exposure level.

Life-safety category	Consequence category		
	C1 (high consequence)	C2 (medium consequence)	C3 (low consequence)
S1 Manned nonevacuated	L1	L1	L1
S2 Manned evacuated	L1	L2	L2
S3 Unmanned	L1	L2	L3

However, the timing of the first periodic level II and level III inspections should be determined from the date of the baseline inspection.

ISO identifies levels of survey as presented in Table 8.32.

A level I inspection consists of an underwater inspection to verify the performance of the CP system (for example, a drop cell), and of a topside visual survey. This inspection includes a general assessment and evaluation of all structural members in the splash zone and above water, concentrating on the condition of the more critical areas, such as topside legs, girders, trusses, etc. If topside structure damage is detected, NDT is used when visual inspection cannot fully determine the extent of the damage. If the level I inspection indicates that underwater damage is possible, a level II inspection should be conducted as soon as conditions permit (Table 8.33).

A level II periodic inspection it will be a general underwater visual inspection. The inspection includes the measurement of cathodic potentials of preselected critical areas. Detection of significant structural damage during a level II inspection initiates a level III inspection. The level III inspection, if required, should be conducted as soon as conditions permit.

The level II inspection shall cover the following as a minimum in the inspection:

- accidental or environmental overloading;
- scour, sea floor instability;
- damage detectable in a visual swim-round survey;
- design or construction deficiencies;
- presence of debris;
- excessive marine growth;
- measurement of cathodic potentials of preselected critical areas.

A level III periodic inspection is mainly an underwater CVI of preselected areas and/or areas of known or suspected damage as presented from the previous level of inspection. The required inspected area shall be cleaned of marine growth to permit thorough inspection. Preselection of areas should be based on results of an engineering evaluation of areas particularly susceptible to structural damage and to areas where repeated inspections, as in the case of cracks due to fatigue, will be important to monitor integrity over time. FMD is more expensive but can supersede the CVI of preselected areas. Engineering judgment should be used to determine

Table 8.33 Maximum inspection intervals for default periodic inspection program.

Exposure level	Level I inspection	Level II inspection (years)	Level III inspection (years)	Level IV inspection
L1	Annual	3	5	Determined from level III inspection results
L2	Annual	5	10	Determined from level III inspection results
L3	Annual	5	Not required	Not required

optimal use of FMD and/or CVI of joints. Detection of significant structural damage during a level III inspection initiates a level IV inspection where visual inspection alone cannot determine the extent of damage. The level IV inspection, if required, should be conducted as soon as conditions permit.

FMD is used to determine the integrity of the tubular bracing members of steel jacket structures. This method relies on the detection of through-wall cracks by the leakage of water into the internal, air-filled space and successful detection of that water. Detection is enabled through the use of gamma radiation or ultrasonic techniques, both of which are applied externally to a tubular member, usually by means of a ROV in the case of gamma FMD, or by a diver, or potentially an ROV, in the case of ultrasonic FMD.

A level IV inspection shall consist of underwater NDT of areas preselected from the results of a level III inspection, in the case of a shallow water platform NDT for the joints is carried out directly as it will provide more accurate results at lower cost than FMD.

The level of inspection identification and scope depends on many factors, one of which is the inspection cost and its level of realism. An example of a survey scope of work is presented in brief in Table 8.34, and it can be considered a guideline in preparing the inspection scope of work.

8.4.5 Inspection and repair strategy

The inspection and repair strategy should be defined based on the probability of failure, the economics of inspection, and minor and major repairs. El-Reedy (2003) presents the optimal inspection and repair strategy.

Inspection alone does not improve reliability unless it is accompanied by corrective action in the event a defect is found. There are some other tactics used in practice in offshore structures, such as:

- Monitoring the crack until its depth reaches a certain percentage of the original thickness, then a repair is performed;
- Immediate repair upon finding the crack;
- Repair at a fixed time period, for example, 1 year after detecting the crack;
- Repair by welding.

In some oil and gas companies, the strategy is to carry out inspections at constant time intervals, as shown in Fig. 8.5, working with a preventive maintenance approach using periodic maintenance with constant inspection intervals to facilitate planning. Inspection intervals are selected using a risk assessment technique to minimize the expected cost of inspection, repair, and failure.

"No repair will be made unless damage is detected" is a very important statement. Most offshore structure inspection techniques are visual or use NDT. It is worth mentioning that the ability to detect damage mainly depends on inspector experience and the accuracy of his tools. A higher quality inspection method will provide a more dependable assessment of damage.

Table 8.34 Inspection survey scope of work overview.

Survey	Generic scope of work	Recommendation
General visual	Underwater general visual inspection of full structure with particular reference to members, joints, and appurtenance connections, to detect the presence of excessive corrosion, accidental or environmental overloading, fatigue damage, design or construction deficiency	All damage and all other anomalies found to be reported in accordance with owner or operating company specification On plan (first level above waterline), confirm or add location of jacket legs, conductor guides, conductors, J-tubes, casings, risers, and boat landings
Marine growth	Measurements of compressed marine growth at different locations that should be defined based on the water depth and the location of the platform	Present schematic for marine growth measurement locations. Visually check for areas of existing or missing marine growth. Document and report, immediately, any locations of missing or ripped marine growth to the company representative
Scour	Visually inspect the sea floor up to 7.5 m (25 ft.) out for possible erosion and scouring or instability. Check if the piles are exposed and whether the mud mat and bottom braces are on the bottom. Take readings of the bottom depths	If the pile is exposed, note if there is any corrosion or damage and check for mud mats. Note any bottom irregularities and bottom depth
Cathodic protection	Readings to be taken on legs on outboard truss chord, legs at the mean water level and halfway between each horizontal framing plan readings	See schematic for CP reading locations Measure all potentials in mV with reference to an Ag/AgCl half-cell
Anodes	Visual examination to locate, count, grade, and confirm the physical condition as loose, missing, or damaged of all original or retrofit anodes. Potential readings and detailed dimensional survey to be taken on two anodes	Grade 4 anodes should be reported as anomalous in accordance with the owner or operator specification Anodes identified as loose, damaged, or missing should be recorded as anomalous

(*Continued*)

Table 8.34 (Continued)

Survey	Generic scope of work	Recommendation
Debris	Visual inspection to record the quantity, type, size, and location of debris hanging on or in the jacket, in contact with the bottom elevation, on the sea floor up to 10.0 m (30 ft.) out or in contact with any risers, pipelines, or conductors	Report the amount of debris inside, on, and around the platform. Note whether the debris is metallic, hazardous, obstructing, or items that could have caused damage. Include a map of debris on the seabed. Remove, subject to confirmation from the company
Risers	Visually inspect the risers Take CP readings between riser clamps. Record riser coating type and depth of termination Inspect the pipelines to the point of entry into the sea floor or 10 m (30 ft.) from platform, whichever is closer	Document and report, immediately to the company representative, any soil disturbance or pipeline distortion within 10 m (30 ft.) of the platform or any hydrocarbon leaks from any source If pipeline suspended, note distance to point of contact and distance away
Caissons	Visual inspection of casings, casing clamps, and intakes. Take CP readings on clamps and casing mid-sections General visual survey of the conductors with particular attention given to examination for conductor movement	Note total number of conductor slots, number of conductors driven, and if any are undrilled Intakes shall be cleaned of marine growth if necessary
Flooded members	Flooded member detection (FMD) for all the members or specific members in the platform	Provide a schematic for FMD locations If flooding is detected, the company representative may request an additional survey to establish the cause

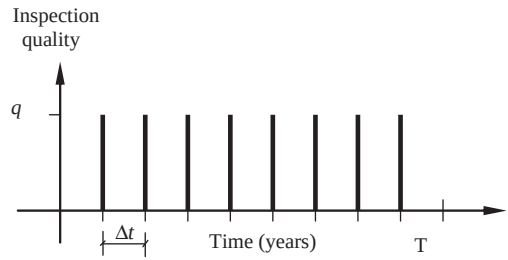

Figure 8.5 Inspection strategy.

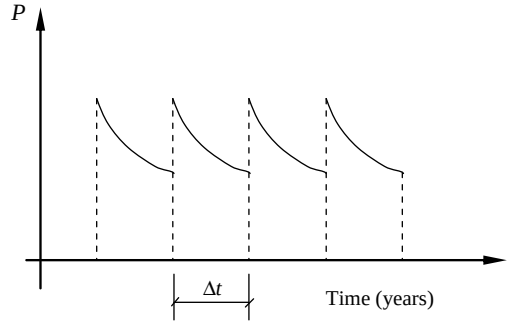

Figure 8.6 Offshore structure performance.

Higher quality inspection may lead to higher quality repair, which could bring the reliability of the structure closer to its original condition (although the reliability of the structure decreases with age). After inspection and repair, the structure's capacity should be the same as the design condition, as shown in Fig. 8.6.

Expected total cost

To calculate the expected cost it is required to determine the service life of the structure. Assuming the service life is 50 years and the routine maintenance (inspection and minor repair) is scheduled to be once every 2 years, it starts at $t = 2$ years and continues until $t = 48$ years. Therefore the preventive maintenance shall be performed 25 times during the life of the structure. The cost of maintenance during the lifetime shall be as follow:

$$C_{FM} = C_{m2} + C_{m4} + C_{m6} + \cdots + C_{m48} \tag{8.10}$$

If the total expected cost in its lifespan (T) is based on the present value, according to Turan (1990) the expected lifetime preventive maintenance cost becomes

$$C_{IR} = C_{IR2}\frac{1}{(1+r)^2} + C_{IR4}\frac{1}{(1+r)^4} + \ldots\ldots\ldots + C_{IR74}\frac{1}{(1+r)^{74}} \tag{8.11}$$

where r is the net discount rate of money.

In general, for a strategy involving, n, number of inspections during lifetime, the total expected inspection cost is

$$C_{ins} = \sum_{i=1}^{n} C_{ins} + C_R\frac{1}{(1+r)^{T_1}} \tag{8.12}$$

where C_{ins} is the inspection cost based on the inspection method, and C_R is the repair cost.

Finally, the total expected cost, C_{ET}, is the sum of the structure initial cost, C_T, the expected cost of periodic maintenance, which is the cost of the inspection and

the repair and maintenance, and the expected cost of failure. Where, C_f is the cost due to the consequence of structure failure, P_f is the structure probability of failure, C_{in}, and C_{re} is the cost of inspection and repair consequently.

Accordingly, C_{ET} can be expressed as

$$C_{ET} = C_T + (C_{in} + C_{re})\,(1 - P_f) + C_f \bullet P_f \tag{8.13}$$

The main objective for the company that the value of C_{ET} to be in the minimum values as possible, on the same time the structure shall be reliable along its life time.

Optimization strategy

The target is to obtain the optimim maintenance strategy plan during the platform lifetime. The following problem must be solved:

$$\text{Minimize } C_{ET} \text{ subject to } P_{f\ life} \leq P_{max}$$

where P_{max} is the maximum acceptable probability of failure during its life time or, considering the minimum accepted reliability index,

$$\beta = \phi^{-1}(1 - P)$$

where ϕ is the function for the standard normal distribution. The optimum inspection strategy during the platform lifetime is obtained by solving the following mathematical problem.

$$\text{Minimize } C_{ET} \text{ subject to } \beta_{life} \geq \beta_{min}$$

By formulating an optimization equation, the optimal inspection strategy plan with respect to cost can be obtained.

Eq. 8.5 presents the objective function (C_{ET}), which is affected by the periodic inspection cost and minor repair costs for the joint or member if applicable, as well as the cost as a consequence of failure occurrence, which includes the cost of major joint or member repair. The inspection periodic time (Δt), which is the optimization variable in this equation, is constrained by the minimum index β specified by the code and the maximum periodic time.

The optimization problem may be mathematically written as: find the Δt that minimizes the objective function

$$C_{ET}(\Delta t) = (C_{IR})(1 - P_f(\Delta t))\left(\frac{(1+r)^T - 1}{\left((1+r)^{\Delta T} - 1\right)(1+r)^T}\right) + C_f P_f(\Delta t)\left(\frac{(1+r)^T - 1}{\left((1+r)^{\Delta T} - 1\right)^T (1+r)^T}\right) \tag{8.14}$$

subject to $\beta(t) \geq \beta_{\min}$, $\Delta t \leq T$, where C_{IR} is the periodic inspection and minor repair cost per inspection, C_f is the cost for major repair, r is the discount rate, and $\beta_{\min}$ is the minimum acceptable reliability index. C_{IR} and C_f are assumed to be constant with time, but these values can escalate with the time factor which is needed for future research. Due to the code requirement it is often necessary to put a constraint on the reliability index.

The above method is matched with the quantitative risk method for the expected probability failure and its consequence. However, from a practical point of view it is easy and not costly to use a qualitative risk assessment approach for a fleet of offshore structure platforms.

8.4.6 Flooded member inspection

The two principal means of FMD are ROV-deployed gamma FMD and diver-deployed ultrasonic FMD.

Gamma FMD requires a gamma source and a detector to be fixed to either end of a yoke that is attached to an ROV. The ROV pilot then positions the yoke over the member and notes the reading count from the detector. This is compared with an expected count that is calculated taking account of the absorption characteristics of water between the yoke and the member, the member steel thickness, and the air within the member. If the member is flooded, the count is lower than expected due to the absorption of gamma radiation by the water and the member is flagged as flooded.

Ultrasonic FMD employs an ultrasound probe that is fixed to the outside of the member after suitable cleaning to provide good acoustic contact (Fig. 8.7 provides a schematic).

Water is a better transmitter of ultrasound than air, and a flooded member is detected by observing echoes that are received back at the probe and viewed on a screen. For an air-filled member, the echo will be that of the back wall. For a water-filled member, the ultrasound is transmitted through the water and a second echo will be generated at the interface between the water and the back face of the tube. This back-face echo is an indication that the member is flooded. Fig. 8.8 shows a typical UT trace for a flooded member.

For gamma FMD, the maximum distance between the source and detector determines the maximum diameter of the member that can be inspected. The distance between the two is limited not only by the size of the yoke, which is dependent on the payload capability of the host vehicle, but also by the strength of the radioactive element relative to the thickness of the steel walls of the members requiring inspection. The size of a gamma source normally varies according to the member diameter and wall thickness. In general, as large a source as possible is used to give meaningful results, but without saturating the detector so that a drop cannot be observed.

The host vehicle should be of sufficient size to allow access and to carry the FMD equipment, and it should be able to operate in the environmental conditions present.

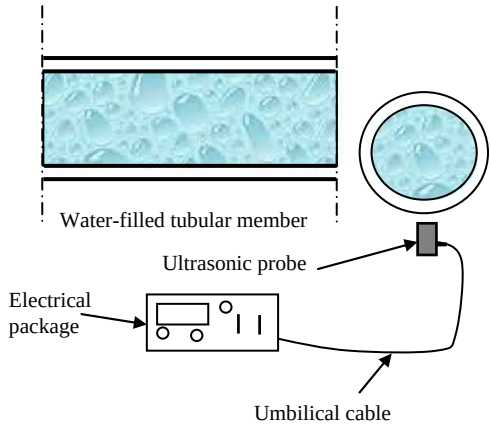

Figure 8.7 Typical arrangement of ultrasonic test flooded member detection (UT FMD) equipment.

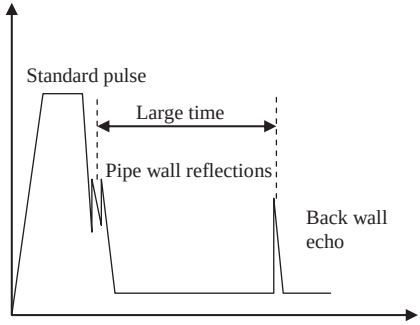

Figure 8.8 Typical ultrasonic test (UT) signal for a flooded member.

The range of member diameters typically surveyed by gamma FMD methods is from 12 inches (0.3 m) to 2.6 m. FMD is currently performed on members with a wall thickness in the range of 8−63.5 mm.

Orientation of the yokes can be adjusted to any position for taking readings on inclined members.

Fig. 8.9 shows that the positions in which readings may be taken on the member can also be varied. Typically, readings are taken at the "6 o'clock−12 o'clock" or the "3 o'clock−9 o'clock" positions. The yoke can be adjusted to make the necessary readings possible.

The majority of flooded or cracked members occur as a result of unforeseen circumstances, such as the presence of a gross defect caused by poor fabrication, poor design practice, or accidental damage. Poor fabrication or design errors manifest themselves in the form of unexpected fatigue cracking where joints crack at a time

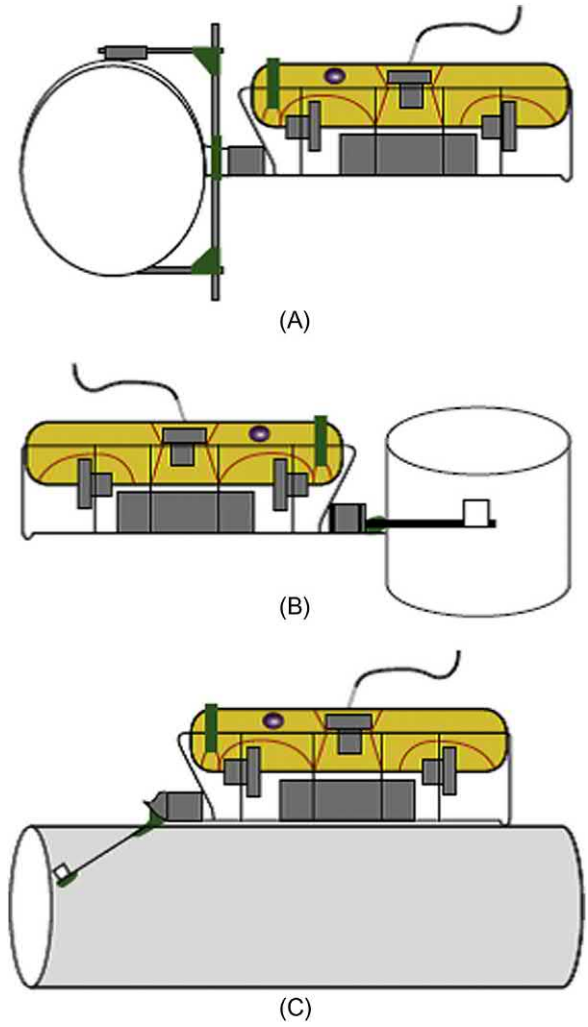

Figure 8.9 (A) Horizontal member standard survey mode for flooded member detection (FMD). (B) Vertical member survey mode for FMD. (C) Horizontal member survey mode for FMD.

well before their design lives. Because the occurrence of this damage is not expected, the inspection strategy should enable detection of unforeseen damage.

Reference to design fatigue lives is not a suitable means of justifying the use of FMD. The traditional S−N fatigue design process does not legislate for large defects or poor design, assuming welded joints to be "nominally perfect." Operationally, it should be assumed that a large defect or design error could potentially exist in every member and could lead to through-thickness failure of the

member and subsequent flooding, and could potentially develop to a size that could lead to final severance.

The most appropriate means of assessing an individual member for the effect of a crack of a size allowing flooding is through a fracture mechanics assessment. A fracture mechanics assessment will determine, for the size of defect, whether failure by fracture or collapse will occur under the prescribed conditions.

It should first be determined that the member can sustain through-thickness damage of a size sufficient to cause leakage without failing completely under the anticipated loading conditions. If this cannot be demonstrated, then FMD is not a suitable method for ensuring that the member's integrity is maintained. If it is determined that through-wall damage is possible but that complete severance is not, then it is necessary to demonstrate that FMD can detect the flooded condition before final severance or some other degree of damage is detected over a particular inspection interval. Given the extreme variability associated with all factors influencing fracture and collapse performance, a probabilistic fracture mechanics assessment should be undertaken to establish the probability of failure of an individual weld and, ultimately, the probability of failure of a complete member.

An alternative method for predicting failure frequencies is the use of historical data. There are many studies of a fracture mechanics approach for calculation of the probability of a member's leaking, and the probability of complete severance. The studies consider member failure rates obtained from a historical review. It should also be noted that other analytical approaches, many of them based on fracture mechanics, may be employed to determine the probability of failure of a member.

It is worth mentioning that the FMD technique is expensive but it is worthy in the case of deep water depth with many tubular joints and with a company that has a fleet of offshore platforms, so the cost will be not very high. However, in the case of a small operating company with only one or two platforms it is more beneficial to do closed visual inspection for every tubular joint using a MPI method. This technique will give direct confidence about the tubular joint condition. Fig. 8.10 presents the MPI for a tubular joint.

Final inspection reporting

The inspection contractor's final report is submitted upon completion of all inspection activities.

The format for the final report is:

- Title page;
- Report title/author/company/date, etc.;
- Contents;
- Summary;
- Contractor's name;
- Dates of survey;
- Inspections completed and inspections omitted and reasons for omission;

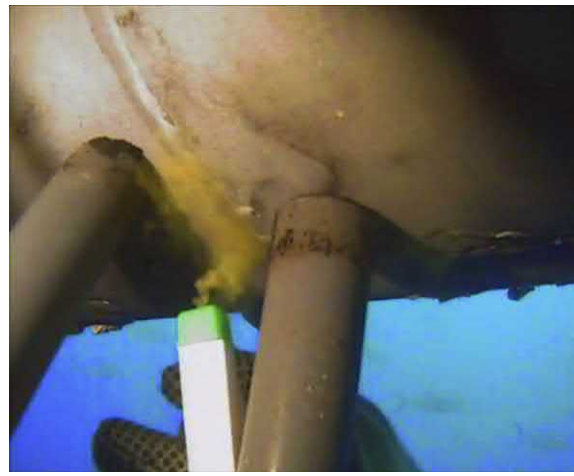

Figure 8.10 Close visual inspection (CVI) by the magnetic particle test (MPI) technique.

- Anomalies found;
- Conclusions;
- Outstanding actions;
- Inspection results by area;
- Written summary;
- Inspection datasheets;
- Drawings;
- Anomaly sheets (including NDT reports where available);
- Photographs/video stills;
- Operations analysis;
- Summary of time breakdown (chart);
- Summary of work breakdown (chart);
- Daily reports;
- Inspection team details;
- Copies of up-to-date CVs;
- Film/video logs;
- Summary of all film/video logs.

Table 8.35 shows an annual summary sheet for each fixed platform. The blank cells in the table indicate that it is not required unless specified by the owner (Table 8.35). Checked items are considered to be minimal requirements for fabrication.

8.5 Anode retrofit maintenance program

As discussed above, the inspection plan includes a survey of the condition of the anodes, which provide the CP to the jacket to prevent corrosion.

Table 8.35 Annual summary sheet for each fixed platform.

General information	**Construction year**	**Water depth**	**Type of platform**	**Conductors**	**Risers**	**Adding riser or conductor**	**Last ROV inspection**	**Other**
Summary								
Topside condition survey								
Subsea inspection								
Structure analysis								
Weight control								
Document control								
Prepared by: Checked by: Approved by:				Date:				

Table 8.36 Anode condition.

Grade of anode	Anode depletion (%)
Grade 4	100 (red cell)
Grade 3	> 50 (yellow cell)
Grade 2	< 50 (yellow cell)
Grade 1	< 10 (green cell)

Table 8.37 Cathodic protection (CP) readings.

CP readings (mV)	Protection condition
<850	Unprotected (red cell)
850–900	Marginal protection (yellow cell)
900–950	Satisfactory (yellow cell)
950–1000	Good (yellow cell)
>1000	Very good (green cell)

Figure 8.11 Depleted anode.

An anode survey during underwater inspection will focus on the condition of the anodes (i.e., whether they are depleted or not; Table 8.36) as well as on a reading of the potential of the CP system (Table 8.37), in order to determine whether the jacket is protected or not.

Fig. 8.11 presents a depleted anode.

The anode condition and the CP reading will have different criticality rankings. For example, if the anode is in a bad condition and the reading is very low, the

jacket is not protected against corrosion. On the other hand, if the CP reading is good but the anode is in bad condition, after a short time the CP reading will be low. The findings of these two factors can define a maintenance plan for anode retrofit of a fleet of platforms. Anode retrofit is expensive because it requires divers and a vessel, which cost a lot more than the anode material itself. Therefore the maintenance plan should be clear, and based on the priority of anode condition and budget.

Ultimately, the integrity engineer should have a table like that in Table 8.38, defining the estimated cost and the status of the anodes for the platforms.

8.6 Assessment process

See Fig. 8.12 for an illustration of the assessment process.

8.6.1 Collecting data

Collecting data is the first step in the assessment process. The required information includes the above-water structure's deck loads, which is obtained from a review of the weight report or comparison of the original facilities, locations, and weights with the current condition. Facilities on the deck may have been changed due to operational requirements. The most common change on the topside is adding a deck extension, new separators, or new compressors, but sometimes the original facilities have been removed.

In addition, jacket structure information will be available from the underwater inspection.

Soil data and metocean data should be available also. Therefore the required information includes:

- deck extensions;
- new conductors or risers;
- additional facilities with their weights and locations;
- soil data;
- metocean data.

8.6.2 Structure assessment

Structure assessment is discussed in detail in Chapter 7, Assessment of existing structures and repairs, but, in general, structure assessment uses different methods according to the structure's condition and the available data.

Simple methods

Simple methods for assessment are used instead of the more complex and time-consuming platform-specific analyses. Simple methods are typically used for a

Table 8.38 Maintenance plan for anode retrofit.

Structure name	WD (ft.)	RA rank	Last inspection	Inspection reading (mV)	Reading condition	Anode condition	Anode installation date	Budget cost	Color code
PL1	123	2	2000	691−708	Unprotected	Grade 4			Red
PL2	123	5	2000	684−690	Unprotected	Grade 4			Red
PL3	123	6	2001	686−699	Unprotected	Grade 3−Grade 4			Red
PL4	113	11	2000	811−907	Unprotected/marginal	Grade 3−Grade 4			Red
PL5	280	16	2002	871−906	Marginal	Grade 4			Red
PL6	127	20	2001	721−739	Unprotected	Grade 4			Red
PL7	155	23	2003	1008−1014	Very good	Grade 3			Green
PL8	130	26	2003	995−1012	Very good	Grade 2−Grade 4			Yellow
PL9	134	27	2001	1004−1020	Very good	Grade 2−Grade 3			Green
PL10	122	32	2001	850−938	Marginal−satisfactory	Grade 4			Yellow
PL11	130	39	2003	954−980	Good	Grade 4			Yellow
PL12	250	40	2003	941−962	Good−very good	Grade 3−Grade 4			Green
PL13	123	44	2001	716−719	Unprotected	Grade 4			Red
PL14	123	45	2001	714−725	Unprotected	Grade 4			Red
PL15	123	46	2001	707−719	Unprotected	Grade 3−Grade 4			Red
PL16	132	47	2003	919−924	Satisfactory	Grade 2−Grade 4			Yellow
PL17	150	104	2002	664−675	Unprotected	Grade 4			Red

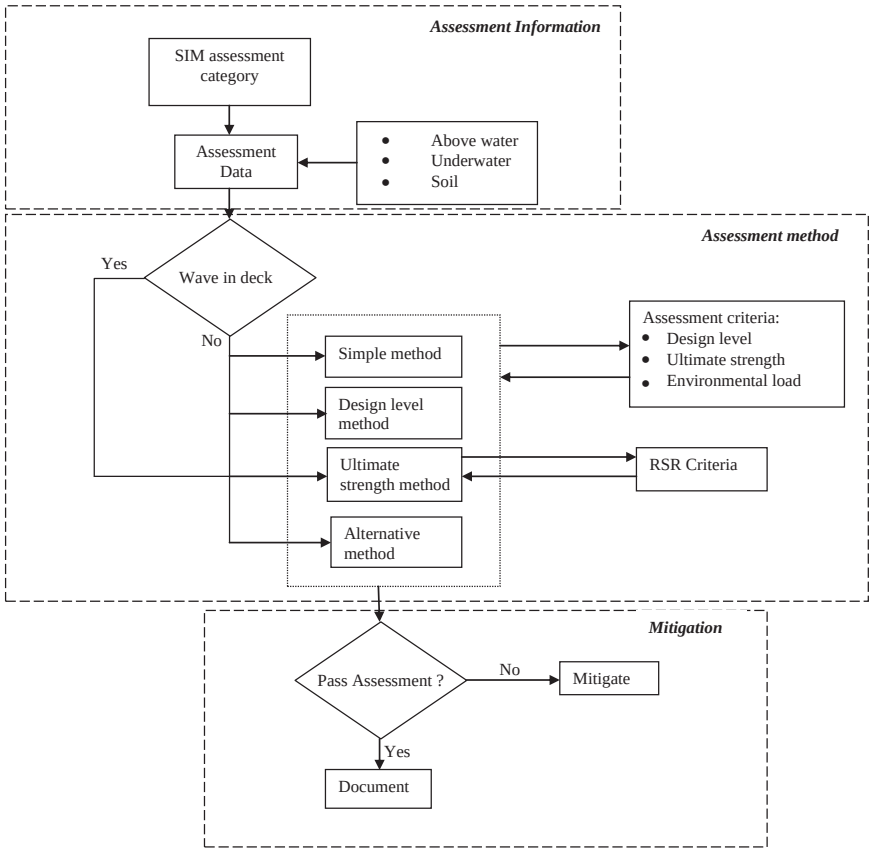

Figure 8.12 Assessment process.

platform in a certain class where prior studies are available or when previous analyses are available. Guidance for simple methods is provided here. If there is any concern that a simple method does not meet the requirements discussed here, then a more detailed assessment approach should be used.

There are three basic types of simple methods.

The *design-level method* (DLM) and *ultimate strength method* (USM) use simple procedures provided that such procedures have been validated. Several investigators have developed simplified procedures for the evaluation of the adequacy of existing platforms. Successful use of these procedures requires intimate knowledge of the assumptions upon which they were based.

The *results from previous analyses* for the platform are used provided that the analysis is representative of the platform's condition at the time of the assessment trigger.

Comparison with a similar platform uses assessment results available from a similar platform.

Design-level method

The DLM involves linear analysis using the standard API RP2A approach for new platform design by checking the platform on a component basis. The same factors of safety used for a new design are used for the DLM. The key difference for assessment is the use of special assessment criteria. The platform must be shown to perform linearly at loads equal to or greater than the assessment criteria.

The DLM is typically the first level of direct analysis of the platform. The DLM is a simpler and more conservative check than the USM, which is more complex and less conservative. It is generally more efficient to begin with the DLM because it is usually simpler to implement.

Ultimate strength method

The USM typically involves the use of nonlinear analysis to determine the maximum environmental loading that the platform can sustain without collapse. The USM is performed using special assessment criteria. A DLM with all the safety factors and sources of conservatism removed is also permitted, as this provides a conservative estimate of ultimate strength. In this case, ultimate strength acceptance criteria must be used. There may also be an existing computer model of the platform that was used for design of upgrades or other modifications that can be readily updated for platform assessment.

The USM is typically used when a platform does not pass the DLM, since it reduces conservatism. A platform that does not pass the DLM may pass the USM.

The USM is always required if the initiating trigger is wave-in-deck loading because this type of stepwise increase in environmental loading is difficult to capture properly with the DLM.

Nonlinear analysis is intended to demonstrate that a platform has adequate strength and stability to withstand the ultimate strength criteria, but accepted local damage or overstresses, but without collapse. At this level of analysis, stresses have exceeded elastic linear limits and during modeling of overstressed members, joints, and foundations, it is important to know its ultimate capacity and also its buckling behavior in this case.

The ultimate strength of a platform is often determined using a nonlinear pushover analysis, which applies an increasing lateral load to the platform until the platform collapses. The lateral pushover load should be representative of the metocean loads acting on the platform at the instance of collapse. The pushover load profile should consider all of the metocean issues for the assessment, including wind, wave, current, marine growth, etc.

There are several structural analysis programs that contain semiautomated approaches to performing a pushover analysis. These programs should always be used and the results should be interpreted by competent personnel.

The following loading guidelines should be considered for the USM.

Gravity loading includes the actual loads on the platform as well as future planned or temporary loads (for example, the drilling rig).

Environmental loading should consider the actual configuration of the structure at the time of the assessment, such as the actual number of conductors or risers, the drill rig, and metocean data. Future planned or temporary loads should also be considered.

If there is a wave-in-deck loading trigger, then the procedures provided should be followed. Alternative wave-in-deck loading methods can be used as long as they are justifiable. Even though there may not be a wave-in-deck loading trigger, wave loads may act on other deck areas, such as sump and spider decks, and the wave loading should be determined in the appropriate manner.

In most cases dynamic effects should be considered for platforms in water depths greater than 400 ft. Dynamic effects should also be considered for damaged platforms that may sustain higher motions in the damaged condition than in the intact condition. This can occur for any water depth platform.

The model of the global structure shall be three-dimensional, the main issue is to represent the damaged or corroded member and also the joint by the actual stiffness. The following guidelines should be considered for the USM.

Damage modeling

The ultimate strength of undamaged members, joints, and piles can be presented by using the formulas from API RP2A with all safety factors taken as equal to 1.0. Nonlinear interactions may also be utilized where justified. For joints, ultimate strength can be calculated using "formula or equation" rather than the lower-bound formulas for joints design. Alternatively, the ultimate strength of a damaged or repaired member or joint may be assessed using a finite element for this member or joint to define its capacity and stiffness.

Actual yield stress

The nominal yield stress is more than the mean yield stress by about 10%, therefore it is possible to use actual yield stress if it is applicable or an expected mean. If the mean yield strength is greater than the laboratory test or mill certificate strength it shall not be used.

The strain hardening phenomena increased strength may also be acknowledged if the section is sufficiently compact, but not rate effects beyond the normal mill tension tests.

Effective length factors

There are many studies and tests that have mentioned that the factor of effective length (K) is substantially lower for elements of a frame subjected to overload than those specified in API RP2A 3.3.1d. Lower values may be used if it can be demonstrated that they are both applicable and substantiated.

Soil strength

For the USM, as we are working at the limit state, it is important to use the best estimation for the soil properties and to avoid the conservative approach. This is particularly true for dynamic analyses, where it is not always clear what constitutes a conservative interpretation.

To simulate the pile response very accurately, it is mandatory to model the pile in sufficient detail. If you use the simplified method for a foundation model you should consider that the model will present the shear and moment at the pile head and the nonlinear behavior of pile and soil shall also be present. In addition, the simplified method can present the collapse of the pile as a failure mode in the case of a weak link in the structure system.

Alternative assessment methods

Alternative assessment methods involve the use of techniques other than a direct structural evaluation to assess an existing platform. There are two basic types of alternative methods.

Historical performance

The platform must have survived, with little or no damage, environmental loading that is as severe as, or more severe than, that required for the USM.

Explicit probabilities of survival

This is a platform assessment using explicit probabilities of survival of the platform for the appropriate assessment criteria.

Acceptance criteria

Two types of acceptance criteria are provided. The first is specific environmental loading criteria, such as wave height, current, etc., that the platform should be shown to withstand without collapse. The second is based upon the RSR, which is a measure of the platform loading relative to loads caused by 100-year environmental conditions used for new platform design.

Environmental lateral loading is computed using API RP2A criteria for a new design.

The required minimum RSR is based upon the platform's exposure category and the version of API RP2A used for design. Platforms designed prior to API RP2A should be considered pre-19th edition. The required minimum RSR for the Gulf of Mexico and other US locations is shown in Table 8.39.

8.7 Mitigation and risk reduction

Structures that do not meet the assessment requirements using any of the methods discussed in this section will need mitigation actions. Mitigation should be considered at all stages of assessment and may be used in lieu of more complex assessment.

Mitigation is defined as modifications or operational procedures that reduce loads, increase capacities, or reduce exposure.

Mitigation includes such measures as demanding, either during a forecast event or completely, a hydrocarbon inventory reduction that reduces the severity and

Table 8.39 Acceptable minimum reserve strength ratios (RSRs).

Offshore location	Assessment category	RSR	
		API RP2A 19th edition and earlier	API RP2A 20th edition and later
Gulf of Mexico	A-1	1.2[a]	1.6 (draft)
	A-2	0.8	1.2 (draft)
	A-3	0.6[b]	1.0 (draft)
Other US offshore areas	A-1	1.6	2.0

[a]This RSR is applicable only for continued use of the platform for its present purpose. Not applicable for change-of-use conditions.
[b]Not to be used for water depths greater than 400 ft.

consequence of platform failure. Mitigations like repairs should be designed to meet the requirements of this section, so that they do not reduce the overall strength of the platform.

Owners or operators who wish to continue to operate structures that have been assessed in accordance with API RP2A Section 6 and do not meet the fitness-for-purpose acceptance criteria appropriate for their consequence of failure category are required to reduce the risk of operating the platform. Either or both of the following can reduce the operating risk:

- Mitigate the consequences of structural failure;
- Reduce the probability of structural failure.

Competent assessment engineering should determine the need for and appropriate selection of risk-reduction options.

8.7.1 Consequence mitigation

If mitigation is an action taken to reduce the consequences of failure of the platform, and if the consequence of failure is related to life safety, then mitigation measures have to reduce the risk to life safety sufficiently to lower the consequence category. For example, implementing operational procedures to evacuate a manned platform such as in the Gulf of Mexico during an extreme event, this procedure reduces the consequence of failure during that event from high to medium. If the consequence of failure is related to environmental impact or some other consequence consideration, then other mitigation measures will be required and may include one or more of the following.

- Shutdown the platform either completely or during extreme events (if operationally feasible for the event);
- Operate subsurface safety valves that are manufactured and tested in accordance with applicable API specifications;

- Remove or reduce hydrocarbon storage or inventory volume;
- Remove or reroute major oil pipelines;
- Remove or reroute large-volume gas flow lines;
- Plug and abandon nonproducing wells;
- Operate pipeline shutting systems to reduce the potential for hydrocarbon release.

8.7.2 Reduction probability of platform failure

Reduction is defined as an action taken to reduce the likelihood of failure of the platform. In general, two methods exist to reduce the likelihood of failure of the platform during an extreme event, as follows:

- Load reduction, which reduces the load to be resisted by the structure during an extreme event, will reduce the likelihood that the platform will fail during the event.
- Strengthening, which increases the global, or system, strength of the structure, will reduce the likelihood that the platform will fail during the event. Competent assessment engineering should determine the need for, and appropriate selection of, either load reduction or strengthening options or both.

Load reduction

Gravity and hydrodynamic loading

During operation of the platform, the actual topside loading may be significantly lower than the loads assumed for the design of the platform. For example, operational procedures can be implemented to reduce and control topside loads by removal of unnecessary equipment or structures, by applying effective weight-control management procedures with defined weight limits, by use of lightweight drilling rigs or operations without a rig, or by using cantilever jack-up drilling operations.

The major effect of load reductions is to reduce leg and pile stresses and pile reactions. Reduced mass generally has a beneficial effect on platform dynamics, although not necessarily for earthquake response, but, in most instances, this effect will generally be small. On platforms with pile tips founded in sand layers, tensile pile capacities may need to be checked. One potential beneficial interaction associated with weight reduction is a possible associated reduction of wind area.

Nonessential components depend on the function and mode of operation, as in some cases there will be a main crude oil pump which is not currently used, but the cost of removing it and the maturity of the structure may make this a good solution for lightening the weight by remove these crude oil pumps, wells, and unused conductors. Since the conductors may contribute to the capacity of the platform foundation, it is often most efficient to remove only the upper section in the wave zone—this should be confirmed during the assessment process.

Removal, or relocation, of equipment on lower deck elevations will significantly reduce loads on the platform in the event of wave inundation of the deck.

In some instances, structural members in the jacket may be removed where it can be shown that the removal results in an increase in the overall system reliability. Examples of structural members that can be removed include launch truss

members and redundant structural members. In the old platform fleet, due to the usual changes to the mode of operation with time, a redundant riser can be found to reduce the load significantly, therefore it is necessary to remove these risers after performing a comprehensive study as this is not easy and may be expensive, on the other hand it can be the best solution to maintaining the structure integrity.

The other solution is to decrease the hydrodynamic load by using marine growth removal as described in Chapter 7, Assessment of existing structures and repairs.

In some cases the surfaces of legs and bracing are painted with a coating that prevents marine growth from accumulating on it.

Other solutions include marine growth removal on a regular basis by means of diver-held water-jetting equipment. There is a new trend to put a piece of plastic about the steel member which rotates due to the movement of waves and which provides a constant clean surface. Inspections of actual growth levels in comparison to design values may sometimes show design values to be incorrect, sometimes positively and sometimes negatively. Marine growth control also has the added benefit of virtual mass reduction on platforms subjected to dynamic excitation by waves or earthquakes.

Raising the deck

In the case that after studying the platform elevation with recent metocean data and it is found that the wave crest is expected to hit the deck, raising the deck out of the wave crest will significantly reduce the structure's global loading. In raising the deck, the effects of increased unbraced deck leg lengths must be evaluated. Due to the high cost and operational impact of raising the deck, the cost−benefit should be considered on a case-by-case basis.

An alternative to raising the deck is to remove or relocate equipment and nonessential structures from the lower deck elevations; this results in lower hydrodynamic forces and will reduce equipment damage from direct wave loads.

The other suitable solution is to install deck grating, instead of plating, which can be beneficial in reducing vertical loads on the underside of the deck by allowing encroaching water and trapped air to dissipate more easily.

In some locations, field subsidence has caused a general settling of the sea floor. Mitigation alternatives for this case often rely on reservoir pressure techniques, such as water or gas injection. This approach does not recover lost height, but can be used to slow future subsidence.

Strengthening

There are many strengthening and repair techniques available, as illustrated in Chapter 7, Assessment of existing structures and repairs. Platform assessment will determine whether platform strengthening or repair is required to meet the assessment acceptance criteria. If strengthening and repair are to be considered, the assessment model should be used to develop strengthening options. Strengthening

and repair of existing platforms requires specialist competence to provide reliable and economical solutions that can be efficiently and safely installed.

The need for accurate inspection data is emphasized; usually, a special inspection with a detailed dimensional survey is required to ensure that no problems are caused by a lack of data during installation.

Some strengthening and repair techniques are discussed in Chapter 7, Assessment of existing structures and repairs, as use of the external bracing which is the most traditional method of strengthening the fixed offshore structure. It is important to recognize that, in all cases, accurate fabrication and clear and efficient installation procedures are as important as the design of the strengthening scheme. Specific design guidance for the techniques discussed is not provided herein but is available in specialist references.

One of the cost-effective methods for increasing the global capacity of the structure is to grout the annulus between the jacket legs and piles. By filling the grout, the grout, pile, and legs will work as a composite section. The effect can be especially pronounced on jackets that have skirt piles, because the increased leg stiffness will tend to take the load from the skirt piles and move it to the jacket main piles. The grout, in effect, mobilizes the pile cross-section and forces the jacket leg and pile to act compositely against joint ovalization, thereby increasing joint capacity for both compression and tension loads. Grouting the annulus will increase the dynamic load so it should be considered also if there is an intention to have a decommissioning process.

The grout causes the pile and jacket leg to act as one unit, as a benefit of this the stresses will be distributed between the two members.

The grouting of the annulus between the jacket legs and piles has the added benefit of locally strengthening the jacket joints for bracing loads.

It is important to consider the impact on the platform in the case of decommissioning and the increase in dynamic mass before applying grout to the main piles.

Member flooding

Intentional flooding of structural members that are subjected to combined structural and hydrostatic loading can be used to increase the load-carrying capacity of the member. The impact of the increased gravity loads and dynamic mass should be considered in the assessment process, as well as possible decommissioning implications.

8.8 Occurrence of member failures with time

The detection of damage is almost entirely a function of when a weld or member is inspected; damage could exist for many years until discovered by the next programmed inspection. Fatigue lives should not be inferred from inspection results unless the inspection intervals are very short. The occurrence of accidental damage is easier to identify because an accidental event will be noted and in most cases investigated.

A review of the data in the context of when the damage was discovered is informative and demonstrates the trends in terms of failure rates.

A study of platforms installed between 1966 and 1977 in the southern sector of the North Sea suggests that the platforms may have been operated for 40 years before damage occurred. However, a major inspection campaign undertaken in the 1980s discovered damage and it is unknown when the members actually cracked.

The structures which were installed from 1971 to 1980 in deep water in the central and northern sectors of the North Sea continue to sustain through-thickness damage. A proposed explanation for this is that while fabrication defects resulted in cracking in the first few years of life that was discovered, assumptions and errors made during design yielded structural defects and stresses that are resulting in ongoing fatigue damage. Structures from this period were designed without the detailed knowledge available at present, particularly analysis software and fatigue design factors.

Structures installed from 1981 to 1985 suggest that an unforeseen problem, such as a fabrication defect, will be exposed at an early stage of the structure's operational life, before it settles into a period when little or no damage occurs unexpectedly. However, with improved analytical techniques and detailing, long-term fatigue performance has improved dramatically and has resulted in no damage being noted after initial fabrication-defect problems have been uncovered.

No gross damage has been noted in structures installed between 1986 and 1995; the explanation for this appears to be good fabrication and design practices and the use of NDE. However, newer structures have seen less service life than older structures.

References

Bea, R.G., Puskar, F.J., Smith, C., Spencer, J.S., 1988. Development of AIM (assessment, inspection, maintenance) programs for fixed and mobile platforms. Offshore Technology Conference, OTC Paper 5703, Houston, Tx, USA.

De Franco, S., O'Connor, P., Tallin, A., Roy, R., Puskar, F, 1999, Development of a Risk Based Underwater Inspection (RBUI) Process for Prioritizing Inspections of Large Numbers of Platforms, Offshore Technology Conference, OTC10846, Houston, Tx, USA.

El-Reedy, M.A., 2003. Life-cycle cost design of deteriorating offshore structures. In: Offshore Mediteranian Conference (OMC2003), Ravenna, Italy.

Gebara, J.M., Westlake, H., DeFranco, S., O'Connor, P., 1998. Influence of framing configuration on the robustness of offshore structures. In: Offshore Technology Conference, OTC Paper 8736, Houston TX, USA.

Puskar, F.J., Aggarwal, R.K., Cornell, C.A., Moses, F., Petrauskas, C., 1994. A comparison of analytically predicted platform damage to actual damage during Hurricane Andrew. In: Offshore Technology Conference, OTC Paper 7473, Houston, TX, USA.

Turan, G., 1990. Engineering Economy for Engineering Managers. John Wiley and Sons.

Further reading

API, 1996. Base Resource Document—Risk-Based Inspection—Preliminary Draft, API 581. American Petroleum Institute, Washington DC.

API RP2A-SIM, 2006. Structural Integrity Management of Fixed Offshore Structures. American Petroleum Institute, Washington DC.

API RP2A-WSD, 2000. Recommended Practice for Planning, Designing, and Constructing Fixed Offshore Platforms, Twentieth Edition, Supplement 1. American Petroleum Institute, Washington DC.

Det Norske Veritas (USA) Inc. (DNV), 2002. Risk Based Underwater Inspection—Phase II, for Amoco, Houston. Document Number 221-8823, 8 February 2002.

Gonen, T., 1990. Engineering Economy for Engineering Managers. John Wiley and Sons, Hoboken, NJ.

PMB Engineering, Inc., 1988. AIM—Assessment, Inspection and Maintenance. Phase III Final Report. San Francisco, CA.

Stahl, B., 1986. Reliability engineering and risk analysis. In: MCClelland, B., Reifel, M.D. (Eds.), Planning and Designing of Fixed Offshore Platforms. Van Nostrand Reinhold, New York.

Stahl, B., De Franco, S. Internal Presentation Material Developed by Amoco. Amoco WE&C, Houston, TX.

Tallin, A.G., Puskar, F.J, Matos, S., 1998. Risk-Based Underwater Inspection. Report for Amoco WE&C, DNV Materials Engineering Consulting Report 232-8507.

Subsea pipeline design and installation

9

9.1 Introduction

Normally, the hydrocarbons from wells (gas, oil, water, and sand) are separated into two streams at the platform (oil and gas), and then delivered to the onshore facilities.

Subsea pipelines can be placed in two categories.

1. *Flowline*
   - **a.** From the wellhead or manifold to the platform;
   - **b.** Carries three phases of oil, gas, and water;
   - **c.** Short lengths of up to 16 km;
   - **d.** Small diameter, ranging from 6 to 12 in
2. *Trunk pipeline*
   - **a.** From the platform to onshore;
   - **b.** Carries one phase of oil or gas;
   - **c.** Long length, up to hundreds of kilometers;
   - **d.** Large diameters used, up to 48 in;
   - **e.** These rigid lines are laid by S-laying.

   Occasionally, the reservoir product and flow rate are such that unseparated gas is sent onshore for processing from unmanned platform. This decision is taken when the whole life capital project or operating costs (capex or opex) have been validated in a feasibility study.

   To start the discussion on pipelines it is very important to identify the main terms used when referring to pipelines. These terms include jumpers, spool pieces, and bundles, which are defined here.

   1. *Jumpers*
   - **a.** Connects the wellhead to the manifold;
   - **b.** Short length of around 100 m;
   - **c.** Flexible or rigid spools.

   2. *Spool pieces*
   - **a.** Rigid or flexible to accommodate thermal changes;
   - **b.** Connects the end of the pipeline to risers.

   3. *Bundles*
   - **a.** Many small-diameter flowlines in carrier pipes, with these pipes between 36 and 48 in;
   - **b.** Used to gather flow from separate wells;
   - **c.** Towed out to the field with the annulus flooded.

Jumpers tend to refer to short lengths of flexible lines and rigid spools may be used to connect the wellhead to the in-field line or manifold.

Offshore Structures. DOI: https://doi.org/10.1016/B978-0-12-816191-3.00009-2

9.2 Pipeline project stages

The first stage after finalizing the feasibility study by the owner is to define the pipeline route. To start with the conceptual design should define the most suitable routes. The conceptual design stage starts by collecting the available data, such as the admiralty chart, block license, and existing nearby developments.

In some countries, such as the United Kingdom, there is a website containing all the existing facilities and geophysical data collected from different companies (www.ukoilandgasdata.com). Therefore local authorities should be queried for any similar data. By collecting all these data, the most suitable route can be calculated. It is important to highlight that in pipeline projects, for 1 day of offshore work, it is required to spend 8 weeks in engineering work after defining the most cost-effective route from the conceptual design.

The most important stage is the survey, of which there are two types: the geophysical survey which defines any obstacles in the seabed and the geotechnical survey which obtains the soil properties enable the most suitable construction method to be chosen. A bathymetry survey is helpful to define the depth of water and seabed shape profile, which are determined by a multibeam system with an echo sound technique which is towed close to the seabed to provide 3D seabed images.

When the distance between the seabed and the sensor is greater, the survey corridor will be wider and the image will be lower resolution. Therefore to obtain higher resolution images the sensor is fixed on an remotely operating vehicle (ROV) which is flown along the route and above the seabed as closely as possible, in most cases only a few meters.

For a bathymetric survey there are two options:

1. Medium resolution
   a. Single beam echo sounder;
   b. Hull mounted;
   c. 750 m wide swathe for best resolution will be 8 m footprint size.
2. High resolution
   a. Multibeam;
   b. Towed close to the seabed;
   c. Much narrower swathe.

A side scan sonar sends sound pulses and receives the echo. This provides details of the gauge contour, wellheads, rock outcrops, wrecks, and similar obstacles.

In addition, manometers can be used to detect metal objects buried beneath the seabed. To understand the soil profile chirpers, pingers, and boomers can be used, these will penetrate the seabed to obtain a reflection from it.

A geotechnical study is carried out to determine the soil types underneath the pipeline along its route. It is usually use a cone penetration test (CPT). This device is described in detail in Chapter 6, Corrosion protection, for geotechnical investigations, but for pipelines they have special requirement which are outlined in Table 9.1, with the sample interval in each case also listed. Vibrocores are used to take a core from the soil for laboratory analysis, the core is taken every 5 or 10 m

Table 9.1 Illustrations of sample intervals.

Route characteristics	Cone penetration test (CPT) interval (km)
Untrenched sections	1−5 km
Offshore trenched sections	0.5−1 km
Shore approach trenched sections	0.3−0.5 km
Soil transition zone	0.3−0.5 km
Pock marks, iceberg scars, etc.	3 per property
Pipeline crossings	2 per crossing

depth and 100 mm diameter. The main data are to define the soil type and strength, with different parameters such as density and porosity.

9.2.1 Pipeline design management

The professional design of the pipeline is essential to have a successful project and the following deliverables are considered as a minimum to be delivered from the engineering firm.

A design basis for a pipeline system should be developed. The document could be a static design basis, prepared by the owner, or it could be a live document, continuously updated whenever design information is received. The choice depends on the project characteristics.

The design document should contain at least the following:

- a full description of the pipeline system and interfaces, pressure-regulating system and other safety issues, functional requirements, system life time, and similar key data;
- design codes and methods for strength and in-place analysis;
- all operational data such as pressures, temperatures, and fluid composition;
- geotechnical investigation data;
- metocean data;
- topographical and bathymetrical conditions along the route;
- The software that will be used during the design.

The deliverables during the design phase, such as design reports, drawings, and specifications shall be review by the owner by carrying out an independent verification, the technical authorities, and third parties, possibly including a certifying agency.

The design should cover all relevant structural and environmental evaluations including, but not limited to, the following checklist:

- pipeline route;
- materials selection;
- pipe wall thickness;
- strength analysis under many loading conditions during installation, hydrotesting, and operation, including installation loads, trawl interaction, forced displacement in trench transitions or over crossings, and others;
- temperature and pressure profiles;

- pipeline expansion force behavior, including buckling;
- risk assessment, quantitative or for selected risks;
- corrosion protection design system and corrosion monitoring;
- pipeline on-bottom stability;
- free span calculation.

The design drawings should be prepared to present the fabrication and installation of the pipeline system, which shall include the following which should be received from the design office:

- Alignment sheet drawings present the pipeline route, including the seabed properties and water depths, existing or planned restrictions and obstructions, such as platforms, shipping lanes, lighthouses, cables, and pipelines; typical pipeline detailed drawings, including coating, field joints, anode fabrication, and fastening;
- Out-of-straightness and span rectification requirements;
- Crossing designs detailed drawings ;
- Tie-in arrangements, including riser detailed drawings;
- Shore approach drawings.

The geotechnical investigation methods and types of soil, metocean data definition and characteristics, and the corrosion protection design use the same approach and methodology as discussed in earlier chapters.

9.3 Pipeline design codes

This book focuses on the offshore pipeline, therefore it is important to identify the codes and standard that control the design, and these codes are as follows:

- ASME B31 Codes started with the first revision in 1926 for pressure piping and later American Society of Mechanical Engineers (ASME) issued B31.8 for gas transmission and distribution, and also published B31.4, which is specific for oil transportation pipelines, in the 1950s. It is important to highlight that, the main design principles for these codes are to assess the pipeline the same as the pressure vessel by controlling the hoop stress.
- ISO Pipeline Code, which is ISO DIS 13623, 1996, allows the use of structural reliability techniques by using the limit state-based design procedures, such as those proposed by SUPERB (Jiao et al., 1996). It is worth mentioning that International Standards Organization (ISO) codes are not traditionally used in practical cases, but they present the basis for the application of the new design approach.
- Det Norske Veritas (DnV) Pipeline Rules are one of the main references used in design, and the first publication was issued in 1976 to cover the design, construction, and inspection of offshore pipelines. In 1996 DnV provided a modification using a new approach to design by the SUPERB project, which considered the failure modes and limit state methodology. Through DnV the pipeline is classified into safety classes according to location, fluid (oil, gas, water, etc.), and likelihood of failure and the impact.
- ABS (2000) is based on the working stress design (WSD) to design offshore pipelines and risers, providing a more conservative approach to wall thickness design, and this standard allows use of the limit state design by considering the risk with a reliability-based method.

- API RP IIII (1998) is a code focused on design of the pipeline and risers that carry a hydrocarbon. In general it focuses on two failure modes—bursting and rupture failure—and uses the limit state methodology in design to define the wall thickness by using the material grade and pipe diameter.

9.3.1 Pipeline route design guidelines

The first step for any pipeline project is to define the route, this route is defined by carrying out a subsea survey and from the bathymetric survey, which will highlight any existing pipelines seabed obstructions, or construction limitations. The seabed obstructions in general include existing platforms, wells, wrecks, pipelines, or cables. Fixed items such as platforms, wellheads, wrecks, and anchors should be passed with a minimum distance clearance of 500 m. As a rule of thumb the number of pipelines and cables crossed should be minimized, and pipelines should be corridored where possible, with anchoring areas and dropped object zones being avoided.

In the case of a corridor with other lines, the typical distance separation is 50−100 m (160−330 ft.). If pipelines are constructed together a separation distance of 20−30 m (65−100 ft.) is required.

Existing pipelines are preferably crossed perpendicularly, with a minimum angle of 30 degrees, as shown in Fig. 9.1. Laying of the pipeline by barge ensures a minimum radius of curves. Typically this is a 1 km radius for a small diameter of 6 in, up to 2 km for a 40 in pipeline. The reason for this is that seabed friction is relied on in order to form the bend.

BS 8010 specifies a crossing height separation of 0.3 m (1 ft.), while in the United States this distance is 0.45 m (1.5 ft.), with this allowance being due to expected settlement. The elevated length depends on the pipe diameter, and the most common supports are mattresses, grout bags, concrete or steel supports. The

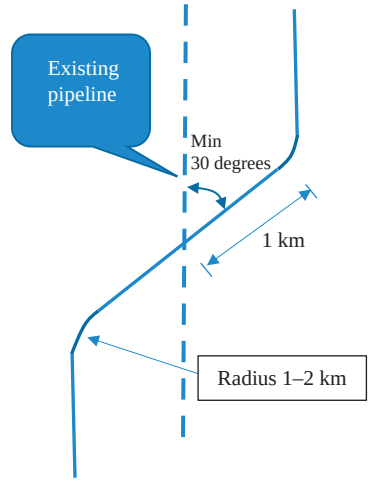

Figure 9.1 Pipelines crossing.

supports should prevent vertex-induced vibration (VIV) or excessive lateral movement of the pipeline. The two ends of the crossing are fixed by a rock dump to fix the main length.

In the case of cables crossing, there are usually a lot of unused cables, but in the case of a live cable, it is important to communicate with the owner to discuss how they wish to carry out the crossing. In the case of soft soil, the simplest method is to lay the pipeline over the cable.

If protective mattresses are required then a long length of cable may need to be protected to allow for uncertainties in the control of laying. Mattresses need to provide sufficient distribution of pipeline weight to prevent damage to the cable.

For bending of the pipeline, the recommended radius depends on the pipeline diameter. The pipeline configuration in Fig. 9.2 presents the required minimum length before and after the pipeline bending radius. The relation between the pipe diameter and the bending radius is shown in Table 9.2.

9.4 Design deliverables

The main drawing of the pipeline project is the alignment sheets. This drawing sheet presents a length of 2−3 km of the pipeline with key features. There will be

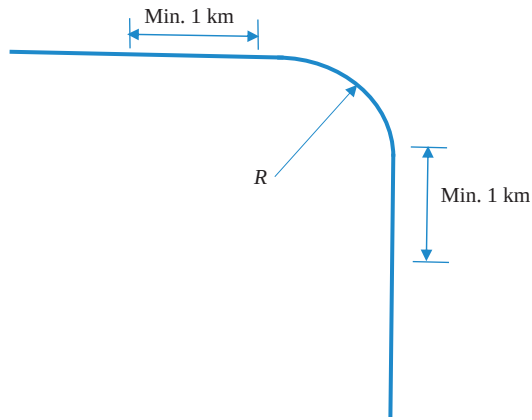

Figure 9.2 Plan for pipeline bend radius.

Table 9.2 Relation between pipeline diameter and bend radius.

Pipeline diameter (in)	Bend radius, km (miles)
6	1 (0.6)
12	1.5 (0.9)
24	2.0 (1.2)
36	2.5 (1.5)

an overlap between the sheets to avoid any conflict. These sheets contain information about seabed survey data, pipeline features, and installation requirements. The following data shall be illustrated on the alignment sheet:

- bend radius;
- lay tolerance;
- pipe OD and wall thickness;
- crossing coating;
- field joint coating;
- backfill and protection details;
- soil description;
- corrosion coating.

If the drawing will be used by installation contractors, it includes the required lay tension, location of crossings, tolerances on pipelays, backfills, or trenches. It also includes obstruction such as platforms, pipelines, and cables.

9.4.1 Pipeline design

The pipeline diameter will be defined by the process engineer depending on the fluid pressure, volume/h, and the pressure at the two ends, and whether the fluid is single-phase flow, two-phase flow, or multiple-phase flow.

To start the stress analysis, the first step is to define the loads that affect the pipeline, which are as follows:

1. internal pressure;
2. external hydrostatic pressure;
3. temperature;
4. bending.

It is worth mentioning that, based on the loads, there are three main modes of failure:

1. burst;
2. collapse;
3. buckle.

Pipeline bursts

A burst is caused by excessive internal pressure. The pressure definition is illustrated in Fig. 9.3. The maximum pressure of the field pipeline is equal to the shut in pressure of the highest pressure well. The maximum allowable operating pressure (MAOP) is different to the design pressure due to the tolerance on the pressure control mechanism. It is possible for the design pressure to be equal to the MAOP in the case that the pressure is driven by a shut in the wellhead pressure, which can be seen from the reservoir properties. Incidental pressure refers to a short-term transient condition which may exist primarily due to a surge condition in the pipeline, and the pipeline is designed to withstand this pressure.

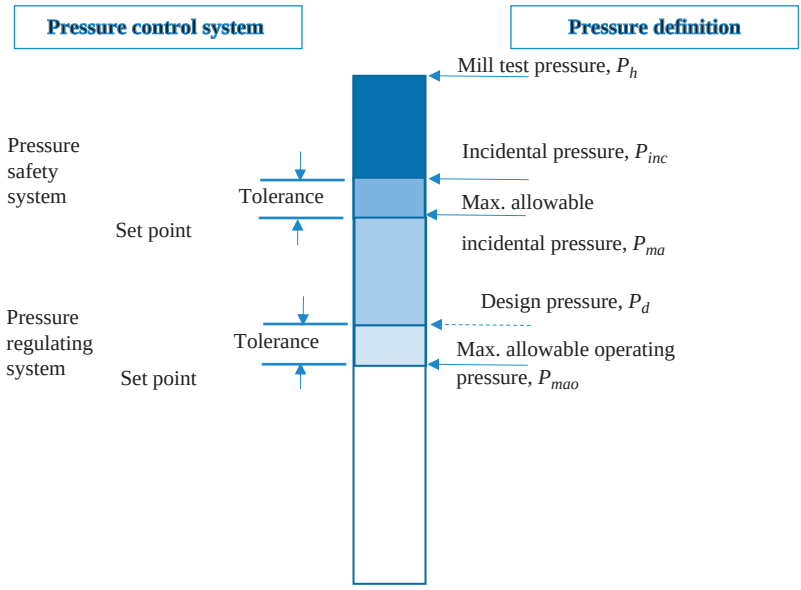

Figure 9.3 Relation between the pressure definition and control system.

The hydrotest requirements normally cover the following:

- A mill pressure test on every joint during fabrication to be 0.96 SMYS (specified minimum yield stress);
- A strength test of the final pipe system during commissioning to at least 1.25 MAOP;
- During the hydrotest the minimum shall be
  - 1.5 MAOP
  - 0.9 SMYS;
- A leak test is normally undertaken at lower pressure;
- PD 81010 requires a strength test for 24 hours and a leak test.

An allowable stress design (ASD) is used to design the pipeline and there are many codes with formulas and parameters. Table 9.3 presents the difference between each code in calculating the hoop stresses.

The equation of the hoop stress is as follows:

$$\sigma_{hp} = (P_i - P_e) \cdot D/2t$$

where P_i and P_e are the internal and external pressures, respectively, D is the internal pipe diameter, and t is the pipe wall thickness.

The maximum hoop stress shall not exceed the following:

$$\sigma_{hp} = F_h \cdot \sigma_y$$

where σ_y is the SMYS at the maximum design temperature; $F_h = 0.77$ for the general route; $F_h = 0.67$ for risers, pig traps, and landfalls; and F_h can be increased to 0.83 for less critical fluids.

Table 9.3 Comparison between different codes in formulas and allowable hoop stress.

Design code	Hoop stress formula	Maximum allowable hoop stress (specified minimum yield stress, SMYS)
USA ASME B31.4 and BS31.8	$= P \cdot \mathrm{OD}/(2 \cdot t_{\min})$	0.72
UK PD8010	$= P \cdot (\mathrm{OD} - t_{\min})/(2 \cdot t_{\min})$	0.72
Netherlands NEN 3650	$= P \cdot (\mathrm{OD} - t_{\min})/(2 \cdot t_{\min})$	0.72
Canada CSA-Z183 and Z184	$= P \cdot \mathrm{OD} - /(2 \cdot t_{\mathrm{nom}})$	0.8
ISO 13623	$= P \cdot (\mathrm{OD} - t_{\min})/(2 \cdot t_{\min})$	0.77

The fluid pressure must fulfill the following equation as per DnV 2000:

$P_{li} - P_e \leq P_b(t)/\gamma_{sc}\gamma_m$

where P_{li} is the local incidental pressure, P_e is the external pressure, P_b is the pressure contaminated resistance based on the minimum wall thickness t, γ_{sc} is the safety class resistance factor, and γ_m is the material factor.

The safety class is identified as described below.

Location class 1

This class characteristics include that there is not frequent human activity in the location. For most offshore pipelines there is little risk of human injury in the case of failure, and the majority of the pipeline route is therefore normally assigned to location class 1.

Location class 2

This class is for locations which are near to manned platforms or areas with frequent human activity (e.g., landfalls). The distance of a location class 2 from these areas is typically a minimum of 500 m.

The extent of the location class 2 would normally be reckoned from the center, or the closest accommodation module, of the platform, but DNV has clarified that 500 m should be taken from the riser touch-down point on the seabed.

As per ISO 13623 there is another definition which uses five location classes, covering both onshore and offshore pipelines. The offshore pipeline design based on ISO 13623 is covered by location classes 1 and 2.

The adoption of DNV location class 1 offshore is normal practice. Offshore human activities and numbers shall be assessed, estimating the number of ships passing a given area can be considered an analysis of human activity. The outcome "frequent human activity" might result, but in reality even heavy ship traffic normally does not translate into a permanent population density warranting use of location class 2. There are, of course, special considerations, such as harbor areas, offshore mining, or intense ferry traffic, that could alter this conclusion.

The designation of safety classes also involves a classification of the medium being transported. The fluid category with regard to toxicity and environmental

impact upon release also needs to be addressed. For instance, one fluid category covers nontoxic, single-phase gas, which is mainly methane, and is hence nontoxic, but flammable. For operation class 1 is considered medium and class 2 is high for installation.

Therefore $\gamma_{sc} = 1.046$ for safety class low, $\gamma_{sc} = 1.138$ for safety class medium, and $\gamma_{Sc} = 1.308$ for safety class high.

For materials, a partial safety factor γ_{m} is equal to 1.15 for service limit state, ultimate limit state, and accidental limit state, and equal to 1.0 for fatigue limit states

The local incidental pressure is given by

$$P_{li} = P_d \gamma_{inc} + \rho_c \cdot g \cdot H$$

where p_d is the design pressure at the reference point; γ_{inc} is the incidental pressure to design pressure ratio; ρ_c is the density of the content; g is the acceleration due to gravity; and H is the height difference between the chosen point and the reference point.

The factor γ_{inc} shall take a minimum value of 1.05. In DNV OS-F101 Section 3 B305, this is allowable provided the pressure safety system is specified to ensure that the local incidental pressure cannot be exceeded.

$$P_b(t) = Min\left(P_{b,s}(t), P_{b,u}(t)\right)$$

Yield limit state

$$P_{b,s}(t) = 1.15\ \left(2t/(D-t)\right) \cdot f_y$$

Bursting limit state

$$P_{b,u}(t) = \left(2t/(D-t)\right) \cdot f_u$$

where f_y is the design yield stress; f_u is the design tensile strength; and D is the nominal outer diameter.

The design yield stress and the design tensile strength can be found as:

$$f_y = (SMYS - f_{y,temp})\alpha_U$$
$$f_u = (SMTS - f_{u,temp})\alpha_U \cdot \alpha_A$$

where $f_{y,temp}$ is the temperature derating value, and is 0 if the design temperature is below 50°C; $f_{u,temp}$ is the temperature derating value, and is 0 if the design temperature is below 50°C; α_U is the material strength factor, and is 0.96 for normal and 1.00 for supplementary requirements, suffix U; α_A is the anisotropy factor, and is 1.00 for the circumferential direction; *SMYS* is the specified minimum yield stress; and *SMTS* is the specified minimum tensile strength.

The collapse

External pressure to the pipeline will cause the collapse of the pipeline, and so the limit state equation for collapse failure is covered by the following equation:

$$P_e \leq P_c/(1\cdot 1\gamma_{sc}\gamma_m)$$

Characteristic resistance for external pressure P_c given by:

$$(P_c - P_{el})\cdot\left(P_c^2 - P_p^2\right) = P_c\cdot P_{el}\cdot P_p f_0\left(D/t'\right)$$

$$P_{el} = 2E\left(t'/D\right)^3/\left(1-\upsilon^2\right)$$

where $t' = t - t_{corr}$; E is the Young's modulus of the pipe materials (N/m^2); t is the pipeline wall thickness, m; D is the pipeline diameter, m; υ is the Poisson's ratio of pipe materials; and P_{el} is the elastic collapse pressure for a perfect tube, MPa.

$$P_p = 2f_y\alpha_f(t'/D)$$

where P_p is the plastic collapse pressure for a perfect tube. α_f is the fabrication factor, which depends on the pipeline manufacturing process and allows for the effects of cold working, giving a variation between tensile and compressive strength and the values of these factors depend on the pipe manufacturing process:

Seamless = 1.0;
UO manufacturing process = 0.93;
UOE manufacturing process = 0.85.

It is worth mentioning that for most large-diameter pipes greater than 16 in for offshore pipeline in most cases they are manufactured through a UOE process using cold formed plates.

The plate is crimped along its edges, formed into a U-shape, and then pressed into an O-shape between two semicircular dies. The expression UO comes from the manufacturing process. To obtain a highly precise circular shape the pipe is welded closed and then circumferentially expanded.

As per Herynk (2007) collapse tests results revealed that, these processing steps, especially the final expansion, shall produce a reduction in its collapse pressure upwards of 30%.

The ovality is calculated from the following equation

$$f_o = (D_{max} - D_{min})/D$$

Buckle propagation

The external pressure required to cause a buckle to propagate is less than that to cause a pipe to collapse.

If the pipe is designed to resist buckle propagation any local buckle accidentally introduced will not propagate. This is a common result for pipelines installed in shallow water, where wall thickness is govern by internal pressure containment. As water depths increase, buckle propagation design begins to dominate.

The buckle propagation also occurs during installation when the pipe is empty.

The buckle propagation equation is:

$$P_b = 35 f_y \alpha_f / \left(\gamma_m \cdot \gamma_{sc}\right) \cdot \left(t'/D\right)^{2.5}$$

We can do the following to reduce the buckle effect by strengthening the pipe with buckle arrestors such as:

- internal ring;
- welded external ring;
- welded external sleeve;
- heavy walled pipe joint;
- grouted external ring.

Buckling

Buckling occurs due to excessive bending at the sag bend during laying. It can occur due to bending moment and axial force which can be due to a thermal effect as occurs also due to excessive bending at touchdown during laying.

Local buckling depends on a combination of longitudinal load, pipe bending moments, and hoop stresses. As the pipe bends, it places the extreme fibers in tension and compression. To partially release these stresses, the pipe deflects, ovalizing to flatten the area under stress. The ovalization reduces the bending stiffness of the pipe. Eventually, a runaway point is reached and the pipe buckles, forming "pinch points" that may tear or fracture, with the potential loss of the contents. Any axial compression in the pipe adds to the tendency to form a buckle.

The combined stresses are based on the ASD in the following formula for von Mises criterion

$$\sigma_{eq} = \sqrt{(\sigma_h^2 + \sigma_l^2 - \sigma_h \sigma_l + 3\tau^2)}$$

where σ_{eq} is the equivalent stress; σ_h is hoop stress; σ_l is longitudinal stress; and τ is the shear or torsion stress.

There are different acceptance criteria for von Mises as per the code that is being used as presented in Table 9.4.

The maximum allowable bending moment for a spool piece is when subject to hoop stress due to hydrostatic pressure and there is no axial or torque therefore the simplified von Mises equation will be as follows:

$$\sigma_{eq} = \sqrt{\sigma_b^2 + 0.75\sigma_h^2}$$

Table 9.4 Maximum allowable combines stress for von Mises for different codes.

Design code	Maximum allowable combined stress	
	Construction phase	During operation (specified minimum yield stress, SMYS)
ASME B31.4&B31.8	–	0.9
PD8010	SMYS	0.96
DNV96	0.96 SMYS	0.96
Netherlands NEN 3650	0.8 to 1.0 SMYS	0.8−1.0
Canada CAS-Z183 and Z184	0.9 SMYS	0.9
ISO 13623	SMYS	0.9

Table 9.5 Pipeline coefficient of friction as per BS (2015).

Soil type	Lateral		Axial	
	Min.	Max.	Min.	Max.
Sand	0.5	0.9	0.55	1.2
Clay	0.3	0.75	0.3	1.0

Most oil pipelines are under high temperature, therefore there will be an axial compressive force on the pipeline which is a function of the seabed irregularities and the expansion analysis which depend on the pipeline route.

To do the buckling analysis from a practical point of view the following load cases are considered:

1. *Case 1*: the pipeline under operating conditions is uncorroded and under the maximum effective compressive axial force.
2. *Case 2*: the pipeline under operating conditions is corroded to its full corrosion allowance value and under the maximum effective compressive axial force.

The coefficient of friction between the pipeline and the soil is as illustrated in Table 9.5.

Hobbs' (1984) analytical method provides the minimum load for induced buckling for the pipeline as it defines four modes of buckling mode.

$$P = k_1\left(EI/L^2\right)$$

$$P_o = P + K_3\ \mu wl[(1 - k_2 AE\ \mu wL^3/(EI)^2)^{0.5} - 1.0]$$

The maximum amplitude of the buckle relative to the original axis is

$$Y = k_4\ \mu wL^4/EI$$

While the maximum bending moment is

$$M_b = k_5\ \mu w L^2$$

where I is the moment of inertia; E is the elastic modulus; W is the pipeline weight; μ is the coefficient of friction as in Table 9.5; and k_1, k_2, k_3, k_4, and k_5 the Hobbs coefficient as in Table 9.6.

On-bottom stability

The main element of design for an offshore pipeline is to maintain the pipeline stability on the seabed under wave and current loads. Moving the pipeline will cause fatigue and then failure with time, and can cause cracking of the concrete coating.

In 1976 the basis of the design of submarine pipelines was delivered through DNV rules for submarine pipeline systems. The loads that affect the pipeline stability are as shown in Fig. 9.4.

A number of research projects have been undertaken in order to understand the hydrodynamic forces on pipelines with the purpose of developing rational

Table 9.6 Constants for lateral buckling modes.

Mode (1)	**Constants**				
	k_1	k_2	k_3	k_4	k_5
1	80.76	6.391×10^{-3}	0.5	2.407×10^{-3}	0.06938
2	$4pi^2$	1.743×10^{-4}	1.0	5.532×10^{-3}	0.1088
3	34.06	1.668×10^{-4}	1.294	1.032×10^{-2}	0.1434
4	28.20	2.144×10^{-4}	1.608	1.047×10^{-2}	0.1483
Infinity	$4pi^2$	4.7050×10^{-5}		4.1195×10^{-3}	0.05066

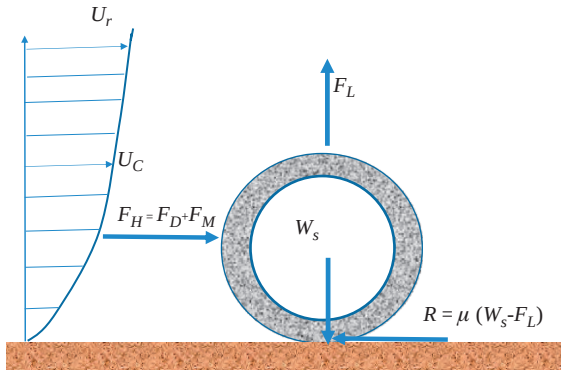

Figure 9.4 Bottom stability.

methodologies for on-bottom stability design. The two most extensive are PIPESTAB (Wolfram et al., 1987) and the On-bottom Stability Project by Pipeline Research Council International (PRCI) (Ayers et al., 1989).

As discussed in earlier chapters there are drag force, F_D, inertia force, F_M, lifting force, F_L, submerged weight, W_S, and the friction resistance force, R, with the coefficient of variation, μ.

Morrison's equation is applied here for drag, inertia, and lifting forces as follows:

Drag force:

$$F_D = 0.5\rho C_D D V^2$$

Inertia force:

$$F_M = \pi\left(D^2/4\right)\rho C_M a$$

Lift force:

$$F_L = 0.5\rho C_L D V^2$$

where the lift force present at the seabed provides a symmetry between the flow over the top of the pipe and the flow underneath. This causes no flow or possibly slower flow underneath the pipeline and higher velocities over the top with lower pressures, which produces the lift force.

In practice, the coefficients of the hydrodynamic forces are $C_D = 0.7$, $C_M = 3.29$, and $C_L = 0.9$.

The pipeline is considered stable vertically if the submerged weight is greater than the maximum lifting weight. The submerged weight is the weight of the pipe and the coating.

The submerged weight; WS = pipe own weight-buoyancy

The pipe own weight depends on the pipe materials (steel, concrete) and the coating thickness and density.

The resistance force is calculated simply by Coulomb friction by multiplying the vertical load by the friction coefficient. The friction coefficient, μ, is equal to 0.2−0.4 in clay soil and 0.5−0.9 in sand soil.

In weak clays or silty sands, there is significant potential for the pipe to embed itself into the seabed. It is therefore likely under these conditions that the stability of the pipeline will be considered higher than would have been predicted. In the case of stiff clay, dense sand, or bare rock, the potential of the pipe to embed into the seabed is low. The allowance for the pipeline to undergo small displacements within a defender corridor means that improvements over a traditional stability analysis technique may still be obtained.

Pipeline stability depends on the load from the oceanography data, which have the same terminology as that discussed in Chapter 2, Offshore structures loads and strength, about waves and currents. The pipeline is different to a fixed offshore structure as the trunk lines can be hundreds of kilometers which therefore changes the oceanographic data due to these distances and also needs a numerical model to hindcast or extrapolate from known storms to a sufficient number of locations along the pipeline.

As has been presented earlier it is required to define the velocity and acceleration to calculate the drag and inertia force. The most common wave theory is the Airy wave as it has good accuracy as the pipeline is on the seabed giving better results than those from the surface.

Seabed currents in design data are always considered at 5 m above the seabed. This is used to integrate the velocity over the height of the pipe to give an effective steady current.

The current can be calculated as per the 1/7th power law as presented in Chapter 2 as per API or can be calculated using the following formula from DNV RP E305

$$\frac{U_c}{U_r} = \frac{1}{ln\left(\frac{Z_r}{Z_o} + 1\right)} \left[\left(1 + \frac{Z_o}{D}\right) ln\left(\frac{D}{Z_o} + 1\right) - 1 \right]$$

where

U_c is the average velocity over the pipe taking account of bottom roughness, Z_o; and U_r is the reference velocity at height, Z_r, above the seabed which is measured by a current meter.

For the DNV formula the rougher the seabed, the thicker the boundary layer and the lower the average velocity over the pipeline.

The bottom roughness can be obtained from Table 9.7 from DnV RP F109.

As per DNV76, the stability factor of safety, FS, is 1.1 as a minimum. The significant wave height, H_s, is normally used for the force balance for long pipelines

Table 9.7 Seabed roughness.

Seabed	Grain size d_{50} (mm)	Approx. roughness Z_o (m)
Silt and clay	0.0625	5×10^{-6}
Fine sand	0.25	1×10^{-5}
Medium sand	0.5	4×10^{-5}
Coarse sand	1.0	1×10^{-4}
Gravel	4.0	3×10^{-4}
Pebble	25	2×10^{-3}
Cobble	125	1×10^{-2}
Boulder	500	4×10^{-2}

but in the case of spools and jumpers, which are not allowed to move, it is used at the maximum wave height, H_{max}, in the stabilization calculation:

$$FS = (W_s - F_L)/(F_D + F_M) \geq 1.1$$

The hydrodynamic loads effect on a pipeline could be very much higher than the DnV76 model which was obtained by experimental tests. Based on that, in 1981 revised rules published by DnV provided a more realistic hydrodynamic calculation model to match with the experimental tests.

As per above, the pipeline that was designed by DNV76 raised some concerns but these are not dangerous as annual surveys have been undertaken to ensure there are no major problems.

American Gas Association (AGA) stability design software covering the outcomes from experimental tests in the case of a storm on a pipeline show a small displacement due to the wave forces which will result in the pipeline gradually digging itself into the seabed and it has small berms from both sides which increase the resistance to movement and provide hydrodynamic shielding.

The most comprehensive design is to do a dynamic analysis. This considers the pipeline as a compliant structure with short crested waves acting randomly along its length. Localized movement of the pipeline is determined and resultant strains are calculated. Limiting criteria are based on a maximum permissible movement, with the limit at 20 m and operating stresses. The dynamic analysis required the use of finite analysis. The analysis includes random waves, a long compliant pipeline model, and a realistic seabed resistance model, including the effects of embedment, that is, increased resistance as the pipeline moves. Dynamic analysis is permitted by DNV RP E305, the PRCI, and AGA. There is a great deal of software that can do this analysis based on the codes that are used. PRCI provides three levels of analysis. Level 1 is a static calculation by force balance and verifies the FS. Level 2 is a quasistatic approach; this approach considers the soil interactions model and the past cyclic loading and the model storm build up followed by design storm, and calculates the FS. Level 3, which is a dynamic analysis, provides the instant value of the FS, pipe displacement, embedment, and the stresses. The significant wave height, wave period, and spectral peak parameters are input to deliver an idealized spectrum from which the seabed bottom water velocity time history can be derived. The software provides a better result using Morrison's equation only, as its simplest form provides accurate results.

There are two main load cases to consider in the design, as follows:

1. *Load case 1*: the pipeline is empty and resting on the seabed, uncorroded, and the wave and current are as follows:
   - **a.** One-year storm wave considering the significant wave height and spectral peak period associated with a 10-year storm current
   - **b.** Ten-year storm wave and 1-year storm current;
2. *Load case 2*: The operation condition is the pipeline full of liquid with its density considering the marine growth if it affects the result and the following combination of analyses as per DnV-RP-F109 are carried out:

a. One-hundred-year storm wave and 10-year storm current
b. Ten-year storm wave and 100-year storm current.

9.4.2 Near-shore pipeline

Waves refract as they come into shallow water, which means that they approach the shore in a direction close to a right angle. As shown in Fig. 9.5 pipelines tend to approach perpendicular to the shoreline for stability.

High wave particle velocities are associated with breaking waves in the same direction as the waves, therefore routing the pipeline perpendicular to the shoreline minimizes the destabilizing cross-velocities. In addition, it is normal to bury the pipeline on its final approach and across the beach in the surf zone. These inshore sections of pipeline often have increased concrete coating thickness or density. The attack wave angle is also lower inshore, and the wave destabilizing force tends to be greater in shallower water.

As discussed earlier, for offshore omnidirectional waves and the corresponding current should always be considered in order to ensure the stability of the pipeline.

In case of the shore approach, it will be over design for pipeline coating, if the design calculation consider the wave omnidirectional.

The US Army shore protection manual provides graphical methods based on Snell's law to determine the refraction of waves. If there is no other information, it is normal to consider extreme wave fronts which are normal to the coastline from either direction. Allowance should be made for tides and the knowledge that these chart have been produced for shipping, and so show the shallowest points rather than the average water depths.

There is software called SWAN developed by Delft University of Technology which is accepted as the standard for nearshore refraction used by industry.

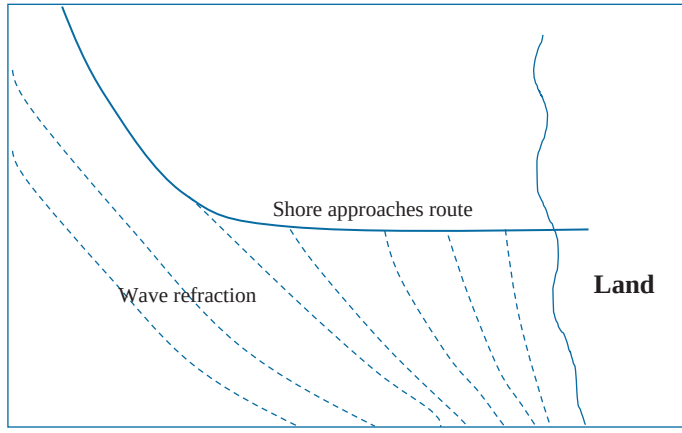

Figure 9.5 Pipeline near-shore approach.

It is important to highlight that the hydrographic chart which is used by shipping is different to the topographic survey described earlier in defining the depth of the seabed, as the hydrographic survey provides a seabed higher by 0.5 m as it provides a FS of 0.5 m to allow for ship draughts.

9.4.3 Methods of stabilization

There are many methods of stabilization. The most common is to use steel coated with concrete, as shown in Fig. 9.6. The density of the concrete is 2.5 t/m^3 and by adding hematite, which is iron ore, the density can reach 3.04 t/m^3.

Concrete coating is normally applied either using the wrap or impingement method. The coating thickness tolerance is about ± 5 mm, therefore the pipe weight is uncertain, and this should be considered in addition to the fact the testing after fabrication will include weighing the pipe.

When creating a trench it is good from a stabilization point of view to provide shielding from hydrodynamic forces, and in the case of the drag force there will be a higher resistance and so it is necessary to move the pipe up. The coefficient of friction will increase as presented in Fig. 9.7.

The effective friction due to seabed inclination is:

$$\mu_e = \frac{tan\theta + \mu}{1 - \mu tan\theta}$$

Figure 9.6 Pipeline coating.

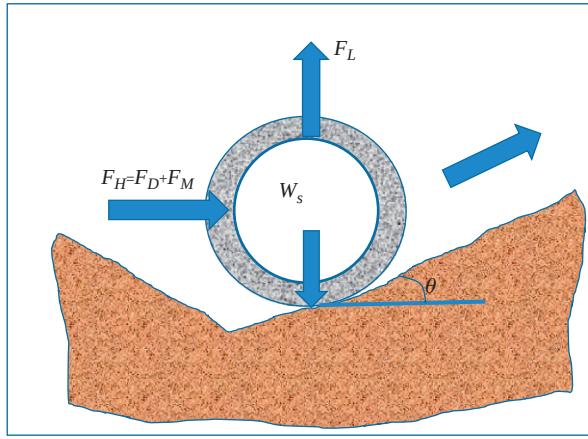

Figure 9.7 Pipeline trench.

where θ is the slope angle of the seabed from the horizontal, μ_e is the effective friction coefficient, and μ is the friction coefficient constant as per the soil type.

Due to cyclic loading on the pipeline, the pipe will be embedded in the seabed and create a small berm over time which will increase its stability. From a practical point of view, the pipeline can be moved laterally up to 20 m but there should be no obstructions or facilities in the seabed within 500 m.

In addition to the cyclic load there will be some settlement due to pipeline weight and the nature of the soil. In case of calculating pipeline settlement, the pipeline is considered theoretically as an infinity long foundation and perform calculation based on this assumption.

It is important to take care in calculating the submerged weight as the fluid during operations may change over the lifetime of the pipeline as the water cut will increase with time, which is normal practice, or the gas oil ratio may increase and the variation of the submerged load should be considered also. In one case study the company changed the pipeline services from oil to gas without carrying out any management of change policy resulting in the pipeline floating on the sea surface—this is a clear result of stabilization not being considered.

Mattresses can be used to stabilize the pipeline. Concrete mattresses are widely used as they are cheap and simple, however there are some disadvantages as they are not fixed to the pipeline, therefore in the case of severe adverse sea conditions, the edge may be lifted and the mattress may be moved from over the pipeline. Concrete mattresses are illustrated in Figs. 9.8 and 9.9.

Another method of stabilization is using a rock dump, as presented in Fig. 9.10.

In the case of a rock seabed, anchor bolts can be used to fix the pipeline. These will fix the anchor by grouting after drilling the rock, as shown in Fig. 9.11. The anchor bolts are installed after the pipelaying at a spacing of around 20 m.

Figure 9.8 Concrete mattress.

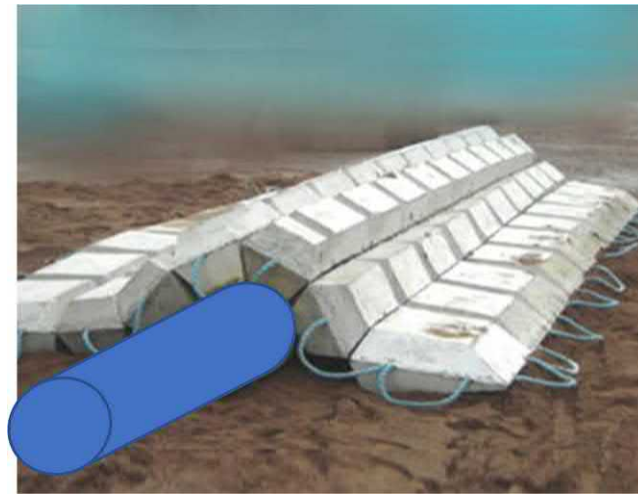

Figure 9.9 Mattress on the pipeline.

Figure 9.10 Rock dump for stabilization.

9.4.4 Combined current and wave in pipeline

High currents can be generated during storms and affect a wave break onshore. Longshore currents form to permit water from reaching the rips. The latter form at regular intervals along a beach but are aligned normal to the beach. The longshore

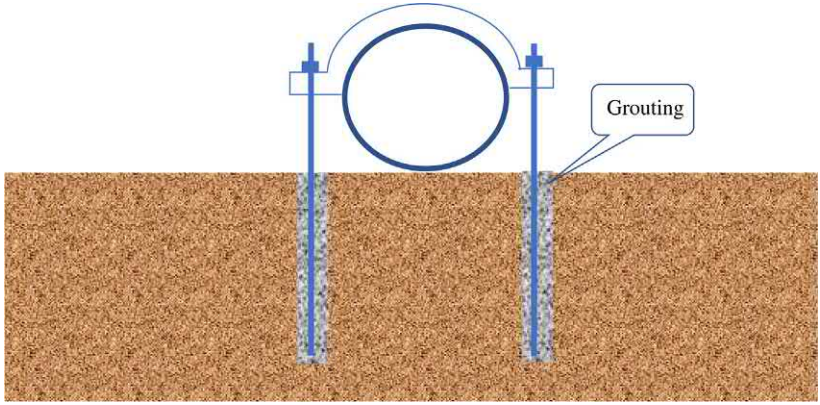

Figure 9.11 Anchor bolts for pipeline stabilization.

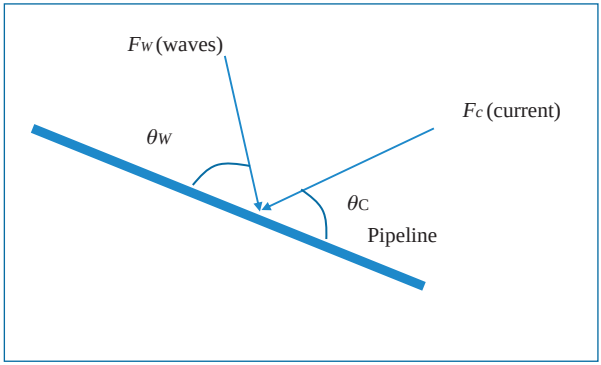

Figure 9.12 Combined current and wave forces.

currents will be aligned normal to the beach and be aligned at 90 degrees to the pipeline and can reach high velocities of up to 1 m/s.

The combined forces are presented in Fig. 9.12 and calculated as follow:

$$F = F_w sin\ \theta_W + F_c sin\theta_C$$

These combined forces are calculated and define the required rock dump for stability.

9.4.5 Impact load

The impact load is considered in the design of the pipeline. The most commonly dropped object characteristics are shown in Tables 9.8 and 9.9. The impact load is due to the dropped object, which includes tubular or bulky objects.

Table 9.8 Most commonly dropped objects.

Tubular objects	OD, mm (in)	WT, mm (in)	*L*, mm (ft.)	Mass, ton	Velocity, m/s (ft./s)	Impact energy (kJ)
Drill collar	280 (11)	102 (4)	9450 (31)	4.2 (4.63 US ton)	22.4 (73.5)	1050
Scaffold pole	48 (1.9)	4.5 (0.18)	6400 (21)	31 kg	66 (216.5)	70
Drill casing	760 (30)	9.5 (0.37)	13100 (43)	2.32 ton (2.6 US ton)	11.9 (39.0)	164

Table 9.9 Most commonly dropped heavy objects.

Object	Length, m (ft.)	Width, m (ft.)	Height, m (ft.)	Weight ton (US ton)
Container	6.1(20)	2.4(7.87)	1.2 (3.9)	15.0 (16.5)
Skid-mounted generator	5.25 (17.2)	1.91(6.3)	2.95 (9.7)	10 (11)

The other effect of impact is trawling, which is regularly used in the fishing activity. Example of dropped tubular objects and bulk objects are listed in Tables 9.8 and 9.9.

The dropped object has a velocity in air that after landing in water will be reduced due to resistance from the water due to the jet force, friction force, and buoyancy force. It will reach the pipe and transfer its energy to the pipeline.

When there is a large diameter with a higher value of D/t the majority of the energy is absorbed by the pipe wall, for smaller pipes with lower D/t the energy will be absorbed globally by the soil and pipe.

The dent energy is the proportion of the impact energy that is actually dissipated during dent deformation. From the numerous impact tests performed, conclusions have revealed that no more than 50% of the kinetic energy is actual dissipated in dent deformation. A more accurate assessment could be done by detailed finite element analysis simulation of the global and local bending mechanisms.

The Ellians−Walker equation for bare pipes is as follows:

$$d_i = \sqrt{D_m\left(\frac{E_d}{25\sigma_y t^2}\right)}$$

where E_d is the denting kinetic energy (J) (lbf.ft.); D_m is the mean diameter (m) (ft.); σ_y is the yield stress (N/m^2) (lbf/ft.^{2}); and t is the wall thickness (m) (ft.).

DNV modified this equation to the following formula:

$$H_p = \left[\frac{F_{sh}}{5\sigma_y t^{1.5}}\right]^2 - \frac{F_{sh}\sqrt{0.005D}}{5\sigma_y t^{1.5}}$$

where

$$F_{sh} = \left(37.5E_I\sigma_y^2 t^3\right)^{0.333}$$

H_p is the permanent plastic dent depth; F_{sh} is the maximum impact force experienced by the pipe shell; σ_y is the pipe material yield stress; t is the pipe wall thickness (steel); D is the steel pipe nominal outside diameter; and E_I the is impact energy absorbed locally by the pipe shell and coating.

There have been many impact tests on coated pipes and it is possible to draw some conclusions on the benefits offered by coatings. There are, however, few tests on uncoated pipes or thin coatings.

Concrete coating is effective in protecting pipelines from denting due to impacts from otter trawls and beam trawls. Tests were performed by Shell in the mid-1980s with a rigidly restrained pipe impacted by a pendulum. They showed that 8−10 blows of 17 kJ were needed to penetrate 75 mm concrete coating and expose the ant-corrosion coating underneath. Field trials carried out at the same time with beam trawls at 3.5 and 3.8 tonnes towed at 4.5 and six knots showed only superficial scratching of the coating, with no observable spalling or penetration of the concrete.

The laboratory tests were therefore seen as conservative.

9.4.6 Pipeline free span

The main problem with the pipelines is the free span as it produces a lot of stresses on the pipeline. Free span is caused by the following:

- uneven seabed on selected route;
- rock dump;
- sandwave;
- scour;
- rocks;
- coral outcrop.

The free span shown in Fig. 9.13 is causing a load due to self weight and external load, in addition to VIV as discussed in earlier chapters.

The portion of the pipeline that spans is subjected to its own weight, fluid loading, or other vertical loading. This could cause a higher bending moment and corresponding higher stress can result in failure due to high bending stresses at the middle of the span.

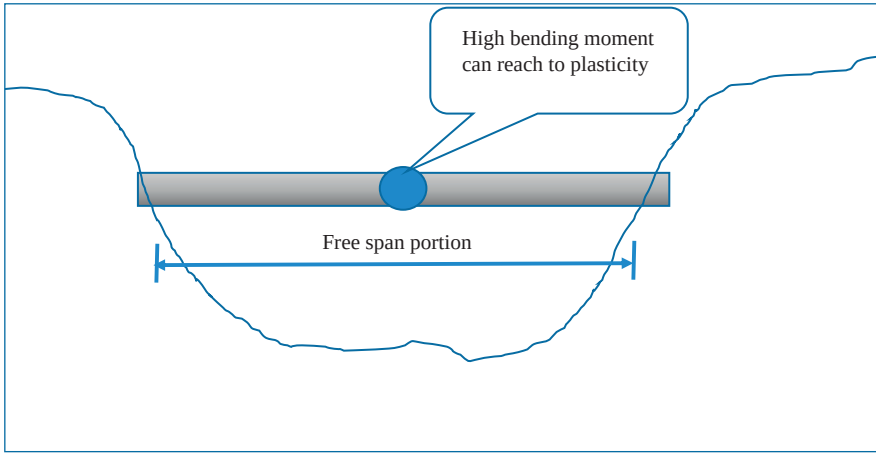

Figure 9.13 Pipeline free span.

A second mode of failure in this case is fatigue due to VIV. These types of vibration induced in the span are due to the passage of the current perpendicular to the pipeline. As per the VIV phenomena discussed earlier, oscillation of the pipeline may reach close to the natural frequency of the pipeline and cause failure due to fatigue. Free span can be identified during visual inspection by divers or ROV. The normal mitigation is to put a sandbag underneath the pipeline.

For free span analysis, it is important to carry out a static analysis, and a dynamic analysis will be applied. Based on that the following load cases will be applied.

The free span analysis shall consider the following load cases as an example applicable along the pipeline design life.

Load case 1—Static analysis:

Empty pipeline with no corrosion allowance or marine growth taken into consideration.

Load case 2—Static analysis:

The pipeline under pressure/temperature loading, with full corrosion allowance is conservatively deducted from the pipe nominal wall thickness, subjected to the most onerous axial force due to pressure/temperature loading; marine growth shall be considered only when it results in more stringent allowable free-span lengths.

Load case 3—Dynamic analysis:

Empty pipeline resting on the seabed, under 1-year storm wave, with no corrosion allowance or marine growth taken into consideration.

Load case 4—Dynamic analysis:

The water-filled pipeline resting on the seabed, under 1-year wave storm, with no corrosion allowance or marine growth taken into consideration.

Load case 5—Dynamic analysis:

The pipeline in operation under a 100-year storm wave, with the full corrosion allowance conservatively deducted from the pipe nominal wall thickness, and

subjected to the most onerous axial force due to design pressure and temperature loading; marine growth shall be considered only when this results in more stringent allowable free-spans lengths.

As per Fig. 9.12, the end support cannot be considered as a hinge support and cannot be considered as 100% fixed support, so in this case the bending moment will be calculated from:

$$M_{max} = w \cdot L^2/10$$

where M_{max} is the maximum bending moment, w is the total gravity load, and L is the free-span length.

To model the pipeline one end is hinged and the other end is fixed, providing suitable assumptions and realistic calculations.

The combined stress by von Mises criteria are calculated in this case and compared with the allowable stresses:

$$\sigma_e = \sqrt{\sigma_{axial}^2 + \sigma_{hoop}^2 - \sigma_{axial}.\sigma_{hoop} - 3\tau^2}$$

where σ_e is the equivalent stress.

VIV is critical for the free span, so it should be checked against the fatigue effect. The natural frequency is calculated from the following equation and there are alternative methods using instruments can be mounted on an ROV to measure the natural frequency of the existing spans.

$$f_o \cong C_1.\sqrt{1 + CSF}\sqrt{\frac{EI}{m_e L_{eff}^4}.\left(1 + C_2\frac{S_{eff}}{P_E} + C_3\left(\frac{\delta}{D}\right)^2\right)}$$

$$CSF = K_c(EI_c/EI_s)^{0.75}$$

The coefficients, C_1, C_2, and C_3 are presented in Table 9.10.

where

E is the Young's modulus of steel; I is the moment of inertia; CSF is the concrete stiffness enhanced value; K_c is an empirical constant to account for deformation of concrete corrosion coating and cracking of concrete, which is equal to 0.33 for asphalt and 0.25

Table 9.10 Boundary condition factors.

Boundary condition	C1	C2	C3	C6
Pin−pin	1.57	1.00	0.8	5/384
Fix−fix	3.56	0.25	0.2	1/384
Single span on seabed	3.56	0.25	0.4	1/384

for/P_P/P_E; L_{eff} is the effective span length; S_{eff} is the effective axial force negative in compression; P_E is the Euler buckling load = $(1 + CSF)\pi_2\ EI/(L_{eff})^2$; and δ is the static deflection due to self weight in cross-flow direction or hydrodynamic drag in an in-line direction limited to $4D$ where D is the pipe diameter.

The static deflection is calculated from the following formula.

$$\delta = C_6 \frac{q.L_{eff}^4}{E{\cdot}I{\cdot}(1 + CSF)\left(1 + C_2{\cdot}\frac{S_{eff}}{P_E}\right)}$$

where q is the deflection load per unit length.
The effective length, L_{eff}, is calculated as follows:

$$\beta = log_{10}\left(\frac{K{\cdot}L^4}{(1 + CSF)EI}\right)$$

where K is the relevant soil stiffness.

For determination of the vertical soil stiffness K_V, the following expression may be applied:

$$K_V = 0.88\ G/(1 - \upsilon)$$

where G is the soil shear modulus. This formula is based on elastic half space theory for a rectangular foundation under assumption of a pipe length that equals 10 times the contact width between the pipe and soil.

For lateral soil stiffness K_L the following equation can be applied

$K_L = 0.76G(1 + \upsilon)$

Poisson's ratio υ and other soil data can be calculated approximately from Tables 9.11 and 9.12 for sand and clay soil, respectively, as guidelines only and in the case of preliminary engineering designs until the geotechnical data are obtained for verification.

In the case of $\beta \geq 2.7$

$$\frac{L_{eff}}{L} = \frac{4.73}{-0.066\beta^2 + 1.02\beta + 0.63}$$

Table 9.11 Guidelines for geotechnical parameters for sand.

Soil type	ϕ_s **(degrees)**	γ_s **(kN/m^3)**	υ
Loose	28–30	8.5–11	0.35
Medium	30–36	9.0–12.5	0.35
Dense	36–41	10–13.5	0.35

Table 9.12 Guidelines for geotechnical parameters for clay.

Soil type	S_u (kN/m^2)	γ_s (kN/m^3)	υ
Very soft	<12.5	4–7	0.45
Soft	12.5–25	5.0–8.0	0.45
Firm	25–50	6–11	0.45
Stiff	50–100	7–12	0.45
Very stiff	100–200	10–13	0.45
Hard	>200	10–13	0.45

In the case of $\beta < 2.7$

$$\frac{L_{eff}}{L} = \frac{4.73}{0.036\beta^2 + 0.61\beta + 1.0}$$

In general; in the case of $L/D < 30$, normally it is not required to perform a comprehensive fatigue check. If $30 < L/D < 100$; the natural frequencies are sensitive to boundary conditions and axial force. For $100 < L/D < 200$ it is applicable in the case of free spans on an uneven seabed in temporary conditions. Natural frequencies are sensitive to boundary conditions, effective axial force, and pipe feed in. If $L/D > 200$ is applicable in case of temporary condition for small pipe diameter. It is important to highlight that natural frequencies in general are affected by the shape of deflection and the applied axial force.

9.5 Concrete coating

The aim of the concrete coating is to provide adequate weight to overcome buoyancy. In some old pipelines the concrete weight coating was executed by pouring concrete inside shutters around the pipe.

Nowadays it is usual to apply concrete by impingement, which is similar to a shotcrete but with another methodology, a process whereby dry concrete mix is thrown at a rotating pipe. Other methods include wrapping concrete around the pipe, the mix being supported by a carrier tape, or casting in a sliding form.

The coating will stop at a distance of around 360 mm from the spool end to achieve welding of the pipes. The reinforcement steel which is installed in the concrete will be from prefabricated cages or using a welded wire mesh, which is fixed around the pipe at the same time as the concrete is applied. As per DNV OS-F101, there is a required minimum reinforcement of 0.08% in the longitudinal direction, and 0.5% circumferentially. Standard 17 gauge reinforcing net may be user in sheltered waters, but the performance of such coatings has been less than satisfactory in more harsh marine environments, and better results are obtained with heavy-gauge welded wire mesh. Alternatively, high-quality coatings are reinforced with re-bar cages, which may be bent from standard welded mats or tailormade as spot-welded

spiral cages. The reinforcement cages are placed on the pipe joint prior to concrete application.

DNV OS-F101 provides the concrete coating specifications and guidelines.

In general, the reinforced concrete density is around 2.5 t/m^3 and when using iron ore aggregate the density can reach 3.04 t/m^3 noting that by using the slip-forming method, densities of 3.3−3.4 ton/m^3 can routinely be achieved, and it is possible to reach 3.800 ton/m^3.

It is normally required to use a low-alkali, sulfate-resistant cement in the concrete mix. Slag furnace cement can also be used and has a good track record in marine applications, and the minimum cement content is 300 kg/m^3 with a maximum cement ratio of 0.4. Pipe coaters traditionally use drilled-out cores for this purpose, and DNV OS-F101 requires a minimum core strength of 40 MPa, determined according to the standard ASTM C39.

As the density and coating weight in general are the main governors of the pipeline stability calculation, the stresses on the pipe during installation are also affecting by the pipe weight and so accuracy of the coating thickness and density is required. The density can be control by continuous measuring by testing and comparing between dry and wet concretes regularly to obtain a better measurement of the concrete density. The tolerance for the pipe weight is between −10% and +20% on individual pipes and from 0% to 4% on daily production.

For design purposes, water absorption is normally taken at 2% by weight, but it may well be higher, thus DNV OS-F101 allows up to 8% by volume. The coating absorption shall be tested by the immersion of samples as complete coated pipe joints for 24 hours at the coating yard.

The reinforcement may consist of wire mesh, which is spirally wrapped around the pipe simultaneously with the application of the concrete.

In general, materials used for the coating and insulation of pipelines are principally characterized by their density and/or thermal conductivity. Some typical values are given in Table 9.13.

Table 9.13 Insulation and coating properties.

Materials	**Density (kg/m^3)**	**Thermal conductivity (W/m °C)**
Concrete coating	1900−3800	1.5
High-density polyoleofins	Variable	0.43
Fusion-bonded epoxy (FBE)	1500	0.3
Polychloroprene	1450	0.27
Solid polyolefins	900	0.12−0.22
Asphalt enamel	1300	0.16
Syntactic foams	Variable	0.1−0.2
Alumina silicate microspheres	Variable	0.1
Polyolefin foams	Variable	0039-0.175

Fusion-bonded epoxy (FBE) is used as an anticorrosion coating in three-layer coatings. This system, to be effective in corrosion prevention, should have at least 400 micron thick FBE dry film. The high-temperature tolerance of FBE in three-layer coatings is due to the fact that it is essentially dry. As a stand-alone coating in contact with water, fusion-bonded epoxy should not be used at service temperatures exceeding 70°C.

Thin film coatings are vulnerable to mechanical impact, and an unacceptable number of holes is likely to occur during handling and transport, unless the coating is protected with an overlay, for example, of fiber-reinforced cement mortar or liquid-applied polymer concrete.

An *asphalt enamel system* is a hot-applied coating consisting of bitumen enamel reinforced with one or more layers of fiberglass tissue inner wrap, and provided with an outer wrap of bitumen-impregnated fiberglass felt.

In most cases, the thickness will be 5−6 mm, but recent specifications allow 4 mm, provided that it is achieved over the weld seam also. The hot enamel is prepared from oxidized bitumen mixed with mineral fillers to the specified hardness and softening point, and stored at a temperature of approximately 220°C.

Modern three-layer coatings consist of an epoxy primer, a copolymer adhesive, and a top layer of polyethylene (PE), polyurethane (PU), or polypropylene (PP).

The main difference between the three options is increasing temperature tolerance, which is matched by increasing price levels. PE should not be used for service temperatures exceeding 85°C, whereas up to 100°C can be permitted for PU systems, and PP coatings perform satisfactorily between 75°C and 140°C. However, these temperature limits are indicative only, as polyolefin coatings are constantly being developed by manufacturers.

9.5.1 Inspection and testing

Determination of the compressive concrete strength represents some difficulty. Conventionally, structural concrete strength is specified as the compressive strength of standard 300 mm by 150 mm cylinders according to the American Concrete Institute code or 150 mm cubes based on the British Standard, tested at 28 days, and such specimens are routinely cast and tested to monitor the quality of the concrete coating. However, due to the method of application and the dryness of the mix (particularly for impingement) the values may not be representative of the finished coating, and in situ testing is required to document the strength of the concrete actually applied on the pipe.

The visual inspection includes girth tape measurements along the pipe. Normally, a maximum outer diameter and a minimum submerged weight will have been specified (for on-bottom stability), and the coater will have determined a nominal concrete thickness based upon the design concrete density. The concrete coating should be concentric with the pipe, and free of excessive undulations, typical tolerances on the nominal coated pipe diameter being −10 to +20 mm. If the pipeline is to be installed by conventional pipelaying, it is important that the concrete coating cannot slip over the anticorrosion coating, which is documented by push-off tests on the finished coating. A length (typically 1.5−2 m) of concrete coating at

each end of a pipe joint is separated by a circumferential saw cut, and pushed off by hydraulic jacks, the required failure strength depending upon the envisaged lay barge tensioner force.

Push-off tests are normally carried out at room temperature, but for asphalt enamel coatings to be used at the upper limit of the temperature range it might be appropriate to verify the shear strength at the topical temperature. Cases have been recorded of steel pipes creeping out of concrete coatings restrained by soil friction.

The interface shear strength between concrete and hot applied enamel coatings will normally be sufficiently large to ensure that failure occurs in the anticorrosion coating, which has a shear strength of approximately 0.1 MPa at ambient temperature.

For coatings such as FBE or three-layer polyolefins, which are more slippery, special measures must be introduced, such as mechanical roughening, embedding of sand grains, etc.

In most cases it will be an impact due to fishing gear so the concrete should be able to withstand the impact load so it is important to carry out an impact test. A pipe joint is adequately supported, for example, by a sand berm or a massive rig, and hit with a hammer at a specified impact energy. The mass and striker edge of the hammer represent typical trawl equipment, and common tests are: 75 mm flat face hammer of 1000 kg, traveling at 2.0 m/s (four knots); 10 mm radius hammer of 2680 kg, traveling at 2.76 m/s.

For the former test the acceptance criterion would be that no reinforcement is exposed by 60 repeated blows at the same spot. For the latter, more severe test, the anticorrosion coating should suffer no damage, and the radius of spalling should not exceed 300 mm, after five blows. The impact angle is at 90 degrees to the pipe axis, but oblique impact testing (e.g., at 60 degrees) may also be specified.

In general the anodes are placed on the pipe joint prior to the application of a concrete coating, and shielded from contamination by cement or concrete. For concreting by slip forming it may be more practical to install the anodes afterward.

9.6 Installation

The principal unit of any pipeline is the pipe joint, which is an approximately 12.2 m length and is called a “linepipe.”

The following items shall be applied to the pipe joint as per the design stage specifications before being assembled into pipe strings and installed on the seabed:

- internal coating;
- external anti-corrosion coating;
- thermal insulation;
- sacrificial anodes;
- concrete weight coating.

The pipe laying is performed using a lay barge, in general, the offshore pipeline is produced by welding every piping spool to another into a pipe string, the most common methods being S-laying or J-laying.

Smaller diameter pipe strings may also be fabricated onshore and spooled onto a reel, which is then installed by a reel barge. The two methods may be combined in the simultaneous laying of a large and a small diameter pipeline, with the latter piggy-backed on the former. In some cases the pipelaying may be initiated at the shore or at an intermediate shore point.

A dead man anchor is a high holding anchor with a chain, laid down on the seabed to provide the required lay tension. In congested areas, however, it may not be feasible to place an anchor chain on the seabed, and instead start piles may be installed, using a subsea hammer.

The tubular steel piles may be 15−20 m long, and are driven in until only the attachment wire is above the seabed, to avoid the need for subsequent removal. The laying of the pipe string is terminated with a lay-down head.

In the absence of lateral pipe supports the maximum horizontal curvature that can be achieved during pipelaying depends on the seabed friction and the lay tension. It is recommended that one have a straight section of a length at least equal to the water depth between two curves in opposite directions, and both at initiation and at termination the pipeline should be straight for a distance of 500−1000 m.

The conventional and old lay barges move forward by pulling on the anchor cables, which are moored to eight or 12 anchors. The tugboat, with the supply ship, survey boats, and in some cases a diving boat, is hired with the laying barge.

Recently lay barges are stable by dynamic positioning (DP), and can keep station by powerful thrusters. However, DP is most mandatory in deep water, where the suspended pipe string is flexible enough to prevent any small displacements at the surface without causing buckling.

9.6.1 S-lay

A lay barge is a floating factory where the pipe joints are welded on to the pipeline as it is installed. From the lay barge the pipeline describes an S-curve on the seabed, as shown in Fig. 9.14. In the upper part, which is called the overbend, the

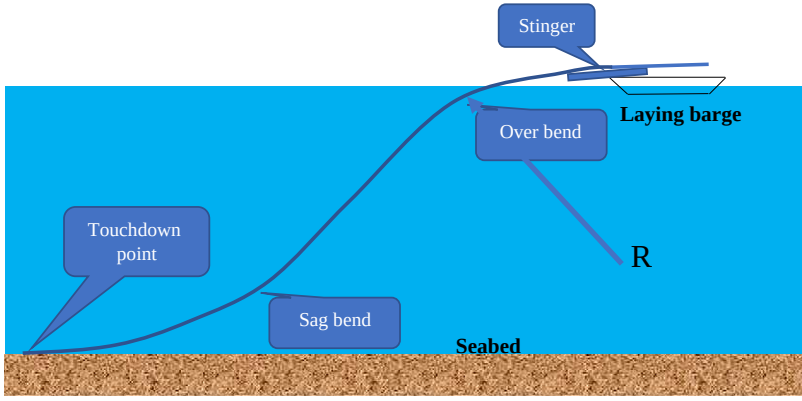

Figure 9.14 S-lay.

curvature profile depends on the stinger of the lay barge and the steel structure is controlled by the lay barge stinger, a steel structure protruding from the stern of the vessel, that supports the pipeline on rollers. The lower part of the curvature is governed by lay tension that is transferred to the pipeline by tension machines gripping the pipe string on the lay barge.

The coated line pipe is transferred to the lay barge using a material barge or supply boat to be stored on the lay barge. Some major lay barges have double jointing facilities, meaning that two 12.2 m pipe joints are welded together, in most cases the automatic submerged arc welding, and then it transfers to the end of the pipe string and is welded on to the pipeline.

Before the stinger the field joint coating is applied. To save time, which directly affects cost offshore, the welding on the pipe stinger is done at a number of stations and as the weld is completed the pipeline goes into the tensioners, which are equipped with rolling tracks to allow movement of the pipeline whilst under tension.

At the final one or two stations, the field joint coating is performed, and the lay barge advances one pipe joint, moving under the pipeline, which goes out over the stinger. The lay rate is highly dependent on the pipe size, welding conditions, etc., but under optimal conditions a daily production rate (working 24 hours) of 4−5 km is not unusual.

The installation contractor checks the stresses in the lay curve, and from this determines the optimum stringer settings and the tension to apply based on the water depth.

The S-lay technique provides higher residual tension stresses on the pipeline in comparison to other pipelaying techniques.

There will be also tension on the touchdown point, and as a rule of thumb the maximum tension bending stresses on the touchdown is 0.6 Fy. This lower allowable stress allows for the dynamic effect during installation. The dynamic effect results in wave motions which cause movements of the laying barge. There is a great deal of software that can calculate the stresses on pipe laying, such as Orca Flex, ABAQUS, ANSYS, Offpipe.

The bending stresses due to curvature on the stringer are calculated from the following formula and the limited bending stress is 0.9 Fy:

$$\sigma_b = E \cdot r/R$$

where σ_b is the bending stresses, r is the pipe outside radius, R is the stringer radius, and E is the Young's modulus.

9.6.2 J-lay

The name J-laying comes from the shape, as shown in Fig. 9.15. S-laying is feasible in water depths of up to approximately 700 m. At greater depths the weight of the suspended pipe string makes it impossible to maintain a stinger supported overbend, and J-laying becomes the best option. This method of laying depends on the pipe

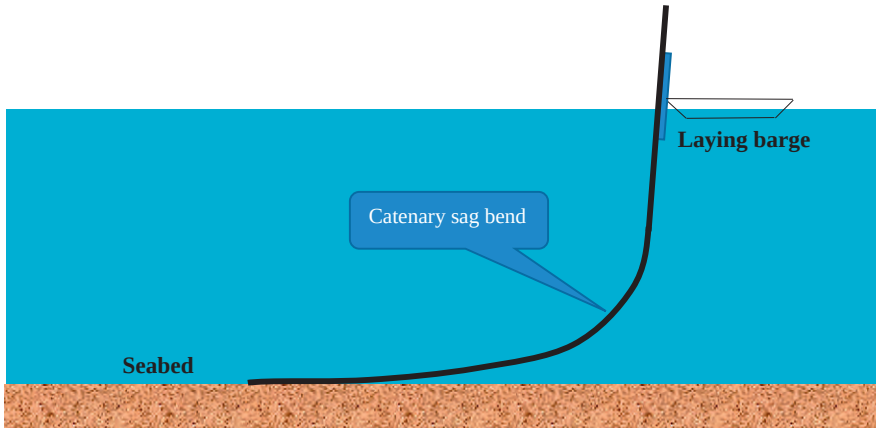

Figure 9.15 J-lay.

Table 9.14 Sample projects for J-laying.

Contractor	Operator	Pipe OD	Water depth (m)	Year
J.R. McDermott	Shell	12″	830	1993
	Shell	18″	1210	1999
	Shell	8/12″	1210	1999
	Shell	8/12″	1350	2001
	Shell	20″	110	1996
Saipem	Exxon	18″	1460	1998
	Gasprom	24″	2150	2002
Stolt offshore	Snepco	10″	1110	2003
Coffexip steria	Kerrmcgee	6″	1130	2001
Saipem	Totalfina Elf	12″	2215	2002

string entering the water in a vertical or nearly vertical position. This eliminates the pipe string, which means that girth welding and field joint coating must take place in one or at most two stations only. For this method of laying the pipe diameter ranges from 4 to 32 in.

Table 9.14 presents sample projects that used the J-laying method.

Thus, traditional welding procedures are too time consuming, and sophisticated methods such as friction welding, electron beam welding, or laser welding are used. To have a reasonable lay rate use double, triple, or quadruple jointing. J-lay barges are therefore equipped with a high tower to support 2−4 pipe joints while they are being added to the pipe string.

Since there is no horizontal stinger there is no need for the pipe to enter the water at the stern of the vessel, which instead may have a mid-ships moon pool.

Alternatively, a drillship may be converted to J-laying. The average pipelay speed is up to 2.3 km/day, which is around half the speed of the S-lay method. The vessel

cost is round 350,000 USD per day. Using J-laying, pipelines may be installed in water depths exceeding 2000 m. At such depths DP is the only feasible method of keeping station, otherwise the operations, including abandonment and recovery procedures, are similar to those for S-laying. Due to deep water, extra weight for stability is not required so there is no concrete coating in the case of the J-lay method. In J-laying the free span is reduced and there are smaller curves on the seabed compared to S-laying and less strain hardening when compared with reel-laying.

9.6.3 Reel-lay

Reel-laying is the process where rigid or flexible pipe is spooled from a drum, passing through tensioners a J-lay tower and then laid over a ramp to the seabed, as shown in Fig. 9.16. The pipe string is unwound from a vertically or horizontally mounted reel of diameter up to 30 m, pulled through a straightening device, and leaves the vessel over the stern. As the pipe enters the water at a steep angle the requirements for stinger support are minimal, and the sagbend is controlled by lay tension imparted by the reel.

So far the largest diameter used has been 18 in to avoid buckling on the reel ($D/t < 22$), and the maximum water depth applied by this method is 2165 m. The installation rate is approximately 1.25 km/h, and the vessel cost is about 200,000 USD/day.

Obviously, there is a limit to the diameter of the pipe that can be spooled, and currently the maximum feasible size for reel barge installation is 16 in, although some examples of 18 in pipe reeling have been reported. The wall thickness of a reeled pipeline will normally be governed by the strains imposed during installation, and depend upon the diameter of the reel. The pipeline cannot be provided with concrete weight coating, but adequate negative buoyancy is ensured by the heavy wall thickness, at least in deep waters which are not subject to much wave and current action. Indeed, reeling is most suitable for pipelines subjected to high pressures or large water depths, where the thick steel wall demanded by the installation method is also required to resist the functional or environmental loads.

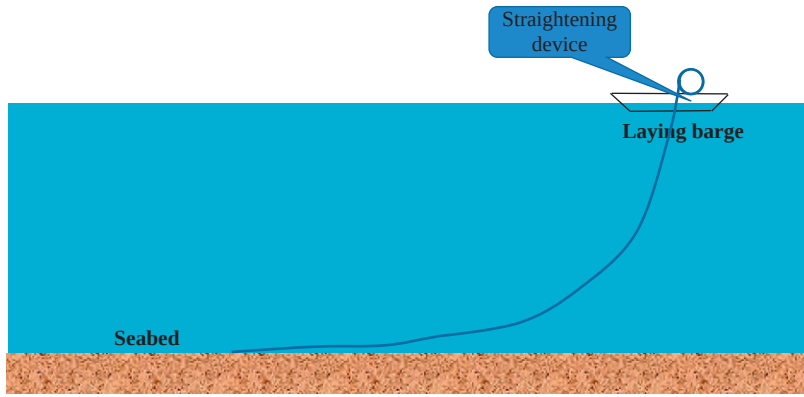

Figure 9.16 Reel-lay.

The pipe string is manufactured onshore and spooled onto the reel. The individual string length depends upon the diameter, for a 12 in pipeline it may reach 10 km. Such spools are too heavy to be transferred offshore, so the reel barge has to return to base to load a new string. In the meantime the pipeline is temporarily abandoned on the seabed.

Once the new spool is joined to the pipeline the reeling only has to stop for the installation of sacrificial anodes at the spacing determined by the design. Bracelet anode half-shells for offshore mounting may be hinged together on one side to minimize the amount of field welding. On the other hand, this can reduce the clamping force, causing the anode to be sheared off during laying or trenching. The electrical cable connections are welded onto doubler plates.

9.6.4 Piggyback installation

In some cases it is required to install two or more pipelines between platforms that may be small services pipelines, such as injection water or gas lift, or a power cable or communication line.

Therefore it is economical to do the installations for all at the same time.

For the past 20 years, the practice of installing two or more pipes has become an established practice in the North Sea.

The lay barge may have room for two lines, but typically the secondary lines would be fabricated onshore and wound onto spools, whereas the main pipeline could be suitable for reeling or S-lay.

From this point the S-lay barges shall be equipped with a smaller stinger on the side from which a secondary pipeline can be paid out during the laying of the main line, however it is more common to clamp the smaller lines on to the larger in piggyback fashion. For this purpose specially designed saddles are used, usually elastomer blocks strapped to the main pipeline by means of aramid fiber (Kevlar) or stainless steel bands.

The piggyback saddles may accommodate several smaller pipelines or cables, depending upon the individual sizes. As the main pipeline is being laid, the secondary lines are unreeled and clamped to the pipeline as is goes over the stinger. In addition to the mechanical attachment by the clamps, the secondary pipelines must be electrically connected to the main pipeline. In order to be covered by the cathodic protection, the sacrificial anodes are designed to include the smaller pipelines also. Alternatively, the piggyback will also have to be fitted with anodes. Two pipelines of similar size may also be clamped together using elastomer or rubber spacers, and laid in one operation.

9.7 Installation management

If you separate the pipeline project for engineering and installation and not EPC, you need an interface management. As some installation procedures and sequences match with the design, the interface is very important for this project.

The installation procedure is dependent on the size and complexity of the pipeline project, a number of specifications will be required to be made by the contractor, based on the owner's specifications for the work.

To identify possible critical items or activities it may be beneficial to carry out systematic analysis of installation operations and equipment, so-called hazard and operability (HAZOP) studies and failure mode effect analyses (FMEA), and an installation risk assessment.

The following documents should be review by the owner or the technical authorities before starting the installation:

- Health, safety, and environmental specification;
- Survey procedures detailing survey requirements, including equipment for the various stages of the work;
- Installation procedures for all the construction methods applied, including monitoring and acceptance criteria, validation of equipment and vessels, qualification of operators such as welders, and all documents to be delivered;
- Trenching specification;
- Shore approach construction works procedures;
- Subsea structures fabrication and installation procedures;
- Pipe protection and seabed intervention procedure;
- Hydrotest procedure;
- Dewatering and drying procedure.

The installation manual in the prelay phase, including supporting specifications, for an offshore prelay survey includes the following as a minimum:

- Survey equipment and software details, specifications for key equipment;
- Equipment calibration procedures and checklists;
- Vessel acceptance trial procedures;
- Manning levels;
- Prelay survey procedures;
- Tidal model;
- Any special procedures for location of live cables;
- Procedures for obstruction identification and removal;
- Procedures for minor re-routing around obstructions;
- Contingency procedures;
- Details of all reporting formats;
- Results of prelay HAZOP and associated FMEA studies performed.

The installation manual shall be included the following information to be reviewed and accepted by the owner:

- General arrangement and elevation drawings of the laybarge, showing locations of all major equipment required for installing the pipeline; elevation drawings to include pipelay configuration drawings and details of the stinger for all configurations to be adopted during the work with sufficient information to enable review of roller heights and positions;
- A schedule of proposed tensioner settings for the entire pipeline;
- Calibration of tensioner and constant tension winch;
- Ranges of permissible roller reactions for critical rollers;
- Verification of roller friction;

- Predicted location of pipe catenary touchdown point, and prediction of suspended pipeline configuration;
- Tension requirements for abandonment and recovery operations testing and inspection of tensioning equipment;
- Cable payout/position of laydown head during abandonment and recovery operations;
- Assessment of station-keeping performance in high currents;
- Local buckling unity checks for the different stages of the installation and for each coating configuration, pipe wall thickness, and water depth combination encountered;
- Local buckling unity checks during retrieval of a dry buckled pipe from the maximum water depth along the route;
- Local buckling unity checks during retrieval of a wet buckled pipe from the maximum water depth along the route;
- Buckle detection system details;
- Laybarge- and anchor-positioning procedures, anchor patterns, and graphs;
- Survey equipment and software details and matrix of key equipment;
- Procedures for pipelay initiation, normal lay, and laydown;
- Contingency procedures;
- Procedures for pipelay at crossings, including contingency procedures in the event that the pipeline is not bearing on the prepared supports or significant settlement takes place;
- DP operating procedures;
- Diving manual;
- Vessel and equipment acceptance trials program;
- Details of all quality assurance (QA) reporting formats that are to be used;
- Production welds test proposals;
- Material handling and repair procedures;
- Field joint coating procedures;
- Wrapping tape/heat shrink sleeve data sheets;
- Infill system data sheets;
- Infill system handling procedure;
- Results of pipelay HAZOP and associated FMEA studies performed.

References

Ayers, R.R., Allen, D.W., Lammert, W.F., Hale, J.R., Jacobsen, V., 1989. Submarine pipeline on-bottom stability: recent AGA research. In: Proceedings of Eighth Offshore Mechanics and Arctic Engineering Conference, The Hague, OMAE, vol. 5, pp. 95–102.

Herynk, M.D., Kyriakides, S., Onoufriou, A., Yun, H.D., 2007. Effects of the UOE/UOC pipe manufacturing processes on pipe collapse pressure. Int. J. Mech. Sci. 49 (5), 533–553.

Hobbs, R.E., 1984. Inservice buckling of heated pipeline. J. Transp. Eng. ASCE 110 (2), 175–189.

Jiao, G., Sotberg, T., Bruschi, R., Verley, R., and Moerk, K. (1996). The SUPERB project: wall-thickness design guideline for pressure containment for offshore pipelines', proc. of OMAE96.

Wolfram, W.R., Getz, J.R., Verley, R., 1987. PIPESTAB project: improved design basis for submarine pipeline stability. In: Proceedings of the Nineteenth Annual Offshore Technology Conference, Houston, TX, OTC 5501, 27–30 April 1987.

Further reading

DNV-RP-F105, 2006. Free spanning pipelines, February 2006. Høvik: Det Norske Veritas.
DNV-RP-F109, 2010. On-Bottom Stability Design of Submarine Pipelines, October 2010. Høvik: Det Norske Veritas.
PD8010-2, 2015. Code of practice for pipelines – Subsea pipelines. British Standard Institutes, March 2015.

Index

Note: Page numbers followed by "*f*" and "*t*" refer to figures and tables, respectively.

Q

OFFSHORE STRUCTURES
DESIGN, CONSTRUCTION AND MAINTENANCE

MOHAMED ABDALLAH EL-REEDY

Offers up-to-date and cost-effective approaches for designing, constructing, and maintaining the integrity for offshore systems that will withstand all types of environments

Key Features

- Describes the latest updates with subsea pipeline design and installation
- Proposes step-by-step approach to structural and design system analysis
- Includes design consideration for all types of environmental conditions
- Illustrates up-to-date maintenance planning and inspection programming
- Provides special procedure for fabrication and installation of offshore platforms
- Presents risk-based underwater inspection techniques

One of the only references available that takes into account the full range of complexities inherent in offshore construction operations, *Offshore Structure: Design, Construction, and Maintenance,* Second Edition, provides a road map for designing structures that will withstand even the harshest offshore environment, making it the ultimate reference for selecting, operating, and maintaining offshore structures. Updated to reflect the latest research in the construction, analysis, and design of offshore structures, this new edition evaluates and addresses the structural concerns that plague offshore structural designers and engineers throughout a structure's operational lifecycle. This book includes three new chapters regarding design analysis modeling, decommissioning and removal of offshore structures, and subsea pipeline design and modeling.

Packed with charts, tables, and diagrams and written with clear and concise language on the advantages and disadvantages of the various types of offshore structures and platforms currently in operation around the world, this book provides engineers the most up-to-date methods for performing a structural life-cycle analysis and enables them to implement maintenance plans for topsides and effectively employ nondestructive testing techniques. Underwater inspection is discussed for hundreds of platforms in detail with information on repair methodology for scour, marine growth, and damaged or deteriorating members. Risk-based underwater inspection techniques are explored from a practical point of view.

Related Titles

El-Reedy, Marine Structural Design Calculations
978-0-08-099987-6

Chakrabarti, Handbook of Offshore Engineering
978-0-08-044381-2

Bai and Jin, Marine Structural Design
978-0-09-099997-5

Technology and Engineering / Construction / General

ISBN 978-0-12-816191-3

9 780128 161913

ELSEVIER

Gulf Professional Publishing
An imprint of Elsevier
elsevier.com/books-and-journals